Modelling, analysis and optimisation of energy systems on offshore platforms

Nguyen, Tuong-Van

Publication date:
2014

Document Version
Publisher's PDF, also known as Version of record

Modelling, analysis and optimisation of energy systems on offshore platforms

PhD Thesis

$$(EIv'')''=q-\rho A\ddot{v}$$

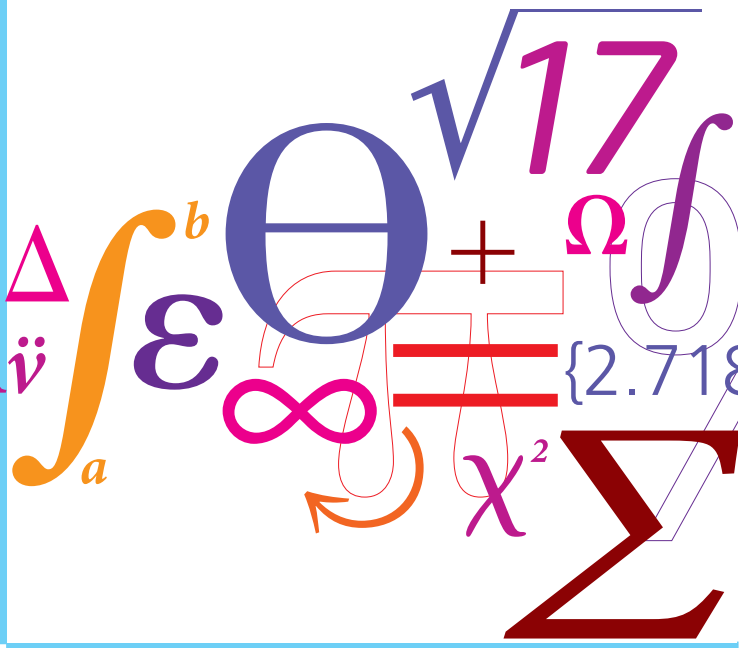

Tuong-Van Nguyen
DCAMM Special Report No. S170
October 2014

DTU Mechanical Engineering
Department of Mechanical Engineering

Modelling, analysis and optimisation of energy systems on offshore platforms

PhD Thesis
submitted the 31st of October 2014
and defended the 19th of December 2014
at the
TECHNICAL UNIVERSITY OF DENMARK

for the degree of Doctor of Philosophy

by
Tuong-Van Nguyen

under suggestion of:
Associate Professor Brian Elmegaard (DTU), main supervisor
Chief Scientist Peter Breuhaus (IRIS), co-supervisor
Associate Professor Fredrik Haglind (DTU), co-supervisor

and under recommendation of:
Associate Professor Gürkan Sin (DTU), examiner
Vice President Per Bagge Angelo (Mærsk Oil), examiner
Associate Professor Silvio de Oliveira Júnior (USP), examiner

Modelling, analysis and optimisation of energy systems on offshore platforms

PhD Thesis
DCAMM Special Report no. S170
Printed by Rosendahls – Schultz Grafisk A/S
Font: Utopia typeset with LaTeX 2ε

DTU Mechanical Engineering
Section of Thermal Energy
Technical University of Denmark

Nils Koppels Allé, Bld. 403
DK-2800 Kongens Lyngby
Denmark
Phone: (+45) 4525 4131
Fax: (+45) 4525 4325
www.mek.dtu.dk
ISBN: 978-87-7475-392-6

to my friends
for the dreams and tears we've shared

It is good to have an end to journey toward;
but it is the journey that matters, in the end.

— Ursula K. Le Guin

Preface

The present thesis was prepared at the Section of Thermal Energy, Department of Mechanical Engineering, Technical University of Denmark (DTU). It is submitted as a partial fulfilment of the requirements for the degree of Doctor of Philosophy and is written as a monograph.

The work was carried out for three years, from November 2011 to October 2014, under supervision of Associate Professor Brian Elmegaard (DTU) and co-supervision of Chief Scientist Peter Breuhaus (International Research Institute of Stavanger, IRIS) and Associate Professor Fredrik Haglind (DTU).

An external research stay was undertaken at the Industrial Process & Energy System Engineering group (IPESE), Institute of Mechanical Engineering, École Polytechnique Fédérale de Lausanne (EPFL), under guidance of Adjunct Professor François Maréchal, from June 2013 to January 2014.

The funding was ensured by the Technical University of Denmark and the Norwegian Research Council, through the Petromaks programme and within the project 2034/E30 led by Teknova. Support was also received from the Otto Mønsted A/S Fond in the frame of the ECOS 2013 and PRES 2014 conferences, and of the PhD exchange in Switzerland.

København, 31st October 2014 Tuong-Van Nguyen.

Acknowledgements

The completion of this dissertation has been an enriching journey that could not have been achieved alone. Choosing the 'right words' to thank all the persons met in this time of doubts was incredibly difficult. As I look back and read, these words still cannot express how grateful I feel, but I am glad that they pay homage to all the ones who have made a difference.

First of all, I thank Brian Elmegaard, my main supervisor, for having chosen me for this project. His confidence in my skills, his scientific curiosity, and the freedom he has given me have been essential for keeping me going. My gratitude also goes to my co-advisor Peter Breuhaus, who has admirably managed to supervise me at a distance, always coming up with constructive feedback, and to my co-supervisor Fredrik Haglind, for interesting conversations.

It has been an honour to have Gürkan Sin, Per Bagge Angelo and Silvio de Oliveira Júnior in my thesis committee. I have truly appreciated their time and the efforts spent in evaluating this manuscript, improving its quality and challenging me in engaging discussions.

This PhD project has led to cooperation with skilled researchers at other institutions. Mari is thanked for having invaluably contributed to the present work with inspiring and passionate talks, sharing her knowledge and easing my research. Laurence is thanked for her outstanding help with modelling issues, encouraging me when needed.

These three years would not have been as enjoyable without my colleagues. In particular, I thank Andrea, for his constant good mood and many entertaining moments a bit everywhere in the world. Jorrit, for a lot of 'hygge' behind and beyond the doors of the university. Jesper, for all the good laughs, productive conversations and one-day hikes. Thomas, for many fun times and gaming weekends. Peam, for his patience and the sometimes serious discussions. Abid and Elham, for the convivial working environment. Leonardo, Ulrik and Francesco, for many fruitful collaborations and interesting work suggestions.

Part of my project took place at the École Polytechnique Fédérale de Lausanne, and I thank François Maréchal for this opportunity. I also thank Nicolas, Elfie and Leandro, for the lively atmosphere in our office. Matthias and Myriam, for the warm welcome and constant teasing. Emanuela, Priscilla and Manuel, for cheering and backing me up, and for plenty of fond memories. And all the other ones next doors, for having made these eight months a blast.

Acknowledgements

However, these acknowledgements would be incomplete if my students were not mentioned, since they have shaped my time as a PhD candidate. Tomek[1], as my 'first student', deserves the first mention. I have been lucky to know and work with someone as keen to listen and learn as you. Thanks for being such a tireless, devoted and kind person.

Gabi[2], thank you for your care, not to leave out your maddening sense of humour, and the non-neglectable amount of hours discussing all types of matters. I also have a thought for the other Ghost House people, who have been present in the good and in the demanding times as well[3]: Timi, for trusting and giving me the right push when needed. Maria and Toni, for bringing so much energy in every moment spent together. Federico, for making all of them a lot funnier. Gianluca, for keeping the spirits up. Maria, for being so gentle.

It has been a chance to be the supervisor of many other talented students. I thank Mathies, for being a determined and motivated person, and for the exciting conversations over Internet. Friedie, for constantly pushing the boundaries of our knowledge, and for the countless and gripping exchanges of views and ideas. Þór, for his interest in this novel field, and for a lot of moral support in the endless working nights. Dennis, for his general awesomeness skill, making the end of this project much more pleasant. And the others: Ray, Erik, Eileen, Elena, Alejandra, Hugo and Seif, for having broadened several aspects of this work.

My former Energy Systems students, especially the Greek Crew and Davide, are thanked for having helped me become a better teacher. My Summer School mates are likewise thanked for the great kick-start into the research world, starting from our Polish nights. I have a special word for Αντώνης, my 'lazy bastard'. Thank you for having given me a friendly hand from the start, never letting me aside – it has meant much and has made my way a lot easier.

Je ne peux continuer sans un mot pour mes vieux compagnons de route qui m'ont soutenu toutes ces années. Merci, en particulier, à Aurélie et Antoine, pour avoir cru en moi et m'avoir suivi sur la voie du doctorat. Ma famille est également remerciée pour leur aide tout ce temps, et ma gratitude va à Chantal, qui a été une tante attentionée et à l'écoute.

Quand je suis arrivé à Lausanne durant l'été 2013, je ne pouvais imaginer que je m'y plairais autant. Y revenir, et me promener le long des berges du lac, au versant des montagnes, est toujours un moment spécial. Merci, Bernard, Ursula, Dominique, Laurent et Pierluigi, pour avoir fait de cet endroit un nouveau chez moi.

Unfortunately, most of the ones I care about may never see these pages – they cannot imagine how glad I feel having them by my side, so I will let them realise how important they are, and I will conclude by this blunt sentence:

[1] Dziękuję mój przyjacielu, teraz jestem w połowie Polakiem.
[2] Egyetlen sünnek sem esett bántódása a disszertáció dolgozat írása alatt.
[3] Winter is coming, and with a lot of agua fresca, m**** and love.

Il y a des rencontres qui marquent,
et qui ne s'oublient pas.

Abstract

Nowadays, the offshore production of oil and gas requires on-site processing, which includes operations such as separation, compression and purification. The offshore system undergoes variations of the petroleum production rates over the field life – it is therefore operated far from its nominal operating conditions, which results in poorer performance.

The present thesis addresses the question of how offshore platforms should be modelled, analysed and optimised from an energy system perspective. The research challenges can be classified into three main areas: (i) the simulation and assessment of oil and gas facilities, (ii) the means to reduce their performance losses, and (iii) the systematic design of future plants.

This work builds upon a combination of modelling tools, performance evaluation methods and multi-objective optimisation routines to reproduce the behaviour of five offshore platforms, quantify the potentials for energy savings, and design more efficient conversion units.

The findings show that the differences in the field and operating conditions directly impact the energy demand and performance profiles of these facilities. Most inefficiencies are associated with the combustion, pressure-change and cooling operations, but these processes are ranked differently depending on the plant layout and on the field production stage.

The most promising improvements consist of introducing a multi-level production manifold, avoiding anti-surge gas recirculation, installing a waste heat recovery cycle, and implementing a CO_2-capture unit. The benefits of such measures vary widely across offshore platforms, pinpointing that no generic improvement can be proposed, and that caution should be exercised when giving recommendations to the stakeholders.

Finally, the several studies stress the importance of developing site-scale solutions, which account for the synergies between the processing and utility plants, to enhance the overall platform performance and intensify the petroleum production.

Keywords. Oil and gas platforms, energy systems, process modelling, exergy and pinch analyses, site integration, multi-objective optimisation, waste heat recovery, CO_2-mitigation.

Resumé

Produktionen af olie og gas på offshore platforme involverer processer såsom separation, behandling og kompression. Indvindingen udviser markante variationer fra år til år, hvilket resulterer i højere energiintensitet, lavere effektivitet og muligvis større energiforbrug.

Formålet med dette projekt er at bidrage til en bedre forståelse af hvordan offshoreanlæg skal modelleres, analyseres og optimeres fra et energiperspektiv. Forskningsmæssige udfordringer knytter sig til (i) simulering og evaluering af olie- og gasprocessering, (ii) analyse af tiltag for at opnå energieffektivisering, og (iii) anlægsdesign af fremtidige platforme med henblik på at reducere energiforbrug, omkostninger og CO_2-udledninger.

Dette arbejde er baseret på en grundig undersøgelse af performance af forskellige platforme: deres forbedringspotentialer er estimeret ved hjælp af avancerede modelleringsmetoder, performance-analyseværktøjer og multi-objekt optimeringsprocedurer.

Resultaterne indikerer, at forskellene i felt- og driftstilstand på tværs af platforme har en klar indflydelse på deres energi- og exergiforbrugsprofiler. De fleste ineffektiviteter er forårsaget af forbrændings-, trykændrings- og varvemevekslingsprocesser, men deres betydning er forskellig fra anlæg til anlæg og varierer med oliefeltets alder.

De mest lovende forbedringer består i at introducere en produktionsmanifold med flere trin, at undgå anti-surge gasrecirkulering, at implementere varmegenvinding, og at indbygge et CO_2-separationsanlæg. De potentielle reduktioner af energiforbrug og CO_2-emissioner varierer dog væsentligt fra platform til platform, hvilket viser at et generelt gyldigt forslag er svært at give, og at forsigtighed skal udvises, når anbefalinger til anlægsdesign gives.

Dette bidrag viser, igennem både modelsimuleringer og optimeringer, at en systematisk systemtilgang, der ikke kun fokuserer på at forbedre performance af en enkelt proces, kan øge procesintensivering og føre til en mere effektiv og bæredygtig olie- og gasproduktion.

Nøgleord. Olie- og gasplatforme, energisystemer, procesmodellering, exergi- og pinchanalyser, systemintegration, multi-objekt optimering, varmegenvinding, CO_2-reduktion.

Papers and Presentations

Part of the work performed during the PhD project resulted in peer-reviewed publications and presentations, which are listed hereafter in the order of acceptance and by category. They are directly or indirectly related to the main topics of this thesis, and all of them have been accepted and published by the end of that project.

Archival papers

(1) **Tuong-Van Nguyen**, Leonardo Pierobon, Brian Elmegaard, Fredrik Haglind, Peter Breuhaus and Mari Voldsund. Exergetic assessment of energy systems on North Sea oil and gas platforms. Energy, vol: 62, pages: 23–36, 2013.

(2) Leonardo Pierobon, **Tuong-Van Nguyen**, Ulrik Larsen, Fredrik Haglind and Brian Elmegaard. Multi-objective optimization of organic Rankine cycles for waste heat recovery: Application in an offshore platform. Energy, vol: 58, pages: 538–549, 2013.

(3) Ulrik Larsen, **Tuong-Van Nguyen**, Thomas Knudsen and Fredrik Haglind. Optimisation and system analysis of a Kalina Split-cycle for waste heat recovery on large marine diesel engines. Energy, vol: 64, pages: 484–494, 2014.

(4) **Tuong-Van Nguyen**, Tomasz Jacyno, Peter Breuhaus, Mari Voldsund and Brian Elmegaard. Thermodynamic analysis of an upstream petroleum plant operated on a mature field. Energy, vol: 68, pages: 464–469, 2014.

(5) Mari Voldsund, **Tuong-Van Nguyen**, Brian Elmegaard, Ivar S. Ertesvåg, Audun Røsjorde, Knut Jøssang and Signe Kjelstrup. Exergy destruction and losses on four North Sea offshore platforms: A comparative study of the oil and gas processing plants. Energy, vol: 74, pages: 45–58, 2014.

(6) **Tuong-Van Nguyen**, Thomas Knudsen, Ulrik Larsen and Fredrik Haglind. Thermodynamic assessment of the Kalina split-cycle concepts for waste heat recovery applications. Energy, vol: 71, pages: 277–288, 2014.

(7) **Tuong-Van Nguyen**, Mari Voldsund, Brian Elmegaard, Ivar S. Ertesvåg and Signe Kjelstrup. On the definition of exergy efficiencies for petroleum systems: Application to offshore oil and gas processing. Energy, vol: 73, pages: 264–281, 2014.

(8) **Tuong-Van Nguyen**, Tamás Gábor Fülöp, Peter Breuhaus and Brian Elmegaard. Life performance of oil and gas platforms: site integration and thermodynamic evaluation. Energy, vol: 73, pages: 282–301, 2014.

(9) **Tuong-Van Nguyen**, Laurence Tock, Peter Breuhaus, François Maréchal and Brian Elmegaard. Oil and gas platforms with steam bottoming cycles: system integration and thermoenvironomic evaluation. Applied Energy, vol: 131, pages: 222–237, 2014.

(10) Mari Voldsund, **Tuong-Van Nguyen**, Brian Elmegaard, Ivar S. Ertesvåg and Signe Kjelstrup. Thermodynamic performance indicators for evaluation of North Sea oil and gas platforms. Journal of Oil and Gas facilities, vol: 3, pages: 51–63, 2014.

(11) Leonardo Pierobon, **Tuong-Van Nguyen**, Andrea Mazzucco, Ulrik Larsen and Fredrik Haglind. Part-Load Performance of a Wet Indirectly Fired Gas Turbine Integrated with an Organic Rankine Cycle Turbogenerator. Energies, vol: 7, pages: 8294–8316, 2014.

Conference publications

(12) **Tuong-Van Nguyen**, Leonardo Pierobon and Brian Elmegaard. Exergy analysis of offshore processes on North Sea oil and gas platforms. Proceedings of CPOTE 2012 - The 3rd International Conference on Contemporary Problems of Thermal Engineering. Gliwice, Poland.

(13) **Tuong-Van Nguyen**, Brian Elmegaard, Leonardo Pierobon, Fredrik Haglind and Peter Breuhaus. Modelling and analysis of offshore energy systems on North Sea oil and gas platforms. Proceedings of SIMS 2012, the 53rd Conference on Simulation and Modelling. Reykjavik, Iceland.

(14) Ulrik Larsen, **Tuong-Van Nguyen** and Fredrik Haglind. Development of a multi-level approach to model and optimise the Kalina Split Cycle for marine diesel engines. Proceedings of SIMS 2012, the 53rd Conference on Simulation and Modelling. Reykjavik, Iceland.

(15) Leonardo Pierobon, Ulrik Larsen, **Tuong-Van Nguyen** and Fredrik Haglind. Optimization of Organic Rankine Cycles for Off-Shore Applications. Proceedings of ASME Turbo Expo 2013. American Society of Mechanical Engineers, 2013.

(16) Mari Voldsund, **Tuong-Van Nguyen**, Brian Elmegaard, Ivar S. Ertesvåg, Audun Røsjorde, Knut Jøssang and Signe Kjelstrup. Comparative study of the sources of exergy destruction on four North Sea oil and gas platforms. Proceedings of ECOS 2013 - The 26th International Conference on Efficiency, Cost, Optimization, Simulation and Environmental Impact of Energy Systems. Guilin, China.

(17) Mari Voldsund, **Tuong-Van Nguyen**, Brian Elmegaard, Ivar S. Ertesvåg, Audun Røsjorde, He Wei and Signe Kjelstrup. Performance indicators for evaluation of North Sea oil and gas platforms. Proceedings of ECOS 2013 - The 26th International Conference on

Efficiency, Cost, Optimization, Simulation and Environmental Impact of Energy Systems. Guilin, China.

(18) **Tuong-Van Nguyen**, Laurence Tock, Peter Breuhaus, François Maréchal and Brian Elmegaard. Thermo-economic assessment of the integration of steam cycles on offshore platforms. Proceedings of ECOS 2014 - The 27th International Conference on Efficiency, Cost, Optimization, Simulation and Environmental Impact of Energy Systems. Turku, Finland.

(19) **Tuong-Van Nguyen**, Laurence Tock, Peter Breuhaus, François Maréchal and Brian Elmegaard. Thermo-Economic Modelling and Process Integration of CO_2-Mitigation Options on Oil and Gas Platforms. Chemical Engineering Transactions - The 17th Conference on Process Integration, Modelling and Optimisation for Energy Saving and Pollution Reduction, vol: 39, pages: 1081-1086, 2014. Prague, Czech Republic.

Poster presentations

(20) **Tuong-Van Nguyen**, Leonardo Pierobon and Brian Elmegaard. Towards energy-efficient offshore platforms. Energieffektivisering for fremtiden, 2012. Kongens Lyngby, Denmark.

(21) **Leonardo Pierobon**, Tuong-Van Nguyen. Technologies for waste heat recovery in offshore applications. Energieffektivisering for fremtiden, 2012. Kongens Lyngby, Denmark.

(22) **Leonardo Pierobon**, Tuong-Van Nguyen. Waste Heat Recovery for Offshore Applications. International Symposium on Advanced Waste Heat Valorisation Technologies, 2012. Kortrijk, Belgium.

The author of the present thesis is responsible, if main author, for most work carried out in the corresponding papers. All the co-authors of the publications listed in this chapter have contributed with scientific feedback on the content of the articles.

Contents

Nomenclature

Abbreviations

ABC	Air bottoming cycle
AC	Alternative current
ACD	Acidification
API	American Petroleum Institute
ATR	Autothermal reforming
BAT	Best available technologies
BCC	Balanced composite curve
BK10	Braun K10
CAPEX	Capital expenditures
CC	Combined cycle
CC	Composite curve
CCR	Carbon capture rate
CEPCI	Chemical engineering chemical plant index
CIT	Compressor inlet temperature, °C or K
CMP	Compressor
COE	Cost of electricity
CS	Chao-Seader
DEPG	Dimethyl ether of polyethylene glycol
DNA	Dynamic Network Analysis
EES	Engineering Equation Solver
EG	Exhaust gases
EI99	Ecoindicator 99
EOR	Enhanced oil recovery
EOS	Equation of state
EUT	Eutrophication
FPSO	Floating production, storage and offloading unit
FU	Functional unit
GCC	Grand composite curve
GE	Exported gas
GHG	Greenhouse gas
GOM	Gulf of Mexico
GOR	Gas-to-oil ratio
GS	Grayson-Streed
GT	Gas turbine
GWP	Global warming potential
HEX	Heat exchanger
HHV	Higher heating value, J/kg
HP	High pressure
HTS	High-temperature shift
HVAC	Heating, ventilation and air conditioning
HVDC	High voltage direct current
IAPWS	International Association for the Properties of Water and Steam
ICC	Integrated composite curve
IPCC	Intergovernmental Panel on Climate Change
LCA	Life cycle assessment

LCI	Life cycle inventory
LHV	Lower heating value, J/kg
LNG	Liquefied natural gas
LP	Low pressure
LTS	Low-temperature shift
MAETP	Marine aquatic ecotoxicity potential
MDEA	Methyldiethanolamine
MEA	Monoethanolamine
MEG	Monoethylene glycol
MEX	Mexogenous
MILP	Mixed integer linear programming
MINLP	Mixed integer non linear programming
MOO	Multi-objective optimisation
NG	Natural gas
NGL	Natural gas liquids
NHV	Net heating value, J/kg
NPD	Norwegian Petroleum Directorate
NRTL	Non-Random Two-Liquid
OE	Exported oil
OPEX	Operational expenditures
ORC	Organic Rankine cycle
PC	Perturbed chain
PR	Peng-Robinson
PSA	Pressure swing adsorption
RVP	Reid vapour pressure
SAFT	Statistical Associating Fluid Theory
SEC	Specific exergy consumption
SED	Specific exergy destruction
SEU	Specific energy use
SMR	Steam methane reforming
SR	Schwartzentruber-Renon
SRK	Redlich-Kwong-Soave
TCC	Twu-Coon-Cunningham
TEA	Triethanolamine
TEG	Tri-ethylene glycol
TIT	Turbine inlet temperature, °C or K
TP	Test pressure
TSA	Total site analysis
VDW	Van der Waals
VHP	Very high pressure
VSC	Voltage source converter
WGS	Water-gas-shift
WOR	Water-to-oil ratio

Greek letters

α	Off-design factor (heat exchanger)
α, β	Shape parameters for beta distributions
α_1	Cost factor (contingencies and fees)
α_2	Cost factor (auxiliary facilities and site development)
β	Chemical exergy correction factor
Δ	Absolute variation
δ	Efficiency defect
δ	Relative variation
δ	Volume-dependent parameter of the attraction contribution
δ_{1-4}	Empirical parameters specific to each EOS
ϵ	Relative error
η	Energy efficiency
η^*	Relative efficiency
ι	Intensity factor
λ	Irreversibility ratio
μ	Mean value
ω	Rotational speed, rpm
ω	Waste factor
Φ	Mass flow ratio

π^*	Relative pressure ratio
ρ	Variance
σ	Specific power consumption
σ	Standard deviation
υ	Molar volume, m^3/mol
ε	Exergy efficiency
$\dot{\omega}$	Corrected rotational speed
$\dot{\omega}^*$	Relative corrected rotational speed

Roman letters

$\bar{e}$	Molar exergy, J/mol
$\bar{x}$	Mole fraction
$\dot{C}$	Cost rate, \$/s
$\dot{E}$	Exergy rate, W
$\dot{F}$	Standard volume flow, Sm^3/h
$\dot{G}$	Corrected mass flow
$\dot{H}$	Enthalpy rate, W
$\dot{I}$	Environmental impact
$\dot{I}$	Irreversibilities rate, W
$\dot{m}$	Mass flow, kg/s or t/h
$\dot{n}$	Molar flow, mol/s or kmol/h
$\dot{Q}$	Thermal energy rate, W
$\dot{S}$	Entropy rate, W/K
$\dot{V}$	Standard volume flow, Sm^3/s
$\dot{Z}$	Investment cost rate, \$/s
A	Capacity/size factor
A	Heat transfer area, m^2
a	Attraction parameter
a, b	Lower and upper bounds for uniform distributions
b	Volume parameter
b_{1-2}	Cost factors (bare module costs)
c	Exergetic cost, \$/kJ
c	Volume-translation parameter
c_{1-4}	Rotational speed factors
c_{trb}	Turbine constant
e	Specific exergy, J/kg
f	Exergoeconomic factor
f_T	LMTD correction factor
f_{Cu}	Copper losses (fraction)
f_{m}	Material factor (bare module costs)
f_{p}	Pressure factor (bare module costs)
g	Gravitational acceleration
g	Process equation vector
h	Specific enthalpy, J/kg
I	Ideal gas constant, J/(mol·K)
i	Chemical compound
i	Measured variable
i_r	Interest rate
j	Stream
j	Unmeasured variable
k	Component
k	Observation
k_{1-3}	Cost factors (purchased equipment costs)
l	Generator load
m	Number of unmeasured variables
m, p	Compressor map scaling factors
n	Number of years
N_{obs}	Number of observations
N_{stages}	Number of stages
N_{wells}	Number of wells
P	Power, W
p	Number of model equations
p	Pressure, Pa
p_{1-4}	Off-design factors (pumps)
R	Ratio of chemicals, mol/mol or kg/kg

R	Redundancy level
r	Recovery ratio
r	Relative cost difference
r	Splitting fraction
s	Specific entropy, J/(kg·K)
T	Temperature, K or °C
T^*	Corrected temperature, K or °C
U	Overall heat transfer coefficient, W/(m^2·K)
u	Estimate of an unmeasured variable
V	Velocity, m/s
w	Weight of the measurement accuracy
x	Mass fraction
x	Measured value
x^*	Reconciled value
y	Component/sub-system exergy ratio
y	Integer activation variable
y^*	Relative component/sub-system exergy ratio
z	Specific pollutant fraction

Subscripts

χ	Exergy-based
v	Volume-based
h	Energy-based
0	Dead state
air	Air
bm	Bare module
C	Cooling demand
c	Critical
cnd	Condensate
cold	Cold stream
cond	Condensation
cool	Cooling medium
cv	Control volume
cw	Cooling water
d	Destruction
dc	Discounted
des	Design
dr	Driver
el	Electric
eq	Equivalent
evap	Evaporation
exh	Exhaust
exp	Export
f	Fuel
feed	Feed
fg	Fuel gas
fn	Furnace
gen	Generation
gen	Generator
gr	Grassroot
gtc	Gas-to-condensate
H	Heating demand
hea	Heavy hydrocarbons
heat	Heating medium
hot	Hot stream
hyp	Hypothetical
i	Inside
id	Ideal
imp	Import
in	Inflow
is	Isentropic
l	Loss
lift	Lift
lig	Light hydrocarbons
liq	Liquid

LMTD	Logarithmic mean temperature difference
MEAN	Mean temperature difference
mec	Mechanical
min	Minimum
mix	Mixture
mn	Maintenance
mol	Molar
mt	Metal
o	Outside
off-des	Off-design
OP	Overall Plant
out	Outflow
p	Product
pc	Purchase cost
pol	Polytropic
PP	Processing Plant
pp	Pump
reb	Reboiler
ref	Reference
res	Residual
rf	Reservoir fluid
rw	Rejected water
sep	Separation
sta	Stabilisation
sub	Subcritical
task	Task
th	Thermal
total	Total
tr	Transcritical
transit	Transit
trs	Transmission
tx	Tax
u	Useful
UT	Utility Plant
ut	Utilities
vol	Volume
w	Waste
wall	Wall
wt	Weight

Superscripts

*	Unsymmetric reference state
Q	Heat transfer
W	Work transfer
+	Exergy increase
+	Material-/Energy-flow entering the system
-	Exergy decrease
-	Material-/Energy-flow leaving the system
0	Reference year
AV	Avoidable
ch	Chemical
EN	Endogenous
EX	Exogenous
kn	Kinetic
lc	Local contribution
m	Mechanical
m	Mixing
PDH	Pitzer-Debye-Hückel
ph	Physical
pt	Potential
rec	Recompression
sep	Separation
sta	Stabilisation
t	Thermal
tre	Treatment
UN	Unavoidable

1 Introduction

1.1 Background

1.1.1 Outlook

The world energy use is projected to increase by 56 % over the next three decades [1], which is largely due to the significant population growth and rising prosperity in the developing countries. Nowadays, fossil fuels (oil, gas and coal) represent almost 80 % of the total energy supply and will continue to represent its lion's share in the near-future, despite their scarcity and the increasing use of renewable resources in our energy systems [2].

The International Energy Agency has forecast that natural gas will become the most predominant fossil fuel in the coming decades [3], but that oil will remain important in transport applications and as a feedstock in the chemical and petrochemical industry. The exploitation of other resources such as shale gas, tar sand and heavy oil have raised interest in the last decades because of the increasing scarcity of the conventional fossil fuels. However, the several environmental studies conducted these last years have led to controversial results, with some claiming that the life cycle emissions of shale gas were as high as those of conventional natural gas, and others stating that they were as high as those of coal, i.e. twice greater.

In all cases, these resources are finite and are characterised by a high carbon content ($\simeq 15$ kg C/GJ for natural gas and $\simeq 20$ kg C/GJ for oil). There is a clear need for a long-term energy strategy that addresses the following challenges:

- climate challenge (reduction of the environmental impact of the energy conversion and use);
- resource challenge (developing an energy system that is independent on finite energy resources on the long-term);
- development challenge (supply of a sufficient amount of energy to satisfy standards of living).

The first issue may be solved by mitigating the anthropogenic greenhouse gas emissions, which arguably contribute to a greater global warming effect and an increase of the mean Earth surface temperature. These emissions can be mitigated by (i) decreasing the energy intensity of human activities such as road industry, (ii) shifting from high CO_2-emitting energy sources to lower ones, or by (iii) capturing and storing the carbon dioxide released to the air. The second one may be addressed by improving the performance of the various energy-using processes by increasing the efficiency of power and heat generation systems.

These challenges have been extensively debated, in particular since the ratification of the Kyoto's Protocol and the subsequent climate commitments. It is now clear that environmental policy instruments should be used together with strong political incentives to encourage investments from privates and industries. For instance, one of the former Norwegian governments has levied a carbon tax on the petroleum sector to motivate the oil and gas companies to develop more energy-efficient processes and reduce the environmental impact of oil and gas facilities. Carbon taxes also exist in the other Nordic countries (Denmark, Finland and Sweden), as well as in Ireland and Switzerland.

1.1.2 Motivation

At present, Norway ranks as Europe's largest oil producer oil (about 3 % world share, 1st Russia) and the world's 3rd largest natural gas exporter [4]. It ranks as well in the top 10–20 for the proven oil and gas reserves. The hydrocarbon production peaked about a decade ago and currently declines [5]. In consequence, the Norwegian governments have encouraged longer exploitations of mature fields and development of heavy oil ones. Such processing is more energy-intensive, and the power consumption and the carbon dioxide emissions on offshore platforms may increase over time [6, 7].

This work focuses on the Norwegian oil and gas extraction sector, which has been responsible for 25 to 30 % of the country's CO_2 and aggregated greenhouse gas emissions in the last decades (Figure 1.1) [8]. The term *oil and gas extraction* commonly refers to the exploitation of petroleum fields (exploring and operating wells), including the associated service activities such as oil loading, but does *not* include the construction of the offshore facilities. The greenhouse gas (GHG) emissions from this sector have steadily increased from the 1990s, both in terms of absolute emissions and relative share.

The emissions caused by the oil loading activities and produced from the onshore installations are lower than the ones produced offshore, and they have represented less than 20 % of the aggregated greenhouse gas emissions of the oil and gas extraction sector in the five last years. Most emissions associated with the offshore petroleum activities (Figure 1.2) are caused by the combustion of natural gas in gas turbines ($\simeq$ 60–70 %) to satisfy the on-site power demand. The share of CO_2- and CH_4-emissions due to flaring and venting have decreased by 5 %-points in the last 35 years. About 94.5 %, 5.2 % and 0.2 % of the total greenhouse gas emissions, in CO_2-equivalent units, are CO_2-, CH_4- and N_2O-emissions, respectively.

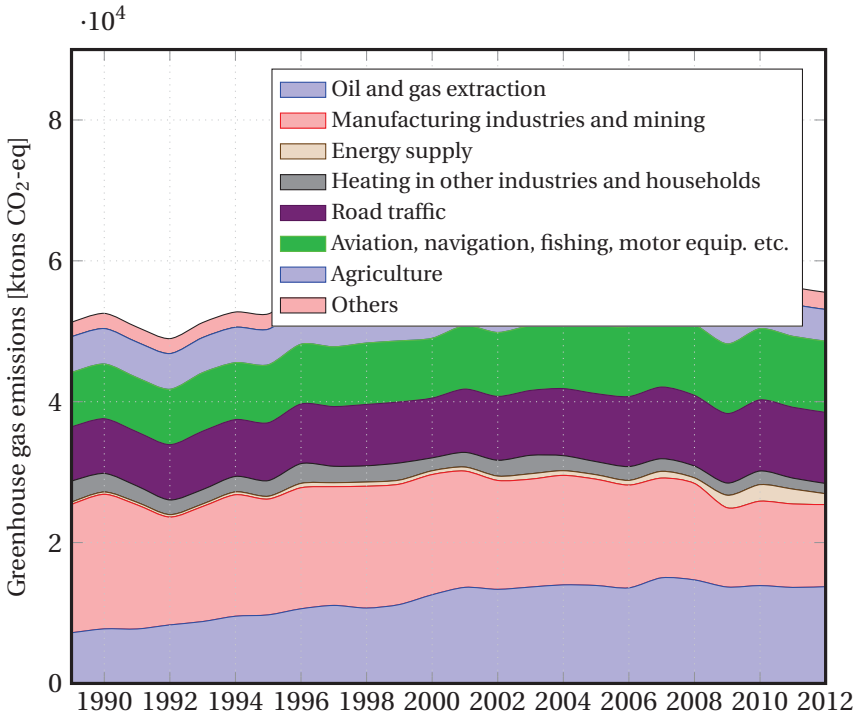

Figure 1.1: Greenhouse gas emissions in Norway from 1987 to 2012 [9].

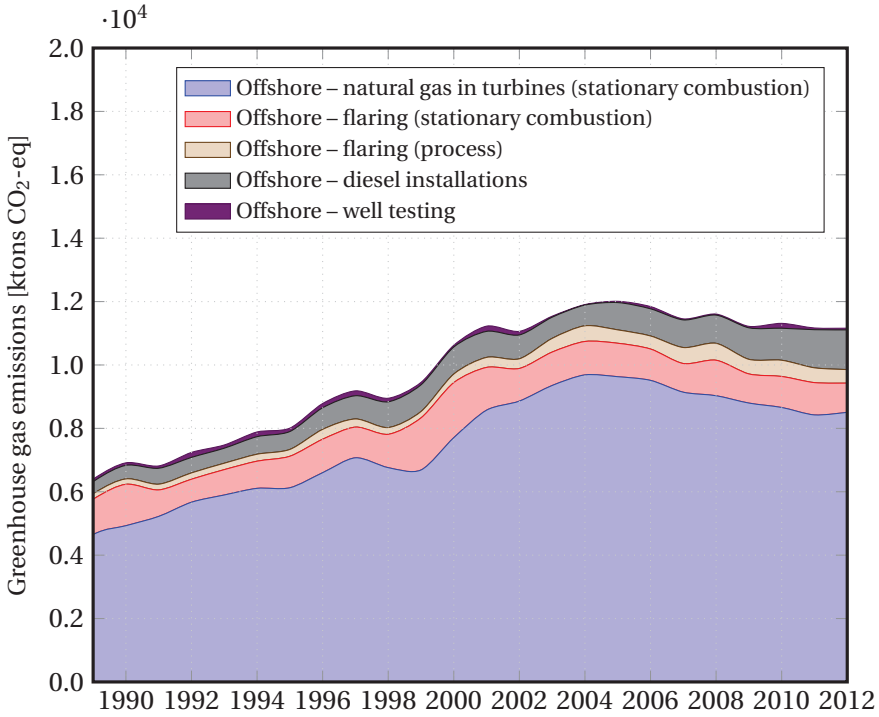

Figure 1.2: Greenhouse gas emissions of the Norwegian offshore oil and gas extraction sector from 1987 to 2012 [9].

1.1.3 Project

The continuous exploitation of petroleum reservoirs results in changes in the field conditions (e.g. flows, pressures, temperatures), and the processes present on oil and gas platforms become less efficient over time. It may be feasible to improve the overall performance of these offshore facilities, by reducing the power consumption of the petroleum processing plant, or by increasing the efficiency of the power generation section, thus mitigating the emissions of carbon dioxide.

The present project is two-sided: it focuses on the performance evaluation of existing platforms and on the development of a methodology for designing future ones. In a first step, this thesis deals with the modelling of several offshore facilities, and the relevant data were given by the project partners or presented in the scientific literature. In a second step, this work investigates various technologies that could be integrated on future platforms to increase their energy efficiency and economic profitability, while decreasing their environmental footprint.

1.2 Oil and gas platforms

General

The purposes of an oil and gas platform (Figure 1.3 and Figure 1.4) are to:

(1) extract petroleum from the exploited reservoir;

(2) separate the oil, gas and water phases;

(3) treat the oil for further export onshore, which may comply with the saleable product specifications;

(4) purify the gas for either export, injection or lift uses;

(5) clean the water before reinjection into the reservoir or discharge into the sea.

The present work focuses on the *processing* plant, where oil, gas, and produced water are processed, and on the *utility* plant, where air, fuel gas and cooling water are used. Sub-systems such as the heating, ventilation and air conditioning (HVAC) are not considered.

The offshore processing of oil and gas may be *minimal*, in the sense that the produced oil, gas and water are separated and sent to an onshore terminal for further and final processing, or may be *complete*, in the sense that the products leaving the offshore facility are meeting the saleable product specifications. The overall design set-up of an oil and gas platform is, nonetheless, similar from one facility to another, although the platform size and system complexity may be highly different. The choice of one option rather than another depends on the proximity of other and existing infrastructures and on the engineers' experience.

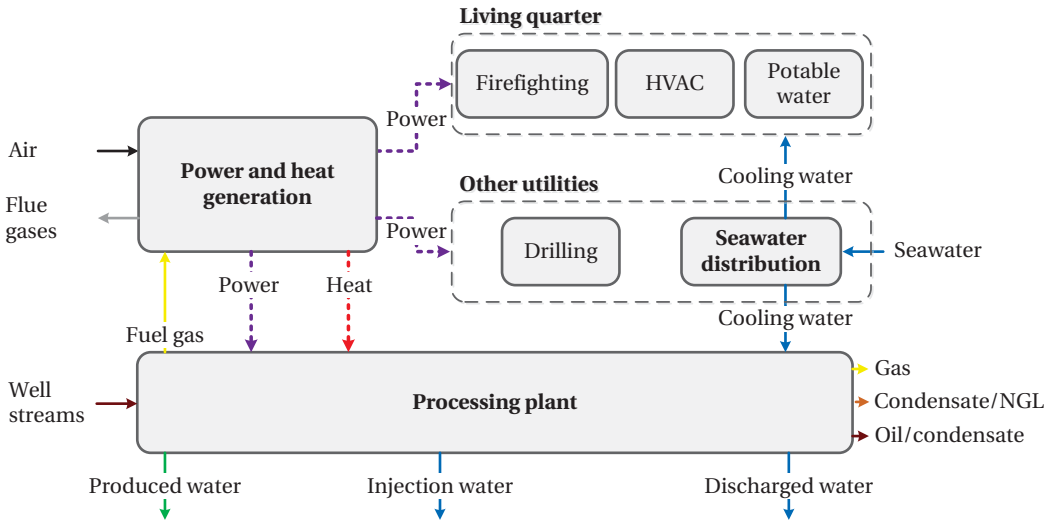

Figure 1.3: A generalised overview of an oil and gas platform.

Figure 1.4: Picture of the Draugen platform [10].

Characteristics

Different platforms may differ by their [11–18]:

- reservoir characteristics (e.g. initial temperature and pressure);
- fluid properties (e.g. chemical composition, gas- and water-to-oil ratios;
- product requirements (e.g. export pressure and temperature, chemical purity);
- operating strategies (e.g. oil and gas recovery, gas treatment, condensate export).

The reservoir properties are subject to significant variations over the lifetime of a petroleum field, and it is generally expected that the reservoir temperature and pressure decrease. Moreover, the oil and gas production flows typically increase until reaching their peaks, and then decrease, while the water extraction continuously rises.

The product requirements are supposedly not varying with time, as they are fixed by the export specifications related to the pipeline (e.g. gas) or shuttle tanker (e.g. oil) systems. The operating strategies may change: there may not be any type of oil recovery method at the beginning of the field exploitation, and gas, water or carbon dioxide injection may be implemented at a later point of time. These differences imply that the heating, cooling and power requirements may vary significantly from one platform to another, and from the beginning to the end of the field exploitation.

Two reference petroleum production areas can be defined, according to Bothamley [11], which are, namely, the Gulf of Mexico and the North Sea regions. Facilities present in other parts of the world present characteristics similar to these ones. In general, the oil and gas streams exported to the shore should be further treated in refining facilities before sales.

North Sea platforms differ from Gulf of Mexico (GOM) ones by, for instance, the feed temperature, which is lower in the second case, and by the constraints on the water content of the exported oil, which can be more stringent.

The type of process equipment is also different, as most compressors are of the reciprocating type for platforms located on the GOM Shelf, rather than centrifugal, and the cooling medium is generally air, rather than seawater.

Several characteristics are similar across North Sea oil platforms, such as the number of separation stages, the export level pressures of the oil and gas streams, the limitations on the water content and true vapour pressure, and the type of turbomachinery equipment. On the other hand, some of the typical differences are whether the exported oil is stabilised before export, and if the exported gas is dehydrated.

Energy performance

Few works in the scientific literature deal with the energy performance of oil and gas platforms, and the main studies in this field are conducted or ordered by oil and gas companies. Bothamley [11] investigated the offshore processing options for oil platforms, comparing the processing schemes between the platforms in the Gulf of Mexico and in the North Sea regions. The heating demand was mainly related to the crude oil stabilisation, the cooling demand to the oil and gas handling processes, and the power demand to the gas compression.

Similarly, Svalheim and King [19] stressed the large energy demand of the compression, pumping and injection (gas or seawater) processes and pointed out the benefits that resulted from applying energy-efficiency measures (e.g. operating gas turbines at high load and reducing flaring practices). Vanner [20] focused on the energy use drivers over the lifetime of an offshore facility, and illustrated the main field events that have an impact on the energy intensity of the oil product. The general trend is a higher energy intensity with time, because of the variations of the gas- and water-to-oil ratios, as well as the use of operating strategies such as gas lift and water injection, which are employed to enhance the production.

Environmental impact

The environmental impact of offshore platforms is expected to increase in the coming years, as a direct consequence of greater energy use on-site to separate and transport oil and gas to the shore and to inject gas or water into the reservoirs for improving the oil recovery [19, 21]. The direct emissions of carbon dioxide are mainly associated with the exhaust gases leaving the natural gas turbines, boilers and burners installed on the facility to produce the necessary power or high-temperature heat required in the processing plant.

The emissions of other greenhouse gases with flaring and venting have significantly decreased in the North Sea region [22]. However, these emissions are expected to increase worldwide, and they are generally produced from the storage tanks, dehydrators, and centrifugal compressors [23]. The ones associated with the centrifugal compressors are caused by the degassing of wet oil. The emissions related to the storage tanks and dehydrators correspond to the necessary venting of the gas recovered from, among other components, the crude oil tanks used for storage purposes.

Chemicals are also used on-site, such as glycol [24, 25] to reduce the risks of freezing and hydrate formation in the gas pipelines, or methanol as corrosion inhibitor [26, 27]. The seawater processed for cooling and/or injection purposes is likewise treated to avoid bacteria growth formation in the reservoir and to prevent reservoir pollution with, among others, biocides (e.g. glutaraldehyde), anti-foaming substances (e.g. alkylsulphates), oxygen scavengers (e.g. ammonium bisulphites), emulsion breakers and scale inhibitors [28]. The produced water extracted along with the oil and gas should comply with the restrictions on the concentration of pollutants such as hydrocarbons, organics and metals before being rejected to the sea [18].

1.3 Statement

It is believed that the key for improving the performance of oil and gas systems is hidden in the understanding of the factors responsible for the inefficiencies of the processes taking place on-site, and in the combined application of multidisciplinary tools covering process, thermodynamic, economic and environmental aspects.

1.3.1 Research questions

The present work aims to complement the previous research in this field and to answer to the multiple research questions that arise:

- How is it possible to derive generic rules of thumbs for estimating the power consumption of oil and gas platforms with different boundary conditions?
- What are the sources and the locations of the performance losses on such plants, and what are the corresponding energy saving potentials?
- Which similarities and differences can be found between facilities operating in various oil regions and processing different petroleum fluids?
- How do these differences across oil and gas fields impact the design of oil and gas systems and their actual performance?
- How do the energy requirements and performance of an offshore platform vary over time, and which are the main causes for such changes?
- Which indicators are suitable or irrelevant when comparing different offshore platforms, and how can they be implemented in practice?
- What are the possibilities for improving the system performance and how can they be optimised, with respect to thermodynamic, economic and environmental criteria?

At the beginning of this project, very few works on the performance of oil and gas platforms have been conducted, as illustrated with the previous literature review, and as shown in Chapter 2. None of the previous studies investigates or addresses in details all these aspects.

1.3.2 Objectives

The main objective of this research is to demonstrate how system modelling, thermodynamic analysis and process integration tools can be combined to assess consistently the performance of oil and gas platforms. It shows, among other points, that the application of such methods is relevant not only for analysing existing facilities, but also for designing future ones and proposing system improvements.

The challenges associated with this goal are, based on the prior research questions, to:

(1) apply a systematic framework for modelling, analysing and optimising existing and future oil and gas platforms;

(2) develop generic and specific models that describe adequately the global behaviour of such systems;

(3) evaluate the performance of existing offshore plants at their current operating conditions;

(4) investigate the changes in energy demands and the performance trends of these facilities over time;

(5) develop consistent performance indicators and efficiency assets for comparing platforms exploiting different fields;

(6) identify the possible system improvements using several advanced methods based on the pinch, energy and exergy concepts;

(7) carry out consistent economic assessment, uncertainty analysis and comparisons between different solutions;

(8) perform life cycle analyses to depict the possible environmental benefits and drawbacks of integrating additional processes on-site;

(9) investigate the thermodynamic, economic and environmental trade-off for each category of system improvements by multi-objective optimisations.

1.3.3 Approach

The present work is exclusively numerical and does not include any consideration on experimental aspects. However, it builds partly on the data obtained from real case studies, which were provided by the project partners. Several of the works included in this thesis consist of numerical simulations, taking, among other cases, the Draugen platform as reference, as pinpointed later. The processing and power plants of oil and gas platforms only are considered, meaning that the energy systems related to the air conditioning and well drilling are *not* considered within this study. They are regarded as *stand-alone* systems, in the sense that each platform is studied separately, without focusing on the possible integration with other facilities. Steady-state or quasi-steady-state conditions are assumed, and issues related to the dynamic behaviour of oil and gas processing are not taken into consideration. The application of detailed risk assessment analysis methods is out of scope of this work.

1.4 Outline

The present thesis consists of 12 chapters:

Chapter 1 introduces the present project, along with the motivation, statement and outline of this study.

Chapter 2 sets the scientific background for this thesis (e.g. description of oil and gas processing) as well as the state-of-the-art of the research conducted in this area;

Chapter 3 outlines the methodology applied throughout this project, from the general strategy to an overview of the system modelling methods, the performance analysis techniques and the optimisation routines;

Chapter 4 presents a generic model of an offshore oil and gas platform operating in the North Sea region, to emphasise the impact of the boundary conditions and to pinpoint the major power consumers and sources of irreversibilities;

Chapter 5 describes the core case study of this work, from the description of the processing and power plants to a thorough analysis of the Draugen facility. The energy flows are tracked, the energy requirements are assessed and the system inefficiencies are pinpointed, based on pinch, total site, energy and exergy analyses.

Chapter 6 focuses on a comparison between several oil and gas facilities located in the North Sea and in the Brazilian Basin, with a strong emphasis on their specificities.

Chapter 7 consists of an application of advanced thermodynamic tools on offshore platforms operated at different life stages, to define more accurately the sources and causes of performance losses, and improvements on the processing plant are simulated.

Chapter 8 includes a review and the development of sets of performance indicators for assessing and comparing consistently petroleum separation systems.

Chapter 9 builds on the modelling and optimisation of different waste heat recovery systems, such as steam networks and organic Rankine cycles, which are integrated either as a bottoming cycle of the power generation or processing plant.

Chapter 10 shows an evaluation of the different ways to mitigate carbon dioxide emissions, e.g. electrification, carbon capture and sequestration, and waste heat recovery, based on process integration and life cycle assessment studies.

Chapter 11 demonstrates the advantages of combining mass- and energy-flow models, together with energy integration tools and multi-objective optimisation routines for designing oil and gas processing plants that meet the export quality requirements.

Chapter 12 concludes the present thesis, summarising the main findings of this work and pinpointing possibilities for future one.

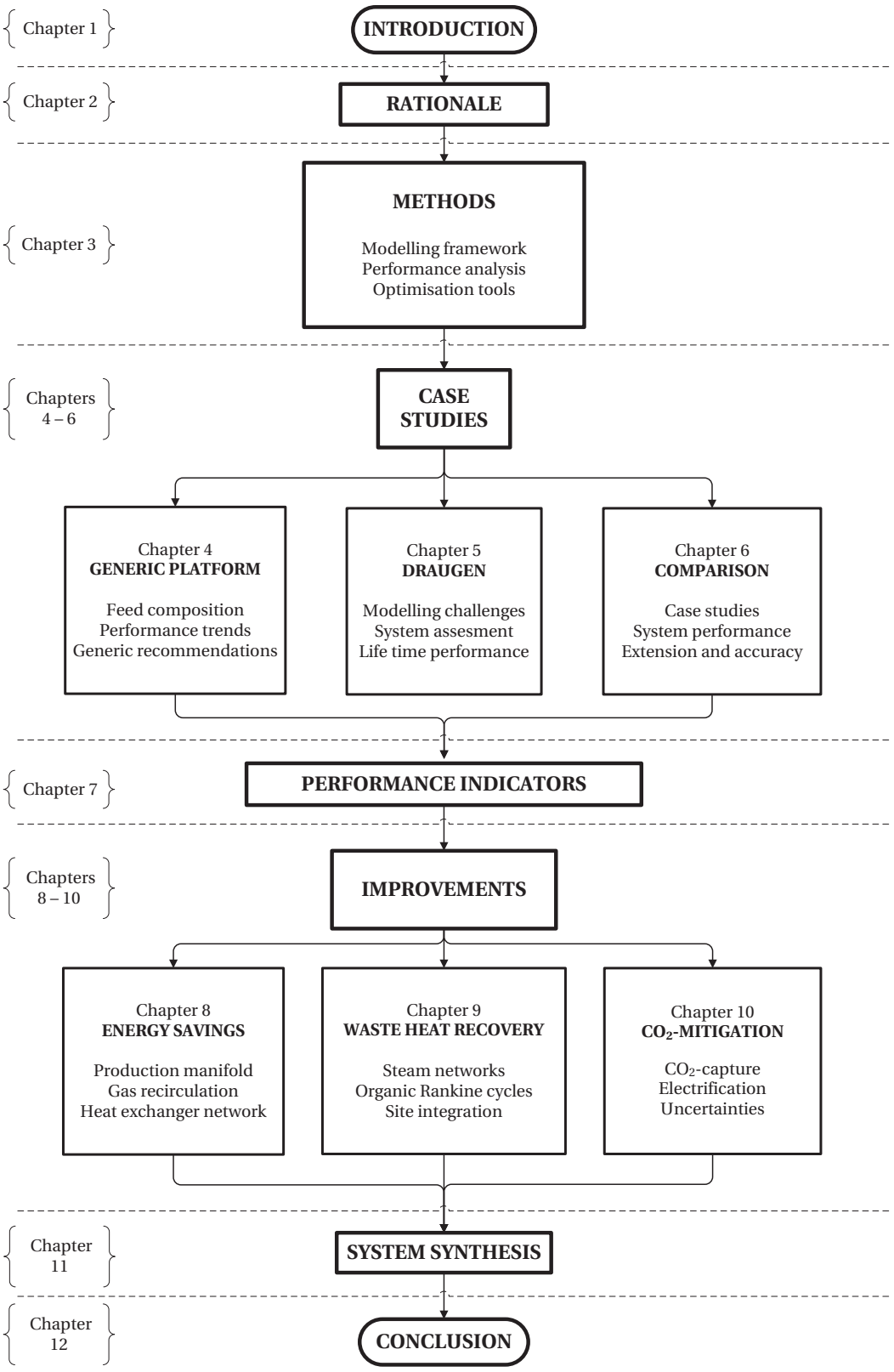
Chapter 1
INTRODUCTION
Chapter 2
RATIONALE
Chapter 3
METHODS
Modelling framework
Performance analysis
Optimisation tools
Chapters 4 – 6
CASE STUDIES
Chapter 4
GENERIC PLATFORM
Feed composition
Performance trends
Generic recommendations
Chapter 5
DRAUGEN
Modelling challenges
System assesment
Life time performance
Chapter 6
COMPARISON
Case studies
System performance
Extension and accuracy
Chapter 7
PERFORMANCE INDICATORS
Chapters 8 – 10
IMPROVEMENTS
Chapter 8
ENERGY SAVINGS
Production manifold
Gas recirculation
Heat exchanger network
Chapter 9
WASTE HEAT RECOVERY
Steam networks
Organic Rankine cycles
Site integration
Chapter 10
CO2-MITIGATION
CO2-capture
Electrification
Uncertainties
Chapter 11
SYSTEM SYNTHESIS
Chapter 12
CONCLUSION

2 Rationale

This chapter presents the background information related to oil and gas platforms, as well as the most relevant studies on the topics investigated in this work. The main scope is formulated based on the outcomes of the literature survey, and this chapter should serve as a basis for understanding the research questions and challenges encountered in this project.

2.1 Introduction

The last decades have seen the development and application of energy efficiency tools for various thermal systems and industrial applications, with only a few studies on the specific case of oil and gas platforms. Most applications have focused on an improved utilisation of primary resources and on a reduction of the environmental burdens.

This chapter provides an overview of the most relevant research works, to illustrate the existing gaps or lacks in the literature, and to outline the challenges to address. The state-of-the-art research related to this project can be classified into five main subjects, which consist of:

(1) the description of oil and gas offshore platforms and of the associated technologies;

(2) an overview of the tools used for modelling and simulating such systems;

(3) the definition of relevant performance evaluation methods;

(4) the identification of the sources of performance losses and their trends over the lifetime of petroleum fields, and across different facilities;

(5) the analysis of potential process and system improvements that would minimise their energy use and environmental impact.

2.2 Oil and gas offshore platforms

2.2.1 Crude oil, gas and reservoir fluid

Reservoir fluids are complex multiphase mixtures containing a large variety of chemical components, and their composition and properties differ significantly from one reservoir to another. They mainly consist of hundreds to thousands of hydrocarbons, i.e. organic compounds made up of hydrogen and carbon, in gaseous, liquid and solid forms. They are extracted along with impurities such as nitrogen, carbon dioxide and hydrogen sulphide, as well as with subsurface formation water. The hydrocarbons present in the reservoir fluids can be classified into four main categories [29]:

- saturated hydrocarbons (also named alkanes or paraffins, with the formula C_nH_{2n+2}). Examples are methane (CH_4) and ethane (C_2H_6), which are mostly in gaseous form in the reservoir and on the offshore facility, and pentanes (C_5H_{12}) and hexanes (C_6H_{14}), which are generally found in the liquid phase. Paraffins with a carbon number higher than 7, i.e. heavier than heptanes (C_7H_{16}), can be in solid form or particularly viscous;
- unsaturated hydrocarbons (e.g. alkenes), which are characterised by non-single covalent bonds between carbon atoms;
- cycloalkanes (also called naphthenes), which have at least one ring of carbon atoms. Examples are cyclopentane (C_5H_{10}) and cyclohexane (C_6H_{12});
- aromatic hydrocarbons (also called arenes), with alternating single and double covalent bonds between the carbon atoms forming rings. Examples are benzene C_6H_6 and toluene C_7H_8.

The reservoir fluids can be classified into five to six main categories [30], depending on the pressure, temperature and composition, which are, from the lightest to the heaviest:

- dry gas (all the hydrocarbon compounds are in the gas phase);
- wet gas (the hydrocarbons are present in the gas phase in the reservoir, but a fraction may condense at the offshore processing conditions);
- gas condensates (similar to wet gas, but liquid in the reservoir)
- volatile oil (the hydrocarbons are present in the liquid phase, but a fraction may change from liquid to gaseous phase as the reservoir pressure declines);
- black oil (mostly intermediate weight hydrocarbons);
- heavy oil (mostly heavy weight hydrocarbons).

This classification is directly related to the gas-to-oil ratio (GOR) of the reservoir and the oil gravity.

2.2.2 Processing plant

The present section goes through the presentation of the several sub-systems implemented on a typical oil and gas platform (Figure 2.1).

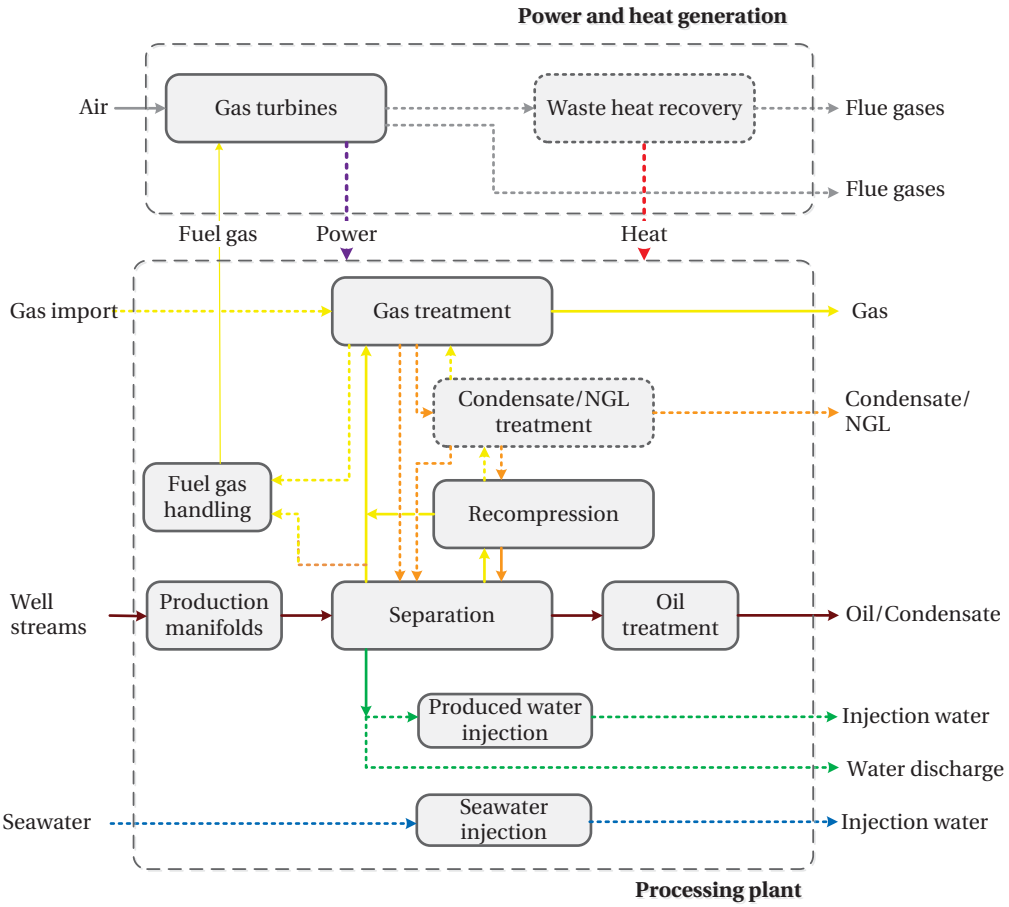

Figure 2.1: A general overview of an oil and gas platform.

Production manifold

The reservoir fluid is transferred to the platform complex via a network of pipelines and a sub-system of production manifolds operating at different pressure levels. The individual well-streams pass through choke boxes, which consist of valves and chokes, in which they are mixed and depressurised to ease further gas and liquid separation in the separation train. Ethylene glycol and methanol may be added to prevent freezing. The operating settings for each well are fixed to ensure an optimum production and recovery rate.

Separation

Oil, gas and water are separated by gravity (Figure 2.2) in a certain number of stages (2–3 for North Sea platforms and 4–5 for Gulf of Mexico facilities). Well-streams from the high-pressure manifold enter the 1st stage separator, while the ones from the low-pressure manifold may be routed to the 2nd stage. A fraction of the well flows may be processed in a test separator to allow for detailed flow measurement and analyses. Since low pressures and high temperatures

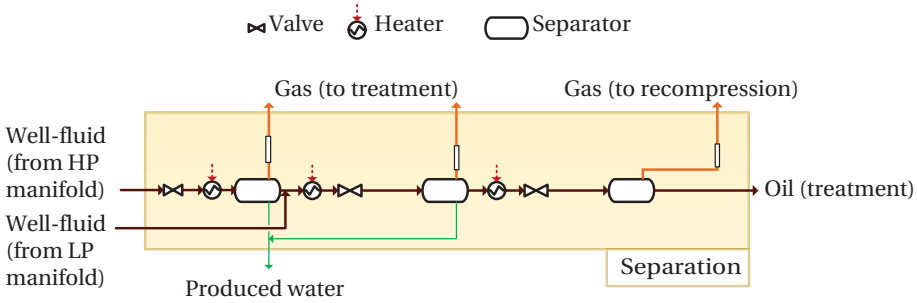

Figure 2.2: A generalised overview of a separation sub-system.

ease the separation of these three phases, the pressure of the well-fluid is decreased in several stages by using throttling valves. In some cases, if the feed temperature is too low or if the oil is viscous, the oil temperature may be increased by preheating at the inlet of each stage, either before or after the de-pressurisation. The oil flow may be split into two or more streams, and only a fraction is then heated before entering the separator of the next stage, while the other fractions bypass the heater.

The separators can be either of the three-phase (gas/liquid/water) or two-phase (gas/liquid or liquid/liquid) type. The separator placed at the first separation stage is generally of the three-phase type, and it should be designed to ensure that minimum amounts of liquid are carried over with gas, that minimum quantities of hydrocarbons are transported with the produced water, and that the oil flow is adequately degassed and dry. The separators implemented at the other separation stages may be either two- or three-phase, depending on the processing plant and the oil properties. The separator placed at the last separation stage is generally a liquid/liquid separator, such as an electrostatic coalescer, and is designed to reduce the water content of the oil flow and to meet the export specifications.

Crude oil typically contains dissolved gases such as impurities (e.g. sulphur hydrogen H_2S) or low and medium-weight hydrocarbons (e.g. methane CH_4). These gases should be removed to avoid corrosion issues in storage tanks or pipelines, which, in other words, means that the oil should be *stabilised* and that its vapour pressure should be decreased. It may be controlled by heating the oil flow at the inlet of the final separation stage, which operates at nearly-atmospheric conditions, to remove the remaining volatile components.

Oil treatment

The oil from the separation section enters the oil treatment and export sub-system (Figure 2.3), after having been mixed with the heavy hydrocarbons that are removed in other parts of the processing plant. It is then pumped and either stored in a tank, where the last traces of gas and water are removed by flashing, or directly exported onshore.

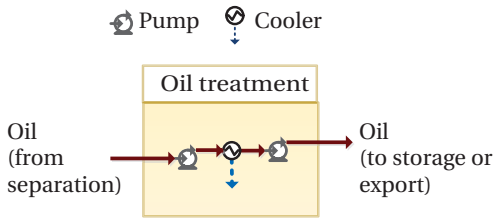

Figure 2.3: A generalised overview of an oil treatment sub-system.

Condensate treatment

In some cases, the typical processing scheme, which combines multi-stage separation and multi-stage recompression sub-systems, may not be sufficient to reach the desired oil export specifications. A more complex processing scheme may then be integrated to control the vapour pressure, by for instance integrating a separate condensate treatment section (Figure 2.4). This sub-system may consist of a stabiliser, where the condensate recovered from the several compression stages is treated apart to allow for a better separation between the light- and medium-weight hydrocarbons, and of a dehydrator and other scrubbers.

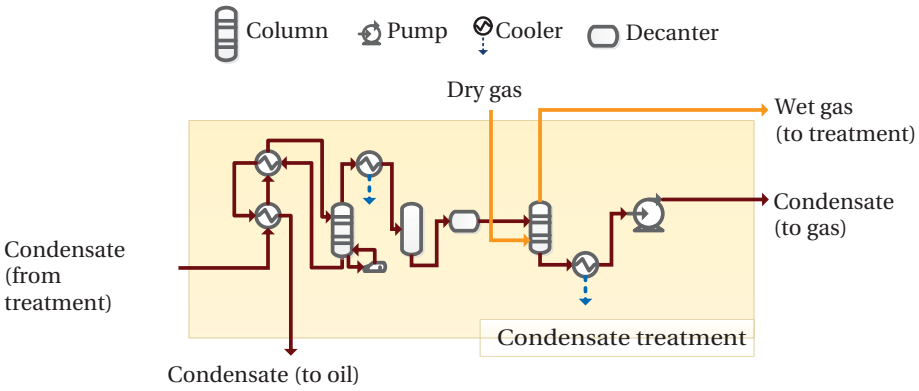

Figure 2.4: A generalised overview of a condensate treatment sub-system.

Recompression

The gas recovered from each separator, excluding the first one, enters the recompression sub-system (Figure 2.5). It generally consists of several stages, each stage processing the gas from the previous stage, and in some cases, from other parts of the processing plant. A typical stage consists of a cooler, a scrubber and a compressor. The cooler and scrubber ensure that the gas temperature and hydrocarbon content are low enough to avoid a too high power demand of the compressors, as condensate and water droplets are condensed and removed, while avoiding hydrate formation. The gas exiting the recompression process has approximatively the same pressure as the feed, and it is mixed with the gas from the 1st separation stage before entering the gas treatment section.

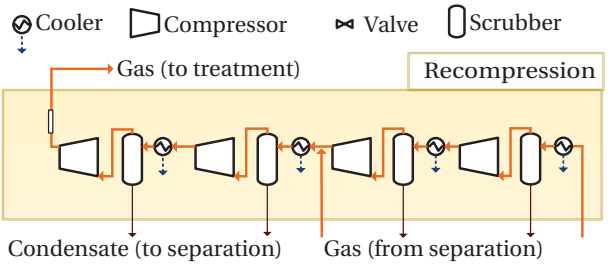

Figure 2.5: A generalised overview of a recompression sub-system.

Gas treatment

As for the recompression sub-system, the gas treatment also consists of several stages, each including a heat exchanger, scrubber and compressor. In some cases, there may be a dehydration stage (Figure 2.6), in which the water content of the gas streams is reduced to prevent further hydrate formation in the pipelines. Wet gas enters a packed contactor, in which water is captured by physical absorption, using an hygroscopic solvent such as liquid triethylene glycol (TEG). The water content of the gas after this dehydration is usually below 0.01 mol. %. The wet glycol is depressurised and cleaned of water vapour in a desorption column, quipped with a condenser and a reboiler. Regenerated glycol is pumped, preheated and reintroduced into the absorber. Most dry gas is further compressed, where it is cooled and scrubbed to further remove heavy hydrocarbons, and compressed for storage and possibly export.

Fuel gas handling

A fraction of the produced gas may be used for on-site power generation after processing in a fuel gas handling sub-system (Figure 2.7). It is most often heated, scrubbed and then expanded through a succession of valves, before final combustion with air in gas turbine engines.

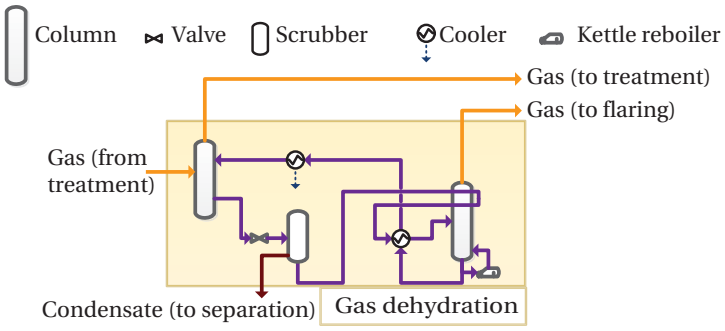

Figure 2.6: A generalised overview of a glycol loop sub-system.

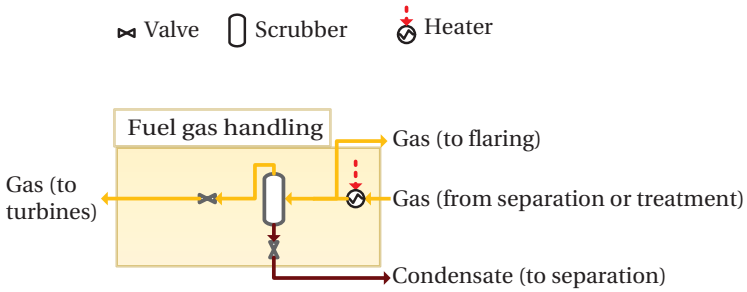

Figure 2.7: A generalised overview of a fuel gas handling sub-system.

Produced water treatment

The water from the separation and purification trains, also denoted produced water, enters hydro-cyclones in which suspended particulates and dissolved hydrocarbons are removed. It then passes through valves and flows through degassers where the last oil and gas traces are recovered before disposal to the sea.

Seawater injection

In parallel with the oil and gas processing, seawater may be treated on the platform for further injection into the reservoir, in order to sustain high pressure conditions. The injection fluid must meet strict quality requirements to prevent corrosion and reservoir degradation: it is thus cleaned before being pumped into the reservoir, using a succession of filters to remove solid impurities such as sand particles and algae.

2.2.3 Utility plant

Power generation

The electrical power required on-site can be produced by gas turbines, generally fuelled with a fraction of the natural gas extracted on the platform, and atmospheric air (Figure 2.8). These engines are typically selected on the basis of the maximum expected power demand. They should ideally, because of the specific features of an offshore plant, have high compactness (e.g. small weight and footprint), high reliability and availability (e.g. robust gas turbine operation), and high fuel flexibility (e.g. adaptability to different types of fuels).

Hence, the selection of a gas turbine for offshore applications may be a compromise between these three criteria and the engine thermal efficiency. In a few cases, the power required may be produced on another platform by gas turbines, or alternatively transmitted from the shore.

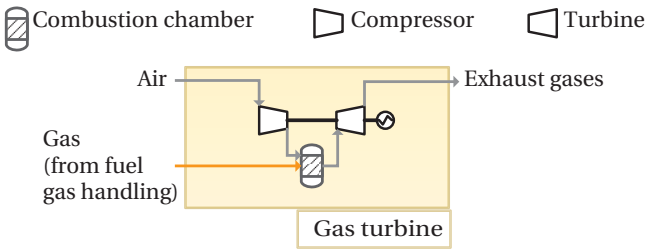

Figure 2.8: A generalised overview of a power generation sub-system.

Shelf electrification is currently under study, because the CO_2-emissions from the power generation system would decrease, compared to the conventional case with on-site gas-fired power generation. In this case, the required power will originate either from electricity generation based on renewable sources such as hydropower or from combined cycle power plants, which display a higher electrical efficiency [31].

The possibility to supply power from offshore wind farms to oil and gas platforms has also been investigated, as it may be an economic and more environmental-friendly solution [32–34]. These studies considered different case studies in the North sea region, and they suggested that implementing wind farms was theoretically feasible, but that further design studies and economic analyses should be conducted.

Waste heat recovery

Heat may be required in the processing plant for, for instance, preheating the crude oil prior to a separation stage. In these cases, heat may be recovered from the exhaust gases leaving the power generation sub-system, using an intermediate heating loop with tri-ethylene glycol or liquid water at high pressure (Figure 2.9). On some platforms, a bottoming cycle, such as a

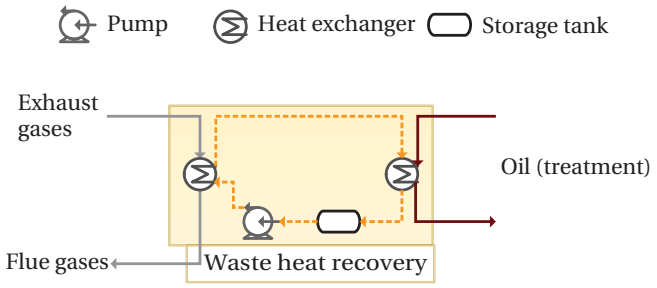

Figure 2.9: A generalised overview of a waste heat recovery sub-system.

steam Rankine cycle, is installed, utilising the waste heat contained in the turbine exhausts at moderate to high temperatures, in order to produce power that can be either used on-site or exported. The current research on offshore platforms, at present, evolves towards the development of electrified oil and gas plants, which are either connected to the shore or are regrouped in power islands.

Seawater distribution

The cooling requirements may be either satisfied by seawater or by air (Figure 2.10), using a direct media or an intermediate cooling loop (e.g. glycol and water, to prevent freezing in the pipelines). Seawater is also pumped for the user needs, and possibly for the firewater headers.

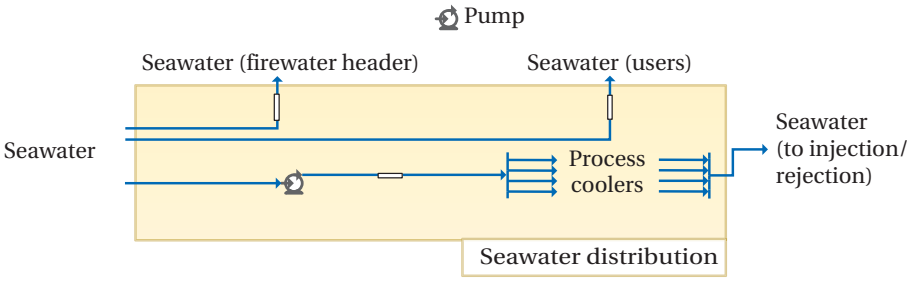

Figure 2.10: A generalised overview of a seawater distribution sub-system.

The cooling water processed on-site may in a further step be injected to sustain the reservoir pressure, as done on, for example, the Draugen platform. This cooling water may be used for condensing the steam produced in a waste heat recovery cycle, if there is a combined cycle on-site.

2.3 Modelling and simulation

2.3.1 Definitions

Practical experiments are empirical procedures, which aim at verifying the validity of a new hypothesis by conducting *laboratory* or *field* tests. On the contrary, *simulations* consist of *virtual* experiments, based on the tuning of models developed with software technologies. The following definition of the term *simulation* was proposed by Thomé [35].

Simulation is a process of designing an operational model of a system and conducting experiments with this model for the purpose either of understanding the behaviour of the system or of evaluating alternative strategies for the development or operation of the system.

Process simulations imply the flowsheeting of the process under investigation, and Westerberg et al. [36] defined the term of flowsheeting as *the use of computer aids to perform steady state heat and mass balancing, sizing and costing calculation for a chemical process.*

Flowsheeting may serve different objectives: a *design* approach, where the simulation aims at proposing a *new* system that complies with the fixed requirements, or an *operation* approach, and the simulation aims at reproducing the behaviour of an already existing plant. The simulation model may be *steady-state* or *dynamic*.

2.3.2 Tools

The history of flowsheeting programs starts in the period 1960–1980, with the development of in-house tools in engineering and manufacturing companies, and of the flowsheeting packages such as PROCESS, DESIGN and ASPEN (later Pro/II [37], Design II [38] and Aspen Plus [39]). Nowadays, there exists a large variety of process simulation tools, which differ by the main developer (e.g. Aspen Technology for Aspen Plus), the area of application (e.g. data reconciliation for Vali [40]), the software architecture (e.g. equation-oriented for gPROMS [41]), and the integration of the database environments. The software architecture is closely related to the resolution strategy of the problems (e.g. sequential, equation-oriented, simultaneous modular).

The selection of one software rather than another seems to be mostly dependent on the engineering experience, the specifications of the clients, and the field of application. Aspen Plus is one of the most popular process simulation software: it has mostly been used for simulations of chemical plants because of the numerous add-ons and features that can be added, and is claimed to be particularly suitable for the modelling of electrolyte and/or non-ideal chemical systems. Pro/II and Hysys are preferred for applications related to the oil and gas industry: Pro/II seems to be more used for refining applications, and Hysys for oil and gas separation, for instance on offshore platforms. Other software such as Aspen Energy [42] and Aspen Flare System Analyser [43] may be used in some specific applications.

2.4 Performance evaluation methods

2.4.1 Thermodynamic assessment

Energy and exergy analyses

The 1st Law of Thermodynamics indicates that energy can neither be created nor destroyed, and it allows therefore for tracking energy flows in the forms of power, heat or matter. However, it does not account for the thermodynamic quality of different forms of energy, implying that all forms are taken as equivalent. It yields only limited information on the maximum system performance that could be reached in theory. Processes such as isenthalpic expansion with throttling valves or heat transfer in adiabatic heat exchangers seem to not present any potential for improvement.

In contrast, the 2nd Law of Thermodynamics addresses these gaps, as it asserts that in real energy transformations, a particular system spontaneously evolves in a given direction, towards thermodynamic equilibrium. Real processes are therefore irreversible, and the measure of these internal inefficiencies can be performed by using the property of *entropy*. Entropy is generated as a system undergoes transformations until reaching equilibrium, implying that the equilibrium state is attained as the entropy reaches a maximum. It indicates that the heat input into a given system cannot fully be converted into useful work, and that the possible uses of energy from sources such as low-temperature heat are limited, unlike electricity.

The combination of these two laws leads to the concept of exergy, and the following definition has been proposed by Szargut et al. [44]: *Exergy is the amount of work obtainable when some matter is brought to a state of thermodynamic equilibrium with the common components of the natural surroundings by means of reversible processes, involving interaction only with the abovementioned components of nature.* As real processes are, in essence, irreversible, exergy is destroyed as the system evolves towards equilibrium, and the quantity of destroyed exergy accounts for the system inefficiencies, while giving a clear picture of the resources that are consumed and degraded.

The concept of exergy goes back to the contributions of Clausius, Thomson, Gibbs, Gouy and Stodola in the 19th century, where the term of *available energy* was first used. The modern development of this type of analysis was initiated by Bosnjakovic in Europe around the 1940s and the term of *exergy* was coined by Rant in the 1950s to denote the *capability for work extraction*. The exergy analysis method is closely linked to the concept of exergy-based performance criteria, which would provide a more consistent measure of the resource use, and which would thus be more appropriate for evaluating process performances. This concept has strongly evolved, with the contributions of Grassmann [45] and Nesselmann [46] in the 1950s, of Baehr [47, 48] in the 1970s, of Kostenko [49], Tsatsaronis [50] and Szargut et al. [44] in the 1980s, to the most recent ones of Lazzaretto and Tsatsaronis [51, 52] in the last decade.

A significant number of studies on the exergetic performance of industrial processes and

systems was published from the 1970s, along with several reference textbooks on the matter (see e.g. Szargut et al. [44], Moran [53] and Kotas [54]). The application of exergy analyses to petroleum systems was more recent, starting from the 1990s, and primarily focused on crude oil distillation processes, with the studies of Rivero and Anaya [55], Cornelissen [56], Demirel [57] and Al-Muslim and Dincer [58].

The first work on the thermodynamic performance of oil and gas offshore processing was the exergy analysis of de Oliveira Jr. and Van Hombeeck [59], which deals with the case of a Brazilian facility, where petroleum is extracted at a low temperature and exported ashore, along with gas. The separation sub-system was the most inefficient process, and the crude oil heating was the most exergy-destroying one.

Pinch and total site analyses

The pinch analysis method builds as well on the 1st and 2nd Laws of Thermodynamics and takes its roots in the work of Linnhoff [60], who pointed out some of the limitations of the exergy concept when applied to the case of heat exchanger networks. The main focus is on targeting the heat integration potential in the system under study. These methods are suitable for designing new processes (grassroot) [61] or for improving existing ones (retrofit) [62]. The pinch analysis method has been extended from the analysis of an individual process [63] to the assessment of a total site [64–67]. The energy saving opportunities are assessed at the site-scale, rather than at the level of a single process. The opportunities for inter-process integration, through a common utility system, can be identified [68].

Process integration tools for improving the energy efficiency of industrial sites have been applied to different sectors, ranging from the pulp and paper sector to the petrochemical and fine chemical industry. Parallels have been developed for other types of networks, such as distillation systems, water distribution [69, 70] and hydrogen refineries [71, 72], with the constant aim of using more efficiently raw materials or energy, while reducing the environmental impact and emissions of the diverse process operations.

The application of these methods to petroleum and large-scale plants has grown recently. Feng et al. [73] investigated possible retrofit schemes for heat exchanger networks of petrochemical plants and pinpointed the importance of choosing the relevant boundaries (process or site). Matsuda et al. [74] applied the total site approach to a large-scale plant, revealing the significant energy saving potential of the facility, despite the high efficiency of each individual process. Chew et al. [75] discussed the implementation issues of this method when applied in practice. However, there is no study dealing with the energy integration of oil and gas facilities.

As emphasised in Bejan et al. [76], the use of pinch analysis may be limited for detecting improvement opportunities in systems in which chemical reactions are involved. Pinch and exergy assessment methods should therefore be considered as complementary, since they both provide deeper insights into the performance of energy systems.

2.4.2 Economic analysis

An economic analysis may be defined as:

The systematic approach in which economists and other professionals will estimate the economic environment and its strengths and weaknesses.

Evaluating the economics of chemical processing plants has been the subject of a wide range of scientific literature in the last decades, and the purchased costs of the equipment items can be deduced from estimating charts, such as the ones presented in Timmerhaus et al. [77] or in Ulrich [78], or capacity-based correlations, such as the ones presented in Turton et al. [79].

In general, these works pinpoint that the evaluation of the economics of a chemical process, new or existing, builds on the assessment of the capital and operating costs associated with the construction, operation and decommissioning.

The economic evaluation of oil and gas platforms is trickier and calls for flexibility when investing in a new facility [80], as there are significant uncertainties associated with, for instance [81]:

(1) the oil and gas prices [82], and the financial market volatility [83];

Volatility in the oil prices has a clear negative impact on investment measures, and these prices may vary significantly over the lifespan of the petroleum field, because of politic (e.g. potential market disruption because of wars and geopolitical tensions) and economic factors (e.g. economic crisis). This uncertainty should therefore be considered to assess reasonably the project profitability.

(2) the investment (CAPEX) and operating (OPEX) costs, as well as the inflation rate;

(3) the production profiles and reserves of petroleum [84];

The production profiles strongly depend on the reserves and reservoir conditions. Not all the oil present in the reservoir is recoverable technically, because of the reservoir geological conditions and limitations in the extraction technologies.

(4) the number of wells and the associated capital costs and production profiles [85];

Similarly, only a fraction of the oil that can be technically recovered is actually economically interesting to extract, because of the additional investment costs that would be induced if new wells were drilled.

(5) the start and development of the production.

Finally, there are uncertainties associated with the production volumes during the build-up, plateau, decline and abandonment phases: each life stage presents different uncertainties, and the durations of each phase vary from one field to another.

2.4.3 Environmental assessment

Senécal et al. [86] proposed to define *environmental impact assessment* methods as:

The process of identifying, predicting, evaluating and mitigating the biophysical, social and other relevant effects of development proposals prior to major decisions being taken and commitments made.

Such methods aim at addressing environmental considerations in decision-making processes, in order to evaluate the sustainability of a given project or plan. An example of such a method is the life-cycle analysis, mainly developed from the mid-1980s, which consists of evaluating the environmental impacts during all the life stages of a product or process.

The term *life cycle* refers to the main lifespan stages, from the processing of raw materials to the waste management and disposal. The exact procedure is at present standardised by [87] and is well-described in e.g. Rebitzer et al. [88, 89]. It consists of an inventory of the relevant inputs and outputs of material and energy streams, the environmental impacts associated with each flow, and an interpretation of the results. In general, the latter include the consumption of material and energy resources, and an assessment of the environmental impacts.

However, a large range of methodological issues has raised, as different practitioners use different assumptions for the same type of problem (e.g. system boundaries and information sources), leading to inconsistent results [90]. Finnveden et al. [91] discussed the most recent developments of this technique and pinpointed the need for an extensive amount of data and the uncertainties caused by the methodological choices.

McCann and Magee [92] performed a comparison of the life cycle of seven different crude oils, which have different origins and chemical properties, implying that the processing schemes are different, especially when it comes to the refinery treatment.

The U.S. Environmental Protection Agency [93] conducted an extensive study of the environmental impacts of oil and gas production, based on a regional analysis of some of the U.S. states. They reported that the main environmental impacts were associated with the air emissions, produced water effluents, and drilling waste flows, because of the emissions of nitrogen, sulphur oxides, methane and carbon dioxide from the combustion sources and separation vessels.

Venkatesh et al. [94] analysed the uncertainties related with the estimations of greenhouse gas emissions during the life cycle of petroleum-based products and showed that the crude extraction and transport sector represented about 10 % of the total $CO_{2,eq}$ emissions for such fuels, and that the coefficient of variation was about 43 %.

Burnham et al. [95] compared the sources and extents of greenhouse gas emissions for hydrocarbon fuels, applying a life-cycle analysis. In the case of natural gas, most CH_4 emissions were caused by the liquid unloading, while most CO_2 effluents were related to the fluid processing.

2.4.4 Hybrid methods

Exergy and economics

Several methods have been developed these last years as combinations of thermodynamic, economic and environmental evaluations. The term *thermoeconomic* stands for the combination of thermodynamic and economic variables, while the term *exergoeconomics* was coined by Tsatsaronis [50] to denote the particular combination of an exergetic and an economic assessment. The main idea lies on valuing energy and material flows based on their associated exergy to design a system. The exergetic cost [96] represents the quantity of exergy that is needed to produce a given flow or product.

These methods have been extended to analyse and optimise existing energy systems [97], and to detect operation anomalies [98, 99]. The application of exergoeconomic and thermoeconomic tools to oil and gas systems is limited. Rivero et al. [100] evaluated a crude oil combined distillation unit, while Nakashima et al. [101] performed an exergoeconomic evaluation of the Marlim platform to compare two production techniques. Silva et al. [102] derived the production costs of petroleum-derived fuels.

Exergy and environment

The exergy concept may also be used to assess the ecological cost of using raw materials or the impact of waste emissions. Rosen and Dincer [103, 104] suggested that a large number of environmental issues can be correlated to the conversion of energy sources. Dewulf et al. [105] suggested to (i) evaluate environmental impacts by calculating the quantity of exergy required to abate the corresponding emissions in waste treatment plants, or (ii) by evaluating the losses of exergy due to health effects [106].

Szargut and Morris [107] introduced the concept of *cumulative exergy consumption*, which is defined as the consumption of energy carriers in all the steps of the production processes from natural resources to final products. More specifically, Szargut et al. [108] defined the term *thermo-ecological cost* as the cumulative consumption of *non-renewable* exergy.

Gong and Wall [109] stressed that the concept of exergy can be embedded in the life cycle analysis method under the name of *exergetic life cycle analysis*, in order to assess the exergy inputs and outputs during the construction, operation and clean-up phases. Cornelissen and Hirs [110] noticed that this method could be used to determine the *consumption* and the *depletion* of natural resources. De Meester et al. [111] suggested calculation improvements, as the current datasets given in the literature might have resulted in significant uncertainties.

Meyer et al. [112] developed the *exergoenvironmental analysis*, which combines the outputs from the life cycle and exergetic assessments, but focuses on the environmental impact formation at the level of the plant components. Dewulf et al. [113] reviewed the different applications of exergy and argued that using this concept in efficiency accounting is appropriate.

2.5 Performance considerations

The energy requirements and the possibilities for improving the performance of such systems are expected to be highly different from one platform to another, because of the differences in the field and operating conditions. Although the main energy-intensive processes are well-known, there is a lack of knowledge about the impact of the field and export conditions on the performance losses of oil and gas facilities.

2.5.1 Field conditions

Petroleum reservoirs may be classified according to their formation conditions (e.g. sizes and shapes of the geologic structures), or to their reservoir drive mechanisms, i.e. the mechanisms responsible for displacing the oil from the reservoir to the surface [114]. Abdel-Aal et al. [17] mentioned three main mechanisms:

(1) the *solution-gas-drive*, also called *depletion drive*;

Gas is initially dissolved into the oil. The reservoir pressure is then decreased below the bubble point as the reservoir depletes, for instance because of the well drilling. Gas is then released from the petroleum and its expansion lifts the oil to the surface. The expected recovery factor is about 15 % to 25 %, implying that gas and water may be injected at a later stage to increase the reservoir pressure, resulting in an increase of the recovery factor by about 20 % points.

(2) the *gas-cap-drive*;

Free gas exists as a gas cap above the oil, and the expansion of this gas cap pushes the oil into the pore spaces that were occupied by the already produced oil. The expected recovery factor is about 25 % to 50 %, and may be increased by using secondary recovery techniques, as for *solution-gas-drive* reservoirs.

(3) the *water-drive* or *aquifer*;

The formation under the oil is saturated with salted water, and the production of oil and gas results in an expansion of the water, which moves upward, maintaining the oil and gas pressure. The expected recovery factor can reach up to 50 %, and may as well be increased by water and gas injection as pressure support.

These differences in driving mechanisms illustrate the various needs for recovery techniques, implying that reservoirs that are water-driven may have a lower need for gas and water injection, and the energy requirements over the life cycle may be smaller.

2.5.2 Fluid composition

The decisions that should be taken regarding the recovery method (e.g. water and gas injection) and the process inventory (e.g. size and type of the equipment items) may change depending on the type of reservoir fluids, which are closely linked to the reservoir properties [114].

For instance, *heavy oil* reservoirs display a small initial gas-to-oil ratio, and their temperatures and saturation pressures are particularly low. Heavy oils have a high density and viscosity, implying that they have a low mobility in the reservoir, and that significant quantities of gas need to be injected through a high number of wells to lift these fluids. Heating may also be required in the processing step to enhance the oil, gas and water separation.

The content of medium-weight hydrocarbons may also have an impact on the processing scheme. For example, if the reservoir fluid has a high propane content, the typical processing design would not be cost- and energy-effective, because significant amounts of propane may be scrubbed and recirculated, and the power demand of the compressors would be greatly increased. In this case, additional gas processing, by integrating supplementary equipment items and recovering the natural gas condensates separately, may be required.

2.5.3 Outlet specifications

The export specifications have a direct impact on the design of the processing plant and on the energy requirements. For instance, depending on whether oil is further processed onshore, the crude oil and gas recovered on-site may be stabilised and dehydrated. The vapour pressure requirements are generally more stringent if oil is exported by tanker loading and unloading, and CO_2 and other impurities such as H_2S may be removed from the gas flows to meet the pipeline specifications and avoid corrosion. The water content of the exported oil should generally be smaller than 1–2 %, on a volume basis, and its true vapour pressure lower than 10 bar [11].

There are as well constraints on the pressures of the oil and gas flows used for lift and injection. Their pressure should be higher than the well and reservoir pressure to improve the oil recovery. This results in a possibly large demand for compression and cooling, and possibly in a need for pumping and injecting seawater for additional pressure maintenance. The exact specifications are specific to the platform characteristics and to the field properties.

2.5.4 Equipment redundancy

A common operational strategy on offshore plants is to share the power generation between several gas turbines run at part-load, while keeping one in standby mode. This control strategy allows for more operational flexibility and a faster reaction to possible system failures. However, this results in a reduced efficiency of these engines and thus higher fuel consumption and greater CO_2-emissions.

2.6 Improvement measures

The monetary values of natural gas and of the CO_2-tax in the upstream petroleum sector have increased these last years [8, 22, 115, 116], and designing more efficient offshore platforms has raised a bit of interest. A greater system efficiency can be achieved by improving the performance of the processing plant or by increasing the efficiency of the utility plant. The first possibility has been investigated in a few works by de Oliveira Jr. and Van Hombeeck [59] and by Voldsund et al. [117]. The second route has been considered in works that suggested to integrate a bottoming cycle, as proposed in the works of Nord and Bolland [118, 119].

2.6.1 Heat exchanger network

Heat integration is not common on North Sea offshore platforms, because there is generally a low demand for heating. They are typically satisfied by using electric heaters, and the major ones by waste heat recovery. On the contrary, heat-recovery by back-exchange (i.e. between the reservoir fluid and the separated oil or produced water streams) is more frequent on the platforms located in the Gulf of Mexico, because the well-head temperature is generally much lower and should be increased for oil stabilisation purposes. In most cases, cooling is done by using seawater or an indirect cooling medium, implying that large quantities of heat are dumped into the environment [11].

2.6.2 Waste heat recovery

Steam Rankine cycles

The integration of waste heat recovery cycles has been performed on at least three North Sea platforms, based on steam Rankine cycles. Kloster [120, 121] noted that they have been implemented as a retrofit option, i.e. after that the facility was operated in a certain amount of time. The economic benefits were emphasised, as the fuel and CO_2-tax costs decreased sharply, while the thermodynamic efficiencies of the retrofitted cycles were greatly enhanced.

Kloster [120, 121] mentioned that the most extensive measure for promoting the energy efficiency of an oil and gas facility has been to adapt gas turbine cycles into combined cycles or combined heat and power plants, by integrating a bottoming steam cycle. A steam bottoming cycle was installed on the Oseberg, Eldfisk and Snorre facilities. The steam networks integrated on the Oseberg Field Center and Snorre B include a steam turbine with extraction, which allows for transferring heat if required.

Nord and Bolland [118] investigated the challenges associated with integrating offshore steam bottoming cycles, and they pinpointed the clear compromise between the weight and the efficiency of these systems. They suggested that the most optimum design of the heat recovery steam generator includes a single pressure level, uses a once-through boiler, to avoid steam drums, and to allow for dry operation, to avoid bypass stack. In a later work, Nord and Bolland

[119] focused on these proposed designs and performed design and off-design simulations of these installations. They showed that such set-ups can allow for high flexibility, with respect to changes in the power demand and gas turbine load.

Organic Rankine cycles

There are, at the moment, no organic Rankine cycles installed on offshore platforms. Walnum et al. [122] analysed the integration of CO_2 bottoming cycles on oil and gas platforms, as these systems may be more compact and have a lower weight and smaller cost. They suggested that CO_2 may be a relevant alternative to steam, although the net power output can be up to 16 % lower, and that the off-design performance of such cycles is promising.

Rohde et al. [123] assessed the possibility for recovering heat from the gas treatment subsystem, implying that the waste heat recovery cycle is integrated to the processing plant, and *not* to the gas turbines, at the difference of the previous studies. Three cycles, using propane, CO_2 and a mixture of propane and ethane, were analysed. The efficiency of the last cycle was higher because of the evaporation gliding profile of the hydrocarbon mixture.

2.6.3 CO_2 sequestration

The integration of carbon capture and storage on oil and gas platforms is uncommon, with the particular cases of Sleipner and Snøhvit [124] in Norway, and In Salah in Algeria [125, 126].

Pre-combustion. The term *pre-combustion* refers to the removal or separation of the carbon present in the fuel prior to the combustion process. For instance, natural gas can be converted into CO_2 and H_2 by steam reforming, and the hydrogen is then used as fuel in a further combustion step, while the carbon dioxide is sequestrated. In the case of the Sleipner project [127], which is the first offshore carbon capture and storage (CCS) plant worldwide, the Sleipner field processes a natural gas with a CO_2 content of up to 9.5 %, which is far higher than the required export specifications of about 2.5 %. Carbon dioxide is separated *offshore* from the hydrocarbons and injected into the Utsira saline formation. The CO_2-removal takes place at high pressure ($\simeq$ 100 bar), based on scrubbing with a methyldiethanolamine-water solution.

Post-combustion. Post-combustion capture technologies are at present the most mature ones, but they have not been implemented on offshore platforms. However, there have been projects for capturing the carbon dioxide emitted in stationary energy sources (e.g. power plants) and transporting it offshore, where it would be injected. The direct integration of carbon capture on the exhaust gases from the turbines installed on-site was discussed in Falk-Pedersen et al. [128], where it was suggested that the combination of an amine absorption process using monoethanolamine (MEA) and a gas absorption membrane was a promising solution for CO_2-removal.

2.7 Overview

The field of oil and gas processing is not new: the first oil wells were drilled in the 19th century, and the general structures of the conventional modern platforms date back to the late 1940s. The overall processing schemes are relatively well-understood, but the foreseen depletion of the oil and gas resources has driven the current scientific research towards the exploitation of unconventional resources (e.g. shale and extra heavy oils), and towards the development of novel technologies and processes (e.g. carbon capture and gas liquefaction).

In this perspective, an accurate modelling and simulation of oil and gas processes is of high interest. It would allow for (i) a better prediction of the production flows and energy demands, (ii) a consistent evaluation of the effects of varying operating and boundary conditions, and (iii) a better overview of alternative system configurations. Very little information is available in the scientific literature, possibly because of confidentiality issues, and the information that are obtained from such studies cannot easily be used or compared with each other. Different methodologies are applied, the modelling bases are not discussed, and the impact of choosing a particular thermodynamic model is not systematically explained.

The literature review shows that few studies deal with the performance of oil and gas platforms, with regards to thermodynamic, economic and environmental criteria. There is no study that actually addresses all these aspects simultaneously, and, at the beginning of this project, there was only one work that investigated the thermodynamic efficiency of offshore processing. The other studies focused on a qualitative assessment of the variations of the energy demands with changes in the field operating conditions and strategies.

Several methods can be applied to identify appropriate system designs or to suggest possible revamping, such as (i) advanced thermodynamic tools (ii) economic evaluations, based on estimations of the grassroot and retrofit costs, and (iii) calculations of the environmental impacts, both at a local level and over the life time of the facility. The development and the application of these tools is therefore essential to make a consistent assessment of offshore platforms and to investigate the possibilities for designing and improving the future ones.

The objectives of the present work are therefore to address these gaps, by:

(1) making a systematic comparison of the simulation tools for oil and gas processing;

(2) proposing meaningful performance indicators;

(3) analysing the performance of existing plants operating in various conditions;

(4) assessing appropriate system improvements, considering consistent criteria;

(5) drawing possible suggestions for designing more efficient systems in the future.

The state-of-the-art research in these fields (Table 2.1) has evolved these three years, particularly with the contributions of this work or of similar research groups.

Table 2.1: Summary of the main works in the state-of-the-art research on the performance of oil and gas platforms.

Author	Year	Topic	Findings
Manning and Thompson [129]	1991	Offshore processing of petroleum	The major energy users are pointed out.
de Oliveira Jr. and Van Hombeeck [59]	1997	Exergy analysis of offshore platforms	The exergy analysis pinpoints the heating operations as major exergy consumers.
Rivero et al. [130]	1999	Exergy of petroleum	A calculation procedure of chemical exergy of petroleum is proposed.
Kloster [120]	1999	Energy optimisation of offshore platforms Analysis of existing facilities	The installation of cold flares and steam cycles is a viable energy conservation measure.
Rivero [131]	2002	Exergy analysis in the petroleum sector	The exergy concept helps improving the energy use in the petroleum energy-intensive sectors.
Svalheim [21]	2002	Environmental impacts and measures Energy use on offshore platforms	The installation of combined cycles and the constant turbine monitoring have greatly improved the energy performance of North Sea facilities.
Bothamley [11]	2004	Offshore processing of petroleum	General petroleum processing is similar from one oil region to another, with minor differences.
Nakashima et al. [101]	2004	Exergoeconomic analysis of offshore platforms	Exergoeconomic tools are powerful for comparing different technology options on oil facilities.
Vanner [20]	2005	Energy use on offshore platforms Efficiency trends with time	The energy intensity increases with time, because of e.g. the variations in GOR.
Voldsund et al. [132]	2010	Exergy analysis of offshore platforms	The exergy analysis pinpoints the gas compression operations as the most exergy-destroying ones.

3 Methods

This chapter presents the methodology applied throughout this project, from the general strategy to an overview and theoretical background of the system modelling methods, the performance analysis techniques and the optimisation routines.

3.1 Introduction

This study deals with the specific case of oil and gas platforms. There is, at the knowledge of the author, no unified and consistent approach for modelling, analysing and optimising such complicated and complex systems. A systematic methodology has therefore been developed throughout this study, based on the generic approach proposed by Bolliger [133].

This approach relies on the separation of the models of the systems under study (physical models) from the models used for analysing their performance (analysis models). The main advantage of this decomposition is that models developed with different software can be reused and assembled to generate large system superstructures, by transferring information from one model to another. Multiple system configurations can therefore be generated and optimised.

Several performance assessment tools (e.g. energy [76, 134–136], exergy [44, 54, 137, 138], pinch [64, 139–141] and life cycle [142]), which were developed during the last decades, were considered when building the analysis models. These tools have been applied for studying systems as small as human metabolisms, and as big as ecosystems. They illustrate different aspects of the performance of the energy system under study, and they should therefore be applied consistently to allow for sound conclusions.

Such a systematic methodology has been applied for the conception and analysis of energy conversion systems such as heat pumps [143], power plants with CO_2-sequestration [144], geothermal systems [145] and fuel cells [146]. Building on these methods, this chapter presents the basis of the strategy applied throughout this project.

3.2 Strategy

The backbone of this methodology consists of a combination of (i) system modelling, using flowsheeting tools, (ii) system analysis, applying advanced evaluation methods, and (iii) system optimisation, based on powerful search heuristics such as genetic algorithms (Figure 3.1). The corresponding models are separated from one another, and, if needed, the data are structured and transferred through a Matlab-language based platform, which was developed at the École Polytechnique Fédérale de Lausanne for this specific purpose.

The first step (**Modelling**) consists of developing a *physical model* of the system of interest (Section 3.3). It builds *either* on the collection of data (*pre-processing*) provided by the project partners (*retrofit study*), *or* on the development of superstructures (*grassroot study*). A superstructure embeds all the necessary unit operations and possible technologies to reach the desired target, and is constructed in a way to include all possible options and connections.

The modelling and simulation tools used in this work are, namely, Aspen Plus® [39], Aspen Hysys® [147], Aspen Energy® [148], Dynamic Network Analysis (DNA) [149], Engineering Equation Solver (EES) [150], Belsim Vali® [40] and Matlab® [151]. The strengths and weaknesses of each tool, as well as their applications in the frame of this project, are explained and detailed further. Data such as temperatures, pressures, mass and heat flows are extracted from the process models (*post-processing*) and sent to the next computing step.

The second step (**Analysis**) relies on a thorough analysis of the system performance, based on thermodynamic, economic and environmental assessment tools. The thermodynamic performance was evaluated by means of energy, pinch and total site, exergy and advanced exergetic analyses (Section 3.4). The economic aspects were addressed by performing an economic evaluation (Section 3.5). The environmental impacts were estimated by conducting a life cycle assessment (Section 3.6). Other methods were also used (Section 3.7).

The third step (**Optimisation**) aims at defining the system configurations that, for example, simultaneously minimise the economic costs or environmental impacts, while maximising the internal heat recovery and the thermodynamic performance [152].

The optimisation problem is based on *decision variables*, which can be changed in practice (for example, the design temperature at the outlet of a heat exchanger), and on *performance indicators* (Section 3.8), which express how well the system performs (e.g. the energy efficiency of a power cycle). For each evaluation, these indicators are re-computed, and an evolutionary algorithm is used to emulate the values of the decision variables (Section 3.9).

This mathematical problem includes discrete and continuous variables, as well as linear and non-linear relationships among them. It is therefore a Mixed Integer Non-Linear Programming (MINLP) problem, decomposed in this work into two sub-problems, namely a *master* and a *slave* problem (Figure 3.1). As this optimisation includes possibly conflicting objectives, the results do not consist of a single solution but as a set of Pareto-optimal ones.

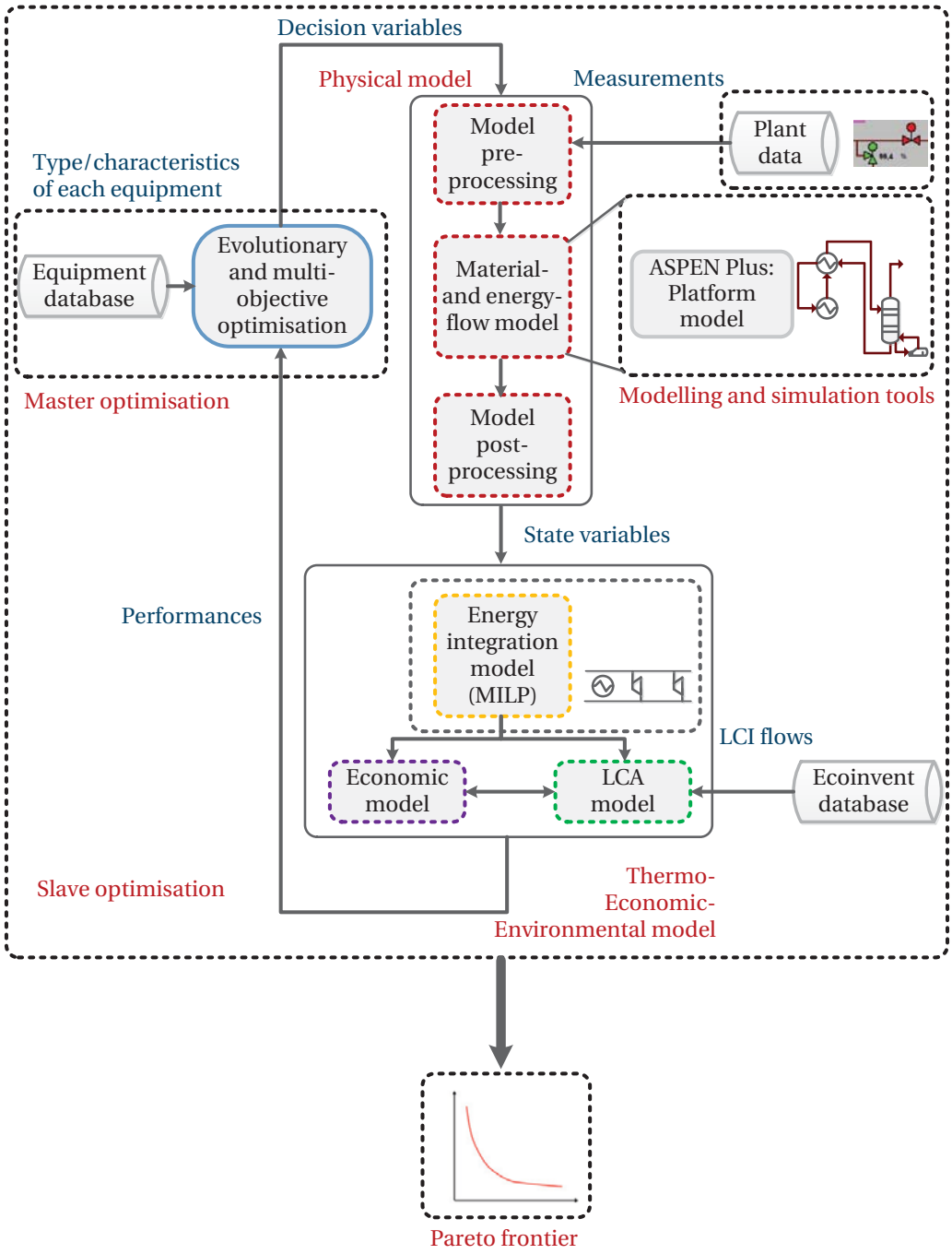

Figure 3.1: Conceptual structure of the general methodology and computational framework, illustrated with the analysis of oil and gas platforms.

3.3 Physical model

The main goal of developing physical models is to compute the mass flows at the level of each equipment item and to determine the possible energy requirements (e.g. power) for each process transformation. These models are developed in specific programming languages or simulation software, in which sets of equations (e.g. material and energy balances) are implemented and solved with the use of mathematical algorithms (e.g. Wegstein and Newton-Raphson methods) [153].

A process design approach can either consist of designing new facilities (grassroot) or of modifying existing ones (retrofit). In both cases, the overall aim is to design the processes with the appropriate physical and/or chemical transformations that are necessary to produce the desired outputs [154].

The main step is therefore to establish an inventory of the available resources (material and energy), identify the product (and possibly by-products) requirements and specifications, and investigate the possible pathways between the inputs and outputs, with respect to operating conditions that are feasible in practice and thermodynamically consistent. The different process alternatives, which are deduced from an extensive literature review and a survey of the technologies currently used, can be evaluated simultaneously and be embedded in a general block flow superstructure [155–157].

The physical model follows a sequence in three steps:

(1) *pre-processing*;

The model to be investigated is called, and the parameters that are required to run it are transferred or directly calculated from the input data given by the model user. For instance, when designing a new oil and gas separation process, the parameters that can be chosen are the operating pressures and temperatures of the vapour-liquid separators.

(2) *simulation*;

The model is solved numerically based on the pre-processed data and the selected equation solver, which can be, in this work, either Aspen Plus or Aspen Hysys (sequential) or Belsim Vali [40] (simultaneous).

(3) *post-processing*;

The results of interest are organised for further use in the analysis and optimisation routines. For example, data such as temperatures, heat capacities, mass and heat flows should be extracted to perform a pinch or energy integration analysis.

3.3.1 Thermochemical modelling

Chemical modelling. The reservoir fluids extracted from petroleum reservoirs contain a large variety of hydrocarbons, and complete compositional analyses are rarely conducted. The crude oils, as processed at the outlet of the offshore facility, are therefore characterised by their bulk and distillation properties, rather than by their chemical compositions. *Bulk properties* refer to properties measured when analysing the complete crude. *Distillation properties* refer to properties measured when analysing individually smaller fractions of the crude mixture [14, 17].

These fluids are thus modelled as mixtures of known and unknown, named *hypothetical* or *pseudo*-components. Light fractions, also called light ends, because they contain low-weight hydrocarbons, are represented by known components such as methane, ethane and propane. Hydrocarbons forming the heavy fractions are lumped into hypothetical components, each representing a certain number of real chemical compounds. Pseudo-properties such as the acentric factor are derived from the true boiling curve of the mixture [158].

Thermodynamic modelling. The calculations of the physical (e.g. density) and thermodynamic (e.g. internal energy) properties of each substance require information such as the pressure, volume and temperature (PvT). These properties are predicted using chemical thermodynamic models, which are based on either *equations of state* (EOS) or *activity coefficient* methods. The several chemical systems encountered in oil and gas modelling, and for which different models are applied, can be grouped into:

- ideal gases (e.g. air processed through the gas turbines): the Van der Waals (VDW) [159] EOS is applied, as it is satisfactory for predicting the thermodynamic properties of gases with perfect behaviour, but not near the critical point and not for phase equilibria [160];
- pure water, in liquid, vapour and supercritical states (e.g. water in a steam cycle): the tabular properties derived by the International Association for the Properties of Water and Steam (IAPWS) [161] are used;
- hydrocarbons in vapour phase (e.g. light gases, mostly containing methane and ethane): the Redlich-Kwong with Soave modifications (SRK) [162] EOS is applied, as it predicts more accurately the vapour-liquid critical properties of light gases than the VDW EOS;
- hydrocarbons in liquid phase (e.g. gas condensate, composed of propane and butane, and oil): the Peng-Robinson (PR) [163] EOS is chosen, as it is significantly more reliable than the SRK EOS for the calculations of liquid volumes of hydrocarbons [164, 165];
- non-ideal mixtures of polar compounds (e.g. water-glycol solutions in dehydration processing): the Twu-Coon-Cunningham (TCC) [166] EOS is considered, because it is more accurate than the PR EOS for estimating the interactions between polar compounds;

- non-ideal mixtures of polar and non-polar compounds at high temperature and pressure (e.g. hydrocarbons, water and glycol in gas absorption): the Schwartzentruber-Renon (SWR) [167, 168] EOS is taken into account, as it is as accurate as activity-coefficient models for predicting the thermodynamic properties of such non-ideal solutions;

- non-ideal single- or two-liquid phase mixtures at low pressure (e.g. treated water with methanol): the Non-Random-Two-Liquid (NRTL) [169] activity model is applied, as water-methanol mixtures at normal conditions are highly non-ideal;

- non-ideal aqueous and mixed-solvent electrolyte solutions at low pressure (e.g. salts, amines and carbon dioxide): the Electrolyte Non-Random-Two-Liquid (eNRTL) [170] activity model is preferred because of the presence of electrolytes;

- non-ideal solutions at low to high pressures without ion formation but with physical absorption (e.g. methanol solvent and carbon dioxide): the Perturbed-Chain Statistical Associating Fluid Theory (PC-SAFT) [171] EOS is more appropriate for modelling systems with important anisotropic association and electrostatic interactions.

3.3.2 Process modelling

Data collection

The data used for the calibration and validation of the process model came from various sources, such as (i) archived data (former measurements), (ii) component data-sheets, (iii) engineering manuals (documentation of the anti-surge recycling), (iv) engineering assumptions (hypotheses on heat and pressure losses), (v) fiscal and online measurements (data subject to taxation or for monitoring purposes), (vi) process flow and instrumentation diagrams (plant processes and major equipments), (vii) public domain (estimations of the oil flows), and (viii) reference textbooks (general descriptions of oil and gas processing).

The evaluation of the data quality from the online measurements showed that, (i) when several sensors are placed at the same location (e.g. venting and flaring systems), a single averaged-value was stored, and no information on the averaging algorithm was available; (ii) some values were kept as constant values inside the database (e.g. volumes of flared gases at high-pressure), as long as the standard deviation of the new measurement did not exceed a certain threshold limit; (iii) it was not possible to identify if the updated values were measured and registered at the same point in time, and this generated an additional uncertainty.

The data used for the model calibration and validation consisted mainly of values received from the process database. These values were *not* the values directly received from the sensors, but they were values that were received after post-processing between the sensor and the database. They were given on a rate of 1/s and had an accuracy of up to 15 digits, in the case of the Draugen platform. Time intervals with stable conditions were considered, and the data were time-averaged to reduce the impact of transient conditions on the system modelling.

Most data used for the calibration of the Draugen platform, which is the core case study of this work, were received between the middle and the end of this project. They were used to adjust the preliminary values deduced from the authors' experience and literature studies. The data related to the other case studies are available in Voldsund et al. [172, 173].

Data adjustment

The chemical compositions of the feed streams, i.e. at the *inlet* of the processing plant, were deduced and adjusted from the crude oil, fuel gas and water compositions and rates, as measured at the *outlets*. This backward approach was suggested by the platform engineers and was successfully applied in the work of Voldsund et al. [172]. A direct and forward approach may be inappropriate, as there is a lack of knowledge on the properties of each well-stream. On the contrary, the application of a backward approach is eased by the measurements of the oil, gas and produced water flows. These measurements were available for each case study, as they are made obligatory by the Norwegian Petroleum Directorate (NPD).

The same reasoning was applied at the level of each chemical compound, as a detailed compositional analysis was not available for the reservoir fluids. In the case of the platforms investigated in this work, the chemical compositions of the fuel and export or injected gas streams were available: they were measured several times in the recent years, and crude oil assays were made available by oil companies or by their industrial partners. This approach was found to be easier to apply if no information was available on the uncertainties of the measurements and on the reliability of the sensors.

Data reconciliation

The measurements on the platform inflows have significant uncertainties, because of the multiphase properties of the well-streams and the changes in the field conditions over its lifespan [174, 175]. They can help in monitoring the well performance but are generally recommended for use along with measurements on the platform outflows [176]. These ones are constrained by the the Norwegian Petroleum Directorate: limitations on the maximum uncertainties that can be allowed were set, for fiscal reasons [177, 178]. The uncertainty levels at 95 % confidence stated by the NPD [177–179] are 0.30 % for oil, 1.8 % for fuel gas, 1.0 % for sales gas and 5 % for flared gas. Values for lift gas and for vented gas were not found and were assumed to be 1.8 % and 5 %, respectively, as for fuel and flared gas. Data were therefore reconciliated when possible to improve the consistency of the models.

3.3.3 System simulation

The processing plant was simulated using Aspen Plus® [39], Aspen Hysys® [147], and Vali® [40]. The power generation plant was simulated by using the in-house tool Dynamic Network Analysis (DNA), which is a program developed at the Technical University of Denmark [149].

3.4 Thermodynamic assessment

The next step consists of developing a thermodynamic model, based on the selection of the process model and on the computation of all the state variables. It includes (i) a mapping of the energy (*energy analysis*) flows, (ii) an assessment of the system inefficiencies (*exergy analysis*), and (iii) an investigation of process integration opportunities (*pinch* and *total site* analyses), based on an estimation of the system requirements.

Based on the results from this analysis, the unit operations and heat recovery within the plant can be improved, by for instance adapting the operating conditions or by integrating combined heat and power. The selection of the utilities and their configuration can be determined by including the several options in a superstructure, and the problem is thereby formulated as a Mixed Integer Linear Programming (MILP) problem, with the purpose of minimising the system inefficiencies, external energy use, operating costs, etc. The different analysis methods are presented in the following.

3.4.1 Energy analysis

Energy may be transformed from one form to another and transferred between systems, but can neither be created nor destroyed. An energy analysis indicates therefore changes from one form of energy to another and allows the tracing of energy flows throughout a given system. The energy rate balance at steady state is:

$$0 = \dot{Q} - \dot{W} + \sum_{\text{in}} \dot{m}_{\text{in}} \left(h_{\text{in}} + \frac{1}{2} V_{\text{in}}^2 + g z_{\text{in}} \right) - \sum_{\text{out}} \dot{m}_{\text{out}} \left(h_{\text{out}} + \frac{1}{2} V_{\text{out}}^2 + g z_{\text{out}} \right) \tag{3.1}$$

where:

$\dot{Q}$ and $\dot{W}$ account for the net rates of energy transfer by heat and work;

$\dot{m}$ represents the mass flow rate at an inlet or outlet port;

h denotes the specific enthalpy of a stream of matter;

V, g and z stand for the velocity, the gravitation constant and the height, respectively.

As suggested in Kotas [54], the specific enthalpy h of a material stream j can be defined as the enthalpy change observed, i.e. the energy released, when the stream is brought from its temperature and pressure to the reference conditions (physical enthalpy) and reacts with the environment (chemical enthalpy). The physical enthalpy depends on the environmental conditions, while the chemical enthalpy depends on the choice of the reference species.

In the case of an offshore platform, energy enters and exits this system with material streams (e.g. petroleum feed, imported gas, fuel air, as well as oil, gas and produced water), with

power (e.g. imported or exported electricity from the mainland or to other platforms) and with heat (e.g. heat losses by component radiation). Without considering the special cases with imported gas (e.g lift purposes) or power import (e.g. electrification), the energy balance for a generalised offshore platform can therefore be expressed as:

$$\dot{H}_{\text{feed}} + \dot{H}_{\text{imp}} + \dot{H}_{\text{air}} + \dot{H}_{\text{cw}} + \dot{W}_{\text{imp}} = \sum_{k} \dot{H}_{k} + \dot{H}_{\text{exh}} + \dot{H}_{\text{rw}} + \dot{W}_{\text{exp}} \tag{3.2}$$

where:

$\dot{H}$ stands for the energy rate carried with the ingoing material flows (feed denoting the feed streams from the wells, imp the imported gas for injection or power generation, air for the air processed through the gas turbines);

or for the outgoing streams (cw for the seawater used for cooling needs, exh for the exhaust gases, rw for the treated and rejected cooling water, and k for the several oil and gas streams);

$\dot{W}$ for the energy transported with power, imported or exported to the mainland or other platforms.

Most oil and gas platforms do *not* import gas ($\dot{H}_{\text{imp}} = 0$) and are stand-alone systems ($\dot{W}_{\text{imp}}$ and $\dot{W}_{\text{exp}} = 0$): the power required on-site for compression and heating purposes is produced by burning a fraction of the gas extracted from the field. The energy balance for the processing and utility plants of the oil and gas facility can then be expressed as:

$$\dot{H}_{\text{feed}} + \dot{W}_{\text{UT}} + \dot{Q}_{\text{UT,heat}} = \sum_{k} \dot{H}_{k} + \dot{Q}_{\text{PP,cool}} \tag{3.3}$$

$$\dot{H}_{\text{k,fuel}} + \dot{H}_{\text{air}} = \dot{Q}_{\text{UT,cool}} + \dot{Q}_{\text{UT,heat}} + \dot{W}_{\text{UT}} \tag{3.4}$$

where:

$\dot{W}_{\text{UT}}$ is the power consumed within the separation and treatment modules, as well as in electric heaters, which is produced in the utility plant;

$\dot{Q}_{\text{PP,heat}}$ is the heat entering the processing plant, generally by direct heat exchange with the exhausts of a gas turbine, or by indirect heat exchange, by using a heating medium (e.g. hot water or hot glycol);

$\dot{Q}_{\text{PP,cool}}$ is the heat entering the processing plant, generally by direct heat exchange with the exhausts of a gas turbine, or by indirect heat exchange, by using a heating medium (e.g. hot water or hot glycol);

$\dot{Q}_{\text{UT,cool}}$ is the energy transferred from the power plant to the cooling medium (e.g. cooling air, seawater or glycol-water mixtures) in, for instance, a steam condenser.

3.4.2 Exergy analysis

Exergy accounting. *Exergy* may be defined as the *maximum theoretical useful work (shaft work or electrical work) as the system is brought into complete thermodynamic equilibrium with the thermodynamic environment while the system interacts with it only* [76]. Unlike energy, exergy is destroyed via conversion technologies and losses in real processes. The amount of exergy destroyed throughout successive processes accounts for the additional fuel use because of the system imperfections [54, 180–182], and an exergy accounting reveals the locations and extents of the thermodynamic irreversibilities of the system under study [76, 183]. The exergy balances are similar in essence to the energy balances, the differences lie on the use of an exergy basis and on the inclusion of an exergy destruction term to account for the thermodynamic irreversibilities of the system.

$$\begin{aligned}\dot{E}_\mathrm{d} &= \sum \dot{E}_\mathrm{in} - \sum \dot{E}_\mathrm{out} \\ &= \sum_j \left(1 - \frac{T_0}{T_j}\right) \dot{Q}_j - \dot{W} + \sum_\mathrm{in} \dot{m}_\mathrm{in} e_\mathrm{in} - \sum_\mathrm{out} \dot{m}_\mathrm{out} e_\mathrm{out}\end{aligned} \tag{3.5}$$

where:

$\dot{E}_\mathrm{d}$ is the destroyed exergy, also defined, from the Gouy-Stodola theorem [183], as:

$$\dot{E}_\mathrm{d} = T_0 \dot{S}_\mathrm{gen} \tag{3.6}$$

$\dot{E}_\mathrm{in}$ is the inflowing exergy;

$\dot{E}_\mathrm{out}$ is the outflowing exergy;

T_j and T_0 are the instantaneous and ambient temperatures;

e denotes the specific exergy of a stream of matter.

The exergy balances for the three control volumes considered in Section 3.4.1 can be expressed as:

$$\dot{E}_\mathrm{feed} + \dot{E}_\mathrm{imp} + \dot{E}_\mathrm{air} + \dot{E}_\mathrm{cw} + \dot{E}^W_\mathrm{imp} = \sum_k \dot{E}_k + \dot{E}_\mathrm{exh} + \dot{E}_\mathrm{rw} + \dot{E}^W_\mathrm{exp} + \dot{E}_\mathrm{d,OP} \tag{3.7}$$

$$\dot{E}_\mathrm{feed} + \dot{E}^W_\mathrm{UT} + \dot{E}^Q_\mathrm{UT,heat} = \sum_k \dot{E}_k + \dot{E}^Q_\mathrm{PP,cool} + \dot{E}_\mathrm{d,PP} \tag{3.8}$$

$$\dot{E}_\mathrm{k,fuel} + \dot{E}_\mathrm{air} = \dot{E}^Q_\mathrm{UT,cool} + \dot{E}^Q_\mathrm{UT,heat} + \dot{E}^W_\mathrm{UT} + \dot{E}_\mathrm{exh} \tag{3.9}$$

where:

$\dot{E}$ denotes the exergy flow associated with a given stream of matter;

$\dot{E}^W$ denotes the exergy transferred with power, and has the same value than its energy;

$\dot{E}^Q$ denotes the exergy transferred with heat, and has a smaller value than its energy, as it depends on the temperatures of the environment and at which the heat transfer takes place;

$\dot{E}_\mathrm{d}$ is the exergy destroyed in the overall (OP), processing (PP) and utility plants (UP).

Dead state. The concept of exergy is only relevant when an appropriate dead state is defined, i.e. when the thermodynamic system cannot further exchange mass, heat and work with its surroundings. The dead state pressure is 1 atm and 8 °C.

The ambient water is a few degrees colder than the ambient air in the North Sea region, when taking the average values over a year. For simplicity, it is assumed that the ambient air and water are in thermal equilibrium at 8 °C, since the measurements conducted by the operators indicated ambient temperature values oscillating around 7 and 9 °C.

Three main works can be found in the scientific literature for the definition of the chemical composition of the reference environment, namely the studies of Ahrendts [184], Szargut et al. [44] and Kotas [54]. The model of Kotas [54] is based on the first models of Szargut, which have been updated in the last decades. The models of Szargut et al. [44] and of Kotas [54] are the most commonly used in the recent exergy analysis studies. The model of Szargut et al. [44] is considered in this work, as the value of the reference atmosphere humidity is closer to the one that can be expected in seaside conditions.

Exergy components. The exergy rates are equal to the product of the specific exergy of a given stream (material or energy) and the mass or energy rate. In the absence of nuclear, magnetic and electrical interactions, the exergy associated with a stream of matter is a function of its physical e^{ph}, chemical e^{ch}, kinetic e^{kn} and potential e^{pt} components [76], and is expressed as:

$$e = e^{\mathrm{ph}} + e^{\mathrm{ch}} + e^{\mathrm{kn}} + e^{\mathrm{pt}} \tag{3.10}$$

Physical exergy accounts for temperature and pressure differences from the environmental state and can be further divided into thermal (temperature-based) e^{t} and mechanical (pressure-based) e^{m} exergies [185]:

$$e^{\mathrm{ph}} = (h - h_0) - T_0(s - s_0) \tag{3.11}$$

$$e^{\mathrm{t}} = \big(h - h(T_0, p)\big) - T_0\big(s - s(T_0, p)\big) \tag{3.12}$$

$$e^{\mathrm{m}} = \big(h(T_0, p) - h(T_0, p_0)\big) - T_0\big(s(T_0, p) - s(T_0, p_0)\big) \tag{3.13}$$

Chemical exergy accounts for deviations in chemical composition from reference substances present in the environment. In this work, the specific chemical exergy of real chemical com-

pounds is derived from the *standard chemical exergy* of the reference compounds present in the environment of Szargut et al. [44]. The specific chemical exergy of hypothetical components $e^{\text{ch}}_{\text{hyp}}$ is computed with the heuristic correlations of Rivero et al. [130]:

$$e^{\text{ch}}_{\text{hyp}} = \beta LHV_{\text{hyp}} + \sum z_{\text{mt}} e^{\text{ch}}_{\text{mt}} \tag{3.14}$$

where:

z_{mt} stands for the mass fraction of metal impurities;

$e^{\text{ch}}_{\text{mt}}$ for the corresponding chemical exergy; and

β for the chemical exergy correction factor.

The specific chemical exergy of a given mixture $e^{\text{ch}}_{\text{mix}}$ is expressed as a function of the chemical exergies of each individual chemical compound in the mixture, and of a reduction of exergy caused by the mixing effects [186]:

$$e^{\text{ch}}_{\text{mix}} = \sum_i x_i e^{\text{ch}}_{i,\text{mix}} \tag{3.15}$$

$$= \sum_i x_i e^{\text{ch}}_{i,0} + \left(\sum_i x_i \left(h_{i,\text{mix}} - h_{i,0} \right) \right) - T_0 \left(\sum_i x_i \left(s_{i,\text{mix}} - s_{i,0} \right) \right) \tag{3.16}$$

where:

the mass fraction, the chemical compound and the mixture are denoted by x, i and mix;

the specific exergy of a given chemical compound is written $e^{\text{ch}}_{i,\text{mix}}$ when it is in the mixture, and $\bar{e}^{\text{ch}}_{i,0}$ when it is in a pure component state;

the term $\sum_i x_i e^{\text{ch}}_{i,0}$ is called the *pure-component* chemical exergy;

the term $\sum_i x_i \left(h_{i,\text{mix}} - h_{i,0} \right) - T_0 \left(\sum_i x_i \left(s_{i,\text{mix}} - s_{i,0} \right) \right)$ is called the *compositional exergy* [130].

Exergetic fuel, product, destruction and losses. Tsatsaronis [187] introduced the concepts of *fuel* and *product* exergy. The *product exergy* ($\dot{E}_{\text{p}}$ on a time rate basis) represents the desired result of the system and includes, according to Lazzaretto and Tsatsaronis [51, 52]:

- all the exergy values to be considered at the outlet;
- all the exergy increases between inlet and outlet (i.e. exergy additions to material streams) that are in accordance with the purpose of operating the system under study.

The *fuel exergy* stands for the necessary resources used to drive the process under consideration to generate the product exergy. It does *not* always correspond to a given fuel such as

natural gas, oil or diesel but represents the exergetic resources utilised within the system and includes, according to Lazzaretto and Tsatsaronis [52]:

- all the exergy values to be considered at the inlet (e.g. exergy of the fuel gas entering a gas turbine);
- all the exergy decreases between inlet and outlet (i.e. exergy removals from material streams).

Hence, the exergetic balance becomes [76, 187]:

$$\dot{E}_{\mathrm{p}} = \dot{E}_{\mathrm{f}} - \dot{E}_{\mathrm{l}} - \dot{E}_{\mathrm{d}} \tag{3.17}$$

The term exergy loss, as named in Bejan et al. [76] refers to the exergy discharged to the environment without any practical use (e.g. exergy lost with cooling water). This wasted exergy is destroyed when mixed irreversibly with the environment and is denoted *external exergy losses* in the works of Szargut [188] and Kotas [54], by opposition to the term of exergy destruction, which refers to the *internal exergy losses*. The lost exergy is destroyed by reaching equilibrium when being mixed into the environment.

However, care should be exercised when using the term exergy losses, as this may refer to thermodynamic irreversibilities in a wide sense [44, 54, 189], i.e. the sum of the exergy destruction and losses. In the rest of this work, the terms *exergy destruction* and *exergy losses* are used to denote the internal and external irreversibilities of the system under study, respectively.

3.4.3 Advanced exergy analysis

Approach. One of the interests of an advanced exergetic analysis over a conventional one is the higher level of details: the exergy destruction in each system component is split into its *endogenous* and *exogenous*, as well as into its *unavoidable* and *avoidable* parts.

The separation between *unavoidable* and *avoidable* exergy destruction lies on the accounting for technological and economic constraints, such as the availability and cost of materials and manufacturing methods. A part of the exergy destruction cannot be avoided with the current limitations (*unavoidable*), and an example is the irreversibilities of the combustion reactions.

The division in *endogenous* and *exogenous* exergy destruction arises from the interactions between different components. A part of the exergy destruction taking place in a given component may result from the non-ideal operation of another one (*exogenous*). For instance, the gas flow rate into a cooler, and thus, its exergy destruction, depends on the degree of gas recirculation around the compressor it serves.

The *endogenous* exergy destruction of the kth component ($\dot{E}_{d,k}^{\mathrm{EN}}$) is associated with the irre-

versibility of the component being considered, when it operates with its real characteristics, while the remaining ones operate ideally. The *exogenous* part ($\dot{E}_{d,k}^{\mathrm{EX}}$) is therefore associated with the effect of the irreversibilities of the other $n-1$ components on the exergy destruction of the kth component [190]. The difference between the sum of all the exogenous exergy destruction per component, and the total exogenous exergy destruction, is named the *mexogenous* exergy destruction ($\dot{E}_{d,k}^{\mathrm{MEXO}}$). This effect is caused by the combined interaction of three or more components.

The *unavoidable* exergy destruction ($\dot{E}_{d,k}^{\mathrm{UN}}$) is the exergy destruction that cannot be further reduced because of technological limitations, such as the availability and cost of the materials and manufacturing methods. On the contrary, the *avoidable* exergy destruction ($\dot{E}_{d,k}^{\mathrm{AV}}$) can be decreased by improving either the kth component or the remaining components, and efforts should thus focus on reducing these inefficiencies.

$$\left(\dot{E}_{d,k}\right) = \begin{cases} \dot{E}_{d,k}^{\mathrm{AV}} + \dot{E}_{d,k}^{\mathrm{UN}} & \text{and } \dot{E}_{d,k}^{\mathrm{UN}} = \dot{E}_{p,k}^{\mathrm{real}} \left(\frac{\dot{E}_{d,k}}{\dot{E}_{p,k}}\right)^{\mathrm{UN}} \\ \dot{E}_{d,k}^{\mathrm{EN}} + \dot{E}_{d,k}^{\mathrm{EX}} & \text{and } \dot{E}_{d,k}^{\mathrm{EX}} = \sum_{i=1, i\neq k}^{n-1} \dot{E}_{d,k}^{\mathrm{EX},i} + \dot{E}_{d,k}^{\mathrm{MEXO}} \end{cases} \tag{3.18}$$

The calculation of $\left(\frac{\dot{E}_{d,k}}{\dot{E}_{p,k}}\right)^{\mathrm{UN}}$ is conducted by simulating a system where only unavoidable exergy destructions take place within each individual component.

Combination. Based on the reasoning presented in Kelly et al. [190], Tsatsaronis and Park [191], Tsatsaronis et al. [192] the exergy destruction is then split into four subsequent parts, namely:

- the *unavoidable exogenous* part of the exergy destruction ($\dot{E}_{d,k}^{\mathrm{UN,EX}}$), which cannot be reduced because of the technological limitations related to the remaining components of the overall system, for the given structure;
- the *unavoidable endogenous* part of the exergy destruction ($\dot{E}_{d,k}^{\mathrm{UN,EN}}$), which cannot be reduced because of the technological limitations of the kth component;
- the *avoidable endogenous* part of the exergy destruction ($\dot{E}_{d,k}^{\mathrm{AV,EN}}$), which can be reduced by improving the performance of the kth component;
- the *avoidable exogenous* part of the exergy destruction ($\dot{E}_{d,k}^{\mathrm{AV,EX}}$), which can be reduced by improving the efficiency of the remaining system components.

3.4.4 Pinch analysis

Pinch-based analysis methods belong to the category of energy and process integration methods [193], which aim at minimising the use of external energy utilities by maximising the internal heat recovery of the system under study. The thermodynamically attainable energy targets are calculated, respecting the 2nd Law of Thermodynamics, and the ways to achieve them are determined, by optimising the use of the different heating and cooling sources, with respect to economic aspects.

When applied to large-scale facilities, this energy-integration problem may be solved by applying a total site analysis (TSA), considering heat exchange restrictions between different sub-systems, and/or by mathematical programming, since a high number of process streams, and thus, a significant amount of heat exchange possibilities, would result in combinatorial challenges. The aim of this problem is to obtain a configuration that aims, for example, at minimising the external utility costs.

The energy integration model is based on several steps [63, 68], which consist of:

(1) defining the hot and cold streams and extracting the appropriate data (e.g. temperatures and heat capacities);

A *stream* is a flow that requires either heating or cooling, without any change in composition. It is called a *hot stream* if it needs to be cooled down (heat excess) and a *cold stream* if it needs to be heated up (heat deficit).

(2) choosing a minimum temperature difference, correcting the stream temperatures;

The concept of minimum temperature difference (ΔT_{min}) is based on that minimum driving heat transfer forces are required in practical heat exchangers, and the process temperatures are corrected in function. It is either global (e.g. entire system or small sub-systems [194]) or individual (e.g. each stream [140]).

The selection of individual temperature differences ($\Delta T_{min}/2$) accounts for various film coefficients for different types of streams, and they are taken to be 2, 4 and 8 K for phase-changing, liquid and gaseous flows. The optimal values of ΔT_{min} may be found by evaluating the variations of the annualised costs of heat exchangers (supertargeting) [195].

$$T^*_{hot} = \left(T_{hot} - \frac{\Delta T_{min}}{2} \right) \tag{3.19}$$

$$T^*_{cold} = \left(T_{cold} + \frac{\Delta T_{min}}{2} \right) \tag{3.20}$$

(3) determining the pinch point and setting the energy targets;

This step can be performed either graphically (composite curves) or numerically (problem table algorithm) [193]. The *composite curves*, which are specific temperature-

enthalpy diagrams, are plotted by combining the heating demand of each cold stream into a single curve (*cold* composite curve) and of each hot stream (*hot* composite curve), with their respective supply and target temperatures, and their energy requirements.

The *pinch point* is the point where the two curves are the closest, i.e. where the temperature difference between the hot and cold streams is at its minimum. The maximum heat recovery corresponds to the area limited by the two curves, and the overall system is defined into two sub-systems that should be treated independently to minimise the external energy use. The pinch golden rules state that only external heating should be supplied above the pinch point, only external cooling should be provided below the pinch point, and no heat should be transferred from one system to another.

An alternative way is to formulate the problem mathematically as a linear programming transshipment model [196], based on the principles that the entire temperature range can be divided into temperature intervals, in which the number of streams is constant, and that heat can only be cascaded from one temperature interval to one under. The heat surplus (or residual) is calculated for each interval, yielding the minimum external heating and cooling demands. This formulation is more adapted for further computational implementation.

(4) designing a heat exchanger network that satisfies the energy requirements (*grassroot*) or improving a current one (*retrofit*) by investigating the possible process changes and the integration of external utilities;

External heating may be satisfied by recovering the waste heat from the exhausts of a heat engine, using the latent heat from steam at different pressure levels, or by converting primary energy sources through electric heaters or furnaces. External cooling may be met by using cooling water or air or by refrigeration utilities.

(5) suggesting system improvements to minimise, for instance, the operating costs, the thermodynamic irreversibilities or the total costs.

These options include the integration of gas turbines and steam cycles, co-generation of heat and power and heat pumping. This problem is in essence complex as attention should be paid to the choice of the utilities, the design of the heat exchanger network and to the system operational constraints. It is formulated as a Mixed Integer Linear Programming problem, and the selection of the objective functions depends on the trade-off that one wants to investigate.

The energy demands of each process are illustrated via means of the *Composite Curves* (CC) and *Grand Composite Curve* (GCC). The composite curves can be re-plotted including the temperature-enthalpy profiles of the utility streams that are used to satisfy the process energy demand: this means that the GCC is closed at each end, because the heat loads of the utilities *balance* the heating and cooling consumptions of the process. These resulting composite curves are named the *Balanced Composite Curves* (BCC) [63].

3.4.5 Total site integration

The total site analysis (TSA) method [64, 67] builds on the pinch analysis: this methodology is extended to an entire plant or site, which consists of several individual processes, with their own utilities. It also considers that the several processes cannot directly exchange heat because of operational reasons (e.g. distance), and that energy delivery from one process to another takes place though a common utility plant, based on steam or another heating medium. The overall procedure to address the site-scale energy integration problem stays similar, with a few variants depending on the research groups, and consists of:

(1) calculating the energy demands for each individual process and drawing the corresponding grand composite curves;

(2) identifying the heating and cooling requirements of the total site by building the site source and sink profiles;

Conventional total site analyses generally assume that the heat exchanges taking place between two process streams are accepted as they are, and that they are excluded from the site integration study. In practice, this means that the *self-sufficient pockets*, which correspond to the non-monotonic parts of the grand composite curves, are removed. However, the energy available in these self-sufficient zones could be used for co-generation purposes, depending on the temperature levels, and it has been argued that they should be considered carefully [154, 197, 198].

(3) setting set-wide targets for co-generation, external heating and cooling, based on the resulting site source and sink profiles;

This approach presents the advantage of identifying the site pinch point rather than focusing on the pinch point of each individual process, and system modifications will therefore improve the overall energy performance of the total site.

As for a conventional pinch analysis, the process improvements can be drawn from a set of temperature-enthalpy diagrams, such as the *Single Source and Sink Profiles* (SSSP) proposed by Dhole and Linnhoff [64] and the *Integrated Composite Curves* (ICC) introduced by Maréchal and Kalitventzeff [140]. The latter are temperature-enthalpy diagrams that assess the integration of a particular system within the remaining processes, and they help in suggesting process improvement options that are not necessarily obvious, on an energy or exergy basis (Carnot diagrams).

The data required for analysing the energy requirements include, in general, the heat load associated with the cooling or heating demand, as well as their temperature levels. However, the data collection process may be difficult or time-consuming, as an important amount of information should be gathered (Figure 3.2). Different approaches found in the literature can be applied [64, 67]:

- *black-box* approach, where the site is represented only by the temperature levels of the utilities (e.g. cooling water and steam) and the corresponding energy demands;
- *grey-box* approach, where the heat exchanges between two process streams are ignored, and where only the process-utility heat exchanges are considered;
- *white-box* approach, where all heat exchanges are considered;
- *detailed* approach, where the heat exchanges associated with non-isothermal mixing and chemical reactions are included.

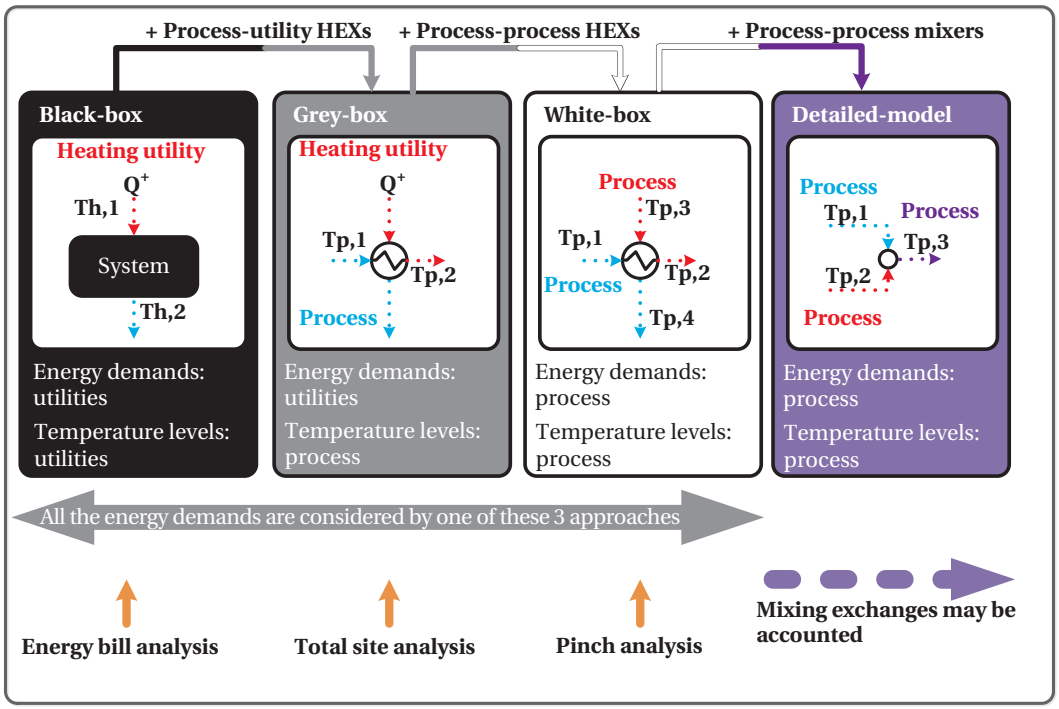

Figure 3.2: Possible data collection approaches in energy-based analyses (energy bill, total site, pinch and detailed).

In practice, most TSA studies have built on the grey-box approach. On the contrary, a conventional pinch analysis is generally based on a white-box approach, as this level of details is required to analyse properly a thermal system and its energy requirements. The application of a black-box approach is generally not recommendable, as possibilities for improvement may be missed.

The next step, after data extraction, is to represent each energy requirement with the most suitable level of details (Figure 3.3), as proposed in Brown et al. [199]:

- *utility* level, where the site is represented only by the temperature levels of the utilities;

For example, the heat used for petroleum heating in the separation process of an oil and gas platform is recovered from the turbine exhausts and is available at a temperature exceeding 300 °C.

- *technology* level, which illustrates how the energy demands are satisfied, and which technologies are actually used;

  In the above-mentioned case, the heat recovered from the flue gases is not directly delivered to the heating process, but an hot water or an hot oil loop is implemented in-between, operating between 120 and 250 °C.

- *thermodynamic* level, which defines precisely the thermodynamic requirements of the system under study.

  For the same example, the energy requirement is represented by the temperature level at which heat is required, i.e. with the temperature levels of the oil and condensate streams, which are in the range of 60 to 220 °C. The energy demand is therefore represented by the temperature level of the low-grade heat instead of the high-grade one.

These energy requirements are equivalent on an *energy* basis, but they differ by their temperature profiles, which implies that the corresponding *exergy* needs are different.

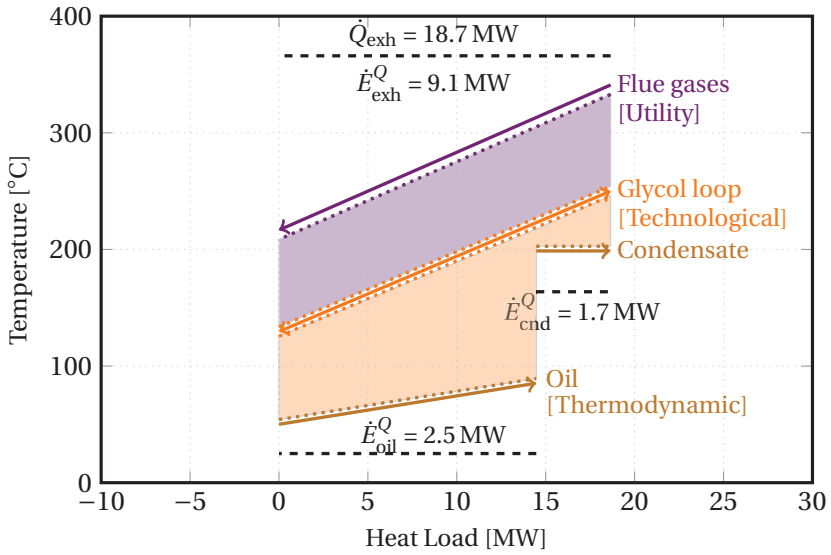

Figure 3.3: Multiple representation of the same energy requirements (utility, technological, thermodynamic).

The application of the thermodynamic requirement approach is more difficult because it may require extensive simulations and/or experiments. In a final step, the composite curves of relevance can be drawn to assess the potentials for energy savings and enhanced process integration (Figure 3.4).

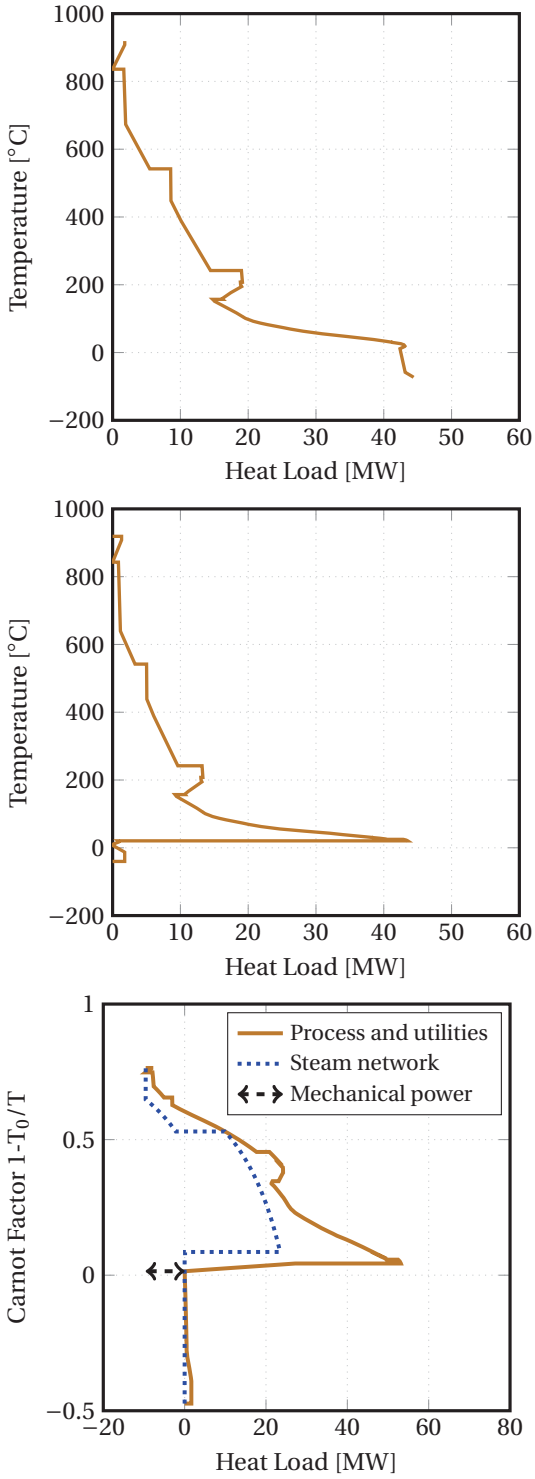

Figure 3.4: Examples of Grand Composite Curve (top), Balanced Grand Composite Curve (middle) and Integrated Composite Curves (bottom).

3.5 Economic evaluation

The economic cost of a given item consists of fixed (i.e. investment) and variable (i.e. operation and maintenance) costs. It is difficult to perform accurate cost estimates, as the fixed costs vary depending on the manufacturers and little commercial data is available. Similarly, the variable costs are subject to high uncertainties since the market prices of fuels such as natural gas are highly variable with the time and geographical location.

The total investment costs are calculated, in this work, following these four steps:

(1) the purchased-equipment costs of each item C_{pc} are estimated by cost correlations, such as the ones of Turton et al. [79], which have an uncertainty of ± 30 %, or by estimation charts, assuming atmospheric pressure conditions and carbon steel construction:

$$\log_{10} C_{\text{pc}} = k_1 + k_2 \log_{10} A + k_3 \left(\log_{10} A\right)^2 \tag{3.21}$$

where k_1, k_2 and k_3 are constants and A is the capacity or size parameter specific to the component under study (e.g. heat transfer area for heat exchangers).

(2) the bare module costs C^0_{bm} are obtained, adjusting the purchased-equipment costs with pressure (f_p) and material (f_m) factors:

$$C^0_{\text{bm}} = C_{\text{pc}} \left(b_1 + b_2 f_m f_p\right) \tag{3.22}$$

where b_1 and b_2 are constants. In some cases, these correlations should be adapted to include design-type and temperature factors to correct these base costs.

(3) the actualised bare module costs C_{bm} are computed, considering the inflation between the reference year of the cost data and the date of the estimate with the chemical engineering plant costs indexes (CEPCI):

$$C_{\text{bm}} = C^0_{\text{bm}} \left(\frac{\text{CEPCI}}{\text{CEPCI}^0}\right) \tag{3.23}$$

(4) the grassroot costs C_{gr}, i.e. the total investment costs when installing the equipment items on a new production site, are deduced from:

$$C_{\text{gr}} = (1 + \alpha_1) \sum_i C_{\text{bm},i} + \alpha_2 \sum_i C^0_{\text{bm},i} \tag{3.24}$$

where the factor α_1 (≃0.18), which depends on the process conditions, accounts for the contingencies (≃0.15) and fees (≃0.03), and the factor α_2 (≃0.35), which is independent of the process operation, accounts for the auxiliary facilities and site development.

3.6 Environmental assessment

Life cycle assessment is a well-established method to evaluate the environmental impacts of the life stages of a product or process, from cradle-to-grave, i.e. from the resource extraction to the final disposal, including all the steps along the production chain. It takes into account all the relevant material and energy flows over the full life cycle of the system under study, which helps considering all the potential environmental impacts, and thus making more informed decisions.

A conventional life cycle analysis consists of four steps:

(1) definition of the goal and scope;

The service delivered, or function, of the studied system is explicitly defined, providing a reference to which all inputs and outputs are scaled linearly. It is quantitatively described by the *functional unit* (FU), which can be defined in relation to a given input (e.g. 1 kg of petroleum entering the oil and gas platform) or output (e.g. 1 kg of oil exiting the facility). Systems that present the same functions can therefore be compared based on this metric.

The system boundaries (e.g. geographical, life-cycle, technosphere–biosphere) are clearly stated, illustrating the assumptions and limitations of the study, and which materials, energy flows, and processes, are included (Figure 3.5). They are typically defined so that the ones contributing significantly to the analysed product or system are considered, and that the alternative ways to provide the same products or functions can be evaluated consistently.

In the case that the system under study provides multiple products, an issue to address is the partitioning of the several environmental impacts for each individual output, and a relevant allocation method (e.g. division per mass, energy, exergy, area, volume...) should be chosen.

(2) inventory of in- and outflows to the nature (Figure 3.6);

The inputs of raw materials and energy are identified and quantified, as well as the outputs to air, land and water: this accounting is generally performed by developing a flow model of the technical system under study, where all the activities that should be assessed, based on the system boundaries defined earlier, are included. For example, particulate matters are emitted during the production process of oil and gas.

(3) impact assessment;

The environmental impacts that one wants to investigate are selected, each inflow and outflow is assigned to the relevant impact category (e.g. carbon dioxide and methane flow is classified into the global warming potential category), and each flow is quantitatively characterised, using a common equivalence unit (e.g. 1 kg of CH_4 has a global warming potential equivalent to about 24.5 kg of CO_2 over a horizon of 100 years).

(4) interpretation.

The main environmental issues of the product or system under study are identified, and the assessment is completed by sensitivity and consistency analyses, verifying the assumptions and limitations.

Life cycle assessment tools are embedded in the computational framework used in this work, following the approach of Gerber et al. [200], taking 1 Sm^3 of oil equivalent exported to the shore as functional unit, because:

- the function of an offshore platform is to separate and purify the petroleum into its oil and gas phases;

  The relative yields of these potential products depend on the initial composition of the reservoir fluid entering the platform, and on the separation efficiency of the plant.

- choosing one unit of oil only as FU may not be suitable for oil and gas facilities where most production consists of gas, which is then exported via pipelines and further sold;

  Moreover, choosing this FU would unfairly penalise oil and gas platforms where significant amounts of heat and electricity are used to purify and dehydrate the gas.

- similarly, the choice of one unit of gas only as FU may not be relevant, as several oil plants aim at at maximising the oil production by injecting back the produced gas into the reservoir;

  Using this FU would imply that the impacts of storing and transporting oil are allocated to the produced gas, which seems inappropriate as the oil export process is independent of the gas production system.

- taking a unit of oil and gas equivalent presents the advantage of considering both gas and oil as potential products. It ensures that the effects of changes in the process design and in the energy conversion technologies are taken into account and allocated properly.

The inventory of the in- and outflows is based on the data and results obtained from the physical model (e.g. material and energy flows, design, size and operational characteristics of the equipments). The data from the Ecoinvent® database [201] are used when conducting the impact assessment phase. All options are compared by considering the following categories: the climate change impact, based on the methods proposed by the Intergovernmental Panel on Climate Change (IPCC), the eutrophication and acidication potentials, the terrestrial and human toxicities, and, finally, the endpoint eco-indicator 99, which lumps all environmental impacts on a single score.

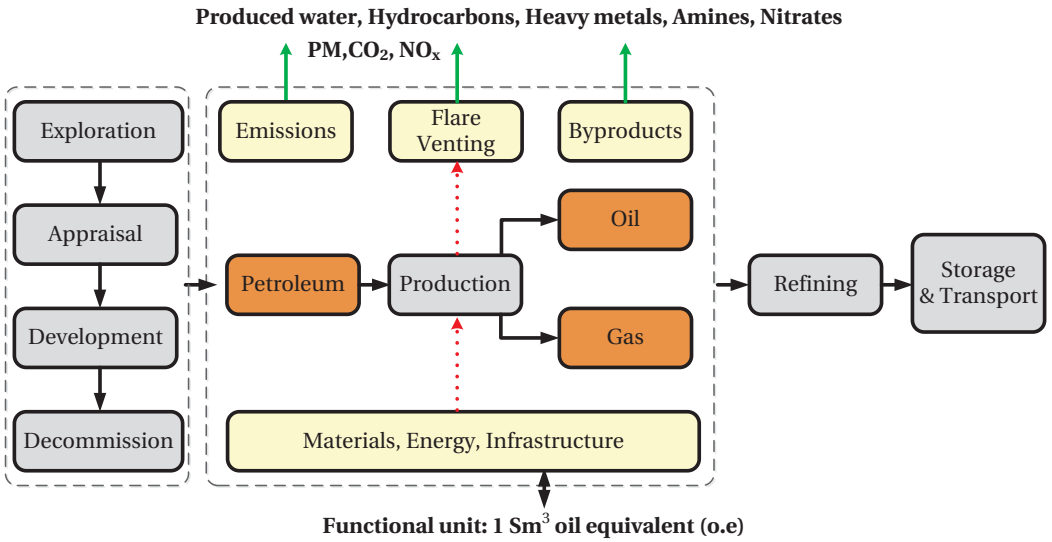

Figure 3.5: Conceptual boundary system for the life cycle analysis of the oil and gas platform.

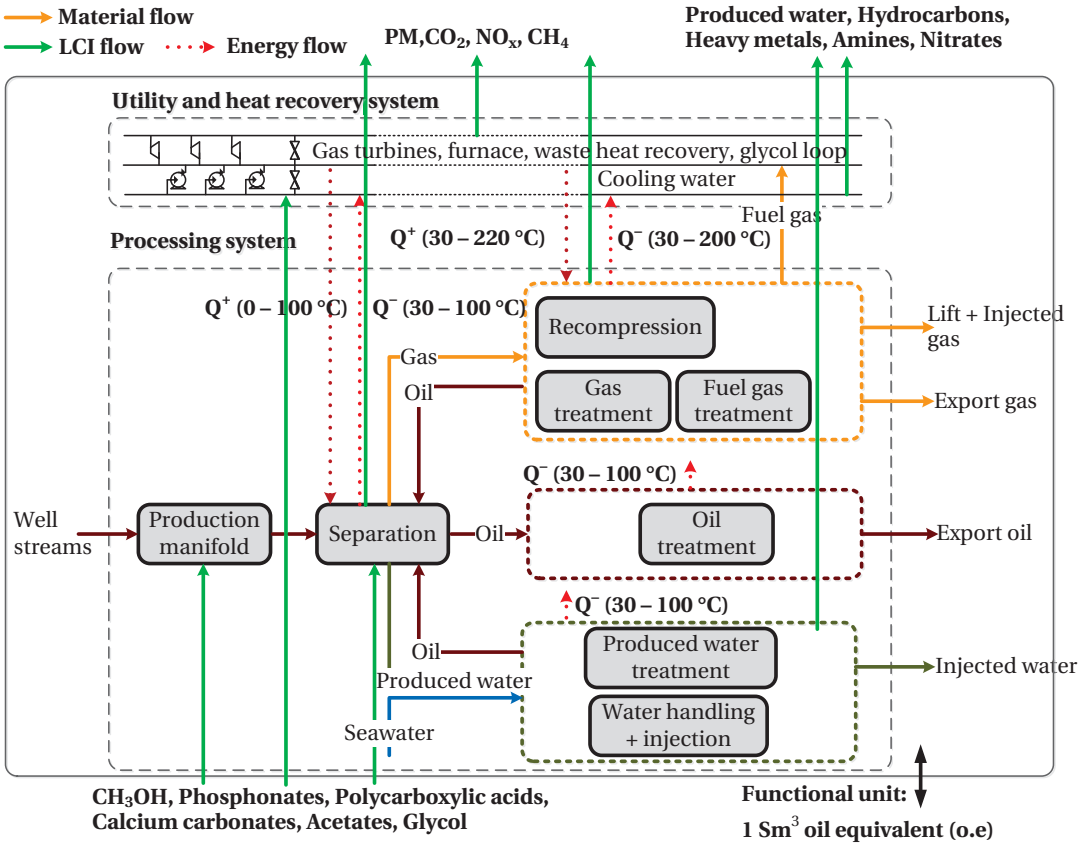

Figure 3.6: Conceptual boundary system for the life cycle inventory of the oil and gas platform.

3.7 Hybrid analyses

3.7.1 Exergoeconomic analysis

Exergoeconomics is a a combination of exergy and economic analysis tools: it aims at providing information on the cost of generating a given product and on the cost of the thermodynamic inefficiencies of a given system. The performance improvements deduced from an exergoeconomic analysis can help designing a more cost-effective system.

The exergoeconomic balance is similar to a conventional exergetic accounting, with the inclusion of economic terms. The exergoeconomic balance can be expressed with the cost rates $\dot{C}$ or with the products of the specific exergetic costs c and exergy flow rates $\dot{E}$:

$$\sum_{\text{in}} \left(\dot{C}_{\text{in}}\right)_k + \dot{C}_k^Q + \dot{Z}_k = \sum_{\text{out}} \left(\dot{C}_{\text{out}}\right)_k + \dot{E}_k^W \tag{3.25}$$

where $\dot{C}_{\text{in}}$, $\dot{C}_{\text{out}}$, $\dot{C}_Q$ and $\dot{C}_W$ are the cost rates that enter and exit the kth component with streams of matter, heat and power, and $\dot{Z}$ the associated capital and operation costs.

The capital costs are considered as sunk costs when evaluating the performance of an already existing system. The associated specific costs are the average costs per unit of exergy. Equation 3.25 states that the total costs of the outflowing exergy transfers are equal to the total costs of the inflowing ones, to which the capital and O&M costs are added.

However, this approach considers that the physical and chemical exergy are supplied or generated at the same unit cost, but it is possible to rewrite the same cost rate balance after a further decomposition of the exergy flows into the physical and chemical exergy terms. This results in a more accurate analysis, at the expense of greater computational efforts:

$$\sum_{\text{in}} \left(\dot{C}_{\text{in}}^{\text{ph}} + \dot{C}_{\text{in}}^{\text{ch}}\right)_k + \dot{C}_k^Q + \dot{Z}_k = \sum_{\text{out}} \left(\dot{C}_{\text{out}}^{\text{ph}} + \dot{C}_{\text{out}}^{\text{ch}}\right)_k + \dot{C}_k^W \tag{3.26}$$

where $\dot{C}^{\text{ph}}$ and $\dot{C}^{\text{ch}}$ are the cost rates of physical and chemical exergy.

The further splitting of the physical and chemical exergies into their mechanical, thermal, non-reactive and reactive terms is not considered in this study, because of the lack of theory on how to apply such decomposition for hydrocarbon and hypothetical compounds.

The exergoeconomic balances for an offshore plant can therefore be expressed as:

$$\dot{C}_{\text{feed}} + \dot{C}_{\text{air}} + \dot{C}_{\text{cw}} + \dot{C}_{\text{imp}} + \dot{C}_{\text{imp}}^W = \sum_k \dot{C}_k + \dot{C}_{\text{exh}} + \dot{C}_{\text{rw}} + \dot{C}_{\text{exp}}^W \tag{3.27}$$

$$\dot{C}_{\text{feed}} + \dot{C}_{\text{UT}}^W + \dot{C}_{\text{UT,heat}}^Q = \sum_k \dot{C}_k + \dot{C}_{\text{PP,cool}}^Q \tag{3.28}$$

$$\dot{C}_{k,\text{fuel}} + \dot{C}_{\text{air}} = \dot{C}_{\text{UT,cool}}^Q + \dot{C}_{\text{UT,heat}}^Q + \dot{C}_{\text{UT}}^W + \dot{C}_{\text{exh}} \tag{3.29}$$

where each superscript and subscript correspond to the ones presented in Equation 3.7.

The introduction of the cost rate expressions is generally not sufficient for calculating all the specific costs, as there may be more than one stream (material or energy) exiting the kth component. Auxiliary equations are thus required to make the problem solvable, and they are established with regards to the purpose of operating the component under consideration.

As for an exergetic analysis, an exergoeconomic analysis deals with the concepts of fuel and product, and the cost rate balance can be rewritten as:

$$\dot{C}_{\mathrm{p},k} = \dot{C}_{\mathrm{f},k} - \dot{C}_{\mathrm{l},k} + \dot{Z}_k \tag{3.30}$$

The costing of the exergy losses is open to different interpretations. Assuming that the concept of exergy losses is only meaningful at the system level, the costs of each loss are derived from the cost rate balances and are thereby allocated to the final products.

3.8 Performance evaluation

3.8.1 Thermodynamic indicators

Energy-based indicators. There exist numerous metrics that characterise the performance of industrial processes, with regards to their energetic performance:

- the energy efficiency η, defined as the ratio of the desired product to the spent resources, in terms of energy;
- the energy intensity ι_h, defined as the ratio of the resources consumed on-site, to the energy content of the desired product;
- the energy waste ω_h, defined as the ratio of the energy content of the waste streams per unit of product;
- the specific power consumption, defined as the power consumed on-site per unit of product.

The first indicator is widely used in the power and gas industry, while the three latter are mostly used in the chemical sector.

Exergy-based indicators. Similar indicators to the energy intensity and waste parameters may be developed on an exergy basis. For instance, performance parameters related to the exergy destruction and losses [54, 76, 181, 182] were developed to illustrate the possibilities for improvement and indicate the components and sub-systems on which attention should be focused:

- the exergetic efficiency ε, which reflects how the system under study performs compared to a thermodynamically perfect one:

$$\varepsilon_k = \frac{\dot{E}_{\mathrm{p},k}}{\dot{E}_{\mathrm{f},k}} = 1 - \frac{\dot{E}_{\mathrm{d},k} + \dot{E}_{\mathrm{l},k}}{\dot{E}_{\mathrm{f},k}} \tag{3.31}$$

  The fuel and product exergies are not necessarily equal to the exergy flows entering $\dot{E}_{\mathrm{in},k}$ and leaving $\dot{E}_{\mathrm{out},k}$.

- the exergy destruction ratio y^*_{d}, which illustrates the relative importance of the kth component compared to the whole system, in terms of exergy destruction:

$$y^*_{\mathrm{d},k} = \frac{\dot{E}_{\mathrm{d},k}}{\dot{E}_{\mathrm{d}}} \tag{3.32}$$

- the exergy loss ratio y^*_{l}, which indicates the relative importance of the kth component or material stream compared to the whole system, in terms of exergy losses:

$$y^*_{\mathrm{l},k} = \frac{\dot{E}_{\mathrm{l},k}}{\dot{E}_{\mathrm{l}}} \tag{3.33}$$

- the irreversibility ratio λ, named exergy loss ratio in Kotas [54, 182] and derived from the exergetic efficiency definition proposed by Grassmann [45], which represents the fraction of the total input exergy that is destroyed through irreversibilities:

$$\lambda = \frac{\dot{I}}{\dot{E}_{\mathrm{in}}} \tag{3.34}$$

- the efficiency defect δ_k, which corresponds to the fraction of the total input exergy that is destroyed in the kth component or subsystem:

$$\delta_k = \frac{\dot{I}_k}{\dot{E}_{\mathrm{in}}} \tag{3.35}$$

The concept of *irreversibility rate*, as mentioned in Kotas [54], is strictly equivalent to the concept of *exergy destruction* used in other works in the field of exergy.

Based on the conclusions drawn from an advanced exergetic analysis, it is possible to use two alternative performance indicators, in addition to the ones used in a conventional exergy assessment:

- a modified exergetic efficiency, denoted ε^*_k, which focuses on the avoidable part of the exergy destruction within the kth component, and that allows therefore for comparing

components with different functions:

$$\varepsilon_k^* = \frac{\dot{E}_{p,k}}{\dot{E}_{f,k} - \dot{E}_{d,k}^{\mathrm{UN}}} \tag{3.36}$$

- the potential for enhancing the system performance by improving the kth component, denoted $\dot{E}_{D,k}^{\mathrm{AV},\Sigma}$, and which consists of the avoidable endogenous exergy destruction, summed to the avoidable exogenous exergy destructions in the other components, caused by the component under study:

$$\dot{E}_{d,k}^{\mathrm{AV},\Sigma} = \dot{E}_{d,k}^{\mathrm{AV,EN}} + \sum_{r=1, r\neq k}^{n} \dot{E}_{d,r}^{\mathrm{AV,EX},k} \tag{3.37}$$

3.8.2 Economic indicators

The economic aspects are assessed by calculating the investment C_{inv} and operating C_{op} costs, using the cost correlations of Turton et al. [79] for the first ones. The operating costs are related to the number of operators, the replacement and maintenance of the several components, and the taxes paid because of the emissions of carbon dioxide.

If the integration of an additional process is investigated in a retrofit situation, for instance, with the implementation of a steam cycle, the investment costs are taken to be the additional investment costs. The supplementary operating costs are neglected, assuming that there is neither an increase of the number of operators, nor a higher operator's salary.

In this specific case, the economic performance can be assessed with regards to the potential fuel gas savings and reductions in CO_2-taxes, or, in other works, with the relative increase in exported gas δ_{NG}:

$$\delta_{\mathrm{NG}} = \frac{\dot{m}_{\mathrm{NG}} - \dot{m}_{\mathrm{NG,ref}}}{\dot{m}_{\mathrm{NG,ref}}} \tag{3.38}$$

The economic value of the exported gas streams cannot be precisely estimated. For instance, for the case of the Draugen platform, which is one of the facilities investigated in this thesis, the exported gas is sent through the Åsgard pipeline system. It is mixed with natural gas from the other petroleum fields located in the northern part of the North Sea, and these flows have different chemical compositions (e.g. light- and medium-weight hydrocarbon contents) and physical properties (e.g. viscosity and heating value).

The mixed streams are then treated at the Kårstø plant, in which they are split and refined into a large variety of hydrocarbons (natural gas and liquid petroleum gases) that are exported worldwide. Calculating the economic value of a single natural gas stream is therefore difficult. The flow rates and compositions of the gas streams from the other facilities should be known, and there are high economic uncertainties on the market. On the contrary, the relative increase

of the export gas flow is a clearer and less controversial performance indicator, which depends solely on the facility under study.

For these reasons, economic indicators such as the net present value or the payback time, which combine in a single metric the capital and operating costs, are not considered in this study. They would require a precise knowledge of the economic benefits made by the platform operators for exporting additional gas, which are difficult to estimate for the reasons mentioned above, and which most likely would not be given by the companies for confidentiality reasons. The decommissioning costs have not been included in the economic evaluation, since these costs are site-specific and vary from one plant to another.

3.8.3 Environmental indicators

The environmental aspects are investigated by calculating several factors related to the emissions of pollutants during the operation (local emissions) and during the life cycle of the facility. The reduction of the local CO_2-emissions, δ_{CO_2} can be calculated as:

$$\delta_{CO_2} = \frac{\dot{m}_{CO_2} - \dot{m}_{CO_2,\text{ref}}}{\dot{m}_{CO_2,\text{ref}}} \tag{3.39}$$

Similarly, the reduction of the global warming potential effects $\delta_{I_{\text{GWP}}}$, over the life cycle of the facility, corresponds to the difference in global warming potential impact, expressed on a CO_2-equivalent basis, and it can be calculated with:

$$\delta_{I_{\text{GWP}}} = \frac{I_{\text{CO}_2-\text{eq,ref}} - I_{\text{CO}_2-\text{eq}}}{I_{\text{CO}_2-\text{eq,ref}}} \tag{3.40}$$

The acidification, eutrophication and marine water ecotoxicity impacts, denoted I_{ACD}, I_{EUT} and I_{MAETP}, and expressed on equivalent SO_2, PO_4 and 1,4-DB, are calculated as:

$$\delta_{I_{\text{ACD}}} = \frac{I_{\text{SO}_2-\text{eq,ref}} - I_{\text{SO}_2-\text{eq}}}{I_{\text{SO}_2-\text{eq,ref}}} \tag{3.41}$$

$$\delta_{I_{\text{EUT}}} = \frac{I_{\text{PO}_4-\text{eq,ref}} - I_{\text{PO}_4-\text{eq}}}{I_{\text{PO}_4-\text{eq,ref}}} \tag{3.42}$$

$$\delta_{I_{\text{MAETP}}} = \frac{I_{1,4-\text{DB}-\text{eq,ref}} - I_{1,4-\text{DB}-\text{eq}}}{I_{1,4-\text{DB}-\text{eq,ref}}} \tag{3.43}$$

In the specific case of the integration of CO_2-capture technologies, the potential for mitigating the CO_2-emissions can be evaluated with the CO_2-capture rate (CCR), defined as the ratio of the CO_2-captured to the carbon entering the power and heat generation plant with the fuel gas:

$$\text{CCR} = \frac{\dot{n}_{CO_2,\text{out}}}{\dot{n}_{C,\text{in}}} \tag{3.44}$$

3.8.4 Hybrid indicators

Exergoeconomic indicators. There exist as well exergoeconomic indicators, which take into account economic aspects when carrying out a performance analysis of a given system:

- the cost rate $\dot{C}_{\mathrm{d},k}$ associated with exergy destruction, which reveals the expenses related to the additional fuel required to cover the system imperfections:

$$\dot{C}_{\mathrm{d},k} = c_{\mathrm{f},k}\dot{E}_{\mathrm{d},k} \tag{3.45}$$

- the relative cost difference r_k:

$$r_k = \frac{c_{\mathrm{p},k} - c_{\mathrm{f},k}}{c_{\mathrm{f},k}} = \frac{1-\varepsilon_k}{\varepsilon_k} + \frac{\dot{Z}_k}{c_{\mathrm{f},k}\dot{E}_{\mathrm{p},k}} \tag{3.46}$$

- the exergoeconomic factor f_k, which illustrates the relative importance of the investment and O&M costs compared to the exergy destruction costs:

$$f_k = \frac{\dot{Z}_k}{\dot{Z}_k + c_{\mathrm{f},k}\left(\dot{E}_{\mathrm{d},k} + \dot{E}_{\mathrm{l},k}\right)} \tag{3.47}$$

Ecoenvironmental indicators. Similarly, there are eco-environmental indicators, which, by definition, consider both economic and environmental aspects. An example is the CO_2-avoidance cost (CAC), which evaluates the economic penalty of reducing the CO_2-emissions when compared to a reference plant (Figure 3.7). This penalty is evaluated in terms of production costs $\dot{C}$, which are higher when CO_2-capture is implemented ($\dot{C}_{CO_2-\mathrm{capture}}$) than in the baseline case ($\dot{C}_{\mathrm{ref}}$), because of the additional investment costs and power consumption.

$$\mathrm{CAC} = \frac{\dot{C}_{CO_2-\mathrm{capture}} - \dot{C}_{\mathrm{ref}}}{\dot{m}_{CO_2,\mathrm{ref}} - \dot{m}_{CO_2,CO_2-\mathrm{capture}}} \tag{3.48}$$

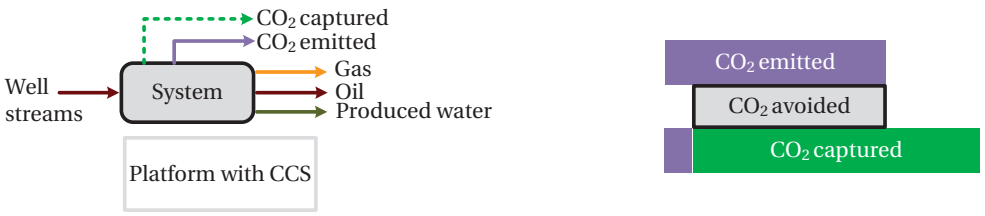

Figure 3.7: Emitted, avoided and captured CO_2.

3.9 Optimisation

3.9.1 Multi-objective optimisations

A multi-objective optimisation (MOO) problem belongs to the area of mathematical programming where several objective functions should be optimised simultaneously, and an example of such problems is the minimisation of the total costs of a combined cycle against the maximisation of its thermodynamic efficiency. An increase of the investment costs results in a more performant system, meaning that these objectives are conflicting. There is no single solution that leads to an optimum for both objectives, and there exists a possibly infinite set of Pareto-optimal solutions. A solution is called Pareto-optimal if a better-off with respect to one objective results in a worse-off with respect to another one. The list of these solutions can be displayed in the form of a Pareto-optimal frontier (Figure 3.8) [202].

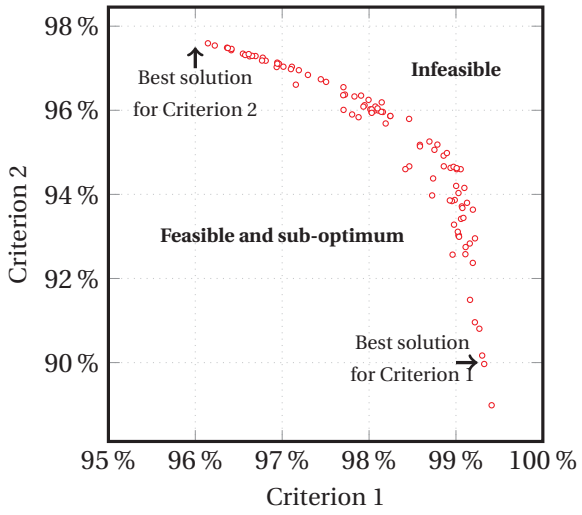

Figure 3.8: Example of Pareto-optimal frontier.

3.9.2 Evolutionary algorithms

Evolutionary algorithms (EAs) have been widely used for solving multi-objective optimisation problems: they are preferred compared to standard conventional algorithms, because several elements can be generated in a single run. They are also more suitable for solving problems in which the parameters and objective functions are non-linear, non-continuous, and non-modal [203]. Heuristics of genetic algorithms are mainly based on the process of natural selection. By analogy, a solution represents a given individual in a population, and a new generation of individuals is used in the next algorithm iteration. Each solution is produced from at least a pair of parent solutions and shares some of their characteristics. The first set of individual solutions is generated randomly to cover the solution domain and the new generation of candidate solutions is produced from some of the previous ones.

3.9.3 Objective functions

The performance of petroleum systems can be evaluated with regards to thermodynamic, economic, environmental and hybrid indicators, as the ones listed in the previous section. The thermodynamic indicators are sensitive to the system efficiency on itself, and to the power and heating demands, and their values are mainly impacted by the field (natural) and operating (process) conditions. The economic indicators depend on the costs of the technologies that are implemented, and the environmental indicators are related to the *local* emissions and *global* ones, i.e. the ones taking place over the system life cycle.

The selection of appropriate objective functions should be evaluated carefully. For instance, for a system where only power and no heat are required, minimising the power demand and minimising the exergy consumption are strictly equivalent, whilst, for a system where both power and heat are needed, choosing the minimisation of the energy use or of the exergy consumption as objective function may return different sets of Pareto-optimal solutions.

Two approaches can be applied when using economic and environmental indicators for formulating the objective functions. The first one is an *absolute* approach, which consists of considering the total economic costs and environmental impacts. For instance, when designing a new system, attention should be paid both to the capital and fuel-related costs to evaluate its economic viability. The second one is an *incremental* approach, which takes into account only the additional costs, benefits or penalties. For example, when retrofitting an existing system, one may consider that the capital investments of the equipments already installed on-site represent *sunk* costs, and the optimisation may focus on minimising the additional costs only.

3.9.4 Decision variables

The decision variables are the numerical quantities for which values should be chosen in the optimisation problem, implying that each has a certain impact on the values of the objective functions. The degrees of association between the decision variables and optimisation objectives can be statistically characterised by the Pearson's linear correlation coefficients ρ. They measure the influence of a decision variable on a given objective: 1 denotes a positive correlation, 0 the absence of a correlation, and -1 a negative correlation. The Pearson's partial linear correlation coefficients measure the influence of a given decision variable on each objective when the effects of all other decision variables are removed, i.e. when all other decision variables are fixed [204, 205].

The dispersion of the optimal values of the decision variables, in relation to a particular objective, can be assessed by plotting an histogram of the number of observations in the Pareto set. The bar lengths are proportional to the number of points on the Pareto frontier for a subinterval of the decision variable, and the colour shadings are related to the ranking of a given Pareto point, with respect to the objective of interest.

3.10 Conclusion

The present thesis builds on a large variety of modelling, analysis and optimisation tools: it uses commercial flow-sheeting software together with a Matlab-based platform, which gives the possibility to connect models developed on different software, while making a common and systematic analysis. Process integration, exergy, economic and life cycle assessment models are included in this framework, and this allows for analysing directly the performance of different oil and gas platforms under various sets of operating conditions. The use of multi-objective optimisation techniques based on a genetic algorithm allows for identifying the trade-off between different objectives and provides guidelines for targeting promising energy efficiency improvements.

4 Generic platform

This chapter presents a generic system analysis of oil and gas platforms, with a particular focus on the facilities located in the North Sea region. The present work builds on models developed from an extensive literature study and general performance trends are shown. Most results are presented in Nguyen et al. [206].

4.1 Introduction

Offshore platforms are usually designed for the peak production of a petroleum field: the on-site processes suffer from changes in production flows and operating conditions over time. They become inevitably less performant, besides the normal process of efficiency reduction due to ageing. A few research studies pinpointed the interest of conducting thermodynamic-based methods such as exergy analyses to depict the inefficiencies of such systems.

de Oliveira Jr. and Van Hombeeck [59] carried out an exergy analysis of a Brazilian petroleum plant, and they showed that the most exergy-consuming process was the petroleum heating step. Voldsund et al. [172] used a similar approach for a Norwegian facility and demonstrated that the largest exergy destruction took place in the gas compression processes.

These studies focus on specific facilities, making an extension of their results difficult. They do not consider both the processing and utility plants, nor investigate the effects of different reservoir fluid compositions. In this context, the objective of this work is to derive generic conclusions on the performance of oil and gas platforms. Three main steps were followed:

(1) development and validation of a generic model of North Sea oil and gas offshore platforms to generate realistic and reliable production profiles;

(2) simulation of various operating conditions and well-fluid flows to investigate the overall system behaviour and evaluate the material and energy flows;

(3) analysis of the energy use patterns with variations of the reservoir fluid composition.

4.2 Generic case

Variations and differences across oil and gas platforms may be related to:

- reservoir characteristics (e.g. temperature and pressure, gas-to-oil (GOR) and water-to-oil (WOR) ratios);
- reservoir fluid properties (e.g. chemical composition, thermophysical properties, critical point);
- technical requirements (e.g. crude oil content of gas and water, export temperature and pressure);
- technological choices (e.g. number of trains, gas export, gas lift, system consideration).

However, the conceptual design of these offshore facilities stays similar: although design differences exist from one platform to another, gas purification and exportation, wastewater treatment and seawater injection are the most common gas and water processing technologies in the North Sea region. Moreover, as North Sea crude oil and natural gas have a low content of carbon dioxide, hydrogen sulphide and salt, neither desalting nor sweetening units are necessary on-site. There are a few exceptions, with some platforms on which advanced gas and condensate processing is integrated.

The model of the generic offshore platform developed within this study builds on the studies of Bothamley [11] and on data from the Danish Energy Agency [12] and the Norwegian Ministry of Petroleum and Energy [13]. It was built based on the system configurations presented in the open literature, such as the works of Manning and Thompson [15], Lyons and Plisga [16], Abdel-Aal et al. [17] and Jones and Pujadó [14]. The validity of this generic model has also been verified by a further comparison with real-case oil and gas facilities present in the North Sea region, such as the ones presented in the rest of this thesis. The HVAC system and the connected utilities are not considered (Figure 4.1 and Figure 4.2), because they may differ significantly from one platform to another. Gas lift and injection were not considered within this study.

The approach of this work assumes an oil and gas processing plant designed for each simulation case investigated, as one of the goals of this study is to provide a basis for comparison between various reservoir fluid compositions. The effects of processing heavy, volatile, and near-critical oils are compared based on the same design set-up, which is a reasonable assumption as the overall process scheme is similar.

The off-design behaviour of the processing plant was not investigated because it is assumed that this part of the platform is designed independently for each feed, whereas the part-load behaviour of the gas turbines was considered. The design conditions for each component and sub-system modelled in this work are presented further (Table 4.1).

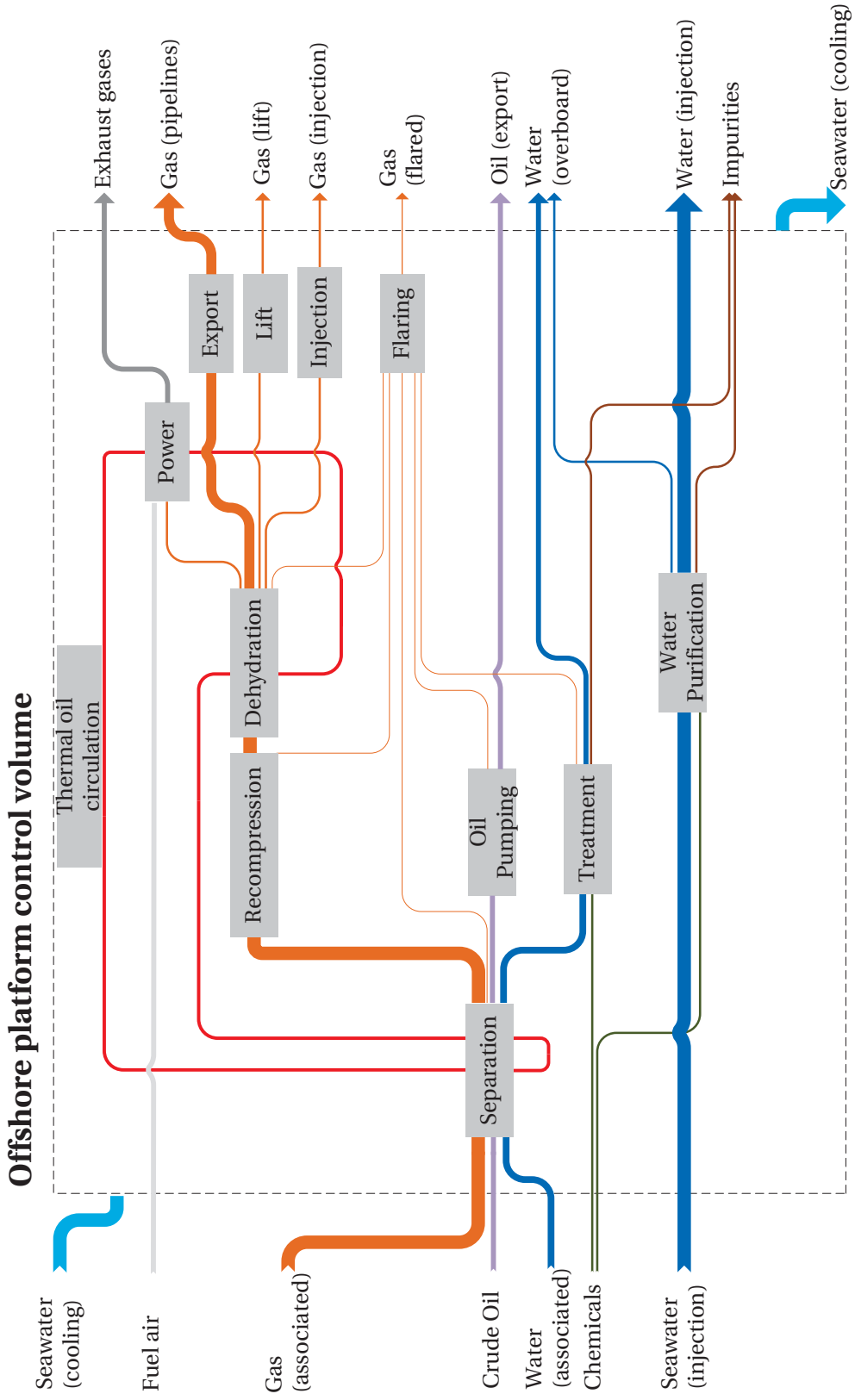

Figure 4.1: Conceptual layout of processes on North Sea oil and gas platforms.

4.3 Modelling and simulation

4.3.1 Fluid modelling

In this study, crude oil was modelled as a mixture of 83 chemical compounds: CO_2, H_2O, O_2, N_2, Ar, H_2S, 47 hydrocarbons and 29 pseudo-components. It had the following bulk properties: an American Petroleum Institute (API) gravity of 39.9, a specific gravity of 0.826, a density of 825.5 kg/m^3 and a content of light hydrocarbons of 27.2 vol %. It was assumed that it is extracted along with associated free gas, with this molar composition: 4.37 % N_2, 1.34 % CO_2, 75.7 % CH_4, 7.22 % C_2H_6, 6.70 % C_3H_8, 3.89 % n-C_4H_{10} and 3.70 % n-C_5H_{12}. The properties of the gas and oil streams were derived from the composition of the feed streams on the Draugen platform as start guesses.

Standard air, with a molar composition of 77.29 % N_2, 20.75 % O_2, 1.01 % H_2O, 0.92 % Ar and 0.03 % CO_2, and standard seawater, with a molar concentration, in mol/L, of 0.002 HCO_3^-, 0.525 Cl^-, 0.024 SO_4^{2-}, 0.045 Mg^{2+}, 0.013 Ca^{2+}, 0.450 Na^+ and 0.01 K^+, were considered. The reservoir fluid compositions are presented further in this work (Table 4.2).

4.3.2 System modelling

Processing plant model

The reservoir fluid is transferred to the platform complex via a network of pipelines and a system of production manifolds. The individual streams pass through choke boxes, are mixed and depressurised before entering the separation section.

Oil, gas and water are separated by gravity in three stages. Since low pressures and high temperatures ease the separation of these three phases, the pressure of the well-fluid is decreased by throttling valves and its temperature is increased by preheating with a heat medium at the inlet of each stage.

The two first stages consist of three-phase separators, the third one consists of a two-phase separator and an electrostatic coalescer. It was assumed that the gravity separators are continuously operated, that physical equilibrium is reached and that no solids are entrained in the gas vapour phase. The power needed to sustain the electric field in the coalescer is ignored, because its contribution to the total power consumption is negligible.

The oil from the separation train enters the export pumping system, after having been mixed with oil and condensate that is removed in other parts of the processing plant. It is then pumped and exported ashore. The recovered gas is recompressed to the pressure of the previous separation stage after scrubbing and cooling. Wet gas enters at the bottom of a packed contactor, in which water is captured by physical absorption with liquid tri-ethylene glycol (TEG).

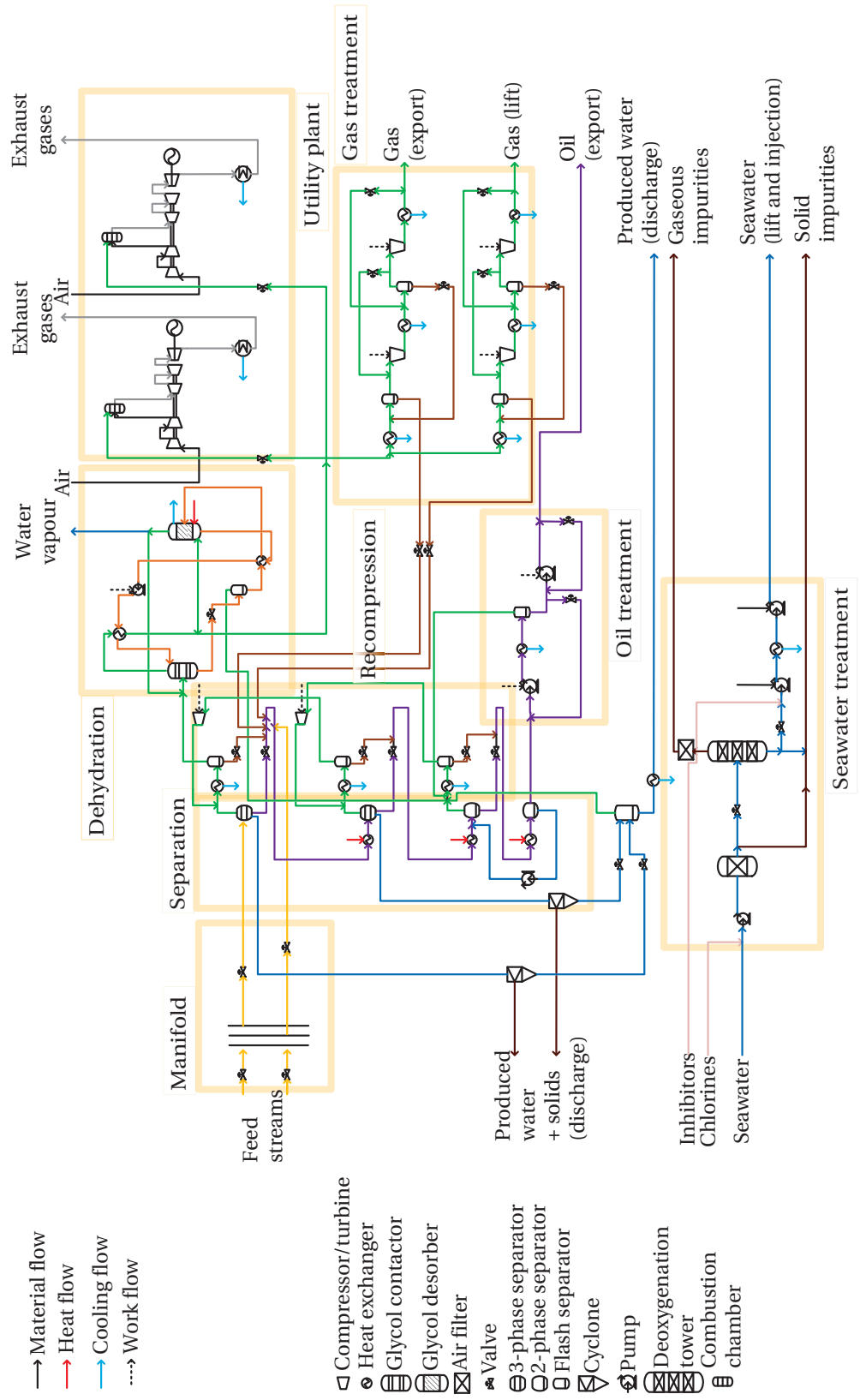

Figure 4.2: Simplified flow diagram of the offshore platform model.

Most dry gas is sent to the compression train for storage and export to the shore. A certain fraction of the dry gas is usually recycled to control the volume of gas entering the compressors and to prevent surge issues. The remaining gas that is not processed is used for power generation directly on-site. It is expanded through a succession of valves and combusted with air in gas turbine engines.

The water from the separation and purification trains, also denoted produced water, enters hydrocyclones in which suspended particulates and dissolved hydrocarbons are removed before disposal to the sea. In parallel with the oil and gas processing, seawater is treated on the platform for further injection into the reservoir, in order to sustain high pressure conditions and to enhance oil production.

Utility plant model

In this study, the utility system was modelled as two twin-spool gas turbines complemented by power turbines sharing equally the electrical power supply. They are based on the performance characteristics of the SGT-500 engines developed by SIEMENS [207], which are claimed to be highly suitable for offshore and marine applications.

The waste heat from the exhaust gases is partly used to increase the temperature of a heating medium, such as glycol-water or hot oils, and the remaining is released to the atmosphere via the stack. The heating medium circulates in a closed-loop system and provides the heat required on the platform.

4.3.3 System simulation

Simulation basis

The assumptions and parameters are based on the compilation of various data from literature [12, 14–16, 19, 30, 129, 208] (Table 4.1).

Case studies

Six cases were investigated within this study, corresponding to the same processes and operating conditions – but with different reservoir fluid compositions and loads (Table 4.2). As emphasised by Svalheim and King [19], production flows are strongly time-dependent: it is thus unlikely to find, for one platform, six distinct situations with sensibly similar flow rates and sensibly different gas-to-oil (GOR) and water-to-oil (WOR) ratios.

In practice, the operating pressures and temperatures of the separation train are adapted to the reservoir fluid composition. Each simulation case was defined on the same well-fluid molar flow rate, fixed at 18,450 kmol/hr, as well as identical design conditions (Table 4.1).

Table 4.1: Process design assumptions.

Reservoir fluid	71 °C and 16.5 MPa
Production manifold	Pressure levels: 12 MPa and 7 MPa
Separation train	Pressure levels: 7 MPa, 2.9 MPa, 0.72 MPa and 0.18 MPa Temperature levels: feed temperature (1st stage), 65 and 85 °C (others) Pressure drops: 0.5-0.3-0.05 bar (3-phase separators), 0.05-0.02 bar (mixers), 0.25-0.1-0.025 bar (heat exchangers), 0.5-0.3-0.05 bar (flash separators)
Crude oil/glycol heat exchangers	Temperature increase (cold side): 5 K, ΔT_{min} = 10 K
Compression train	Intermediate pressure level: 11.4 MPa Recycling: 75 m^3/hr
Gas/seawater heat exchangers	Temperature outlet (hot side): 30-20 °C, ΔT_{min} = 10 K
Centrifugal compressors	η_{is} = 63-67 %, η_{mec} = 93 % (recompression train), η_{is} = 65 %, η_{mec} = 95 % (compression train)
Centrifugal oil pumps	η_{pp} = 62 %, η_{dr} = 98 % (export train)
Centrifugal water pumps	η_{pp} = 81 %, η_{dr} = 98 % (injection train)
Produced water/seawater heat exchangers	Temperature outlet (hot side) = 25 °C, ΔT_{min} = 10 K
Skim vessel/degasser	Operating pressure: 1.2 bar
Glycol contactor	Packed column, operating pressure: 7 MPa
Glycol regenerator	1.2 bar, 5 stages, kettle reboiler: 204.4 °C, overhead condenser: 98.5 °C
Glycol/glycol heat exchangers	Pressure drops: 0.2-0.025 bar
Waste-heat recovery system	Temperature outlet (cold side): 210-220 °C
Seawater injection	Standard volume flow rate: 1300 Sm^3/h
Seawater quality	Oxygen level: 10 ppb, solids content: 5 ppm
Cooling water	Standard volume flow rate: 2400 Sm^3/h
Flaring-to-fuel gas ratio	12.4 %vol [12]
Export and injection pressures	12.5 MPa (seawater), 14.5 MPa (oil) and 18.5 MPa (gas)

Case 1, referred as the baseline case in the rest of this study, was intended to represent a reservoir fluid containing oil, associated free gas and water with a cut of 15 % on a molar basis. Gas- and water-to-oil ratios were chosen based on the production data of different oil platforms operating in the North Sea region in order to simulate a volatile oil. Case 2 and Case 3 differ from Case 1 by the content of water, which was increased by 10 mol % points and decreased by 5 mol % points, respectively.

Cases 4, 5 and 6 were intended to represent three different types of oils, respectively black, near-critical (NC) and condensate, which differ in their content of heavy hydrocarbons [30]. Black oil has a low API gravity, a large fraction of heavy hydrocarbons, and a relatively low content of methane, whereas near-critical and condensate oils are characterised by a high API gravity (≥ 40 °) and light hydrocarbons content. The latter are generally located at greater depths, which results in higher reservoir pressures [30]. These differences in physical properties across petroleum reservoirs were not considered in the process modelling.

Table 4.2: Simulation specifications – reservoir fluid properties.

	Case 1	Case 2	Case 3	Case 4	Case 5	Case 6
Flow						
$\dot{m}$ [t/h]	738	757	963	1783	649	543
$\dot{V}$ [m^3/h]	2044	1750	2153	2567	2093	2147
Mole fraction [%]						
y_{CH_4}	49.2	42.9	49.0	29.5	59.0	62.2
$y_{C_2H_6}$	4.70	4.10	6.30	3.60	6.72	6.64
$y_{C_3H_8}$	4.70	4.10	4.03	2.00	3.82	3.18
$y_{n-C_4H_{10}}$	3.40	3.00	3.53	3.90	3.09	2.26
$y_{n-C_5H_{12}}$	1.40	1.20	2.35	3.30	2.21	1.52
$y_{n-C_6H_{14}}$	0.60	0.50	2.36	2.80	1.55	1.12
y_{CO_2}	0.90	0.80	0.02	0.02	1.11	0.26
y_{N_2}	2.80	2.50	1.55	0.30	0.47	2.01
$y_{C_{7+}}$	12.3	10.7	15.9	39.6	7.01	5.81
y_{H_2O}	20.0	30.2	15.0	15.0	15.0	15.0
Exergy						
$\bar{e}^{\text{ch}}$ [GJ/kmol]	1.88	1.64	2.31	4.32	1.54	1.37
$\bar{e}^{\text{ph}}$ [MJ/kmol]	7.87	6.90	7.81	6.26	8.66	9.04
$\dot{E}$ [GW]	9.62	8.40	11.9	22.2	7.91	7.04

4.4 Performance evaluation

4.4.1 Simulations

Baseline cases

The offshore platform model was used to investigate the six case studies in order to obtain the net oil, gas and water production flows (Table 4.3) and the electrical energy demand of each module (Figure 4.3). The power consumption of the offshore platform ranges from 22.6 to 31.1 MW and the maximum value is obtained with black oil as input (Case 4), as the power demand of the oil pumping section increases sharply. Results indicate that the major electricity consumer is generally the compression train, which is responsible for 42 % to 56 % of the total power demand in the remaining cases.

The seawater injection process ranks second with a share of 17 % to 23 % and a power demand of about 5.3 MW. Seawater pumped to a pressure of 12.5 MPa for further injection into the reservoir is not extracted through the oil and natural gas wells and does not enter the separation train. As the water purification and injection processes are not integrated within the other on-site systems, crude oil, produced oil, gas and water do not flow through this section of the platform. The electrical energy demand of this process is therefore independent of the composition and flow rate of the reservoir fluid. It depends exclusively on the flow rate of the seawater required for pressure maintenance and on the pressure level requirements.

Table 4.3: Net oil, gas and water production flow rates of the offshore platform system.

	Case 1	Case 2	Case 3	Case 4	Case 5	Case 6
Oil (export)						
Molar [Mmol/h]	3.2	3.0	4.5	9.9	2.3	1.7
Volume [Sm^3/h]	614	548	843	1962	407	316
Mass [t/h]	508	451	686	1628	325	255
Gas (export)						
Molar [Mmol/h]	11.1	9.7	10.8	5.9	12.9	13.6
Volume [kSm^3/h]	262	228	255	139	305	319
Mass [t/h]	234	203	223	118	267	273
Produced water						
Molar [Mmol/h]	3.4	4.7	2.1	1.7	2.3	2.3
Volume [Sm^3/h]	60.9	85.2	38.0	30.2	41.4	41.6
Mass [t/h]	61.0	85.3	38.0	30.2	41.5	41.6

The third greatest power demand of the offshore facility is either the gas recompression process or the oil pumping, depending on the amount of gas extracted along with oil. The power consumption of these compressors is smaller in the cases with a high gas-to-oil ratio (Cases 5 and 6). This suggests that most associated gas, rich in light hydrocarbons such as methane and ethane, exits the separation train at the first stage and bypasses the booster compressors, and this situation may be expected for all types of oil.

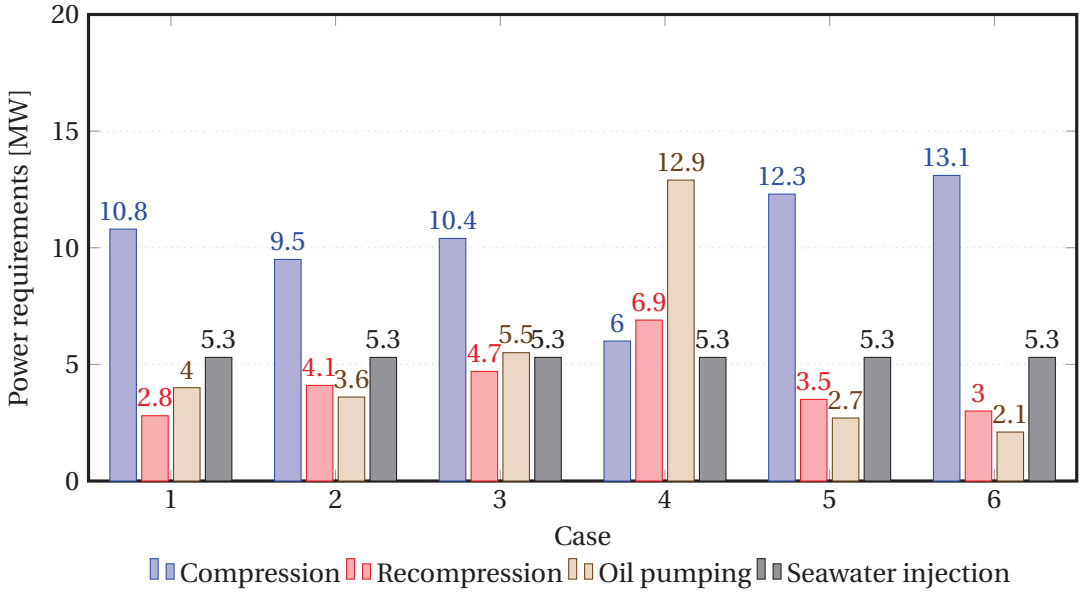

Figure 4.3: Power consumption (values in MW) of the generic offshore platform for the six simulation cases.

Case 4 is characterised by a different power consumption profile: the oil pumping section has the greatest demand, accounting for about 41 % of the total plant consumption. The results suggest that the additional power needed to pump the surplus of oil overcomes the decrease of power required in the gas compression section. The duty of the recompression train also increases in this specific case, because hydrocarbons of intermediate molecular weight (e.g. butane, pentanes and hexanes) are not flashed at the first separation stage but at the second and third ones. This results in larger recycle flows between the separation and recompression modules and thus in a significant increase of the power and cooling demands.

In contrast, a greater water fraction has a negative feedback on the electrical energy demand of the processing plant, since water is directly removed in the three-phase separators and only small amounts are carried through the plant. The effect of a higher water fraction in the wet gas leaving the recompression train is limited: the power demand of the dehydration process slightly increases because of the larger glycol flow in the absorption-desorption loop to reduce the water content of gas to the required specification.

Sensitivity

Operating parameters, such as gas and oil export pressures, seawater injection flow rate, and pressure differ from one platform to another, depending on the physical properties of the oil field and on the pipeline network requirements. Moreover, different technological choices such as the selection of the gas compressors (e.g. centrifugal, radial or axial, depending on the volume flow and pressure ratio per stage) and of the oil pumps (e.g. centrifugal or positive displacement) apply.

The effects of these different characteristics were investigated in a parametric study based on the values discussed in de Oliveira Jr. and Van Hombeeck [59], Voldsund et al. [117, 132], Ingeniøren/bøger [209] and Sulzer Pumps [210]. The pump efficiency, η_{pp}, was varied between 55 % and 78 % and the isentropic efficiency of the compressors, η_{is}, between 63 % and 80 %.

The results suggest that the total power demand is mostly sensitive to the efficiency of the gas compressors in the compression train. The power demand between a state-of-the-art centrifugal compressor and a poorly designed one, or operated at part-load, can vary from 3 to 9 MW. This difference is significant in all cases but is particularly marked in Case 5 and Case 6, where near-critical and condensate oils are processed.

The variations in power demand with the efficiencies of the oil pumps are comparatively small, with the exception of the black oil case where the electrical power demand of the export train is much more significant. Similar, but smaller, trends are found with the variations of efficiencies of the gas recompressors.

However, the compression and pumping power demands reveal to be particularly sensitive to the anti-surge recycling fraction, since gas and liquid flows are expanded to a lower pressure, and are then re-entering the turbomachinery components.

4.4.2 Exergy analysis

Exergy flows

The results of the combined process simulations and exergy accountings (Table 4.4) indicate that the produced water and exhaust gases from the power generation system have a small specific exergy content. Operations such as compression and pumping, which aim at increasing the physical exergy of the gas and oil flows, have a minor impact on the total specific exergy of these streams. The input and output exergies of the offshore platform system are dominated by the chemical exergy content of the oil and gas streams, which ranges from 43 to 48 MJ/kg and is at least 100 times as great as their physical exergy (Table 4.2). Most of the exergy found at the outlet of the offshore platform system is thus carried by these two streams, independently of the case considered.

Exergy destruction, losses and efficiencies

The total destroyed exergy on the overall offshore platform, i.e. including both the processing and the utility plant, is between 68 and 84 MW, with 62-65 % of this being attributable to the gas turbines and waste heat recovery and 35-38 % to the oil, gas and seawater processing plant (Table 4.5).

The largest exergy destruction of the *complete* system lies, in *all cases*, in the combustion chambers of the gas turbines and amounts to almost 50 % of the total exergy destruction of the platform. It can be split into thermodynamic irreversibilities due to mixing of natural gas and compressed air and to the combustion process by itself. This exergetic analysis demonstrates that the variability of the well-fluid composition has a moderate effect on this result, but, on the other hand, has a significant impact on the share of exergy destruction across the processing plant.

The total exergy destruction of the processing plant exclusively is between 24 and 32 MW. The maximum exergy destruction is found in Case 4 (31.6 MW), which is characterised by a crude oil poor in light hydrocarbons, while the minimum is found in Case 6 (23.9 MW), featured by a crude oil with a high gas content. A comparison of the specific exergy destruction per unit of mass, actual volume and exergy input is presented further (Table 4.6).

The results also indicate that the largest thermodynamic irreversibilities of the processing plant occur in the production manifold and in the gas compression systems, followed by the recompression and separation modules (Figure 4.4).

In contrast, the contributions from the wastewater treatment and the seawater injection processes are negligible, and the exergy destruction taking place in the oil pumping step is moderate in most cases. The latter is significant only when black crude oil enters the platform (Case 4) because of the higher content of heavy hydrocarbons and larger oil flow at the inlet of the export pumping section.

Stream number (type)	Case 1		Case 2		Case 3		Case 4		Case 5		Case 6	
	$\dot{n}$	$\bar{e}$	$\dot{n}$	$\bar{e}$	$\dot{n}$	$\bar{e}$	$\dot{n}$	$\bar{e}$	$\dot{n}$	$\bar{e}$	$\dot{n}$	$\bar{e}$
1 (Reservoir fluid)	18.5	1.88	18.5	1.64	18.5	2.31	18.5	4.32	18.5	1.54	18.5	1.37
2 (Reservoir fluid)	18.5	1.87	18.5	1.63	18.5	2.30	18.5	4.31	18.5	1.53	18.5	1.36
3 (Separated oil)	3.7	6.42	3.2	6.48	4.8	6.52	10.2	7.18	2.5	6.07	1.8	6.36
4 (Pumped oil)	3.2	7.17	3.0	6.77	4.5	6.80	9.9	7.37	2.3	6.40	1.7	6.63
5 (Recompressed gas)	11.7	0.96	11.6	0.96	11.9	1.04	6.4	0.99	13.6	1.00	14.9	1.02
6 (Dry gas)	11.4	0.97	9.9	0.97	11.0	1.00	6.1	1.00	13.1	1.00	13.8	0.98
7 (Compressed gas)	11.1	0.99	9.7	0.99	10.8	1.02	5.9	1.02	12.9	1.02	13.6	1.00
8 (Fuel gas)	0.18	0.97	0.17	0.97	0.19	1.00	0.22	1.00	0.18	1.00	0.18	0.98
9 (Produced water)	3.4	≥ 0.001	4.7	≥ 0.001	2.1	≥ 0.001	1.7	≥ 0.001	2.3	≥ 0.001	2.3	≥ 0.001
10 (Injected water)	71.1	≥ 0.003	71.1	≥ 0.003	71.1	≥ 0.003	71.1	≥ 0.003	71.1	≥ 0.003	71.1	≥ 0.003
11 (Air)	20.5	≥ 0.001	20.3	≥ 0.001	21.4	≥ 0.001	22.8	≥ 0.001	20.9	≥ 0.001	20.7	≥ 0.001
12 (Exhaust gases)	20.5	0.003	20.4	0.003	21.4	0.003	22.9	0.004	21.0	0.003	20.8	0.003
Flared and vented gases	0.02	0.96	0.02	0.96	0.02	0.99	0.03	0.99	0.02	0.99	0.02	0.97

Table 4.4: Flow rates and associated specific exergies (values in Mmol/h and GJ/kmol, respectively) – stream numbers refer to Figure 4.2.

Table 4.5: Exergy destruction and losses (MW) of the generic offshore platform.

Sub-system, component	Case 1	Case 2	Case 3	Case 4	Case 5	Case 6
Production manifold	6.01	5.25	6.10	6.07	6.32	6.75
Separation	3.49	3.60	4.36	8.41	2.37	1.82
Heaters	0.85	0.73	1.16	2.32	0.63	0.47
Throttles	1.87	1.62	2.56	5.40	1.19	0.92
Mixers & others	0.77	1.25	0.64	0.69	0.55	0.43
Recompression	2.88	4.85	3.54	3.32	3.61	3.30
Coolers	1.92	3.00	1.80	1.23	2.10	2.07
Throttles	0.15	0.20	0.13	0.07	0.18	0.11
Compressors	0.62	0.82	1.04	1.58	0.74	0.60
Mixers & others	0.19	0.82	0.57	0.44	0.58	0.52
Glycol dehydration	3.18	3.23	2.75	1.76	3.24	3.68
Fuel gas and flaring	1.23	1.39	1.48	1.42	1.52	1.53
Gas compression	4.78	4.20	4.62	2.61	5.48	5.80
Coolers	1.57	1.35	1.50	0.69	1.86	1.95
Compressors	2.92	2.57	2.83	1.63	3.33	3.56
Mixers	0.02	0.02	0.02	0.02	0.02	0.02
Throttles	0.27	0.27	0.27	0.27	0.27	0.27
Oil pumping	2.29	2.29	2.94	7.69	1.06	1.12
Pumps	1.14	1.02	1.60	3.64	0.73	0.60
Coolers	1.03	1.27	1.34	4.05	0.33	0.52
Throttles & others	0.12	0.10	0.12	0.21	0.07	0.05
Wastewater treatment	0.11	0.20	0.07	0.06	0.07	0.07
Seawater injection	0.23	0.23	0.23	0.23	0.23	0.23
Processing plant	24.2	25.2	26.1	31.6	23.9	24.3
Power generation	40.8	40.2	43.4	47.8	41.5	41.3
Compressors	2.87	2.82	3.12	3.61	2.92	2.92
Turbines	4.55	4.51	4.74	5.00	4.59	4.59
Combustion chamber	33.0	32.6	35.1	38.7	33.4	33.2
Others	0.40	0.40	0.43	0.47	0.41	0.41
Heat carrier circulation	3.41	3.37	3.55	3.79	3.43	3.42
Utility plant	44.2	43.6	47.0	51.6	44.9	44.7
Platform destruction	68.4	68.8	73.1	83.2	68.8	69.0
Exhaust gases	18.5	18.3	20.4	23.4	19.1	18.9
Cooling water	2.46	2.81	2.80	5.17	2.21	2.09
Flared gases	10.5	10.4	11.4	13.0	10.8	10.7
Wastewater	0.85	1.21	0.33	0.28	0.36	0.37
Platform losses	32.3	32.7	34.9	41.9	32.5	32.1
Platform destruction and losses	100.7	101.5	108.0	125.1	101.3	101.1

The exergy destruction within the production manifold is caused by the well-fluid depressurisation from 16.5 to 7 MPa without any conversion of physical and potential exergies into any other form. The second greatest irreversibilities are found at the gas compression section: they are mainly due to the poor performances of the gas compressors and to the recycling around these components to prevent surging. Significant exergy destruction also takes place in the recompression step, because the streams flowing out of the separation train are mixed at different temperatures and compositions before scrubbing and throttling.

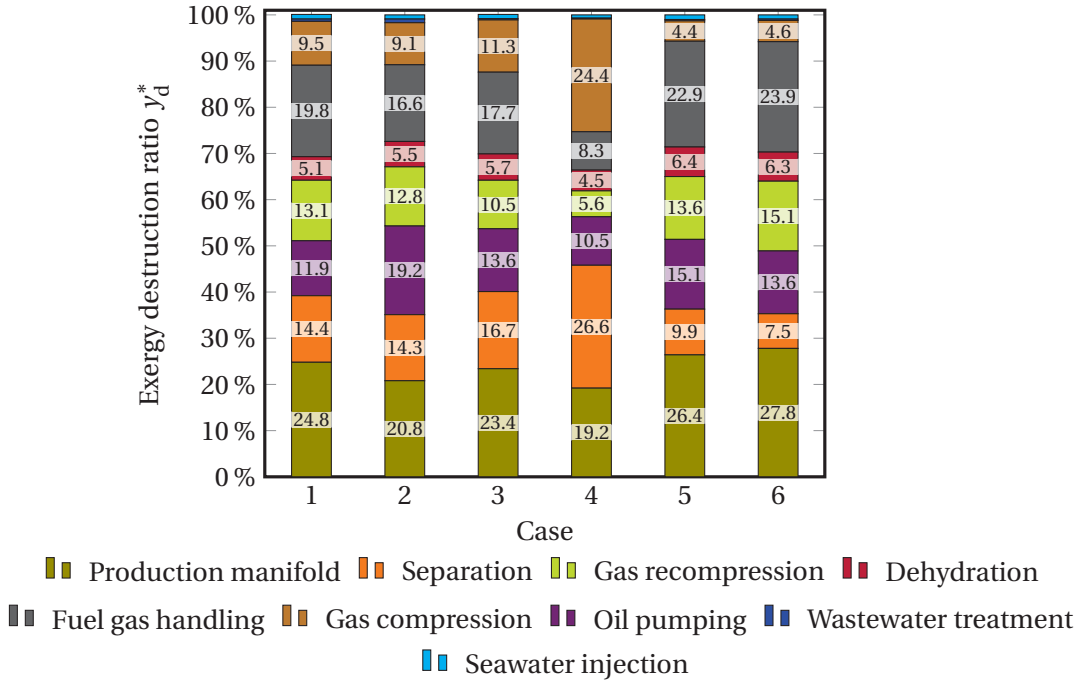

Figure 4.4: Exergy destruction ratio of the generic offshore platform (excl. utility system) y_d^*.

The exergy losses of the offshore platform are nearly constant in all cases: they are related to effluent streams rejected into the environment without being valorised, such as flared gases, discharged seawater, wastewater and exhaust gases from the gas turbine systems. The exact values depend on the choice of the reference environment (e.g. humidity level).

Approximatively 60 % of the total exergy losses are due to the direct rejection of high-temperature exhaust gases to the environment, while about 30 % are associated with the flaring and ventilation of natural gas throughout its processing. The remaining 10 % are related to the exergy content of cooling and wastewater discharged overboard: these exergy losses are comparatively small, as the discharged streams are rejected at nearly environmental conditions (Figure 4.5). The exergy losses associated with exhaust gases are higher in Case 3 and Case 4, as the mass flow rate of exhaust gases increases with the power demand of the processing plant.

A comparison based on the irreversibility ratio λ suggests that the offshore processing becomes

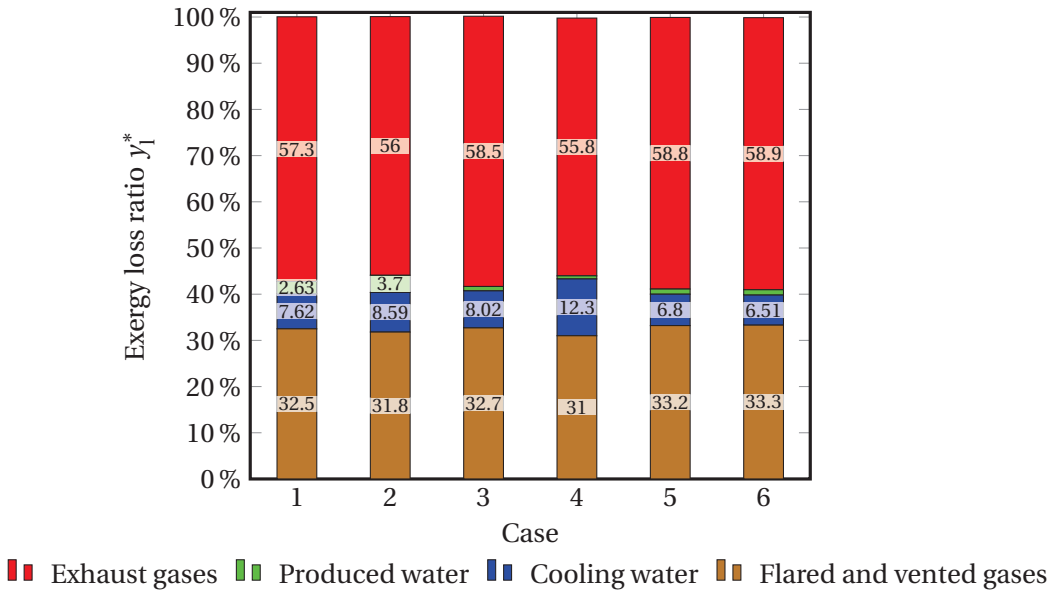

Figure 4.5: Exergy loss ratio of the generic offshore platform y_1^*.

less performant with increasing gas-to-oil and water-to-oil ratios (Table 4.6). It also indicates that the total exergy destruction and losses within the offshore platform represent only 0.5-1.5 % of the total exergy flowing into the system. These values of the irreversibility ratio may be expected not only for North Sea platforms, and can be generalised to all types of petroleum facilities, since hydrocarbons are flowing throughout the whole system in all cases.

In the baseline case, the gas turbine system, the gas compression and the oil pumping processes have a low exergetic efficiency, of about 27 %, 42 % and 37 % respectively, as a result of large thermodynamic irreversibilities associated with chemical reaction and heat transfer in the first process, and with mixing and friction in the second and third ones. No meaningful exergetic efficiency could be defined for the production manifold and the gas flaring modules. They mainly consist of arrangements of mixers and throttling valves, which are dissipative by design: they destroy exergy without generating any useful product. Alternatively, as the exergetic product is null, it may be argued that the exergetic efficiency is 0. This reasoning may not be valid for throttling valves operating across the ambient temperature.

This exergetic analysis shows that exergy is introduced on-site in the form of raw materials (crude oil, fuel air, seawater and chemicals) and exits in the form of valuable products (oil and gas sent onshore) and waste streams (produced water, exhaust and flare gases) (Figure 4.6). The chemical exergy of the reservoir fluid flows through the offshore platform system and is separated into the oil and gas chemical exergies with only minor destruction in the processing plant, as no chemical reactions take place. On the contrary, chemical exergy is consumed to a great extent in the utility plant, as a fraction of the produced natural gas is used and combusted in the gas turbines.

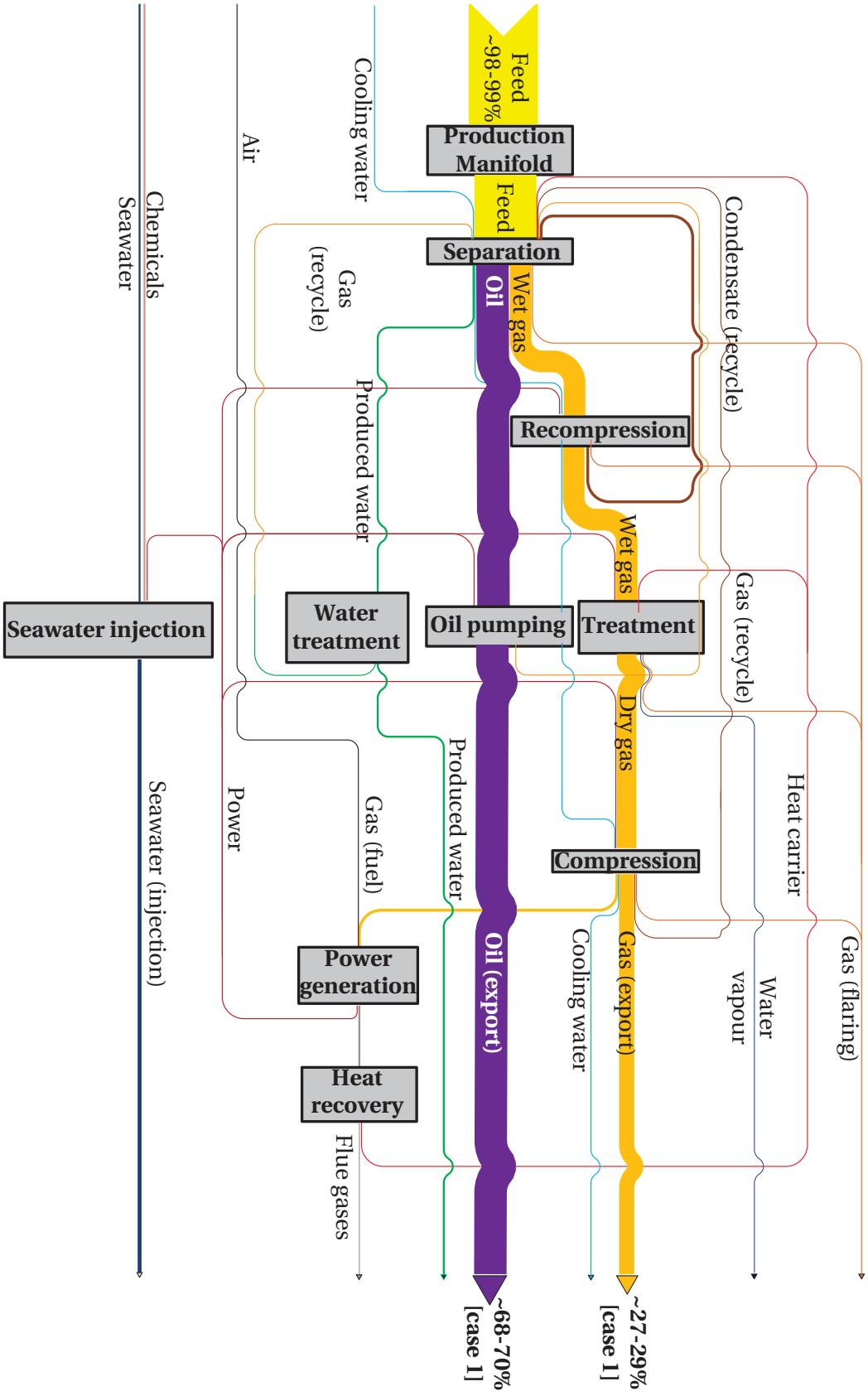

Figure 4.6: Grassmann diagram of the offshore platform system.

Table 4.6: Specific exergy destruction, losses and irreversibility ratios.

Irreversibilities	Case 1	Case 2	Case 3	Case 4	Case 5	Case 6
$\dot{E}_d$ [MW]	68	69	73	83	69	69
e_d [MJ/t_{rf}]	334	327	273	168	382	457
e_d [MJ/m^3_{rf}]	120	142	122	117	118	116
$\dot{E}_l$ [MW]	32	33	35	42	33	32
e_l [MJ/t_{rf}]	158	156	130	85	180	213
e_l [MJ/m^3_{rf}]	57	67	58	59	56	54
Total [MW]	101	102	108	125	101	101
Total [MJ/t_{rf}]	491	483	404	253	562	670
Total [MJ/m^3_{rf}]	177	209	181	175	174	170
λ [%, internal]	0.71	0.82	0.61	0.37	0.87	0.98
λ [%, total]	1.05	1.21	0.91	0.56	1.28	1.43

Possibilities for improvement

Generic rules of thumbs and recommendations may be derived from the exergy analysis. The overall goal is to reduce or eliminate the exergy destruction and losses of the plant and the main ones are ranked as follows:

- combustion chambers of the gas turbines (chemical reaction, mixing, friction, heat transfer);

  These inefficiencies are likely to be significant for all oil and gas facilities for which power is produced in internal combustion engines. They may not easily be reduced, as combustion is in essence an irreversible process.

- exhaust gases from the waste heat recovery system (large physical exergy);

  These losses are mainly related to the high temperature of the exhaust gases, implying that a fraction of the waste heat could be recovered and used for generating power in a bottoming cycle, for example.

- flared and vented gases from the processing plant (large chemical and physical exergy contents);

  Flaring systems are connected to the processing and power plants for safety reasons, and a straightforward way to reduce these losses is to limit flaring by implementing gas recovery systems.

- production manifold (mainly due to depressurisation);

  The typical design set-up of an oil and gas facility involves pressure reduction in the production manifold, and this results in larger destruction of exergy as the pressure differential between the reservoir and the separation sub-system increases.

- compressors in the gas recompression and treatment sections.

  Significant inefficiencies may be associated with the compression operations because of the large pressure ratios and the high gas flows.

Major issues are (i) whether these irreversibilities can be avoided or reduced with the current technological achievements, (ii) how sensitive they are to the variations of the hydrocarbon production over the life span of a petroleum field, and to the reservoir properties and outlet specifications, and (iii) how the design set-up and operating conditions actually affect them.

The present results help to predict *qualitatively* the major sources of thermodynamic irreversibilities of an oil and gas platform with a minimum of information, but they cannot be used for predicting them *quantitatively*. Several limitations should be pointed out, which justify why caution should be exercised when applying the reasoning presented in this study.

Limitations

Firstly, temperatures and pressures of the separation train are not fixed in practice, as assumed in this work, and they are adapted to the type of reservoir fluids. Pressure and temperature levels in the reservoir are generally lower as the API gravity of oils increases (heavy oils) [30, 129]. This suggests that the exergy destruction in the production manifold, the separation train and the recompression system may be slightly underestimated in this study.

Secondly, caution should be exercised in drawing conclusions for cases presenting different design set-ups. Although gas export is the preferred gas processing technology in the North Sea oil region [11], processing routes such as gas injection are practised on several platforms [12] to support the reservoir pressure and enhance oil recovery.

This is, for instance, the case of the oil platform investigated in Voldsund et al. [117, 132]. It may be difficult to estimate the exergy destruction profile for these cases, since it depends on factors such as the injection pressure, the compression train efficiency and the gas recirculation. The power demand and the exergy destruction are nonetheless expected to increase, because the injected gas must be compressed to a higher pressure than in the reservoir to induce oil flowing [211]. Similar reasoning applies to the gas lift process: the difference being that the gas is injected into the well flow in the well-head to decrease the specific gravity of the reservoir fluid.

Thirdly, de Oliveira Jr. and Van Hombeeck [59] investigated a real-case Brazilian oil platform and stressed the great power demand and the significant exergy destruction associated with the gas compression step. However, the authors pointed out the importance of the crude oil heating operations taking place within the separation module, which are not present in most petroleum facilities of the North Sea type. These differences suggest that offshore platforms located in different oil regions (e.g. North Sea, Gulf of Mexico, Brazilian Basin) may, with respect to process and exergy considerations, present highly different characteristics.

4.5 Conclusion

A generic North Sea offshore platform was modelled in order to establish rules of thumbs for oil and gas platforms of that region. The material outflows and energy requirements under different sets of production flows were predicted and validated. This overall model includes power generation, oil and gas processing, gas purification and seawater injection sub-models. The first sub-model was calibrated by use of published data from SIEMENS [207] while the others were verified by comparison with open literature.

Six simulation cases were investigated to analyse the effects of different gas-to-oil and water-to-oil ratios on the thermodynamic performance of this integrated system, based on the exergy analysis method. Exergy is destroyed with a split of about 65 %/35 % for the utility system (power generation and waste heat recovery) and the oil, gas and water processing, respectively. Exergy losses are mostly due to the rejection of high-temperature exhaust gases from the cogeneration plant to the environment and on flaring practices. However, the exergy destruction and loss rates represent only 0.5 to 1.5 % of the total input exergy because of the inherently large chemical exergy content of oil and natural gas.

At identical design conditions, the irreversibility ratio of an offshore platform is higher with increasing gas-to-oil and water-to-oil ratios, suggesting that the thermodynamic performance of this overall system is optimal with low well-fluid contents of gas and water. Although the exact values of exergy destruction would differ from one platform to another, it is suggested that significant inefficiencies and possibilities for performance improvement of the system exist. Recovering more thermal exergy from the exhaust gases, limiting or eliminating flaring practices and monitoring the gas compression trains could increase the thermodynamic performance of conventional oil and gas offshore platforms.

The generic results presented in this work are compared against and validated with a performance assessment of a real-case oil and gas platform located in the Norwegian part of the North Sea (Chapter 5) and other cases, which process different types of reservoir fluids (Chapter 6). A conventional exergy analysis, as conducted in this work, does not allow for evaluating the interactions and cost flows among the system components and processes, as it does not consider their mutual interdependencies [190]. Such issues can be addressed by, for instance, applying the exergoeconomic [212, 213] and the advanced exergy-based analyses [112, 190], which are used further in this work.

5 Draugen

This chapter introduces the Draugen platform, which is the core case study of this PhD project. The performance of this plant is assessed, using the same methods as in the generic study presented in Chapter 4. The first part of the results, which deals with the analysis of the current oil and gas processing plant, is discussed in Nguyen et al. [214]. The second part, which investigates the interactions between the processing and the power plants, is presented in Nguyen et al. [215].

5.1 Introduction

At the beginning of this PhD project, very few projects and publications dealing with the thermodynamic performance of offshore platforms could be found in the scientific literature. The only studies on this topic were the analyses of a Brazilian facility by de Oliveira Jr. and Van Hombeeck [59] and of a Norwegian one by Voldsund et al. [132]. They have shown that such analyses were useful for evaluating the performance of petroleum systems, as also suggested by Rivero [131]. The first study recommends to focus on the oil heating and separation, whilst the second one brings attention to the gas compression operations.

The Draugen facility is similar to other plants in the North Sea [11–13], with two main differences: (i) the oilfield is characterised by a high propane content of the reservoir fluid and a small gas-to-oil ratio, and (ii) oil is not exported continuously via pipelines but in batch operation. The oil recovery rate is expected to reach 65–75 %, which is much higher than the typical rate of 45–50 % for Norwegian fields. This has encouraged an extended exploitation of this petroleum field, although the plant is already now run far from its nominal conditions.

The main objective of this research is to assess the thermodynamic performance of the Draugen platform, while gaining further insights into the efficiency of offshore processes. Special attention is given to the different operating modes of this platform, the end-life production aspects, and the specific process requirements.

5.2 Case study

5.2.1 General overview

The Draugen field is located in the Norwegian Continental Shelf region [9]. The construction of the platform was finalised in 1993 and the oil production started the same year. This facility is characterised by the seven oil tanks located at the base of the structure and operates on two different deposits (Garn and Rogn).

The aim has been to maximise the oil production: associated gas was used for petroleum lift, and gas export only started in 2000. Water injection started in 1994 to sustain a high reservoir pressure: seawater was filtered, treated by addition of chemicals and injected into the reservoir at high pressure. Water production started in 1998 and has drastically increased, reaching a water cut above 90 % in the last years. Produced water reinjection is considered, and may be mixed with seawater for further re-injection. The oil production peak was reached between 2000 and 2002 (Figure 5.1).

At present, stabilised oil is stored in the tanks in the base of the facility, and exported to the shore once every single or other week via shuttle tankers that load the oil at the floating buoy. Produced gas is (i) mainly used for gas lift, i.e. is injected into the oil wells to ease the reservoir fluid lift and maximise oil production, or (ii) transported to the shore through the Åsgard pipeline system, or (iii) used as fuel in the gas turbines. The gas-to-oil ratio has decreased these last years: gas injection is not practised, there is a foreseen gas deficiency, and the operators plan to shut-down the gas export system in the near-future. Produced gas may be used only for gas lift, and diesel oil may be imported to fuel the gas turbines.

The possibilities of electrifying the platform and of importing carbon dioxide from the shore to enhance oil recovery were discussed [216–218]. However, feasibility studies showed that these projects, though technically feasible, would be uneconomical in the current context. The additional oil production would not be high enough to justify such investments, and platform modifications would require production shut-down.

5.2.2 System layout

The structural design and general building blocks of oil and gas processing plants stay similar across platforms [11–13], but differences in the detailed design exist from one processing plant to another (Figure 5.2), depending on the reservoir characteristics (e.g. temperature and pressure), reservoir fluid properties (e.g. chemical composition and thermophysical properties), technical requirements (e.g. need for dehydration and compression) and operating strategies (e.g. gas export and water injection). The field produces oil from two reservoirs located at about the same depth, which is extracted via seven platform- and six subsea-wells connected to the platform. The initial hydrostatic pressure and reservoir temperature were about 165 bar and 71 °C.

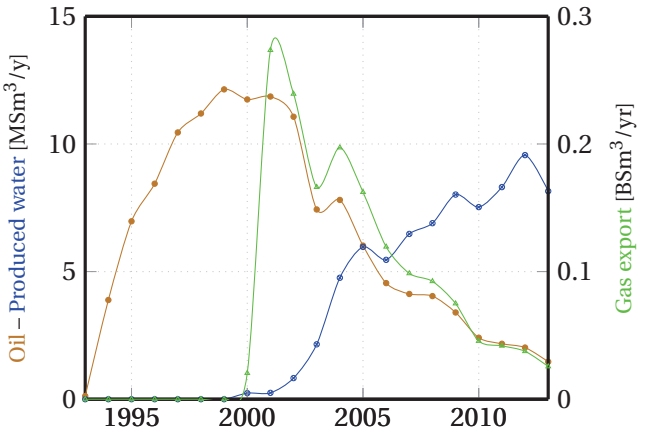

Figure 5.1: Oil, gas and water production and exports for the platform under study, from 1993 to 2013.

The facility can be divided into two main plants, namely the *processing plant*, which includes the production manifold, separation, recompression, condensate treatment, gas treatment, fuel gas handling, oil export, wastewater purification and seawater injection sub-systems, and the *utility plant*, which consists of the gas turbines, waste heat recovery and cooling sub-systems. Other utilities, such as the ones related to the drilling operations or to the living quarters, are out of scope of this work. The same subdivisions are considered for the other oil and gas platforms investigated in this project.

Production manifold

The well-streams are gathered and transported to the main production facility via a network of pipelines and manifolds. They are mixed and depressurised by choke valves, which are set to control both flows and pressures. A fraction of the well streams, usually from a dedicated well, is placed in a test manifold and processed in a test separator, to allow further flow analysis. The other fraction is placed in production manifolds and is normally processed in two three-phase separators run in parallel.

Four platforms wells (named afterwards Wells 1, 2, 3 and 4) are connected to the same 3-phase separator at the 1st stage, while the seven subsea wells (named Wells 7 to 13) are connected to another one. There are two other platform production wells (named Wells 5 and 6), that can be connected to the test manifold and separator, or to any of the two regular 3-phase separators. Well-streams from Well 5 are generally routed to the test separator, while the well-streams from Well 6 are generally sent directly to the 1st stage separator connected to the platform wells. Some wells only extract gas, some extract mainly oil and water, and a few are not operated at the period of analysis. The water cut is slightly higher for platform wells, resulting in a greater water production from the 1st stage separator connected to Wells 1 to 4.

Separation

Oil, gas and water are separated by gravity in two stages, operated at two different pressure and temperature levels. The 1st stage consists of two three-phase separators run in parallel and at similar operating conditions, at a temperature of about 55–65 °C and an absolute pressure of about 8 bar. The 2nd stage consists of a two-phase separator operated at about 65–75 °C and 1.6–1.8 bar. The pressure is decreased by throttling valves, the oil streams from the three 1st stage separators are mixed, and their temperature is increased in a crude heater from the 1st to the 2nd stage, easing recovery of light hydrocarbons.

Oil export

The crude oil leaving the separation system enters a storage and pumping section. It is first mixed with condensate removed in other sections of the processing plant, cooled by seawater, and placed in tanks located at the bottom of the sea. Stabilised oil is pumped later for export onshore, and additional power is therefore required during the loading periods. Two main operating modes can be defined, depending on whether oil is stored or exported.

Gas recompression

The gas recovered from the 2nd separation stage is sent to the recompression system, where it is cooled to 30–35 °C, sent to a scrubber, where condensate and water droplets are removed, and recompressed to the pressure of the 1st separation stage. It is then mixed with the gas recovered from the 1st separation stage and enters the gas treatment and compression train.

Gas treatment and compression

This system is divided in three stages operated at 19–23, 57–60 and 179–189 bar. Each stage includes a cooler operated with seawater, a scrubber to separate liquid droplets from the gaseous phase, and a compressor, as in the recompression process. The 2nd compression stage also includes a dehydration process to prevent corrosion issues and hydrate formation in the gas pipelines. In a packed contactor, wet gas flows counter-currently to liquid and dry TEG (triethylene glycol).

The glycol-water mixture is then depressurised, flashed and heated before entering a desorption column where water and glycol are separated. Liquid TEG exits at the bottom of the desorber while water vapour exits at the top, along with hydrocarbon impurities. Dry gas from the 2nd stage of the compression train is introduced in the desorber to increase the glycol purity to about 99–99.5 % on a weight basis. The temperature of the bottom stage is controlled by a reboiler and is about 205 °C, which is the highest temperature level of the processing plant. The temperature of the top stage is controlled by a reflux condenser and is about 95 °C to prevent excessive glycol losses with the vented gases.

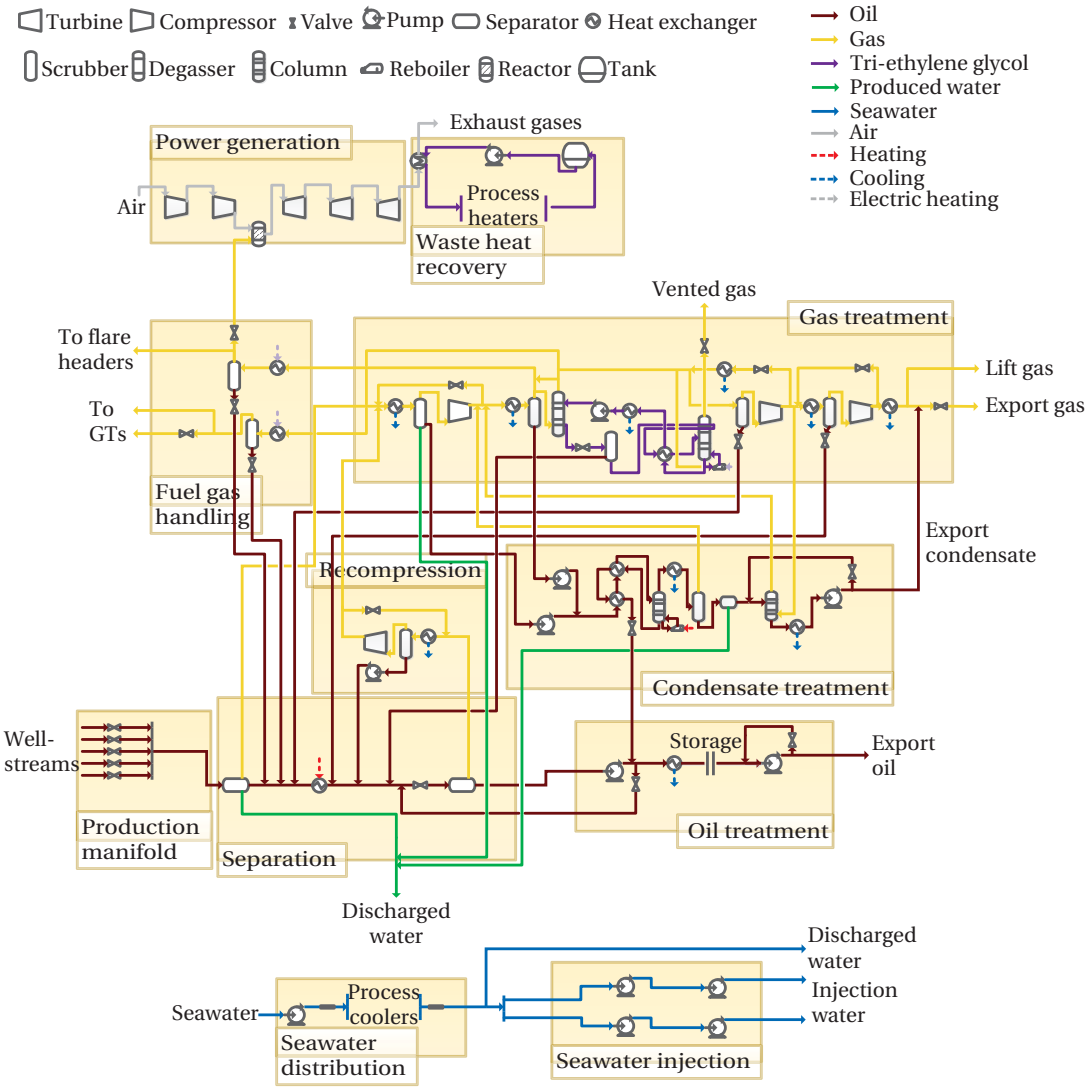

Figure 5.2: Process flow diagram of the Draugen offshore platform, based on input by Norske Shell A/S. For ease of reading, only the most important recycling loops are drawn. Control valves, connections to pilot flares, storage units and shaft connections are not presented. Addition of chemicals such as biocides and methanol is not indicated. The hydrocyclones of the produced water handling system are merged into two, the scrubbers of the fuel gas treatment into one, and the oil and condensate pumps are shown as a single pump per two pumps run in parallel. Only one gas turbine is shown, and the waste heat recovery system is simplified for readability.

Regenerated glycol is pumped to the pressure of the 2nd compression stage and is recycled to the absorber. Most high-pressure dry gas is used for gas lift, while the remaining is sent onshore via pipelines.

Fuel gas handling

A certain fraction of the wet and dry gases from the 2nd separation stage is processed through the fuel gas system: it is heated in electric heaters, scrubbed in three parallel trains and is combusted in three gas turbines installed on-site for power generation. Two are used to generate the power required in the oil and gas processing section while the third one is dedicated to the water injection train.

Condensate stabilisation

Condensate recovered from the 1st and 2nd stages of the gas compression system is not sent to the crude separators, as done on most offshore platforms, but is handled in a separate process. This avoids recycling of propane, butanes and pentanes between the separation and gas treatment sections, and reduces significantly the power demand of the recompression train. The recovered condensate is pumped to a pressure of 21–25 bar, heated by integration with other process streams, and sent to a fractionation column.

At the difference of conventional scrubbers, which operate without any heat addition, this condensate scrubber is equipped with a reboiler: the heat input is regulated to control the temperature at the 15th stage, and therefore to achieve the desired separation between light and heavy hydrocarbons.

Liquid hydrocarbons exiting this column are mixed with the crude oil entering the cooler of the oil pumping section, while gaseous ones are processed further in the condensate treatment system. They are cooled and dried in a condensate dehydrator, using stripping gas from the 3rd stage of the gas compression train as a drying agent. The dry condensate is then cooled, pumped and finally mixed with the gas for export. Wet gas from the condensate dehydrator is reprocessed through the gas treatment system at the inlet of the 2nd stage.

Produced water treatment

Produced water from the oil and gas processing sections enters a wastewater handling train. Suspended particulates and traces of dissolved hydrocarbons are removed by hydrocyclones operated in parallel, and entrained gases are removed in degassers. Most cleaned produced water is discharged into the sea. This sub-system is connected to the seawater injection process, as produced water may be injected for improving oil recovery. At present, produced water is not used at all for such purposes, but it may be done in the future, together with seawater.

Seawater handling and injection

Seawater is processed to meet the cooling demand on-site, and a large fraction is filtered and used for further injection into the oil reservoir. The cooling water system was originally designed for processing water with temperatures increasing from 5–10 °C to 30–35 °C, which corresponds to an average flow rate of 1500 to 2000 Sm^3/h.

Flaring and venting

The introduction of an offshore CO_2-tax by the Norwegian Authorities in 1991 [219] and stricter environmental regulations under the Petroleum Act [8, 22, 115] have encouraged efforts to reduce flaring practices [13, 19]. However, the possibility of releasing gas by flaring in emergency and shut-down situations is essential. The 1st stage separators, as well as the gas treatment and fuel gas processes, are connected to high-pressure flares. The 2nd stage separator and the produced water handling system are connected to low-pressure ones.

Gas turbines

Five gas turbines are installed on-site, of which three are of the SGT-500 type, and two of the SGT-200. Two of the SGT-500 turbines are running, sharing about half of the processing plant power demand, without including the seawater injection process. They provide the power required to run the compressors of the gas recompression and treatment sections, as well as the pumping demand associated with the oil export. The last SGT-500 is generally on stand-by and is run in case of failure of one of the two others. These gas turbines are un-cooled and can be operated with various fuels, which explain the low turbine inlet temperature and thus the low exit one. One of the SGT-200 turbines is used for satisfying the power demand of the seawater injection plant, and the last one is used in emergency cases only.

Only the three SGT-500 gas turbines are equipped with waste heat recovery: the current temperature of the exhausts, before waste heat recovery, is about 330 °C, which can be considered as a low exhaust temperature compared to other gas turbines, such as the LM2500+, which are installed on other oil platforms in the North Sea region. This temperature is supposed to be higher in case of greater power demand, since the turbines are run at loads as low as 50 %.

Waste heat recovery

An intermediate heating loop of tri-ethylene glycol, heated up to 220 °C, operates in-between, flowing first through the condensate treatment and then to the separation sub-system. The return temperature was controlled to vary between 120 and 140 °C when the oil production reached its peak, and currently varies between 180 and 200 °C, as the need for heating has decreased. Tanks are implemented in this loop, and the flowrate of glycol is also controlled to match the heating demand.

5.3 Modelling and simulation

5.3.1 Fluid modelling

The reservoir fluid processed on this platform is a light volatile crude oil [30]. The term *volatile oil* implies that the hydrocarbon compounds are mostly present in the liquid phase, but that large quantities of light hydrocarbons may, as the reservoir pressure declines, evolve out of the liquid phase to the gaseous one. The chemical composition of this reservoir fluid, excluding the subsurface water, is remarkable. The propane fraction is as high as 9 % on a molar basis, and the content of medium-weight hydrocarbons such as butanes and pentanes is significantly higher than in most conventional volatile crude oils [220].

In this study, crude oil was modelled as a blend of 82 chemical compounds, including 29 hypothetical components, which properties were calculated by using the analyses and assays from 2002. The following bulk properties were considered: an API (American Petroleum Institute) gravity of 39.9, a specific gravity of 0.826, a density of 825.5 kg/m^3 and a light ends fraction of 27.2 % in volume. The API gravity varied between 39 and 41 ° this last decade. Thermophysical properties of the whole crude oil (e.g. density and kinematic viscosity) were similar from one assay to another with a deviation of ± 2 %, and the kinematic viscosity at 20 °C is around 4 cSt. Sulphur and nitrogen concentrations varied within a range of ± 5 %, and vanadium and nickel contents by ± 0.03 ppm.

5.3.2 System modelling and simulation

Yearly analysis

Average daily measurements of several temperatures, pressures and flows throughout the offshore plant were provided for the year 2012, including as well the estimations of the energy exported, used on-site and flared as calculated in the monitoring system.

The measurements on the outflows show that the processing plant was shut-down about 6 to 7 times in that year. The water production is, despite several local fluctuations, slightly increasing over the year, while the opposite trend can be observed for the gas production. The energy export profile follows closely the gas export profile.

The rate of gas used for lift purposes is maintained constant, around 875 to 925 kSm^3 per day, with the exception of some stages at 500 and 700 around the 150th and 180th days, which are due to the shut-down of some lift wells (Wells 1 to 6). The gas consumption profile can be divided into four typical stages, depending on whether the seawater injection pumps are operating, and on whether oil is exported to the shuttle tankers. The case where none of these two processes are run is by far the least frequent, and oil was exported about 25 times in the whole period, which corresponds to the sharp peaks. The rate of flared and vented gas is nearly constant and leads to an energy waste of about 6 MW (Figure 5.3).

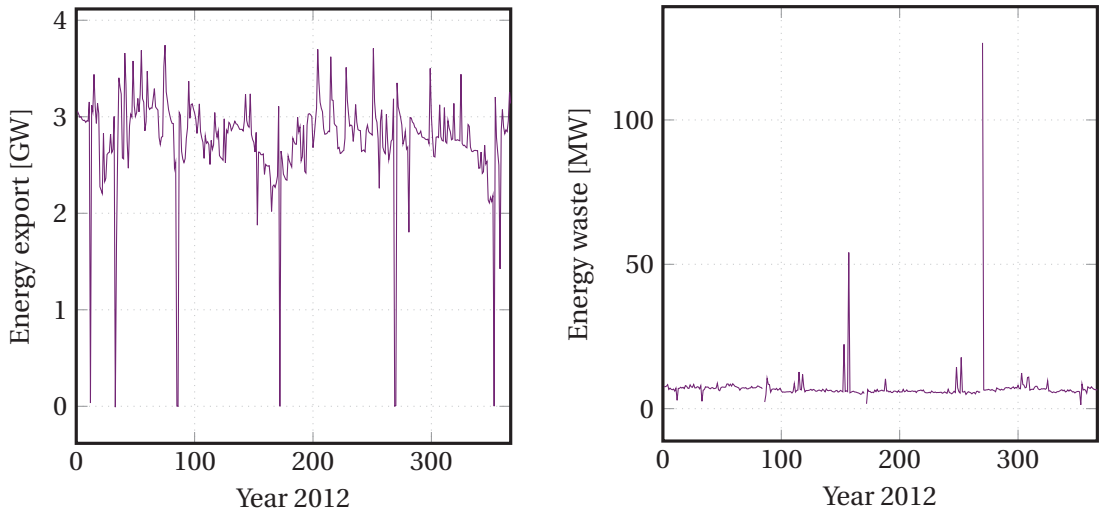

Figure 5.3: Energy export and waste.

Although the processing plant undergoes changes in the production rates of oil and gas over the year, the gas flow rate through the compressors is nearly constant, illustrating the recirculation of gas around the compressors to prevent surge and the nearly constant power demand of these components (Figure 5.4).

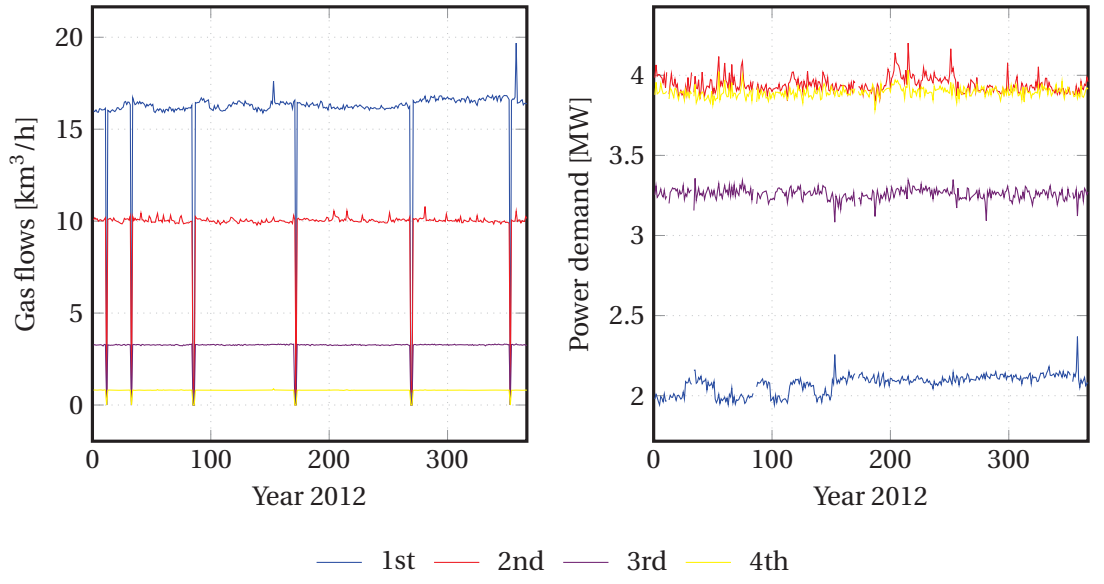

Figure 5.4: Gas flows and power demands of the four compression stages.

Typical production days

Process data was measured and available from 2000 to 2013, showing that operating conditions and process variables change considerably from year to year because of variations in the well-fluid composition and flow rates. However, variations on an hourly, daily or weekly basis were not significant, with the exceptions of urgency or shut-down situations, as well as cases where load set-points were changed by the operators. If the seawater injection system is operating, normal production days can be grouped into two different categories.

The first one is called *low-energy use* production days: oil, gas and water are processed and treated on-site, and oil is stored in the storage tanks located at the bottom of the plant. The second one is denoted *high-energy use* production days: oil, gas and water are processed on-site, and oil is pumped from the storage tanks to the floating loading buoys, which results in a greater power consumption. The second operation mode is the least frequent.

A representative day is studied for both cases, but this work focuses mainly on the first type of production day. Neither the energy trends of the other processes, nor their operating temperatures and pressures, change significantly. The days during which seawater lift and injection are not operating are not considered. It is expected that, since the power consumption is lower in such cases, the gas flow through the compressors in the gas treatment process will be slightly higher, resulting in additional cooling and compression demands of this processing section.

A more thorough analysis of the average values and standard deviations (Table 5.1), for some pertinent process variables, illustrates that the pressures and temperatures thorough the process are overall constant, while the flows of oil and gas can vary significantly over time. The operating conditions throughout the processing plant remain fixed. The separation pressures are controlled by the opening of the valves in the production manifold and at the 2nd separation stage.

Lifetime analysis

Three base simulation cases were considered in this study, each corresponding to a different stage in the lifespan of the oilfield. The first case corresponds to the *early-life* production: the oil rate increases, while the gas and water production are negligible. Gas and condensate were re-injected into the reservoir through dedicated wells, as there were no pipelines for exporting them. The second case corresponds to a *plateau* case, where the oil rate has reached its maximum. Most equipments are designed for this point of time, and this case determines the maximum head and power requirements of the system. The third and final case corresponds to an *end-life* case, where the oil and gas productions have sharply decreased, and the water content of the feed is greater than 85 %, on a molar basis (Table 5.2).

In the early- and end-life situations, the mass flow of the produced gas is significantly lower than what the process was designed for. Gas is therefore recycled around the compressors to prevent surge, as a minimum flow rate through the compressors should be maintained.

Table 5.1: Yearly average values and standard deviations for selected process variables.

Process	Variable	Average value	Standard deviation
Gas turbine	Exhaust temperature [°C]	348	13
Waste heat recovery	Supply temperature [°C]	226	5.9
Waste heat recovery	Return temperature [°C]	208	5.8
Waste heat recovery	Loop pressure [bar]	6.5	0.4
Separation	1st-stage pressure [bar]	6.9–7.8	0.6
Separation	2nd-stage pressure [bar]	1.8	0.7
Recompression	CIT [°C]	28.4	1.5
Gas treatment	2nd stage CIT [°C]	27.2	0.9
Gas treatment	3rd stage CIT [°C]	53.9	0.9
Condensate treatment	Fractionation temperature [°C]	160	8.4
Condensate treatment	Dehydration pressure [bar]	24.5	1.7
Condensate treatment	Dehydration pressure [bar]	24.5	1.7
System	Energy export [MW]	2760	510
System	Energy use [MW]	120	30

These three cases are set up to underline (i) the significant differences in operating conditions between each stage, and (ii) the variations of the heating and cooling demands over time, and (iii) the changes in the locations and extents of the system inefficiencies.

Table 5.2: Simulated flow rates of the process streams at the outlet of the offshore platform.

	Variable	Start	Peak	End
Exported oil	$\dot{F}$ [Sm^3/h]	948.1	1325.1	279.1
Exported gas and condensate	$\dot{F}$ [10^3 Sm^3/h]	$\simeq 0$	111.8	23.5
Produced water	$\dot{F}$ [Sm^3/h]	$\simeq 0$	31.6	1128.5

These three cases are derived from the actual production flows at three points of time of the Draugen platform, the *end* case corresponding to the current one, as of 2012–2014, the *start* and *peak* cases corresponding to the actual productions as of 1995–1998 and 2000–2004, respectively. The *start* case is characterised by a high production of oil, low extraction of gas and water, while the *peak* case represents high production of oil and gas.

Power and flow measurements were not available for the *start* case, as the new measurement database used by the operators contains data from around 2000. They were therefore extrapolated based on the component maps and case simulations provided by the manufacturers in the component data, as well as on discussions with the platform engineers. Not all data were available either for deriving the *peak* case model, so a similar approach than for the *start* case model was applied. The final results should therefore not be seen as accurate as for the final case, but provide a reasonable basis for comparing different stages in the lifetime of this oil and gas platform. Similar trends can be expected for other oil and gas platforms, but the initial water-to-oil ratio may be much higher than in the Draugen case.

5.4 Performance evaluation

5.4.1 Site-scale analysis

The total heating demand of the site amounts to about 5 MW and can be categorised as follows:

- the largest heating demand is identified as the crude oil heating in the separation process. A fraction of the oil from the 1st separation stage, at 45–55 °C, is heated to 80–90 °C before entering the 2nd separation stage. The fluid viscosity decreases and the vapour fraction increases to 2–5 %. It is then mixed to the oil fraction that has by-passed the heater, and the temperature after mixing is about 70–80 °C. The separation between the gas and oil phases is enhanced to prevent a too high vapour pressure of the oil;
- the second largest heating demand is found at the reboiler of the condensate stripping column. The boiling-off of the light hydrocarbons from the condensate is called *stabilisation* and takes place at temperatures of 180–200 °C.
- other heating demands amount to less than 300 kW each: glycol is used to dehydrate wet gas, and the glycol-water mixture should be heated in a column up to 205 °C to regenerate and re-use the glycol back in the gas treatment section. The fuel gas entering the gas turbines should be heated from 40 to 65 °C.

The total cooling demand amounts to about 27 MW in the current end-life conditions. It has varied between 27 and 44 MW and can be subdivided as follows:

- the gas cooling before each compressor: the gas flows are cooled from temperatures between 70 and 140 °C to about 30 to 50 °C, to condense medium- and heavy-weight hydrocarbons, further removed in the scrubber, and to reduce the compression power;
- the oil cooling after separation: the mixed oil and condensate flow is cooled down to 25–30 °C to reduce the pumping power and ease further export.

The heating and cooling requirements are particularly sensitive to the oil rate, while they are moderately varying with the gas rate (Figure 5.5). The drop of the oil rate of about 80 % between the *peak* and *end-life* productions has resulted in a reduction of 80 % and 40 % of the heating and cooling demands, respectively.

In a *plateau* situation, the large oil throughput results in significant heating in the separation and condensate stabilisation processes, and in high gas recovery. In *start-* and *end-life* situations, the compressed gas should be recycled to prevent compressor surge, implying that the gas rates into each cooler are nearly constant over time. The decrease of the cooling demand results from the lower cooling demand of the oil pumping process.

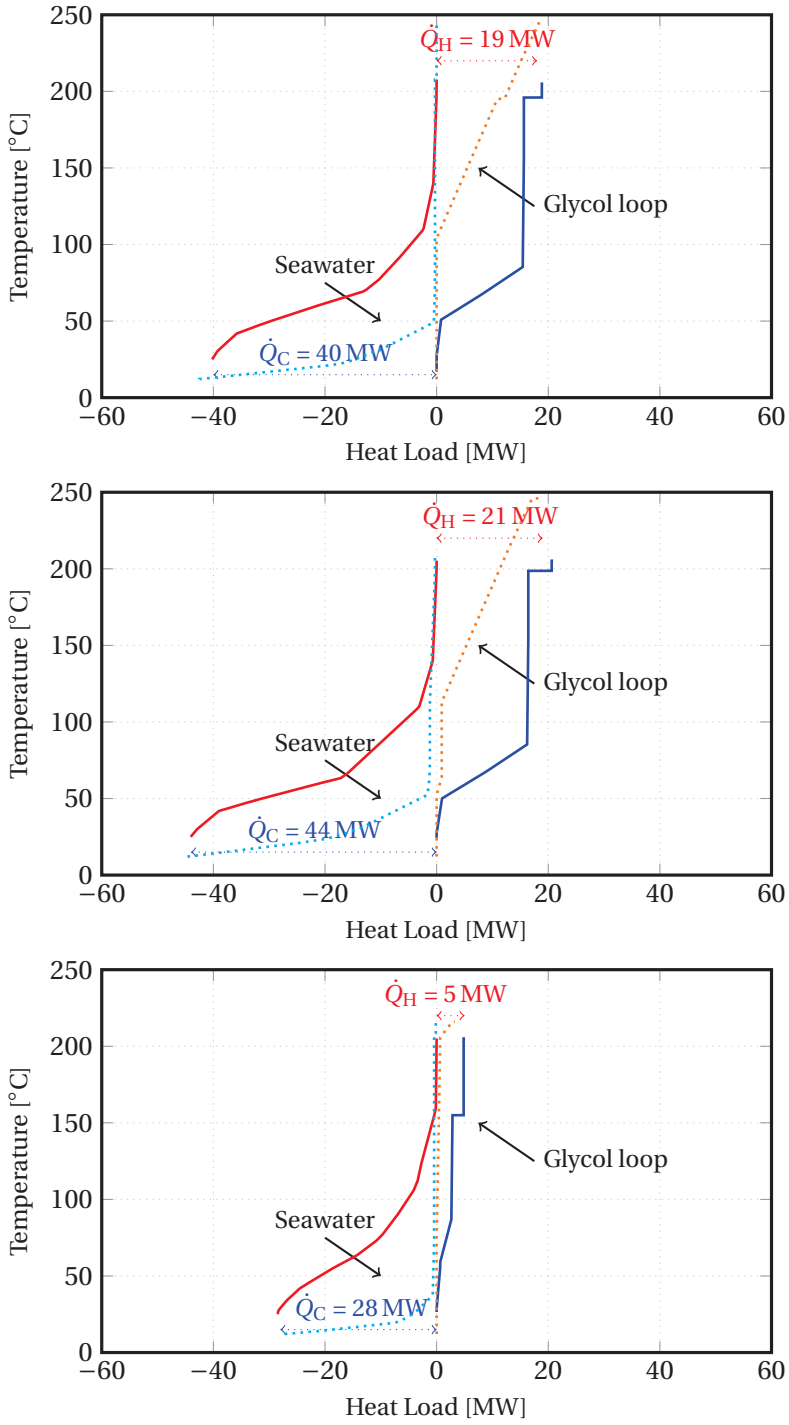

Figure 5.5: Total site profiles of the offshore plant with its current utility system for the *start*, *plateau* and *end-life* productions. The hot and cold process streams are represented by continuous lines, while the hot and cold utility streams are illustrated by dotted ones.

The energy demands can be described by three levels of details, utility, which illustrates the actual energy use from the external utilities, technological, which shows how energy is transferred from the utility plant to the processing one, and thermodynamic, which denotes the heat transfer profile within the heat exchanger. This decomposition shows the degradation of energy when transferred from high to low temperatures (Figure 5.6).

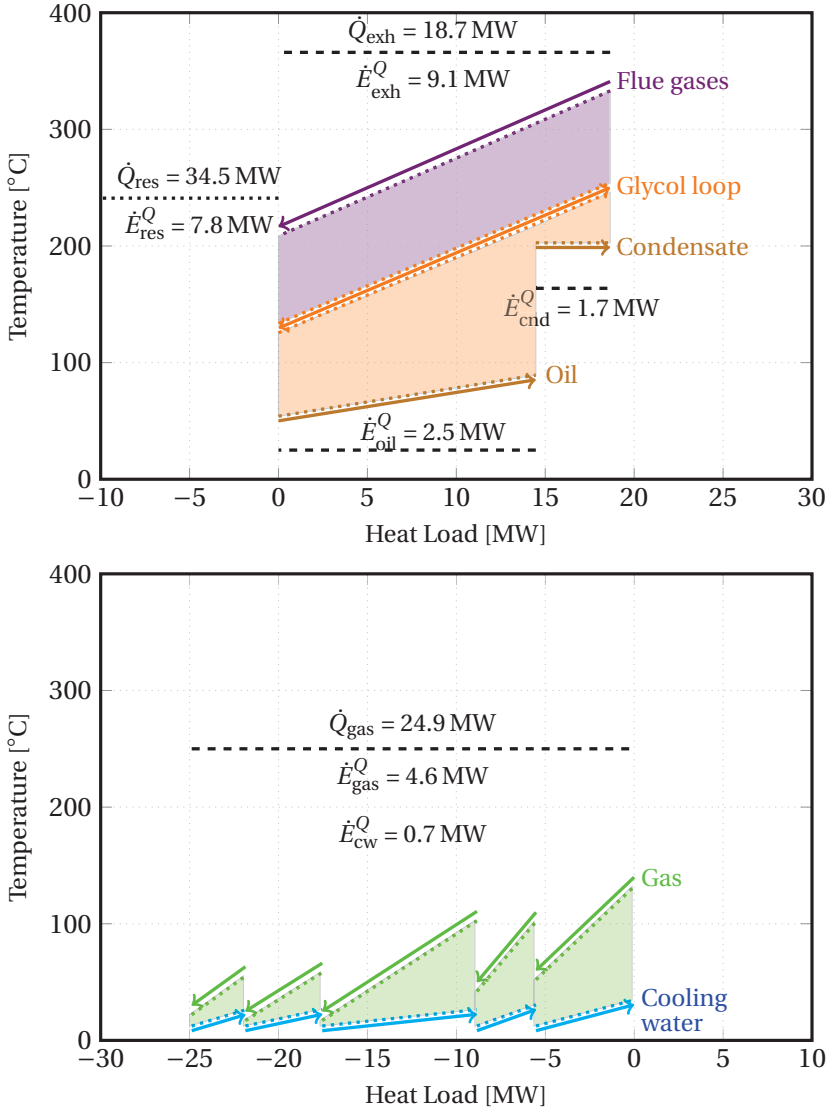

Figure 5.6: Temperature-enthalpy diagrams of the site heating (oil heating and condensate treatment) and cooling demands (gas recompression and treatment) illustrated with the thermodynamic (process), technology (glycol loop) and utility (exhaust gases and cooling water) requirements. The full lines correspond to the real temperatures, the dotted lines to the corrected ones (i.e. adjusted with the individual temperature differences $\frac{\Delta T}{2}$), and the dashed ones to the energy demands.

5.4.2 Energy analysis

Energy flows

At present, about 3870 ± 100 MW of energy enters the oil and gas plant, of which $\simeq 98.5$ % enters with the well-streams, $\simeq 0.5$ % with power and heat. Most inflowing energy is exported to the shore along with oil, gas and condensate (76 % ± 0.4), while a small fraction is used as lift gas (18 % ± 0.2), fuel gas (2.3 % ± 0.1), and injection seawater (0.4 % ± 0.1). Only a small fraction of the total energy input is lost to the environment, along with wastewater (2.0 % ± 0.1), cooling water (0.5 % ± 0.1), injection water (0.4 % ± 0.1), flared and vented gases ($\simeq 0.1$ %).

Energy transformations

Energy flowing through the oil and gas plant is dominated by the chemical energy of the material streams. Electrical energy is converted into physical energy in the recompression, compression and pumping sections, with negligible heat losses, while physical energy is partly dissipated along with cooling water. The total power consumption varies between 18,900 and 25,500 kW, as the oil loading system is not run continuously. For every production day, the gas treatment ranks as the most power-consuming sub-system, representing 44 to 60 % of the total power demand of the processing plant in the current situation, with small oil production. The major power consumers of this system are the compressors, using about 13,300 kW of power (Figure 5.7 and Figure 5.8). The discharge of thermal energy with cooling water amounts to about 18,200 kW.

Energy-based indicators

The energy efficiency η, the energy intensity ι_h and the energy waste ω_h amount to 93.4 % ± 0.25, 2.3 % ± 0.05 and 0.13 % ± 0.03 for a *low energy use* production day, and about 93.2 %, 2.8 % and 0.18 % for a *high energy use* one. These values are fairly constant over time. In all cases, the energy efficiency of the processing plant is lower than the benchmark value, while the energy intensity and waste are higher. The changes of the energy contained in the lift gas are small, as the volume of gas used for lift varies only slightly, while the amount of fuel gas changes from day to day, since the water injection turbines are not operated at a constant load.

These values, as returned by the model, are similar with a deviation of ± 1 % point to the values retrieved by the operators. The largest difference corresponds to the energy intensity factor, and this may be caused by (i) a difference in the litteral expression of this indicator, (ii) discrepancies between measurements and estimations or (iii) deviations between the measured composition at a certain time point and the actual one. The specific power consumption of the processing plant is about 76.5 kWh/$Sm^3_{o.e}$ and 103 kWh/$Sm^3_{o.e}$ of exported oil and gas for *low* and *high* energy use production days. The specific power consumptions of the gas recompression and treatment systems amount to 1060 kJ/Sm^3 and 650 kJ/Sm^3 of processed gas. It has a value of about 57 kJ/Sm^3 of condensate for the condensate treatment process.

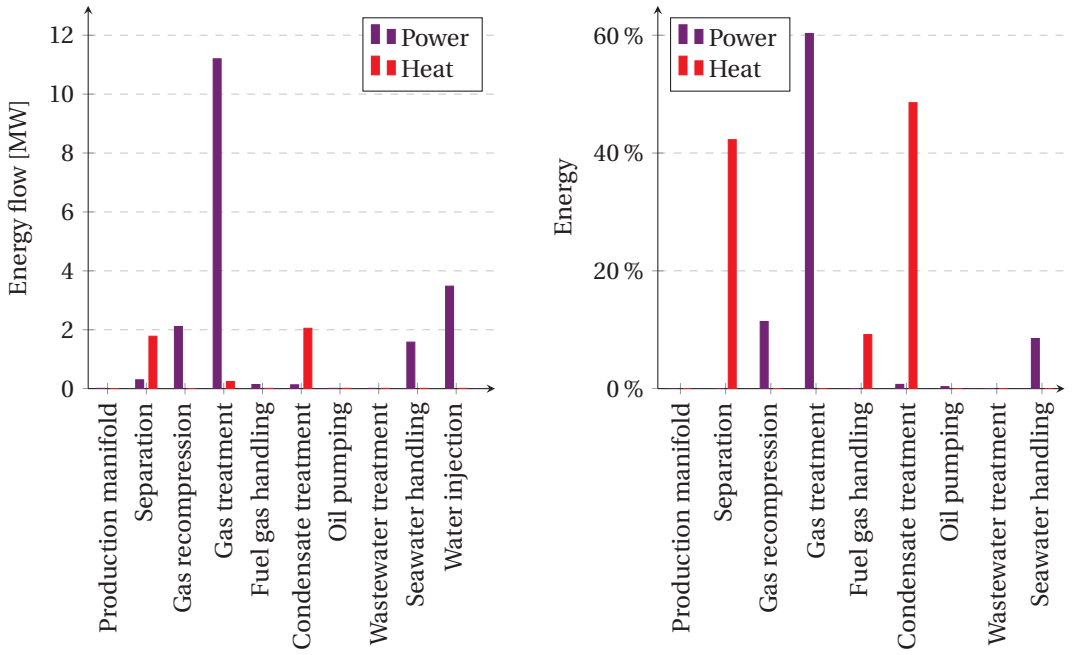

Figure 5.7: Energy demand of the processing plant for a low-energy use production day, expressed in absolute (left) and relative (right) values.

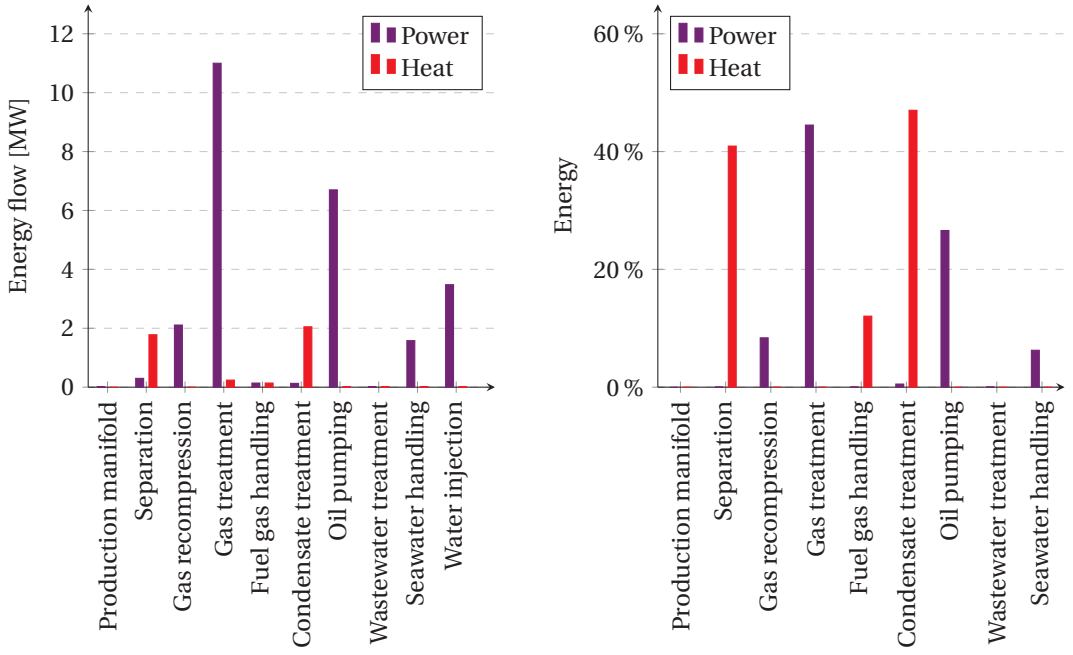

Figure 5.8: Energy demand of the processing plant for a high-energy use production day, expressed in absolute (left) and relative (right) values.

5.4.3 Exergy analysis

Exergy flows

The exergy analysis shows that exergy enters the oil and gas platform along with the hydrocarbons contained in the well-streams, as well as with the seawater and the chemicals imported for water treatment. Similarly, most exergy exits the facility with the oil exported to the shore and with the gas used for lifting the reservoir fluids. The largest contribution to the exergy inflows and outflows corresponds to the chemical exergy associated with the hydrocarbons (Table 5.3 and Figure 5.9): the latter are separated in the processing plant, and consumed, to a minor extent, as fuel gas in the gas turbines. At all times, most exergy entering the offshore platform system transits without being converted or used, giving the misleading impression of a high thermodynamic performance. It is dominated by the chemical exergy associated with the oil and gas streams.

The exergy entering the facility with the well-streams amounts to 10,700 ± 270 MW in the *early-life*, 14,900 ± 370 MW in the *plateau*, and 3800 ± 100 MW in the *end-life* cases. The exergy flowing with the air and cooling water are negligible in comparison, representing less than 50 MW in total. Similarly, the exergy sent to the shore with the exported flows of hydrocarbons in the oil, gas and condensate amount to 9620 ± 240 MW, 14,100 ± 350 MW and 2940 ± 70 MW for the three investigated cases. About 700–900 ± 20 MW of exergy is used on-site for either power generation or gas lift. The exergy entering the system is higher than the corresponding energy, because (i) the chemical energy of hydrocarbons (LHV) is smaller than their exergy and (ii) in the models of Szargut et al. [44], the chemical exergy of water is greater than the enthalpy of devaluation.

The chemical exergy of the hydrocarbons compounds is calculated by using the Peng-Robinson EOS for the computation of the enthalpies and entropies and with correlations from the works of Rivero [131]. This inherent uncertainty of the EOS results in a spin of about 2 to 3 %, which may be higher in the case of oil and gas platforms processing heavy oils. The uncertainties related to the chemical exergy of the well-streams and oil are higher than for the other streams. These flows contain a larger variety of chemical compounds, and their lower heating value is only estimated by correlations. Mixing of the hydrocarbons, water and impurities results in a reduction of the chemical exergy (Term III in Equation 3.16) between 0.11 and 0.23 % for the well-streams, about 0.06 % for the export oil, 0.01 % for the produced water, 0.14–0.24 % for the vented and flared gases, 0.24 % for the export, lift and fuel gas streams.

The physical exergy of the well-streams is generally dominated by the thermal (temperature-based) exergy, as a result of a high water content. The physical exergy associated with the lift, fuel and export gas is dominated by the mechanical (pressure-based) exergy (Term II in Equation 3.13), while it is dominated by the thermal (temperature-based) exergy (Term I in Equation 3.13) for the discharged water. A comparison of the Peng-Robinson EOS with the Setzmann and Wagner EOS, showed that the relative deviation of physical exergy can vary up to 1.6 % for methane [172].

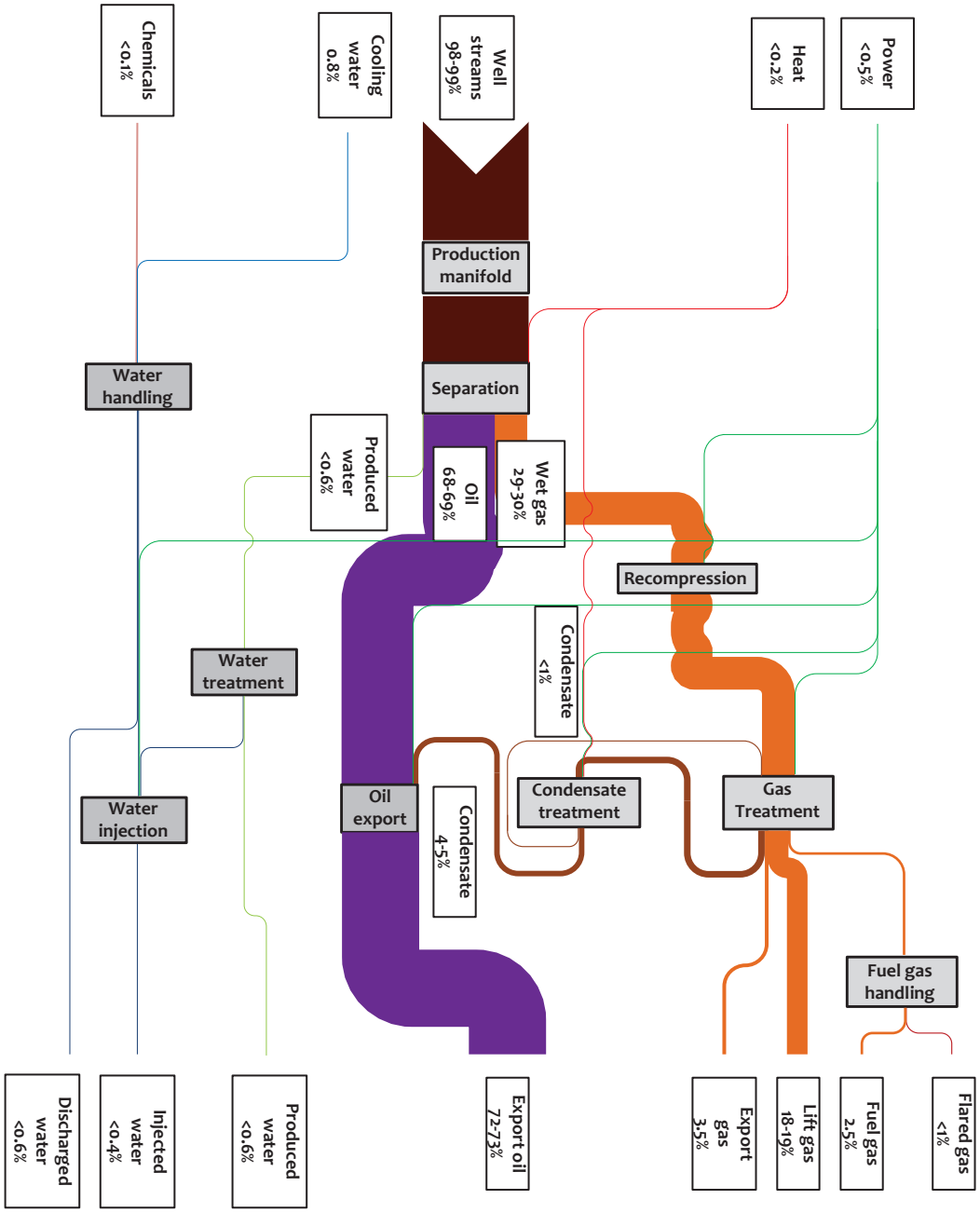

Figure 5.9: Sankey diagram of the processing plant of the Draugen offshore platform.

Exergy transformations

No chemical transformations occur in the processing plant: the changes in chemical exergy are only related to the mixing and separation effects. As emphasised in the work of Kotas [54], chemical exergy is increased at the expense of other forms of exergy [137], such as (i) thermal exergy (e.g. the crude oil mixture is heated) (ii) mechanical exergy (e.g. the pressure of the well-streams is decreased in separation train), (iii) potential exergy (e.g. oil and gas are separated by gravity in the 1st separation stage), (iv) kinetic exergy (e.g. reduction of the mixture velocity) or (iv) a combination of these four.

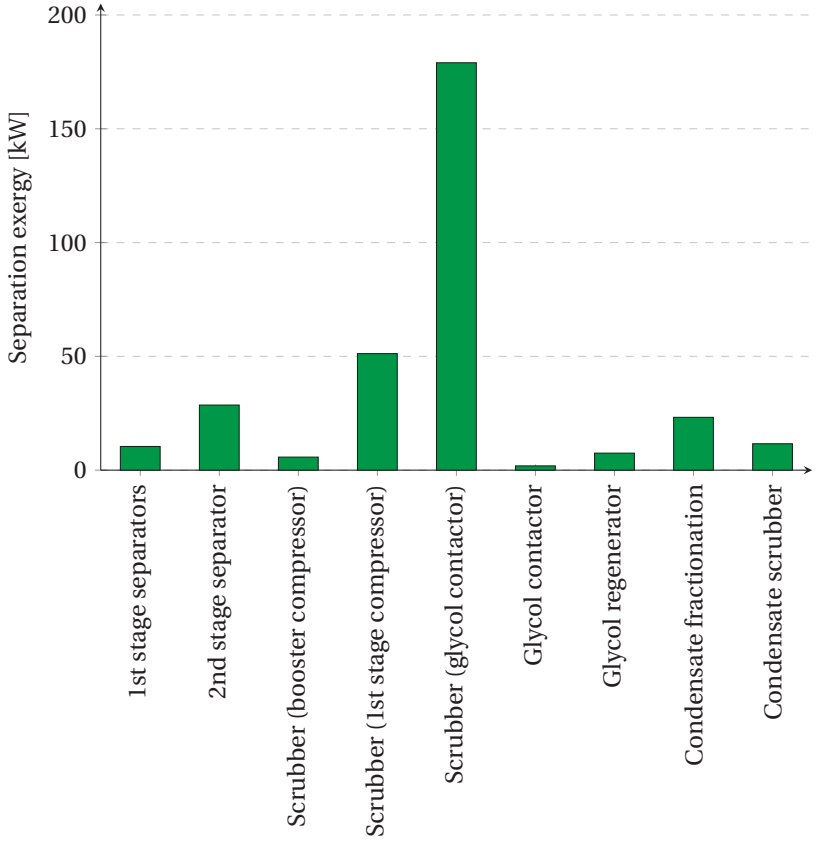

Figure 5.10: Distribution of the separation exergy on the Draugen processing plant for the end-life production case.

The sum of the chemical exergy increases (Figure 5.10) due to the separation effects amounts to about 560 kW for the *start-life* case, of which 50 %, 42 %, 6 % and 2 % take place in the gas treatment, separation, condensate stabilisation and recompression processes. The separation exergy increases to 620 kW in the *peak* case, with a share of 52 %, 39 %, 7 % and 2 %, and decreases to 320 kW in the *end-life* case, with a distribution of 74 %, 12 %, 14 % and 2 %. This illustrates that the gas treatment process is of key importance for achieving the desired separation of the oil and gas phases. In all cases, the components in which most separation

work is performed are the 2nd stage 2-phase separator in the separation train and the two scrubbers prior to the glycol dehydration.

The only chemical transformations (reactions) that take place on an oil and gas platform are the combustion reactions in the gas turbines, i.e. in the utility system. The outflows of the combustion chamber have a low heating value and a high temperature, in comparison to the inflows, illustrating that most chemical exergy is transformed into thermal exergy. In the processing plant, as no chemical reactions occur, the only changes in chemical exergy are associated with the mixing and separation operations.

Exergy destruction and losses

The exergy destroyed on the platform amounts to 65, 64 and 58 MW in the *start-life*, *plateau* and *end-life* cases, while the exergy lost amounts to 28, 29 and 50 MW, respectively. The exergy destruction share between the processing and utility plants is nearly unchanged (65–70 % to 30–35 %) for the *plateau*, *mid-decline* and *end-life* cases (Figure 5.11). However, the distribution of the exergy destruction per sub-system changes significantly. The exergy destruction in the processing plant is highest in the *plateau* case and smallest in the *end-life* situation, ranging from 16 to 19 MW.

Most exergy destruction takes place in the production manifold and gas treatment at the beginning of the field exploitation, while it mainly occurs in the gas recompression as the field approaches its end-life. These findings suggest that the small decrease of the exergy destruction in the *end-life* case, compared to the two others, results from the smaller heating demand in the separation and condensate stabilisation processes, as the irreversibilities taking place in the heaters are reduced by more than 75 %. On the contrary, the exergy losses of the overall platform rise with time (Figure 5.12), because of the greater flow of produced water. Smaller amounts of heat are required: the exhaust gases are therefore rejected with higher temperature and physical exergy.

The total exergy destruction and losses represent more than 150 % of the total power consumption, and a further investigation illustrates in details their locations and causes:

- combustion chambers (chemical reaction, mixing, friction and heat transfer);
- produced water rejection (only in end-life case, because of the large water production);
- exhaust gases exiting the waste heat recovery system (high temperature);
- coolers in the processing plant (large heat transfer across high temperature differences);
- compressors in the gas systems (low isentropic efficiency);
- anti-surge recycling (gas throttling and mixing at different conditions);

- oil pumping (during the loading process);
- valves in the production manifold (depressurisation of the reservoir fluids);
- flaring and venting;
- cooling water.

The specific exergy destruction per unit of produced gas and oil, on a standard volume basis, is about 70, 50 and 210 kWh per Sm^3 of oil equivalent. It decreases as the hydrocarbon production rate rises, and increases sharply after the peak production is passed, because of the gas recirculation around each compressor and the smaller production rate.

Table 5.3: Exergy inflows and outflows of the processing plant of the studied platform for the end-life low-energy production day.

Stream	$\dot{m}$ [10^3 kg/h]	$\dot{E}^{ph}$ [kW]	$\dot{E}^{mix}$ [kW]	$\dot{W}$ [kW]	e^{ph} [kJ/kg]	e^{mix} [kJ/kg]
In						
Well 1	195	1911	-772		35.4	-14
Well 2	227	1709	-574		27.1	-9
Well 3	152	973	-703		23.0	-17
Well 4	167	1273	-616		27.5	-13
Well 6	270	2246	-1091		30.0	-15
Well 7	2	167	-64		292	-112
Well 8	133	1700	-294		46.0	-8
Well 9	162	1553	-466		34.5	-10
Well 10	53	252	-675		17.2	-46
Well 13	71	554	-133		28.2	-7
TEG	255	11,258	0		159	0
Seawater	2302	0	0		0	0
Power				18,929		
Out						
Well 1	9	914	-291		354	-113
Well 2	11	1123	-359		354	-113
Well 3	8	731	-241		343	-113
Well 4	4	407	-135		341	-113
Well 6	11	1000	-325		343	-111
Well 7	2	169	-66		291	-113
Well 8	6	649	-204		360	-113
Well 9	4	444	-139		360	-113
Export wet gas	10	774	-322		276	-115
Wasted gas	0	25	-11		193	-85
TEG	255	9577	0		135	0
Fuel gas	7	492	-214		261	-113
Injection water	860	3607	0		15	0
Discharged water	1441	637	0		2	0
Produced water	1126	6156	-1		20	0
Oil	231	301	-2898		5	-45

At present, the total exergy destruction within the processing plant, for a *low-energy use* production day, amounts to 15,290 kW (Figure 5.13). It mostly takes place in subsystems where pressure is decreased (production manifold) or increased (gas compression) significantly. The exergy losses with flared and vented gases amount to about 4934.6 kW, of which chemical losses account for 4910 kW. Physical losses with cooling water amount to 637 kW.

Physical exergy losses with produced water amount to 6150 kW, and most is temperature-based, which implies that these losses may only be reduced by recovering this heat at very low ($\leq 50°C$) and low (50 to 100 °C) temperatures. When it comes to chemical exergy losses, the model of Szargut [221], which estimates the chemical exergy of liquid water to 900 kJ/kmol, predicts that the chemical exergy of the produced water effluent amounts to 15,630 kW. This model may be more appropriate that the model of Kotas [54], which estimates the chemical exergy of liquid water to 3180 kJ/kmol because of a different humidity at the dead state conditions. In all cases, using this exergy with the current technologies is challenging, and would imply exploiting the exergy potential related to the differences in chemical composition between the seawater and the produced water (e.g. salinity and other chemical compounds).

The main difference between low- and high-energy production days lies in the exergy destruction associated with the oil loading process. The overall storage and loading process destroys exergy, in the sense that oil was stored at the bottom and is brought again to the surface, where the potential energy and exergy are null. Similarly, the oil was brought in motion in the pumping process and is stored in shuttle tanks, where the kinetic exergy is dissipated.

The exergy destruction of the complete process operation is equal to 6640 kW for typical high energy production days, and this corresponds to the additional power consumption induced by the oil loading. The actual configuration of the system does not allow improvements, unless if more efficient loading pumps are integrated, and if losses through the pipelines can be reduced, which is hardly feasible in practice.

The exergy losses of the processing plant system do not vary, or very little, with the operating modes. The volumes of flared and vented gas are insensitive to the operation of the oil loading process, unless if more gas needs to be purged from the fuel gas handling process, and the same reasoning applies for the exergy rejected with produced and cooling water.

Potential and kinetic exergies were not considered, as no velocity or height measurements were available. In practice, kinetic exergy is destroyed, because the well-stream velocity is reduced between the wells and the separation plant. Similarly, potential exergy is destroyed when being converted into physical and kinetic exergies within the processing plant. These types of exergy are generally not taken into account, but it may be relevant to include them if alternative technologies exploiting the high pressure and velocity of the well-streams are implemented. Neglecting the contributions from the potential exergy does not have any impact on the overall exergy destruction if the streams enter and leave the platform at the same elevation. However, the height differences between the several process units may result in the assignment of some exergy destruction to the wrong system section.

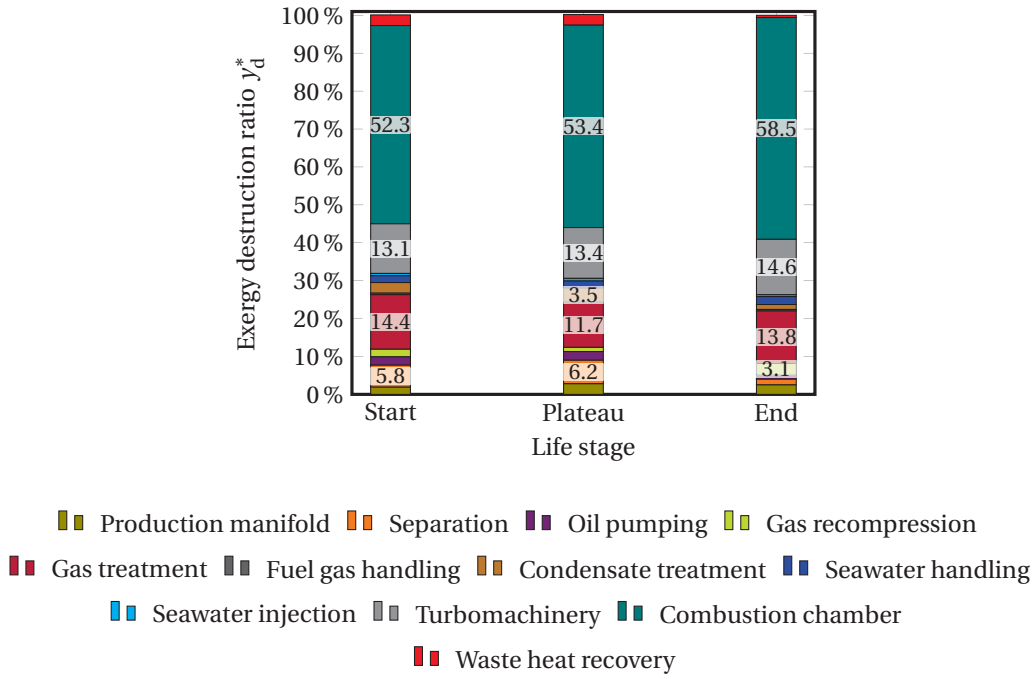

Figure 5.11: Distribution of the exergy destruction on an offshore platform at three life stages of the oil production.

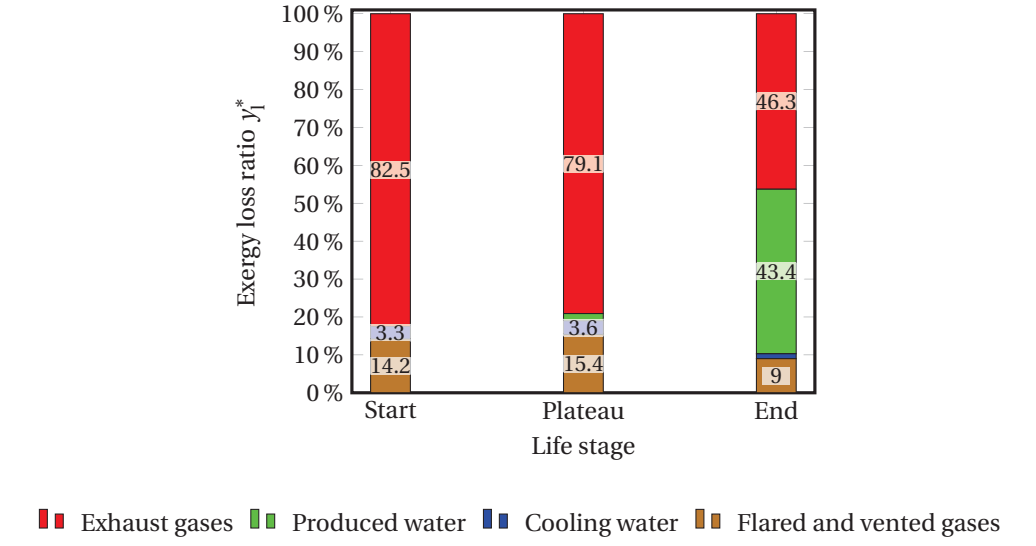

Figure 5.12: Distribution of the exergy losses on an offshore platform at three life stages of the oil production.

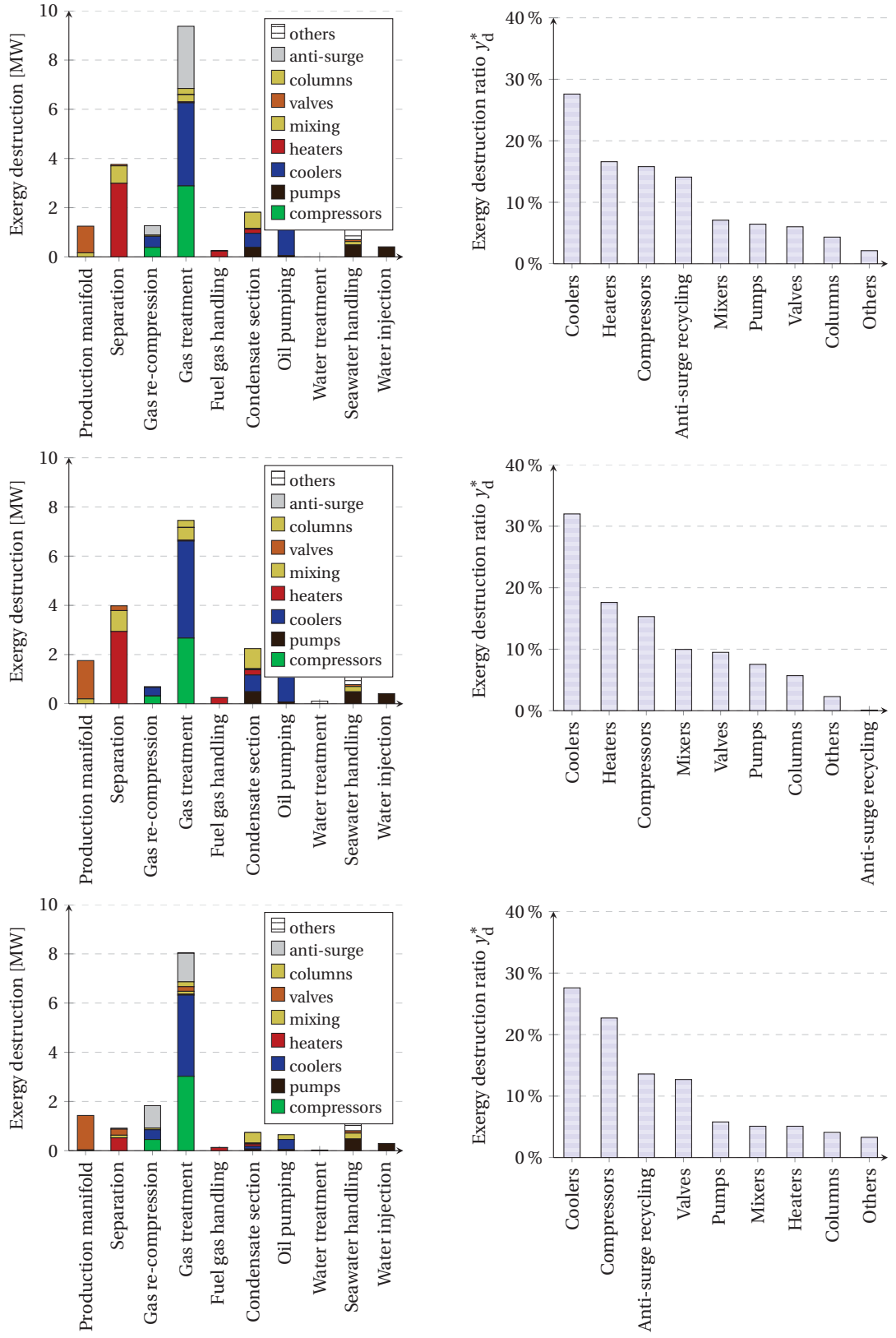

Figure 5.13: Exergy destruction share and ranking for the *early-life*, *peak* and *end-life* production, sorted by processes (left) and components (right), in the processing plant only.

Exergy-based indicators

The exergy intensity ι_χ and the exergy waste ω_χ amount to 2.5 % and 0.17 % for a *low-energy use* production day, and similar values are found for the *high-energy use* one. These values are sensibly similar to the energy intensity ι_h and the energy waste ω_h indicators, because the chemical energy and chemical exergy of hydrocarbons dominate the energy and exergy flows and differ by only ± 1.2 %. The trends are similar for both types of production days, but the oil loading system is responsible for a significant amount of destroyed exergy when operated. It ranks, in this case, as the second most exergy-destroying sub-system.

The four gas compressors have an exergetic efficiency of 79 %, 73 %, 74 % and 72 %, and the corresponding polytropic efficiencies are 74 %, 67 %, 69 % and 61 %. The heat exchangers display a low exergetic efficiency, in the range of 2–17 % for the coolers, as exergy is transferred across a large temperature gap from the hot gases to the cooling seawater. The heaters and internal heat exchangers are more performant, with an exergetic efficiency of 35–65 %, since exergy is exchanged at a higher heat transfer temperature. No meaningful exergetic product can be defined for the throttling valves, since they are operated above the dead state conditions and are therefore dissipative by design. An alternative may be to assume that such components have an exergetic efficiency of 0 %, considering that a throttling valve acts as an expander without any work production. It should be noticed that the most efficient components (e.g. compressors) may also be the most exergy-destroying ones (Figure 5.14).

The four gas compressors in the gas recompression and treatment sections display an exergetic efficiency of 70 to 80 %, which varies in a range of ± 5 % over time. They have the highest performance in the *peak* production case, as they are designed for such operating conditions. The efficiencies for these turbomachinery components do not vary significantly over time, as the gas flow rates at their inlets are adjusted by gas recirculation, and regular service and maintenance activities are targeted to eliminate the negative effects of degradation and fouling.

The seawater coolers have an exergetic efficiency lower than 20 %, while the crude oil heater in the separation process has an efficiency of about 49 % in *peak* conditions, and 37 % in *end-life* ones. This sharp decrease results from the worse matching of the temperature profiles of the glycol loop and of the crude oil, illustrating the unbalanced behaviour of the heat exchanger. The gas turbines, which are run in part-load conditions, have an exergetic efficiency lower than 25 %.

The rest of this study focuses on an improved use of the waste heat from the exhaust gases and hot gases, as these measures could reduce significantly the exergy destruction and losses of an offshore platform. The integration of heat pumping of the low-temperature heat below 130 °C to temperatures above 200 °C is not considered, because of the self-sufficient pocket between 60 and 100 °C and since this would require a significant temperature lift. The use of heat pumping may be relevant for platforms on which low-temperature heating is required, as it is the case for viscous oils.

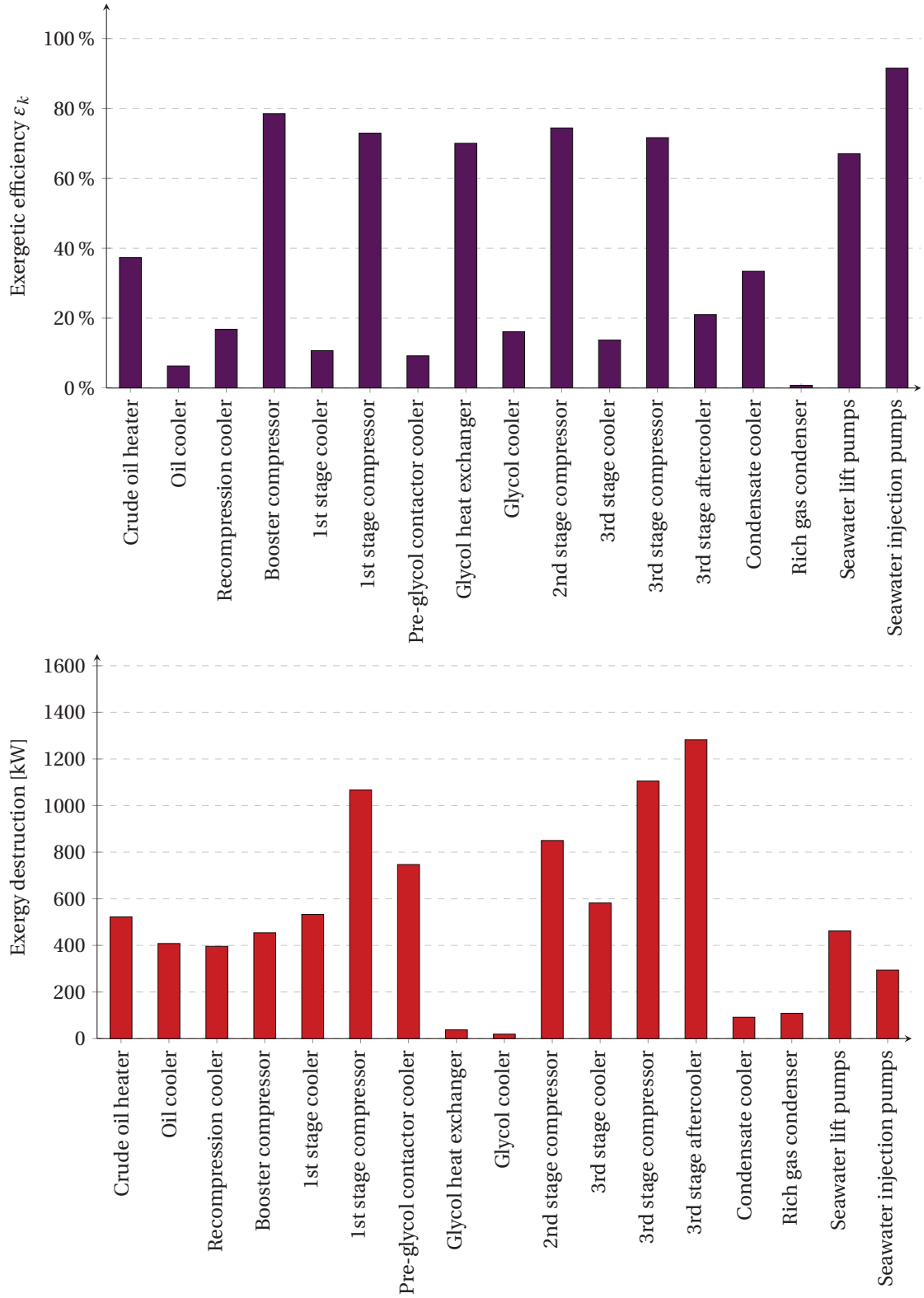

Figure 5.14: Exergy efficiency and destruction of the main processing plant components.

5.4.4 Efficiency trends

The most common field events that have an impact on the efficiency of oil and gas processing are listed as follows, based on the observations of the platform of study. Their consequences are expressed in energy and exergy terms, and possible energy efficiency measures, which shine from the previous comparisons, are proposed.

Boundary conditions

- *Reservoir and export pressures:* a large differential between the reservoir and separation pressures results in (i) high power consumption in the gas treatment process to satisfy the gas export or injection requirements, and in (ii) large exergy destruction in the production manifolds (2–10 MW).

  Two possibilities are (i) to operate the production manifolds at multiple pressure levels, to reduce the compression demand, and (ii) to install multiphase expanders, to produce power from the pressure reduction process. However, *the reservoir pressure decreases over time*, implying that more energy is required to lift the reservoir fluid on-site, and that less exergy could be recovered. The well-fluids could possibly be re-routed from high-pressure manifolds to medium-pressure ones in such cases;

- *Reservoir temperature:* the heating and exergy demands of an offshore platform are directly correlated to the *reservoir temperature*, as the separation between the oil, gas and water phases generally takes place at temperatures between 50 and 100 °C. There may be either gas or produced water streams available in these ranges of temperature, and this suggests that process integration efforts should be regarded carefully from the beginning of the exploitation. Reliability aspects should be considered to ensure a secure oil production;

- *Reservoir fluid composition:* the content of medium- and heavy-weight hydrocarbons has a direct impact on the process design. Significant heating and distillation columns may be required to achieve the desired separation between the oil and gas phases. This heating demand may be important and decreases with the oil production. This indicates that the utility plant should be flexible enough to satisfy both the heating and power requirements. The integration of a steam Rankine cycle can be promising, as this could be combined with steam extraction to satisfy the heating needs of the platform, and the steam network could be run in full condensation mode if the heating demand becomes insignificant;

- *Gas production:* the gas-to-oil ratio generally increases over the field life, but the absolute gas production decreases after reaching a production peak. High gas production leads to high power consumption in the gas re-compression and compression sections because of the large flows to handle. Low gas production, in start- and end-life situations, results in gas recycling around the compressors for operating and safety issues, which

contributes to high exergy destruction in the recirculation loops (valves and coolers) as well as in the compressors. The same effect can be observed for pumps and recirculation to prevent cavitation, although the amount of exergy destroyed is much smaller;

- *Water production:* the water-to-oil ratio continually increases with time, as well as the absolute water production. The exergy destruction in the produced water system is negligible (under a few hundreds kW) at the level of the processing plant, but more separation work should be performed to separate the oil, gas and water phases.

Operating strategies

- *Gas lift and injection:* gas lift and injection are energy-intensive techniques practised to maximise the liquid throughput. Gas should be compressed to a pressure greater than the hydrostatic pressure of the reservoir fluid, and this impacts both the power (compressors) and the cooling demands (seawater);

- *Water injection:* as for gas lift, water injection is an energy-intensive process, as large quantities of power are consumed in the pumping operations. Seawater has been used to support the reservoir pressure and enhance the oil displacement. The use of produced water is challenging: solid sulphates (e.g. $BaSO_4$) may precipitate, and seawater should be added in all cases to avoid reservoir deterioration. The use of cooling water is, on the contrary, already practised on several platforms such as Ekofisk [120]. It allows for smaller power consumption and moderate exergy losses, since the cooling water is already at a pressure higher than the atmospheric one. In the case that a steam cycle is integrated, the cooling water from the steam condenser may also be used for injection;

- *Gas import:* a low gas production may result in gas import from another field, either for gas lift and injection or for power generation purposes. Depending on the import pressure, further compression and cooling may be required;

- *Equipment redundancy:* the use of redundant components in parallel, such as gas turbines, leads to lower efficiencies of these components, and additional power consumption. A different design may be preferable, by using 3 gas turbines instead of 2, which would operate at a better load point and with a higher efficiency, so at the end the losses might be lower. The integration of bottoming cycles to gas turbines may be considered, as it adds more flexibility and stability to the power generation plant.

These trends and variations suggest that a high efficiency over the whole operating range is of interest, rather than a very high efficiency at *peak* conditions, and a significantly lower one in part-load, during the other production phases.

5.5 Conclusion

A real-case offshore platform was modelled using measured and reconciliated data, and its performance was assessed by performing energy-, total site- and exergy-based assessments. The material and energy flows under two types of production days were derived and validated by comparison with the available measurements.

The total power consumption amounts to 18,590 kW and can reach 25,500 kW when oil is loaded and exported to the coast. The heating demand is minor in comparison and is met by electrical heating and heat recovery from a glycol loop. Power is mostly consumed to increase the pressure of the produced gas in the recompression and compression sections, while heat is used for enhancing the hydrocarbon separation in the condensate treatment and glycol regeneration system.

As suggested in related studies, exergy is mainly destroyed in subsystems where the pressure is significantly reduced (throttling in well-heads and production manifolds) or increased (compression in gas treatment and recompression), because of the turbomachinery inefficiencies and the temperature differences in the coolers. The process waste heat can hardly be recovered because of the temperature and enthalpy mismatches between process streams, and the inadequate temperature levels of the utilities.

The exergetic efficiencies ranged between 2–17 % for the coolers, exceeded 35 % for the heaters, 60 % for the compressors and 70 % for the large pumps. Anti-surge recycling around the compressors is practised at a ratio of 17 to 65 % as a consequence of the smaller oil and gas flows entering the plant. Exergy is lost to the environment with flared and vented gases, and with produced and cooling water not used for water injection.

The life performance of an oil and platform was assessed by modelling the same facility in two exploitation periods, using the same tools. The energy demands, exergy destruction and losses change significantly with time, with an absolute variation of about 15, 7 and 22 MW, respectively, because of the variations of the produced oil, gas and water flows, and the changes in operating strategies. Similar trends were identified: the irreversibilities in the heat exchangers were significant during the whole exploitation period, while the ones caused by gas recirculation were remarkable only in the start- and end-life production periods.

6 Comparison

This chapter presents a detailed assessment of four North Sea offshore platforms, of which one is the main case study of this PhD project. They differ by their working and boundary conditions, and their performances are compared, using exergy analysis and system integration methods. The main results of this work are presented in Voldsund et al. [173], and they are used as well in the study described in Nguyen et al. [214]. The present findings are further compared to the ones obtained for two Brazilian platforms described in the literature.

6.1 Introduction

Oil and gas platforms differ by their reservoir characteristics, product requirements and operating strategies. However, the structural design of the processing plant stays similar, as the main purpose of such facilities is to recover oil and gas and to prepare them for export.

The research presented in this chapter aims at comparing systematically different facilities: the platforms analysed by Voldsund et al. [172] (named Platform A in this study) and by Nguyen et al. [214] (Draugen, further called Platform D) are compared against two other offshore platforms operating in the North Sea (Platforms B and C), and with the platforms investigated by de Oliveira Jr. and Van Hombeeck [59] (Platform E) and Barrera et al. [222] (Platform F). The main points of the present work are therefore to:

(1) describe and compare four different oil and gas platforms located in the North Sea, which serve as main case studies in the further chapters;

(2) evaluate their energy demands and investigate the locations and extents of the system imperfections;

(3) quantify to which extent the differences are due to the technologies employed on the facilities and to external factors;

(4) extend the discussion of the results to two other platforms.

6.2 Case studies

6.2.1 Platform A

The first platform investigated in this study, namely *Platform A*, was built and started-up more than 20 years ago (i.e. before 1995), and it operates in the North Sea region. This facility displays the typical processes that are generally present on the platforms located in this oil region [11], with the exception of the gas dehydration module (Figure 6.1).

The main aim has been to maximise the oil production, which is pumped to a nearby platform, and transported through a dedicated system to a terminal in western Norway. The associated gas is compressed and injected at high-pressure in the reservoir for pressure support, and the produced water is cleaned and discharged into the sea. Pressure maintenance is also ensured by water injection into dedicated wells, but this water comes from another facility.

The gas- and water-to-oil ratios currently increase, whilst the oil production decreases. The gas compression trains are therefore run at full-load, while the gas recompression section is run at severe off-design conditions. The reservoir fluid streams enter the production manifolds at high temperatures (80–90 °C) and pressures (80–170 bar), and they are further mixed, resulting in a feed stream with about 80 % of gas and at 71 bar.

The pressure is reduced down to 2.8 bar in the separation sub-system, and produced water is recovered from the three separation stages. The water content is further decreased in an electrostatic coalescer, and the stabilised oil enters the export sub-system, in which the pressure is increased in two steps with a booster and an export pump to 32 bar.

The gas exiting the 2nd and 3rd stage separators enters the recompression train, in which its pressure is increased up to the initial feed pressure of 70 bar. The recompression train consists of three compression stages, each including a cooler, a scrubber and a compressor. The addition of the cooler results in a smaller temperature at the inlet of the compressor, which in turn results in smaller power consumption.

The gas recovered from the separation and recompression sections is sent to the gas treatment sub-system, which consists of three parallel reinjection trains with two stages each. The third re-injection train was installed after the two others to handle greater gas flow rates, since it was decided to extend the exploitation period of the field. Gas is reinjected at 236 bar through five specific wells. The condensate flows from the numerous scrubbers are sent back to the separation train and are, in some cases, processed through a drain section in which their pressure is increased to the 2nd-stage separation pressure. Part of the gas recovered at the 1st-stage separator enters the fuel gas handling, in which it is heated before entering the gas turbines. Gas may be flared in order to keep a safe and stable production.

The power demand of the entire platform amounts to about 34 MW, of which 24 MW are consumed in the oil and gas processing plant.

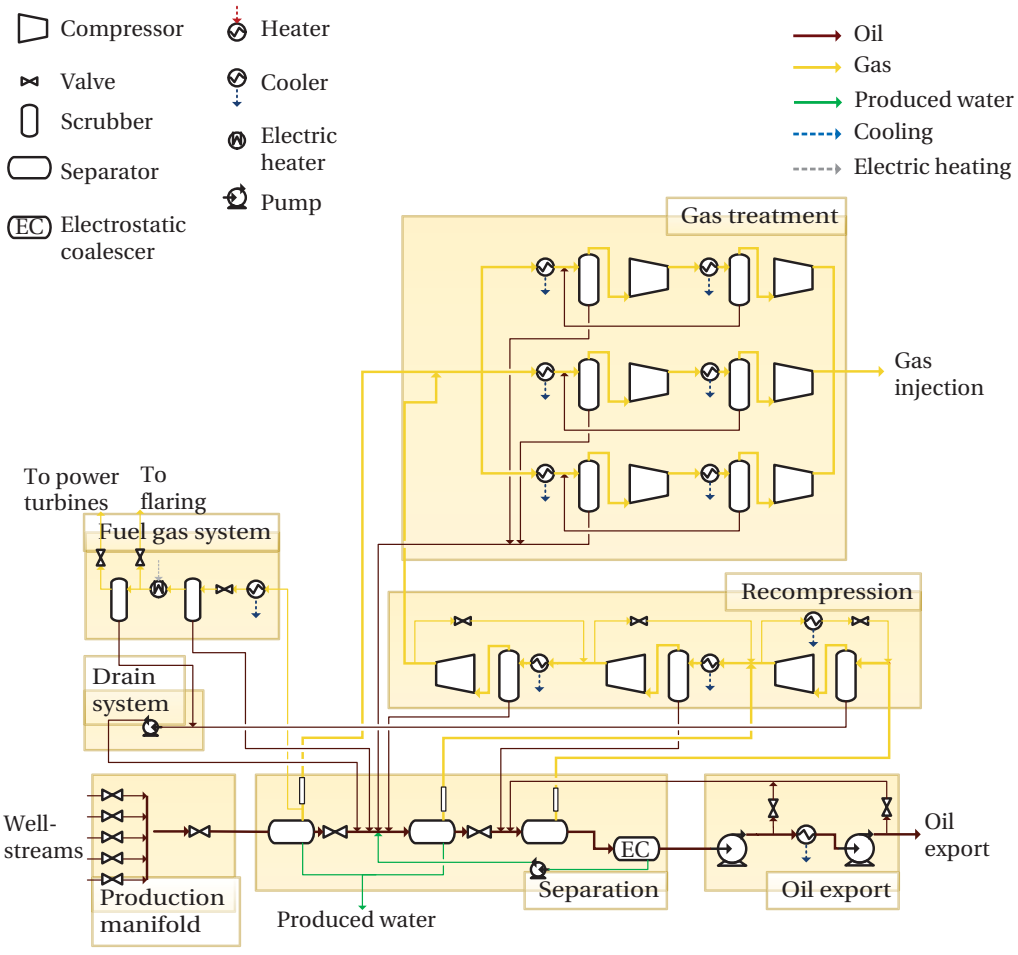

Figure 6.1: Process flow diagram of Platform A.

6.2.2 Platform B

The second platform investigated in this study, namely *Platform B*, is about 10 years old (i.e. was started up in the period 2000–2005), and it lies in the Norwegian North Sea. This facility operates on a gas and light oil (condensate) field, and presents the same processes as on Platform A, but with a smaller number of compression stages (Figure 6.2).

At the difference of Platform A, both gas and condensate are exported: the rich gas is exported through a pipeline network and most is treated in a gas processing plant on-shore, while the condensate is sent to an oil processing plant via other pipelines. The gas and condensate are recovered by pressure depletion, and the produced water is treated and rejected. Neither gas nor water injections take place on this facility.

The gas- and water-to-oil ratios currently increase, but the water production is particularly small, illustrating that the field is between its early- and peak-life phases. The gas recompression trains are run under their nominal loads. The reservoir fluid streams enter the production manifolds at very high temperatures (60–110 °C) and pressures (120–160 bar), and they are mixed before entering the separation sub-system. The resulting feed stream contains about 95 % of gas and is processed in the first separators at a pressure of 134 bar.

The 1st 3-phase separator is complemented upstream by a phase splitter, which was installed later than the other separators, because of a larger gas production than expected. This additional component allowed for a capacity upgrade, because, in design conditions, about 30–50 % of the incoming gas can bypass the 1st-stage separator.

The separation sub-system is divided in three stages and the pressure is reduced down to 2.4 bar. The produced oil is then pumped to 107 bar in two stages, while the produced water is sent to the water treatment. The recovered gas from the 2nd and 3rd stage separators goes through the recompression section, designed with four compression stages, with a cooler, scrubber and compressor. The 4th stage also includes an internal heat exchanger, in which the gas from the 3rd stage is cooled by condensate recovered in another part of the plant.

The gas recovered from the separation and recompression sections is sent to the gas treatment sub-system, which consists of a single stage with a cooler and a scrubber. There is no need for further compression, as the feed pressure complies with the pressure requirements of the pipeline network. The rich gas is exported at a pressure of about 118 bar, after addition of mono-ethylene glycol to prevent hydrate formation in the pipelines, and the condensate flows re-enter the oil and gas separation process. Part of the gas from the recompression section enters the fuel gas handling, in which it is scrubbed, heated and filtered. It is further consumed in two parallel gas turbines. Each has a nominal capacity of 9.8 MW and consists of two stages (low- and high-pressure) compression and expansion, on a single shaft.

The power demand of the entire platform amounts to about 17.9 MW, of which most is consumed for the drilling operations.

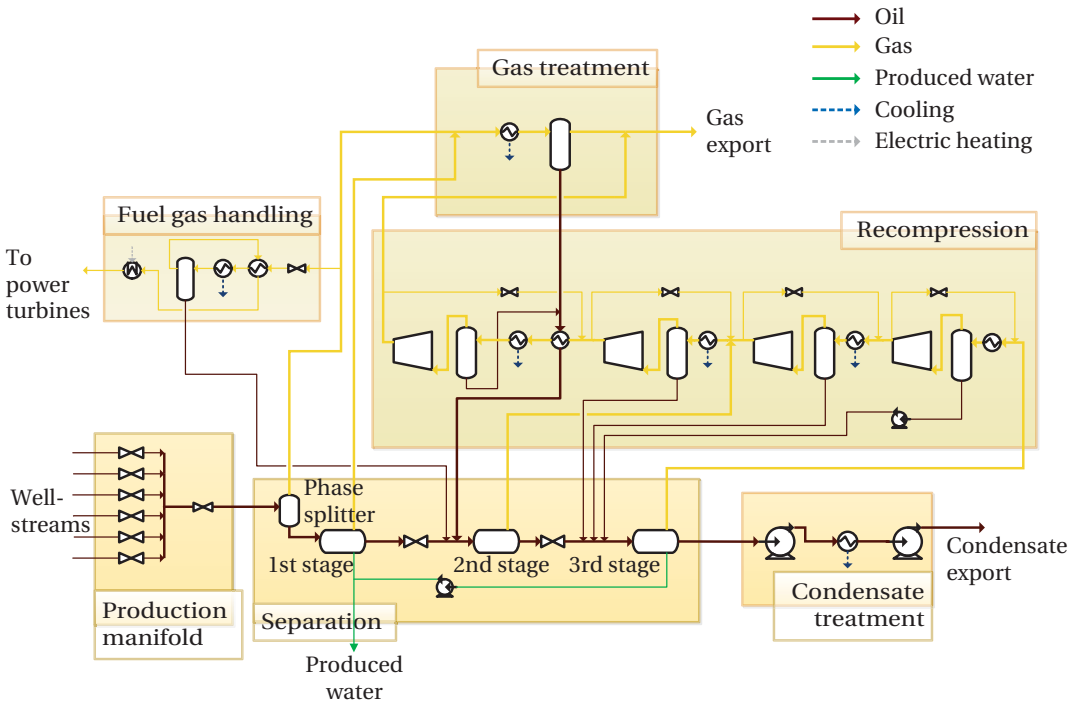

Figure 6.2: Process flow diagram of Platform B.

6.2.3 Platform C

The third platform investigated in this study, namely *Platform C*, is about 10 years old (i.e. was started up in the period 2000–2005). This facility processes heavy oil and gas, and presents the same processes as on Platforms A and B, but the heat exchanger network is more complex, including heaters and internal heat exchangers (Figure 6.3).

Only oil is exported: the associated gas is used for injection and reservoir fluid lift, and additional gas was actually imported from another platform during the first years of exploitation, since the gas-to-oil ratio of this field was initially very small. At present, the gas production is sufficient for oil recovery purposes, and water injection started recently. This analysis deals with data of an old production day, with gas import but without water injection.

The gas- and water-to-oil ratios currently increase, the oil production decreases, and the water extraction has been significant from the first years of exploitation. The reservoir fluid streams enter three production manifolds (high-pressure, low-pressure, and test) at high temperatures (50–75 °C) and at pressures varying between 10 and 110 bar. The high-pressure feed enters the 1st-stage separator at 46 bar, while the feeds from the low-pressure and test manifolds enter the separation train at the 2nd stage at 7–13 bar.

The pressure is reduced down to 2.4 bar, and produced water is recovered only from the 2nd and 3rd separation stages. The oil is heated between the 2nd and 3rd stages in two parallel trains, up to a temperature of about 95 °C, and is further stabilised in an electrostatic coalescer, before being pumped, cooled and exported at 99 bar.

Heating is required on this particular platform because of the heavy and viscous properties of the processed oil. It is ensured, in a first step, by recovering heat from the produced water and oil streams, and, in a second step, by waste heat recovery from the exhausts of the gas turbines on-site. The trains with the heat exchangers in parallel are designed for processing each half of the incoming oil, but they can be run in other modes if the water production is not sufficient. The recompression takes place in three stages.

The gas recovered from the separation and recompression sections is sent to the gas treatment sub-system, which consists of two compression stages. The fuel gas is extracted from the 1st-stage scrubber of the gas treatment, and the condensate flows are re-processed through the separation sub-system. The gas that is imported, if any, enters a parallel train at about 110 bar and is compressed to 184 bar, it is then mixed with the associated gas and used for lift and injection. Three gas turbines are installed on-site, and each has a nominal capacity of 25 MW. The first gas turbine drives the compressors of the gas treatment train, as well as the 2nd and 3rd compressor of the recompression section. The other power demands are satisfied by the remaining two gas turbines.

The power demand of the entire platform is unknown, but the power demand of the processing plant itself is about 30 MW.

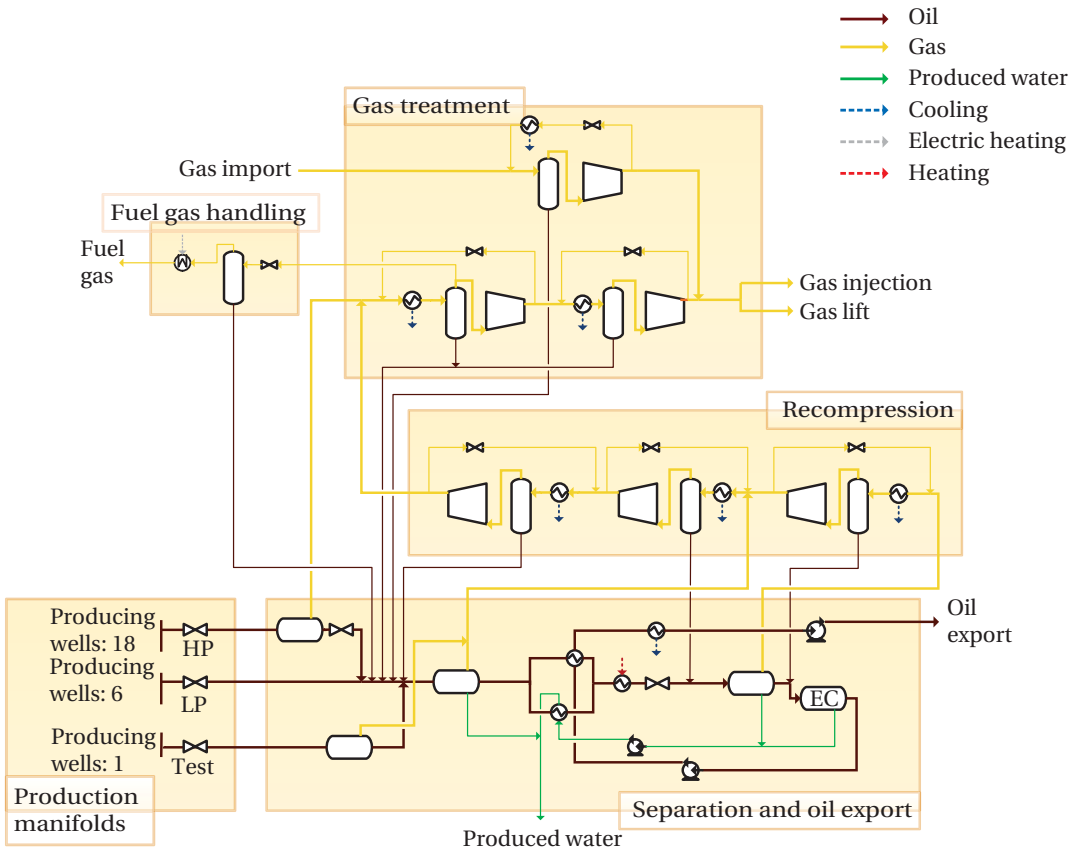

Figure 6.3: Process flow diagram of Platform C.

6.2.4 Platform E

Platform E is an offshore facility studied by de Oliveira Jr. and Van Hombeeck [59] and analysed in the works of Nakashima et al. [101] and Sánchez and de Oliveira Jr. [223], is located in the Brazilian Gulf. This platform is at least 15-20 years old: little information is given on the type of oil and gas extracted in this field. The overall facility presents the same processes as on Platforms A, B and C (Figure 6.4). The petroleum feed enters the processing plant at about 11 bar and 7.4 °C: it is heated by about 85 °C and the separation process includes two stages with a limit of 1.7 bar. Oil is pumped to 8.6 bar, gas is compressed and exported at 174 bar.

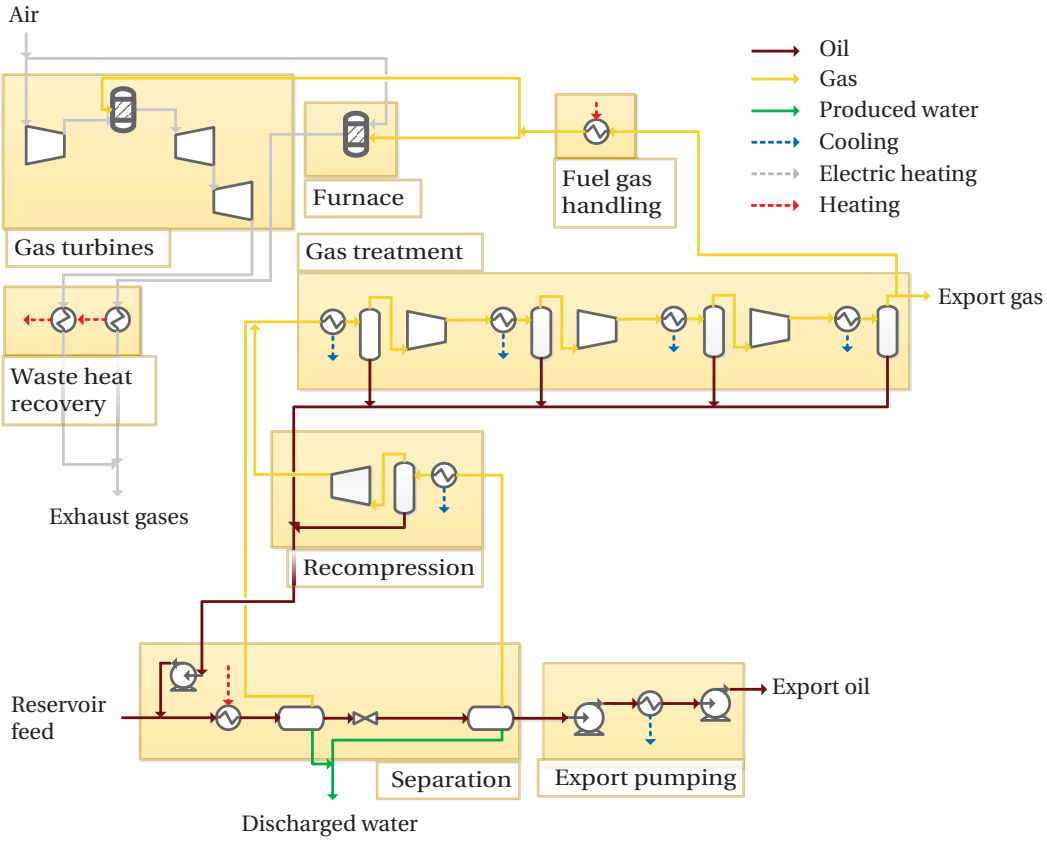

Figure 6.4: Process flow diagram of Platform E.

Heating is required as the initial feed temperature is not high enough to reach the desired degree of separation between the light and heavy hydrocarbons at the last separation stage. The compression sub-system consists of four compression stages, and the fuel gas is extracted at the last stage. At the difference of the four North Sea platforms investigated earlier, the waste heat that can be recovered from the exhaust gases is not sufficient for satisfying the heating needs of the processing plant, and additional fuel gas is therefore burnt in a furnace.

6.2.5 Platform F

Platform F, which is the second platform presented in this work located in the Brazilian oil region (Figure 6.5), is a Floating Production, Storage and Offloading (FPSO) unit operated by Petrobras [222]. Power and heat are generated on-site by combustion of the fuel gas extracted with oil and water. The design set-up is highly similar to the one of Platform C, with heat back-exchange and waste heat recovery from the gas turbines.

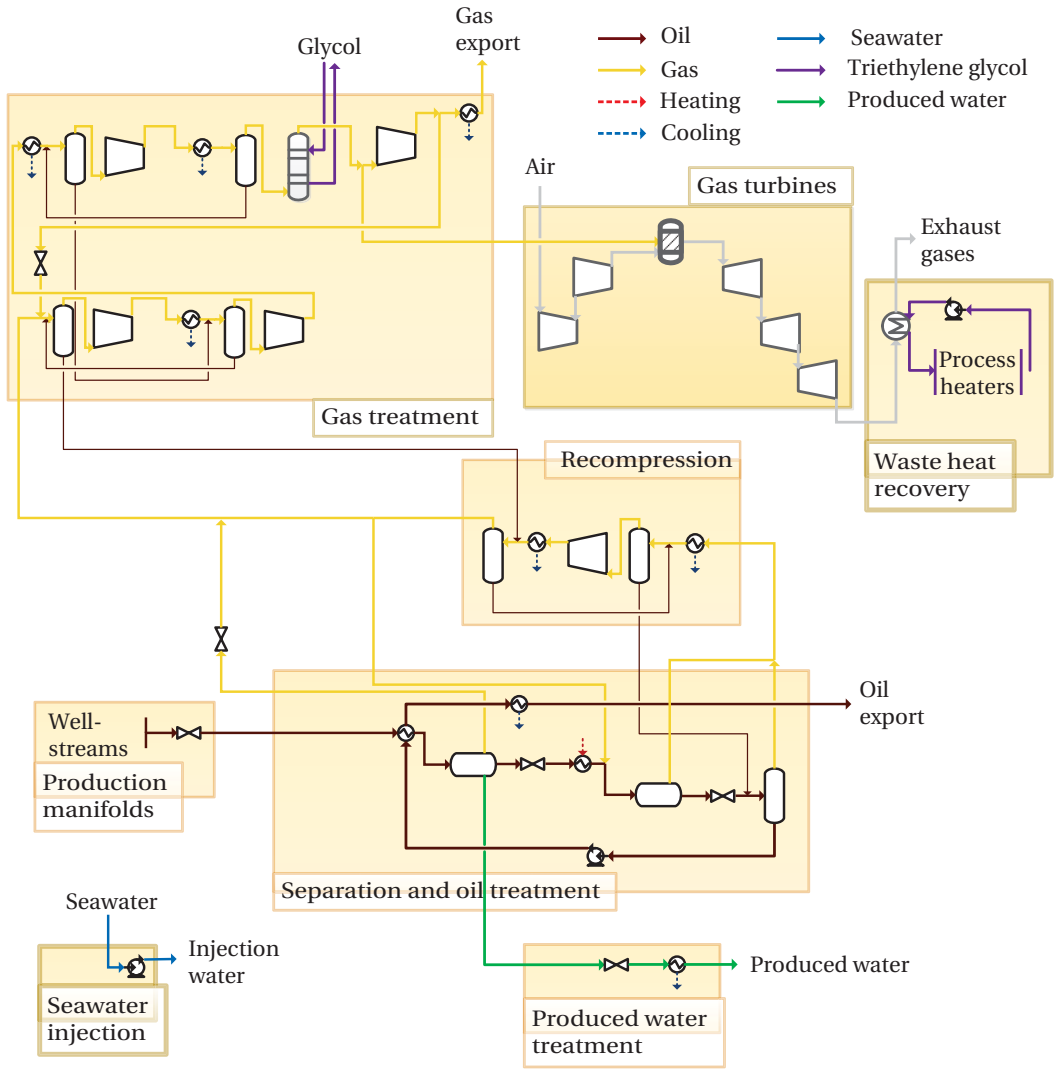

Figure 6.5: Process flow diagram of Platform F.

The petroleum extracted from this field has a temperature in the same order of magnitude as for the one of Platform C, but the viscosity is smaller, with an API of 30, and this classifies this type of oil as volatile. As for Platform D, there is a need for dehydrating the gas before export, and tri-ethylene glycol is used for this purpose.

6.2.6 Comparison

Boundaries

Platforms A, B and C are compared with the Draugen facility, named *Platform D*, and the focus is kept on the oil and gas processing plants (Figure 6.6). The measurements used for Platform D are the ones corresponding to the low-energy use production day, at end-life conditions, since these ones are the most representative of the current situation. Platforms E and F are not as extensively investigated because of the lack of information in the open literature.

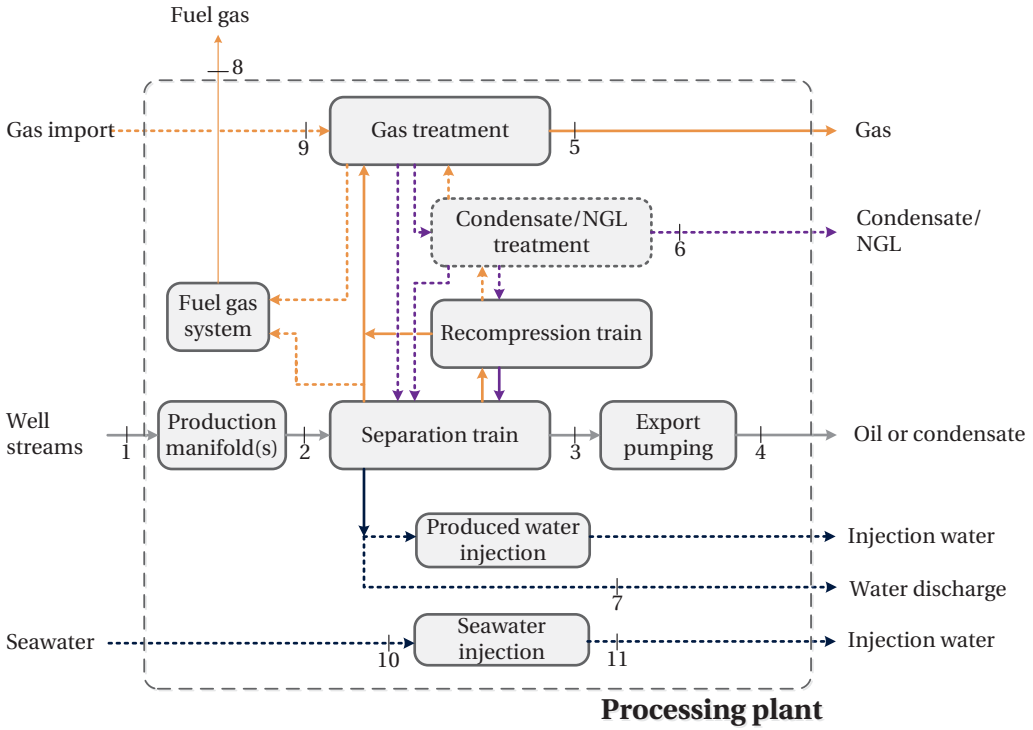

Figure 6.6: Schematic overview of the processing plant of an oil and gas platform.

The following sub-systems are not considered, as they are not part of the processing plant as such, or because they are not characterised by a significant energy use: (i) the seawater lift, which includes the pumps required to lift the seawater on-site; (ii) the cooling water system, where the seawater is distributed; (iii) the pilot flares and flare headers, where the unusable gas from various sections of the plant is burnt off and rejected to the atmosphere; (iv) the produced water treatment, where chemicals such as biocides are mixed with produced water to ease separation with impurities; and (v) the gas lift, where the pressure of the gas streams is reduced for easing petroleum recovery.

Flows

The gas-to-oil ratios and product flow rates vary markedly from one platform to another, illustrating some of the diversity that can be found for fields located in the North Sea oil region (Table 6.1).

Table 6.1: Gas-to-oil ratios and product flow rates for the studied oil and gas platforms. Gas-to-oil ratio is given on a standard volume basis, with a standard temperature of 15 °C and pressure of 1.013 bar.

	Platform A	Platform B	Platform C	Platform D
Gas-to-oil ratio [-]	2800	3200	320	230
Exported oil | condensate [Sm^3/h]	133	239	1147	271
Exported gas [10^3 Sm^3/h]	-	761	-	7.9
Injected gas [10^3 Sm^3/h]	369	-	363	-
Lift gas [10^3 Sm^3/h]	-	-	22	49.4
Produced water [Sm^3/h]	67	12	250	1110
Injected seawater [Sm^3/h]	-	-	-	890

Temperatures and pressures

Similarly, the temperatures (Table 6.2) and pressure (Table 6.3) levels are highly different for each field. The following points are essential for a better understanding of the outcomes of this research:

- pressure is *always* reduced in the production manifold and the separation train. The well-stream (p_1) and inlet separation pressures (p_2) vary between the platforms, while the outlet pressures (p_3) are *always* around 1.5 to 3 bar;
- heating is required, in the case of Platform C, to prevent problems with viscous emulsions and to enhance separation between the oil and water phases;
- the pressure of the produced oil or condensate is increased in the export pumping section (p_3 to p_4), and the final one depends on the export requirements;
- the gas treatment section differs between the platforms, depending on the properties of the incoming gas and on the end-use. For Platforms A, C, and D, the produced gas is compressed for lift and injection (high end-pressure p_5) or for export (low feed pressure p_2), while for Platform B, the gas does not need to be compressed (high initial feed pressure p_2);
- gas is imported and compressed (p_{10} to p_5) in the gas treatment section of Platform C;
- seawater is pressurised for injection on Platform D ($p_{11}$to p_{12}).

Table 6.2: Temperatures in the oil- and gas processing of the studied oil and gas platforms.

Stream number (type)	Platform A T [°C]	Platform B T [°C]	Platform C T [°C]	Platform D T [°C]
1 (reservoir fluids)	80–87	64–111	51–72	49–74
2 (reservoir fluids)	74	106	62[a], 65[b], 69[c]	59[d], 64[e], 63[c]
3 (oil/condensate)	55	62	97	63
4 (oil/condensate)	50	56	76	45
5 (treated gas)	78	35	75	81
6 (condensate)	-	-	-	68
7 (produced water)	73	78	72	55
8 (fuel gas)	54	50	61	59
9 (gas import)	-	-	4.4	-
10 (inlet seawater)	-	-	-	19
11 (injection seawater)	-	-	-	57

[a]From low pressure manifold.
[b]From high pressure manifold.
[c]From test manifold.
[d]From platform manifold.
[e]From subsea manifold.

Table 6.3: Pressures in the oil- and gas processing of the studied oil and gas platforms.

Stream number (type)	Platform A p [bar]	Platform B p [bar]	Platform C p [bar]	Platform D p [bar]
1 (reservoir fluids)	88–165	123–155	13–111	15–187
2 (reservoir fluids)	70	120	46[a], 7.0[b], 13[c]	7.8[d], 7.9[e], 8.0[c]
3 (oil/condensate)	2.8	2.4	2.7	1.7
4 (oil/condensate)	32	107	99	19
5 (treated gas)	236	118	184	179
6 (condensate)	-	-	-	179
7 (produced water)	9	61	7.2	1.3
8 (fuel gas)	18	37	39	21
9 (gas import)	-	-	110	-
10 (inlet seawater)	-	-	-	8.5
11 (injection seawater)	-	-	-	127[f]–147[g]

[a]From low pressure manifold.
[b]From high pressure manifold.
[c]From test manifold.
[d]From platform manifold.
[e]From subsea manifold.
[f]Pressure level 1.
[g]Pressure level 2.

Strategies

Anti-surge. The production flow rates change over the field lifetime, and some sections of the processing plant are run at lower rates than what they are designed for (Table 6.4), but the same final pressure should be kept. Gas needs to be recycled around the compression stages to keep a minimum flow rate through the centrifugal compressors and to prevent surge. The recirculated gas is also cooled and scrubbed to keep a low temperature and to remove the liquid resulting from the expansion.

Anti-surge recycling takes place in the recompression trains of all platforms, while it happens only on Platforms B and D for the gas treatment section, with the recirculation of the imported gas and produced gas. The gas recirculation in the recompression trains illustrates the decreasing oil throughput, whilst the recycling in the gas treatment sections reflects the decreasing gas production. No information on the anti-surge strategies was presented for Platforms E and F.

Table 6.4: Anti-surge recycle rates in the various compression sections of the studied oil and gas platforms, given as percentage of the flow through the compressors.

	Platform A	Platform B	Platform C	Platform D
Recompression train	69–92 %	4–34 %	19–41 %	65–75 %
Gas treatment, produced gas compression	0 %	-	0 %	5–35 %
Gas treatment, import gas compression	-	-	22 %	-

Heat exchanges. For all the North Sea platforms investigated in this work, the heating requirements were smaller than the heat contained in the exhaust gases from the gas turbines on-site, implying that no additional heat production was needed. Heat recovery in all cases was performed using an indirect heating medium, for operational reasons. In most cases, the cooling demand was satisfied by using an indirect cooling medium based on a 70 %wt water–30 %wt glycol to avoid corrosion of the heat exchangers in which hydrocarbons flow.

In the case of Platforms C and D, the heating demand in peak conditions exceeds 10 MW and the processing plant was designed to meet a given temperature specification of the oil entering the 2nd (Platform D) or 3rd separation stage (Platform C), easing the gas, oil and possibly water separation.

On Platform C, the crude oil entering the 3rd stage is preheated in two parallel heat exchangers, by cooling down the oil and produced water streams exiting the 3-phase separator. This *back-exchange* allows for a smaller external cooling demand in the oil treatment section, and for a smaller external heating one. If the water production is not sufficient, which was likely in *early-life* production, a greater oil flow may enter the oil–oil heat exchanger, and more heat may be extracted from the heating medium. On Platform D, only a certain fraction of the crude oil enters the 2nd stage heater, meaning that the remaining flow bypasses this heat exchanger.

6.3 Modelling and simulation

6.3.1 Process modelling

The reservoir fluids were simulated using a mix of real chemical components such as water and methane, as well as hypothetical components that describe the heavier oil fractions. The medium and heavy fractions of the crude oil are represented by 7 hypothetical components for Platform A, 12 for Platform B, 7 for Platform C, and 27 for Platform D. Their properties were given by the platform operators for the three first cases, and they were developed based on the crude oil assay for the last one. The comparison of the properties of the pseudo-components shows that one to two pseudo-components are generally used to model the medium-weight fractions, and one to model the very heavy ones, characterised by a molar mass over 500 g/mol. Only the main impurities, such as nitrogen and carbon dioxide, are considered, since the content of hydrogen sulphide of the petroleum feeds is negligible in all cases. The flows of corrosion inhibitors, such as mono-ethylene glycol, are not taken into account as they are only added in few quantities, and not always continuously.

Platforms A, C and D process oil, gas, and dirty water, and the Peng-Robinson equation of state (EOS) [163] was selected. Platform B processes gas and light oil, so light- and medium-weight hydrocarbons overall, and the Redlich-Kwong EOS with Soave modifications [162] was used. According to the literature, the use of the PR EOS would have been suitable for conducting the simulations of Platform B, while the SRK EOS may not be appropriate for the three other platforms, as the latter processes heavy-weight hydrocarbons. Aspen Hysys [147] version 7.3 and Aspen Plus [39] version 7.2 were used: the four platforms were simulated using both software and returned minor differences.

One typical production day was simulated for each platform, based on measured values, design data in the equipment documentation or values assumed based on discussions with the operators. The measured values are mean values for the simulated day for Platforms A, B and D, while the ones for Platform C are measured at 12:00, as time-averaged values were not available. The simulated days had stable conditions and the standard deviations for the flow rates of gas and oil were lower than 2 % and 3 %, respectively (Table 6.5).

Table 6.5: Standard deviation in measured flow rates of produced oil, condensate and gas for Platforms A, B and D for the simulated days.

		Platform A	Platform B	Platform C	Platform D
Exported oil	[Sm^3/h]	9	7	8*	2.2
	[%]	7	3	0.7*	0.80
Lift-, injected or exported gas	[Sm^3/h]	$\leq 0.8 \cdot 10^3$	$8 \cdot 10^3$	$6 \cdot 10^3$*	$55 \cdot 10^3$
	[%]	≤ 0.2	1.1	1.7*	0.7

The tolerance limits of the process models were set in order to have relative deviations between the in- and outflows smaller than $2 \cdot 10^{-5}$, both for mass and energy for all four platforms.

6.3.2 Exergy and total site analyses

The performance of the oil and gas platforms is analysed by using the same methods used for assessing Draugen (Chapter 5), and the control volume encompasses the processing plant of the oil and gas platforms only, to compare consistently all facilities. An exergoeconomic and an advanced exergy analysis are performed on Platforms A and D.

6.3.3 Exergoeconomic analysis

Platforms A and D are taken as case studies to investigate how the results from the performance evaluation methods resemble or differ with the field and operating conditions. The variability of the production flows over time is treated in two different ways. The first one is to consider three simulation cases with a constant feed volume flow, but with different phase compositions (approach for Platform A) [224]. The second one is to derive three case studies based on actual fiscal measurements, which describe the early-life, plateau and end-life production cases (approach for Platform D). The advantages of such an approach are to investigate at first the sensitivity of these costs to different boundary and operating conditions, and then to assess the changes in cost formation over time for a real case-study. A specific exergetic cost of 1 $/kJ is assumed for all well-streams.

For Platform A, the data used for the *near end-life* case include the measurements and simulation assumptions given in Voldsund et al. [172], while the early plateau and mid-decline cases are fictive simulation cases developed for the present study (Table 6.6). It can be argued that the use of secondary recovery methods results in a roughly constant flow of extracted feed [225], and the water, oil and gas fractions are varied.

Table 6.6: Aggregated fractions of the oil, gas and water phases in the composition of the feed streams, used for the simulation of Platform A.

	Plateau	Decline	End
Oil	115.4	97.1	11.5
Gas	404.1	331.2	40.5
Water	0	64.5	330.6

6.3.4 Advanced exergetic analysis

An advanced exergetic analysis aims, among other goals, at splitting the system inefficiencies into the avoidable, unavoidable, endogenous and exogenous subdivisions. The purpose is thus to assess whether the components to improve are, by priority, the combustion chambers, followed by the compressors and coolers operating in the last stages of the gas treatment process. For example, part of the exergy destruction is unavoidable, because of the current technological limitations related to the availability and/or material costs.

6.4 Performance evaluation

6.4.1 Site-scale analysis

The total heating demands vary greatly across platforms because of the significant differences in the chemical composition of the reservoir fluid:

- the largest heating demand for Platforms C, D and E corresponds to the crude oil heating in the separation process. All (Platforms C and E) or part (Platform D) of the oil from the 1st separation stage is heated to nearly 100 (Platforms C and E) and 70 °C (Platform D) to enhance the gas recovery. This heating demand is only present on these two facilities because of the high oil viscosity (Platform C), the large propane content (Platform D), or the low feed temperature (Platforms E and F);
- in the case of Platform D, the second largest heating demand is associated with stabilisation purposes in the first stripping column of the condensate treatment sub-system (Chapter 5). This heating demand is not found at the other platforms, as the proportion of medium-weight hydrocarbons was not high enough to justify the implementation of a more complex processing scheme;
- these major heating demands are currently covered, at least partially, by waste heat recovery from the exhaust gases of the gas turbines of the power generation sub-system. Waste heat is first transferred to a thermal loop, either with high-pressure water (Platform C), or with medium-pressure tri-ethylene glycol (Platform D), and then to the oil and condensate streams. The types of heating medium used on Platforms E and F are unknown;
- there exists a demand for fuel gas heating, which amounts in all cases between 100 and 500 kW and is performed by electric heating, as a fraction of the processed gas should be heated from 30–40 to 60–70 °C. Electric heating is also done to regenerate the glycol solution if gas dehydration is implemented on-site (Platforms D and F).
- Platform E differs by the use of a furnace to boost the heating production, implying that the natural gas consumption is not determined by the power consumption, at the difference of the five other platforms, but is directly impacted by the heating demand of the oil separation sub-system and the petroleum feed temperature.
- internal heat recovery on-site is not present on Platforms A and E, minor on Platforms B and D (≤ 2 MW), and significant on Platform C (≥ 5 MW). For Platform B, gas circulating in the gas recompression is used to preheat the condensate recovered from the gas treatment, while for Platform C, the oil and produced water recovered from the 2nd separation stage are used to preheat up to 60–70 °C by back-exchange with the reservoir fluid at the same stage. Back-exchange is also performed on Platform F, following the same scheme as for Platform C, but the heat from the produced water is not used.

The total cooling demand exceeds 20 MW, with a maximum of about 50 MW for Platform B and is characterised by:

- the gas cooling prior to the gas treatment section: the gas flows is cooled from temperatures between 70 and 140 °C to about 30 to 50 °C, in order to condense medium- and heavy-weight hydrocarbons, further removed in the scrubber, and to reduce the compression power;
- the gas cooling prior to the export or injection, in the gas treatment section: as in the gas recompression sub-system, the temperature is decreased to allow for condensation of the non-light hydrocarbons;
- the oil cooling after separation and stabilisation, to 25–30 °C, to reduce the pumping power and ease further export;
- the external cooling demand is satisfied by using seawater, either directly (Platform D), or indirectly (Platforms A, B and C), using a seawater-glycol loop as indirect cooling medium. Air is also used on Platform F for cooling down the gas flows within the gas treatment section.

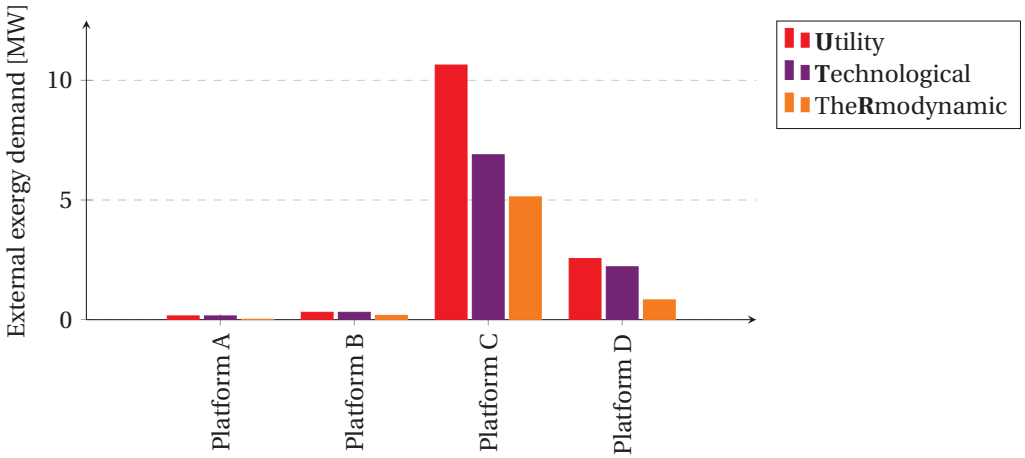

Figure 6.7: Multiple representation of the energy and exergy needs of the processing plants of Platforms A–D.

The representation of the energy needs of the processing plant (Figure 6.7), into its thermodynamic, technological and utility requirements, show that there is a large amount of exergy destroyed in the heat exchanger network. The total site profiles (Figure 6.8) illustrate the large temperature mismatches between the hot and cold streams, and that the integration of the overall system may be improved by a better match of the temperature profiles.

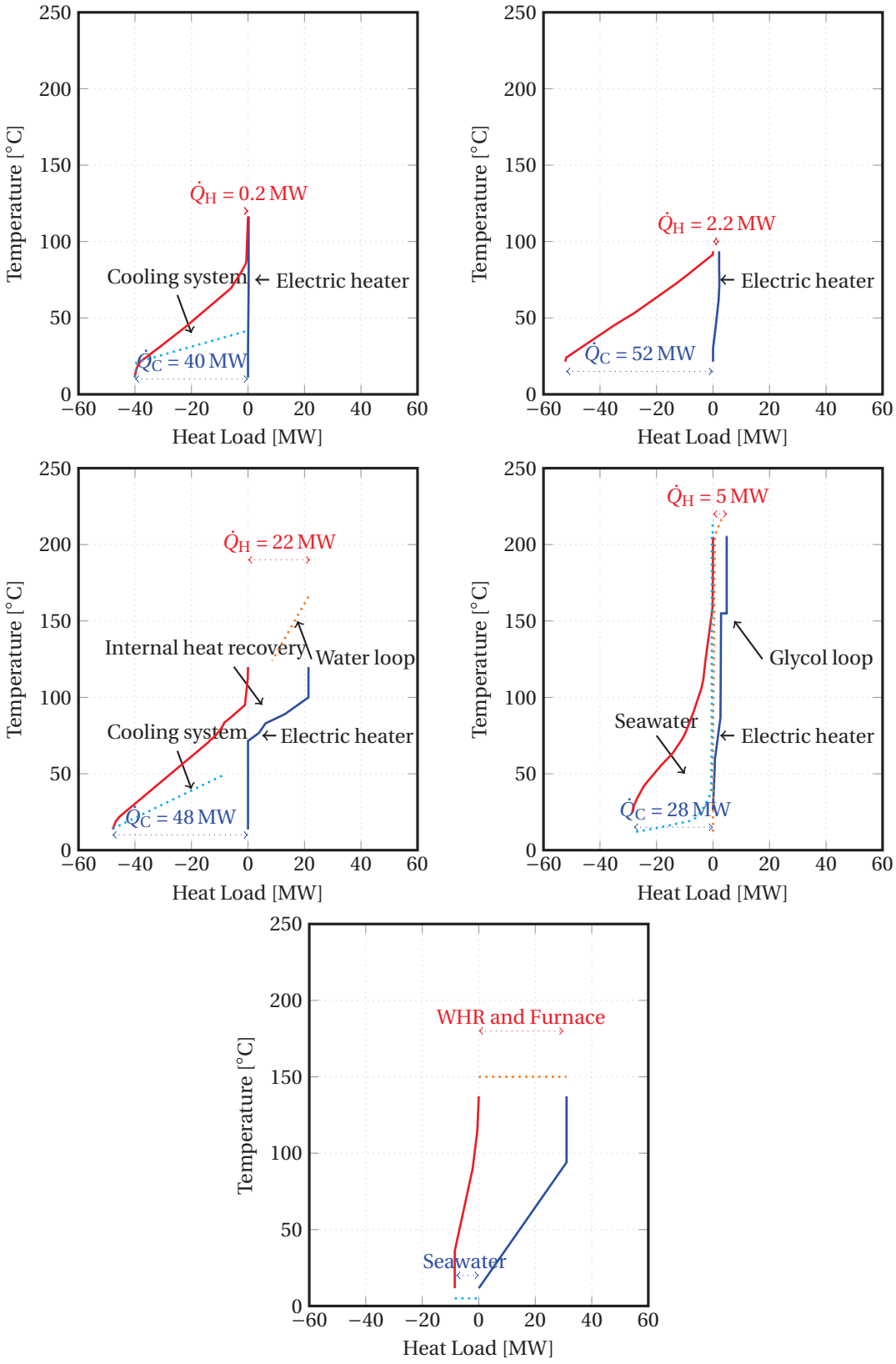

Figure 6.8: Total site profiles of four North Sea and one Brazilian offshore platforms.

6.4.2 Exergy analysis

North Sea platforms

The ambient pressure and temperature were taken as 1.013 bar and 8 °C [226], which is the average air temperature for the North Sea. The chemical exergy of the pure components were taken as presented by Kotas [54] for the real chemical compounds and calculated following the method of Rivero et al. [130] for the hypothetical components. Potential and kinetic exergy were assumed negligible in comparison with chemical and physical exergy. The exergy destruction in the heaters in Platforms B and C is assigned to the separation sub-system, as the heating demand results from the low temperatures in that section. The exergy destruction in the seawater coolers is allocated to the section in which the heat exchanger is integrated.

The amounts of exergy exported from each of the platforms as oil, condensate or gas are always greater than the consumption of exergy with heat and power (Table 6.7). The chemical exergy in the oil and gas that flows through the system is very high compared to the exergy changes within the system. The consumption of power and heat exergy is less than 2 % of the exergy exported for all the platforms.

The main sources of exergy losses on the four studied platforms include the discharge of produced water, the release of flared and vented gases to the atmosphere, and the rejection of cooling water to the sea. The exact amount of exergy losses with flared and vented gases varies from day to day, as gas flaring is not practised continuously. The chemical exergy of the flared gases at Platforms A and D are 4.9 and 4.7 MW for the days under study. Such losses can be reduced with the use of gas recovery systems, as already done on Platform C. Exergy losses with produced water are significant only in the cases of Platforms C and D, because of the high water-to-oil ratio, and this exergy is hardly usable within the processing plant because of the low associated temperature (50–75 °C).

Table 6.7: Exergy flows on the studied platforms (MW).

	Platform A	Platform B	Platform C	Platform D
Well streams and gas import, total exergy	$5.7{\cdot}10^3$	$11{\cdot}10^3$	$17\cdot10^3$	$3.8{\cdot}10^3$
Export streams, total exergy	$1.4{\cdot}10^3$	$11{\cdot}10^3$	$13\cdot10^3$	$3.0{\cdot}10^3$
Gas injection and lift, total exergy	$4.3{\cdot}10^3$	-	$4.3\cdot10^3$	$8.2{\cdot}10^2$
Power consumption	24.6	5.5	30	17.4
Heat consumption	0	0.3	7.2	1.8
Produced water, chemical exergy	0.94	0.17	3.6	16
Produced water, physical exergy	0.54	0.14	2.0	6.1
Flared gas, chemical exergy	4.9	1.1	0	4.7
Flared gas, physical exergy	≤ 0.03	≤ 0.01	0	≤ 0.1
Cooling medium, received thermal exergy	2.2	5.6	1.8	0.7

The power and heat exergy, which are consumed in each subsystem for the four platforms, are presented in absolute numbers and per oil equivalent in Figure 6.9 and Figure 6.10.

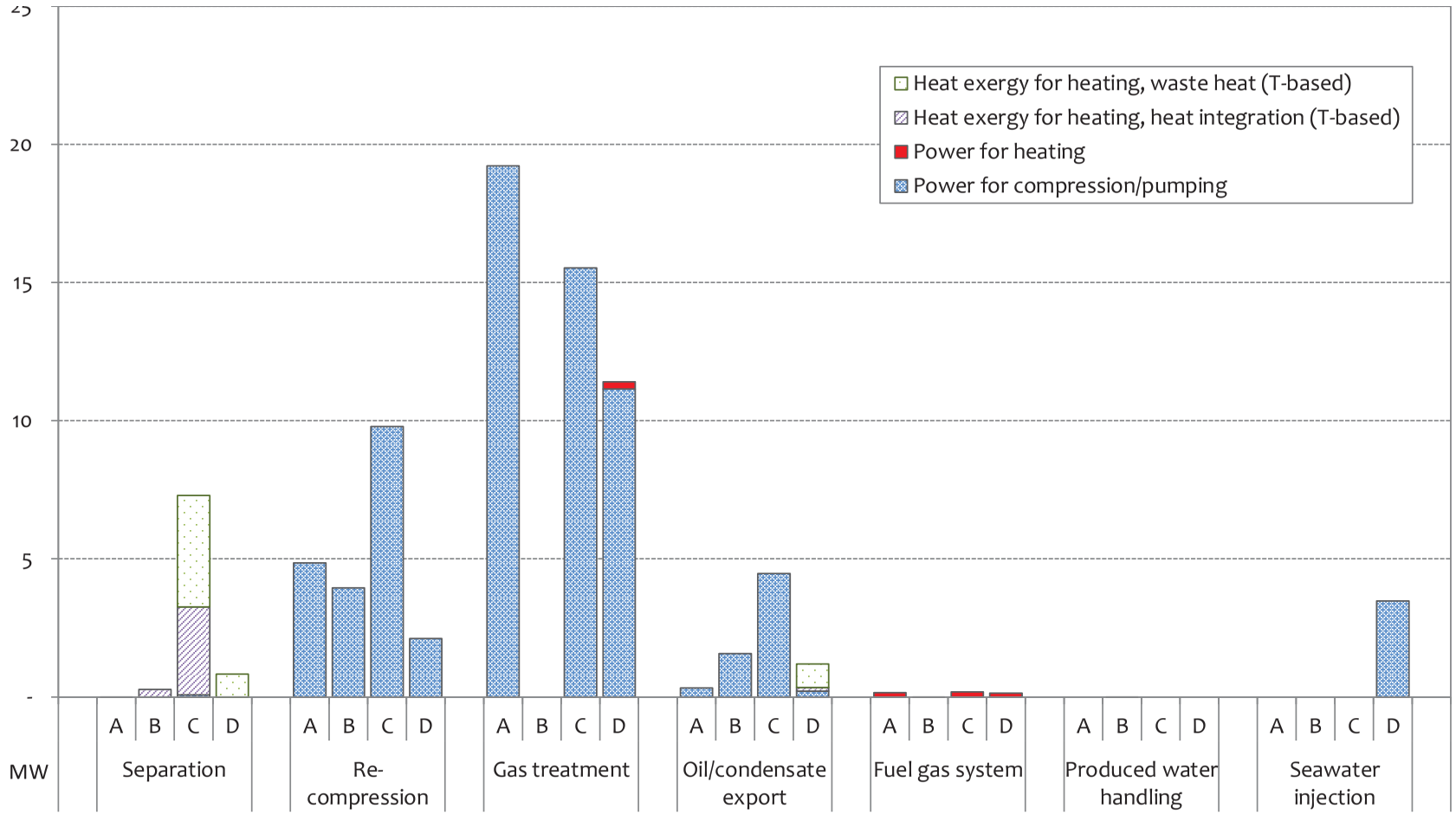

Figure 6.9: Power and heat exergy consumed in each subsystem for the studied platforms (Platforms A–D). The production manifolds are not included, since no power and heat exergy is consumed there. The thermal energy labelled 'waste heat' is from a heating medium that is heated with waste heat from the power turbines. The thermal energy labelled 'heat integration' is from heat integration with other process streams.

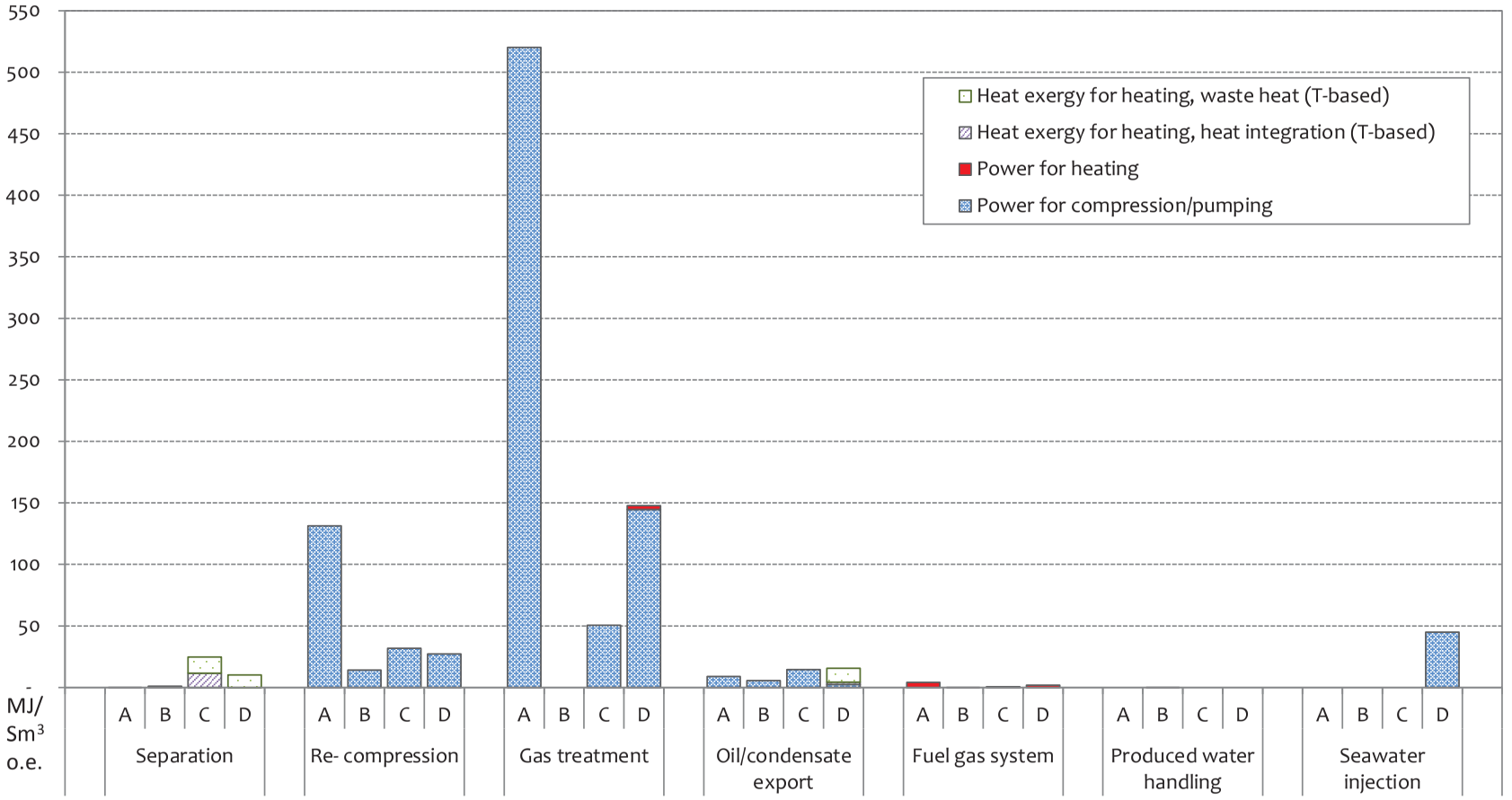

Figure 6.10: Power and heat exergy consumed per exported oil equivalent (o.e.) in each subsystem for the studied platforms (Platforms A–D). The production manifolds are not included, since no power and heat exergy is consumed there. The heat exergy labelled 'waste heat' is from a heating medium that is heated with waste heat from the power turbines. The thermal energy labelled 'heat integration' is from heat integration with other process streams. The following conversion factors are used when converting to o.e: 1 Sm^3 oil = 1 Sm^3 condensate = 1000 Sm^3 gas = 1 Sm^3 o.e.

The main outcomes of the comparison of these four facilities can be summarised as follows.

- power is mainly consumed for gas compression in the recompression, gas treatment and oil/condensate sections;
- the power consumption for increasing the seawater pressure is also significant, representing nearly 25 % of the total power demand;
- on the contrary, no power is required in the gas treatment section on Platform B, as the inlet separation pressure (p_1) is high enough to comply with the export specifications (p_5);
- the heat exergy demand is only significant for Platforms C and D, since heating is required for stabilising the oil and condensate streams;
- in all cases, the power used for electric heating of the fuel gas is negligible compared to the power consumption in the other sub-systems;
- the power and heat exergy consumed per oil equivalent is the highest for Platform A, followed by Platform D, while it is relatively small for Platforms B and C;
- the power exergy consumed per oil equivalent is particularly high in the gas treatment section on Platform A.

The highest contributions to the exergy destruction (Figure 6.11) on each platform are generally related to (i) throttling in production manifolds and separation trains; (ii) heat transfer in coolers, and (iii) compressor inefficiencies and recirculation. A more detailed investigation (Figure 6.12) pinpoints that:

- the exergy destruction in production manifolds represents 11–27 % of the total exergy destruction at the four platforms;
- throttling in separation trains accounts for 2–12 %;
- compressor inefficiencies account for 31–40 %, with the exception of Platform B where it amounts to only 13 %;
- gas cooling in the gas treatment section amounts to 33 % for Platform B;
- pressure loss in recycled streams amounts to 4–13 % for the four platforms;
- the crude oil heater makes up approximately 6 % and 4 % for Platforms C and D;
- the oil/condensate export system of Platform A accounts for 1 %, while for Platforms B–D it accounts for 6–10 %;
- exergy destruction in the fuel gas and water treatment sub-systems is minor.

The exergy destroyed per exported oil equivalent in each subsystem for the four platforms (Figure 6.13) show that Platforms A and D have clearly more inefficiencies per oil equivalent than Platforms B and C. They are older than the other two platforms and have export flow rates that are low compared to their peak production, which results in gas recirculation and thus high performance losses. Platform A has a high gas-to-oil ratio, injects gas and exports only oil. The injection of gas makes a high oil recovery from the reservoir possible but results in very high power consumption and exergy destruction. Platform D has a low gas-to-oil ratio, uses gas and seawater for lift and injection, and exports oil, gas and condensate. The high exergy destruction per exported oil equivalent results from the large amount of power required to compress the gas, and to the recycling of gas around the compressors, which results in nearly power consumption and exergy destruction.

Brazilian platforms

An exergy analysis was performed by de Oliveira Jr. and Van Hombeeck [59] on Platform E and was further conducted in the frame of this work to validate the process model, while it was performed by Barrera et al. [222] for Platform F. The compression operations are as well the main exergy consumers of the offshore plant, and the gas treatment operations are responsible for a a large share of the exergy destruction in the processing plant of an oil and gas platform ($\simeq$ 40 % for Platform F).

The main difference between the Brazilian and Norwegian platforms corresponds to the extent of the irreversibilities in the separation module, which are greater in the first case, both in relative ($\simeq$ 40 % for Platform F) and absolute ($\simeq$ 4 MW for Platform F) values. This trend is due to the petroleum heating operations, as it can also be depicted when comparing Platforms C and D to Platforms A and B.

The utility plant represents in all cases the lion's share of the total exergy destruction on an oil and gas facility, representing more than 65 % for Platforms C and D, and the same results are expected for Platforms A and B. Such conclusions were drawn by the authors of these studies, indicating that the inefficiencies associated with the combustion process on itself cannot be avoided, but that the overall system efficiency could be enhanced by integrating new separation technologies [59] or by a bottoming cycle [222]. The environmental impact of such facilities may be decreased by introducing a CO_2-capture plant, as suggested by Sánchez and de Oliveira Jr. [223].

Finally, all works on this topic conclude that most exergy flowing into an oil and gas platform is under the form of the chemical exergy associated with hydrocarbons, implying that most transits without being transformed into other forms of exergy on-site. The thermodynamic degree of perfection, called in other studies the total or input-output efficiency, reaches 98.99 % for Platform F, meaning that only 1 % of the initial feed exergy is lost in the form of heat losses or irreversibility in the process operations.

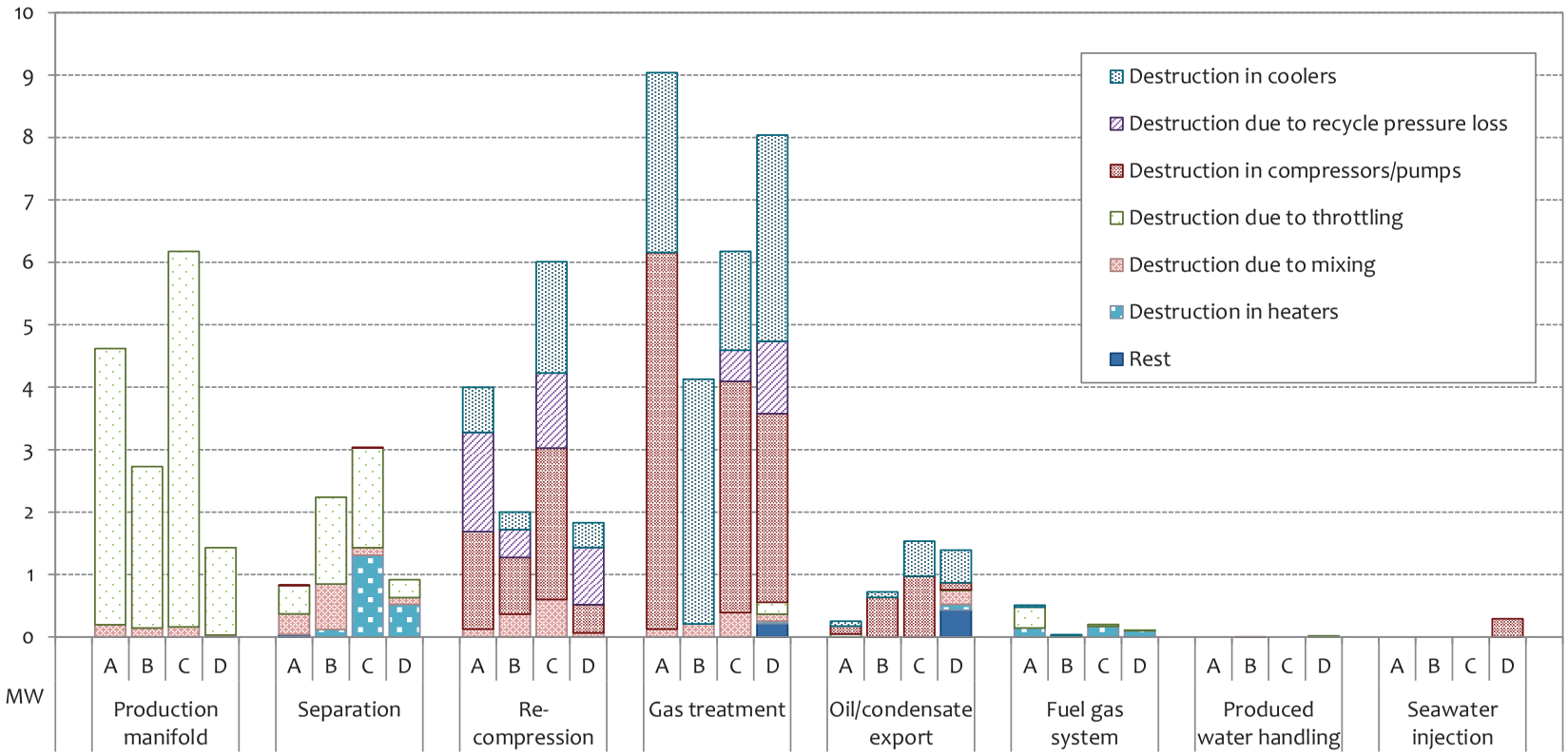

Figure 6.11: Exergy destruction in each subsystem for the studied platforms (Platforms A–D). The main sources of exergy destruction/loss in each subsystem are indicated with different colours, and smaller sources are lumped into 'rest'.

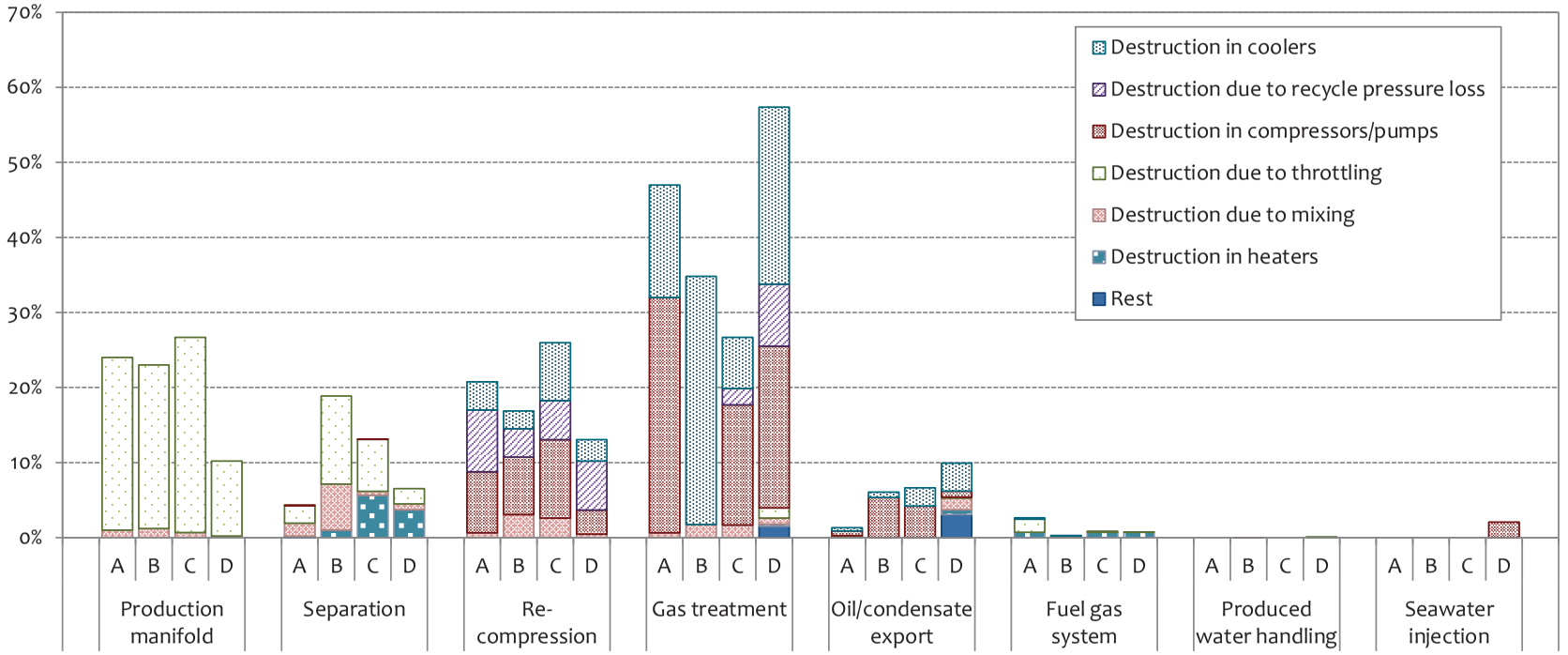

Figure 6.12: Percentage of exergy destruction in each subsystem for the studied platforms (Platforms A–D). The main sources of exergy destruction/loss in each subsystem are indicated with different colours, and smaller sources are lumped into 'rest'.

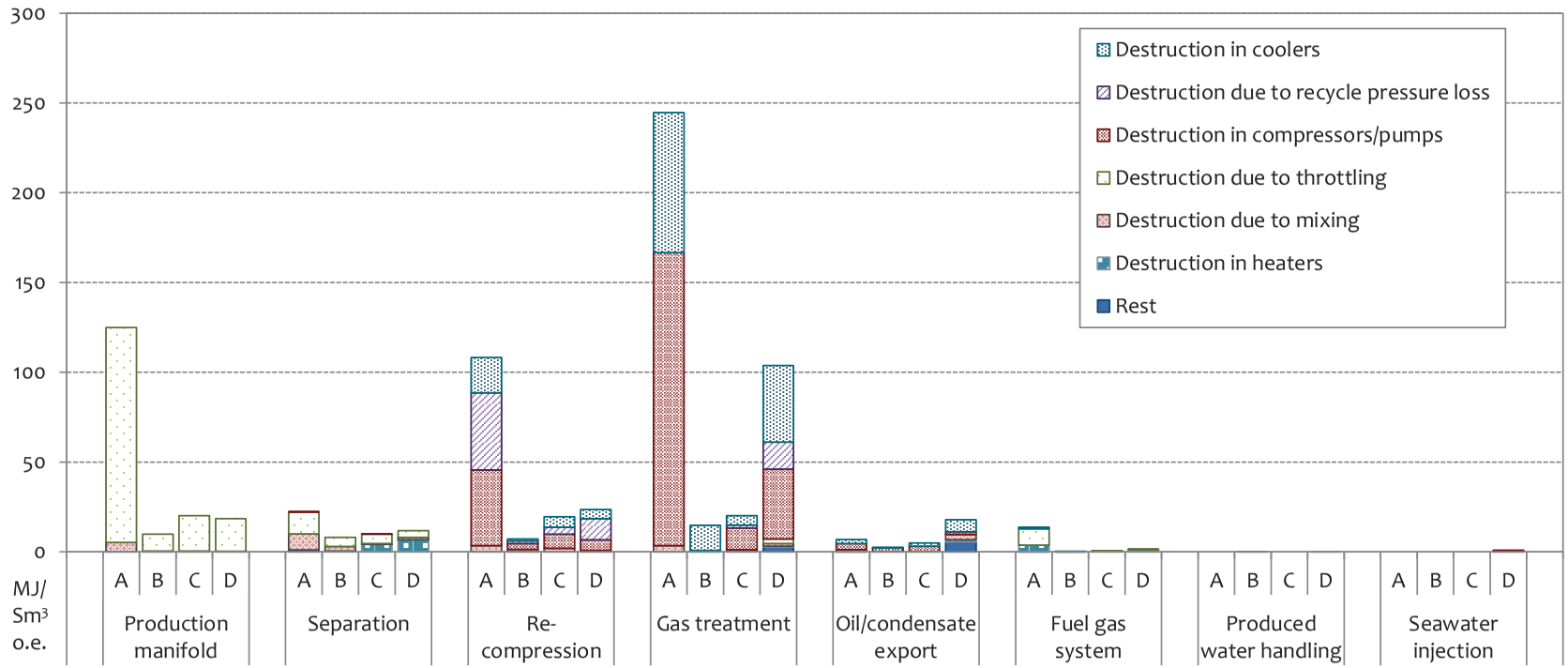

Figure 6.13: Exergy destruction per exported oil equivalent (o.e.) in each subsystem for the studied platforms (Platforms A–D). The main sources of exergy destruction/loss in each subsystem are indicated with different colours, and smaller sources are lumped into 'rest'.

6.4.3 Exergoeconomic analysis

Exergoeconomic flows

Cost formation. The exergoeconomic analysis shows that the main cost flows are associated with the exported oil and injected/exported gas flows. The ones corresponding to the produced water, fuel and exhaust gases are negligible in comparison, in all cases, and at all stages of the field lifetime. The largest contribution to the exergy cost inflows and outflows is related to the chemical exergy of the hydrocarbon compounds, as it could be expected. The cost flows associated with the physical exergy of a stream of matter represent, with the exception of produced water, less than 2–3 % of the total cost flows.

Two different trends can be observed when analysing the cost formation process and comparing Platforms A and D. In the first case, the gas flow display the highest specific c and absolute $\dot{C}$ exergetic costs. In the second case, the crude oil flow has the highest absolute exergetic cost ($\dot{C}_{\text{oil}}$ of 13.3 \$/s against $\dot{C}_{\text{gas}}$ of 1.18 \$/s for the peak case), but the produced gas still presents the highest specific one (c_{gas} of 3 \$/kJ against c_{oil} of 1.3 \$/kJ, for the same case).

The higher specific exergetic price for the gas flows derives from the cost build-up in the gas recompression and treatment processes. Power is consumed to increase the gas pressure, increasing in turn the exergetic value of the gas flows. In comparison, little power is required for pumping the oil flows, as it can be seen with the small increase of the specific exergetic cost of these streams. The produced water flows have the smallest specific and total exergetic costs: this is due to the separation of water from the petroleum feed at an early stage of the processing plant, implying that little, if none, exergy has been consumed.

Costing considerations. Considering different costs of physical and chemical exergy allows for a more accurate assessment of the cost formation process. This differentiation pinpoints that the specific cost of chemical exergy c^{ch} is nearly constant across all processes, varying in a range of ≃ 15–20 %, as the only chemical transformations on such systems are separation, mixing, and combustion reactions in the gas turbines. On the contrary, the specific cost of physical exergy c^{ch} increases sharply, with a rise of ≃ 110–310 % between the production manifolds and the outlet of the oil export and gas treatment sections. This rise is even more marked for the end-life cases, and the specific costs of the oil and gas physical exergy are ≃ 1000–2400 % greater than the feed ones.

Irreversibility costs

Exergy destruction cost. The most costly irreversibilities are related to the operations of the utility plant and gas treatment processes, and the findings suggest that the centrifugal components should be the first components on which improvement efforts should focus on, followed by the seawater coolers. These conclusions are similar for both facilities, and they resemble the ones drawn from a conventional exergetic analysis.

The overall ranking of the process components, sorted by their exergy destruction cost $\dot{C}_{\mathrm{d}}$, does not change over time. For all the studied stages of an oilfield lifetime, the highest exergy destruction cost is associated with the combustion chambers, followed by the crude oil heater in the separation process, the process compressors and coolers, the gas turbine components, the process pumps and, finally, the distillation columns.

The compressors operating in the last stage of the gas treatment process have a slightly higher cost importance than the ones in the low- and medium-pressure stages, with an exergy destruction cost of $\simeq 3$ % greater. The irreversibility costs of the process coolers are in the same order of magnitude, amounting to 80 to 95 % of the irreversibility costs of the compressors they serve.

The only exception to this trend is the aftercooler placed after the high-pressure compressor. Although significant amounts of exergy are destroyed in the production manifolds because of the throttling operations, the exergoeconomic analysis pinpoints the small importance of this sub-system, when it comes to the evaluation of the economic impacts.

However, the absolute values of the irreversibility costs increase with time: less oil and gas are processed throughout the processing plant, but the specific power and exergy consumption actually increase, as a consequence of anti-surge recycling.

Relative cost difference. The components that display the highest relative cost difference, or, in other words, the ones in which the average cost per exergy unit increases the most, are, by category, the process coolers ($\simeq$ 2–12), the pumps ($\simeq$ 1.5–2), the process heaters ($\simeq$ 1.2–1.5), and the compressors ($\simeq$ 0.3–0.5). The large cost differences for the heat exchangers reflect the poor exergetic efficiency of these components, indicating that the increase of thermal exergy on the cooling water side is performed at the expense of a large decrease of thermal exergy on the oil and gas sides, and is ultimately lost to the environment. These findings suggest that the objective of any cost optimisation of the heat exchanger should be to minimise the relative cost difference, which, in other words, implies to better utilise the heat from the petroleum streams.

Exergy and exergoeconomy

In general, the streams exiting the platform system have undergone more physical and chemical transformations than the inflowing ones, and their specific cost is therefore higher. This implies that the economic losses associated with a given component will increase as it is located further from the system inlet. For example, the exergy destruction in the last compression stage has a bigger economic impact than the one occurring in the separation sub-system. Finally, it can the exergoeconomic analysis also pinpoints the importance of the compression operations, as well as the thermodynamic and economic impacts of the anti-surge recycling strategy on the costs of the system inefficiencies.

6.4.4 Advanced exergetic analysis

Combustion chambers. The exergy destruction taking place in the combustion chambers (≤ 40 MW) is mostly *unavoidable*, as it is caused by the chemical reactions, which are irreversible processes. In theory, it could be reduced by adjusting the air-to-fuel ratio near the stoichiometric proportions or by allowing for higher reaction temperatures. However, a stoichiometric air-to-fuel ratio is generally not advisable, as a fraction of the hydrocarbons may be unburned, and an elevated temperature favours the formation of nitrous oxides following the Zeldovich mechanisms (thermal NO_x), while issues with the gas turbine materials may occur (sintering and melting).

Gas turbines. The exergy destruction occurring in the gas turbines ($\simeq$ 40–45 MW) can hardly be reduced, being mostly unavoidable, although the exergetic efficiency of this system is low compared to similar engines. The current power generation strategy of offshore platforms, i.e. the operation of multiple gas turbines at low load, lets little room for optimisation. A possibility is to reduce the power consumption of the oil and gas processing by improving this part of the system, which would in turn reduce the exergy destruction in the gas turbines.

Newer gas turbines, which have higher turbine inlet temperatures (TIT), or gas engines, which are unfortunately heavy, may result in a higher efficiency. The current gas turbines (SGT-500) implemented on the Draugen platform (Platform D) are of the uncooled type and can handle a large variety of fuels: compared to the state-of-the-art gas turbines, their TIT is much lower and so is their exit temperature.

Production manifold. The exergy destroyed in the production manifold (≤ 3 MW), where all streams are mixed and de-pressurised to the operating pressure of the separation system, can be seen as endogenous, since no components interact with the throttling valves and chokes upstream. It may be argued that these inefficiencies are exogenous, because these components serve the phase separators. This exergy destruction may be reduced if multiphase expanders are integrated to make use of the high pressure of the well-streams, but a practical implementation is challenging because these components should be able to handle multiphase (solid, liquid and vapour) streams over time and stand corrosion and erosion.

Separation. The separation sub-system consists of expansion valves and separators, and the exergy destruction in the latter is not meaningful. The irreversibilities of the depressurisation operations could only be reduced if the throttling valves between each separation stage are replaced by expanders. Most water exits the separation sub-system at the 1st stage, even at high water cuts, and the oil composition in the separation system fluctuates less. Designing expanders for this section of the plant is therefore less problematic. As for the production manifolds, these valves serve the phase separators, and their inefficiencies can be regarded as *exogenous*, and *avoidable*, but only if liquid expanders can be integrated.

Gas processing. The inefficiencies of the separators are negligible in comparison to the other ones and are not analysed thoroughly in this work, but in practice, a poorly designed separator would result in a higher liquid entrainment in the vapour phase, impacting negatively the compressor efficiency and causing exogenous exergy destruction in the downstream components.

The irreversibilities occurring in the coolers are caused by two main factors. The first one is the temperature gap between the heat source and sink, implying that exergy is destroyed in the heat transfer process. Smaller amounts of exergy may be destroyed with a better match of the water and gas flow rates and temperatures, but, as the seawater coolers are unbalanced heat exchangers, a fraction of the exergy destruction in these components remains *unavoidable*. The second one is the gas gas recycling around the compressors. These inefficiencies can be regarded as exogenous, as they are attributable to the control strategy of the compressors, which is to prevent surge, and larger gas flow rates need to be cooled before being recompressed.

The exergy destruction in the compressors is mostly endogenous, because higher exergetic efficiencies of the remaining components in each stage do not impact their performance.

Produced and cooling water. The use of the exergy lost with the produced water is challenging. The chemical exergy of water (≤ 16 MW) can hardly be used with the conventional technologies, and the high physical exergy (≤ 7 MW) could only be used, through process integration, if there is a heating demand at temperatures lower than 50 °C. This may be interesting for platforms on which heavy oil is processed, but challenging, as the production of water is significant only in *end-life* cases. The same reasoning applies for the cooling water: the exergy discharged from the gas streams may be recovered, although it may be difficult to recover heat at these temperature levels (30 to 150 °C). These exergy losses may be regarded as *unavoidable* with the current state-of-the-art.

Exhaust gases. Finally, one of the main sources of inefficiencies is the rejection of exhaust gases at high temperature to the environment (≤ 25 MW), combined to the heat transfer over large temperature gaps in the heat exchangers of the processing plant (≤ 15 MW), using a glycol loop and cooling water. This results in significant exergy destruction in the beginning and peak production periods, and large exergy losses with the flue gases throughout the complete exploitation. The current utility system does not allow for recovering and using efficiently the large amounts of waste heat, and these exergy losses are partly *avoidable*, if a bottoming cycle is integrated to the gas turbines.

Flaring and venting. Exergy losses with flared and vented gases are minimal, as gas is only flared during shut-down or emergencies, and vented in small quantities from the glycol regenerator. In general, continuous flaring is forbidden on Norwegian platforms and should be avoided, as it results in unnecessary losses.

6.5 Conclusion

Exergy analyses were performed on the oil and gas processing systems on four North Sea oil and gas platforms, which differ by their operating conditions and strategies. The comparison of the exergy destruction sources illustrated the large exergy destruction associated with the gas treatment and production manifold systems, ranging above 27 % and 11 %, respectively. The fuel gas and seawater injection processes represent less than 3 % each in every case. However, the contributions of the recompression, separation and oil export sections vary significantly across the different platforms. Although the precise values of the exergy destruction rates differ from one platform to another, the main causes can be identified with the depressurisation in the production manifold, the compressor inefficiencies, and the heat transfers processes in the coolers.

The exergy destruction and losses in the oil and gas processing system of four oil and gas platforms were mapped: the findings are in accordance with the results of Svalheim and King [19], who stated that the gas compression step is the most energy-demanding steps. They can also be compared to the previous results of Bothamley [11] who focused on the variety of offshore processing options in different oil regions. However, these results depend strongly on factors such as (i) the efficiency and the control strategies of the turbo-machinery components (ii) the integration of additional subsystems such as condensate export and (iii) the outlet specifications of the processing plant.

In addition, the differences between the platforms analysed in this study and the Brazilian cases [59, 222] show that caution should be exercised when extending the present conclusions to platforms in other regions of the world. Each oil platform should be analysed individually, to pinpoint the major sources of performance losses for each specific facility.

7 Performance indicators

Well-defined performance indicators can allow for sound comparisons of oil and gas platforms and indicate rooms for improvement. This chapter presents the development of such metrics, which mainly focus on energy performance aspects. It includes as well a thorough analysis of possible efficiency definitions for petroleum systems. The major issues and possible interpretations are discussed and applied to the specific case of oil and gas platforms. The main outcomes of this work are underlined in Voldsund et al. [227] and in Nguyen et al. [228].

7.1 Introduction

Performance indicators consist of sets of values that are used to measure the actual performance of a given system and the gap with the objectives that are desirable. They generally belong to the category of management tools and can provide relevant information to the decision-makers. Nowadays, the performance of oil and gas facilities is mainly judged with regards to the oil and gas production and the absence of leakages, but aspects such as the energy use and environmental impact are considered to some extent.

The energy performance is generally evaluated by calculating the *specific energy use* and the *specific power consumption* [19], which are defined as the ratio of the energy contained in the fuel, flared and vented gases, or of the power consumed on-site, to the energy carried with the exported oil and gas.

The use of these metrics can be misleading, as each petroleum field presents specific characteristics (e.g. gas-to-oil ratio, well-fluid composition, field size) and each facility follows a different oil recovery strategy (e.g. gas and water injection). These dissimilarities complicate the comparison across offshore plants, since platforms operating under certain conditions may be favoured, if, for instance, gas does not need to be compressed and injected at a high pressure after the separation step.

These indicators allow therefore for evaluating the performance of a single platform over

its lifetime, but not for establishing consistent benchmarks or for comparing one facility with another. Another approach is to compare the total energy use to the ones if the energy management strategies had been optimal [19], or if state-of-the-art technologies had been implemented in replacement of the current ones [229].

However, they cannot provide information on the extents and locations of the performance losses of the overall plant and subsystems, which can be, on the contrary, illustrated by exergy-based indicators, as suggested by Rivero [131]. Various formulations have been proposed from the 1950s, with, among others, the contributions of Nesselmann [230] and of Fratzscher and Beyer [231]. Both works reported the definition of the exergetic efficiency of a given system as the ratio of its total exergy output to its total exergy input. Grassmann [45] and Nesselmann [46] suggested to define the exergetic efficiency as the ratio of the part of the exergy transfers that contribute to the transformations taking place, i.e. the *consumed* exergy, to the part of the exergy transfers that are generated within the system, i.e. the *produced* exergy. Baehr [47, 48] proposed his own expressions for these two terms. The difficulty of providing a non-ambiguous definition of an exergetic efficiency was stressed, as different views on *consumed* and *produced* exergies may apply.

Further advances within this field include the studies of Brodyansky et al. [137], Szargut et al. [44], and Tsatsaronis [185] in the 1980s. Brodyansky et al. [137] suggested a systematic procedure for calculating the *produced* and *consumed* exergies, without regarding whether they are useful to the owner of the system. His work is based on the concept of *transit exergy* introduced by Kostenko [49]. Szargut et al. [44] and Tsatsaronis [185] proposed to consider only the exergy transfers representing the *desired* exergetic output and the *driving* exergetic input of the system, leading to the concept of *product* and *fuel* exergies.

These concepts have been widely used since then by exergy practitioners. As emphasised in the works of Kotas [181], such considerations should be consistent with the purpose of owning and operating the system of investigation, both from an economic and a thermodynamic prospect. At a process level, a unique formulation may not be available and several formulations may be appropriate [185], but a systematic procedure for defining the exergetic efficiency at a component level has been suggested by Lazzaretto and Tsatsaronis [51, 52]. Finally, in the last decade, Lior and Zhang [232] attempted to clarify the definitions and uses of thermodynamic performance criteria, with the goal of achieving an international standardisation.

The literature seems to contain little, if nothing, on sets of consistent and relevant performance parameters for petroleum processes. The goals of the research presented in this chapter are to:

- perform an extensive review of performance indicators and exergy efficiency;
- evaluate the applicability of such criteria in the case of offshore platforms;
- derive new and relevant parameters, and discuss their advantages and drawbacks.

7.2 Performance metrics

7.2.1 Background

Following the classification of Patterson [233], which is also considered in several works of the International Energy Agency (IEA) [234], indicators related to the energy performance of a given system can be categorised into four main groups. These performance metrics can be applied at different levels, ranging from a particular product or small process, to a large industrial sector or a country.

(1) *thermodynamic*: these indicators derive exclusively from thermodynamic measures, such as the power consumption of a given process, and include, for instance, the 1st- and 2nd-law efficiencies;

(2) *physical-thermodynamic*: these metrics are hybrid, in the sense that they consider terms measured in thermodynamic units (e.g. kW) and in physical ones (e.g. kg), and an example is the energy intensity per unit of oil equivalent ($MJ/Sm^3_{o.e}$);

(3) *economic-thermodynamic*: similarly, these indicators are hybrid, but the unit of product is expressed in monetary terms, with a relation to the market price, as it is the case with the gross energy–gross domestic product (GDP) ratio (MJ/$);

(4) *economic*: for such parameters, the changes in energetic performance are described exclusively in economic terms, with, among others, the energy dollars–GDP ratio.

Each category of indicators faces methodological and practical issues, since the results can be biased depending on the assumptions on the system boundaries (e.g. selection of the energy inputs and outputs to consider) and on the partitioning of a given energy input to multiple system outputs (e.g. allocation to one product or another).

The energy performance metrics currently used in the oil and gas industry, and implemented in the monitoring system, include the *energy efficiency* (η), the *energy intensity* (ι_h), the *energy waste* (ω_h), the *specific power consumption*, and the *energy cost*. The three first belong to the category of *thermodynamic* performance indicators, and are defined as:

$$\eta = \frac{\sum \dot{H}_{\text{exp}}}{\sum \dot{H}_{\text{in}}} \tag{7.1}$$

$$\iota_h = \frac{\sum \dot{H}_{\text{fg}} + \sum \dot{H}_{\text{lift}}}{\sum \dot{H}_{\text{exp}}} \tag{7.2}$$

$$\omega_h = \frac{\sum \dot{H}_{\text{l}}}{\sum \dot{H}_{\text{exp}}} \tag{7.3}$$

The *specific power consumption* is classified as a *physical-thermodynamic* metric, as the output of the oil and gas system is measured in physical units, rather than in thermodynamic ones:

$$\sigma = \frac{\dot{W}}{\dot{V}_{\text{exp}}} \tag{7.4}$$

This indicator still presents the advantage that it can be unambiguously calculated, while it actually reflects that the end-use service of an oil and gas facility is to deliver oil and gas to the shore. In most cases, the volume of the exported oil and gas is expressed on an oil equivalent basis (o.e), and the conversion factor is defined by convention, considering that 1000 standard cubic meters of natural gas equal 1 standard cubic meter of oil equivalent.

The *energy cost* belongs to the category of *economic* metrics, as the energy flows are enumerated in terms of economic value:

$$\dot{C}_h = c_{\text{fg}} \cdot \dot{H}_{\text{fg}} + c_{\text{l}} \cdot \dot{H}_{\text{l}} \tag{7.5}$$

where c_{fg} and c_{l} represent the specific energy costs per unit of fuel and lost gas, and $\dot{C}_{\bar{h}}$ the total energy cost. These specific energy costs measure the economic value of the energy in the fuel gas used in the gas turbines or dissipated by flaring and venting.

Benchmarks have been established, which are, in the case of the Draugen platform, 97 % for the energy efficiency, 2 % for the energy intensity, 0.15 % for the energy waste, and NOK 450,000 per day for the energy cost. These indicators can be complemented by other ones, which reflect more consistently the energy performance of an oil and gas platform.

The criteria (e.g. consistency, credibility, reliability) that define whether a performance metric is appropriate may vary, depending on the field of application. In the case of an oil and gas platform, it is assumed that a useful indicator should:

(1) *evaluate whether the technically achievable potential is utilised:* it should indicate whether the performance of the platform could be further enhanced, if, for instance, state-of-the-art equipments are used, or if the process is better-integrated;

(2) *evaluate whether the theoretically achievable potential is utilised:* a process with a given set of boundary conditions, such as temperatures, pressures, compositions or flow rates, can never consume less exergy than in the reversible case, and this sets an upper theoretical limit. The indicator should then answer whether the studied process is far from this limit;

(3) *evaluate the total use of energy resources:* oil and gas platforms may operate under very different boundary and natural conditions, implying that the total use of energy resources for petroleum processing may vary significantly across oil fields.

The present work mainly focuses on *thermodynamic* and *physical-thermodynamic* indicators.

7.2.2 Energy-based indicators

The performance indicators related to thermodynamic measurements can be further sub-categorised into the ones using an energy or an exergy basis. Energy-based performance parameters are only based on the 1st Law of Thermodynamics, and are presented as follows.

As mentioned earlier, the energy performance of an oil and gas platform can be measured by its energy intensity, which accounts for the energy used on-site with the fuel and lift gases. This indicator gives an overview of the energy resources that have been utilised, but does neither distinguish the processing and power plants, nor considers differently the gas used for driving the processing operations (fuel gas) from the gas used to enhance oil recovery (lift gas).

The oil and gas processing on itself uses heat and power in the heat exchangers, pumps and compressors, implying that the specific energy use (SEU) per unit of oil and gas exported can be defined as:

$$\mathrm{SEU}_v = \frac{\dot{W}_{\mathrm{in}} + \dot{Q}_{\mathrm{in}}}{\dot{V}_{\mathrm{exp}}} \tag{7.6}$$

$$\mathrm{SEU}_h = \frac{\dot{W}_{\mathrm{in}} + \dot{Q}_{\mathrm{in}}}{\dot{H}_{\mathrm{exp}}} \tag{7.7}$$

However, as emphasised by Svalheim and King [19], the calorific value of the oil and gas produced on-site differs with the characteristics of the oil field, implying that the use of an oil-equivalent volume basis (SEU_v) may be misleading, and using an energy basis may be more appropriate (SEU_h). These energy performance indicators cannot be used for comparing consistently different facilities, as they do not account for the particularities of each platform and field.

Margarone et al. [229] proposed to evaluate the plant performance of an upstream gas treatment facility by comparing it against the performance reachable with the best available technologies (BAT). The proposed indicator, called the BAT efficiency, η_{BAT}, is defined as the ratio between the energy content of the fuel required on-site by using the best available technologies, and the energy content of the fuel consumed in the current (reference) case:

$$\eta_{\mathrm{BAT}} = \frac{\dot{W}_{\mathrm{BAT,in}} + \dot{Q}_{\mathrm{BAT,in}}}{\dot{W}_{\mathrm{in}} + \dot{Q}_{\mathrm{in}}} \tag{7.8}$$

The methodological issue, in this case, becomes how to precisely define the state-of-the-art components, which actually differ depending on the time frame. The state-of-the-art compressors are assumed, based on their work, to be inter-cooled compressors, without anti-surge recycling, with an isentropic efficiency of 85 % and inter-coolers with a maximum discharge temperature of 100 °C (if no liquid formation). State-of-the-art pumps are taken as pumps with a mechanical efficiency of 85 %. It is worth noting that state-of-the-art compressors are not centrifugal, which is the most common type for compressors used in offshore applications, because of their low weight and high compactness.

7.2.3 Exergy-based indicators

As pinpointed by Hammond [135], the use of energy (enthalpic) measurements does not take into account the quality of energy, meaning that all the energy inputs are treated as equivalent. The previous indicators can thus be presented on an exergy basis (SEC):

$$\mathrm{SEC}_{\nu} = \frac{\dot{E}_{W,\mathrm{in}} + \dot{E}_{Q,\mathrm{in}}}{\dot{V}_{\mathrm{exp}}} \tag{7.9}$$

$$\mathrm{SEC}_{\chi} = \frac{\dot{E}_{W,\mathrm{in}} + \dot{E}_{Q,\mathrm{in}}}{\dot{E}_{\mathrm{exp}}} \tag{7.10}$$

Since the exergy destroyed in a given system accounts for its performance losses and therefore for the use of primary energy, an indicator that measures these thermodynamic imperfections is the specific exergy destruction (SED):

$$\mathrm{SED}_{\nu} = \frac{\dot{E}_{\mathrm{d}}}{\dot{V}_{\mathrm{exp}}} \tag{7.11}$$

$$\mathrm{SED}_{\chi} = \frac{E_{\mathrm{d}}}{\dot{E}_{\mathrm{exp}}} \tag{7.12}$$

These 2nd-law performance indicators may be less misleading than energy-based metrics for assessing the performance of a wide range of processes, but their applicability may be limited when comparing real processes. Patterson [233] pointed out that their main, but inherent, drawback is that a real process is compared to an ideal one, which in is essence perfectly reversible, i.e. is infinitely slow, and without any exergy destruction. Similarly, the BAT-efficiency proposed in Margarone et al. [229] can be expressed in exergy terms, which leads to:

$$\varepsilon_{\mathrm{BAT}} = \frac{\dot{E}^{W}_{\mathrm{BAT,in}} + \dot{E}^{Q}_{\mathrm{BAT,in}}}{\dot{E}^{W}_{\mathrm{in}} + \dot{E}^{Q}_{\mathrm{in}}} \tag{7.13}$$

7.2.4 Application

Specific energy use and consumption. The performance indicators are calculated for the four platforms that have been introduced in Chapter 6. The two variants of specific energy use and specific exergy consumption are shown for each platform in Figure 7.1, whilst the two variants of specific exergy destruction are illustrated in Figure 7.2. Platform A has the highest specific energy use of the four platforms with 647 $\mathrm{MJ/Sm^3_{o.e.}}$, followed by Platform D with 371 $\mathrm{MJ/Sm^3_{o.e.}}$, Platform C with 139 $\mathrm{MJ/Sm^3_{o.e.}}$, and Platform B with only 19 $\mathrm{MJ/Sm^3_{o.e.}}$.

The ranking of these facilities is identical if the specific energy uses are calculated on an energy basis instead of a volume one. The exported oil from Platform A has a lower energy density than the oils from the three other platforms, meaning that the difference of SEU between Platforms A and D is slightly greater on a volume basis.

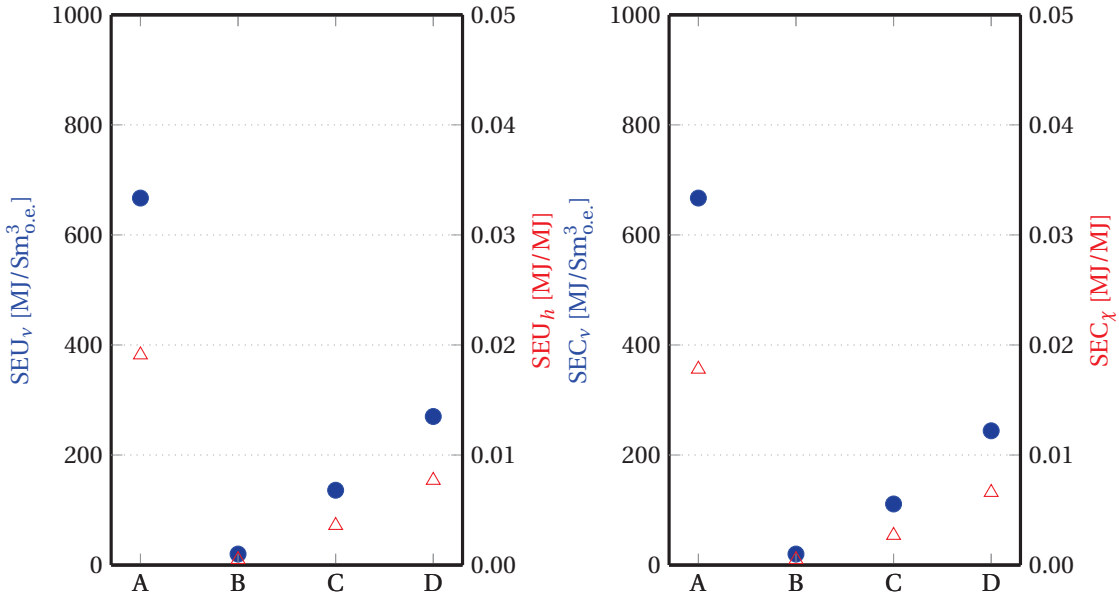

Figure 7.1: Specific energy use (SEU) and specific exergy consumption (SEC) of Platforms A – D, on a volume and on an energy | exergy basis.

The specific exergy consumption and specific energy use, on a volume basis, are strictly equal for Platforms A and B, as only electricity is used in the processing plant, at the difference of Platforms C and D, where heat is used for enhancing the oil and gas separation. This illustrates that the exergy transported with heat is smaller than its corresponding energy.

The dissimilarities between the numerical values of the two indicators, SEU and SEC, are not significant, as little heat is needed. They may be higher in peak production conditions, as a greater amount of heat is required, or for platforms operating in different petroleum regions, if the initial petroleum temperature is much lower. This would be the case, for instance, of the platform investigated by de Oliveira Jr. and Van Hombeeck [59], where additional fuel is consumed in a furnace to sustain the heat demand.

Specific exergy destruction. The specific exergy destruction is highest on Platform A with 156 MJ/Sm$^3_{o.e.}$, followed by Platform D with 84 MJ/Sm$^3_{o.e.}$, and Platforms B and C have nearly the same specific exergy destruction with 17 and 22 MJ/Sm$^3_{o.e.}$. The higher numbers for Platforms A and D are caused by the smaller oil and gas production of these platforms and by the large demand for compression.

The same picture is displayed on a volume or on an exergy basis, and the same trends can be observed when using the specific energy use and specific exergy destruction indicators. These tendencies are also similar to the ones presented with the specific exergy use, illustrating that the more exergy is used, the more exergy is destroyed.

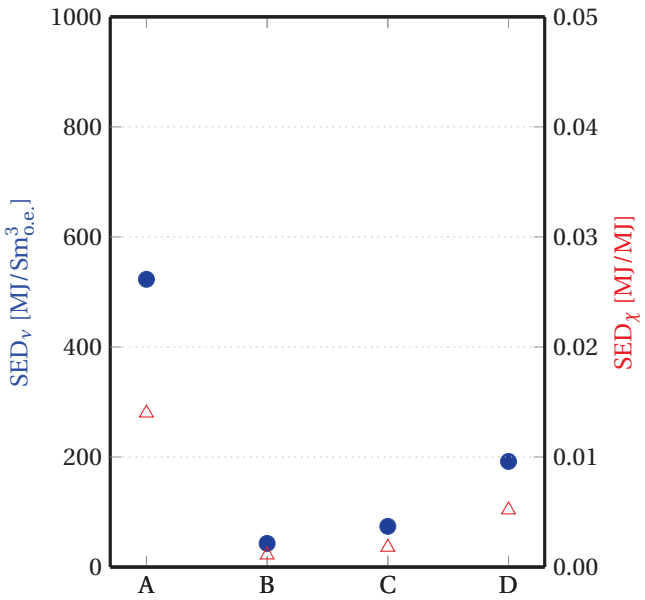

Figure 7.2: Specific exergy destruction (SED) of Platforms A – D, on a volume and on an exergy basis.

The use of exergy-based indicators rather than energy-based ones may be preferred, as they account for the quality of energy and are therefore more consistent. They would, for instance, promote the use of low-temperature heat and discourage the implementation of electric heating, as often done for preheating the fuel gas entering the gas turbines.

These indicators illustrate the total amount of energy resources that are used to extract petroleum, and to separate and process oil, gas and water. They can be calculated easily and rigorously, using temperature and flow sensors already implemented on most offshore facilities, and they can be understood by wide public types. On the contrary, they do not indicate the improvement potentials, neither the technical nor the theoretical ones, and can therefore not be used for establishing consistent benchmarks between different facilities.

Best-available-technology efficiencies. The calculated BAT efficiencies are given in Figure 7.3. All platforms have energy-based BAT efficiencies ranging from 62 % to 79 %, meaning that the energy demand could be reduced to these percentages if state-of-the-art compressors and pumps were integrated to replace the current ones. Similarly, the exergy-based efficiencies range between 62 % and 74 %, implying that the exergy demand could be decreased by 36 % to 48 %.

The results suggest that the platform presenting the largest potential for energy savings is Platform A, followed by Platform B. A different ranking can be observed on an exergy basis, which illustrates that the potential for exergy savings is actually bigger for Platform D than for

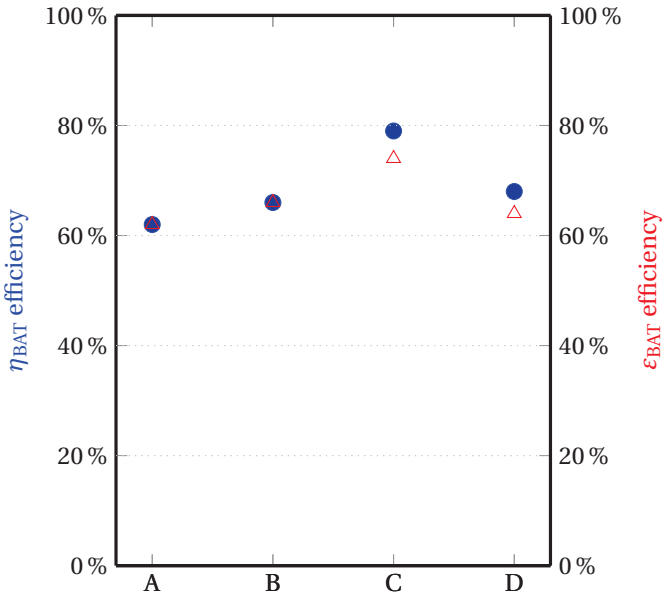

Figure 7.3: Best-available-technology efficiencies of Platforms A – D, on an energy and on an exergy basis.

Platform B. These differences between the BAT efficiencies on energy and exergy bases show that care should be exercised when making comparisons across platforms, as the results may be misleading.

Although the calculations of the BAT efficiencies only require a consistent model, some limitations can be pointed out. First, the efficiency of a compressor depends on the type of fluid processed, the component subclass (e.g. centrifugal, axial, reciprocating, etc.) and the pressure ratio, while the efficiency of a pump depends, among other characteristics, on the magnitude and specific speed of the fluid volume flow. Replacements of heat exchangers and throttling valves with more effective ones and expanders, if possible, were not considered.

Secondly, this parameter compares a specific design set-up with the same one, with state-of-the-art technologies. It does not show any improvement potential for systems where no mature technology is already available. This is the case of production manifolds: depressurisation is achieved by valve throttling, and multiphase expansion of fluids containing sand, water, oil and gas is currently not feasible. Using BAT efficiencies for establishing performance benchmarks may not be transparent, in the sense that they rely on a large set of assumptions.

Finally, technologies evolve over time and may become more efficient with scientific and technical progresses: this implies that the state-of-the-art components are changing, and the values of the BAT efficiencies may therefore be updated regularly for consistency.

7.3 Exergy efficiencies for petroleum processes

7.3.1 Overview

The definitions of exergy efficiency, as presented and discussed in the open literature, can be divided into two main groups, as suggested by Lior and Zhang [232]:

- the *total*, *overall*, *input-output* or *universal* exergy efficiency, which is defined as the ratio of all outgoing to ingoing exergy flows, without regarding whether these flows are actually used or not;

- the *task*, *utilitarian*, *consumed-produced*, *rational* or *functional* exergy efficiency, which is defined as the ratio of the exergy terms associated with the products generated within the system, i.e. the *produced exergy*, to the exergy terms associated with the resources expended to achieve these outputs, i.e. the *consumed exergy*.

The *total* exergy efficiency $\varepsilon_{\text{total,1}}$ is defined as the ratio of all exergy outflows to inflows [56, 134, 232]:

$$\varepsilon_{\text{total,1}} \equiv \frac{\sum \dot{E}_{\text{out}}}{\sum \dot{E}_{\text{in}}} = 1 - \frac{\dot{E}_{\text{d}}}{\sum \dot{E}_{\text{in}}} \tag{7.14}$$

where some authors exclude the exergy associated with waste products [134, 235]:

$$\varepsilon_{\text{total,2}} \equiv \frac{\sum \dot{E}_{\text{out,u}}}{\sum \dot{E}_{\text{in}}} = 1 - \frac{\dot{E}_{\text{out,l}} + \dot{E}_{\text{d}}}{\sum \dot{E}_{\text{in}}} \tag{7.15}$$

The *total* exergy efficiency is claimed to be adequate when (i) the ingoing and outgoing exergy flows are converted to other forms of exergy [56], or (ii) a major part of the out-flowing exergy can be considered as useful, as it is the case of power plants [232], or (iii) for dissipative processes and devices [53, 54].

The concept of *total* exergy efficiency has been criticised, as it takes into account all the exergetic flows entering and exiting a system, without considering whether they are utilised in the thermodynamic conversions. The *task* exergy efficiency, on the contrary, differentiates the exergy flows undergoing transformations from the exergy flows that are not affected, i.e. neither used nor produced.

Grassmann [45] proposed a general formulation for an exergy efficiency: he suggested the ratio of the intended increase to the used decrease in ability to do work. In exergy terms, this means that the exergy efficiency should be defined as the ratio of the production of exergy that is desired, to the reduction of exergy that is utilised. It was emphasised that this performance criterion always has a value between 0 and 1, as the increased ability to do work always is smaller than the decreased ability.

Baehr [48] proposed a variant of this formulation, considering *all* the exergy increases in the numerator and *all* the exergy decreases in the denominator. At the difference of the expression proposed by Grassmann [45], the total production and expenditure of exergy are considered, whether they are actually desired or utilised within the system.

It was pointed out that (i) exergy efficiencies based on exergy differences are more sensitive to changes in the system than the total exergy efficiency and are therefore more suitable and (ii) different numerical values could be obtained with the formulation of exergy efficiency proposed by Grassmann [45], as it depends on whether an exergy difference is considered as *useful, used* or none of those.

Szargut [236] and Kotas [182] argued that the exergy efficiency should be defined as the ratio of the *desired output* or *useful exergetic effect*, and of the *necessary input* or *driving exergy expense*. Other authors name the same terms *exergetic product* $\dot{E}_\mathrm{p}$ and *exergetic fuel* $\dot{E}_\mathrm{f}$ [76, 187]. The global exergetic balance can be rewritten:

$$\dot{E}_\mathrm{p} = \dot{E}_\mathrm{f} - \dot{E}_\mathrm{l} - \dot{E}_\mathrm{d} \tag{7.16}$$

Hence, the task exergy efficiency can be written:

$$\varepsilon_\mathrm{task} \equiv \frac{\dot{E}_\mathrm{p}}{\dot{E}_\mathrm{f}} = 1 - \frac{\dot{E}_\mathrm{l} + \dot{E}_\mathrm{d}}{\dot{E}_\mathrm{f}} \tag{7.17}$$

Brodyansky et al. [137] and Sorin et al. [237] proposed to define the exergy efficiency as the ratio of the total exergy output to the total exergy input, minus the *transit exergy* $\dot{E}_\mathrm{tr}$ in both numerator and denominator:

$$\varepsilon_\mathrm{transit} \equiv \frac{\sum \dot{E}_\mathrm{out} - \sum \dot{E}_\mathrm{tr}}{\sum \dot{E}_\mathrm{in} - \sum \dot{E}_\mathrm{tr}} \tag{7.18}$$

The concept of *transit exergy* was introduced by Kostenko [49] and was further developed by Brodyansky et al. [137]. The transit exergy is the part of the exergy supplied to a system that flows through the system without undergoing any physical or chemical transformation.

This concept is also mentioned by Cornelissen [56], who applied this method to an air separation unit and a crude oil distillation plant. The lack of ambiguity and the complexity of the calculations were underlined, as this method requires a precise decoupling of the exergy flows into their components. This efficiency can also be regarded as a variant of the *total* exergy efficiency. The total and the transit exergy efficiencies strongly differ from each other when a significant fraction of the exergy flows entering the system are not used or transformed.

Several approaches for the exergy efficiencies of petroleum processing systems can be found in the literature [54, 56, 59, 117, 132, 172, 191, 213, 238]. In addition to the *total* exergy efficiency, three different *task* exergy efficiencies are found. For the types of *task* efficiencies where it is possible both to include waste streams as product or as lost, the waste exergy is regarded as a loss.

7.3.2 Total exergy efficiency

The exergy balance for the processing plant of the oil and gas facility can be expressed as:

$$\underbrace{\dot{E}_{\text{feed}} + \dot{E}^{Q}_{\text{heat}} + \dot{E}^{W}}_{\dot{E}_{\text{in}}} = \underbrace{\sum_{k,\text{u}} \dot{E}_{k,\text{u}}}_{\dot{E}_{\text{out,u}}} + \underbrace{\sum_{k,\text{w}} \dot{E}_{k,\text{w}} + \dot{E}^{Q}_{\text{cool}}}_{\dot{E}_{\text{out,l}}} + \underbrace{\dot{E}_{\text{d,PP}}}_{\dot{E}_{\text{d}}} \tag{7.19}$$

The left-hand side terms consist of the exergy associated with the feed entering the processing plant $\dot{E}_{\text{feed}}$ (i.e. reservoir fluid) and the heat exergy $\dot{E}^{Q}_{\text{heat}}$ and power exergy $\dot{E}^{W}$ delivered by the utility plant.

The right-hand side terms consist of the exergy of the useful outlet material streams of the processing plant $\sum_k \dot{E}_{k,\text{u}}$ (i.e. oil, gas, condensate, fuel gas), the wasted outlet material streams $\sum_k \dot{E}_{k,\text{w}}$ (i.e. flared gas, produced water), the exergy lost in the cooling system $\dot{E}^{Q}_{\text{cool}}$ and the destroyed exergy $\dot{E}_{\text{d,PP}}$.

All the left-hand side terms include the input exergy $\dot{E}_{\text{in}}$, while the useful outlet material streams on the right-hand side are counted as useful output exergy $\dot{E}_{\text{out,u}}$. The produced water that is extracted along with oil and gas is normally considered as waste, since it is discharged to the surroundings without being used. The exception to this rule is if the produced water is injected back for enhanced oil recovery, which is a possible plan in the case of Platform D.

The *total* exergy efficiency without differentiating the *useful* from the *waste* streams [230] is:

$$\varepsilon_{I-1} \equiv \frac{\sum_{k,\text{u}} \dot{E}_{k,\text{u}} + \sum_{k,\text{w}} \dot{E}_{k,\text{w}} + \dot{E}^{Q}_{\text{cool}}}{\dot{E}_{\text{feed}} + \dot{E}^{Q}_{\text{heat}} + \dot{E}^{W}} \tag{7.20}$$

while the *total* exergy efficiency considering only the *useful* streams is:

$$\varepsilon_{I-2} \equiv \frac{\sum_{k,\text{u}} \dot{E}_{k,\text{u}}}{\dot{E}_{\text{feed}} + \dot{E}^{Q}_{\text{heat}} + \dot{E}^{W}} \tag{7.21}$$

The total exergy efficiencies of all four processing plants (Table 7.1) range between 99 % – 100 % when waste streams are considered as a part of the product and between 98 % – 100 % when waste streams are considered lost (Figure 7.4). These values are very similar to the values of energy efficiencies used in the monitoring systems of oil and gas platforms. The facility that presents the highest efficiency is Platform B, as gas is not compressed before export and little power is required on-site.

The high numbers are caused by the inclusion of the chemical exergy of hydrocarbons in the formulation of these exergy efficiencies, and the total efficiencies are therefore always high. They can hardly be used to compare the performance of oil and gas facilities, since (i) they give the impression that all platforms are similar in terms of efficiency and (ii) they are poorly sensitive to improvement efforts.

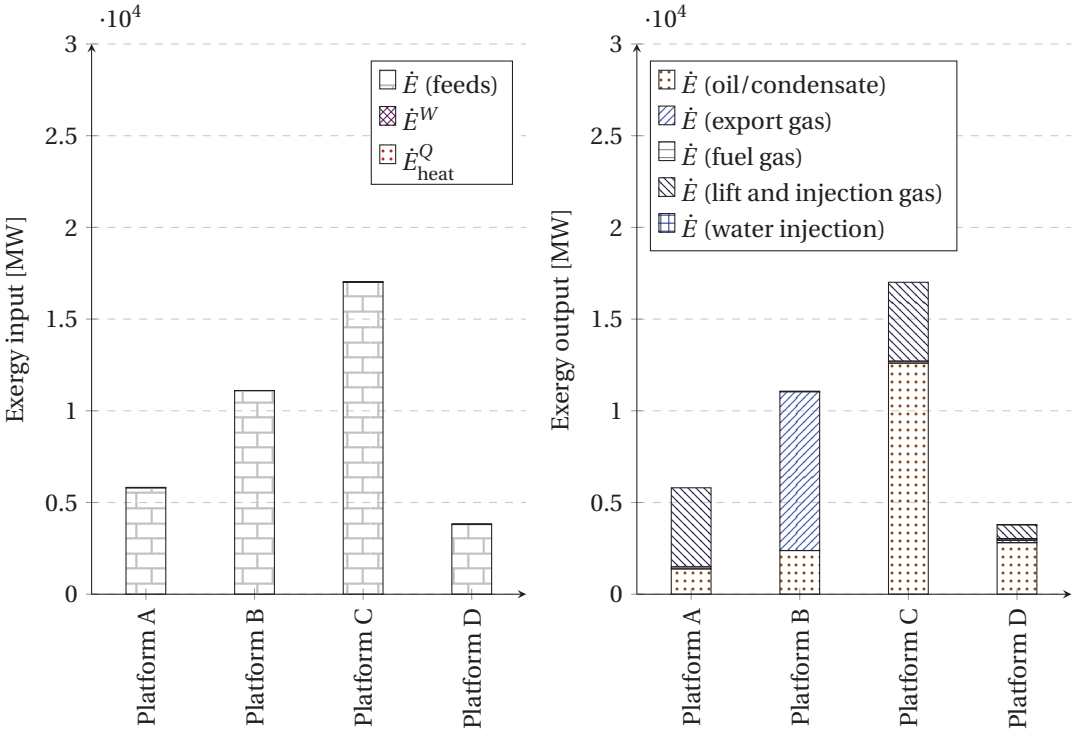

Figure 7.4: Exergy input and useful output flows.

Kotas [54] and Tsatsaronis [185] support this view in their works. They argue that the total exergy efficiencies do not show the potential for reducing the system inefficiencies, and that conclusions based on them would be misleading. Another critique on the total exergy efficiencies is that they do not reflect the *purposes* of operating these facilities, which are to separate the petroleum from the water, and to export the oil and gas to the shore.

The same reasoning can be drawn for the energy efficiency, as formulated and used for the evaluation of some oil and gas platforms: it has, for instance, varied between 92 % and 94 % for Platform D these last years.

An alternative may be to assume that the gas and water used for lift and injection represents an exergy loss, as it is not exported but processed to the reservoir. In such cases, the total efficiencies would amount to 25.8 %, 99.8 %, 74.8 % and 80.0 %.

Table 7.1: *Total* exergy efficiencies (%) without differentiating between waste useful streams and waste streams ε_{I-1} and with waste streams regarded as lost ε_{I-2}.

	Platform A	Platform B	Platform C	Platform D
ε_{I-1}	99.7	99.9	99.9	99.6
ε_{I-2}	99.5	99.8	99.8	98.0

7.3.3 Task exergy efficiency: Kotas for general separation systems, Oliveira and Van Hombeeck for offshore platform

The exergy balance for the processing plant, Equation 7.19, can be rewritten as:

$$\underbrace{\dot{E}^Q_{\text{heat}} + \dot{E}^W}_{\dot{E}_\text{f}} = \underbrace{\left(\sum_k \dot{E}_k - \dot{E}_{\text{feed}}\right)}_{\dot{E}_\text{p}} + \underbrace{\dot{E}^Q_{\text{cool}}}_{\dot{E}_\text{l}} + \underbrace{\dot{E}_{\text{d,PP}}}_{\dot{E}_\text{d}} \tag{7.22}$$

The left-hand side terms can be identified as the resources required to drive the processing plant, i.e. the exergetic fuel $\dot{E}_\text{f}$, while the difference of exergy between the inlet and outlet material streams can be considered as the exergetic product $\dot{E}_\text{p}$. This approach is similar to the one suggested by Kotas [54] for a generalised separation plant and used by de Oliveira Jr. and Van Hombeeck [59] for petroleum separation processes on a Brazilian offshore platform, and by Voldsund et al. [172] for Platform A.

The desired effect of the offshore platforms is taken as the difference of exergy between the inlet and outlet streams, i.e. the exergy increase due to separation, and possibly the exergy increase with physical processes such as compression. In all cases, the increase of chemical exergy represents less than 1 MW, and is often negligible compared to the changes in physical exergy.

The resources required to drive the processing plant and to separate the three phases correspond to the power and heat required on-site. The losses are identified as the exergy lost with the cooling water $\dot{E}_\text{l}$ and the rest is the destroyed exergy $\dot{E}_\text{d}$. The expression for this exergy efficiency, denoted ε_{II-1}, is then given by:

$$\varepsilon_{II-1} \equiv \frac{\sum_k \dot{E}_k - \dot{E}_{\text{feed}}}{\dot{E}^Q_{\text{heat}} + \dot{E}^W} = 1 - \frac{\dot{E}^Q_{\text{cool}} + \dot{E}_{\text{d,PP}}}{\dot{E}^Q_{\text{heat}} + \dot{E}^W} \tag{7.23}$$

The exergy efficiencies, as defined in Equation 7.23, for the processing plants of Platforms A, C and D are low (Table 7.2). This is in accordance with the findings of Kotas [54], who suggested that the rational efficiency of separation processes is often low, because of the large compression work required to compress the gas streams (Figure 7.5).

Platform B presents a negative efficiency, since the exergy of the output streams is smaller than the exergy of the feeds. The pressures and temperatures of the oil and gas are lower than those of the feed since because the feed pressure already complies with the export pressure requirements, implying that there is no need for gas compression before export. On the contrary, the gas pressure must be increased for all other platforms.

The reductions of physical exergy ($\simeq$ 12,200 kW) are thus higher than the increases of chemical exergy ($\simeq$ 300 kW), leading to the negative value. Moreover, for this facility, the exergy destroyed in the processing plant is actually greater than the total power consumption.

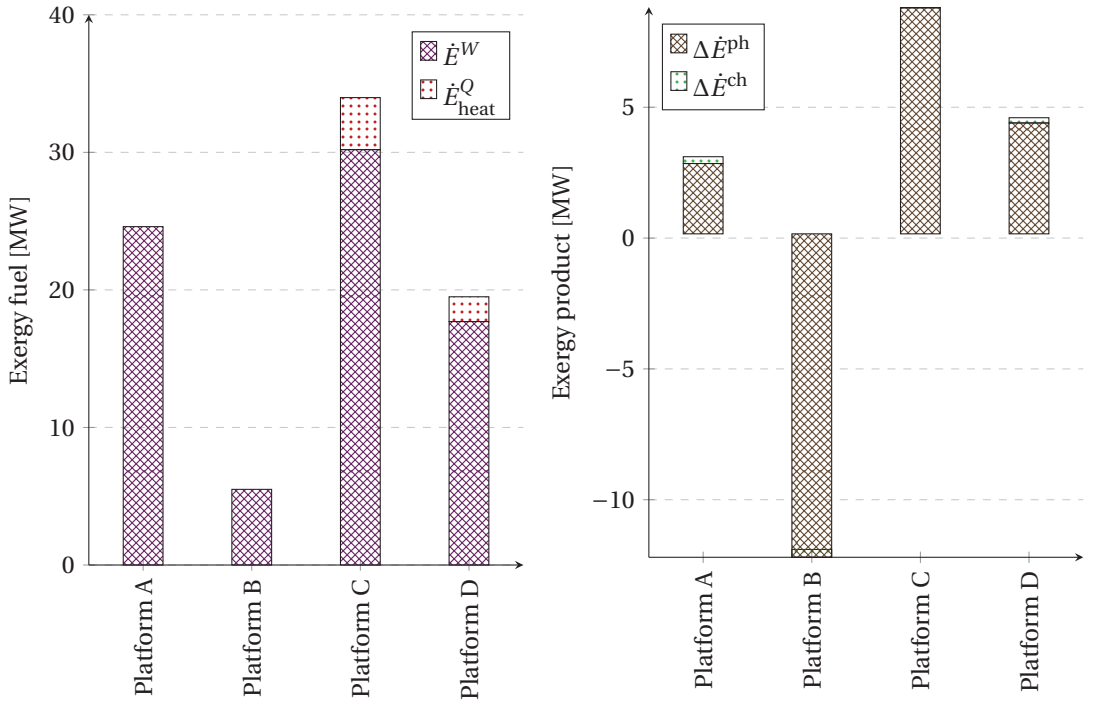

Figure 7.5: Exergy fuels and products, based on the approach of Kotas and de Oliveira Jr. and Van Hombeeck for generic separation systems.

This issue with the negative value was also noted in an earlier work of Voldsund et al. [132], who applied this definition of exergy efficiency to the separation sub-system of Platform A, and found an inconsistent value of -1.7e4.

This case illustrates the limitations of applying this approach to systems where the physical exergy decreases may be significant, and this suggests that the differences of physical and chemical exergy between the input and output streams should be considered apart. The reduction of pressure throughout the platform drives the separation process, and the expense of physical exergy may be accounted as a part of the resources used in the processing plant.

Such inconsistencies may be less remarkable if the variations in potential and kinetic exergies, which also ease the separation between the liquid and gas phases, are accounted, but measuring the height and velocity of the feed streams is challenging.

Table 7.2: Task exergy efficiencies (%) based on the approach of Kotas [54] and de Oliveira Jr. and Van Hombeeck [59] for generic separation systems.

	Platform A	Platform B	Platform C	Platform D
ε_{II-1}	12.7	-215	20.6	23.6

7.3.4 Task exergy efficiency: Cornelissen for crude oil distillation, Rian and Ertesvåg for LNG plant

Kotas [54] suggested an alternative to Equation 7.23 for air distillation plants, where the physical and chemical exergy in the material streams are treated separately:

$$\begin{aligned}\underbrace{\dot{E}^{\mathrm{ph}}_{\mathrm{feed}} + \dot{E}^{Q}_{\mathrm{heat}} + \dot{E}^{W}}_{\dot{E}_{\mathrm{f}}} &= \sum_k \dot{E}^{\mathrm{ch}}_k - \dot{E}^{\mathrm{ch}}_{\mathrm{feed}} + \sum_k \dot{E}^{\mathrm{ph}}_{k,\mathrm{u}} + \sum_k \dot{E}^{\mathrm{ph}}_{k,\mathrm{w}} + \dot{E}^{Q}_{\mathrm{cool}} + \dot{E}_{\mathrm{d,PP}} \\ &= \underbrace{\Delta E^{\mathrm{ch}} + \sum_{k,\mathrm{u}} \dot{E}^{\mathrm{ph}}_{k,\mathrm{u}}}_{\dot{E}_{\mathrm{p}}} + \underbrace{\sum_{k,\mathrm{w}} \dot{E}^{\mathrm{ph}}_{k,\mathrm{w}} + \dot{E}^{Q}_{\mathrm{cool}}}_{\dot{E}_{\mathrm{l}}} + \underbrace{\dot{E}_{\mathrm{d,PP}}}_{\dot{E}_{\mathrm{d}}}\end{aligned} \tag{7.24}$$

The exergetic fuel is now taken as the sum of the exergy transferred as heat and power and the physical exergy of the feed. The exergetic product is taken as the difference of chemical exergies between the inlet and outlets of the processing plant, as well as the physical exergy of the useful output streams.

This approach is similar to the one applied by Cornelissen [56] for a crude oil distillation plant and by Rian and Ertesvåg [238] for an LNG plant, where it is suggested that all physical exergy of the feed streams is consumed along with exergy associated with heat and power. It was therefore applied for chemical systems where the main flow has a very low chemical exergy (air) or a very high one (petroleum and natural gas), and where the needs for heating and cooling utilities were significant.

The desired result is taken as the physical exergy of the outlet streams, as well as the increased chemical exergy due to separation. The expression for the exergy efficiency of the system (ε_{II-2}) is then given by:

$$\varepsilon_{II-2} \equiv \frac{\Delta E^{\mathrm{ch}} + \sum_{k,\mathrm{u}} \dot{E}^{\mathrm{ph}}_{k,\mathrm{u}}}{\dot{E}^{\mathrm{ph}}_{\mathrm{feed}} + \dot{E}^{Q}_{\mathrm{heat}} + \dot{E}^{W}} = 1 - \frac{\sum_{k,\mathrm{w}} \dot{E}^{\mathrm{ph}}_{k,\mathrm{w}} + \dot{E}^{Q}_{\mathrm{cool}} + \dot{E}_{\mathrm{d,PP}}}{\dot{E}^{\mathrm{ph}}_{\mathrm{feed}} + \dot{E}^{Q}_{\mathrm{heat}} + \dot{E}^{W}} \tag{7.25}$$

When applying this approach (Figure 7.6), the exergetic fuel amounts from 33 MW (Platform D) to 110 MW (Platform B). The major contributions to the fuel are the physical exergy of the feeds and the power consumption. Most exergy consumed on the plant is used to produce high-pressure gas, and that the separation effect is negligible in comparison.

The platform that presents the highest exergy efficiency, as defined in Equation 7.25, is Platform B ($\simeq$ 84 %), followed by Platforms A ($\simeq$ 71 %), C ($\simeq$ 71 %) and D ($\simeq$ 33 %). The higher performance of Platform B can be explained by the high rate of physical exergy flowing throughout the plant with the produced gas (Table 7.3).

Gas is exported at nearly the same conditions as it enters, and its physical exergy dominates transformations taking place on-site. At the difference of Platforms A, C and D, the transit exergy in the case of Platform B consists not only of the pure-component chemical exergy.

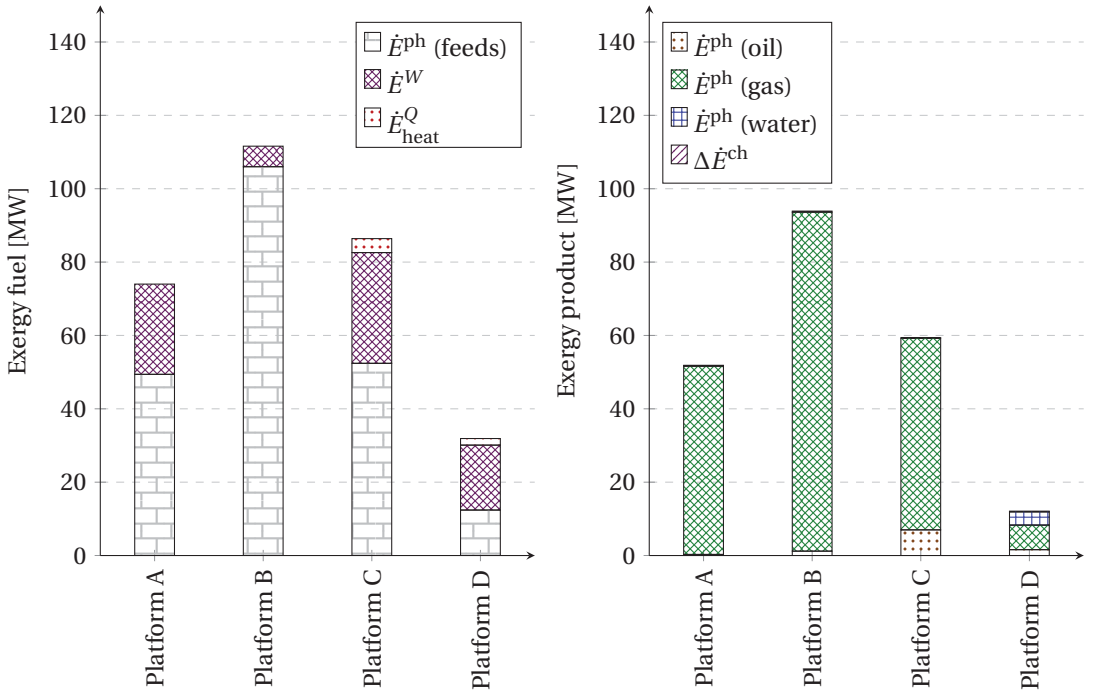

Figure 7.6: Exergy fuels and products, based on the approach of Cornelissen and Rian and Ertesvåg for crude oil distillation and LNG plants.

On the other hand, Platform D presents a smaller exergy efficiency, because the lift and export pressures (≃ 175–180 bar) are much higher than the feed pressures (≃ 11–45 bar) and the separation pressures (≃ 1.7–8 bar). A significant amount of power is required to increase the gas pressure, which results in high irreversibilities in the gas compression section. Moreover, the water cuts of the feeds are much higher, and the produced water is discharged to the sea at high temperatures, without being further used.

This approach was used for an LNG plant, where most physical exergy entering the system was pressure-based, and most leaving the system was temperature-based, since the gas should be cooled down below the ambient temperature (need for refrigeration) and exported at nearly atmospheric pressure.

This is different in the present cases, where most physical exergy that enters and exits is pressure-based, and has not necessarily undergone exergy transformations within the process.

Table 7.3: Task exergy efficiencies (%) based on the approach of Cornelissen [56] and Rian and Ertesvåg [238] for crude oil distillation and LNG plants.

	Platform A	Platform B	Platform C	Platform D
ε_{II-2}	70.9	84.2	71.0	33.2

7.3.5 Task exergy efficiency: Tsatsaronis and Cziesla for distillation columns

In the third alternative formulation of the *task* exergy efficiency, the fuel exergy is defined as the sum of the physical exergy decreases between the inflowing feed and the separated streams with a lower specific physical exergy (k^-) and the exergy with heating and power.

The product exergy is defined as the sum of the physical exergy increases between the inflowing feed and the separated useful products with a higher specific physical exergy (k^+) and the chemical exergy increases between the feed and products.

This approach was illustrated with the case of a generalised distillation plant [213], and by separating between product streams with increased and decreased specific physical exergy, Equation 7.19 can be rewritten:

$$\begin{aligned} &\underbrace{\sum_{k^-} \dot{m}_{k^-} \cdot (e^{\mathrm{ph}}_{\mathrm{feed}} - e^{\mathrm{ph}}_{k^-}) + \dot{E}^Q_{\mathrm{heat}} + \dot{E}^W}_{\dot{E}_{\mathrm{f}}} = \\ &\underbrace{\Delta E^{\mathrm{ch}} + \sum_{k^+,\mathrm{u}} \dot{m}_{k^+,\mathrm{u}} \cdot (e^{\mathrm{ph}}_{k^+,\mathrm{u}} - e^{\mathrm{ph}}_{\mathrm{feed}})}_{\dot{E}_{\mathrm{p}}} + \underbrace{\sum_{k^+,\mathrm{w}} \dot{m}_{k^+,\mathrm{w}} \cdot (e^{\mathrm{ph}}_{k^+,\mathrm{w}} - e^{\mathrm{ph}}_{\mathrm{feed}}) + \dot{E}^Q_{\mathrm{cool}}}_{\dot{E}_{\mathrm{l}}} + \underbrace{\dot{E}_{\mathrm{d,PP}}}_{\dot{E}_{\mathrm{d}}} \end{aligned} \tag{7.26}$$

The approach of Tsatsaronis and Cziesla [213] considers the physical exergy decreases as part of the exergetic fuel, and the increases as part of the exergetic product, which is in accordance with the SPECO method proposed by Lazzaretto and Tsatsaronis [51, 52] and the previous works of Baehr [48] and Grassmann [45]. They define physical exergy decreases and increases by comparing the specific physical exergies of the outlet and inlet streams on a mass basis.

The expression for the exergy efficiency of this system (ε_{II-3}) is then given by:

$$\begin{aligned} \varepsilon_{II-3} &\equiv \frac{\Delta E^{\mathrm{ch}} + \sum_{k^+,\mathrm{u}} \dot{m}_{k^+,\mathrm{u}} \cdot (e^{\mathrm{ph}}_{k^+,\mathrm{u}} - e^{\mathrm{ph}}_{\mathrm{feed}})}{\sum_{k^-} \dot{m}_{k^-} \cdot (e^{\mathrm{ph}}_{\mathrm{feed}} - e^{\mathrm{ph}}_{k^-}) + \dot{E}^Q_{\mathrm{heat}} + \dot{E}^W} \\ &= 1 - \frac{\sum_{k^+,\mathrm{w}} \dot{m}_{k^+,\mathrm{w}} \cdot (e^{\mathrm{ph}}_{k^+,\mathrm{w}} - e^{\mathrm{ph}}_{\mathrm{feed}}) + \dot{E}^Q_{\mathrm{cool}} + \dot{E}_{\mathrm{d,PP}}}{\sum_{k^-} \dot{m}_{k^-} \cdot (e^{\mathrm{ph}}_{\mathrm{feed}} - e^{\mathrm{ph}}_{k^-}) + \dot{E}^Q_{\mathrm{heat}} + \dot{E}^W} \end{aligned} \tag{7.27}$$

Calculating this efficiency on a mass basis (Table 7.4) suggests that Platform C presents the highest performance ($\simeq$ 54%), followed by Platforms A ($\simeq$ 48%), B ($\simeq$ 39%) and D ($\simeq$ 39%). The exergetic fuel includes two major contributions (Figure 7.7), which are the reduction in physical exergy and power consumption. With the exception of Platform B, most exergetic fuel consists of the power input ($\geq$ 55 %). The physical exergy reduction is mainly caused by the decrease of pressure of the produced water (Platform D) and of the exported oil (Platforms A, B and C) compared to the feed pressure.

The exergetic product mainly includes an exergy increase of the gas flows, with the exception of Platform D, where nearly 40 % of the exergetic product consists of the exergy increase of

Table 7.4: Task exergy efficiencies (%) based on the approach of Tsatsaronis and Cziesla for distillation columns.

	Platform A	Platform B	Platform C	Platform D
$\varepsilon_{II-3,mass}$	48.1	39.0	53.9	38.8
$\varepsilon_{II-3,molar}$	38.2	1.7	49.3	39.3

the seawater pumped for injection. Such conclusions may be expected, as the gas products mostly have significantly higher pressures than the feed streams.

An exception is the exported gas from Platform B, which has lower pressure and temperature than the feed streams, but still displays a higher specific physical exergy than the feed streams.

Applying the same expression on a molar basis returns different numerical values and conclusions (Table 7.4). Furthermore, the exergetic fuels and products differ slightly for Platforms A, C and D, and significantly for Platform B. The inconsistencies are due to the different compositions of the feed and product streams that are compared.

For Platforms A, C and D a calculation on a molar basis (Figure 7.8) leads to a somewhat higher or lower value for each exergy increase or decrease. For Platform B, this results in a change from an exergy increase to an exergy decrease, and thus in different calculations of the product and fuel exergies for the gas export stream (Table 7.5). The specific physical exergy of the export gas (507 kJ/kg) is higher than the specific physical exergy of the well streams (447 kJ/kg), whilst the molar physical exergy is lower (10,317 kJ/kmol against 11,082 kJ/kmol).

Table 7.5: Specific and molar physical exergies for Platform B.

	Feed	Exported gas	Fuel gas	Exported oil	Produced water
e^{ph} (kJ/kg)	447	507	337	24	41
$\bar{e}^{\mathrm{ph}}$ (kJ/kmol)	11,082	10,317	8145	2973	734

Effects from this inconsistency may be small for distillation columns that separate similar components. However, these effects may be considerable when applying this formulation to oil and gas platforms, because there are large differences in chemical composition and therefore in molecular weights and densities.

This suggests that comparing the specific exergy of different streams is not appropriate to determine whether an exergetic transfer is an exergetic fuel or product, and that another formulation must be found.

The same approach may instead be applied at the level of each chemical component, to quantify precisely the exergy transfers taking place, rather than at the level of each material stream.

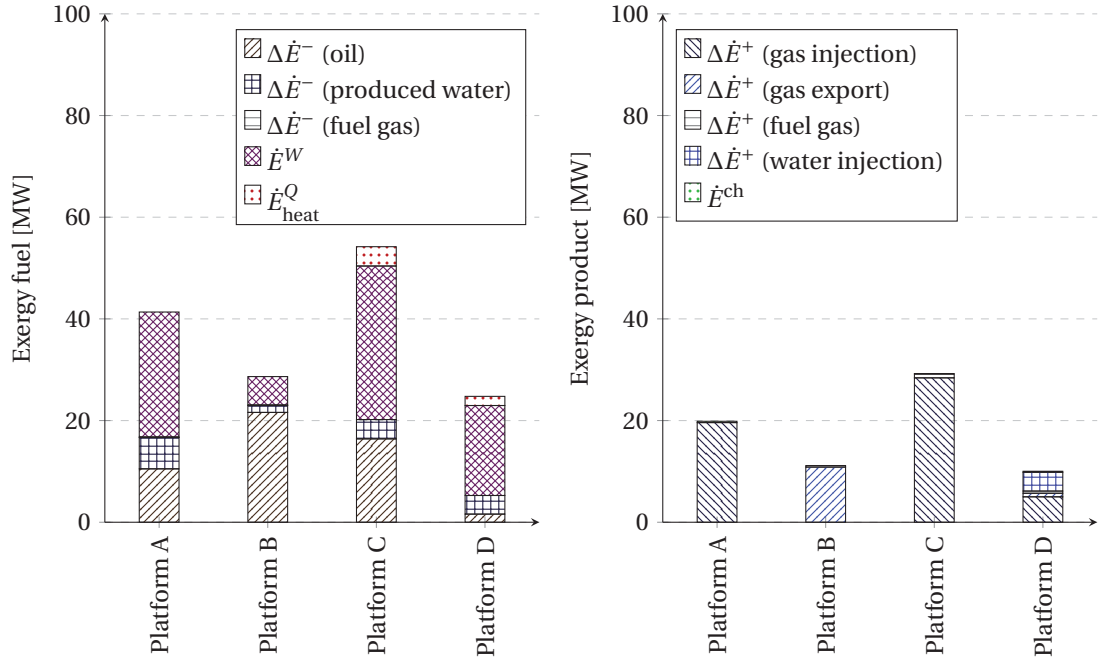

Figure 7.7: Exergy fuels and products, based on the approach of Tsatsaronis and Cziesla for distillation columns, calculated on a mass basis.

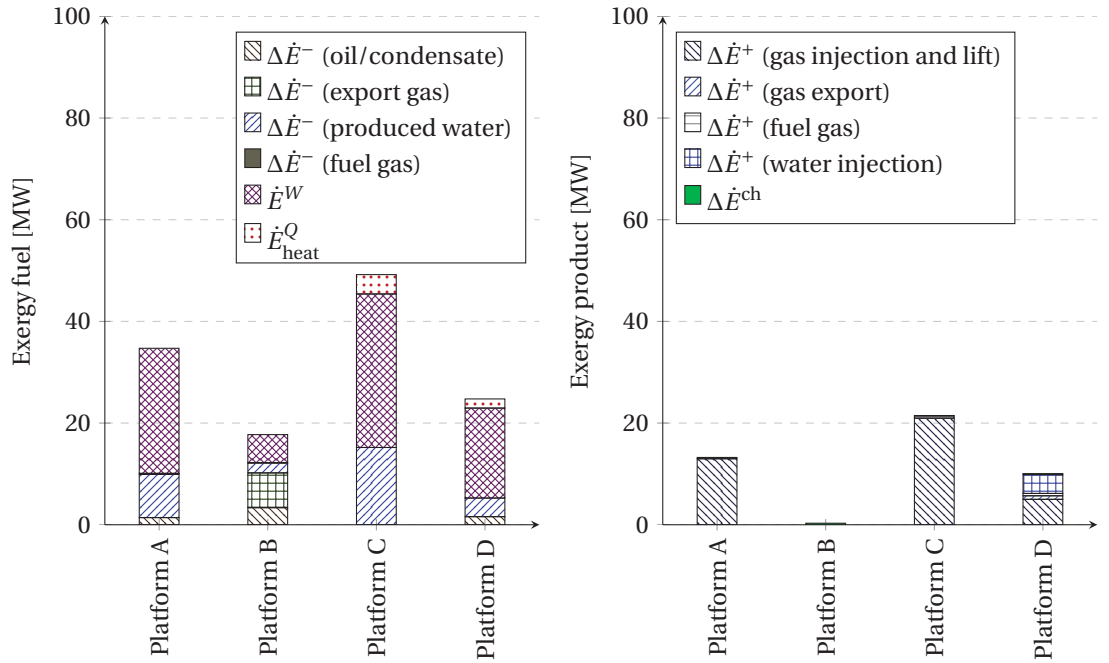

Figure 7.8: Exergy fuels and products, based on the approach of Tsatsaronis and Cziesla for distillation columns, calculated on a molar basis.

7.4 Component-by-component exergy efficiency

7.4.1 Concept

As seen in the previous section, the formulation of an exergy efficiency for oil and gas platforms is not straightforward, because of (i) the high transit chemical (and sometimes also physical) exergy of hydrocarbon components, (ii) the large variety of chemical components and (iii) the differences in process conditions and product specifications among these facilities. The following formulation of exergetic efficiency is proposed, building on the same reasoning as in Tsatsaronis and Park [191].

The increase of chemical exergy between all input and output streams is taken as the first contribution to the exergetic product. The second contribution is related to increases in physical exergy of useful product streams. However, the specific physical exergies of the *entire* streams are not compared with the specific physical exergies of the feed streams. For each feed stream, different parts may end up in different products.

The physical exergy of each part in the feeds is compared against the physical exergy of the corresponding parts in the products. The exergy that is spent in the system is taken as the power and heat exergy consumed onsite, as well as the decrease of physical exergy of fractions that lose physical exergy on the way from feed to product. This concept is similar to the one considering transit exergy [137], but carried out on the chemical component level.

A schematic overview of the component flows for a system with two components, two feeds and two products is shown in Figure 7.9. The physical exergy of each part at the outlet $\dot{E}^{\mathrm{ph}}_{j,k,\mathrm{out}}$, will either have increased or decreased compared to the physical exergy of the same part at the inlet $\dot{E}^{\mathrm{ph}}_{j,k,\mathrm{in}}$. Since the exergetic fuel and the exergetic product are evaluated at the chemical component level, this efficiency is called the *component-by-component* efficiency.

7.4.2 Derivation

The physical exergies of the *part* of a stream coming from feed j, $\dot{E}^{\mathrm{ph}}_{j,k,\mathrm{in}}$, and ending up in product k, $\dot{E}^{\mathrm{ph}}_{j,k,\mathrm{out}}$, are calculated using the following equations:

$$\dot{E}^{\mathrm{ph}}_{j,k,\mathrm{in}} = \sum_i \dot{n}_{i,j,k} \bar{e}^{\mathrm{ph}}_{i,j} \tag{7.28}$$

$$\dot{E}^{\mathrm{ph}}_{j,k,\mathrm{out}} = \sum_i \dot{n}_{i,j,k} \bar{e}^{\mathrm{ph}}_{i,k} \tag{7.29}$$

The symbol $\bar{e}^{\mathrm{ph}}_{i,j}$ denotes the partial molar physical exergy of component i in feed stream j, $\bar{e}^{\mathrm{ph}}_{i,k}$ denotes partial molar physical exergy of component i in product stream k and $n_{i,j,k}$ denotes the molar flow of component i from feed j to product k.

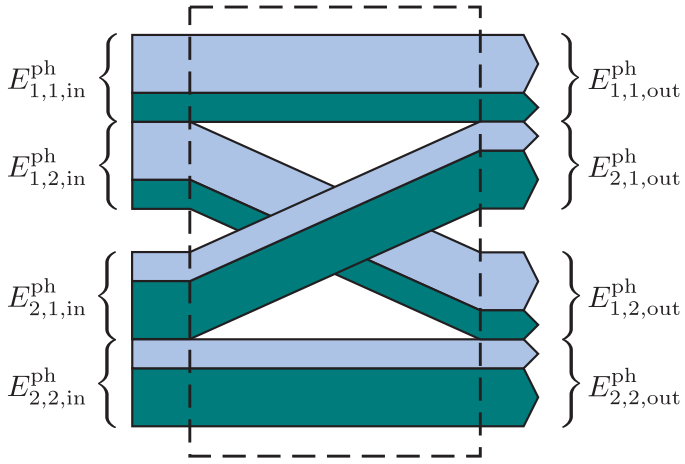

Figure 7.9: Schematic overview of component flows in and out of a control volume for a system with two components, two feeds at the left and two product streams at the right.

The partial molar physical exergy of component i, which should not be confused with the molar physical exergy, is defined as:

$$\bar{e}^{ph}_i = \left(\frac{\partial E^{ph}}{\partial n_i}\right)_{T,P,n_{l\neq i}} \tag{7.30}$$

For each component in each feed stream, it is assumed that the fraction of the component ending up in each product stream is the same as the fraction of the total amount of this component entering as feeds ending up in each product stream.

For instance, for methane in feed 1, it is assumed that the fraction of this methane ending up in product 1 is the same as the fraction of the total amount of methane ending up in product 1.

Physical exergy increases of parts of streams are denoted $\left(\Delta\dot{E}^{ph}_{j,k}\right)^+$ and can be expressed mathematically:

$$\left(\Delta\dot{E}^{ph}_{j,k}\right)^+ = \begin{cases} \dot{E}^{ph}_{j,k,out} - \dot{E}^{ph}_{j,k,in} & \text{if } \dot{E}^{ph}_{j,k,out} > \dot{E}^{ph}_{j,k,in} \\ 0 & \text{if } \dot{E}^{ph}_{j,k,out} < \dot{E}^{ph}_{j,k,in} \end{cases} \tag{7.31}$$

On the opposite, physical exergy decreases of parts of streams are denoted $\left(\Delta\dot{E}^{ph}_{j,k}\right)^-$ and can be expressed:

$$\left(\Delta\dot{E}^{ph}_{j,k}\right)^- = \begin{cases} 0 & \text{if } \dot{E}^{ph}_{j,k,out} > \dot{E}^{ph}_{j,k,in} \\ \dot{E}^{ph}_{j,k,in} - \dot{E}^{ph}_{j,k,out} & \text{if } \dot{E}^{ph}_{j,k,out} < \dot{E}^{ph}_{j,k,in} \end{cases} \tag{7.32}$$

The exergy balance, Equation 7.19, can thus be rewritten:

$$\underbrace{\sum_j \sum_k \left(\Delta \dot{E}^{\mathrm{ph}}_{j,k}\right)^- + \dot{E}^Q_{\mathrm{heat}} + \dot{E}^W}_{\dot{E}_{\mathrm{f}}} = \underbrace{\Delta \dot{E}^{\mathrm{ch}} + \sum_j \sum_{k,\mathrm{u}} \left(\Delta \dot{E}^{\mathrm{ph}}_{j,k}\right)^+_{\mathrm{u}}}_{\dot{E}_{\mathrm{p}}} + \underbrace{\sum_j \sum_{k,\mathrm{w}} \left(\Delta \dot{E}^{\mathrm{ph}}_{j,k}\right)^+_{\mathrm{w}} + \dot{E}^Q_{\mathrm{cool}}}_{\dot{E}_{\mathrm{l}}} + \underbrace{\dot{E}_{\mathrm{d,PP}}}_{\dot{E}_{\mathrm{d}}} \tag{7.33}$$

This result in the following expression for the exergy efficiency (ε_{II-4}):

$$\begin{aligned} \varepsilon_{II-4} &\equiv \frac{\sum_j \sum_k \left(\Delta \dot{E}^{\mathrm{ph}}_{j,k}\right)^+_{\mathrm{u}} + \Delta \dot{E}^{\mathrm{ch}}}{\sum_j \sum_k \left(\Delta \dot{E}^{\mathrm{ph}}_{j,k}\right)^- + \dot{E}^Q_{\mathrm{heat}} + \dot{E}^W} \\ &= 1 - \frac{\sum_j \sum_k \left(\Delta \dot{E}^{\mathrm{ph}}_{j,k}\right)^+_{\mathrm{w}} + \dot{E}^{\mathrm{Q}}_{\mathrm{cool}} + \dot{E}_{\mathrm{d,PP}}}{\sum_j \sum_k \left(\Delta \dot{E}^{\mathrm{ph}}_{j,k}\right)^- + \dot{E}^Q_{\mathrm{heat}} + \dot{E}^W} \end{aligned} \tag{7.34}$$

This approach, at the chemical component level, takes into account the fact that in separation processes the feed and product streams display the same chemical components, but in different quantities.

Gas mostly contains light hydrocarbons, which have much lower molecular weights than the hydrocarbons present in the oil. As different types of chemical components do not have the same thermodynamic properties (enthalpy and entropy) at the same environmental conditions (temperature and pressure), this implies that different components carry different quantities of physical exergy.

Decomposing the physical exergy of a stream into the physical exergy per chemical component allows therefore for more accurate calculations of the exergy fuels and products. This formulation of exergy efficiency is not valid only for oil and gas offshore platforms, but can be generalised to separation processes.

This approach does not depend on whether the partial physical exergies are calculated on a mass or molar basis, meaning that the same results would be found if the partial specific physical exergies are calculated instead:

$$e^{\mathrm{ph}}_i = \left(\frac{\partial E^{\mathrm{ph}}}{\partial m_i}\right)_{T,P,m_{l\neq i}} \tag{7.35}$$

7.4.3 Application

The calculations of the exergy efficiency as given in Equation 7.34 suggest that Platforms D and C present the highest thermodynamic performances, while Platform B presents the poorest performance (Table 7.6). With the exception of Platform B, the major exergy fuel consists of the power required in the pumping and compression operations (Figure 7.10).

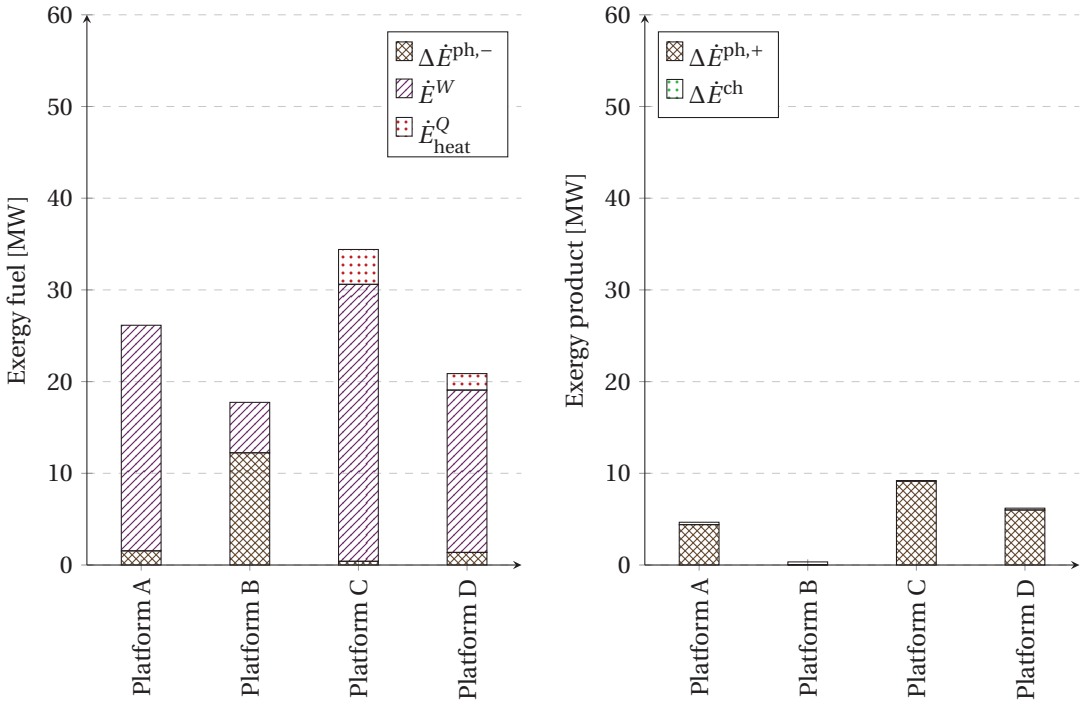

Figure 7.10: Exergy fuels and products, based on the component-by-component approach.

The numerical value of the component-per-component efficiency for Platform B is equal to the task efficiency one, using the approach of Tsatsaronis and Park [191] on a molar basis.

Table 7.6: *Task* exergy efficiencies (%) based on the *component-per-component* approach.

	Platform A	Platform B	Platform C	Platform D
ε_{II-4}	17.9	1.7	26.8	29.6

Oil and gas platforms perform separation, pumping and compression work, but in different magnitudes, and this explains some the large differences in terms of efficiencies between the four facilities. Platform A processes oil, gas and water: the three phases are separated, oil is pumped to another platform, gas is compressed to more than 200 bar for further injection, and water is discharged to the sea at low pressures. The *separation* work is small in comparison to the pumping work, and negligible towards the compression one.

Platform B processes condensate, gas and water: gas and oil exported at a pressure lower than the feed pressure, and the separation work is mostly driven by the decreases in physical exergy. Platform C processes oil, gas and water: oil is exported at a much higher pressure than the feed pressure, and the pumping work on this platform is significantly higher than on Platforms A and B. Platform D processes oil, gas, and significant quantities of produced water. Seawater is pumped for further injection, and small quantities of gas are compressed and exported.

7.5 Applicability

7.5.1 Sensitivity

Despite the significant differences between the four cases under study, the specific power consumption represents less than 2 % of the total energy and exergy leaving the system. This is also reflected by the low specific exergy destruction and high input-output exergy efficiency values, which are below 2 % and above 99 %, respectively, in all cases.

This is characteristic of facilities processing oil and gas, as also shown in the study of Margarone et al. [229], where the specific power consumption is below 1.5 %. Crude oil mixtures have inherently a large chemical energy and exergy content: caution should be exercised when using these parameters alone, as they may give the impression that there is a very small room for improvement.

Such an issue is also discussed in the works of Kotas [54, 181, 182] and Tsatsaronis and Cziesla [213]. Both argued that using the concept of input-output exergy efficiency may be misleading, as it may hide the effects of reducing the system inefficiencies and of integrating improvement strategies. However, it may give an interesting basis for comparison with other methods of oil and gas exploration, such as shale oil and hydrate production. On the contrary, all the *task* exergy efficiencies showed a clear difference between the four facilities, and they are also expected to be sensitive to system improvements.

7.5.2 Feasibility and simplicity

The approaches found in the scientific literature presented all drawbacks compared to the *component-by-component* efficiency, stemming from the fact that they were derived for systems with partly different tasks. However, some of them require significantly less calculation efforts. The use of the exergy efficiencies as defined in the approaches of Kotas [54] and de Oliveira Jr. and Van Hombeeck [59], and of Cornelissen [56] and Rian and Ertesvåg [238], requires flow, temperature and pressure measurements, which are often already conducted, as well as crude oil and gas assays to estimate the composition.

The *component-by-component* efficiency requires significantly more computational efforts than the other definitions, since the calculations are done on a component level, and the partial molar physical exergy of each component has to be calculated.

7.5.3 Transparency

Indicators such as the specific power consumption or specific energy use are already in use in the oil and gas industry, as well as in other industrial sectors. They can easily be controlled, and the results that are obtained are reliable, in the sense that they can be validated by a few practical measurements and are not dependent on different assumptions or approaches.

The case of BAT efficiencies is trickier: Margarone et al. [229] emphasised that the current system layout of the gas treatment facility consumed twice as much power as an improved layout with state-of-the-art technologies. On the contrary, Svalheim and King [19] argued that the oil and gas facilities under study had an excellent energy performance and a small improvement potential.

When it comes to exergetic efficiencies, exergetic efficiencies depend solely on the extent of the irreversibilities of the system under study and take into account pressure reduction due to throttling. They may therefore allow a more adequate comparison between various oil and gas platforms.

In addition to the different efficiencies calculated here, de Oliveira Jr. and Van Hombeeck [59] defined the terms of fuel and product exergies differently, and this definition resulted in another efficiency value in the case of Platform A, as shown in Voldsund et al. [172].

Finally, the expressions and numerical values of exergetic efficiencies are dependent on the selection of the:

- environmental state: the environmental temperature and pressure have a direct impact on physical and chemical exergy;
- system boundaries: the inclusion of the import and export pipelines and of the gas lift system would impact the numerical values of the mechanical exergy increases.

As different considerations on exergetic efficiencies may lead to different deductions, it should be made clear which interpretations and system boundaries are actually used, to avoid misleading conclusions.

7.5.4 Temperature-based and pressure-based exergy

The exergy balances and interpretation of product in the *component-by-component* efficiency can be improved by decomposing the physical exergy term into its temperature-based and pressure-based components. For example, one of the desired outcomes of the processing plant is the export of gas at high pressure, which is equivalent, from a thermodynamic viewpoint, to the production of pressure-based exergy.

The temperature-based exergy of gas streams is a result of the turbomachinery component inefficiencies, and is dissipated to a large extent in the export pipelines. Pressure-based exergy increases should therefore be accounted as a part of the exergetic product (desired outcome of the system), while the temperature-based exergy increases should be considered as a part of the exergetic losses. These considerations were also emphasised in the studies of Kotas [54], Cornelissen [56] for oil and gas distillation systems, and Marmolejo-Correa and Gundersen for LNG processes.

Such decompositions would further increase the required computational efforts [51, 52]. In the present cases, it is expected that the decomposition would only very slightly affect the numerical results, as the pressure-based exergy of gas generally dominates the temperature-based exergy (96 % against 4 % in the work of Voldsund et al. [172] for Platform A). The benefit of such an improvement in the efficiency should be evaluated against the larger required computational efforts.

7.5.5 Theoretical and practical improvement potential

Best-available-technologies efficiencies allow for reasonable estimations of the improvement potential of a given oil and gas platforms, as they are based on the selection of technologies already available on the market. Other reasoning that may be applied are the ones of:

- Tsatsaronis and Park [191], who defined the unavoidable exergy destruction as the exergy that is destroyed when the current components are operated at their maximum efficiency, considering technological limitations that could not be overcome in the near future, regardless of the investment costs;
- Johannessen and Røsjorde [239], who suggested to set a state of minimum entropy production or minimum exergy destruction for a given operation target, and the difference between the current value and this minimum would be considered as an excess loss. This principle has been applied to, for instance, distillation systems.

The main criticisms against these approaches are the degree of subjectivity when defining the state of unavoidable exergy destruction, and the high sensitivity of such targets to future technological achievements. These approaches could anyway give a more realistic target for each platform, and allow for comparison on how well they utilise their practically achievable potential.

On the contrary, the targets suggested by investigating exergy efficiencies may not realistic, as there are practical constraints that should be considered:

- economical – integrating other components or redesigning the system may be costly, and possibly cause shut-downs of the plant during the installation phase;
- technical – the structural design of the processing plant is partly fixed and bound by the field characteristics (e.g. temperatures) and the export conditions (e.g. purity);
- technological – the performance of a process component is limited by the current technological advances (e.g. state-of-the art centrifugal compressors).

This implies that only a part of the thermodynamic inefficiencies taking place in petroleum separation processes can be reduced in practice, whereas another part cannot be avoided.

Bejan et al. [76] emphasised the difficulty of using the exergy efficiency for comparing systems with dissimilar functions, which is the case of oil and gas platforms. All platforms have the functions of separation, compression and pumping.

However, because of differences in operating conditions, some platforms must achieve more compression work (Platform A), others mainly perform pumping work (Platform D), and some may do less of compression and pumping, and thus almost only separation (Platform B). In general, pumps are characterised by a higher exergetic performance than compressors, and the latter are more exergy-efficient than systems with separation tasks. Different systems present different potentials for improvement.

One way to overcome this problem may be to evaluate different sub-processes separately. If for instance the performance of separation was evaluated individually, or similarly the performance of compression or pumping, the platforms could be compared on a similar basis. The issue of comparing systems with dissimilar functions would be eliminated.

Estimating each type of performance individually may be difficult, as several components and sub-systems have several functions. For instance, the integration of a scrubber results in a separation between the liquid and gas phases, increasing the separation work, but also prevents the processing of heavy hydrocarbons in the gas compressors, reducing thus the power requirements.

Another alternatives may be to compare the efficiencies of each sub-system (e.g. separation, re-compression, treatment) between different platforms, or to eliminate from the calculations the processes that are specific to a given one. For instance, for Platform D, the presence of a seawater injection process results in a higher system exergetic efficiency compared to the three other ones, because pumping is generally a more efficient process than compression and separation.

7.5.6 Performance and ageing

It is generally admitted that the performance of oil and gas platforms decreases with time, as a result of ageing and degradation of the on-site components and processes. Therefore, it may be expected that old platforms have a lower BAT efficiency than newer ones, although that, in this work, the platform with the lowest BAT efficiency was one of the newest.

Meanwhile, the main function of an offshore platform may change over time due to varying operating conditions. For instance, an increased gas-to-oil ratio for Platform A resulted in more necessary compression work over the last 20 years, while the increased water-to-oil ratio for Platform D has resulted in a greater pumping demand. Using exergy efficiency to monitor installations over time may give results that are biased by the changes in the relative importance of compression, pumping and separation over time.

7.6 Conclusion

The energy performance indicators currently used in the oil and gas industry present weaknesses, as they cannot be used to compare consistently different facilities and over-predict the performance of all the platforms analysed in this study. They can be improved by considering an exergy basis rather than an oil equivalent volume one, and they can be complemented by additional metrics that provide more in-depth information.

The parameters presented in this work are of two different types, and they belong to the categories of *thermodynamic* and *physical-thermodynamic* metrics. The specific energy use and exergy consumption illustrate the amounts of resources spent to produce oil, gas and condensate, but do not indicate opportunities for enhancing the system performance. On the contrary, the different types of efficiencies and the specific exergy destruction evaluate the actual performance of the system, and they can show either the technical or the theoretical achievable improvement potential.

A use of these parameters in practice, for example in monitoring systems or as general performance metrics, could be discussed. These indicators illustrate different aspects of a platform performance and could be used at different phases of the lifetime of an oil and gas facility, for instance in the early stages of the planning and evaluation of a platform configuration, or at later stages to evaluate the performance of existing platforms. Local or global implementations of these indicators seem feasible, as most can be calculated with only a few measurements and be used for informing a broader audience.

Exergy efficiency definitions found in the scientific literature for similar systems had drawbacks such as (i) low sensitivity to efficiency improvements, (ii) calculation inconsistencies or (iii) favoured facilities with certain boundary conditions when applied to the four offshore processing plants. Based on these experiences, the *component-by-component* efficiency was proposed. This efficiency is sensitive to process improvements, gives consistent results and evaluates successfully the theoretical improvement potential, but requires large computational efforts.

The *component-by-component* efficiency may be of interest for petrochemical systems other than oil and gas platforms. It can be applied to industrial systems where petroleum is fractionated, since similar processes take place (compression, expansion, separation, distillation). However, although oil and gas platforms and oil refineries aim at separating the hydrocarbons composing the oil and gas mixtures, the performance of both systems may not be directly comparable, since the structural design set-up is fundamentally different.

8 Energy savings

This chapter presents the evaluation of possible energy saving scenarios, based on the case studies presented in Chapter 6. The performance losses of oil and gas platforms are assessed and the improvement possibilities on which focus should be set are spotted.

8.1 Introduction

Different strategies can be applied to improve the thermodynamic performance of oil and gas facilities, and they can roughly be classified into two categories. The first possibility is to reduce the *internal* and *external* energy requirements of the processing plant by increasing the efficiency of the most important components and processes, or by promoting energy integration between different sections of the plant. The second one aims at improving the performance of the power generation system, by, for instance, implementing co-generation engines.

The present chapter addresses the first possibility: it focuses on the main components and sub-systems of a petroleum processing plant, from the production manifolds to the gas compression operations. Energy saving opportunities are depicted by changing the operating conditions or modifying the process layouts:

(1) the possibilities for reducing or exploiting the pressure-based exergy of the well-streams in the production manifold and separation sub-systems were analysed, considering the implementation of multi-level production manifolds and multiphase expanders;

(2) the effects of eliminating gas recirculation around the gas compressors were quantified in terms of energy savings and exergy destruction;

(3) the opportunities for energy integration within each sub-system and at the level of the total site were assessed, with and without a central utility loop.

8.2 Production manifolds

There are two main possibilities for improving this sub-system: the first one is to operate the production manifolds with more pressure levels, and the second one is to integrate multi-phase expanders and to utilise the feed energy. First, some platforms include manifolds operated at different pressure levels. The inlet pressure depends on the well pressure and on the necessary pressure drop between the well-head and the production manifold to ease flowing of oil and gas. The outlet pressure depends on the requirements of the 1st stage separation process and on the lowest pressure of the mixed well-streams.

8.2.1 Multi-level production manifold

Background

The integration of an additional pressure level in the production manifolds could result in (i) smaller exergy destruction in this section of the plant, (ii) lower gas recovery at the 1st separation stage, (iii) smaller power demand of the gas compression and thus higher gas export, and (iv) greater system complexity. However, well-stream pressures decrease with time, and therefore the well-streams that undergo a significant reduction in pressure can be re-routed to a production manifold operating at a lower pressure. In practice, the energy savings may not be significant without a tuning of the control system of the compressors. An additional pressure level in the production manifold section results in smaller gas flows in the separation and gas recompression processes. These decreases should be compensated by a greater recirculation rate to prevent surge.

Case studies

The cases of Platforms A and C can be taken as examples (Figure 8.1), because the production manifolds are operating on high-pressure wells, and some of these wells have an inlet pressure higher than the pressure of the gas treatment process at the outlet of the 1st stage. This study analyses only the case of Platform C.

The introduction of an additional pressure level for this facility, presently named *very-high*, could result in a smaller power consumption and thereby greater fuel gas export. It may also allow for smaller loading (unloading) of the separators placed in the 1st and 2nd stage of the separation train, reducing the liquid carry-over with the gas phases. A drawback would be the higher loading of the cooler and separator operating on the stage at which the very-high pressure manifold is connected, and a more in-depth study should be conducted to evaluate the possible liquid carry-over with the gas phase. This retrofit may be interesting, as a large number of processing wells are operating at a pressure higher than the second stage of the gas treatment (≥ 94 bar), and the gas fraction of the reservoir fluids extracted through these wells is higher (≥ 30 %) than for the other.

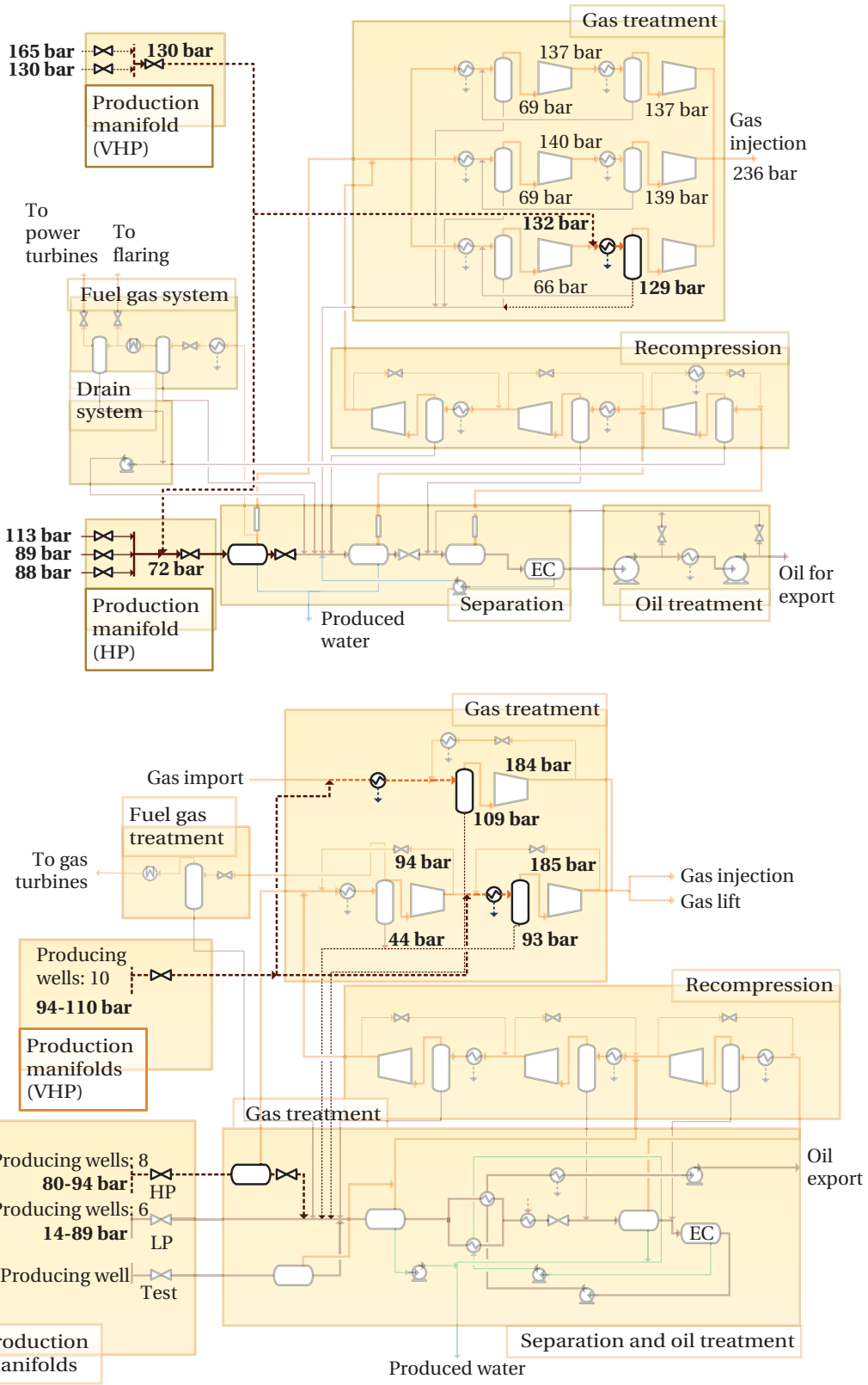

Figure 8.1: Process flow diagram of Platforms A and C with retrofit of the production manifolds.

Perspectives

The introduction of an additional pressure level is relevant only with another control strategy of the compressors on-site. The benefits of the scenarios proposed as follows are therefore evaluated against a base case scenario (Scenario 0), where no gas is recirculated. The first improved scenario (Scenario 1) assumes that the separation pressures are fixed and cannot be optimised. In this case, the very high pressure manifold should operate at the pressure of the 2nd stage of the gas treatment section, i.e. at least at 93 bar, and 10 wells can be rerouted.

The second improved scenario (Scenario 2) assumes that the separation and production manifold pressures can be modified. In that case, all the wells currently connected to the high pressure manifold can be rerouted, and the compressors at the last recompression and first gas treatment stages should be retrofitted to allow for operations at different pressures. Scenario 2 is thus reformulated as an optimisation problem, for which the objectives are to minimise the total power consumption and maximise the oil and gas recovery. The degrees of freedom are of two types: a feed stream from a given well can be connected either to the VHP or HP production manifold, and the outlet pressure of each valve can be varied between the LP and reservoir pressures.

The improved scenarios build on the following assumptions: (i) perfect separation between liquid and vapour phases takes place in the scrubbers, (ii) the feed conditions are identical to the ones given in the original measurements presented in Voldsund et al. [173], and (iii) the flow rate of the cooling water is regulated to ensure the same conditions of the gas streams at the outlet of the seawater coolers.

The introduction of a VHP level at a pressure of 93.9 bar (Scenario 1) is shown to be beneficial, resulting in a net power saving of 1.7 MW. The recovery of medium- and heavy-weight hydrocarbons into the oil stream is nearly identical. However, the recovery of light-hydrocarbons is slightly worse, by 0.2 %-point, because more methane and ethane are entrained with the liquid condensate recovered in the high-pressure scrubber of the last compression stage.

The optimisation of the pressure levels of the VHP and HP production manifolds (Figure 8.2) suggests that greater power savings could be attained by designing and routing properly this section of the processing plant.

The recoveries of light and heavy hydrocarbons are clearly conflictive objectives, since larger liquid throughput results in smaller gas production, and vice-versa. However, the Pareto fronts indicate that the optimal gas and oil recovery vary only in a range of $\pm$ 0.5 %, while the total power consumption varies between 17,000 to 26,500 kW.

The probability of a well to be placed on the very-high pressure level is calculated by analysing the results returned by the multi-objective optimisations. The allocation of a given well to the VHP or HP level production manifold is not clearly distinct for most wells (Figure 8.3).

For example, the findings suggest that the 15th well should rather be connected to the HP level

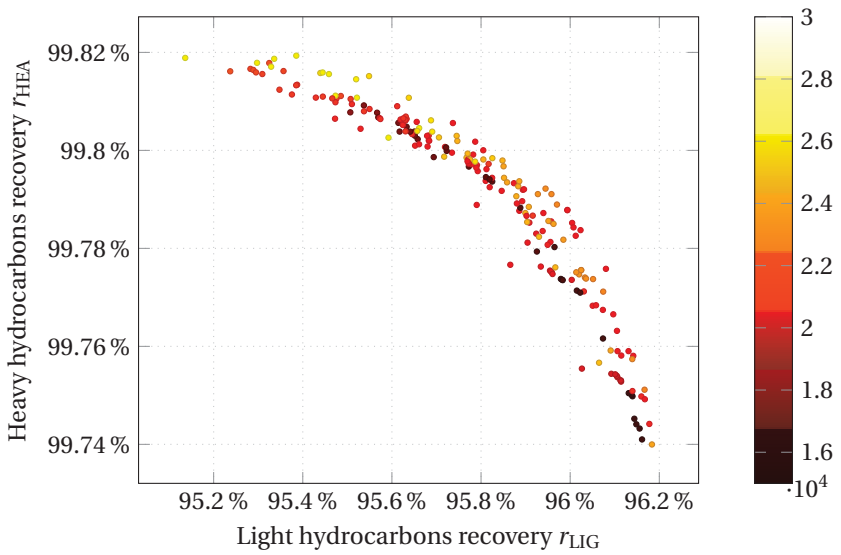

Figure 8.2: Pareto-optimal solutions for an integrated design of production manifolds with an additional pressure level (VHP) in the case of Platform C. The colour bar illustrates the power consumption of each solution, expressed in kW.

because of its low inlet pressure, and, on the contrary, that the 19th well should preferably be linked to the VHP level because of its high inlet pressure. However, the initial oil, gas and water contents of each feed stream have an importance, as suggested with the case of the 26th well. The associated flow has a high pressure, of about 94 bar, but should optimally be placed on the HP level because of the high liquid throughout (oil and water) compared to the gas production. The resulting flow at the inlet of the 2nd stage compression level would then have a higher content of water and heavy hydrocarbons than desired, which would cause a greater power consumption.

The optimum pressure levels, with respect to the maximisation of the oil and gas production, as well as the minimisation of the power consumption, range between 15 and 44 bar for the HP level, and between 34 and 78 bar for the VHP one, with average levels of about 21 and 50 bar, respectively. However, the recoveries of light and heavy hydrocarbons vary only in a range of $\pm$ 0.1% over the whole optimisation domain, and the results indicate that the optimal pressure levels for minimising the total power consumption, which would be around 17,000 kW, are of 16 and 40 bar. It can be noticed that the suggested VHP level is in the same order of magnitude as the HP level in the current situation, and that the proposed HP level is about 8 to 10 bar higher than the LP one.

A similar analysis could be conducted for the case of Platform A, but the energy savings are much likely smaller since the oil and gas flows are not as high, and the number of wells is only 5.

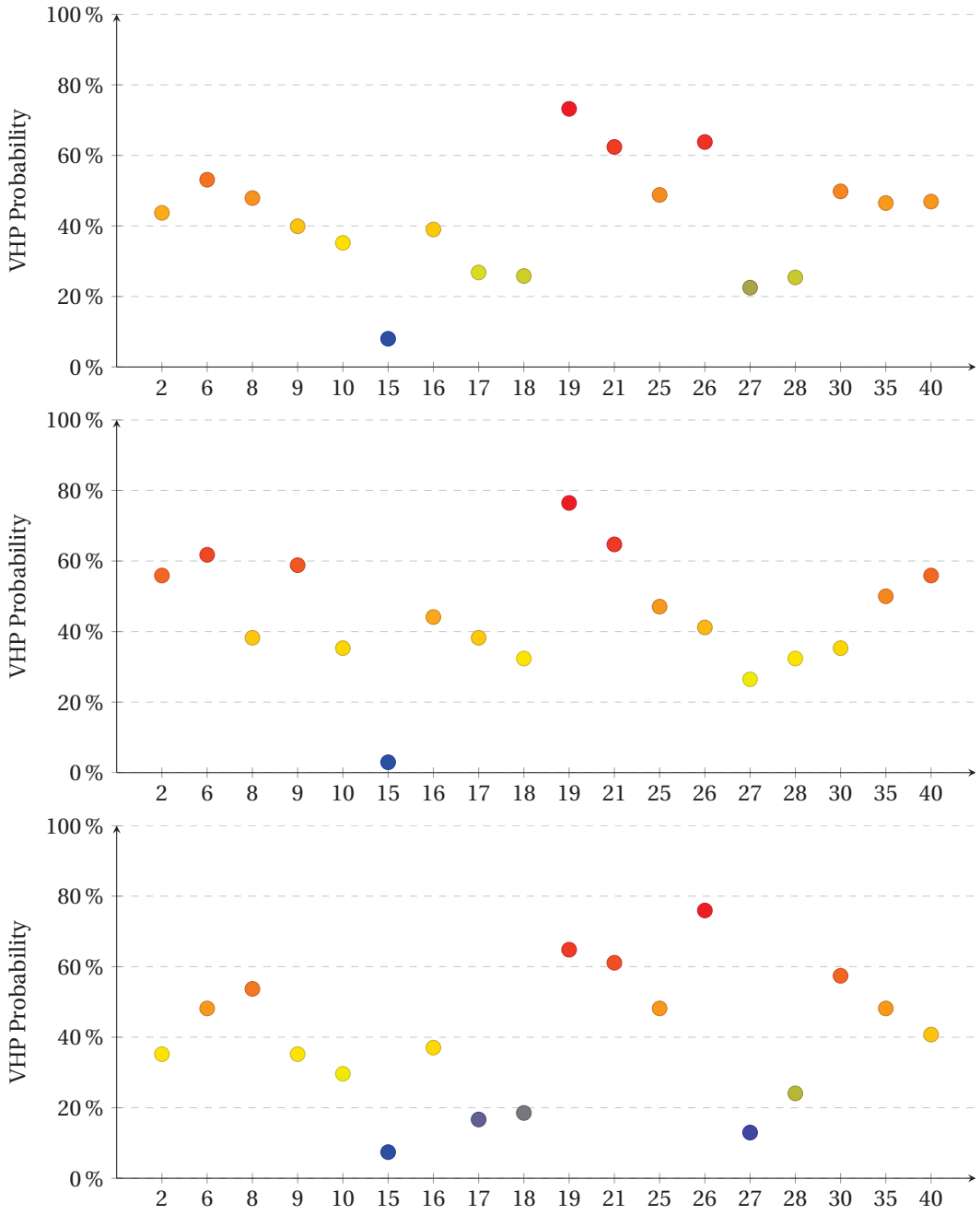

Figure 8.3: Probability for a well to be placed on the very high pressure level production manifold over the whole domain of the optimisation results (top), for a power consumption ranging in the least 25 % (middle) and in the top 25 % (bottom).

8.2.2 Multiphase flow expanders

Background

Multiphase flow expanders may allow for energy recovery from the depressurisation of the well-streams and reduce the quantity of exergy destroyed in the production manifolds. Multiphase flow ejectors would result in higher oil recovery in depleted wells, which is of particular interest for mature oil fields. There are in practice technical challenges in implementing these devices, as the fractions of oil, gas and water vary significantly. The presence of impurities and sand in the reservoir fluids will also complicate the designing task because of the risks of erosion.

In theory, the replacement of choke valves by multi-phase turbines would result in smaller exergy destruction in the production manifolds, which has been shown to be significant for some platforms, and the additional power generation would involve a smaller fuel consumption. It may also be advantageous for fields processing high-temperature and high-pressure petroleums, as the expander outlet temperature would be lower than by an isenthalpic expansion with a choke valve, and the outlet liquid flow rate would be higher. The integration of two-phase turbines has been studied in natural gas liquefaction applications [240].

Case studies

The cases of Platforms A and B are considered, since they both have increasing gas-to-oil ratios. Such improvements may not be effective at the end-life of a field, since lower pressures and higher water cuts result in a lower mechanical exergy of the well-streams, and thus in smaller power recovery.

Estimating the efficiency of multiphase flow expanders is challenging, as there are no practical examples of such applications in oil and gas processing. Hydraulic expanders and turbines are well-known technologies with hydraulic efficiencies exceeding 90 %, but the current literature suggests that the performance of multiphase expanders, using two-phase helico-axial ones, is comprised between 30 and 70 %, depending on the initial feed pressure [241–243]. Since the inlet feed pressures range between 70 and 130 bar, it can be expected that the hydraulic efficiency would be, with the current state-of-the-art technologies, closer to the lower bound.

Perspectives

A preliminary analysis suggests that energy could efficiently be recovered with such technologies (Figure 8.4): the produced power would represent about 6.5 and 16 % of the total power consumption of Platforms A and B, assuming an efficiency of 30 %, and the temperature at the outlet of the expander would be about 3 to 5 °C lower than in the current situation, with a drop of the vapour fraction of less than 5 %. These differences would impact to a minor extent the downstream separation process. A more detailed technical analysis should be conducted, to investigate the practicability of multiphase flow expanders.

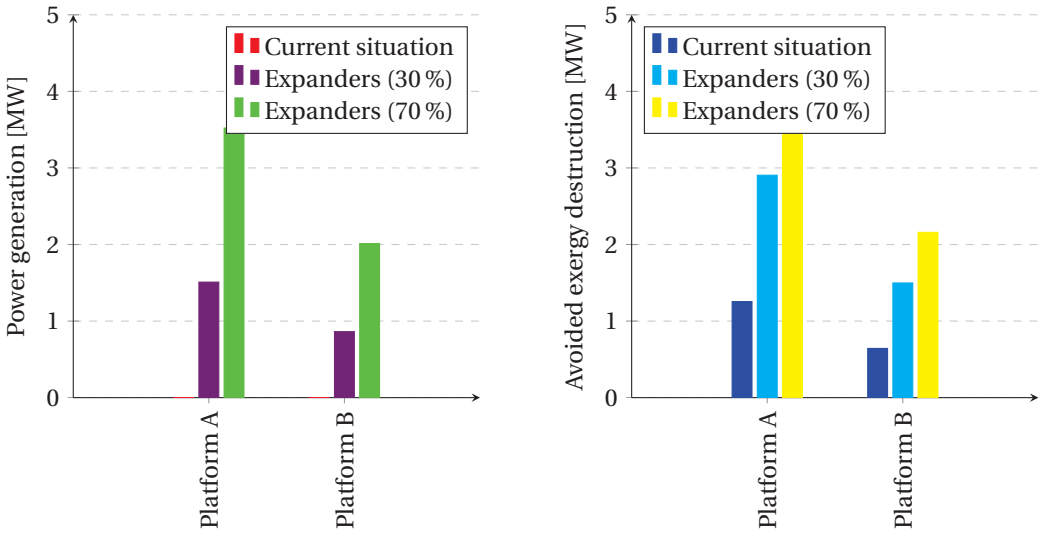

Figure 8.4: Power generation and avoided exergy destruction with integration of multi-phase flow expanders in the production manifolds.

8.3 Separation

Attention may be drawn to the gas fraction of each well-stream entering each separator. Some wells mainly process gas, while some mainly process oil and water. The mixed well-streams at the inlet of the 1st stage separator have different vapour fractions. The possibilities of (i) integrating an extra phase separator or operating the 1st stage separator at a higher receiving pressure, (ii) increasing the number of separation stages, and (iii) by-passing the oil and gas mixing step and treating the gas separately, may be considered for wells processing a high amount of gas.

This would result in a smaller power consumption in the recompression and compression trains, and in a smaller exergy destruction in the separation section. Similarly, the operating benefits of adding more components or integrating more separation stages or parallel trains should be evaluated against their investment costs. The latter are likely to increase, as the foot area and volume taken by the process would be higher. These benefits are also limited for platforms operated on mature fields, as the exergy destruction in the separation process is expected to be smaller than during a peak production.

As for the production manifold, the introduction of multiphase expanders to replace the throttling valves operating between each separation stage may be considered. The benefits are, nonetheless, smaller, since smaller liquid flows are processed, and they generally have lower temperatures and pressures than the reservoir fluid streams entering the separation step. A preliminary analysis performed in this work indicates that the power that could be recovered at the 1st separation stage is equivalent to about 11 and 30 % of the power output of multiphase expanders in the production manifold for Platforms A and B.

8.4 Gas processing and recirculation

Background

Gas recirculation around the compressors is responsible for additional power consumption and cooling demand, as the gas flows in the compressors and heat exchangers is kept constant. Avoiding gas recirculation may therefore be an interesting alternative for increasing the amount of gas exported to the shore, increasing the operational benefits. If gas recirculation cannot be avoided, the integration of expanders in the recirculation loop may be relevant.

There are different ways to avoid such large amounts of exergy destruction and additional power consumption. For instance, some of them include the use of alternative control methods, the downsizing of the compressors, the re-wheeling of these components, or the introduction of parallel but smaller compression trains, as on Platform A. When designing a new offshore compression train, it may be interesting to implement compressors that exhibit an acceptable efficiency when they are operated at their maximum capacity and at part-load conditions, rather than ones that present a high efficiency at their design point only.

The possibility of designing smaller but parallel trains, to delay the start of off-design operations, may likewise be considered. Varying flow rates can then be handled by closing or opening parallel trains, and the compressors will be run for a longer period near their nominal point. This may be the case on Platform A, where the most recent gas train has a capacity of about twice the capacity of each other train.

Case studies

The benefits of such solutions are evaluated for the four North and Norwegian Sea platforms A, B, C and D, and the reductions in power and cooling demands vary significantly across these facilities (Figure 8.5) since they are not at the same oil production stage (e.g. early, peak, decline or end). It is assumed that (i) no recirculation takes place, (ii) the compressors operate with the same polytropic efficiency, and (iii) the cooling source flows (seawater or indirect medium) entering each heat exchanger are regulated to achieve the same temperature levels.

Perspectives

The power consumption of the entire processing plant decreases by 15 to 20 % and the greatest reduction is observed for the platforms that operate the furthest from their nominal point, since more gas is recirculated for anti-surge purposes. The cooling demand of the entire processing plant decreases by more than 10 % for Platforms A, C and D (Figure 8.5). The potential savings are smaller for Platform B, because the major cooling demand, of about 45 MW, corresponds to the gas aftercooling before export. This demand is not impacted by the gas recirculation rates, since there is no compressor operating in the gas treatment section of this platform, and the power consumption is nearly constant.

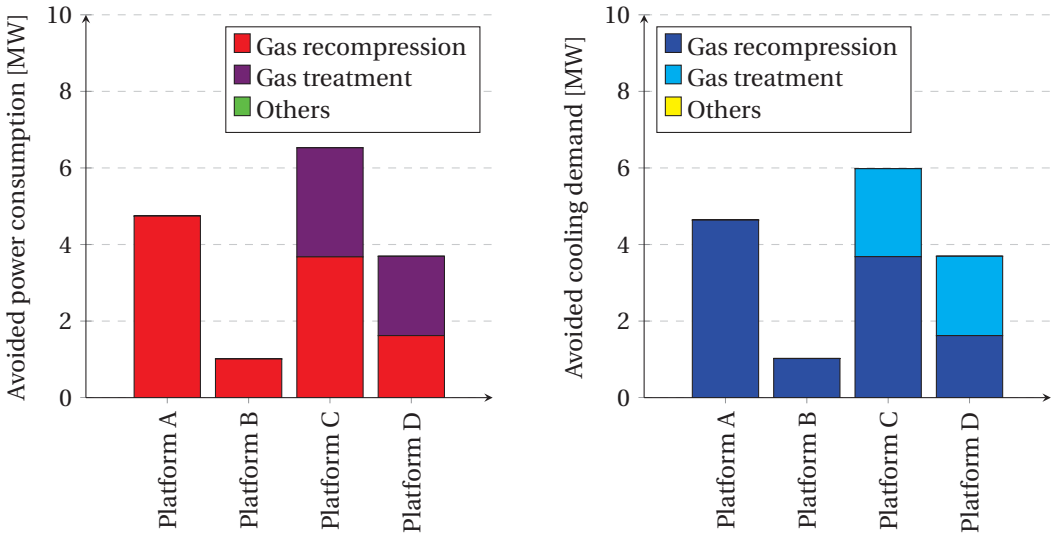

Figure 8.5: Avoided power and cooling demands if no anti-surge recirculation.

The largest savings, on relative values, are found at the gas recompression process (Figure 8.8 and Figure 8.6), and can reach up to 70–80 % of the initial power demand of that process. The savings in the gas treatment process are smaller, which can be explained by the smaller gas recirculation. The cooling demand of the gas recompression process can also be reduced by up to 70–80 % for Platforms A and D. In practice, the total energy savings (Figure 8.6) may be even greater, as a smaller cooling demand results in a smaller power consumption of the seawater lift pumps, which has not been accounted for.

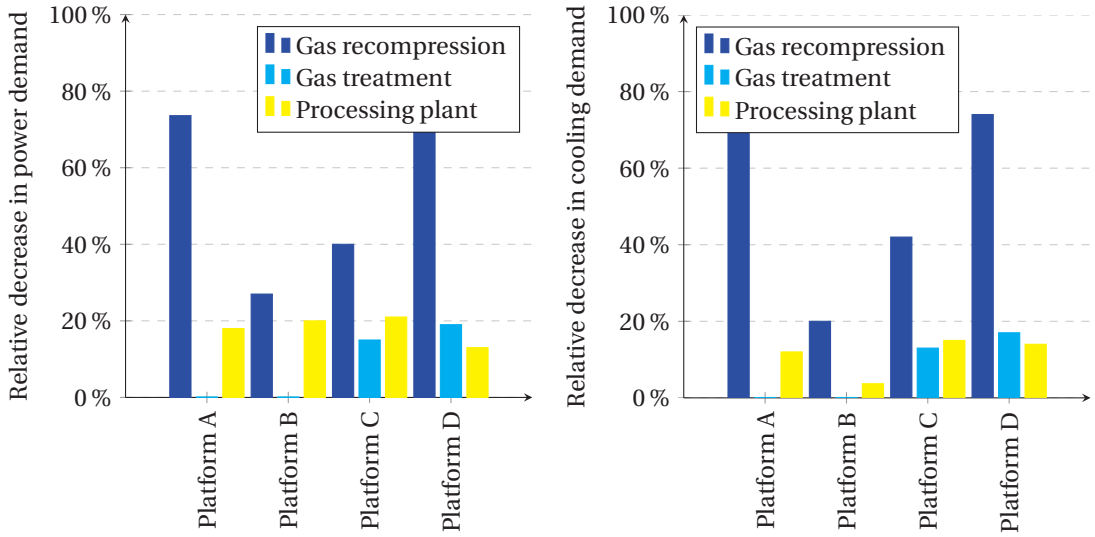

Figure 8.6: Relative changes in energy demands if no anti-surge recirculation.

Avoiding anti-surge recycling results in smaller exergy destruction throughout the processing plant of each facility (Figures 8.7 and 8.8), because of (i) the elimination of the pressure losses through the anti-surge control valves, (ii) the smaller exergy destruction by heat transfer in the coolers, and (iii) the smaller compression inefficiencies. The first amount to about 1600, 450, 1700 and 2000 kW, which corresponds to a decrease of 8.3, 3.8, 7.4 and 14.8 %. The sums of the second and third ones are roughly equal to the first ones. The reductions in exergy destruction due to smaller mixing effects represent less than 50 kW per stage.

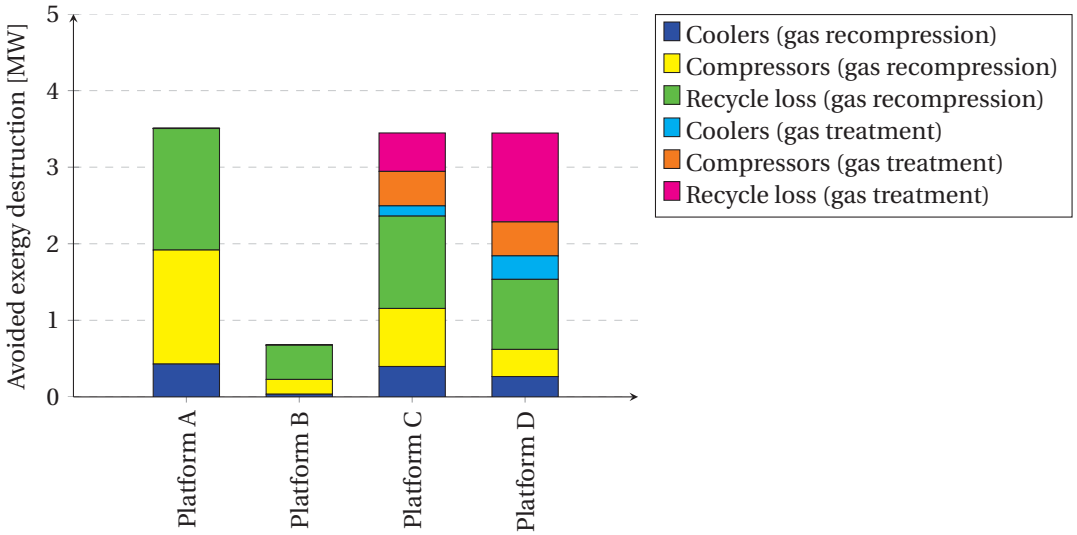

Figure 8.7: Absolute changes in exergy destruction if no anti-surge recirculation.

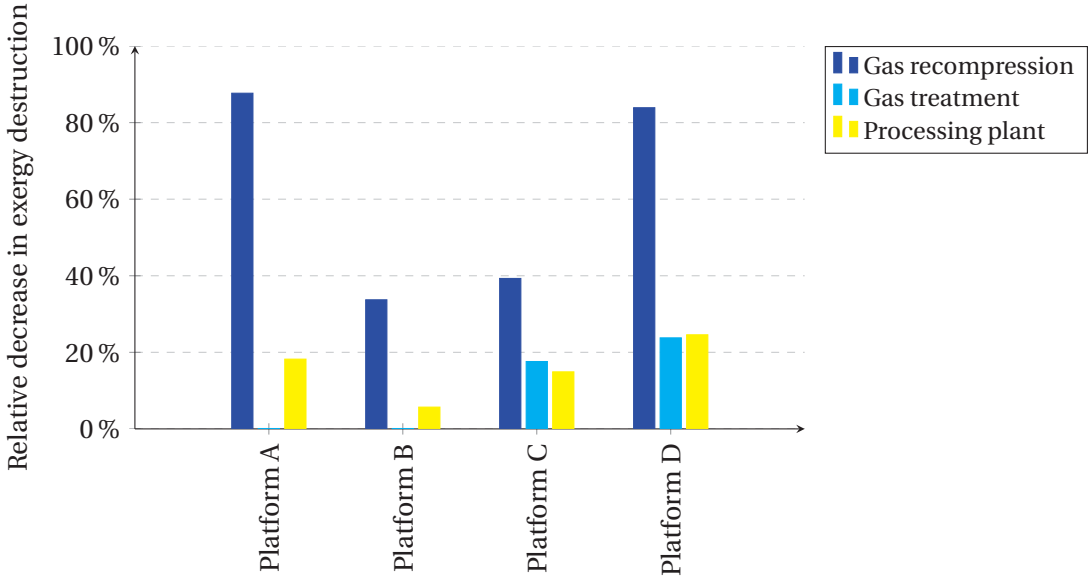

Figure 8.8: Relative changes in exergy destruction if no anti-surge recirculation.

8.5 Site-scale integration

8.5.1 Energy integration

Background

Process integration techniques aim at minimising the energy use of a given system by promoting internal heat exchanges and improving the integration of each individual process with the hot and cold external utilities.

Case studies

The four North Sea oil and gas platforms presented in Chapter 6 (Platforms A–D) and the Brazilian non-FPSO one (Platform E) are taken as case studies, as they present different energy profiles and the utility systems have different layouts.

Minimum energy requirements

A pinch analysis of each individual sub-system shows that some processes such as the oil separation or the condensate treatment require both heating or cooling, while others such as the gas treatment and oil pumping only have a cooling demand. The interest of the total site integration lies in the matching between the heating demands of a given sub-system with the cooling needs of another one. The benefits of such improvements can be observed by comparing the external utility demands resulting from the integration of each sub-system individually to an improved scenario, where the overall site is integrated (Figure 8.9).

The analysis of the entire platform, i.e. of the total site, illustrates therefore two types of problems. The first type, named *threshold*, implies that only one type of external utility (cooling or heating) is required if internal heat exchanges between sub-systems is feasible. This corresponds to the cases of Platforms A and B, where no external heating is required if the system is well-integrated. In the case of Platform E, only external heating, and no cooling, is needed. The second type (non-threshold) corresponds to cases such as of Platforms C and D, where both external heating and cooling are needed (Figure 8.10). These five cases illustrate therefore some of the variety that can be seen with offshore platforms.

Direct heat exchange. Improving the integration of the current site is particularly relevant for Platforms C and D because of the demands for both external heating and cooling. It can be performed by allowing for direct heat exchange between the process streams belonging to different sub-systems. However, this may be challenging for geographical and operational reasons. The site profiles show that all the site cooling demand takes place at temperatures lower than 120 °C, and only the oil heating process takes place at this level.

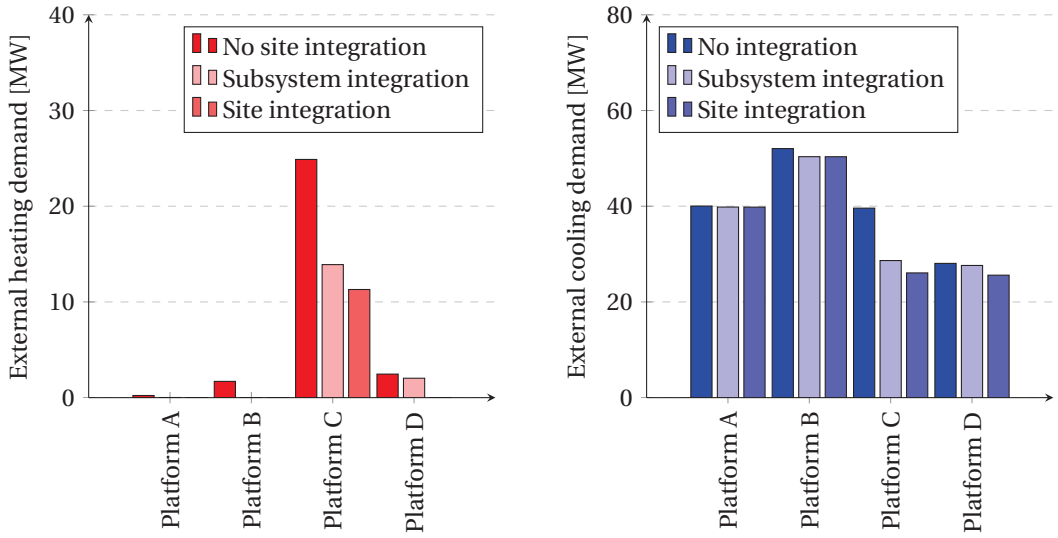

Figure 8.9: External utility demands without integration, with subsystem integration and with site integration.

The integration of gas-oil heat exchangers faces two issues. First, all the gas streams should be cooled down to 20–50 °C, and the oil stream has an initial temperature of 45–55 °C. The gas streams should therefore be cooled in two steps, by first exchanging heat with the oil, and then with cooling water. Secondly, the oil stream cannot be heated by only one gas stream, as the heating demand for the oil can reach up to 12 MW, while the cooling demand for each individual gas stream does not exceed 4 MW. These temperature and enthalpy mismatches suggest that allowing for heat recovery between different sub-systems may result in a complex heat exchanger network and reliability issues, and a fall-back solution should then be implemented to react to possible component failures.

A possibility could be to promote back-exchange, as performed on some oil and gas platforms in the Gulf of Mexico and on Platform C. For instance, on Platform D, the oil recovered from the 2-phase separator can be used to preheat the oil flow exiting the 1st separation stage. This solution has also been proved to be successful for Platform F [222].

Indirect heat exchange. In practice, direct heat exchange between the process streams may not be feasible for operational reasons, and a central utility system may be used, such as a cold water loop. In this case, the potential for heat recovery is limited to less than 2 to 3 MW. However, the use of a central utility system is not beneficial from a process integration perspective, because (i) most heating demands take place at temperatures higher than the temperature of the cooling water utility system; (ii) most cooling demands take place at temperature lower than the temperature of the hot glycol utility system; (iii) two temperature differences should be considered: from the heat source (e.g. hot gas) to the utility stream (e.g. hot water), and from the utility stream to the heat sink (e.g. cold oil).

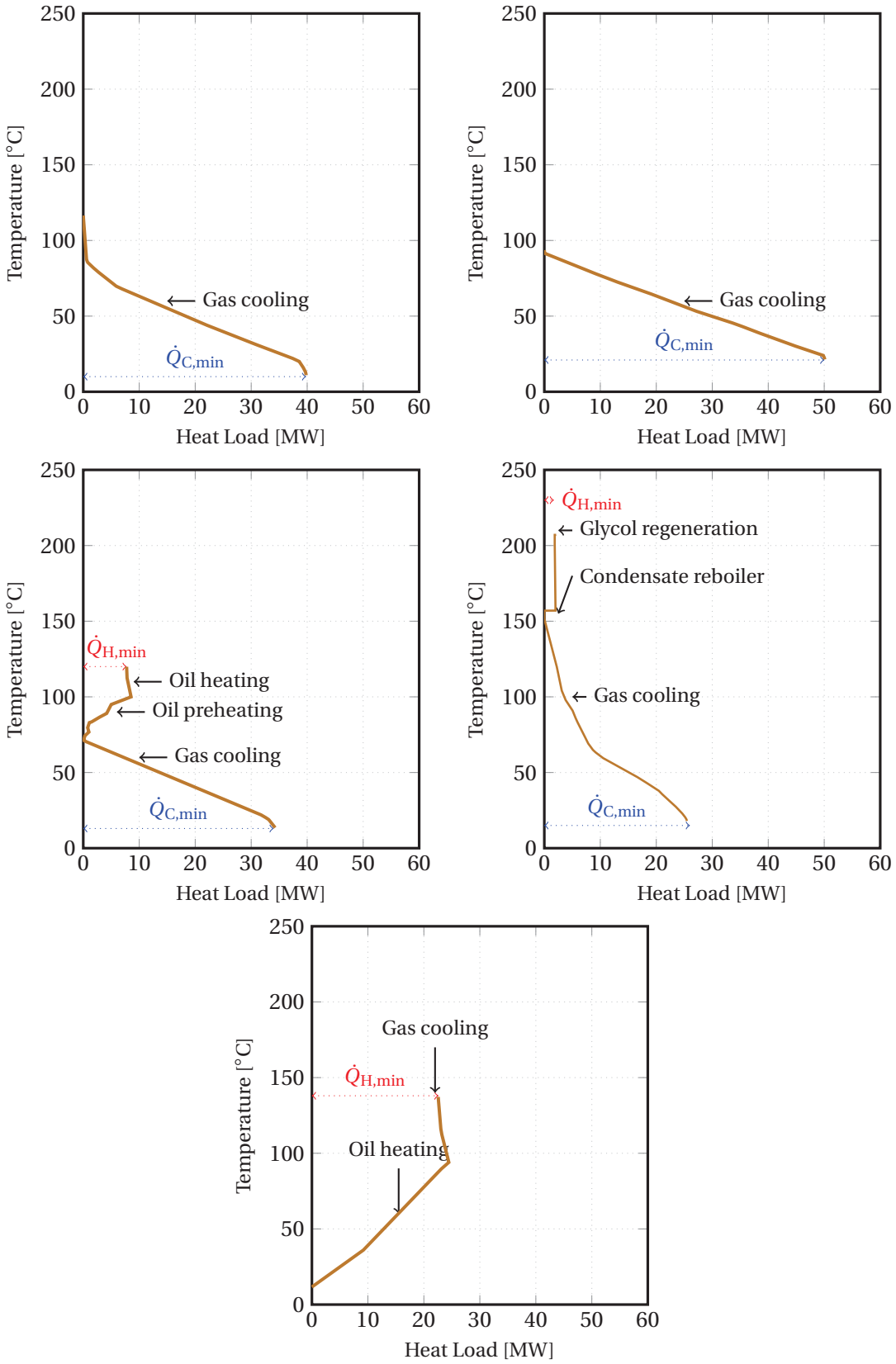

Figure 8.10: Grand Composite Curves of four North Sea and one Brazilian offshore platforms.

Lifetime. However, the opportunities for heat exchange vary with time as a consequence of the changes in energy demands. In the case of Platform D, for all production stages, the pinch point corresponds to a temperature of 150–200 °C (Figure 8.11), which is the reboiling temperature in the stabilisation column. The maximum heating ($\dot{Q}_{H}$) and cooling ($\dot{Q}_{C}$) demands over time amount to 19 and 44 MW. The grand composite curve of the system shows that the minimum demand for external heating ($\dot{Q}_{H,min}$) is smaller than 5 MW, while the minimum demand for external cooling ($\dot{Q}_{C,min}$) is smaller than 30 MW, if heat integration at the total site level can be performed (Figure 8.12).

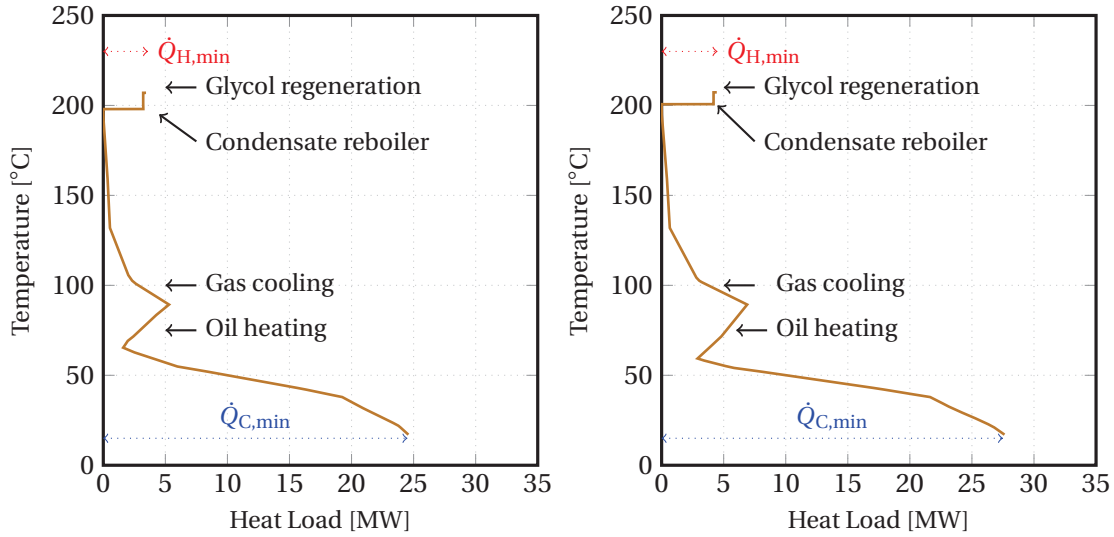

Figure 8.11: Grand Composite Curves of the process streams for the start and plateau productions.

8.5.2 Water integration

Background

Energy in the form of power may be saved, and less exergy may be destroyed if the water network is adequately designed, while satisfying the cooling demand of the processing plant. The introduction of an intermediate cooling loop, as performed on Platforms A, B and C, results in additional exergy destruction, as the consequence of greater pressure drops and heat cascading [244].

Case studies

Platforms A and B are taken as case studies, since they are the two North Sea facilities that do not have a heating demand at low temperatures, implying that all cooling needs should be satisfied by processing an external cooling source such as seawater. The water network may

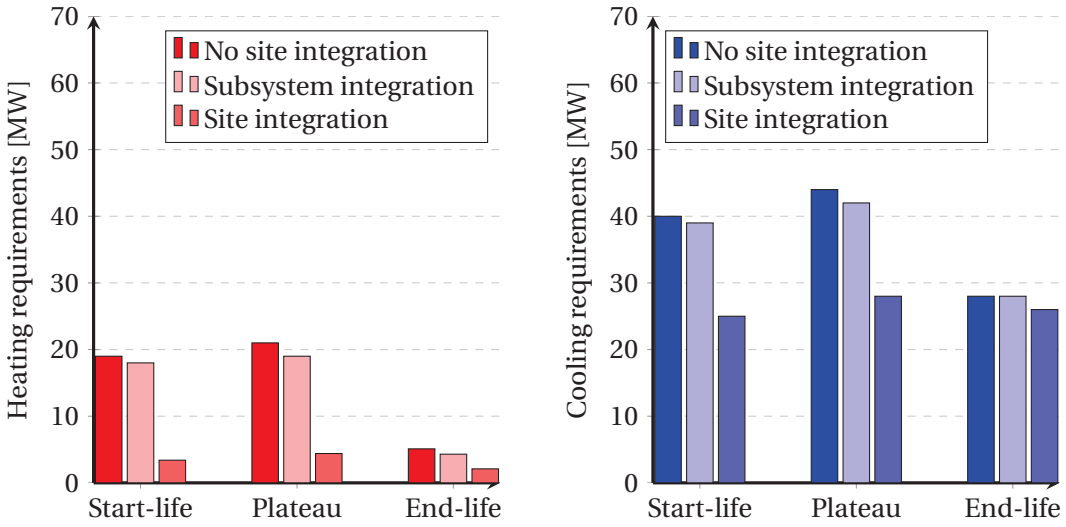

Figure 8.12: Energy requirements and savings by internal heat recovery within sub-systems and within total site.

be designed so that there is an individual cooling water stream for each hot process stream (Scenario 1), for each sub-system (Scenario 2), or for the whole offshore facility (Scenario 3). The dumping temperature is subject to environmental regulations, and higher rejection temperature may be interesting, as this would result in a better match of the temperature profiles and smaller exergy destruction (Scenario 4).

Perspectives

The comparison of the three first scenarios, which differ only by the flow rate of water processed through each heat exchanger, shows that the exergy destruction due to heat transfer through the coolers does not vary over a range of ± 1 %, the minimum being found when a single stream receives all heat discharged from the gas compression operations. Additional, but small, benefits are found with regards to the power consumption, as the pump efficiencies are increased for larger flows, but these minor improvements of performance are outweighed by the economic cost related to the additional space and weight of the pipeline system, and the difficulties to process such great amounts of water through each single heat exchanger.

Higher water temperature rejection results in a smaller water flow rate, which presents benefits with regards to the space required by the heat exchanger network. Eliminating the intermediate heat transfer loop, and allowing for a rejection temperature of 50 °C instead of 20 °C can result in a reduction of about 23 % of the exergy destruction due to heat transfer for Platform B, at the expense of greater exergy losses. The benefits for Platform A are minor in comparison. A more detailed analysis, considering the purity of each water stream, could be conducted by means of a water pinch.

8.6 Conclusion

Several energy saving scenarios were analysed, based on the findings of Chapters 4–6 related to the performance losses of oil and gas platforms. The proposed measures were of different types, aiming either at reducing the electrical or thermal energy use, by re-designing some sections of the processing plant (production manifolds), replacing chokes and valves (separation), changing the operating strategy or redimensioning the compressors (gas recompression and treatment), and promoting energy and process integration (heat exchanger network).

The potentials for each measure differ significantly from one platform to another. The implementation of an additional pressure level is, for example, irrelevant for facilities where the export pressure is below the feed one, and the substitution of throttling valves by multiphase expanders is currently challenging because of technological limitations. Site-scale integration is promising for some of the platforms investigated in this work, because of the demands for both heating and cooling, and can result in a significant decrease of the external heating demand if the plants are fully-integrated.

The greatest energy saving improvement is associated with the limitation, if possible, of anti-surge recycling. This can be achieved, by, for example, adapting the control strategy of the compressors, adding parallel trains or re-wheeling them. The total power and fuel gas consumptions, as well as the exergy destruction within the processing plant, can be reduced by up to 20 %, and this pinpoints the importance of designing and operating adequately this section of a platform.

With regards to these findings, it can be concluded that the priority to give to each measure would be different from one platform to another. Attention should then be given to aspects such as energy efficiency, economic profitability and environmental impact.

9 Waste heat recovery

This chapter presents a detailed process integration and optimisation study of waste heat recovery cycles on offshore platforms. The integration of steam and organic Rankine cycles as bottoming cycles to the power turbines and to the gas treatment process is evaluated and their performances are compared. The main outcomes are emphasised in Nguyen et al. [245].

9.1 Introduction

Designing more efficient power generation systems and reducing the fuel consumption have gained interest in the last years. The use of the waste heat from the turbine exhausts is a standard choice in power plants, but not on oil and gas platforms. This work investigates the possibility of integrating such systems offshore: most works in this field focus on the possible power cycle layouts, without regarding the energy requirements of the oil processing plant and the possibilities for site-scale integration. The power cycles are generally designed and optimised individually, while their economic and environmental impacts are briefly assessed.

The various system configurations and the synergies between each sub-system should be identified to improve the performance of the overall plant, besides focusing on the ways to design compact and low-weight steam cycles. The main objectives of the present work are therefore to:

(1) evaluate the prospects and challenges associated with the integration of waste heat recovery cycles at a site-scale level, by systematic process integration;

(2) estimate the total costs, local and life cycle CO_2-emissions and fuel savings simultaneously, as well as other environmental impacts, by considering the multi-period (design point and part-load) and multi-objective aspects of this optimisation problem;

(3) assess the differences in terms of waste heat recovery potential when comparing different facilities.

9.2 System description

9.2.1 General superstructure

Different scenarios can be drawn when integrating a waste heat recovery cycle, depending (i) on the selection of the waste heat recovery technology, (ii) on the recovery of the waste heat from the turbine exhausts or the processed gas, (iii) on the use, or not, of an intermediary heating loop, (iv) on the choice of the cold utility. All the possible configurations are embedded in a superstructure (Figure 9.1), and the aim is to find the designs that, for example, simultaneously minimise the economic costs or environmental impacts, while maximising the internal heat recovery and the thermodynamic performance.

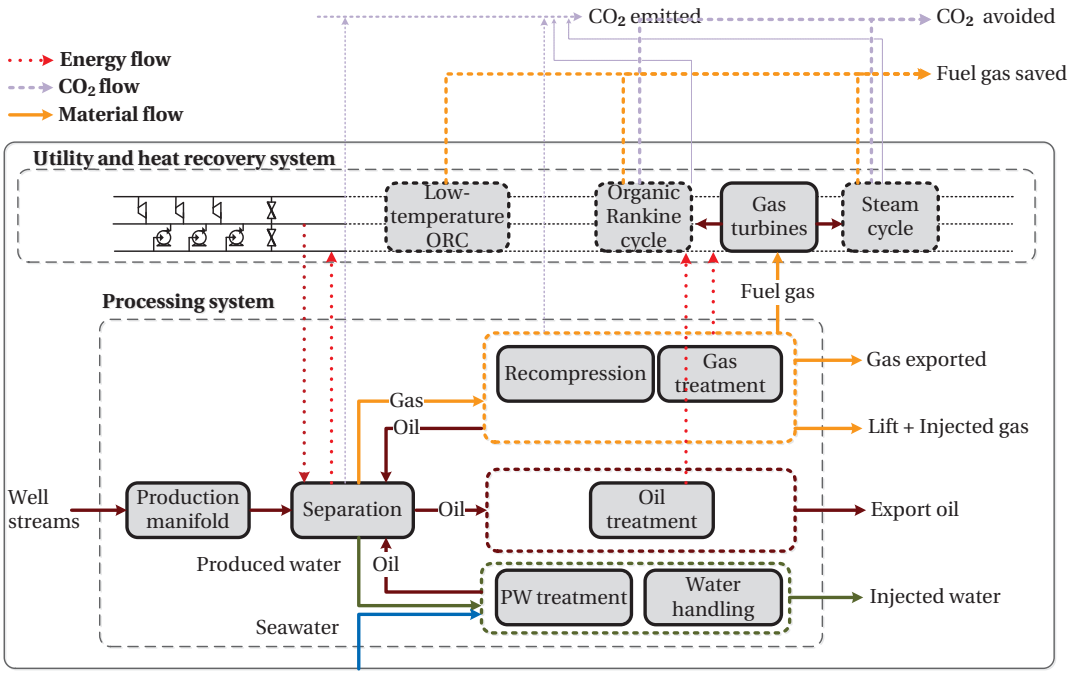

Figure 9.1: Process superstructure for the integration of waste heat recovery cycles on offshore platforms.

The integration of waste heat recovery cycles on oil and gas platforms in the North Sea region is not common, as it is believed that the additional investment costs related to the supplementary weight and space may outweigh the financial gains of exporting a higher amount of gas. The recent researches in this field argued that (i) such cycles could replace one of the gas turbines present on-site, (ii) it could be placed on the top of the facility, and that (iii) new technologies are more and more compact, and their weight has been brought down significantly. The integration of organic Rankine cycles has not been performed up to now, and the implementation of low-temperature cycles for exploiting the waste heat from the processing train has never been achieved.

9.2.2 Process technologies

Heat-to-power technologies are necessary to convert waste heat into power, of which the Rankine cycles are the predominant ones. A Rankine cycle always includes four main steps: pumping, where the working fluid is pumped; heating, where the high-pressure water is preheated, evaporated and possibly superheated; expansion, where the vapour is expanded for power generation; and cooling, where the wet vapour is condensed.

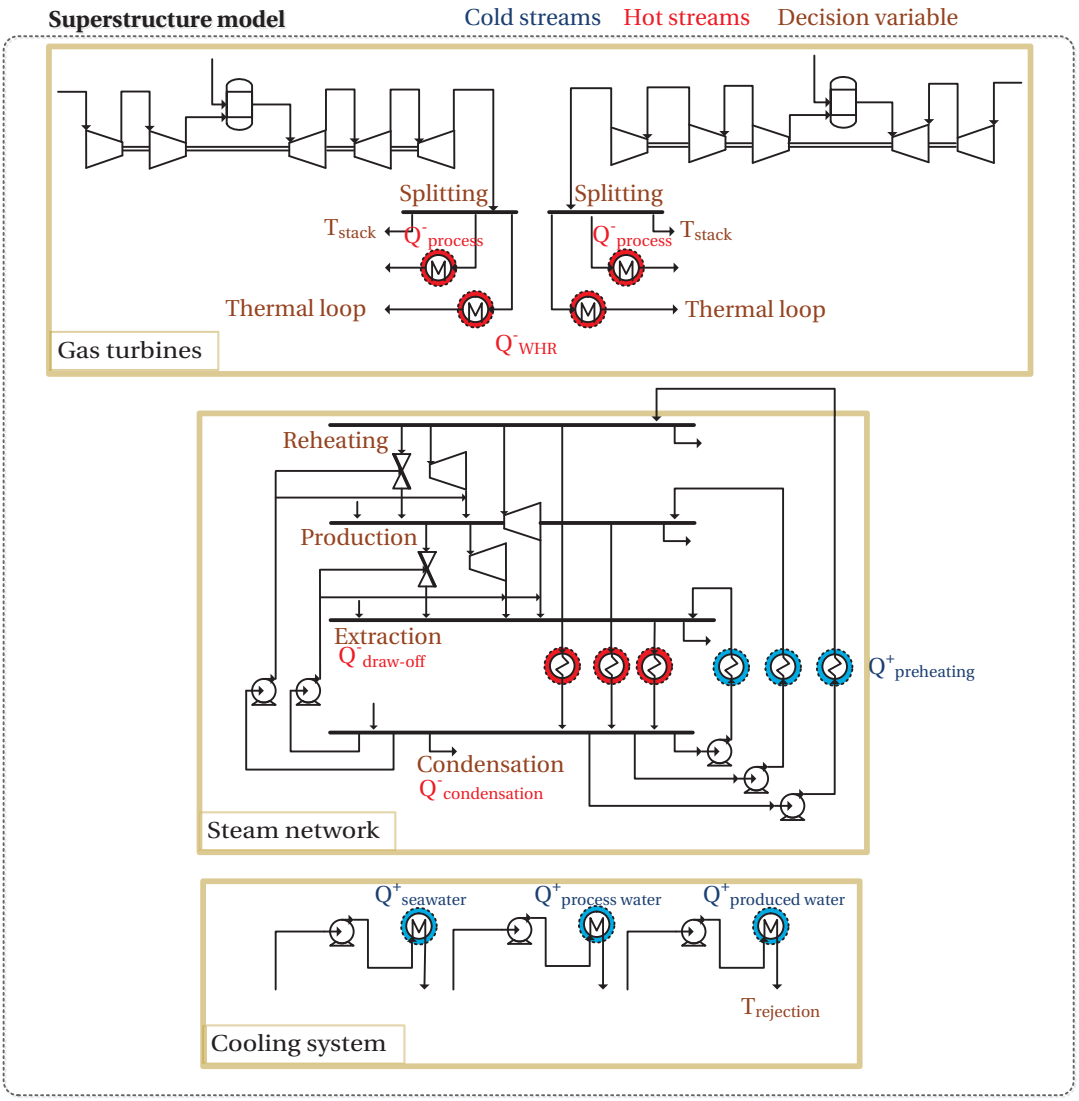

Figure 9.2: Process superstructure for the conversion of waste heat-to-power using Rankine cycles.

Several variations can be found, if for instance extraction is installed to satisfy some heating demands (Figure 9.2).

9.3 Modelling and optimisation

9.3.1 Thermo-environomic modelling

Case study

This chapter focuses mainly on the integration of waste heat recovery cycles in the case of the Draugen platform, with the exception of a few digressions to illustrate how the possibilities for implementing Rankine cycles differ across platforms. The integration of Kalina cycles is out of scope because of the possible risks associated with ammonia-water mixtures. The exhaust gases from the power turbines have a low temperature ($\leq 350\,^{\circ}C$) compared to the other gas turbines used in the offshore industry, such as the LM2500 engine ($\geq 500\,^{\circ}C$) used on Platform C. The implementation on waste heat recovery cycles is investigated only for the power turbines that provide the main share of the mechanical and electrical loads, and the two remaining ones are not considered. The part-load behaviours of the gas turbine and of the Rankine cycles are included in the models in order to predict the possible CO_2-reductions and changes in fuel consumption with the load.

Steam Rankine cycle

Such technologies are mature for onshore applications, while the engineering challenges of installing these cycles offshore are emphasised in Nord and Bolland [118, 119]. A power-to-weight of about 10 tonnes per MW was estimated for the case studies presented in the works of Kloster [120, 121]. The integration of a steam cycle was performed as a retrofit option on existing facilities, as discussed in their studies, and the steam cycle was implemented on either one or two gas turbines. The physical model of the steam Rankine cycle builds on an adapted version of a model previously developed at EPFL on the Matlab® platform.

Organic Rankine cycle

The implementation of organic Rankine cycles for recovering the waste heat from the turbine exhausts may be interesting, as the exhaust temperature of some gas turbines may be relatively low (≥ 350–$400\,^{\circ}C$), especially in part-load conditions. These cycles may be more compact and lighter than conventional steam Rankine cycles, which could make them more competitive for offshore applications where space is limited.

Another possibility is to integrate a low-temperature ORC for recovering heat from the extracted gas (≥ 100–$150\,^{\circ}C$), as large quantities of heat are dumped into the sea during the field exploitation. The exergetic efficiency of the gas coolers is typically small (≤ 15–$20\,\%$) and these components are responsible for a high dumping of heat into the sea. As emphasised by Rohde et al. [123], using this low-grade heat is challenging, because of the low heat source temperature and the variations of the gas flowrate and properties over time.

9.3.2 Thermo-environomic optimisation

The overall thermodynamic, economic and environmental performance is then evaluated based on user-defined indicators, and a multi-objective optimisation is performed using an evolutionary algorithm [203, 246]. The competing objectives and resulting trade-off are identified, and the optimal system configurations are compared and illustrated in the form of Pareto-optimal frontiers.

Performance indicators

Several indicators characterising the performance of the utility plant solely and of the overall plant can be defined to compare the different integration alternatives and scenarios. The indicators considered in this part of the project are:

- the energy intensity [20, 21], based on the lower heating value;
- the combined cycle/cogeneration plant energy efficiency η_{CC};
- the additional investment costs C_{inv};
- the increase of natural gas export δ_{NG};
- the reduction of the local CO_2-emissions $\delta_{I_{\mathrm{CO_2}}}$;
- the decrease in the global warming potential effects $\delta_{I_{\mathrm{GWP100}}}$;
- the acidification potential, the eutrophication impact and the marine water ecotoxicity, I_{ACD}, I_{EUT} and I_{MAETP}.

A detailed analysis of the weight and space occupied by the waste heat recovery cycle is out of scope of the present study. The limitations regarding weight and space may vary significantly from one platform to another, as different facilities present different structures (e.g. floating production, gravity-based, tension-leg, etc.). The weight and space of the WHR cycle depend on the weight and type of each individual component, and on the piping connections that would be required. For instance, for the same requirements, a shell-and-tube or a plate-and-frame heat exchange would not occupy the same volume. The dry weight of the steam cycle is roughly calculated based on the estimations of Nord and Bolland [118] for offshore steam cycles.

There was, at the beginning of this project, no available study on the weight of organic Rankine cycles for offshore applications, but a more extensive work has been conducted in parallel by Pierobon et al. [247]. The comparison of these processes with air bottoming cycles (ABCs) suggests that the ABC is more compact, but that the poor efficiency and payback time make such an option less competitive compared to the two others.

Multi-objective optimisation

The steam cycle operating parameters and strategy, the selection of the cold and hot utilities, and the implementation of a heating loop are defined as master decision variables of the multi-objective optimisation, to ensure that all possible configurations are explored during the optimisation phase, for steam networks (Table 9.1) as well as for medium- (Table 9.2) and low-temperature (Table 9.3) Rankine cycles.

Objective functions. The large variety of performance indicators that can be considered as objectives illustrates that optimal decisions need to be taken with regards to trade-offs between two or more competing objectives. An example is the trade-off between the thermodynamic efficiency of the utility plant, which is improved with the integration of a steam cycle, and the investment costs, which rise because of the greater equipment inventory. The following three objectives are considered:

1. the net power generation of the utility system, which includes the combined cycle and the associated pumping utilities, to be maximised, so that the combined cycle has the capacity to cover the power demand in the different operation modes of the plant;

2. the investment costs C_{inv} of the additional bottoming cycle, to be minimised;

3. the daily local CO_2-emissions, to be minimised. The economic value of the exported gas is difficult to estimate, but maximising the annual profit is equivalent to maximising δ_{NG} and $\delta_{I_{CO_2}}$ simultaneously.

Decision variables. The ranges of values for the decision variables related to the steam network (e.g. production level, degree of superheating, reheating, extraction and condensing levels) are based on a preliminary study of the steam cycles already installed offshore and of the current combined cycles that are typically used in power plants.

The maximum values for the rejection of the seawater, cooling and produced waters are based on the limitations and recommendations presented in the manufacturing data of the separators and heat exchangers for several oil and gas facilities. The minimum gas exhaust temperature is set to avoid possible corrosion issues in the pipes because of the presence of sulphur compounds and other impurities.

The following organic fluids are considered: propane, n-butane, isobutane, n-pentane, isopentane, cyclopentane, cyclohexane, toluene and benzene, because of their suitability for such cycles and their adaptability to low- and medium-temperature heat recovery. Subcritical and transcritical configurations are considered.

Table 9.1: Set of the master decision variables used in the multi-objective optimisation of the steam cycle.

Variable	Type	Unit	Range/Value
Production level	continuous	bar	[9–25]
Degree of superheating	continuous	ΔK	[0–50]
Selection of reheating	integer	-	{0;1}
Reheating level	continuous	°C	[30–300]
Selection of 2nd production level	integer	-	{0;1}
2nd production level	continuous	bar	[90–130]
Selection of extraction level	integer	-	{0;1}
Extraction level	continuous	°C	[30–300]
Condensation level	continuous	°C	[15–75]
Vapour fraction (turbine outlet)	continuous	-	[0.8–1]
Selection of seawater	integer	-	{0;1}
Selection of processed cooling water	integer	-	{0;1}
Selection of produced water	integer	-	{0;1}
Selection of thermal intermediate loop	integer	-	{0;1}
Seawater rejection temperature	continuous	°C	[8–40]
Processed water temperature	continuous	°C	[15–40]
Produced water temperature	continuous	°C	[55–95]
Use of exhaust gases from the 2nd GT	integer	-	{0;1}
Exhaust temperature (after SC)	continuous	°C	[120–180]
Gas turbine load for the SC design point	continuous	%	[40–100]
Power share CC/2nd GT	continuous	%	[50–90]

Table 9.2: Set of the master decision variables used in the multi-objective optimisation of the medium-temperature organic Rankine cycle.

Variable	Type	Unit	Range/Value
Selection of the working fluid	discrete	-	{0 − 11}
Production level (working fluid dependent)	continuous	bar	[10–80]
Condensation level	continuous	bar	[0.05–30]
Degree of superheating	continuous	ΔK	[0–100]
Ethane weight fraction	continuous	%	[0–100]

Table 9.3: Set of the master decision variables used in the multi-objective optimisation of the low-temperature organic Rankine cycle.

Variable	Type	Unit	Range/Value
Selection of the working fluid	discrete	-	{0;1;2;3}
Production level (working fluid dependent)	continuous	bar	[10–80]
Condensation level	continuous	bar	[0.05–30]
Degree of superheating	continuous	ΔK	[0–100]
Ethane weight fraction	continuous	%	[0–100]

9.4 Steam Rankine cycles

9.4.1 Process integration

The performance of the steam Rankine cycle depends on the degree of conversion of the excess waste heat into power and on the level of integration within the total site, which means that the number and levels of the steam production and utilisation should be selected adequately. There is therefore a large number of possible configurations of steam cycle integration within the oil and gas platform (Figure 9.3), which differ by, for example, the use of the exhaust gases from one or two turbines, the direct or indirect heating of the processing plant, the number of stages of the glycol loop, the splitting of the flue gases, etc.

Processing the exhaust gases from the two on-site gas turbines would lead to a greater flow rate at the inlet of the gas–glycol exchanger, and thus in a higher temperature at the outlet and greater power generation of the bottoming cycle, if needed. The net power capacity at the platform operating conditions can be increased by up to about 4500 kW if the waste heat from one gas turbine is recovered, and up to 9000 kW if from the two sub-systems. Such configurations are relevant both if the aim is to increase the power capacity on-site, as no additional fuel gas would be required, or if the goal is to share the power generation load between the gas turbines and the steam network, as less fuel gas would be consumed.

A possible process configuration is to recover the heat from the exhaust gases in three steps: (i) in a *first* glycol loop, to provide heating at high temperatures ($\simeq 200\,^{\circ}C$) for the condensate stabilisation column, (ii) in a *steam network*, to produce additional electricity, and (iii) in a *second* glycol loop, to provide heating at low temperatures ($\simeq 85\,^{\circ}C$) for the crude oil heater.

This design allows for a better match of the temperature profiles between the exhaust gases and the several heating demands, as the oil heating and condensate reboiling take place at dissimilar temperatures. The exhaust temperature at the inlet of the heat recovery steam generator is about 10 to 15 °C higher compared to the current situation, and this results in a better efficiency of the steam cycle and a greater power generation. The increase of the net power capacity is estimated to be about 8 %, for the same temperature approach and pressure level (Figure 9.4) in the HRSG (Heat Recovery Steam Generator).

The integration of such a configuration appears promising, especially in cases where the heating demands of the oil and gas processing plant are minor, or take place at very dissimilar temperature levels. This solution is also interesting from an operational point of view, since the two glycol loops can be run and controlled independently. The total flow of glycol in the waste heat recovery loops is smaller than in the baseline case, meaning that the pumping work is also reduced. It would as well result in a smaller exergy destruction in the heat exchanger network operating between the utility and processing plants because of the better match of the temperature profiles. However, the construction of this double glycol loop may be space-consuming, since the pipeline network would be more sophisticated.

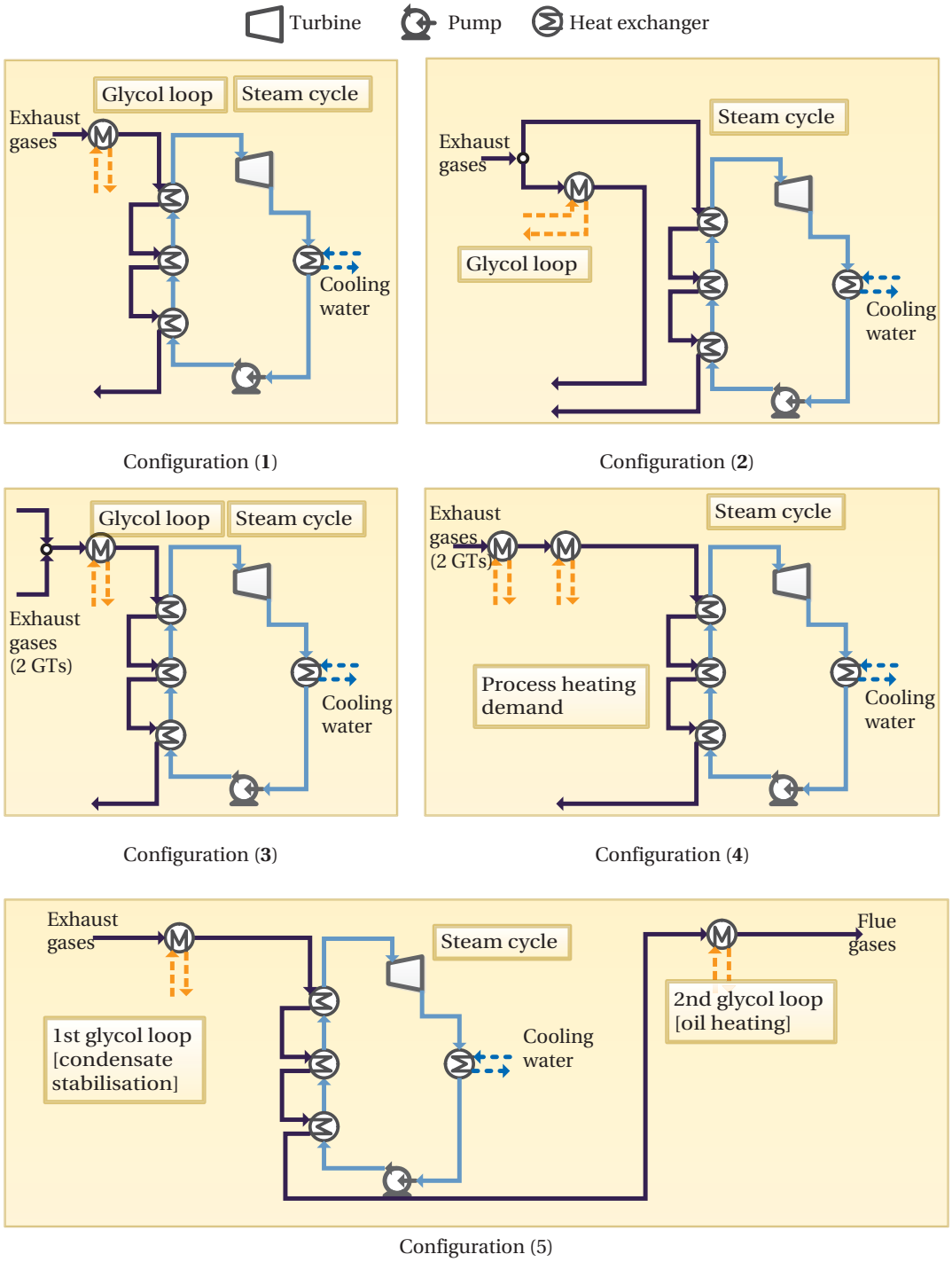

Figure 9.3: Examples of process integration of steam Rankine cycles on offshore platforms, with low heating demand, with possible splitting of exhaust gases, direct or indirect process heating, or with a two-level glycol loop (case study: Platform D).

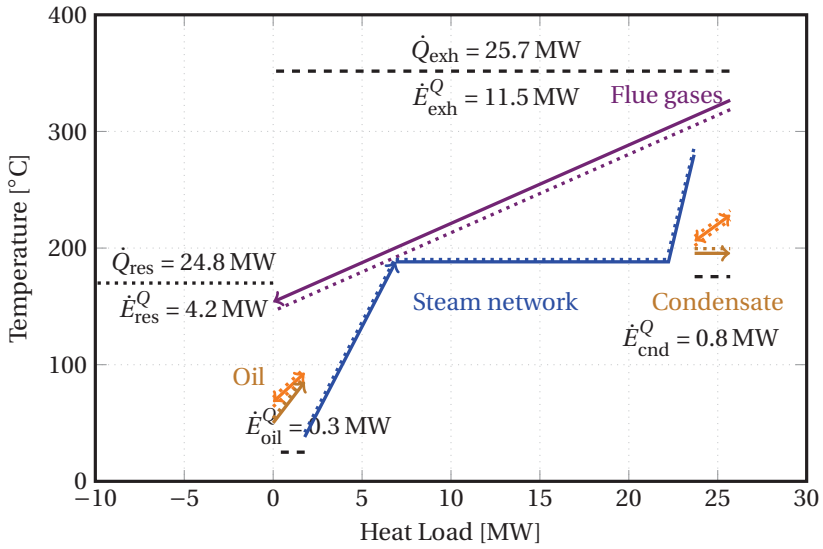

Figure 9.4: Temperature-enthalpy diagram of the site heating demand for the end-life production case, with integration of a steam network and a double circuit glycol loop. They are illustrated with the thermodynamic (process), technology (glycol loop) and utility (exhaust gases) requirements. The full lines correspond to the real temperatures, the dotted lines to the corrected ones (i.e. adjusted with the individual temperature differences $\frac{\Delta T}{2}$), and the dashed ones to the energy demands.

9.4.2 Optimal configurations

The Pareto curves (Figure 9.5) show a net trade-off between the investment costs and the net power generation capacity, as well as with the local CO_2-emissions and operating costs:

- the daily CO_2-emissions and net power generation capacity respectively decrease and increase with higher investment costs, when the waste heat from the exhaust gases of only one gas turbine is recovered;
- the total local CO_2-emissions cannot be decreased further down than 360 tonnes per day;
- when the waste heat from the exhaust gases of two gas turbines is used, an increase of the investment costs beyond 14 M$ only results in an increase of the net power generation capacity above 7 MW, without further decrease of the local CO_2-emissions;
- the steam cycle is not run at its design point or maximum capacity, and an increase of the power capacity of the steam cycle is performed at the expense of a lower thermodynamic efficiency of the combined cycle at their actual operating point.

All the optimal configurations displayed on the Pareto frontier (Figure 9.5) are based on the use of the cooling water recovered from the processing plant at about 16.5 °C, and on, in a few

cases, the lift of additional seawater on-site. The use of *only* seawater at 8 °C is not advisable because the benefits of using a cold source at a lower temperature are outweighed by the additional power consumption to bring this water on-site, and by the supplementary costs for installing water lift pumps. Similarly, the use of the produced water from the oil and gas plant is not recommended, because its temperature (≃ 60–70 °C) results in severe limitations on the condensation pressure and power generation capacity of the steam cycle.

Moreover, none of the optimal design set-ups shown on the Pareto frontier include reheating, extraction, or an additional production level. This suggests that the relatively low temperature of the heat source (exhaust gases at about 330 °C) does not favour the use of more than one production (evaporation and superheating) and utilisation (condensation) level. The production of steam takes place at pressures between 10 and 20 bar, and the implementation of an extraction level to satisfy the heating demand at 200 °C for the glycol reboiler is therefore not feasible.

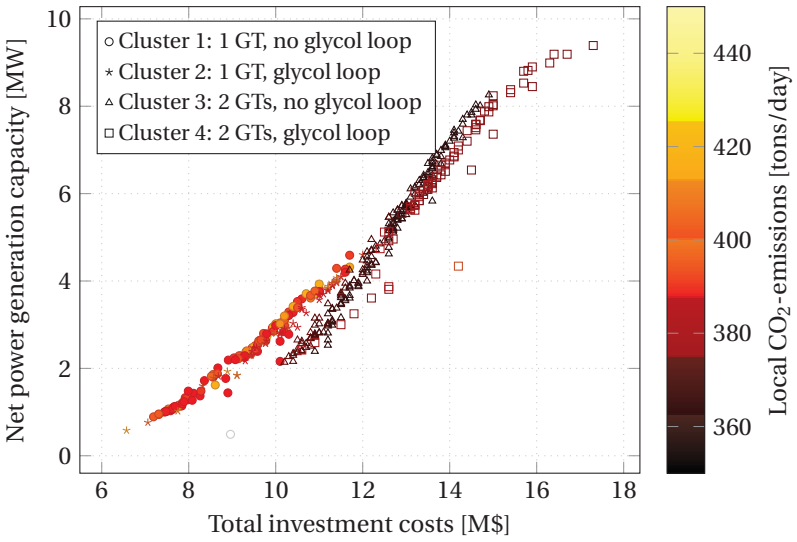

Figure 9.5: Pareto-optimal solutions for the site-scale integration of steam Rankine cycles on offshore platforms: trade-off between the investment costs, CO_2-emissions and net power capacity.

All the Pareto-optimal solutions can be grouped into four major zones, each corresponding to a different configuration:

- **Cluster 1**: the steam cycle is integrated with the exhaust gases coming from only one of the two gas turbines, and the glycol loop is dismantled. This implies that the exhaust gases are directly exchanging heat with the process streams (oil and condensate), which reduces the minimum temperature difference to respect between the heat source and sink.

  The total investment costs vary between 7.2 and 11.7 M$, the net power capacity at

the design point of the steam cycle between 490 and 4600 kW, the daily CO_2-emissions down to 370 tons per day. This corresponds to a reduction of the CO_2-emissions of up to 15 % at the scale of the utility plant, and up to 14 % at the scale of the overall facility. Moreover, this corresponds to an increase of the natural gas exportations by up to 18 %. The rejection temperatures of the cooling water range between 30 °C and 40 °C and the exhaust gas temperatures between 150 and 160 °C.

- **Cluster 2** (Configuration 2 in Figure 9.3): the steam cycle is integrated with the exhaust gases coming from only one of the two gas turbines. A fraction of the exhaust gases is used to satisfy the heating demand of the glycol loop, which is set, in the optimum case, equal to the heating demand of the processing plant.

  The reductions in CO_2-emissions are similar than the ones retrieved from Cluster 1. The exhaust gas temperature are lower by 20 °C in these cases, ranging between 120 and 130 °C, which may be problematic if the gas used in the gas turbines is substituted by a dirtier fuel such as heavy oil or diesel. Power generation is clearly limited by the activation of a utility pinch point at the level of the condensate reboiler, i.e at 250 °C. Producing a greater amount of mechanical power, i.e. above 5 MW, requires that a greater amount of heat is available between the two utility pinch points at 150 and 350 °C.

- **Cluster 3**: the steam cycle is integrated with the exhaust gases coming from the two gas turbines, and the exhaust gases are directly used for meeting the requirements of the processing plant.

  The investment costs are on average greater by about 20 % compared to the previously proposed solutions, but the net power capacity is greatly enhanced, ranging from 2100 to 8260 kW. The daily CO_2-emissions decrease by about 20–30 tonnes per day compared to the two optimal solutions of the two first clusters. The total savings, compared to the baseline case, can reach up to 60–80 tonnes per day. The rejection temperatures of the cooling water and exhaust gases are sensibly similar to the ones in the first cluster of solutions. The implementation of the steam cycle on the two main gas turbines, for the configuration C, results in a greater amount of heat and exergy available between 150 and 350 °C. Steam production takes place at a higher pressure level, in comparison to the previous cases, and the utility pinch point between the condensate reboiler and the steam network is not activated.

- **Cluster 4** (Configuration 3 in Figure 9.3): compared to the third configuration, the main difference lies in the use of the glycol intermediate loop.

  The investment costs are higher by 13 % and the net power generation capacity greater by 36 %. As expected from the comparison between the solutions displayed in Cluster 1 and in Cluster 2, the stack temperature of the exhaust gases is lower by about 10 °C and the rejection temperature of the cooling water slightly higher. Both the steam production and condensation take place at lower pressure levels, and the power production is again constrained by the activation of the utility pinch point at 150 °C.

An example of configuration for each cluster is further studied (Table 9.4), together with the integrated composite curves of the steam cycle (Figure 9.6). They highlight the thermodynamic benefits of the introduction of a steam network, and the area between the steam network and the other process stream curves corresponds to the exergy that cannot be further recovered in the heat exchanger network [140, 152].

It is observed that (i) the production level ranges between 8 and 20 bar; (ii) the condensation level is comprised between 0.05 and 0.3 bar; (iii) the vapour fraction at the turbine outlet is always close to its lower bound of 0.85; and (iv) the stack temperature is not necessarily reaching the minimum allowable temperature of 120 °C, because it is limited by the minimum temperature approach in the heat recovery steam generator of 10 °C (phase change and gas).

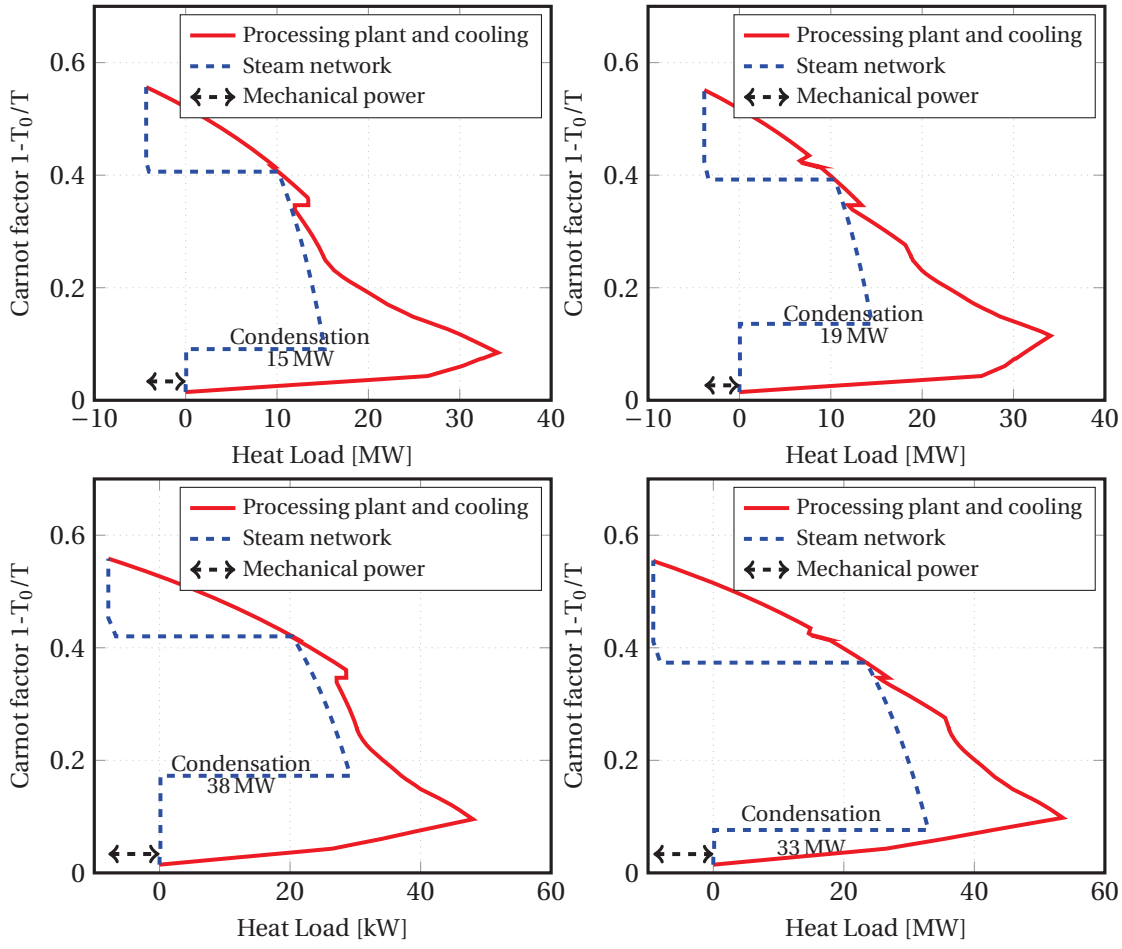

Figure 9.6: Integrated Carnot Composite Curves (ICC) of the steam network for an optimum case of each cluster.

Table 9.4: Selection of thermo-environomic optimal configurations. - stands for non-relevant, y for included, n for not-included, and * for the gas turbine characteristics, before integration of the steam cycle.

Case Steam cycle		Reference	1	2	3	4
Parameters (design point)						
Production level	[bar]	-	15.6	12.3	19.7	9.01
Superheating	[ΔK]	-	15.1	25.6	28.9	28.1
Reheating		-	n	n	n	n
Extraction		-	n	n	n	n
Seawater		-	n	n	n	n
Process water		-	y	y	y	y
Produced water		-	n	n	n	n
Glycol loop		y	n	y	n	y
Condensation level	[bar]	-	0.07	0.15	0.29	0.05
Vapour fraction (turbine outlet)	[-]	-	0.86	0.87	0.85	0.87
Gas turbines		-	1	1	2	2
Stack temperature	[°C]	330	173	123	174	123
Seawater rejection temperature	[°C]	-	-	-	-	
Process water rejection temperature	[°C]	16.5	29.8	40.2	33.5	34.4
Power share CC/2nd GT	-	-	54.5	60.7	75.0	55.6
Power production [design point]						
Steam network generation	[kW]	-	4320	3840	7840	9190
Pumping consumption	[kW]	-	0	0	0	0
Net power generation	[kW]	-	4320	3840	7840	9190
Thermodynamic performance						
η_{cc} [steam cycle design point]	[-]	33.7*	34.1	32.6	38.5	39.9
η_{cc} [operating point]	[-]	23.3*	31.2	32.4	30.4	30.4
σ	[%]	4.6	4.1	4.0	3.4	3.4
Economic evaluation						
Investment costs	[M$]	-	11.6	11.1	15.1	16.6
δ_{NG}	[%]	0	9.5	10	20.3	20.2
Environmental impact						
Daily emissions	[tons/day]	450	398	396	362	362
$\delta_{I_{\mathrm{CO_2}}}$	[%]	0	8.7	9.2	16.9	16.8
$I_{\mathrm{GWP100,FU}}$	[$\mathrm{kg_{CO_2-eq}}$]	40.8	38.0	37.8	35.6	35.5
$I_{\mathrm{ACD,FU}}$	[$\mathrm{kg_{SO_2-eq}}$]	0.15	0.14	0.14	0.13	0.13
$I_{\mathrm{EUT,FU}}$	[$\mathrm{kg_{NO_x-eq}}$]	0.30	0.28	0.27	0.25	0.25
$I_{\mathrm{MAETP,FU}}$	[$\mathrm{kg_{1,4-DCB-eq}}$]	65.6	65.7	65.7	65.7	65.7
Eco-Indicator 99	[points]	2.20	2.10	2.10	2.09	2.09
Other characteristics						
Dry weight	[tons]	-	43	38	78	92

9.4.3 Interdependency analysis

The sensitivity of the optimisation results can be analysed by plotting the Pearson's coefficients (Figure 9.7). The latter give a statistical indication of how each optimisation objective is correlated to each decision variable, and the main findings can be summarised as follows:

- the condensation level and the allowable vapour fraction at the turbine outlet are the decision variables having the greatest negative influence on the total investment costs, as the cost of the steam turbine increases with the pressure ratio;
- designing the steam cycle for a low steam production level is generally beneficial, because of the greater recovery of the heat from the exhaust gases;
- the selection of the gas turbine loads, at which the steam cycle is designed, is critical: it illustrates a clear conflict between the minimisation of the economic costs and the maximisation of the power capacity;
- the power share between the combined cycle and the 2nd gas turbine has a moderate effect on the investment costs and on the total CO_2-emissions: it should be chosen appropriately, considering operational matters (e.g. avoiding surge or choking of the 2nd gas turbine);
- the rejection temperature of the process water impacts mainly the total investment costs, as a smaller temperature difference in the steam condenser results in a larger heat transfer area;
- the influence of the stack temperature is more marked when there is an intermediate heating loop installed on-site, since the glycol medium circulates between 200 and 220 °C, and the waste heat is available at lower temperatures;
- processing seawater in addition to the process cooling water is not particularly beneficial;
- the main difference between the cases where heat is recovered from one stream of exhaust gases, or from two, lies in the importance of the production level and of the degree of superheating;

  In the first case (Clusters 1 and 2), there is, apparently, no direct correlation between these two decision variables and the optimal configurations found on the Pareto frontier.

  On the contrary, in the second case (Clusters 3 and 4), these variables and the optimisation objectives seem interdependent. This can be explained by the larger amount of energy/exergy available for power production, and the selection of appropriate production and superheating levels becomes critical.
- the trends are overall similar for all clusters, and for all decision variables.

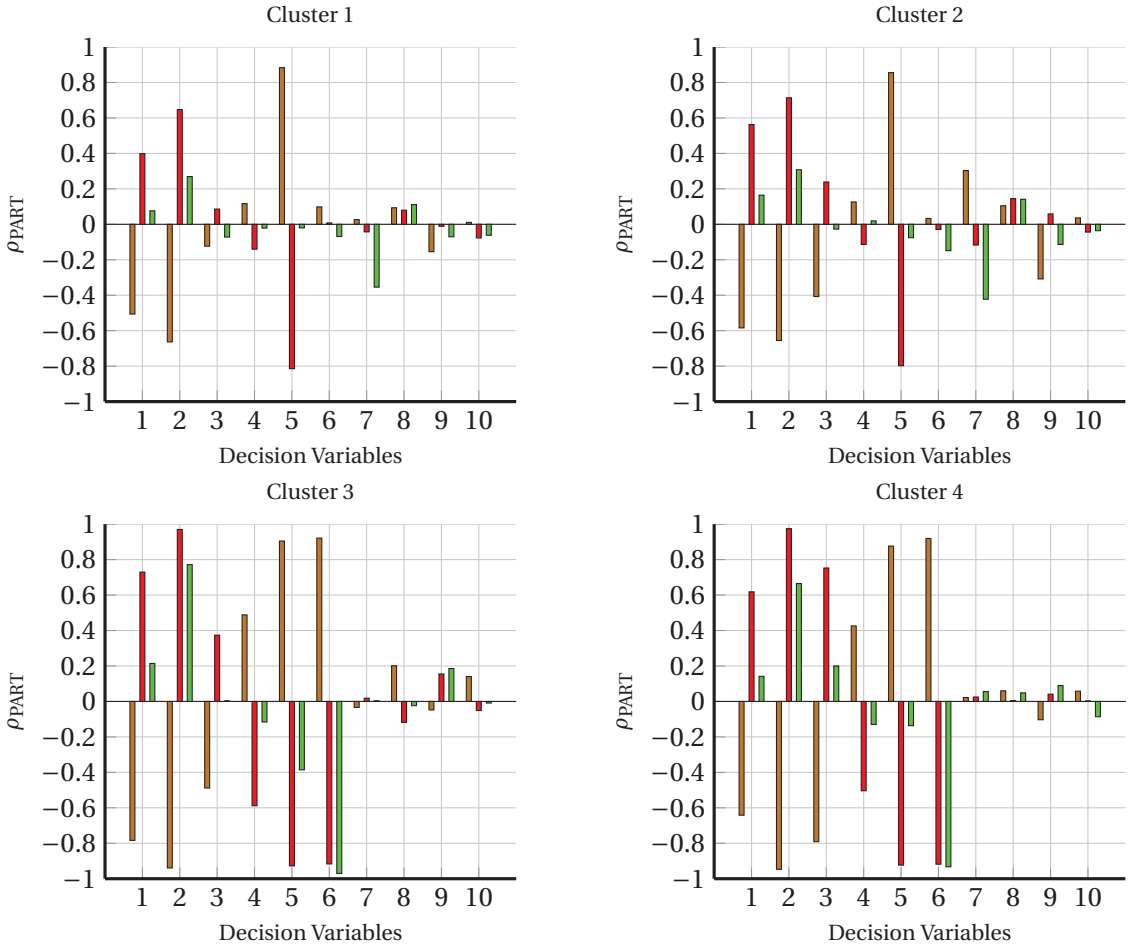

Number	Decision variable	Unit
1	Condensation level	bar
2	Vapour fraction (turbine outlet)	-
3	Production level	bar
4	Degree of superheating	K
5	Load of the 1st gas turbine	-
6	Load of the 2nd gas turbine	-
7	Power share between the CC and the 2nd GT	-
8	Rejection temperature of the process water	K
9	Rejection temperature of the exhaust gases	K
10	Rejection temperature of the additional seawater	K

Figure 9.7: Interdependencies between the master decision variables and optimisation objectives for the integration of steam Rankine cycles, characterised by the Pearson's partial correlation coefficients. Brown denotes the total investment costs, red the power capacity, and green the CO_2-emissions.

9.4.4 Environmental assessment

A comparison of the environmental impacts of each configuration with the current facility shows that the main contributions to the global warming effect of an oil and gas plant are associated with the CO_2-emissions with the exhaust gases of the power turbines (Figure 9.8). Such a conclusion is supported by the annual measurements and data provided by the Norwegian government [13]. The incentives to reduce flaring [22] in this oil region seem to have been effective, since the equivalent CO_2-emissions associated with such practices are negligible.

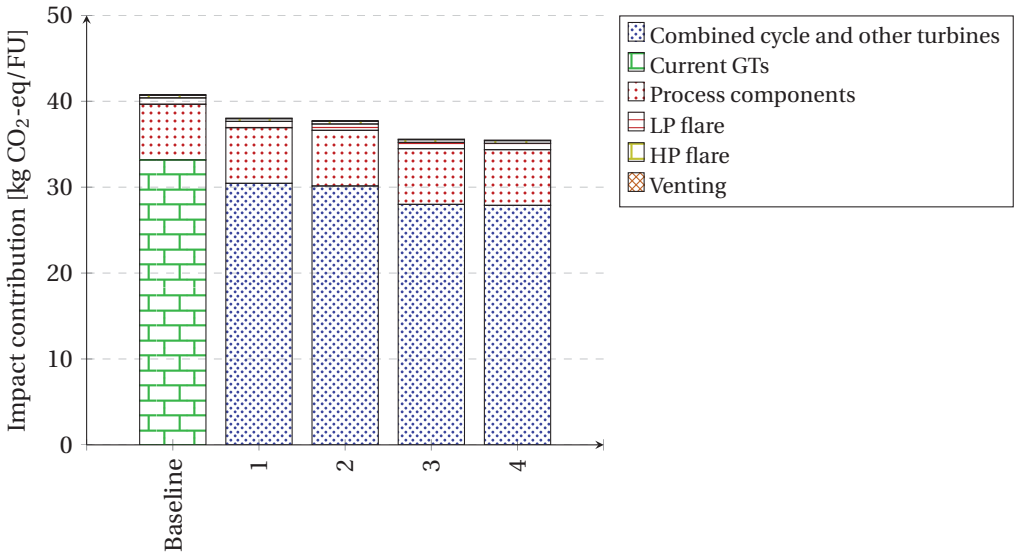

Figure 9.8: Impact contribution of each process and component on-site, expressed in kg CO_2-eq per functional unit, based on the IPCC-07 method. The global warming potential is shown with an horizon of 100 years.

The positive environmental effect of the integration of a steam cycle is also clearly visible when conducting a life cycle assessment. The emissions related to the operation of the steam cycle components, and to the construction and maintenance of this process, are greatly compensated by the benefits induced by the reduction in fuel gas consumption and CO_2-emissions.

The exact values of the environmental impacts are subject to uncertainties and to several environmental factors. However, the estimation of the eco-points illustrates the same trends, although the difference between the 4 cases is minor ($\pm$ 0.01 eco-point). The major contribution to the eco-points is associated with the environmental impact of the process components (about 58 %), followed by the impacts of the NO_x (about 23 %) and CO_2-emissions (about 15 %). The acidification and eutrophication impacts of the platform are also reduced, as the emissions of nitrogen oxides decrease with a smaller consumption of fuel gas. The platform impact related to the toxicity effects to the marine environment does not vary.

9.4.5 Technological constraints

In practice, there may be technological constraints on the selection of the cooling utility for the steam condensation. Moreover, the use of an intermediate glycol loop may be favoured for safety issues, and in some cases for heat buffering. Finally, the space and volume available on an offshore platform are limited, and the addition of a steam cycle may be both costly and problematic.

The multi-objective optimisations were run in a further step by adding these constraints into the mathematical problem, the resulting Pareto frontiers (Figure 9.9) illustrate the penalties these constraints induce. The optimal solutions derived in the ideal cases are compared to the solutions obtained when introducing an operational constraint in the system. The use of additional seawater, lifted and pumped on-site displays a clear penalty with regards to thermodynamic and economic aspects, with an average increase of 10 % of the investment costs for the same net power capacity, and an average decrease of 20 % of the net power capacity for the same investment expenses. These trends are confirmed and amplified if the steam cycle operates on the exhaust gases of two gas turbines.

These aspects are of particular importance if the space and allowable weight on the facility are limited. They are generally related to the number of components that should be added on-site, as well as to the power generation capacity of the process. A steam cycle using seawater presents the drawbacks of possibly requiring an additional lift pump and having a smaller power capacity for an equal investment expense.

As expected, the glycol loop results in greater investment costs, because the steam cycle operates with a heat source at lower temperatures, and more waste heat needs to be recovered. It allows nevertheless for a greater flexibility of the heating system, since the flow of circulating glycol can be regulated by using storage tanks, at the expense of greater weight and space.

The penalty of using seawater instead of process water is also depicted with regards to environmental aspects (Figure 9.10). Higher investment costs result in smaller CO_2-emissions, and the difference between optimum cases with process water or seawater reaches up to 20 tonnes CO_2 per day at low investment costs, and decreases to about 20 tonnes CO_2 per day for investment costs greater than 14 M$. However, it can be seen, in all cases, that the CO_2-emissions cannot be reduced below a threshold value of about 360 tonnes CO_2 per day. The penalty related to the glycol loop is not significant in comparison.

These differences in the economic performance of these cases are mainly related to the lower exhaust gas temperatures, and therefore to the higher heat transfer areas of the heat exchangers. Similarly, using exclusively seawater for the steam condensation is not promising, as the investment costs for the lift pumps and steam turbines increase, and the net power capacity of the steam cycle may decrease.

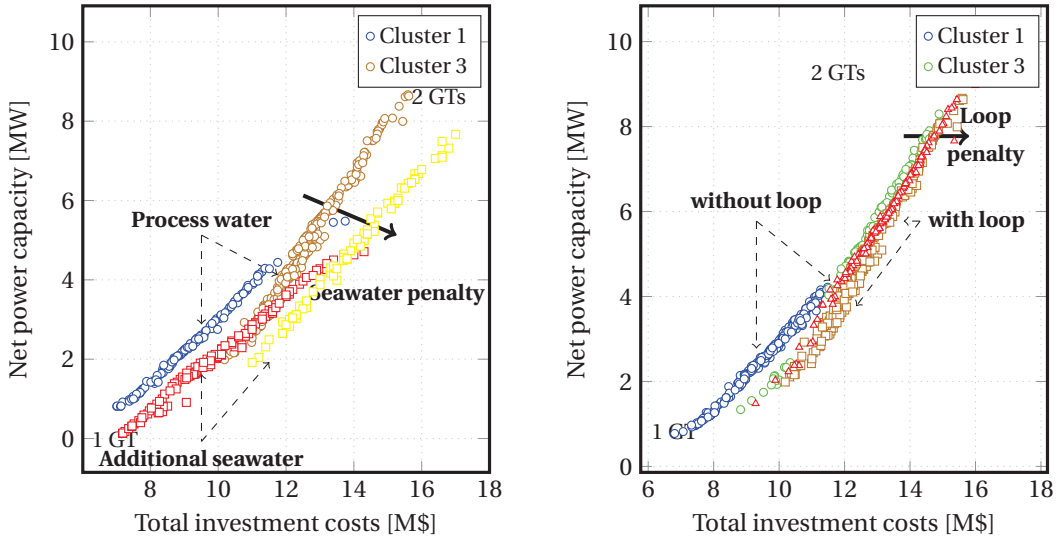

Figure 9.9: Evolution of the thermo-economic Pareto-fronts with practical constraints: process water against seawater (left), with or without glycol intermediate loop (right).

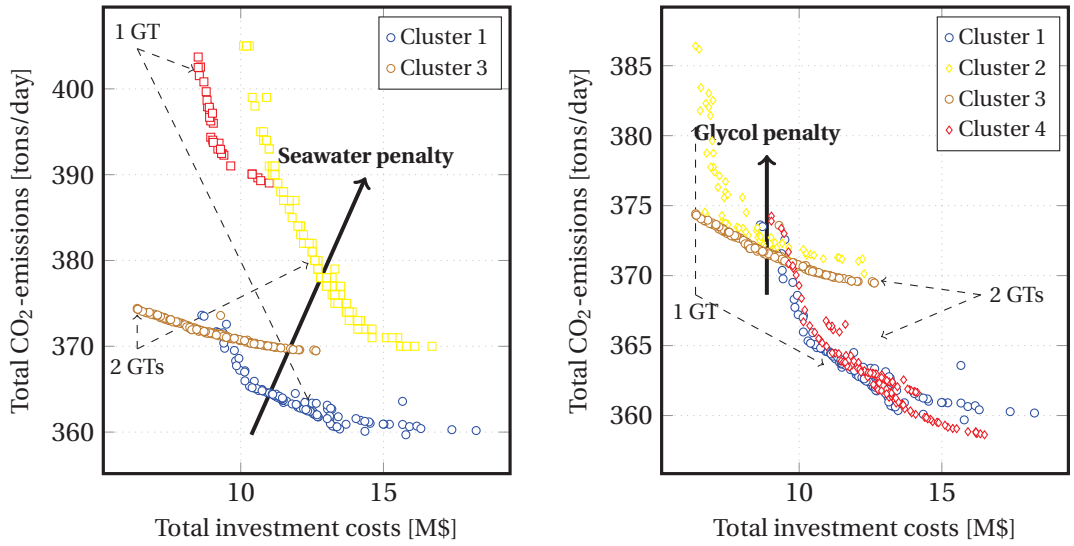

Figure 9.10: Evolution of the thermo-environomic Pareto-fronts with practical constraints: process water against seawater (left), with exhaust gases from one or two gas turbines (right).

9.4.6 Lifetime effects

The integration of steam Rankine cycles is investigated optimising simultaneously the grass-root costs (minimisation), the power capacity (maximisation) and the local CO_2-emissions (minimisation) for different production periods, since the heating and cooling demands are changing, as well as their temperature levels. The comparison of the optimal solutions is based on the *peak* and *end-life* production cases, as these two situations present the biggest differences with regards to their oil, gas and water production rates.

The introduction of steam extraction is not recommended for any of these cases as the heating demand of the stabilisation process at about 200 °C would force the operation of a steam draw-off at a pressure of at least 17 bar for the peak-case, while it would be only 11 bar in the end-life situation. Such a solution is sub-optimum because the net power generation is maximised for a production level of 9 to 12 bar. Two configurations are preferred : the first one consists of implementing the steam network after the waste heat recovery loop, while the second one relies on a splitting of the exhaust gas flow, a fraction being routed to the heat recovery steam generator, the remaining one being used for process heating. The first possibility may be preferable in practice, as it allows for steam production whichever gas turbine is in operation.

The two cases that are shown correspond to two steam network configurations present on the Pareto frontier, for which the net power capacity ranges in the top 5 % of all the displayed solutions. They show that solutions that may be optimum for the *peak* case may not be optimum for the *end-life* case, and vice-versa (Figure 9.11).

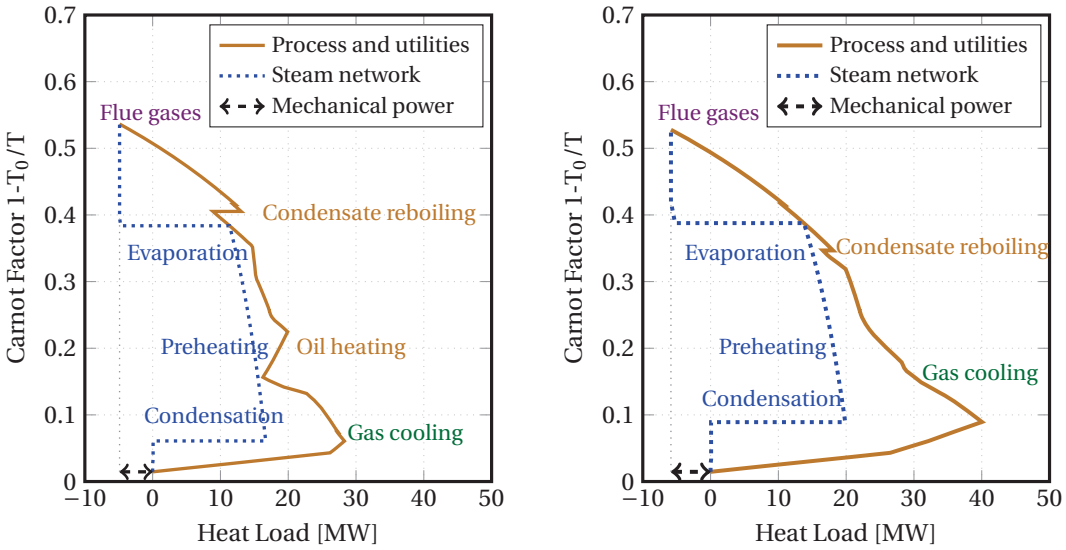

Figure 9.11: Integrated composite curves, on an exergy basis, of the steam Rankine cycle within the oil and gas platform, for the peak (left) and end-life (right) productions, without heat exchange restrictions.

In the 1st case, the steam production (evaporation) takes place *below* the temperature of the condensate reboiling process. The steam generation, and therefore, the power production, are limited by the heating demands of the condensate reboiling and oil heating demands, as indicated by the two utility pinches located at about 55 °C and 190 °C. In the 2nd case, the steam production takes place *above* the condensate reboiling temperature, and the power production is limited by the low temperature of the flue gases. These differences illustrate the impact of large heating demands on the optimal operating conditions of the SRC.

As emphasised earlier, the net power capacity of the steam Rankine cycle is particularly sensitive to the evaporation and condensation pressures, as well as the allowable vapour fraction at the outlet of the steam turbine (Table 9.5). The standard deviations for the superheating approach is higher than for other parameters: this suggests that the maximum power capacity of the steam network and the superheating temperature are not directly correlated.

For all life stages, the steam production level varies in the range 9–12 bar, while the condensation level varies between 0.05 and 0.10 bar. The steam is condensed using cooling water from the processing plant, rather than using additional seawater, which has a lower temperature but should be lifted on-site. The maximum power capacity of the steam network ranges between 4800 and 5800 kW, and the smallest maximum corresponds to the *peak* case, as there is a greater heating demand, and thus a smaller quantity of waste heat in the exhaust gases.

Table 9.5: Optimal design parameters for the steam Rankine cycle, for each production period. These numbers are the average means of the decision variable values for the configurations yielding the greatest power generation. The numbers in parentheses correspond to the standard deviations.

	Production [bar]	Superheating [ΔK]	Condensation [bar]	Vapour fraction [%]
Begin	10.6 (14 %)	24.0 (18 %)	0.07 (43 %)	86 (1 %)
Peak	9.8 (13 %)	12.9 (71 %)	0.05 (30 %)	86 (1 %)
End	11.8 (12 %)	20.6 (30 %)	0.11 (35 %)	87 (1 %)

In the case that direct heat recovery between process streams is not feasible, the integration of the steam Rankine cycle is more challenging in *plateau* production cases. The external heating demand is higher and the amount of heat available for steam production is smaller, resulting in a temperature drop at the outlet of the waste heat recovery system with the heating medium. The integration in *end-life* cases is generally less challenging, as the heating demand has decreased with the oil production. In this situation, the temperature at the inlet of the steam boiler was about 25 to 30 °C lower, resulting in a subsequent drop of the stack temperature.

In general, the integration of the steam Rankine cycle results in a drop of the exergy lost with the exhaust gases of about 10 ± 1.5 MW, while the exergy lost with cooling water increases by 1.2 ± 0.2 MW. Exergy is destroyed in the cycle at rates of about 1.5 ± 0.3 MW, 1.2 ± 0.2 MW and 0.7 ± 0.1 MW in the steam boiler, turbine and condenser.

9.4.7 Comparison

Background

The integration of steam Rankine cycles and their design is likely to be different from one platform to another, as suggested by the works of Kloster [120, 121]: the utility plant was converted into a cogeneration unit for the Oseberg platform, based on steam extraction to provide heat at 90 °C, while it was designed as a combined cycle for Eldfisk. The bottoming cycle was added considering a heating demand of 11.65 MW.

The introduction of a steam network as a bottoming cycle may be of interest for Platform C, since the external heating demand, at present, is of about 15 MW. The following work focuses on that specific platform: the possibility for steam extraction (Figure 9.12) to replace the current hot water loop is considered. The utility plant on that platform consists of two main gas turbines of the LM2500, and the total flow rate of exhaust gases amounts to about 119 kg/s, with a temperature at design point of 566 °C, and at the simulated current conditions of 515.5 °C.

Approaches

Two main approaches can be followed, depending on the final use of the power produced by the steam network:

Power export. The first one assumes that power can be exported from this facility, as it is located in a region where other offshore plants from the same company are operating, and since it already interacts with them by importing gas when the current production is not sufficient. The gas production for this platform is low, and the fuel gas consumption is assumed to be the same as in the baseline case simulated in Chapter 6, and the additional power is exported. In such a case, the aim is to evaluate the trade-off between the investment costs associated with the waste heat recovery cycle and the total power generation, which would result in a smaller fuel gas consumption on other facilities (Figure 9.13). Opening the possibility for steam extraction results in sub-optimum solutions with respect to the maximum power capacity, as it can be seen by the closeness of the two Pareto fronts.

Steam extraction (Figure 9.14) can be used for covering the heating needs of the processing plant, and this allows for a better match of the temperature levels. However, this is performed at the expense of a significant power penalty, because of the lower steam production pressure ($\leq$ 10 bar) compared to a case where no steam is extracted ($\simeq$ 18–20 bar).

Power substitution. The second one considers that electrification between different platforms is currently infeasible, and the steam Rankine cycle is installed to complement the gas turbines for the same baseline power consumption.

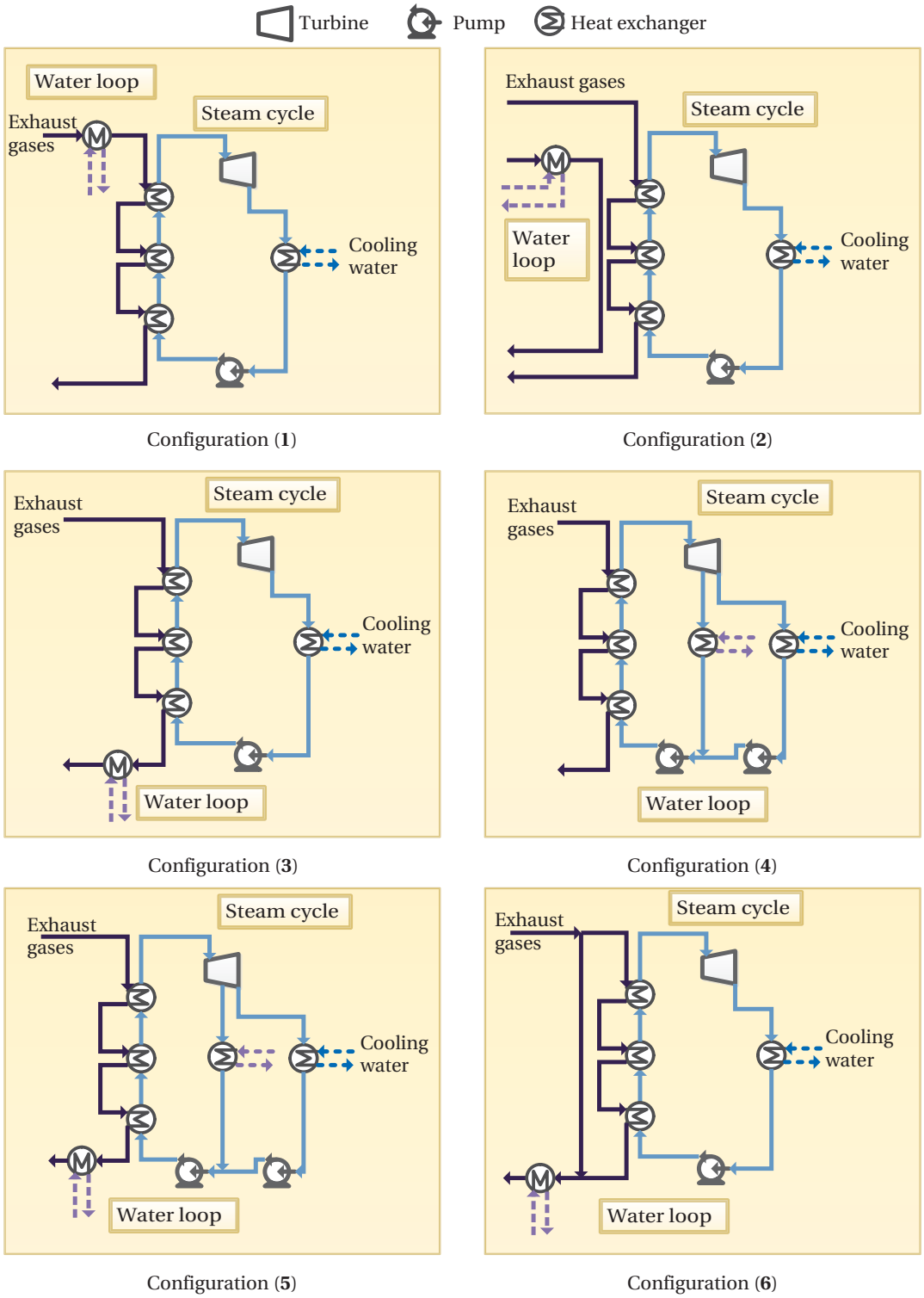

Figure 9.12: Examples of process integration of steam Rankine cycles on offshore platforms with high heating demand, with possible splitting of exhaust gases and indirect process heating (case study: Platform C).

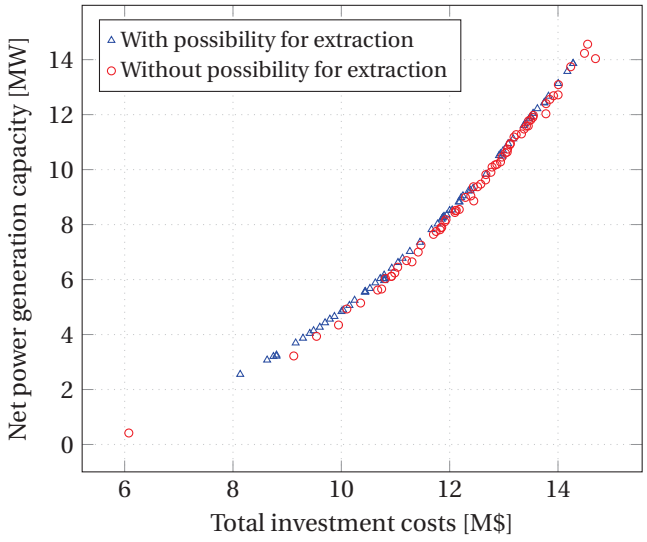

Figure 9.13: Pareto-optimal solutions for the site-scale integration of steam networks for platforms with high heat demand, with possibility for power export.

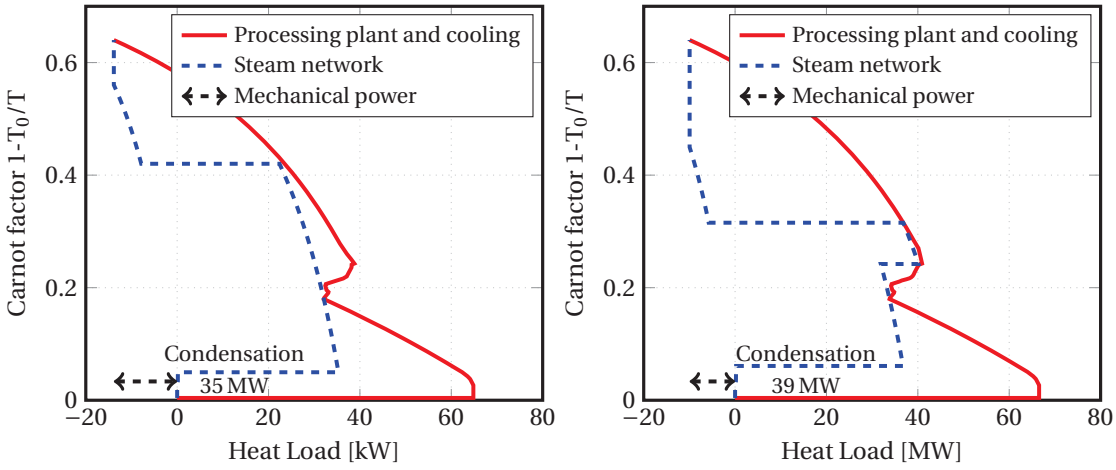

Figure 9.14: Integrated Carnot Composite Curves (ICC) of the steam network for an optimum case without (left) and with (right) steam extraction.

The findings related to Chapter 5 suggest that the greatest heating demand takes place between the early-life and peak production stages, as a consequence of high oil and gas production. The steam network should then be designed for these conditions, which are unknown because of the lack of public information. The oil, water and gas flows simulated for the early case, which represents the design point for the steam network, have been assumed based on the production profiles of three platforms located in the North Sea that process heavy oil [248].

In this case, the design layouts presented earlier (Figure 9.12) may not all be implemented in practice because of thermodynamic and practical limitations:

- **Cluster 1** (Configuration 1): the flue gases from both gas turbines are mixed and run first through the gas-water loop heat exchanger, followed by the heat recovery steam generator. This layout results in a gas temperature of about 240 °C at the HRSG inlet, which severely limits the steam production pressure and a maximum power production of the steam turbine to about 5.5 MW.

- **Cluster 2** (Configuration 2): the flue gases from the first gas turbine, which produces electrical power, are processed through the heat recovery steam generator. This configuration is not feasible in practice, as the waste heat from the exhaust gases of the second gas turbine is not sufficient to satisfy the heating demand.

- **Cluster 3** (Configuration 3): the flue gases from both gas turbines are mixed and processed at first through the heat recovery steam generator, and then through the gas-hot water heat exchanger. The gas temperature at the HRSG inlet is then constrained by the heating demand and the temperature profile of the water loop.

- **Cluster 4** (Configuration 4): all flue gases are processed through the heat recovery steam generator, and steam extraction is used to satisfy all the heating needs. However, this configuration is impracticable because most steam should then be extracted at about 30 bar and cannot be run through the last turbine stage.

- **Cluster 5**: part of the heating demand may be satisfied by processing a fraction of the exhaust gases, and the remaining one by steam extraction, but this configuration is not considered within this work, as it is seen earlier that the thermodynamic benefits of such operation are minor.

- **Cluster 6** (Configuration 6): part of the exhaust gases is processed through the heat recovery steam generator to satisfy the power demand, and is mixed with the remaining flue gases at high temperature, before entering the gas-water loop heat exchanger. In such a configuration, the splitting ratio at the design point is fixed to avoid water condensation in the flue gases, and the final discharge temperature is set to match a temperature approach of 12 °C.

The optimal and most feasible configurations correspond therefore to Clusters 1 and 6, as they both allow for satisfying the heating and power demands in all cases. However, the latter may be preferable from an economic perspective, since a smaller flow of gases is processed through the HRSG, and the costs of the steam cycle are smaller. In this case, the power production from the steam turbine is then equal to 5.8 MW, resulting in the corresponding decrease of the electrical and mechanical loads of the gas turbines. The reductions in fuel consumption range between 11 (design point, early production) and 14.5 % (baseline case, towards peak production).

9.5 Medium-temperature organic Rankine cycles

9.5.1 Process integration

As for steam Rankine cycles, the performance of the organic Rankine cycle depends on the degree of conversion of the waste heat into power and on the level of integration with the remaining processes. The large variety of fluids that can be selected when designing an organic Rankine cycle allows for an additional degree of freedom in the design process. The maximum power capacity is directly related to the selection of the working fluid. At the difference of steam Rankine cycles, extraction is not common for organic Rankine cycles, implying that the heat demand should be satisfied by heat exchange with the exhaust gases, possibly with the glycol loop, and that the cycle expander is single-stage (Figure 9.15).

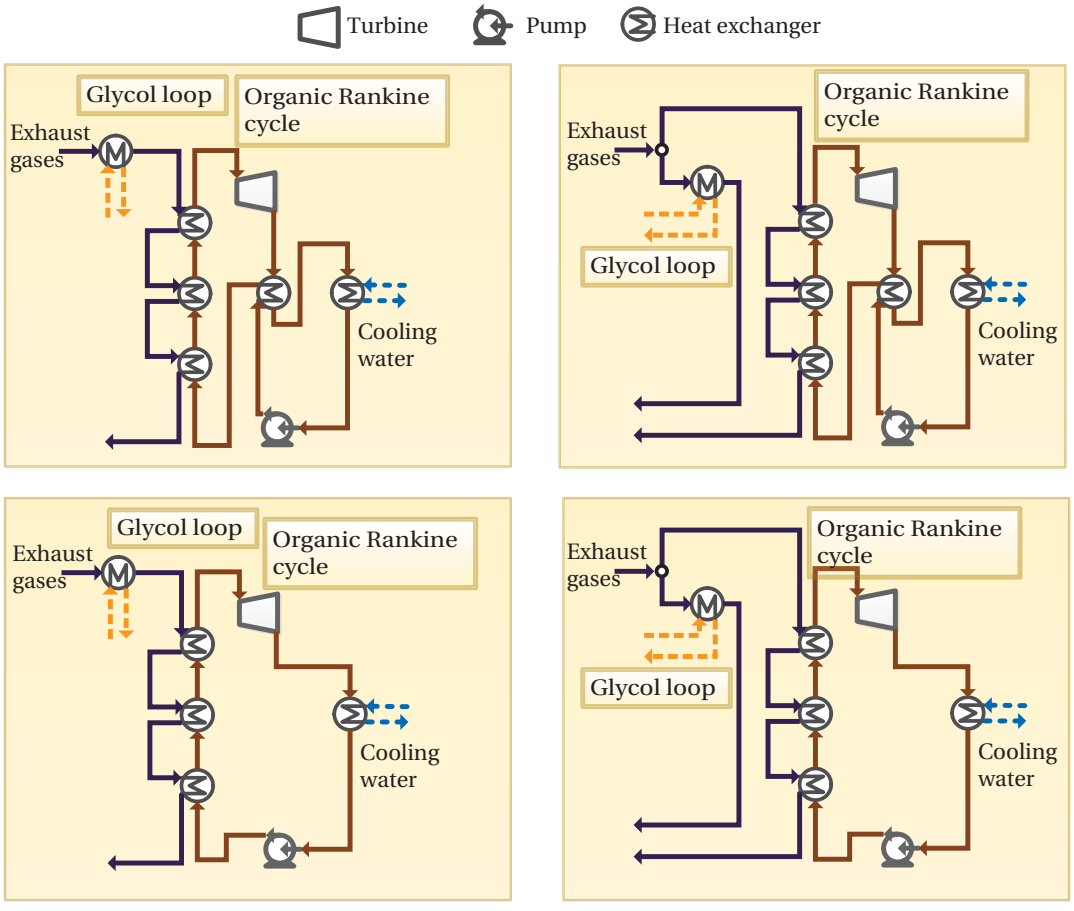

Figure 9.15: Examples of process integration of organic Rankine cycles on offshore platforms with possible splitting of exhaust gases and indirect process heating.

Most investigated fluids are dry fluids, implying that the slope of the T-s diagram on the

right-hand side of the critical point is positive, unlike water. In such cases, superheating is generally not beneficial with respect to the cycle thermal efficiency [249].

9.5.2 Process optimisation

The Pareto curves illustrate the trade-off between the economic, thermodynamic and environmental performance, while pinpointing the differences between the working fluids. There are no significant differences between the different working fluids, considering subcritical configurations (Figure 9.16), with regard to the required economic investments and maximum power capacity.

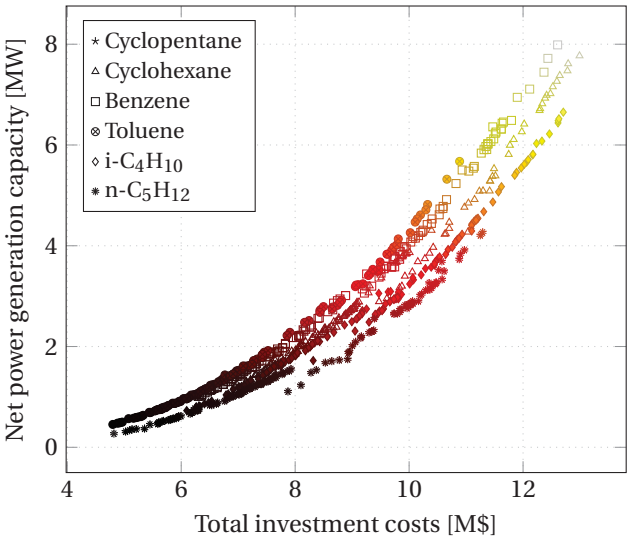

Figure 9.16: Pareto-optimal solutions for the site-scale integration of subcritical organic Rankine cycles on offshore platforms: trade-off between the investment costs and net power capacity.

The maximum thermal efficiency of the organic Rankine cycles on themselves strongly differs from one fluid to another [250], and it is generally comprised between 10 and 25 % (Table 9.6). Transcritical configurations generally result in higher efficiencies and net power output for most fluids [251], at the expense of slightly higher investment costs (Figure 9.17). The advantage of such design layouts can be visualised with the corresponding integrated composite curves, where a better match between the temperature profiles is observed (Figure 9.18).

The selection of one substance rather than another should be performed considering other criteria, such as the process operating conditions (Table 9.7) and, in the case of offshore platforms, the weight and volume of the cycle, as well as the possible hazards and risks. The optimum condensing pressure for fluids such as benzene and toluene is near the atmospheric pressure and below if the aim is to maximise the design power capacity or to minimise the CO_2-emissions, and there is therefore a higher risk of air infiltration. The evaporation pressure

Table 9.6: Maximum thermal efficiency and CO_2-abatement potential for selected working fluids in subcritical and transcritical configurations.

	$\eta_{ORC,sub}$	$\delta_{CO_2,sub}$	$\eta_{ORC,tr}$	$\delta_{CO_2,tr}$
Cyclohexane	23.4 %	21.4 %	24.0 %	23.8 %
Benzene	26.6 %	22.4 %	25.8 %	20.2 %
Toluene	26.5 %	16.4 %	25.6 %	15.1 %
i-C_5H_{12}	18.2 %	21.7 %	20.4 %	21.8 %

Table 9.7: Characteristics and optimal process conditions for selected working fluids, aiming at power maximisation in subcritical configurations.

Fluid	T_c [°C]	p_c [bar]	p_{cond} [bar]	p_{evap} [bar]
Cyclohexane	280.35	40.74	0.17	27.7
Benzene	288.95	49.24	0.27	46.1
Toluene	318.85	42.15	0.16	17.6
i-C_4H_{10}	134.98	36.48	9.24	29.8
n-C_5H_{12}	196.63	33.75	4.12	28.4
i-C_5H_{12}	187.25	33.34	1.00	26.5

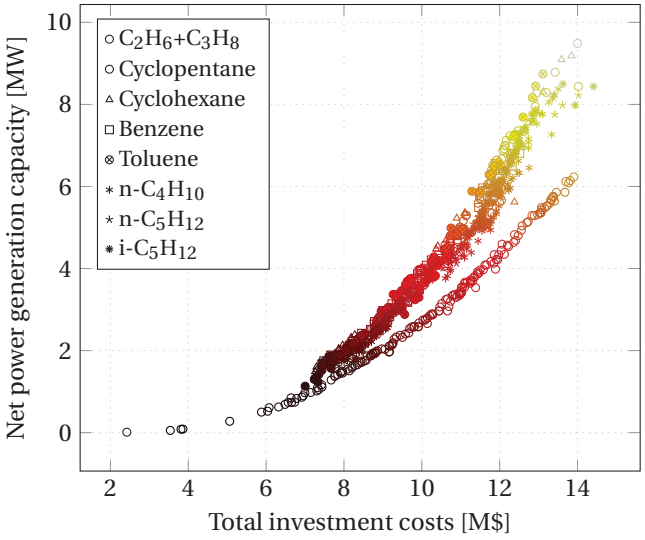

Figure 9.17: Pareto-optimal solutions for the site-scale integration of supercritical organic Rankine cycles on offshore platforms: trade-off between the investment costs and net power capacity.

may be constrained for safety and cost concerns [252], and there are similarly legal limitations in a few countries [253]. The upper pressure may not exceed 20 to 25 bar, which would impede the maximum heat recovery for fluids such as benzene.

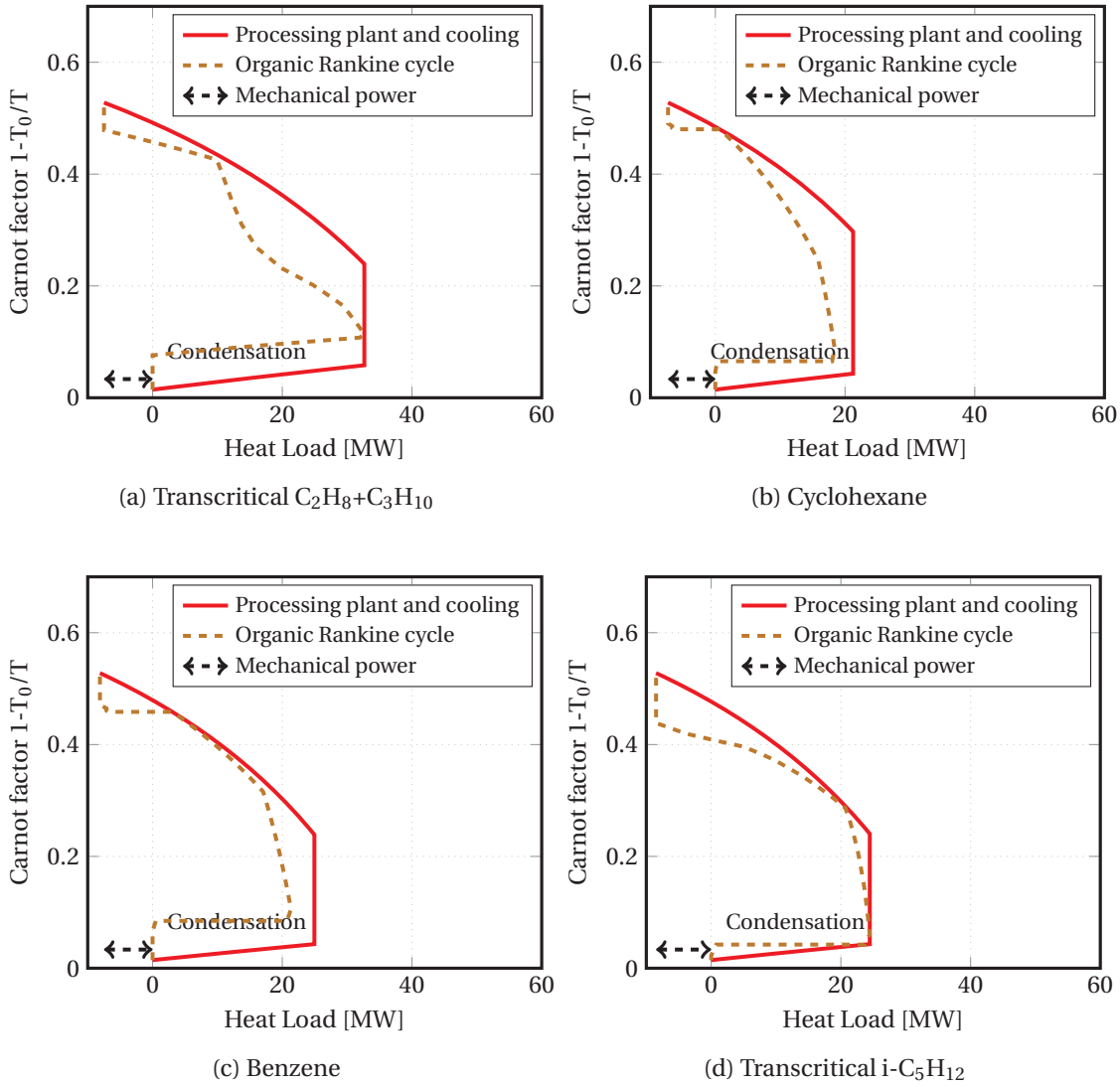

(a) Transcritical C_2H_8+C_3H_{10}

(b) Cyclohexane

(c) Benzene

(d) Transcritical i-C_5H_{12}

Figure 9.18: Integrated Carnot Composite Curves (ICC) of the organic Rankine cycle for an optimum power generation case. The processes belonging to the oil and gas processing plant are omitted for clarity.

Environmental hazards, such as global warming and ozone depletion potentials, may be problematic for the working fluids belonging to the categories of chlorofluorocarbons, but not for substances such as hydrocarbons. Flammability and fire hazards may be of concern, and most hydrocarbons would be discarded since they are characterised by a low flash point. Thermal stability is as well an important criterion, and toluene and benzene present a low decomposition rate in medium- to high-temperature applications. There is no organic fluid that is satisfying with regards to these aspects, which underlines the difficulty of selecting a relevant working fluid.

9.6 Low-temperature organic Rankine cycles

9.6.1 Process integration

A second possibility for improving the thermodynamic performance of this system is to valorise the heat and exergy available at moderate temperatures from the *produced* gas ($\leq 150\,^{\circ}C$), using a low-temperature power cycle using carbon dioxide, propane, or a mixture of hydrocarbons. The cycles can operate either on sub-critical or transcritical conditions, as indicated in Rohde et al. [123]. Similarly, there is a large number of possible system layouts, depending on the selection of the hot and cold sources. In theory, heat from the gas coolers in the gas recompression and treatment sections can be exploited by using a single cycle (Figure 9.19), at the expense of a complex process scheme.

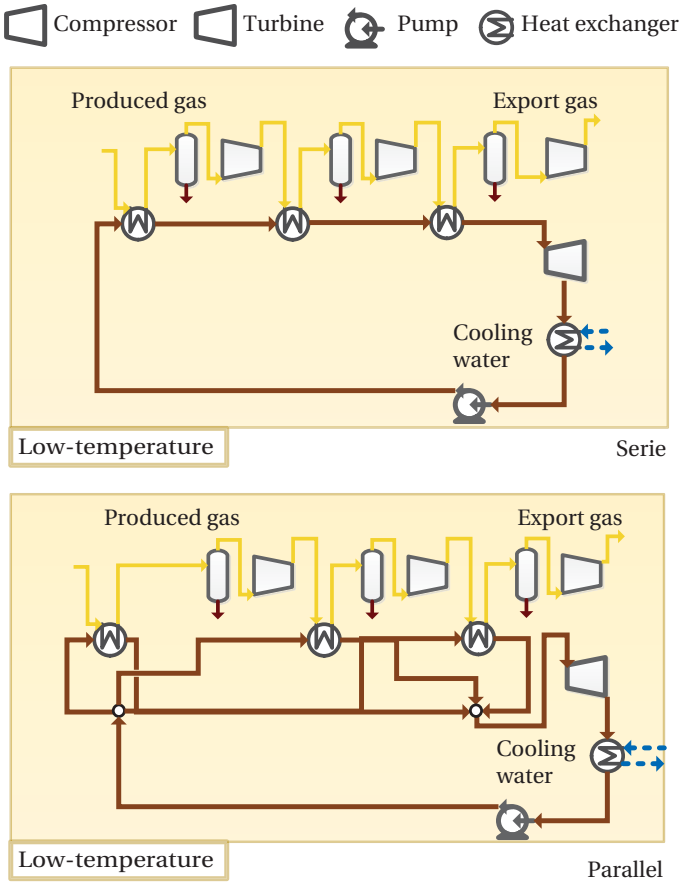

Figure 9.19: Examples of process integration of low-temperature organic Rankine cycles on offshore platforms, in serie or in parallel.

The addition of a recuperator generally improves the thermodynamic efficiency, but its integration may be an issue because of the extra space required.

9.6.2 Process optimisation

The optimisation results suggest that the most efficient cycle would be a trans-critical cycle using a mixture of ethane and propane, in proportions, on a mass basis, varying between 50 %–50 % to 30 %–70 %. Although these cycles display a thermal efficiency as low as 10 %, their integration can result in an additional net power generation of 1.5 to 3.5 MW, depending on the life production stage and on the rate of the produced gas (Figure 9.20).

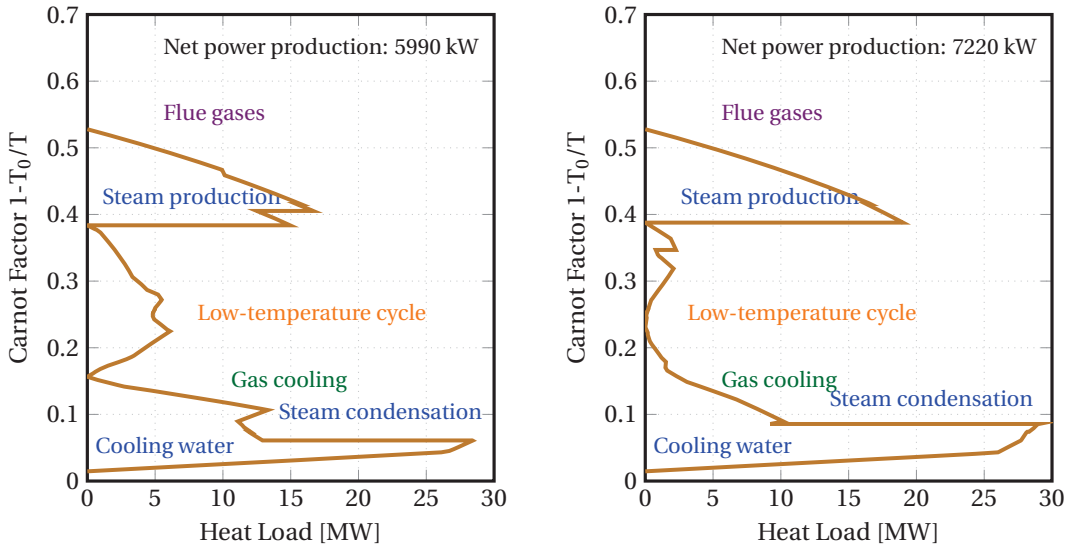

Figure 9.20: Balanced Grand Composite Curves, on an exergy basis, of the oil and gas platform system, including a steam Rankine and a low-temperature power cycles.

As for the steam Rankine cycle, the performance of the low-temperature power cycle is directly correlated to a few design parameters, such as the condensation and production levels, the temperature after superheating and the ethane fraction (Table 9.8). The optimal low-temperature power cycles, i.e. the ones with the greatest power generation, operate between 20 °C and 170 °C, and recover heat from the gas streams in the treatment process. In practice, the design of such a cycle would be challenging and costly, as the working fluid should be evaporated and superheated in several heat exchangers.

Table 9.8: Optimal design parameters for the low-temperature power cycle, for each production period. These numbers are the average means of the decision variable values for the configurations yielding the greatest power generation.

	Condensation [°C]	Production [bar]	Superheating [°C]	C_2H_6 [% molar]
Begin	19.2 (2.8)	77.5 (4.0 %)	174 (6.1)	80 (21 %)
Peak	23.1 (2.6)	77.2 (3.6 %)	177 (14)	73 (21 %)
End	20.4 (4.1)	69.9 (11 %)	162 (9.2)	51 (6 %)

The integration of a steam network, without any low-temperature power cycle, allows for a greater power production, ranging from 3 to 8 MW at design conditions for a total investment cost between 6 and 14 M$. There are no further increases in operating costs, as no additional fuel is required, and the number of operators is assumed to be constant. The thermal efficiency increases to about 35–40 % when the steam cycle is run at full-load conditions, and between 28 and 33 % when run for the normal operating conditions.

The integration of a low-temperature power cycle besides a steam network results in an additional power generation of up to 3.5 MW, which should be added to the additional 3 to 8 MW of the steam network. These numbers can be attained only if heat can be recovered from all the coolers located in the gas recompression and compression sections. Although the heat exchangers are already installed, such solutions may be problematic as further retrofit of the pipeline connections and of the heat exchangers may be necessary.

The total investment cost ranges between 5 and 7 M$, and the preferred low-temperature cycle for these applications is the ethane-propane cycle, as suggested previously in the work of Rohde et al. [123]. As expected, the economic and environmental benefits related to the decrease of the fuel gas consumption are smaller, and the reductions in natural gas consumption and CO_2-emissions are smaller by at most 8 % in all cases.

9.6.3 Comparison

In the case that no heat recovery is feasible between the oil and gas streams, a cost-efficient alternative is to utilise the waste heat from one single hot stream, using the heat from the gas to be exported in the final heat exchanger. Additional power can be generated, while having a relatively compact and light system including only four components.

In the case of Platform D, and considering the end-life conditions, the working fluid, with a composition of 40 % ethane and 60 % propane, should operate between 23 °C (19.5 bar) and 144 °C (56 bar). The cycle can provide a net supplement of power of 590 kW, which corresponds to a thermal efficiency of 8.3 %. For the latter case, exergy is destroyed at rate of about 250, 210 and 200 kW in the boiler, turbine and condenser, while the exergy lost with the additional cooling water amounts to nearly 120 kW. However, setting the low-temperature power cycle only on the after-cooler placed at the outlets of the gas treatment process may not be viable, because the gas flow through this heat exchanger is already small (lower than 2 kg/s) and is expected to decrease with time.

This solution may, on the contrary, be of particular interest for platforms processing and cooling high quantities of gas. It seems a priori interesting for Platform B, because the quantity of heat discharged in the gas aftercooler currently exceeds 40 MW. In practice, the gas inlet and outlet temperatures are around 100 and 32 °C, respectively, and these requirements restrict severely the evaporation level on the organic fluid side and the maximum power output.

9.7 Conclusion

Integrating a waste heat recovery cycle results in a greater power capacity, if required, or in a lower fuel gas consumption and smaller CO_2-emissions. The introduction of these processes is a complex design task, as many layouts can be suggested, depending on the energy requirements of the platform and on the plant layouts. The use of multi-objective optimisation procedures helps discarding sub-optimum solutions, while illustrating the trade-offs between the investment costs, operational savings and maximum power capacity.

The implementation of steam Rankine cycles on oil and gas platforms is discussed in the works of Kloster [120, 121], and the engineering challenges are emphasised in Nord and Bolland [118, 119]. These cycles present a satisfying behaviour at design and part-load conditions, if they are properly designed and integrated within the offshore system. The heating demand, if any, can either be met by recovering the waste heat from the exhaust gases, adjusting the temperatures of an intermediate heat transfer loop (e.g. glycol or pressurised water), or by using steam extraction [120, 121].

The installation of organic Rankine cycles on offshore facilities has never been performed. The high compactness and low weight compared to a conventional steam Rankine cycle may favour the implementation of such cycles because of the stringent space and weight constraints on offshore platforms. However, the comparison of several possible working fluids illustrates that none can satisfy simultaneously efficiency, safety, risk, operational and environmental criteria.

Steam networks may therefore be preferred against organic Rankine cycles, since these processes are well-known and already implemented offshore. Thorough techno-economic assessments should be conducted to analyse the compactness and economic viability of these installations, with regards to the specific features of each facility.

In all cases, the integration of these cycles allows only a partial recovery of the waste heat and exergy contained in the flue gases. Substantial exergy pockets are found at temperatures as low as 20–80 °C, and they can most likely be exploited by integrating a low-temperature power cycle to recover heat from the produced gas.

Finally, this outlook on waste heat recovery technologies illustrates the potential of applying a site-scale approach, as it shows possibilities for creating and exploiting synergies between several processes, which results in a more efficient and profitable oil and gas processing. However, a close integration could result in reduced availability: a smaller level of integration is associated with an efficiency penalty, but at the benefit of reduced unforeseen outages.

10 CO_2-mitigation

This chapter details a systematic comparison of existing and future CO_2-mitigation options for oil and gas platforms, using thermodynamic, economic and environmental performance indicators. It builds partly on CO_2-capture models developed prior to this thesis, and a strong focus is on the specificities and requirements of offshore facilities.

10.1 Introduction

The extraction and processing of oil and gas on offshore fields is an energy-intensive sector that represented up to 26 % of the total CO_2-emissions of Norway in 2011. These emissions are caused by the combustion of diesel, gas or oil for power generation on-site and are subject to a hydrocarbon fuel tax that has increased these last years, from 210 ($ 35) to 410 NOK ($ 67) per ton of CO_2 [13, 254].

In this context, reducing the CO_2-emissions has become more and more interesting from both an environmental and an economic prospective. This goal can be achieved (i) by integrating a waste heat recovery unit, which would result in a smaller fuel gas consumption, by (ii) implementing a carbon capture process, or by (iii) connecting the local power generation system to the ashore electric grid, which would lead to lower emissions on-site. The main objectives of the work presented in this chapter are therefore to:

(1) compare the prospects and challenges of integrating CO_2-capture processes on existing oil and gas platforms;

(2) design and optimise such systems at a site-scale level, by systematic process integration;

(3) estimate the total costs, energy penalties and environmental benefits simultaneously.

10.2 System description

10.2.1 General superstructure

The different technological options that can be implemented to reduce the CO_2-emissions of the oil and gas plant (waste heat recovery and CO_2-capture) are investigated and included in a general system superstructure, considering that carbon dioxide may be captured prior to the combustion process (pre-combustion) or after (post-combustion).

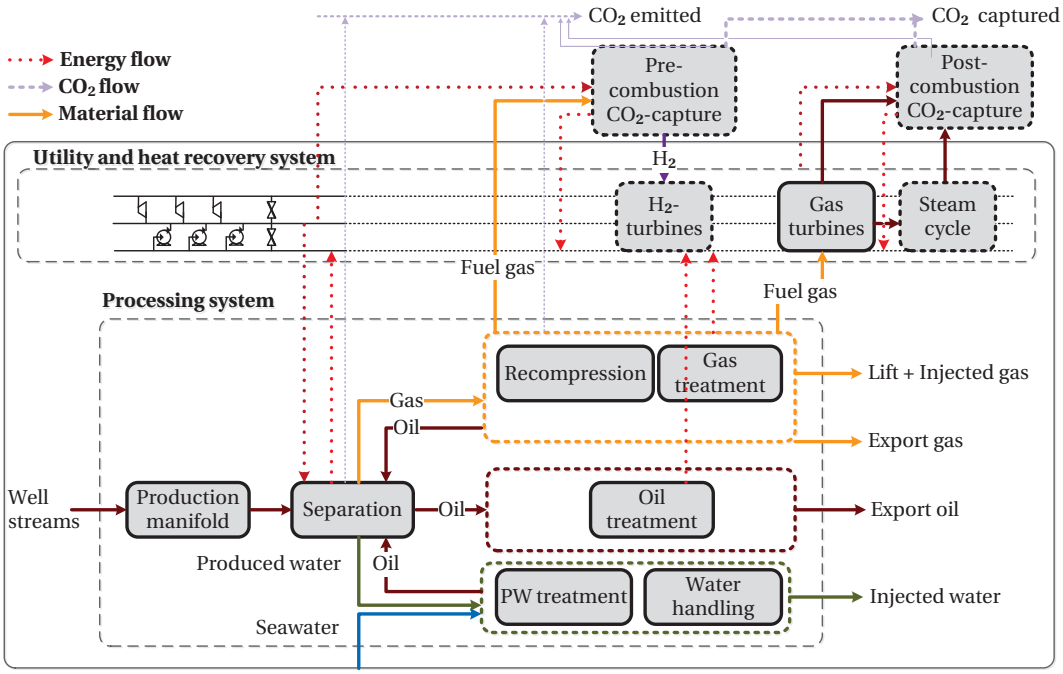

Figure 10.1: A generalised superstructure for integration of CO_2-capture on offshore platforms.

The integration of CO_2-capture on oil and gas platforms is not common, as it faces several technical and economical challenges. CO_2-separation with acid gas (i.e. CO_2 and H_2S) removal is a mature technology, and it is widely applied in hydrocarbon processing industries such as refineries. It is also a common process for purifying hydrogen after steam reforming processes, such as in integrated gasification combined cycle plants. Most applications are nevertheless onshore, and CO_2-separation offshore is limited to the natural gas offshore platforms if the initial CO_2-content is considered too high for export in the pipelines.

Electrifying the platform implies that the electricity required offshore is produced onshore, supposedly in more efficient energy systems such as high-efficiency combined cycles or hydroelectric plants.

10.2.2 Process technologies

Waste heat recovery

As discussed in Chapter 9, waste heat from the turbine exhausts or from the processed gas can be recovered by integrating a bottoming cycle. The same technologies are considered in this part of the work.

CO_2-capture

There exists a large variety of CO_2-separation technologies, which can be classified into four main categories:

- absorption;

  Acid gases such as CO_2 are bound to an organic solvent, either chemically (chemical absorption), based on the CO_2-dissociation into hydrogen carbonates (HCO_3^-), or physically (physical absorption), based on the solubility differences of CO_2 in the feed gas and the liquid solvent [255].

  This process takes place in two main columns: an absorption column, in which the solvent circulates at counter-current of the feed gas, removing CO_2, and a regeneration one, in which CO_2 is recovered at high purity, generally by heating up and/or depressurising the solvent-CO_2-mixture.

- adsorption;

  CO_2-molecules (adsorbate) are bound to a solid surface (adsorbent) because of the selective effects of the surface forces (weak such as van der Waals or intermolecular such as covalent) [256, 257].

  This process is cyclic, with a first step (adsorption), in which CO_2 is removed from the feed gas and adheres the solid adsorbent, and a second step (desorption), in which CO_2 is separated from the adsorbent by either changing the pressure (pressure-swing) or the temperature (temperature-swing) conditions.

- cryogenic distillation;

  This process builds on the differences of boiling point temperatures between the various constituents of the feed gas. The separation takes place at low temperatures, and the carbon dioxide is liquefied and separated from the other compounds [258].

- membrane separation.

  Selective membranes, either organic or polymeric, are used to separate CO_2 from the remaining chemical compounds [259, 260], based on different mechanisms such as the Knudsen or surface diffusion. The performance of this technology is linked to its capacity to let CO_2 only pass through the membrane (selectivity and permeability).

There exist different pathways of CO_2-capture [261] based on these separation technologies:

- pre-combustion;
- oxy-combustion;
- post-combustion.

It may be argued that oxy-combustion by, for instance, chemical looping, is a sub-category of the pre-combustion pathway, as CO_2 is inherently separated from the other gases prior or during the combustion process. The rest of this work focuses on the pre- and post-combustion paths, as the oxy-combustion one is the least mature and requires, by definition, production of pure oxygen, which is generally done by cryogenic air separation at very low temperatures. This separation involves a refrigeration demand, which corresponds to the main energy penalty of the oxy-combustion path.

Pre-combustion. The term *pre-combustion* CO_2-capture refers to the CO_2-removal from carbonaceous fuels before combustion (Figure 10.2), by, for instance, converting the primary fuel such as natural gas or biomass into hydrogen and carbon dioxide [144, 262, 263]. Hydrogen is then burnt to generate electricity or used in other applications such as fuel cells, while carbon dioxide is sequestrated apart after compression. These processes can only be implemented to new power generation systems, since they should be directly integrated together with the combustion processes [264].

Smaller installations may be expected compared to post-combustion ones, because of the smaller fuel flow rate in the gas turbines and the higher partial pressure of CO_2. However, the addition of components such as water-gas shift reactors may lead to an overall bigger process, and a detailed study should be conducted.

The major challenges encountered with these technologies are namely their high investment costs, their applicability to new plants only (grassroot), and the difficulties associated with hydrogen combustion. The first hydrogen-fired gas turbines will likely run on hydrogen combustion with air, as the production of pure oxygen is costly and hydrogen premixed combustion is challenging. With some exceptions, the current turbine materials cannot withstand temperatures above 1500 °C [265, 266]. Other issues that may be encountered are the flame stability and the production of nitrogen oxides, and research on these topics is currently on-going.

Pre-combustion technologies vary widely, from integrated gasification techniques to membrane modules. In general, natural gas is first converted into a synthesis gas with carbon monoxide, hydrogen, water and carbon dioxide, by partial oxidation, steam reforming, au-

tothermal reforming, which is a combination of the two previous paths, or cracking.

$$\mathrm{CH_4} + \tfrac{1}{2}\mathrm{O_2} \rightleftharpoons \mathrm{CO} + 2\mathrm{H_2}$$
$$\mathrm{CH_4} + \mathrm{H_2O} \rightleftharpoons \mathrm{CO} + 3\mathrm{H_2}$$
$$\mathrm{CH_4} \rightleftharpoons \mathrm{C} + 2\mathrm{H_2}$$

Partial oxidation is an exothermic reaction which requires oxygen, either pure, after air separation by cryogenic distillation, or diluted with nitrogen, by processing directly air. Steam reforming is an endothermic reaction taking place in fuel-lean conditions, and cracking consists of a decomposition of heavy hydrocarbons into hydrogen and carbon. The carbon dioxide and hydrogen contents of the syngas are increased by water-gas shift, which is a mildly exothermic reaction.

$$\mathrm{CO} + \mathrm{H_2O} \rightleftharpoons \mathrm{CO_2} + \mathrm{H_2}$$

Finally, CO_2 is removed by physical or chemical absorption, yielding a H_2-rich fuel gas. Depending on the system specifications, the synthesis gas can be further purified into near-pure hydrogen by pressure-swing adsorption. The higher CO_2 partial pressure eases the separation process and make it less energy-intensive. High CO_2 partial pressures (≥ 7 bar) favour the introduction of physical absorption, while low ones push towards the implementation of chemical absorption with aqueous TEA solutions. Other solvents may be considered, based on other amines (MDEA) or chemicals (potassium carbonate and aqueous ammonia).

The use of membranes in pre-combustion processes may be more economically effective than in post-combustion ones, because the volume flow rates are smaller, implying that the membrane area will be smaller as well. In this case, the number and arrangement of membrane modules, as well as the operating pressures are decision variables that can be optimised to reach a high separation performance and low investment costs.

The energy penalty of pre-combustion CO_2-capture processes is generally associated with the need for high-temperature heat in the steam reforming process and the demand for auxiliary steam in the water-gas shift reactors. At the moment, the combination of autothermal reforming, two-step water-gas shift, physical absorption and hydrogen-fuelled gas turbine seems to be the most adapted option.

Post-combustion. The term *post-combustion* CO_2-capture refers to the removal of carbon dioxide from the flue gases of a power plant (e.g. coal- or gas-fired), i.e. after the combustion process (Figure 10.3). At the difference of coal-fired plants, the exhausts from a gas turbine have a low CO_2-concentration, of about 3 to 5 %, as well as a relatively low pressure (near atmospheric). Separation technologies such as physical absorption, adsorption, cryogenic refrigeration and membrane diffusion are therefore not suitable, and the CO_2-removal step is then achieved by chemical absorption, preferably with alkanolamines [267]. The major

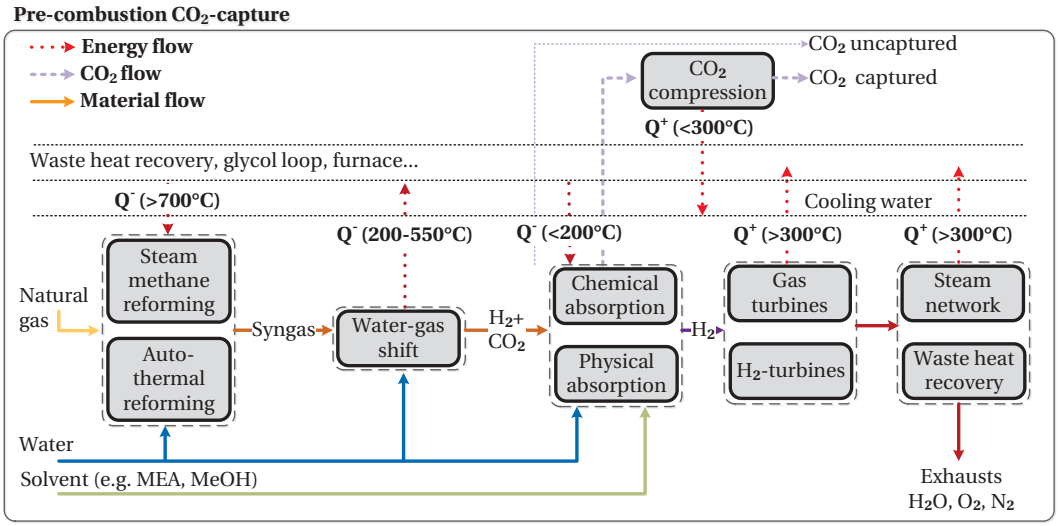

Figure 10.2: A generalised superstructure for integration of pre-combustion CO_2-capture on offshore platforms.

challenges are namely the large heat and power consumptions, which induce a significant energy efficiency penalty, as well as the large volume flow of the exhaust gases, which implies large units for CO_2-separation.

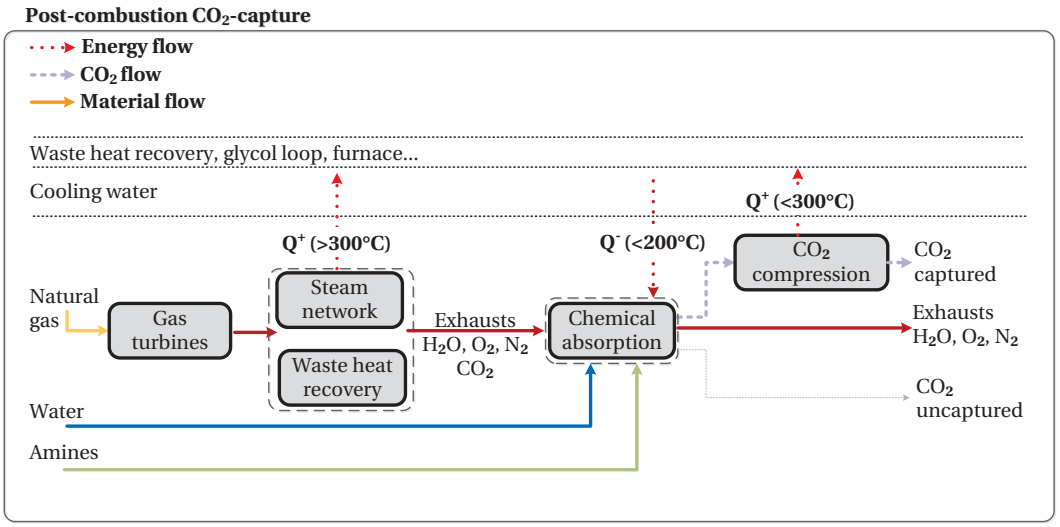

Figure 10.3: A generalised superstructure for integration of post-combustion CO_2-capture on offshore platforms.

Electrification. The term *electrification* refers to the supply of electricity from *shore* to offshore oil and gas installations. The power duty originates from land-based installations, such as hydroelectric facilities or combined cycle plants, and is transmitted by either alternative current (AC), or by high-voltage direct current (HVDC). HVDC systems may be preferable for long-distance applications, since they suffer lower electrical losses, and may be more economical in such situations. As a consequence, depending on the distance between the offshore platform and the shore, and on the acceptable utility frequency, one topology may be preferred. Power transmission based on voltage source converter (VSC) seem to be promising.

Offshore electrification is claimed to present several technical and operational benefits, such as higher facility availability, lower maintenance costs, and higher system efficiency, as well as environmental benefits, with a cut-down of the greenhouse gas emissions. The operational costs are supposed to be much lower, as the natural gas consumption is much smaller. One challenge with platform electrification is their high investment costs.

A few offshore platforms located in the North and Norwegian Seas are currently electrified, and new projects on the electrification of other ones are ongoing. The Troll A platform is at present connected to the Norwegian onshore grid using a 70-km long HVDC cable, using mostly hydropower from the mainland, which is used to drive the compressors on-site. The Valhall platform is completely electrified, and is connected via a 290-km long DC cable. On the contrary, the Gjøa platform is connected via a 100-km long AC cable. A platform can be *partly* or *fully* electrified, depending on whether the heating demand, if any, is satisfied by electric heaters or by gas-fired burners, and on part of or all the electrical consumption is supplied by land-based electricity (Figure 10.4).

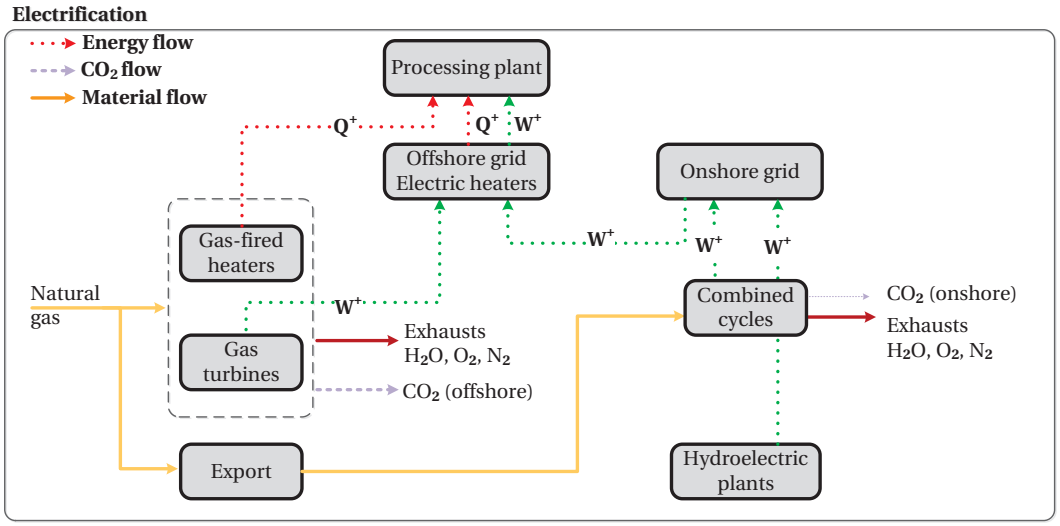

Figure 10.4: A generalised superstructure for integration of electrification on offshore platforms.

10.3 Modelling and optimisation

10.3.1 Thermo-environomic modelling

Baseline plant

The Draugen platform is taken as a baseline case study, with the corresponding power demand. The exhaust gases from the power turbines are characterised by a relatively low temperature ($\leq 350\,^{\circ}C$), pressure ($\simeq 1$ bar) and CO_2-content (≤ 3 %-weight). The integration of post-combustion CO_2-capture may be challenging because of the low CO_2-partial pressure, and the implementation of pre-combustion CO_2-capture costly because of the equipment to install for replacing the existing gas turbines.

Natural gas reforming

Synthesis gas production by steam-methane reforming (Figure 10.5) is modelled as an isobaric reaction taking place with steam at a temperature between 700 and 1000 °C, and at a pressure between 3 and 25 bar. This reaction is endothermic and is by definition favoured at high temperatures: the heat supply is modelled as a heat source at constant temperature, implying that heat is consumed in isothermal conditions as the reaction proceeds. The use of a metal-based catalyst such as nickel, to improve the reaction kinetics, is not modelled explicitly, but it is assumed that the reaction reaches thermodynamic equilibrium.

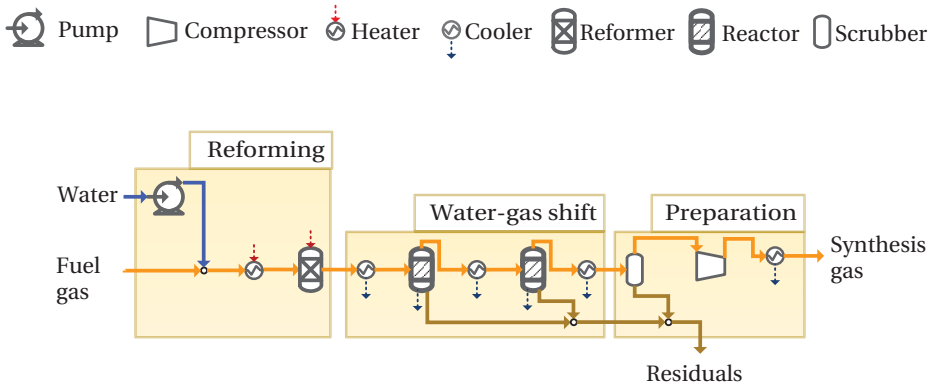

Figure 10.5: A generalised overview of a steam methane reforming system for pre-combustion CO_2-capture.

Similarly, natural gas reforming by partial oxidation is modelled as an isobaric reaction occurring with limited quantities of oxygen at a temperature of 900 to 1100 °C, and the operating pressure can be increased up to 100 bar (Figure 10.6). This reaction, at the opposite of SMR, is exothermic: the heat release is modelled as a heat discharge at constant temperature, implying that heat is removed in isothermal conditions as the reaction evolves. However, partial oxidation is characterised by better kinetics than the steam-methane reforming reaction.

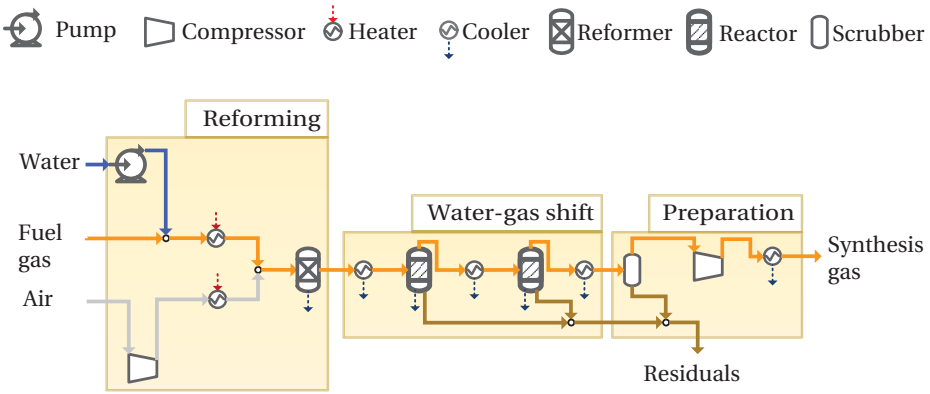

Figure 10.6: A generalised overview of an autothermal reforming system for pre-combustion CO_2-capture.

Water-gas shift

The water-gas shift reaction follows the SMR and ATR reactions and allows for controlling the H_2/CO ratio by a further reaction between carbon monoxide and steam. It may take place in a one- or two-step reactor at high and low temperatures, but most industrial applications consist of a high-temperature shift (HTS) followed by interstage cooling and low-temperature shift (LTS). This reaction is therefore modelled as a two-stage isobaric reaction: the HTS takes place at a temperature between 300 and 450 °C, while the LTS operates between 200 and 250 °C. The operating pressure can be varied between the atmospheric one and up to 80 bar.

The water-gas-shift reaction is mildly exothermic, meaning that it is thermodynamically favoured at low temperatures but kinetically favoured at high ones. Carbon monoxide is therefore not completely converted in the HTS (2–4 %) and nearly reaches total conversion in the LTS (≤ 1%). As for natural gas reforming, the use of catalysts, which are iron (Fe_2O_3) and chromium (Cr_2O_3) oxides for HTS, and copper (CuO), zinc (ZnO) and aluminium (Al_2O_3) oxides for LTS, is not modelled explicitly, but the WGS reactions are assumed to reach thermodynamic equilibrium at the temperature operating conditions.

Chemical absorption

The feed gases enter an absorption column in which an aqueous mixture with an amine concentration of 30–35 %-wt flows counter-currently. The amine acts as a weak base, neutralising acid compounds such as CO_2 and recombining them into HCO_3^- ions, which are soluble in the cold aqueous solution. The CO_2-rich mixture is preheated before entering the regeneration column, with a condenser at the top stage and a reboiler at the bottom one. The chemical bounds are then broken: the regenerated amine solution is recycled back to the absorber, while the carbon dioxide at high purity is dehydrated and compressed.

For a primary amine such as MEA, the overall reaction can be written as:

$$CO_2 + R{-}NH_2 + H_2O \rightleftharpoons R{-}NH_3HCO_3$$

It is slightly different for tertiary amines (e.g. TEA), since the latter cannot react directly with carbon dioxide [268]:

$$CO_2 + R_3{-}N + H_2O \rightleftharpoons R_3NH^+ + HCO_3^-$$

The most often used amines in commercial applications are mono- (MEA) and tri- (TEA) ethanolamines, the first one is preferred for low temperature and pressure applications, while the second is recommended for cleaning H_2-rich fuels, although it has become less attractive because of its low absorption capacity. Other amines such as methyldiethanolamine (MDEA) have also gained interest recently because of the greater loading in aqueous solutions and higher degradation resistance, but their higher selectivity towards hydrogen sulphide (H_2S) makes them more interesting for acid gas removal in gas processing applications. Potassium carbonate solutions are promising because of the high chemical solubility of CO_2, low solvent costs and low energy requirements in the regeneration process. The main challenge is the lower reaction rate in the liquid phase. Piperazine may be used to improve the reaction kinetics, but the degradation of this component raises health end environmental concerns [269, 270].

MEA is characterised by a significant heating demand in the regeneration process, an issue encountered for most CO_2-solvents, which amounts to 3–5 GJ/t_{CO_2}, a low CO_2-loading capacity, as well as thermal, oxidation degradation and corrosion issues. The solvent regeneration also takes place at low pressures, near-atmospheric, compared to the ones required for CO_2-storage and transport, implying that the CO_2-rich off-gas should be further compressed. The model of the CO_2-capture units with monoethanolamine (Figure 10.7) is developed using the commercial flowsheeting software Aspen Plus® version 7.2 [39], based on the electrolyte NRTL method [271] for the liquid phase and the Redlich-Kwong [272] EOS for the vapour phase.

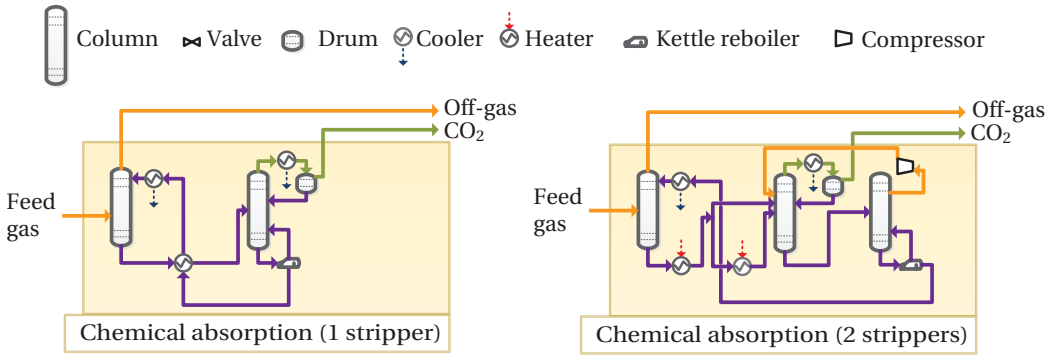

Figure 10.7: A generalised overview of a chemical absorption sub-system for CO_2-capture.

The solution chemistry is defined by the interactions between carbon dioxide, water and monoethanolamine, and the sulphur chemistry is not considered.

$$2H_2O \rightleftharpoons H_3O^+ + OH^-$$
$$CO_2 + 2H_2O \rightleftharpoons H_3O^+ + HCO_3^-$$
$$HCO_3^- + H_2O \rightleftharpoons H_3O^+ + CO_3^{2-}$$
$$MEAH^+ + H_2O \rightleftharpoons MEA + H_3O^+$$
$$MEACOO^- + H_2O \rightleftharpoons MEA + HCO_3^-$$

The absorber and desorber are modelled as rate-based, by opposition to steady-state equilibrium, taking into account the reaction kinetics: each column is modelled as a a number of control volumes where each phase is perfectly mixed in each volume, vapour-liquid equilibrium is assumed only at the contact interface, the heat-tranfer coefficients are assumed constant, and the mass transfer is assumed to be limited by the low-flux mass-transfers.

Physical absorption

Unlike the absorption process with amines, where CO_2 is involved in parallel chemical reactions, the absorption with solvents such as methanol does not imply the formation of HCO_3^- ions. The overall process set-up is nonetheless similar: the feed gas enters an absorption column, where an aqueous solution flows counter-currently and absorbs CO_2. This CO_2-rich solution is then regenerated in a different column operating at different pressure and temperature conditions, cooled and pumped before re-entering the absorption column.

The implementation of physical rather than chemical absorption is preferred at high pressures, as the CO_2-capture is driven by the CO_2-solubility in the physical solvent, which depends on the partial pressure and temperature. The most common solvents are methanol (MeOH) and mixtures of polyethylene glycol esters (DEPG) [255]. There is a large variety of process design set-ups investigated in previous works, and the two main ones, already under commercialisation, are the Rectisol® (methanol) and Selexol® (polyethylene glycol esters) schemes.

The Rectisol® process layout is highly flexible. The number of stripping stages can for example be adapted to the system needs and water washing can be integrated to reduce the methanol vapour losses (Figure 10.8). It requires less thermal energy than chemical amines in the regeneration step, but the solvent should enter the absorption column at low temperatures, typically below -30°C. The Selexol® process, in comparison, can operate at temperatures up to 175 °C, does not require water wash, and not necessarily refrigeration, but has a much higher viscosity, impeding mass transfer and lowering tray efficiencies.

The models of the CO_2-capture units with methanol and DEPG are developed using the commercial flowsheeting software Aspen Plus® version 7.2 [39], based on the PC-SAFT equation of state [171].

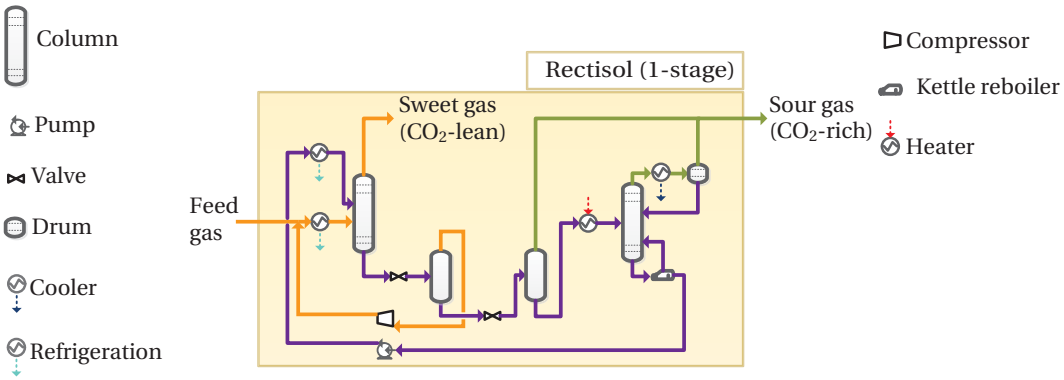

Figure 10.8: A generalised overview of a physical absorption sub-system based on methanol (Rectisol) for CO_2-capture.

H_2-fuelled turbines and refrigeration cycles

Finally, the hydrogen-rich gas can be processed in a gas turbine where the power required on-site is produced (Figure 10.9). A simple and generic cycle layout is adopted for this study, assuming that the turbine inlet temperature is constrained by blade cooling limitations and is controlled by using cooling air from the compressor outlet, while the temperature in the combustion chamber is regulated by the air excess. A generic propane refrigeration cycle is considered for the refrigeration needs of the Selexol® and Rectisol® processes. The optimisation study may be further improved by considering different types of refrigeration cycles.

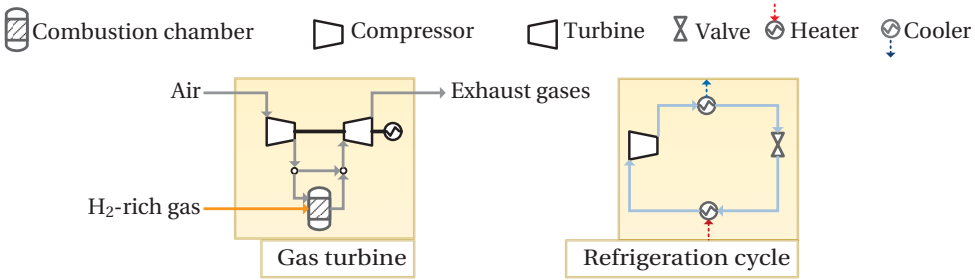

Figure 10.9: A generalised overview of the utilities implemented on the pre-combustion CO_2-capture path.

The steam Rankine cycle is modelled as explained in Chapter 9 considering the integration of production (i.e. steam production), usage (i.e. steam extraction) and condensation (i.e. steam condensation) headers. The same process characteristics are taken, but it is assumed that a post-combustion CO_2-capture plant would process the exhaust gases produced from the two gas turbines that are currently in operation.

Electrification

Unlike CO_2-capture processes, there are several platforms receiving power from shore, and new projects with onshore electrification are on the plan. The system set-up of an electrified platform can differ from one facility to another, but, for simplicity, and because this thesis does not aim at investigating all the electrical engineering aspects, the transmission losses are assumed constant and equal to 8 %. In practice, they vary with the power duty of the platform, on the type and geometry of the power transmission cable. Different electrification scenarios can be proposed, depending on how the power is supplied offshore:

- *no electrification*: all the power demand is satisfied by on-site utilities such as gas turbines;
- *partial electrification*: part of the power duty is met with power produced on onshore facilities;
- *total electrification*: all the required power is imported from the shore.

and on how the heating needs are met:

- *internal heat recovery* between process streams;
- *electric heaters* fuelled with on- or offshore power;
- *heat pumps* driven by on- or offshore power;
- *burners and furnaces* fuelled by natural gas.

Two electrification scenarios are considered in the rest of this study, referred as Scenario 1, where all the power demand is satisfied with power from the mainland, but the heating demand is ensured by natural gas combustion in heaters, and Scenario 2, where the heating demand is satisfied by electric heating, and all power is supplied from shore.

Different electrification sources can be considered, depending on the case study and country of interest. However, only the hydro- and combined cycle power plants options are regarded in this work, as these possibilities are the ones that are mostly discussed in the literature. Gas-fired power plants are taken as examples since they present the highest efficiency compared to the ones driven with coal.

It is assumed that the electrification of current and future platforms will not result in the construction of new power and thermal plants, and that the power demand of offshore facilities will belong to the baseline load category. This assumption is open to discussions, because some platforms have a power demand greater than 50-70 MW, and electricity may be imported from neighbouring countries.

10.3.2 Thermo-environomic optimisation

Performance indicators

The overall performance can be evaluated by a large variety of thermodynamic and economic parameters, and this study focuses on:

- the energy efficiency of the cogeneration plant η;
- the investment costs C_{inv} of the CO_2-capture unit;
- the relative variation of natural gas δ_{NG} exported to the shore (increase or decrease);
- the reduction of CO_2-emissions δ_{CO_2} caused by the decrease of fuel gas consumption and/or the possible integration of a CO_2-mitigation plant;
- the changes in operating costs C_{op}, due to the replacement of monoethanolamine, methanol and DEPG because of degradation issues;
- the CO_2-avoidance cost CAC, defined as the ratio of the increase in investment costs over the decrease of CO_2-emissions;
- the power capacity or consumption of the additional systems $\dot{W}$.

Multi-objective optimisation

Objective functions. Several objectives can be considered, based on the numerous performance indicators: they illustrate that decision-makers need to evaluate the trade-off between two or more competing objectives (e.g. limitation of the investment costs versus reduction of CO_2-emissions). The objectives considered in the optimisation procedure are the maximisation of the power capacity $\dot{W}$, the minimisation of the investment costs C_{inv} and the minimisation of the CO_2-emissions δ_{CO_2}.

Decision variables. The optimal system configurations are computed by performing a multi-objective optimisation and displaying the solutions under the form of a Pareto optimal frontier. The master decision variables amount to 48, of which 18 are related to the operation of the steam cycle (e.g. pressures, temperatures, vapour fraction) and 5 to the selection of the cooling utility (e.g. process water and temperatures).

The decision variables related to the CO_2-capture processes are related to the selection and configuration of the CO_2-capture unit (e.g, equipment sizes) and amount to 15 in the case of a chemical absorption unit with MEA (Table 10.1), 7 in the case of a physical absorption module with MeOH (Table 10.2), 7 with DEPG (Table 10.3), 6 with TEA (Table 10.4). 13 other decision variables (Table 10.5) are related to the design of the natural gas pre-processing and of the associated utilities in the CO_2 pre-combustion path.

Table 10.1: Set of the master decision variables used in the multi-objective optimisation of the CO_2-capture unit based on chemical absorption with an aqueous solution of monoethanolamine.

Variable	Type	Unit	Range/Value
Lean solvent CO_2 loading	continuous	kmol/kmol	[0.18–0.25]
Rich solvent CO_2 loading	continuous	kmol/kmol	[0.4–0.5]
Split fraction	continuous	-	[0;1]
Rich solvent preheat temperature	continuous	°C	[95–105]
Rich solvent reheat temperature	continuous	°C	[115–125]
LP stripper pressure	continuous	bar	[1.7–2.1]
HP/LP pressure ratio	continuous	-	[1–1.5]
Number stages absorber	continuous	-	[10–17]
Number stages HP stripper	continuous	-	[8–15]
Number stages LP stripper	continuous	-	[6–10]
Absorber diameter	continuous	m	[6–12]
LP stripper diameter	continuous	m	[2–5]
HP stripper diameter	continuous	m	[3–6]
MEA concentration (solvent)	continuous	wt %	[30–40]

Table 10.2: Set of the master decision variables used in the multi-objective optimisation of the CO_2-capture unit based on physical absorption with methanol.

Variable	Type	Unit	Range/Value
MeOH/CO_2 ratio	continuous	kmol/kmol	[10–15]
Absorber temperature	continuous	°C	[-70–0]
Absorber pressure	continuous	bar	[15–60]
Absorber packing	Ceramic intalox saddles		
Number stages absorber	continuous	-	10
Regenerator pressure	continuous	bar	[1–10]
Regenerator temperature	continuous	°C	[20–100]

Table 10.3: Set of the master decision variables used in the multi-objective optimisation of the CO_2-capture unit based on physical absorption with DEPG.

Variable	Type	Unit	Range/Value
DEPG/CO_2 ratio	continuous	kg/kg	[8–14]
Absorber temperature	continuous	°C	[-18–173]
Absorber pressure	continuous	bar	[10–60]
Absorber packing	Pall ring		
Number stages absorber	continuous	-	10
Regenerator pressure	continuous	bar	[1–10]
Regenerator temperature	continuous	°C	[25–100]

Table 10.4: Set of the master decision variables used in the multi-objective optimisation of the CO_2-capture unit based on chemical absorption with an aqueous solution of TEA.

Variable	Type	Unit	Range/Value
TEA concentration	continuous	kg/kg	[0.25–0.40]
H_2-TEA ratio	continuous	kg/kg	[0.035–0.055]
Absorber temperature	continuous	°C	[20–45]
Absorber pressure	continuous	bar	[15–30]
Number stages absorber	continuous	-	25
Regeneration pressure	continuous	bar	[1-130]
Regeneration temperature	continuous	°C	[25–120]

Table 10.5: Set of the master decision variables used in the multi-objective optimisation of the pre-combustion CO_2-capture path.

Variable	Type	Unit	Range/Value
SMR temperature	continuous	°C	[450–950]
ATR temperature	continuous	°C	[500-950]
Reforming pressure	continuous	bar	[1–30]
Air-to-carbon ratio (ATR)	continuous	kg/kg	[3–4.5]
Steam-to-carbon ratio (ATR & SMR)	continuous	kg/kg	[1.5–6]
High-temperature water-gas-shift	continuous	°C	[250–420]
Low-temperature water-gas-shift	continuous	°C	[150–250]
Water-gas-shift pressure	continuous	bar	[1–30]
CO_2-capture unit	discrete	-	$\{0-3\}$
Oxygen-to-hydrogen ratio	continuous	kmol/kmol	[0.4–0.7]
H_2-combustion temperature	continuous	°C	1500
H_2-turbine inlet temperature	continuous	°C	1300
H_2-turbine combustion pressure	continuous	bar	[5–50]
Exhaust gas temperature	continuous	°C	[100–200]
Low-pressure level (refrigeration cycle)	continuous	bar	[0.1–5]
High-pressure level (refrigeration cycle)	continuous	bar	10

10.4 Pre-combustion CO_2-capture

10.4.1 Process integration

Reforming technology

The comparison of the reforming technologies (Figure 10.10) illustrates the differences between the autothermal and steam reforming processes with regards to their energy demands. An advantage of ATR over SMR is that the water- and air-to-gas ratios can be varied, which gives more flexibility for controlling the hydrogen-to-carbon ratio of the synthesis gas.

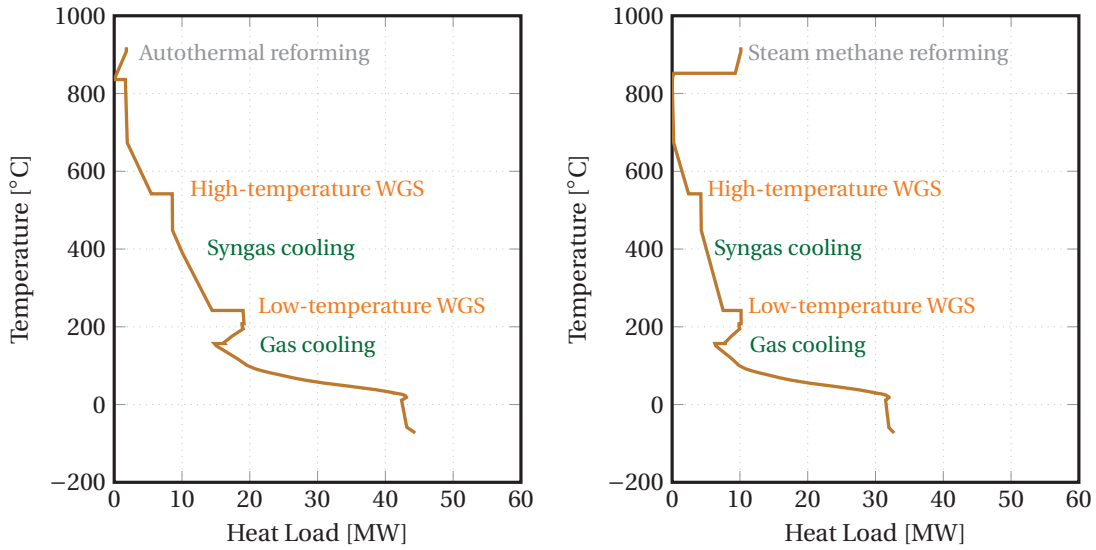

Figure 10.10: Grand Composite Curves for an oil and gas platform with ATR (left) and SMR (right) using Selexol as CO_2-capture technology.

The first layout (ATR) has (i) smaller steam consumption, because oxygen is used to generate the synthesis gas, (ii) lower high-temperature heating demand, since partial oxidation takes place in the reforming reactor, but (iii) higher electricity consumption, as air compression is required. Bigger equipment is required to produce the same quantity of hydrogen since nitrogen is present in the reforming air. On the contrary, the second configuration (SMR) results in a nitrogen-free synthesis gas.

In both cases, the grand composite curves of the entire system, including the oil and gas processing plant together with the fuel gas reforming, illustrate that the external cooling demand is increased, compared to the case without pre-combustion CO_2-capture, at high ($\geq 350\,^{\circ}C$), moderate ($\simeq 150$–$350\,^{\circ}C$), low ($\leq$,$150\,^{\circ}C$) and very low ($\leq 8\,^{\circ}C$) temperatures. They are related to the syngas cooling, water-gas shift reactions, gas cooling and physical solvent regeneration processes. The cooling water demand is increased by about 5 to 10 MW with SMR and by 10 to 20 MW with ATR, which represent 20 to 80 % of the initial requirements.

CO_2-capture technology

The introduction of CO_2-capture processes by physical absorption (Figure 10.11) results in different conclusions whether the Rectisol® or Selexol® technology is integrated. The first one systematically implies a need for cooling down the solvent (methanol) and the feed gas below ambient temperatures, increasing the electricity consumption as a refrigeration cycle should be implemented. The second one creates a refrigeration demand only if high CO_2-capture rates are of interest, since the CO_2-solubility in DEPG is higher at low temperatures.

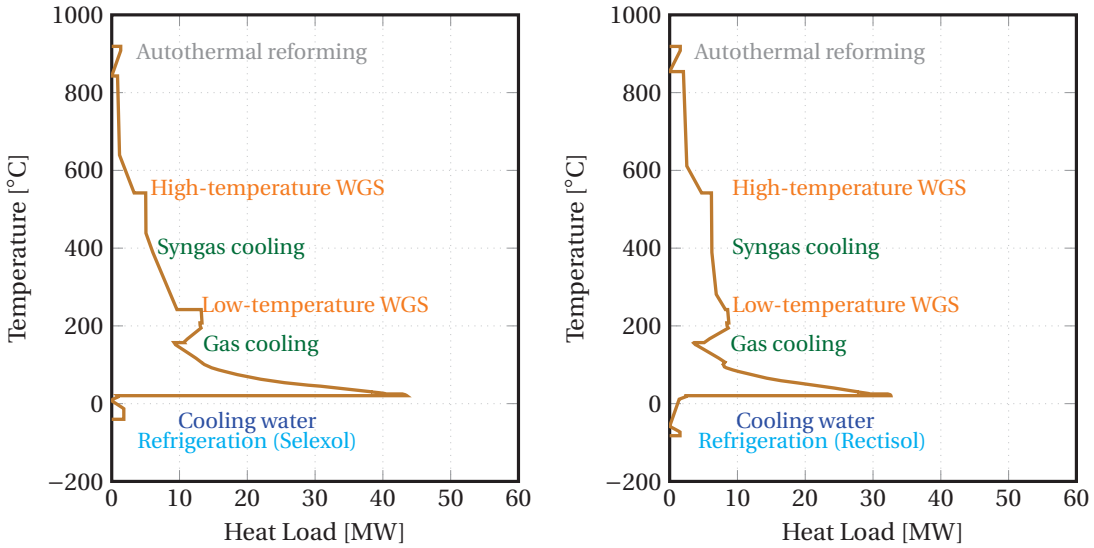

Figure 10.11: Balanced Composite Curves for an oil and gas platform with pre-combustion CO_2-capture based on autothermal reforming and using Selexol (left) and Rectisol (right).

In terms of power consumption, the differences between the Selexol and Rectisol processes are minor, because the synthesis gas should preferably be compressed at pressures higher than 40–50 bar in both cases to ensure high CO_2-partial pressure, and the solvent pumping process has a negligible power demand in comparison to the CO_2-compression. Power may be recovered by integrating a gas expander between the hydrogen-fuelled gas turbines and the CO_2-capture process, or with a radial liquid expander driven by the depressurisation of the CO_2-rich solvent.

There is a large variety of sets of operating conditions for which a CO_2-capture rate can exceed 80 %. It is assumed in the following examples that the H_2-fuelled gas turbines replace the current SGT-500, which satisfy the baseline power demand of 16,500 kW and the additional power consumption, which can be split (Figure 10.12 and Figure 10.13) into the power demands of the synthesis gas preparation process, the DEPG pumping in the Selexol process, the CO_2-compression and the refrigeration cycle . The same trends are found with system configurations based on Rectisol, with a higher share of the refrigeration cycle because of the lower temperatures of the methanol solvent (≃ -70°C) compared to the DEPG (≃ -10°C).

Syngas composition (mol %)	After preparation	After Selexol
H_2	54.4	64.4
CO	1.74	-
CO_2	17.9	3.6
N_2	25.7	30.0
H_2O	0.2	-

DEPG purity (solvent, before absorber): 97.1 mol %

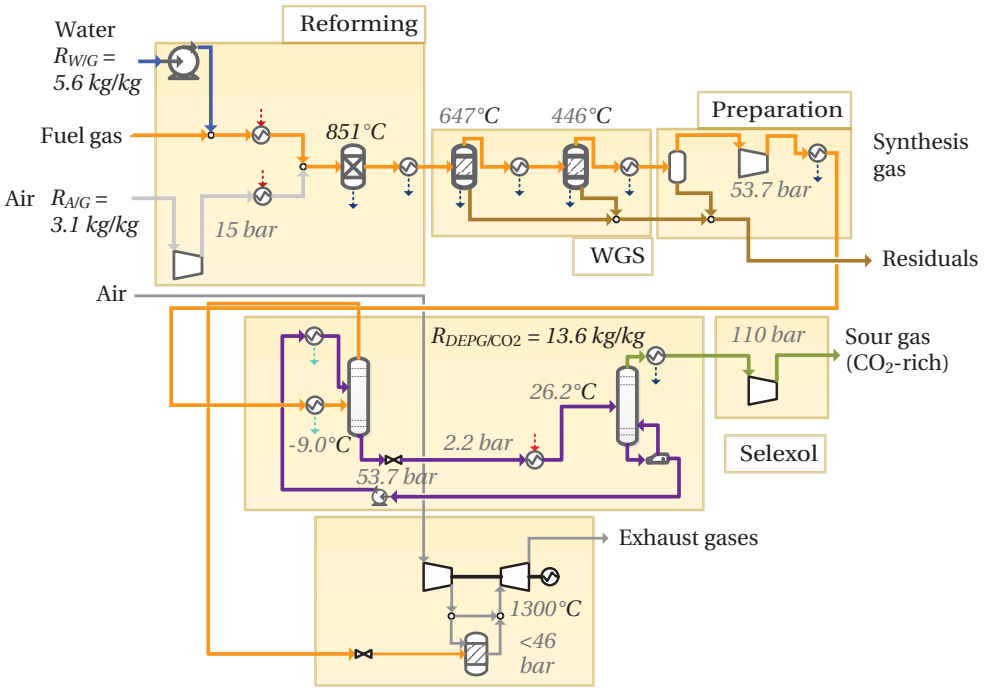

Figure 10.12: Example of configuration of pre-combustion CO_2 capture with ATR and Selexol.

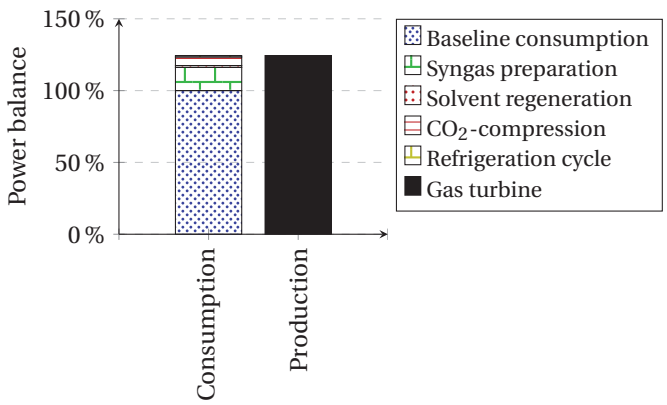

Figure 10.13: Power balance for an example of layout with ATR and Selexol.

Chemical absorption processes with TEA (Figure 10.14) may also compete with physical absorption ones since the CO_2-content may be as high as 25 % for a H_2-purity of 75 %. The heating requirements at low temperatures ($\leq 150°C$) increase in such cases, as a chemical absorption unit is always characterised by a heating demand (Figure 10.15) for regenerating the amine solvent. The highest H_2-purity is reached for chemical absorption with TEA along with steam methane reforming: it can exceed 90 % because the produced syngas is not diluted with nitrogen, while it is limited to 65–70 % if the reforming process is autothermal. The use of chemical absorption avoids large pressure drops in the CO_2-capture unit and the need for refrigeration (Figure 10.16), which explains the slightly higher electrical efficiency of pre-combustion CO_2-capture processes with amines in the later optimisations.

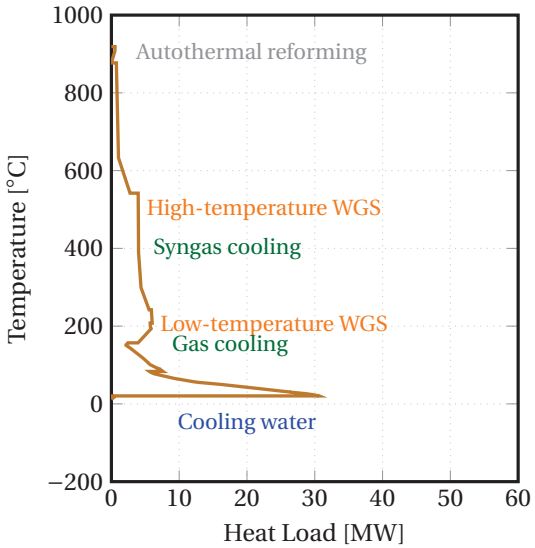

Figure 10.14: Balanced Composite Curve for an oil and gas platform with chemical absorption based on TEA.

Moreover, the energy required to regenerate the chemical solvent can be covered by utilising the heat from the water-gas shift reactors and syngas coolers, and that results in a smaller demand for cooling water compared to the process layouts with physical absorption. The introduction of a cogeneration utility together with a chemical absorption plant with TEA can be beneficial since it would result in a better match between the temperatures of the regeneration process and the hot utilities. However, the maximum amount of electricity that can be generated is smaller than if a physical absorption unit is integrated, because less heat is available in the temperature range of 300 to 600 °C.

The losses of carbon dioxide with the knock-out water are negligible in all cases, representing less than 0.5 % of the total carbon entering the capture unit. However, there are losses of hydrogen with the carbon dioxide sent to sequestration, which limit the CO_2-purity to an upper bound of 96–97 %. The implementation of a 2-stage regeneration plant may be beneficial, but this configuration is not further studied in this work.

Syngas composition (mol %)	After preparation	After TEA
H_2	53.4	63.9
CO	0.4	-
CO_2	18.8	3.4
N_2	27.2	32.7
H_2O	-	-

TEA purity (concentration, before absorber): 24.4 wt %

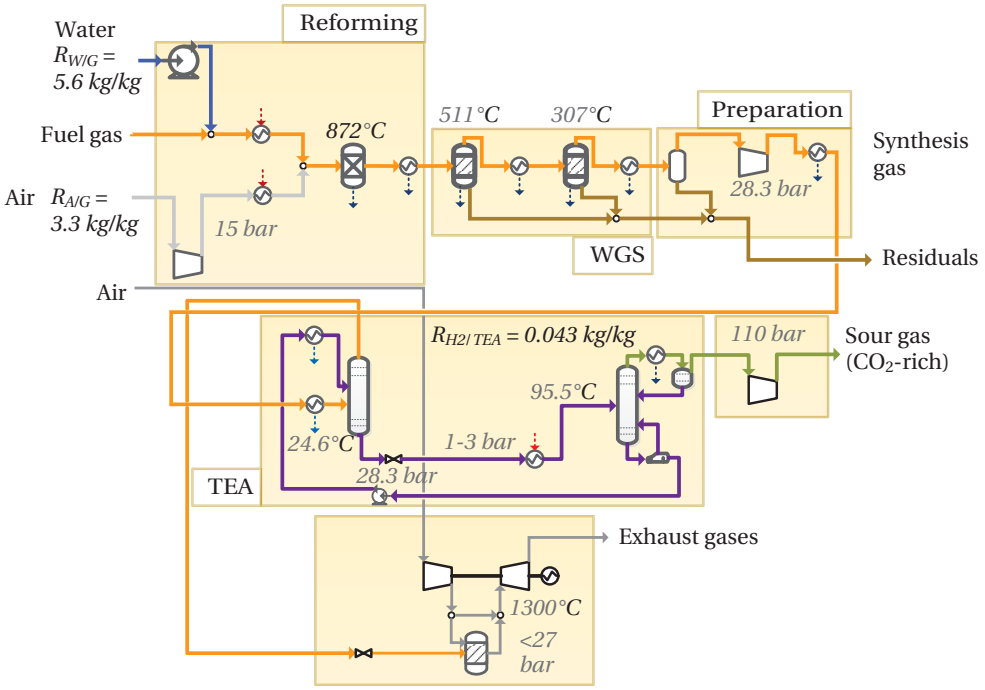

Figure 10.15: Example of configuration of pre-combustion CO_2 capture with ATR and TEA.

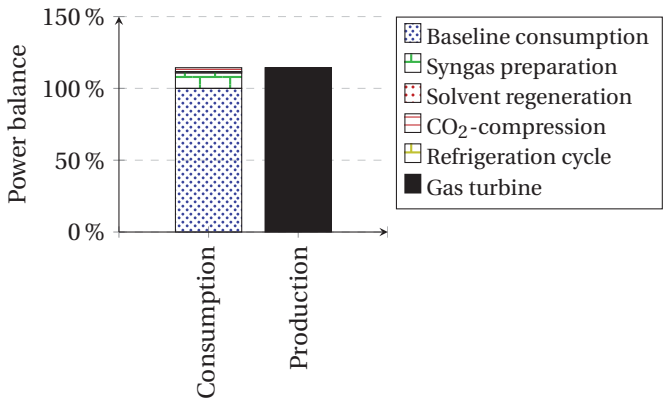

Figure 10.16: Power balance for an example of layout with ATR and TEA.

Utility integration

The integration of pre-combustion CO_2-capture affects significantly the possibilities for energy integration on-site and with the utilities such as the gas turbines. The pinch point of the overall site is determined by the operating conditions of the reforming process, illustrating the need for an external hot utility above 900 °C. The reforming temperature is about 600 to 700 °C higher than the oil and gas temperatures in the processing plant, and the heat demand can thus be satisfied only by (i) burning a fraction of the H_2-rich synthesis gas, (ii) recovering heat from the combustion chamber of the H_2-fuelled gas turbines, (iii) combusting a fraction of the produced natural gas, or (iv) if possible, using the off-gases from the flashing operations in the purification steps.

The first option, i.e. burning the H_2-rich syngas in an additional furnace, is considered in this work, because the flow rate of the off-gases is never sufficient for producing enough heat in the cases with steam methane reforming, and burning natural gas would result in fuel CO_2-emissions, which should be avoided. The gas cooling and water-gas-shift operations are responsible for a large heat release below the pinch point, which is sufficient for covering the heating needs associated with the oil and gas processing plant, and should be treated by using cooling water or air. However, the large temperature gap between these processes (350–900 °C compared to 100–250 °C) indicates that power can be cogenerated in a steam Rankine cycle, valorising this excess thermal exergy and increasing the efficiency of the utility plant.

Additionally, the gas turbine configuration has an effect on the perspectives for integrating a waste heat recovery cycle, since the exhaust gases exiting this section of the system have a temperature generally higher than 300–400 °C. There are therefore different possibilities for integrating a cogeneration plant, which are denoted in the rest of the study *simple*, if only heat from the exhaust gases is recovered in the steam network, and *advanced*, if heat from several process sections can be utilised as well. A main issue to be addressed is the flame stability, which may be a critical point for pre-combustion CO_2-capture systems including SMR, TEA-based absorption and PSA, since the hydrogen purity can exceed 90-95 % at the gas turbine inlet.

10.4.2 Process optimisation

The impact of pre-combustion CO_2-capture technologies on the performance of the oil and gas platform and on its utility plant can be assessed by performing a multi-objective optimisation, analysing the trade-off between the exergy efficiency and the CO_2-capture rate. For simplicity, the possibility of purifying the H_2-rich fuel obtained after the CO_2-capture process, by integrating pressure swing adsorption (PSA), is not investigated. It is claimed in the literature that the additional power that is generated in the gas turbines is counterbalanced by the need for compressing the gas flow before the pressure swing adsorption process. In theory, the purity of the H_2 and CO_2 streams is dependent on the durations of the adsorption, recycling and purging steps.

In a first step (Figure 10.17), the impact of integrating a simple steam Rankine cycle, which utilises the heat from the gas turbine exhausts only, is investigated. The advantage of such configuration can be visualised by the horizontal shift of the Pareto frontiers, which illustrate that the gain in exergy efficiency is about 15 to 20 %-points, whether physical or chemical absorption is implemented.

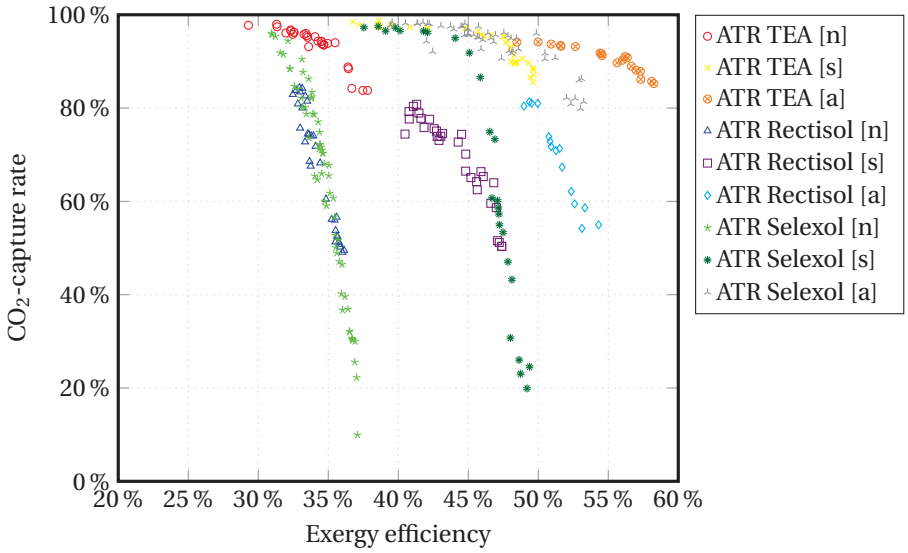

Figure 10.17: Pareto-optimal solutions for the site-scale integration of pre-combustion CO_2-capture processes on offshore platforms: trade-off between the CO_2-emissions and exergy efficiency, without steam cycle [n], with simple [s] and advanced [a] steam cycle.

In a second step, the possibility of recovering heat from the several sections of the system is analysed, and the corresponding gain in efficiency is about 5 %-points. In all cases, the comparison of the CO_2-capture technologies indicates that the Rectisol process presents the highest energy penalty, followed by the Selexol process and the TEA-based units, because of the demand for refrigeration in the solvent regeneration process. For a capture rate aiming at more than 80 %, this penalty is about 1 to 2 %-points between each process.

These advanced steam cycle configurations allow for valorising the waste heat present in the system at all temperature levels, under the condition that the production and condensation levels are selected appropriately. The amount of heat available that can be exploited in a Rankine cycle is directly correlated to the rejection temperature of the exhaust gases after the waste heat recovery unit and not to the selection of the solvent used for CO_2-capture (Figure 10.18 and Figure 10.19). Assuming that the gas turbine is designed to satisfy by itself the baseline power consumption of 16.5 MW, the addition of such advanced configurations could result in an additional power capacity of up to 15 MW, which may be of interest if power export is feasible.

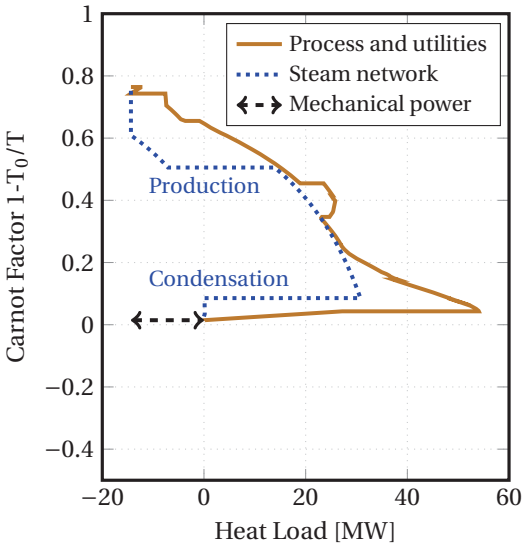

Figure 10.18: Integrated Composite Curves, on an exergy basis, of the steam Rankine cycle within the oil and gas platform with pre-combustion CO_2-capture based on TEA.

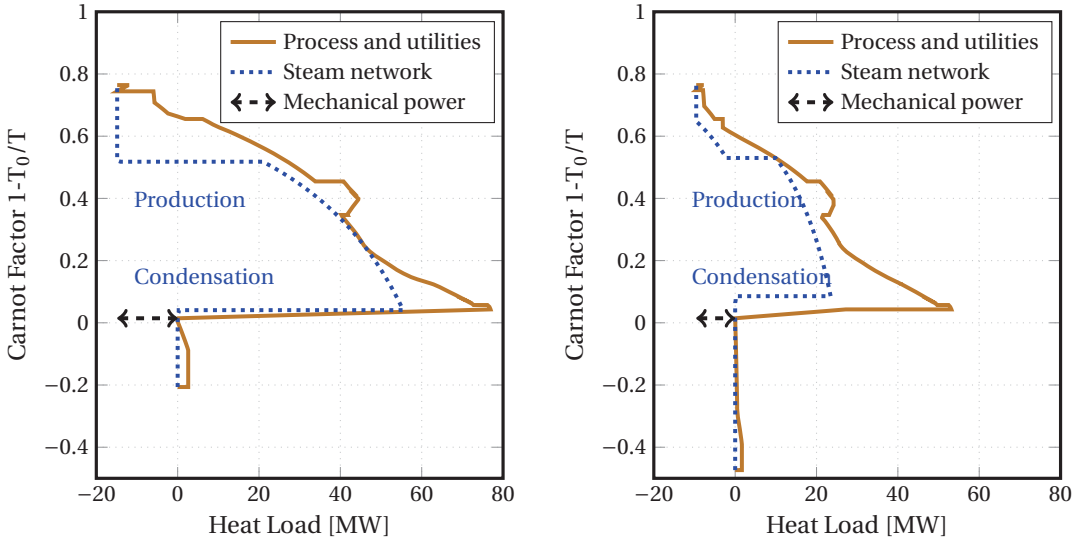

Figure 10.19: Integrated Composite Curves, on an exergy basis, of the steam Rankine cycle within the oil and gas platform with pre-combustion CO_2-capture based on Selexol (left) and Rectisol (right).

10.5 Post-combustion CO_2-capture

10.5.1 Process integration

The integration of a post-combustion CO_2-capture plant results in a significant energy penalty, which is directly correlated to the CO_2-capture rate. It includes two contributions: the electricity consumption increases because of the power requirements of the CO_2-capture unit (solvent pumping, blower and compressor) and of the cooling water plant (water lift). The thermal energy use is greater because of the heat demand of the solvent regeneration step in the chemical absorption process. In this regard, the implementation of a MEA-based unit for post-combustion CO_2-capture purposes is similar to the introduction of a TEA-based one for pre-combustion.

Flue gas cooling results in a lower temperature at the inlet of the absorber (Figure 10.20), which is thermodynamically and kinetically favourable for removing CO_2 with amine solvents and thus maximising the capture rate. It may be performed by air or water cooling, at the expense of an additional power consumption for driving the fans and seawater pumps (Figure 10.21). However, the preferred option is to implement a waste heat recovery cycle before further cooling, since it would allow for higher power generation and smaller fuel consumption.

Compared to the pre-combustion CO_2-capture path, the introduction of post-combustion CO_2-capture does not change significantly the overall energy profile of an oil and gas platform. The overall heating demand stays minor and is located at temperatures lower than 300 °C, with an additional requirement at the level of the desorption reboiler of the chemical absorption unit. The impact of these additional energy requirements is clearly visualised with the integrated composite curves of the overall offshore system (Figure 10.22). They also indicate that a pinch point is activated at about 120 °C, which illustrates that heat from the exhaust gases is required to satisfy the reboiler demand, limiting the net power output from the steam network.

The CO_2-recovery is directly related to the quality of the absorption process by MEA, which is mainly affected by the solvent loading and the operating temperature conditions. The low CO_2-concentration of the exhaust gases results in a higher MEA processing that what could be expected for modern gas turbines, where the air-to-fuel ratio is smaller than for the studied one.

The integration of a steam turbine with extraction at about 8 bar may be relevant (Figure 10.23), since steam is produced at pressures over 10 bar and the heat demand for the amine regeneration process is at about 110–120 °C. Such a design improves the integration of the post-combustion unit within the offshore system, and may result in greater power generation. However, it is not favoured in the further optimisations, as the thermodynamic benefits of such an option are outweighed by the additional investment costs, the greater system complexity and the reduced availability.

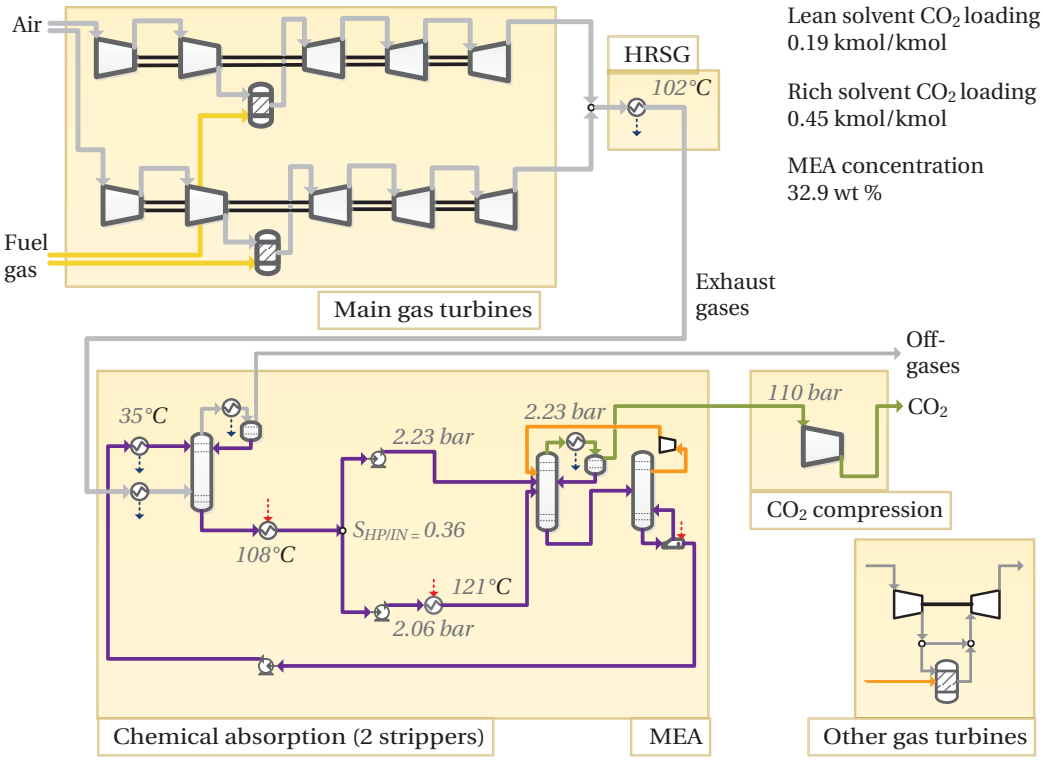

Figure 10.20: Example of configuration of post-combustion CO_2 capture with MEA.

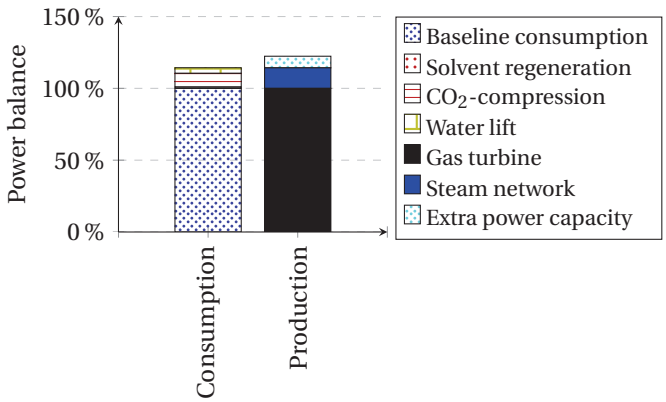

Figure 10.21: Power balance for an example of layout with MEA.

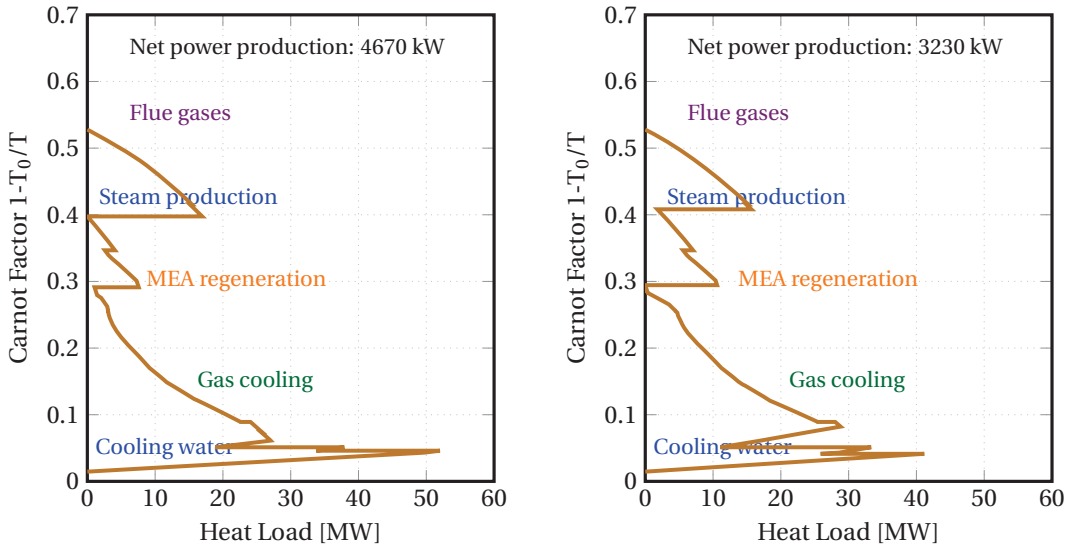

Figure 10.22: Balanced Grand Composite Curves, on an exergy basis, of the oil and gas platform system, including a steam Rankine and a post-combustion CO_2-capture unit, with low (left) and high (right) CO_2-capture rate.

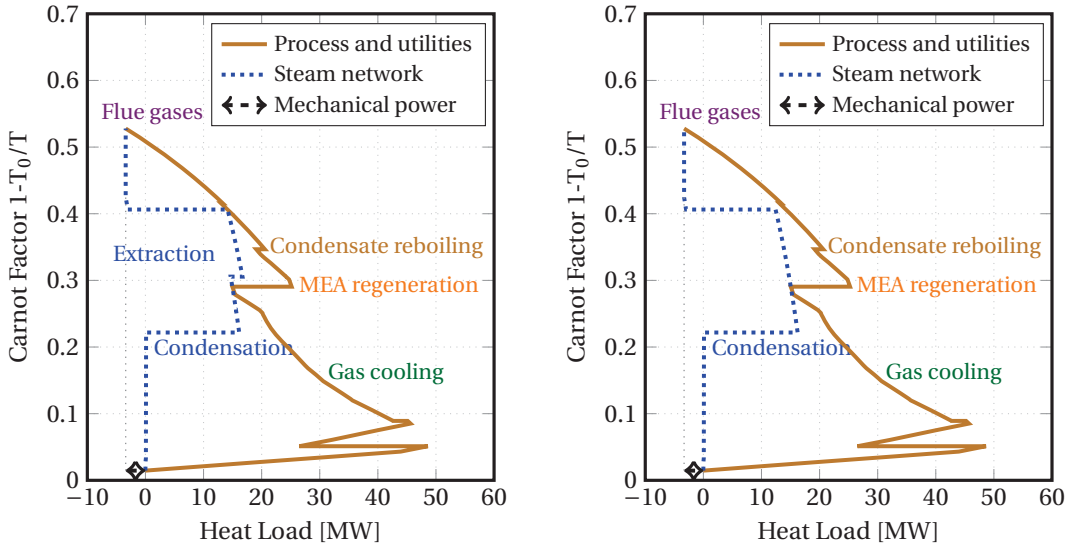

Figure 10.23: Integrated Composite Curves, on an exergy basis, of the steam Rankine cycle within the oil and gas platform system, with (left) and without (right) extraction.

10.5.2 Process optimisation

The installation of CO_2-capture plant together with a steam cycle presents by far the greatest potential for CO_2-reduction, but only reduces the exergy losses with the exhaust gases taking place at temperatures of 100 to 330 °C. There is a potential for recovering exergy at low-temperatures, which is, in the proposed configurations, dissipated with cooling water, but such option may be particularly challenging. Smaller quantities of heat are dissipated into the environment with cooling water for the process designs including CO_2-capture, as a fraction of the heat contained in the exhaust gases is used to regenerate monoethanolamine instead and dissipated into the environment.

The total CO_2-emissions of the platform can be reduced by up to 70 % (Figure 10.24), of which ≃ 10–20 %-points are related to the steam network, and ≃ 50–60 %-points are associated with the CO_2-capture unit. The remaining CO_2-emissions are caused by the flaring and secondary gas turbines on-site. The export of natural gas also increases, although the savings in fuel gas are not as significant as if only a steam cycle was integrated, because of the power demand of the CO_2-sequestration unit. This alternative may be interesting if the facility has a lifetime expected to be short, and the constraints related to the operation of the monoethanolamine system should be evaluated carefully.

The maximisation of the net power capacity and the minimisation of the CO_2-emissions are clearly conflicting objectives, since CO_2-capture is favoured with large flows of solvent and high regeneration temperature. Significant amounts of heat from the exhaust gases are required and cannot be used in the steam network for electricity generation purposes.

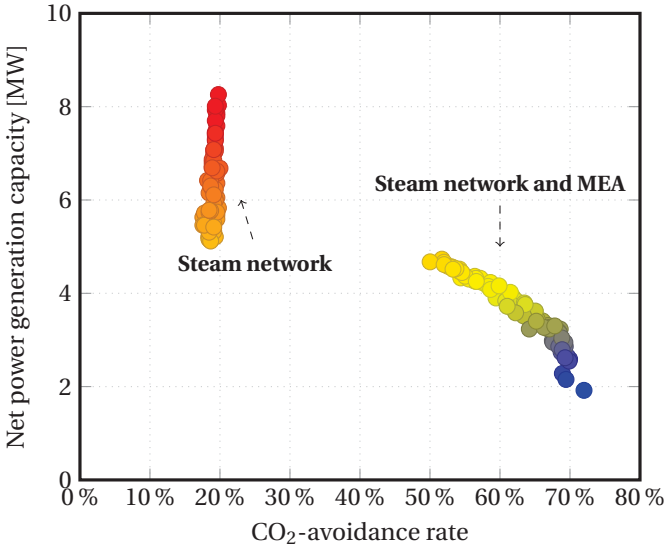

Figure 10.24: Pareto-optimal solutions for the site-scale integration of post-combustion CO_2-capture processes on offshore platforms: trade-off between the CO_2-emissions and net power capacity.

10.6 Electrification

The higher gas export results in larger cooling duty in the gas treatment section and greater power demand (Figure 10.25). However, platform electrification does not change significantly the temperature-enthalpy, or temperature-exergy profiles of an oil and gas platform (Figure 10.26). The exergy destruction and losses in the gas turbines are eliminated, but they are replaced with the ones related to the onshore plants (combined cycles or hydroelectric facilities), to the gas-fired heaters (if any), and to the transmission cables (power losses). The exact values of these irreversibilities are not calculated in this work, but they are expected to be smaller because of the greater efficiency of the onshore power plants and the smaller fuel gas consumption.

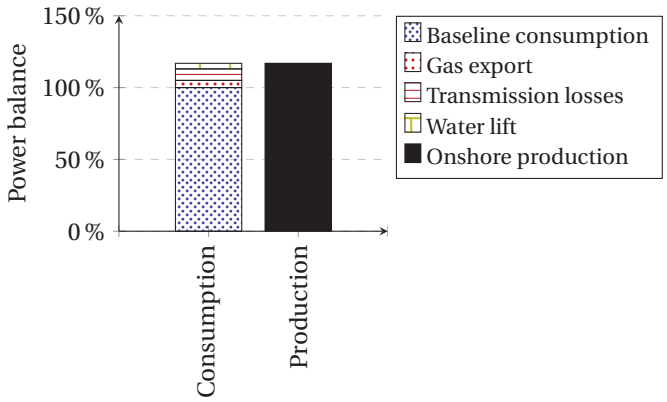

Figure 10.25: Power balance for an example of layout with electrification (Scenario 1).

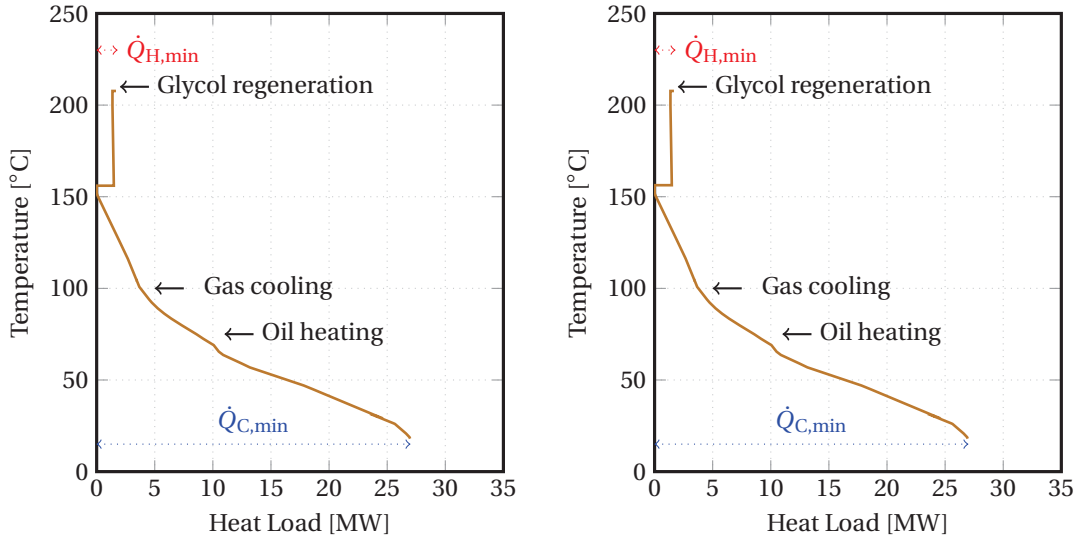

Figure 10.26: Grand Composite Curves of the oil and gas platform system with electrification (Scenarios 1, left and 2, right).

10.7 Economic assessment

10.7.1 Capital cost build-up

A precise economic analysis of a CO_2-capture plant on an offshore platform is difficult because of (i) the very few, if none, studies on this topic, as well as the absence of case studies, (ii) the lack of knowledge on the necessary space and associated cost for installing the equipment items, (iii) the uncertainties on the economic value of the natural gas consumed on-site, and (iv) the different approaches and cost correlations for evaluating the economics of a chemical or physical absorption plant.

A preliminary assessment of the economic build-up of the capital costs of such plants (Figure 10.27) suggests that pre-combustion CO_2-capture processes are more costly than post-combustion ones, which is consistent with the conclusions drawn in the literature. The first have a higher number of equipment items, including costly ones such as the Selexol tower and reforming reactors, for which the grassroot costs are estimated to exceed 1–5 M$.

The additional costs, related to the initial costs of the processes installed on the Draugen platform, vary between 10 to 40 %: the application of the economic correlations suggests that a configuration based on the Selexol process is the most costly, but the differences with the other system layouts are within the range of uncertainty suggested in the work of Turton et al. [79].

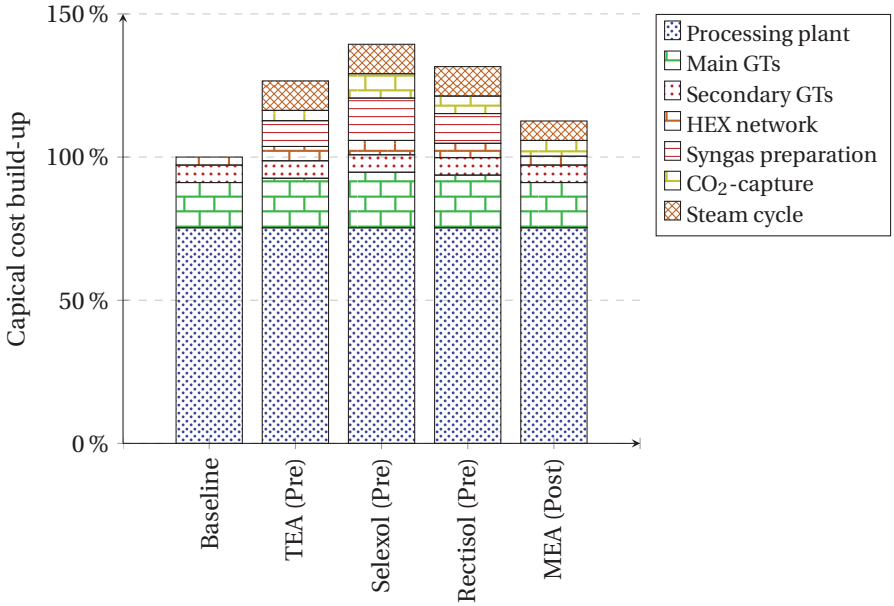

Figure 10.27: Capital cost build-up for offshore platforms with and without CO_2-capture, based on the process equipments of the Draugen platform.

10.7.2 Sensitivity analyses

Economic analyses of carbon capture units may be evaluated using either the electricity (COE) or the CO_2-avoidance (CAC) cost. The first one illustrates the cost of using the produced natural gas in the on-site gas turbines, while the second one reflects the costs of reducing the carbon dioxide emissions. They depend on factors such as the production cost of the fuel gas, the capital costs with the well construction and the CO_2-tax on the hydrocarbon production. The two post-combustion cases investigated previously are used as references for analysing the sensitivity of the electricity and CO_2-avoidance costs for process configurations with medium- and high CO_2-reduction potential. The baseline values assumed for conducting the sensitivity analyses are a natural gas price of 8.08 \$/GJ, a lifetime of 30 years, site-specific costs of M\$ 15, and a carbon tax of 65 $\$/t_{CO_2}$.

Natural gas price. This evolution is difficult to predict, as it is highly different between European and American countries. It is generally projected that this resource price will increase over years, as a result of the depletion of the natural gas resources and of the possible extraction of unconventional resources such as shale gas. The electricity and CO_2-avoidance costs clearly follow a linear dependence on the natural gas price (Figure 10.28). An oil and gas platform without CO_2-capture or waste heat recovery appears to be the most competitive option if no carbon tax is set. The introduction of a carbon tax, in this case of 65 $\$/t_{CO_2}$, decreases the profitability of this system, compared to the ones with CO_2-capture, which become more competitive. The first CCS process configuration appears to be competitive over a large range of natural gas prices, while the second one is only competitive for a resource price below 4 \$/GJ. The same trends can be visualised by analysing the variations of the CO_2-avoidance cost with the natural gas price, which increase more sharply in the second case.

CO_2-tax. Similarly, the taxation on CO_2 depends on the industrial sector and country of application: it is at the moment about \$ 65 per tonne of carbon dioxide in the Norwegian petroleum sector, and it will most likely rank as one of the highest CO_2-taxes in Europe. The foreseen values of the CO_2-taxes range between \$ 20 and \$ 40 in the near-future and between \$ 65 and \$ 75 in the long-term. As suggested by the first sensitivity analysis, the CO_2-tax also has a strong impact on the electricity and CO_2-avoidance costs (Figure 10.29). For a natural gas price of 8.08 \$/GJ, which is in the range of the production costs estimated by the oil companies operating petroleum fields in Norway, the break-even values are about 35 and 100 $\$/tCO_2$ for the first and second configurations, respectively. This large difference between the break-even values illustrates that the implementation of CO_2-capture processes may be feasible or economically profitable only over a certain range of CO_2-capture potentials.

Lifetime. The economic lifetime depends on the expectations on the oil and gas recovery rates, which are likely to change as the field is exploited (Figure 10.30). The current trend

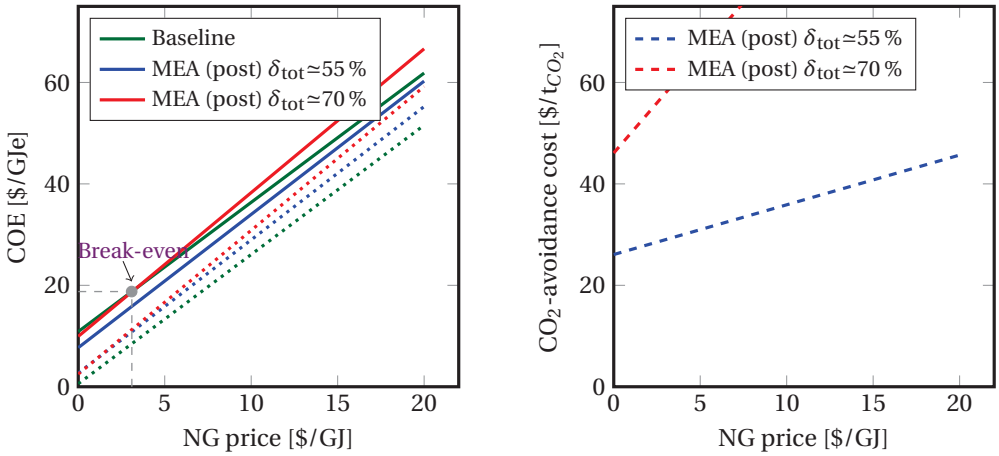

Figure 10.28: Sensitivity of the electricity production (COE) and avoidance (CAC) costs of an offshore platform with and without integration of post-combustion CO_2-capture to the natural gas price, with (solid) and without (dotted) CO_2-tax.

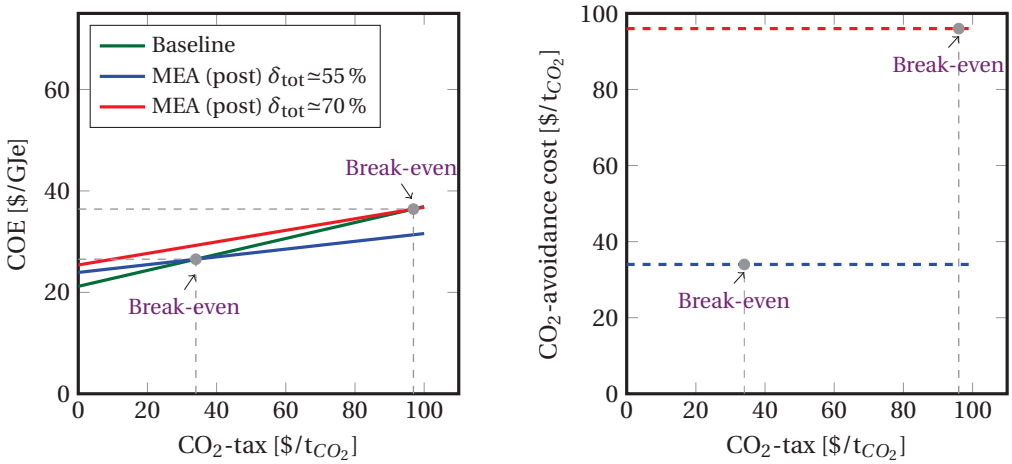

Figure 10.29: Sensitivity of the electricity production (COE) and avoidance (CAC) costs of an offshore platform with and without integration of post-combustion CO_2-capture to the carbon taxation.

in Norway is to extend the exploitation of the already operated fields, but the integration of CO_2-capture during the middle- and late-life phases may not be economically viable. As for power plants, the profitability of carbon capture processes is highest when the facility has high lifetime and availability factor. Integrating a CO_2-capture plant as a retrofit option may be economically challenging, as part of the oil and gas reserves are already depleted, which suggests that the electricity and avoidance costs are higher in these cases.

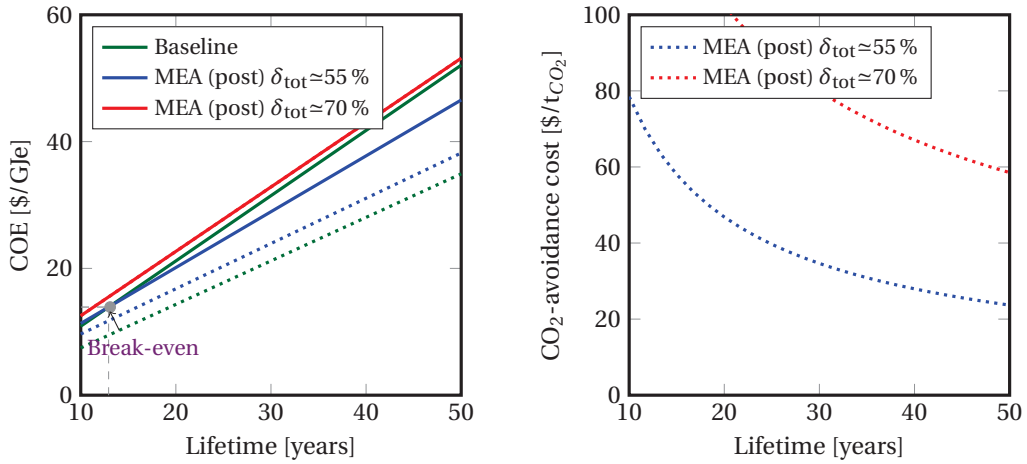

Figure 10.30: Sensitivity of the electricity production (COE) and avoidance (CAC) costs of an offshore platform with and without integration of CO_2-capture to the field lifetime.

CO_2-injection wells. These expenses are site-specific and the cost estimates vary widely from one study to another (Figure 10.31). They consist of the costs for building the injection wells, cementing the wells, installing corrosion resistant casing, drilling and constructing the pipelines, and have been estimated to about 15 M$ in the case of the Sleipner platform. The electricity and CO_2-avoidance costs of the process configurations with CCS are highly sensitive to the site-specific costs, and those sensitivity analyses suggest that an offshore platform with a high degree of CO_2-reduction may only be economically viable, in the future, with a further increase of the CO_2-tax, and unlikely for all petroleum fields.

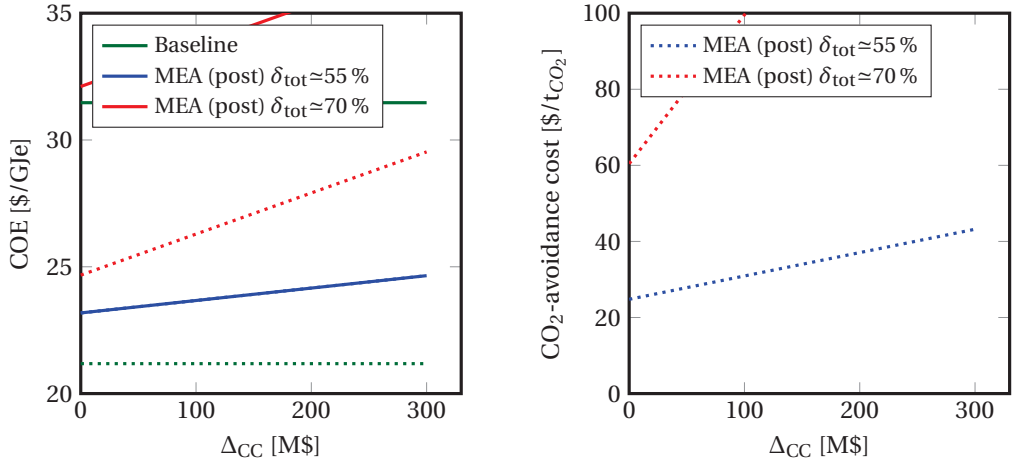

Figure 10.31: Sensitivity of the electricity production (COE) and avoidance (CAC) costs of an offshore platform with and without integration of CO_2-capture to the additional construction and capital costs.

10.7.3 Economic scenarios

There is a clear trade-off between the economic performance and the degree of CO_2-abatement of oil and gas platforms, and the process configurations that are optimal will obviously differ depending on the field and the future economic scenarios (Table 10.6).

Table 10.6: Tested economic scenarios on the post-combustion CO_2-capture unit.

Scenario	Base	Low	High
Natural gas price [$/GJ]	8.08	16.16	4.04
CO_2-tax [$/t$CO_2$]	65.6	0.00	131.2
Expected lifetime [years]	30	20	40
Capital costs (CO_2-wells) [M$]	≥ 15 and ≤ 30	≥ 30	≤ 15

High CO_2-capture rates are favoured with high CO_2-tax, small well capital costs, and low gas costs, because the large economic penalties on the CO_2-emissions compensate the additional investment costs of a CO_2-capture unit and the possible benefits with a greater gas export. Medium CO_2-capture rates, i.e. with a steam cycle only or with a small capture unit capacity, are preferable with high fuel gas production costs, since the integration of a waste heat recovery cycle allows for a smaller gas consumption on-site (Figure 10.32).

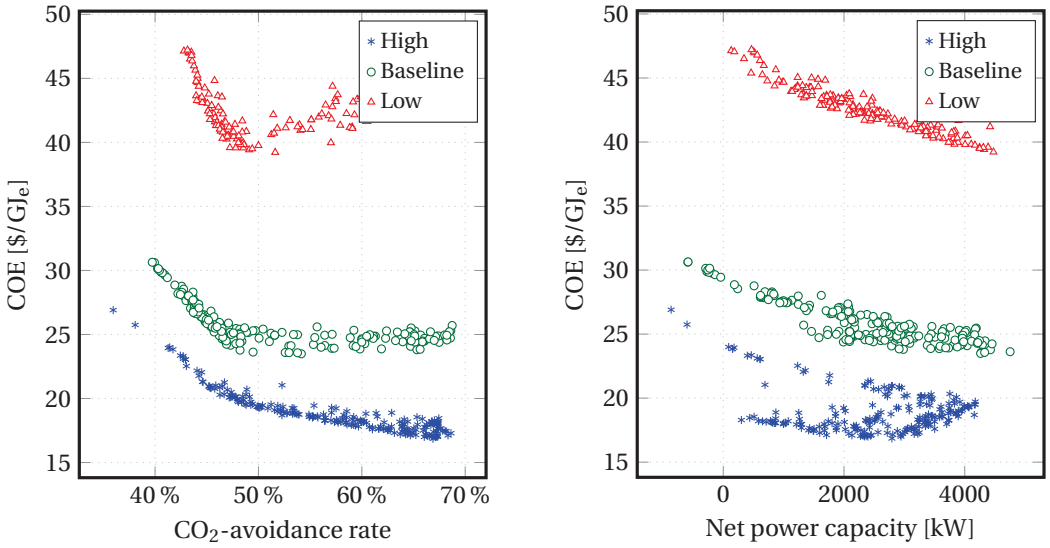

Figure 10.32: Pareto-optimal solutions for the site-scale integration of CO_2-capture with steam networks: trade-off between the electricity cost (with CO_2-tax), CO_2-emissions and net power capacity.

10.8 Environmental impact

There is likewise a lack of knowledge on the environmental impact of CO_2-capture plants on offshore platforms. The integration of such processes obviously results in a reduction of the local CO_2-emissions, but the installation of additional equipment items and the discharge of amines to the environment may have other harmful impacts.

In the case of electrification (Figure 10.33), the local fuel gas CO_2-emissions are completely eliminated in Scenario 2 and decreased by about 90–95 % in Scenario 1. The remaining emissions consist of the release of methane, carbon dioxide and other greenhouse gases by flaring and venting. The global emissions are reduced by up to 45 % in Scenario 2 and by more than 50 % in Scenario 1, if the supplied power comes from gas-fired combined cycle power plants with a thermal efficiency of 55 %. This bigger decrease in Scenario 1 can be explained by the lower transmission and conversion losses. There are, a priori, no CO_2-emissions associated with fuel consumption if hydraulic power is used instead of natural gas.

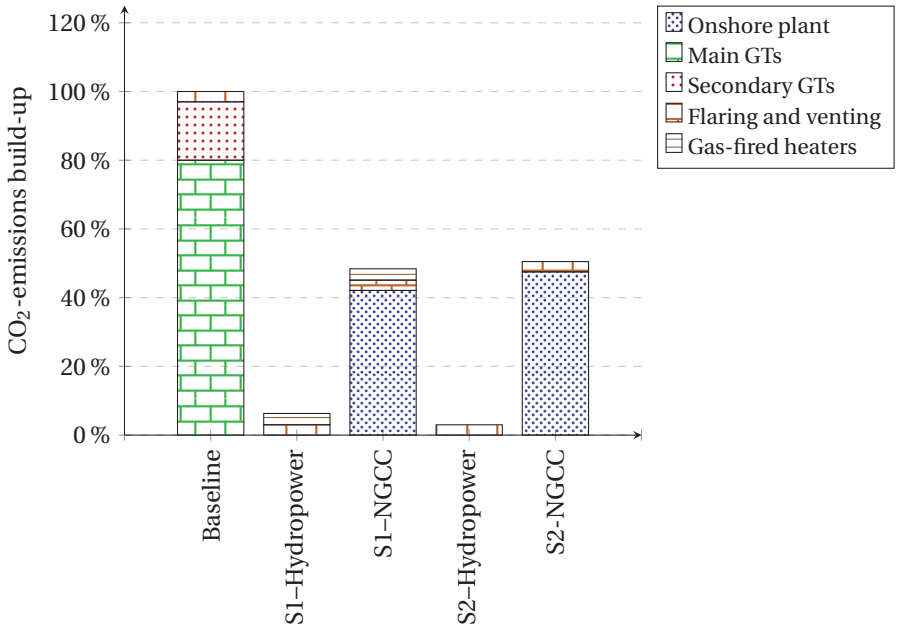

Figure 10.33: CO_2-emissions build-up for offshore platforms with and without electrification.

The environmental performance of the whole process chain, i.e. from the resource extraction to the decommissioning of the offshore platform, can be evaluated based on a life cycle assessment, considering several impacts (e.g. GWP) and various analyses methods (e.g. CML 2001 [142]). An aspect that can be considered, but is not treated in this work, is whether the carbon dioxide can be stored safely in the reservoir: this may be problematic because of plug corrosion aspects and possible geological movements.

All configurations combining a steam network and a CO_2-capture unit have, overall, a benefi-

cial effect with respect to the global warming potential impacts (Figure 10.34), because of the reductions in greenhouse gas emissions over the facility lifetime. The major contribution to the remaining GWP impact corresponds to the fossil CO_2-emissions that are not sequestrated. The global warming potential effects associated with the construction and manufacturing of the process components are negligible in comparison.

Similarly, all configurations including electrification have a beneficial effect with regards the global warming potential impacts, because of the lower CO_2-emissions over the lifetime of the offshore facility. The main contributions to the remaining impacts correspond to (i) the fuel emissions associated with the combustion of natural gas in power plants, (ii) the process components, including the voltage cables, and (iii) the flaring and venting discharges. The contributions from the voltage cables are much smaller than the contributions of the other process components. However, these results build on the assumption that there is enough power on the electrical grid to meet the power demands offshore. The picture would likely be different if additional power plants have to be built as it would require additional resources and materials.

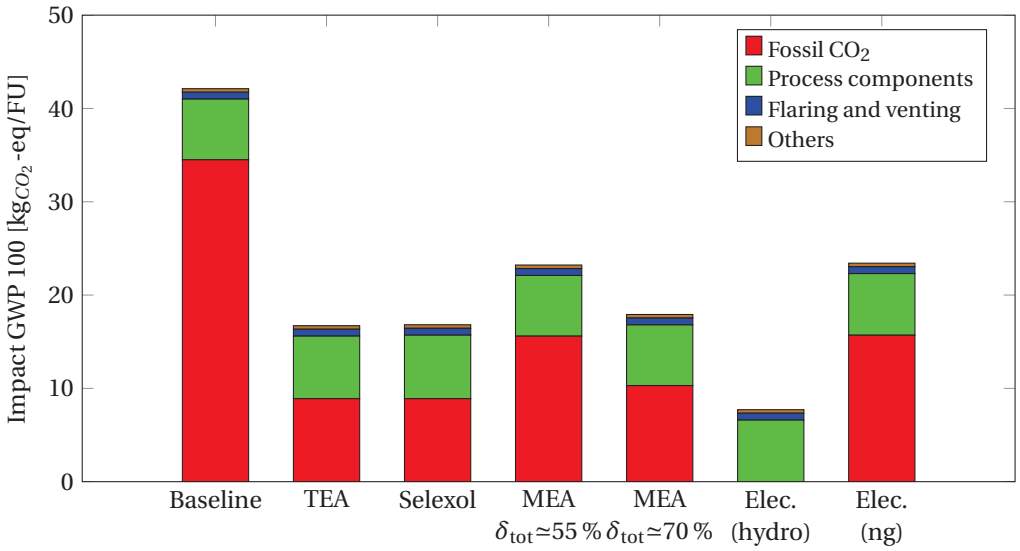

Figure 10.34: Comparison of the scenarios with and without CO_2-capture: IPCC 07 (impact method) – GWP 100 (impact category)

The same trend (Figure 10.35) can be observed if the Impact 2002+ method [273] is applied instead of the IPCC 07 [274]. The Impact 2002+ method applies a combined midpoint and damage-oriented approach: it builds on the results of the life cycle inventory, and the ones with similar impact pathways are allocated to impact categories at midpoint level (e.g. global warming or ozone layer depletion). The midpoint global warming is allocated to the climate change damage category, based on the IPCC source, which explains why the results obtained by both methods are similar.

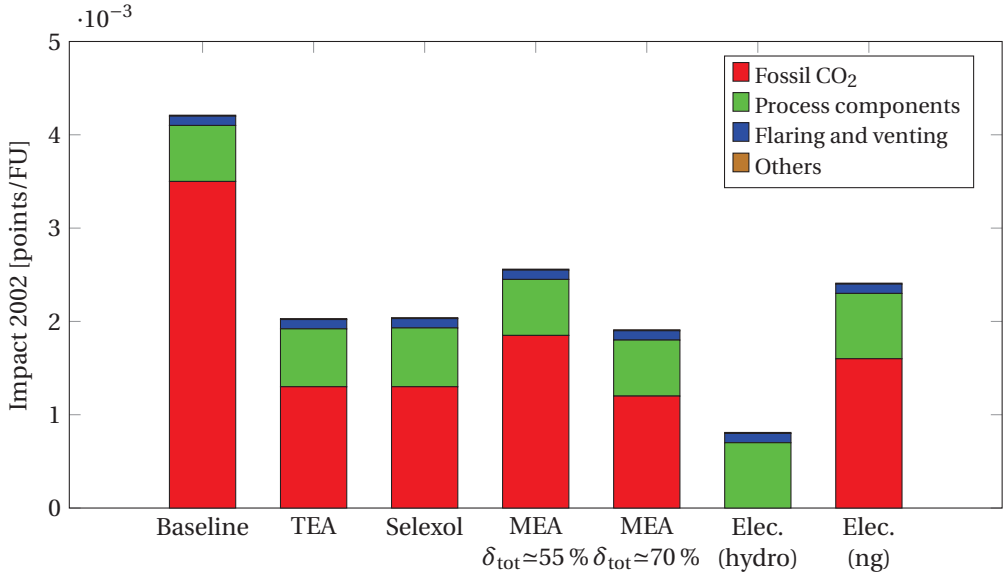

Figure 10.35: Comparison of the scenarios with and without CO_2-capture: Impact 2002+ – Climate change.

The benefits of CO_2-capture processes combined with steam Rankine cycles can also be drawn with regards to the acidification and eutrophication potentials, as the on-site NO_x emissions are decreased by about 25 %. Although the chemical absorption process induces an energy penalty, the overall natural gas consumption for the platforms on which carbon capture is implemented is decreased, because this results in a smaller depletion of the gas resources. Similarly, the impact on human health is reduced because of the smaller emissions of carbon dioxide, nitrous oxides and pollutants, and this is illustrated with both the Ecoindicator 99 [275] and Impact 2002+ methods (Figure 10.36 and Figure 10.37).

For the climate change impact category, the main contributions are caused by the emissions of fossil CO_2 from the gas turbines ($\simeq 85\,\%$). The emissions associated with the manufacturing and installation phases of the system components play the major role ($\simeq 85\,\%$) for the ecosystem impact, and the greatest impact on human health derives from the NO_x-emissions ($\simeq 60\,\%$). The same conclusions can be drawn when applying the Ecoindicator 99 approach. One of the main differences is that the climate change impacts are considered within the human health category, and the impact decrease is more marked as it is affected by the reductions of both carbon dioxide and nitrous oxide emissions.

The comparison of the several system set-ups clearly suggests that the integration of waste heat recovery cycles together with carbon sequestration is advantageous both at local and global levels. The expected environmental benefits are most probably slightly smaller, as the material required to build the additional space on-site has not been accounted for. Similarly, the environmental benefits of electrifying have been demonstrated, although there is a clear difference between the cases with power generation from gas-fired or hydraulic plants.

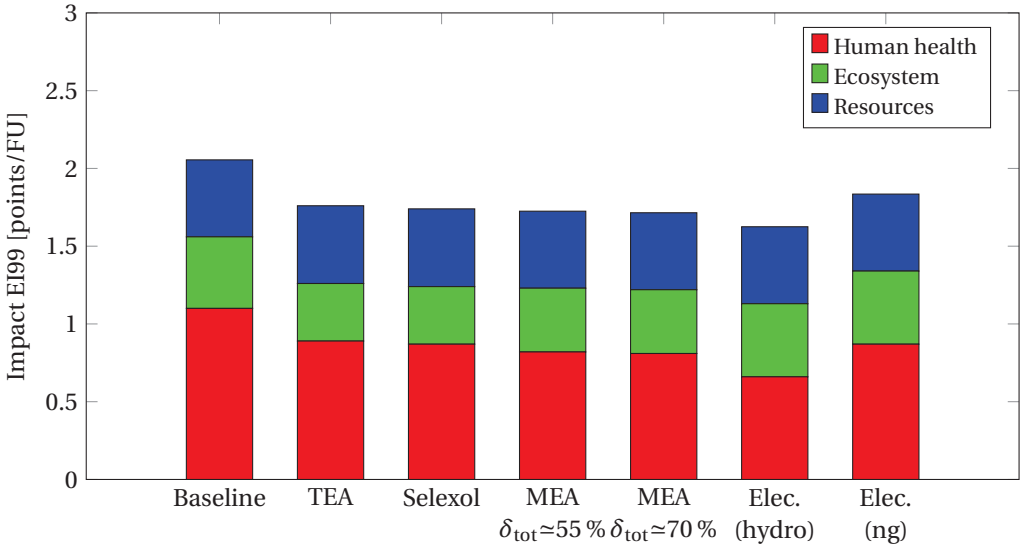

Figure 10.36: Comparison of the scenarios with and without CO_2-capture: EI99 (hierarchical approach).

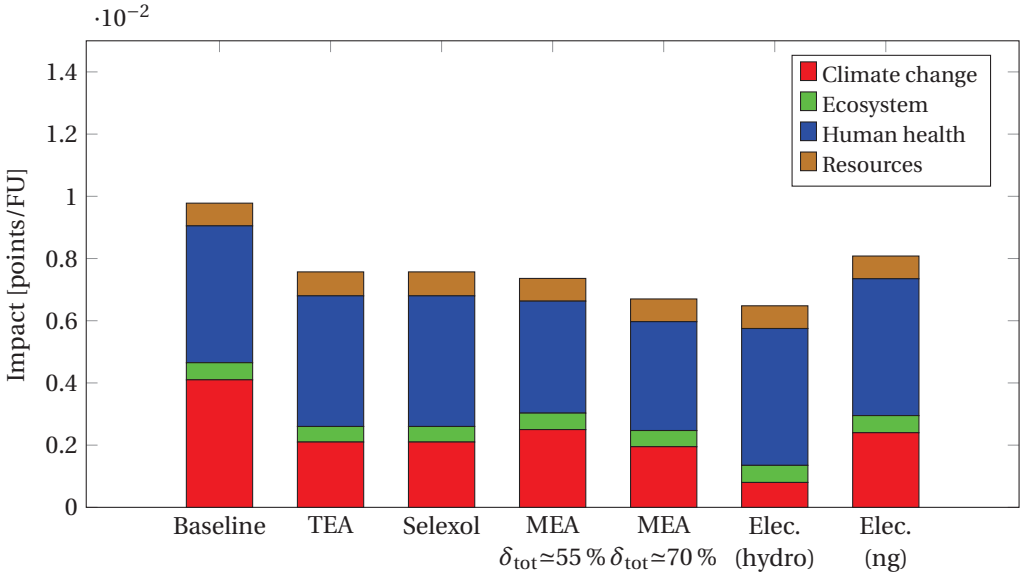

Figure 10.37: Comparison of the scenarios with and without CO_2-capture: Impact 2002+.

10.9 Conclusion

Although CO_2-separation with physical and chemical absorption processes is a well-known process, its integration offshore has been limited to a few case studies, where the produced natural gas has a high CO_2-content and should be treated in consequence. The implementation of CO_2-capture to reduce the fuel emissions associated with the power generation processes has not been performed up-to-now, but the present study suggests that it is possible in theory, at the expense of an efficiency penalty of 5 to 10 %-points depending on the choice of the physical or chemical solvent.

However, the integration of CO_2-capture on oil and gas platforms faces economic and practical challenges, since technologies such as reforming and H_2-fuelled combustion have not been implemented offshore at present. The introduction of post-combustion capture with MEA may be the most practical option for facilities that are already in operation, while the use of pre-combustion capture with Selexol, Rectisol or TEA may be interesting only for new plants. The smaller volume flow rates that are processed in the second case may make such systems interesting in the future, since space and weight limitations on offshore platforms have discouraged the integration of non-conservative technologies.

The economic profitability is mainly impacted by the carbon dioxide tax (positive feedback) and the natural gas sales price (negative feedback), and the assessment of possible economic scenarios has shown that the integration of CO_2-capture is not competitive at present. The environmental analyses have illustrated the benefits of integrating conjointly a waste heat recovery cycle with a CO_2-capture plant, as it results in a reduction of the CO_2 and NO_x emissions.

11 System synthesis

This last chapter deals with the synthesis of petroleum processing systems for offshore applications, and it is believed that the system performance can benefit from process integration measures. The advantages of using mass- and energy-integration models, together with optimisation routines and uncertainty analyses, are therefore assessed by using several case studies.

11.1 Introduction

Process Synthesis is a research area for which interest has grown over the last decades, but very few works deal with the systematic synthesis of an entire oil and gas platform, assessing the trade-off between the separation, thermodynamic and economic performances.

The set-up of an offshore processing plant is determined by the type of petroleum, the export constraints, and the limits on the concentrations of impurities. In practice, the design procedure builds on the technical expertise of process engineers and is subject to uncertainties on, among others, the field economic viability.

The aim of this work is to evaluate the suitability of a combined mass- and energy-integration approach to the design of such facilities, based on multi-objective optimisation routines and uncertainty assessments. The overall approach consists of the following steps:

(1) different process synthesis strategies are compared, focusing on the design of an isolated or integrated separation system;

(2) the compromises between the separation, thermodynamic and economic performance are assessed;

(3) the sensitivity of the optimal process set-ups to the uncertainties related to the petroleum composition and economic scenarios is analysed;

(4) the robustness of these configurations is tested.

11.2 Problem formulation

11.2.1 Background and specifications

The conventional oil and gas processing consists of lifting the well-streams on the facility through production manifolds, separating oil, gas and water, compressing gas and pumping oil, while discharging or injecting the produced water. The presence of sulphur, carbon dioxide and other impurities leads to the possible addition of cleaning steps if the export requirements are stringent. The composition of the final products depends obviously on the feed composition, which is likely to vary over time, and on the operating conditions of the processing plant.

The separation between the light-, medium- and heavy hydrocarbons is limited by the vapour-liquid-liquid equilibrium between the oil, gas and water phases. Low pressures and high temperatures may result in a significant loss of medium- and heavy hydrocarbons from the oil to the gas stream, and to large power consumption for re-compressing the gas. High operating pressures and low temperatures may result in non-negligible residues of light hydrocarbons in the oil stream, which conflicts with the target of low vapour pressures.

The current state-of-the-art research clearly shows that a single separation stage is not satisfying from an operational and economic point of view. Multiple stages, typically between 2 and 4, should be integrated to reach the desired targets in terms of purity, pressure and temperature conditions of the final outputs. However, separation work is also performed in the gas treatment process.

Typical numbers for the external heating and cooling demands cannot be given for an oil and gas processing plant, as these are highly dependent on the feed composition, temperature, and viscosity. Heavy petroleum feeds generally have greater demand for heating, at the opposite of volatile ones.

The exact specifications for exporting oil and gas vary from platform to platform (Table 11.1), depending on whether gas and oil are exported via pipelines or shuttle tankers, the requirements of the pipeline network, the connections to the onshore facilities, etc.

Table 11.1: Typical export specifications for Gulf of Mexico and North Sea offshore platforms.

	GoM Shelf	GoM Deepwater	North Sea
Export gas water content [ppm]	147	42–84	42–84
Export gas pressure [bar]	69–83	103–207	134–187
Export oil water content [% v/v]	1	1	2
Export oil RVP [bar]	0.76	0.76	10.3
Export oil pressure [bar]	69–103	103–207	103–193

11.2.2 Problem definition

The problem can be schematically represented as a black-box, with the feed composition and flow properties as inputs, and the process schemes, operating conditions and external energy demands as outputs. The goals are to satisfy the system outlet specifications, but several challenges need to be addressed: (i) the high uncertainties and variability of the feed properties and economic costs, (ii) the differences across various fields, (iii) the calculation of the minimum energy requirements, (iv) the identification of the fuel alternatives to satisfy these needs, and (v) the resulting high number of possible system configurations.

These issues lead to in a non-trivial problem: it is not possible to suggest a standard configuration of an oil and gas platform, as such a set-up is likely to be technically or economically unacceptable for other locations and boundary conditions. The aim of this research is therefore (i) to investigate the trade-off between the process, thermodynamic, economic and environmental performances for all the possible platform layouts, for a given scenario (*deterministic* solution), and (ii) to evaluate how the uncertainties on the feed properties and resource prices affect the choice of the system layout (solution *under uncertainties*).

11.2.3 Superstructure definition

Data collection

The data required for defining the problem superstructure builds on the open literature. The configurations depicted in previous researches are decomposed into sequences of process steps and transformations, for which different technical and technological alternatives are identified. It is assumed that all the inflowing streams from the wells are mixed at the outlet of the production manifold and treated in a single separation train. Three types of feed compositions (Table 11.2) and two temperature levels (15 and 75 °C) and an initial reservoir pressure of 150 bar are considered, to cover a wide range of feed conditions.

Isolated separation plant

The typical operational scheme of an oil and gas separation system consists of a network of two- or three-phase separators in cascades, where the liquid outlet of each module is connected to the inlet of the next one, and the gas outlet is connected to a mixing point with the gas streams from the downstream modules. The separation modules operate at different temperatures and pressures. The pressure of the liquid streams is decreased from the first to the last stage, implying that expansion is performed in-between by using throttling valves. The option of implementing multiphase expanders is disregarded in this work, because such a technology is currently not mature, and the outlet temperature would be lower, having a negative impact on the gas and liquid separation in the subsequent stage. The pressure of the recovered gas is increased from the last to the first separation module, creating a need for compression, and possibly for cooling.

Table 11.2: Simulated compositions (molar basis) for the flowsheet synthesis problem.

	Composition 1 Volatile	Composition 2 Near-Critical	Composition 3 Black
CO_2	0.009	0.012	0.000
CH_4	0.558	0.660	0.329
C_2H_6	0.072	0.075	0.039
C_3H_8	0.039	0.040	0.010
n-C_4H_{10}	0.020	0.020	0.005
i-C_4H_{10}	0.009	0.008	0.007
n-C_5H_{12}	0.011	0.011	0.002
i-C_5H_{12}	0.007	0.009	0.004
H_2O	0.050	0.050	0.050
N_2	0.002	0.002	0.003
Hypotheticals	0.223	0.110	0.551

Separation cascading in 1 to 3 stages is considered (Figure 11.1), with the possibility of integrating heaters between each module. Recycling of produced water from a separation stage to a previous one is not considered for simplification, since it has a negligible impact on the separation performance of each stage.

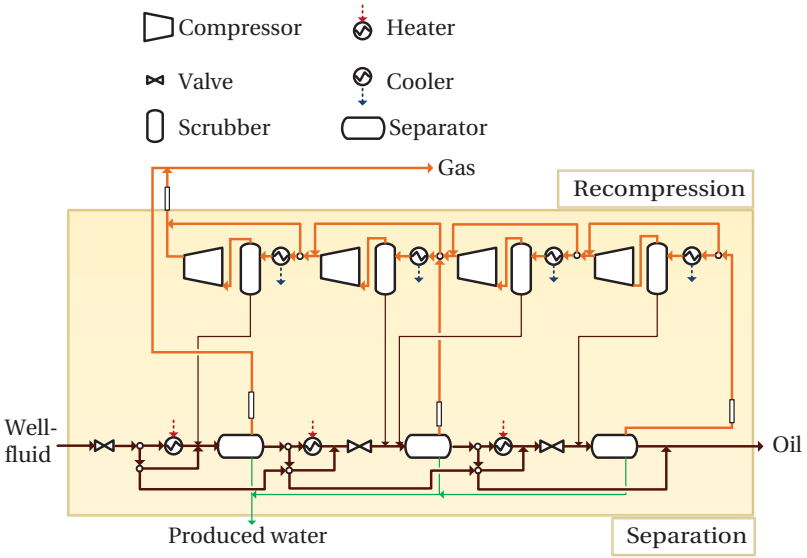

Figure 11.1: Possible layouts of the separation-recompression superstructure.

The decision variables correspond to the operating conditions of all the possible layouts (Table 11.3). They include the operating conditions of each separation and recompression level, which are continuous variables, and the number of stages, which are discrete.

Table 11.3: Decision variables of the separation-recompression system.

Operating conditions	Variable	Unit				
Separation			1-stage	2-stage	3-stage	
Number of stages	N_{stages}^{sep}	-	1	2	3	
Stage pressure 1	p_1^{sep}	bar	1.75	[1.75–70]	[1.75–70]	
Stage pressure 2	p_2^{sep}	bar	-	1.75	[1.75–70]	
Stage pressure 3	p_3^{sep}	bar	-	-	1.75	
Stage temperature	$T_{1,2,3}^{sep}$	°C	[15–95]	[15–95]	[15–95]	
Recompression			1-stage	2-stage	3-stage	4-stage
Number of stages	N_{stages}^{rec}	-	1	2	3	4
Stage pressure 1	p_1^{rec}	bar	p_1^{sep}	[1.75–p_1^{sep}]	[1.75–p_1^{sep}]	[1.75–p_1^{sep}]
Stage pressure 2	p_2^{rec}	bar	-	p_1^{sep}	[p_1^{rec}–p_1^{sep}]	[p_1^{rec}–p_1^{sep}]
Stage pressure 3	p_3^{rec}	bar	-	-	p_1^{sep}	[p_2^{rec}–p_1^{sep}]
Stage pressure 4	p_4^{rec}	bar	-	-	-	p_1^{sep}
Stage temperature	$T_{1,2,3,4}^{sep}$	°C	[15–45]	[15–45]	[15–45]	[15–45]

Integrated processing plant

The separation design model is completed with the addition of the gas and condensate treatment models, as these processes also include two- and three-phase separators, and they can therefore impact the separation efficiency of the overall plant. The gas treatment process includes two to three stages, with possibly a glycol dehydration module at the second one. This network of separators is operated at different pressures and temperatures, and the final stage is generally operated at the pressure required for gas export or injection.

Compression and separation cascading in 1 to 3 stages is considered, with the possibility of introducing coolers at each stage. Recycling of condensate from a compression stage to a previous one is not considered for simplification, and the produced condensate is either recycled directly at the 2nd separation stage or processed through the condensate stabilisation process (Figure 11.2). Two additional synthesis constraints are added based on rules of thumbs derived from the comparison of several oil and gas facilities, and from the works of Manning and Thompson [15] and Bothamley [11]. First, the activation of the condensate treatment process can only be performed if the pressure at which the condensate is recovered is in the range of 20 to 30 bar [220]. Secondly, the integration of a gas treatment process with 2 compression stages is feasible only if the inlet gas pressure is above 20 bar, to prevent excessive compression ratios and significant cooling and compression demands.

The condensate stabilisation process includes at least a stabilisation column, to which the condensate from the gas treatment scrubbers is sent. It operates at a nearly-constant pressure level, but the temperatures thorough this sub-system can be increased or decreased to enhance the separation between the light- and medium-weight hydrocarbons. The recovered waste gas from the stabilisation column may be valuable if further dehydrated, or may be used as fuel for providing high-temperature heat.

The recovered condensate may be valuable if further cooled and mixed with the oil recovered in the separation process. The quality of these two depleted streams is thus important and depends strongly on the location at which they are withdrawn. For example, if the gas recovered from the stabilisation column still contains significant amounts of non-light hydrocarbons that are valuable, a condensate dehydrator and a three-phase separator may be added to recover the medium-weight hydrocarbons in liquid form.

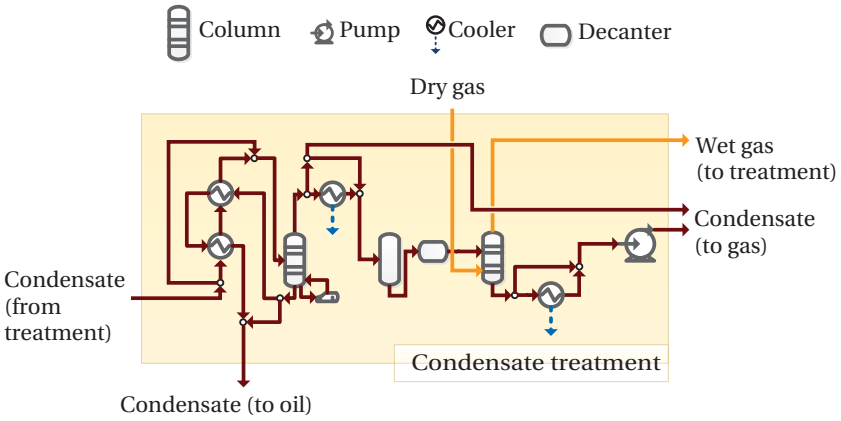

Figure 11.2: Generalised condensate treatment superstructure.

Similarly, the decision variables associated with the gas treatment and condensate stabilisation processes correspond to their operating conditions (Table 11.4, as well as the number of stages and the possible introduction of condensate stabilisation and glycol dehydration modules.

Table 11.4: Decision variables of the gas treatment and condensate stabilisation system.

Operating conditions	Variable	Unit			
Treatment			1-stage	2-stage	3-stage
Number of stages	$N^{\text{tre}}_{\text{stages}}$	-	1	2	3
Stage pressure 1	p^{tre}_{1}	bar	180	$[p^{\text{sep}}_{1}$–180]	$[p^{\text{sep}}_{1}$–180]
Stage pressure 2	p^{tre}_{2}	bar	-	180	$[p^{\text{tre}}_{1}$–180]
Stage pressure 3	p^{tre}_{3}	bar	-	-	180
Stage temperature	$T^{\text{tre}}_{1,2,3}$	°C	[15–50]	[15–50]	[15–50]
Stabilisation activation	y^{sta1}	-	{0;1}	{0;1}	{0;1}
Stabilisation					
Stabilisation pressure	p^{sta}	bar	[20–30]	[20–30]	[20–30]
Stabilisation temperature (feed)	$T^{\text{sta}}_{\text{feed}}$	°C	[75–150]	[75–150]	[75–150]
Stabilisation temperature (reboiler)	$T^{\text{sta}}_{\text{reb}}$	°C	[150–225]	[150–225]	[150–225]
Dehydration activation	y^{sta2}	-	{0;1}		
Dehydration					
Condensate temperature (gas)	$T^{\text{sta}}_{\text{cnd}}$	°C	[40–100]	[40–100]	[40–100]
Gas-to-condensate ratio (dehydration)	x_{gtc}	kg/kg			

11.2.4 Performance indicators

Isolated separation system

The proposed separation plant configurations are compared using process, thermodynamic and economic performance indicators. The process performance is assessed by the recovery indicators of the light r_{lig} and heavy r_{hea} hydrocarbons in the gas and oil streams, as well as by the separation efficiency ε^{sep}, and are defined as:

$$r_{\text{lig}} = \frac{\sum_{n=1}^{3} \dot{m}_{C_nH_{2n+2},\text{gas}}}{\sum_{n=1}^{3} \dot{m}_{C_nH_{2n+2},\text{feed}}} \tag{11.1}$$

$$r_{\text{hea}} = \frac{\sum_{n=4}^{\infty} \dot{m}_{C_nH_{2n+2},\text{oil}}}{\sum_{n=4}^{\infty} \dot{m}_{C_nH_{2n+2},\text{feed}}} \tag{11.2}$$

$$\varepsilon^{\text{sep}} = r_{\text{lig}} \cdot r_{\text{hea}} \tag{11.3}$$

The thermodynamic performance is assessed by calculating the specific energy use SEU and exergy consumption SEC associated with the power and heat consumptions. The specific energy use is calculated to reflect that heat is required besides electrical and mechanical power to enhance the separation performance between oil and gas: the heating demand may be significant for low-temperature feeds, as it was shown with the study conducted by de Oliveira Jr. and Van Hombeeck [59] and the previous chapters.

The exergy concept is preferred for the optimisation calculations to account for the differences between electrical and thermal energy. Optimising with regards to the energy use or exergy consumption does not affect the results when comparing set-ups without any heat exchanger, but favours the use of heaters over large pressure drops between separation stages.

The economic performance is evaluated by calculating the specific separation cost, which is defined to include the investment $\dot{C}^{\text{sep}}_{\text{gr,dc}}$, maintenance $\dot{C}^{\text{sep}}_{\text{mn}}$, utility $\dot{C}^{\text{sep}}_{\text{ut}}$, taxes $\dot{C}^{\text{sep}}_{\text{tx}}$ and waste $C^{\text{sep}}_{\text{w}}$ costs. These variables reflect all the costs associated with the oil and gas processing, from the equipment construction to the maintenance, the site-specific taxes and the hydrocarbon losses to the environment.

$$\dot{C}^{\text{sep}} = \dot{C}^{\text{sep}}_{\text{gr,dc}} + \dot{C}^{\text{sep}}_{\text{mn}} + \dot{C}^{\text{sep}}_{\text{ut}} + \dot{C}^{\text{sep}}_{\text{tx}} + \dot{C}^{\text{sep}}_{\text{w}} \tag{11.4}$$

$$\dot{C}^{\text{sep}}_{\text{gr,dc}} = \frac{(1+i_r)^n - 1}{i_r(1+i_r)^n} \cdot \dot{C}^{\text{sep}}_{\text{gr}} \tag{11.5}$$

$$\dot{C}^{\text{sep}}_{\text{mn}} = 0.05 \cdot \dot{C}^{\text{sep}}_{\text{gr}} \tag{11.6}$$

$$\dot{C}^{\text{sep}}_{\text{ut}} = \left(\frac{\dot{W}}{e_{\text{fg}} \dot{m}_{\text{fg,base}}} + \frac{\dot{Q}_{\text{fn}}}{e_{\text{fg,fn}} \dot{m}_{\text{fg,fn}}} \right) \cdot C_{\text{fg}} \tag{11.7}$$

$$\dot{C}^{\text{sep}}_{\text{tx}} = y_{\text{CO}_2/\text{fg}} \cdot \dot{m}_{\text{fg}} \cdot C_{\text{tx}} \tag{11.8}$$

$$\dot{C}^{\text{sep}}_{\text{w}} = \dot{m}_{\text{pw,lig}} \cdot C_{\text{oil}} + \dot{m}_{\text{pw,lig}} \cdot C_{\text{gas}} \tag{11.9}$$

where:

i_r and n refer to the interest rate and years of operation;

$y_{CO_2/fg}$ to the CO_2-emission factor for the fuel gas and C_{TX} to the CO_2-tax in Norway;

$\dot{W}$ and $\dot{Q}_{FN}$ the power demand and additional furnace consumption;

C_{fg}, C_{oil} and C_{gas} to the sale prices of fuel gas, oil and gas, and the fuel gas price is taken equal to the gas price for simplification.

The maintenance costs are assumed to represent 5 % of the grassroot costs, which are on themselves estimated for a lifetime of 30 years, an availability factor of 95 % and an interest rate of 6 %. The fuel gas price is initially fixed to 8.8 $/GJ, based on the cost estimates of natural gas in Norway. The carbon dioxide taxes are also assumed considering a Norwegian economic environment, with a value of about 65 $ per ton of CO_2. The electricity cost is calculated by assuming that the gas used for power generation is extracted at the final recompression stage, and is combusted in gas turbines displaying an electrical efficiency of 38 % with an exhaust gas temperature of 450 °C.

At this stage, the integration of the heat exchanger network with the processing plant is not analysed yet, and the thermal exergy is estimated assuming that heat is transferred with a minimum temperature difference of 12 °C, which is a conservative approach for liquid-gas heat exchanger. The heating cost is taken to 0 $/kW$_{th}$ if the heating demand can be ensured by waste heat recovery. In the opposite case, the heating cost is calculated by assuming that gas is burnt in an additional furnace with complete fuel combustion and a thermal recovery efficiency of 80 to 90 %, depending on the temperature at which heat is required. The cooling cost is calculated assuming that seawater is processed with a temperature increase of 20 °C, and with an efficiency of the lift pumps of 55 %.

The tax cost are calculated assuming an air-to-fuel ratio of 1.2, which results in an emission factor of the gas turbines of about 2.45 kg CO_2 per kg of natural gas. The waste cost corresponds to the amounts of light and heavy hydrocarbons lost to the oil and gas streams, respectively, as well as with the produced water, since more resources need to be extracted and more energy needs to be used for recovering petroleum if the system is not well-designed. The quantity of hydrocarbon compounds discharged with produced water is generally negligible compared to the rates of oil and gas exported.

Integrated processing plant

The same performance indicators are used for evaluating the performance of the entire processing plant, but the power and exergy consumption terms are completed by the terms corresponding to the energy demands of the gas treatment process. Similarly, the total production costs include the expenses related to the additional equipment items (compressors and heat exchangers).

11.2.5 Uncertainty definition

As mentioned earlier, the feed properties (composition, temperature and pressure) are subject to uncertainties related to the field measurements and the lack of knowledge on the reservoir characteristics and resource availability. Other uncertainties are associated with the selection of the equations of state and activity models that describe the vapour and liquid equilibriums, as well as with the investment and operational costs, which fluctuate with, for example, the natural gas price. This large number of uncertainties results in a complex optimisation problem dealing with a large-scale search space complicated by the presence of integer and non-integer variables, as well as by the non-linearity characteristics of the material-, energy- and economic models.

The uncertainties associated with the feed properties are difficult to estimate, and very little information can be found in the open literature. The upper and lower bounds set in the optimisation problem build on the scenario simulations presented in the component data for two North Sea platforms and on discussions with oil engineers. The distribution function of the feed composition is assumed normal, with a variance equal to 10 % of the value chosen initially for the deterministic cases. Similarly, it is assumed that the feed temperature follows a normal distribution with a variance equal to 5, so that the range of temperatures corresponds roughly to the one considered in the simulations conducted by the processing plant designers.

The uncertainty domain for the economic parameters and type of distribution functions are based on information found in the literature (Table 11.5): for example, the investment costs estimated by the correlations of Turton et al. [79] are claimed by the same author to have an inaccuracy of ± 30 %.

Table 11.5: Uncertainty (process and economic) characterisation for the platform design problem.

	Variable	Distribution	p_1	p_2
Process	Temperature	Normal	75	5
Economics	Resource price	Normal	8.08	2.5
	CO_2-tax	Beta	2	1.5
	Economic lifetime	Beta	5.8	4
	Interest rate	Normal	0.06	0.01
	Investment cost	Uniform	-0.3	0.3

The parameters p_1 and p_2 denote the mean value (μ) and variance (σ) for a normal distribution, the lower (a) and upper (b) bounds for a uniform one, and the shape parameters (α and β) for a beta one. Monte-Carlo simulations are therefore conducted to evaluate the impact of the feed properties and economic assumptions on the selection of the most relevant process configurations, and on the probability that this design set-up is optimal and robust.

11.3 Deterministic solution

The deterministic MINLP model is formulated and solved in Matlab, based on the AMPL modelling language, and the trade-off between the oil and gas recovery rates with the specific energy use and exergy consumptions are investigated. A given set-up is called a *Pareto-optimal* solution if it is optimum with respect to one of the objective functions and performance indicators defined in the MILP problem (light r_{lig} and heavy r_{hea} hydrocarbons recovery, separation efficiency ε_{sep}, specific exergy consumption σ and separation cost C^{sep}).

11.3.1 Feed conditions

Temperatures and pressures

High recoveries of light and heavy hydrocarbons are conflicting objectives, since higher gas production involves lower liquid throughout. The required exergy consumption to achieve the desired recovery of heavy and light hydrocarbons clearly depends on the initial feed conditions. At low feed temperatures, most light- and medium-weight hydrocarbons are in liquid form, implying that very little gas can be recovered at the 1st stage separation stage without either feed preheating or subsequent multiphase expansion and gas recompression.

At high feed temperatures, the same trend can be observed, but the heating requirements are much smaller or insignificant, and the Pareto curves of the recovery of the light and heavy hydrocarbons are shifted upwards or downwards. The exergy consumption is generally dominated by the power consumption, as the need for heating takes place at low to moderate temperatures (20 to 110 °C).

Regarding the economic aspects, a generic trend deduced from the first optimisation routines is that (i) low recovery rates result in high hydrocarbon losses, and thus high waste costs, (ii) high recovery rates correspond to a high number of separation and compression stages, and thus high investment costs, and (iii) high exergy use results in high utility costs and CO_2-taxes because of the greater fuel consumption.

Compositions

These trends are observable for all the feed compositions that were simulated, the only difference being the numerical values of the specific exergy consumption for reaching the same degree of separation. These values are higher in the heavy oil cases, illustrating that larger quantities of heat and power are required to separate the gas and liquid phases. The maximum gas recoveries are smaller (97.5 % against 99.3 %) when processing heavy oil, which can be explained by the high viscosity of the petroleum, while the opposite conclusion can be drawn for the maximum oil recovery, which is smaller when processing near-critical feeds (96 % against 99.8 %).

11.3.2 Isolated separation plant

Separation and recompression stages

The comparison of the various separation layouts (Figure 11.3) illustrates the limits in terms of recovery rates associated with each configuration, for each type of petroleum and different feed conditions.

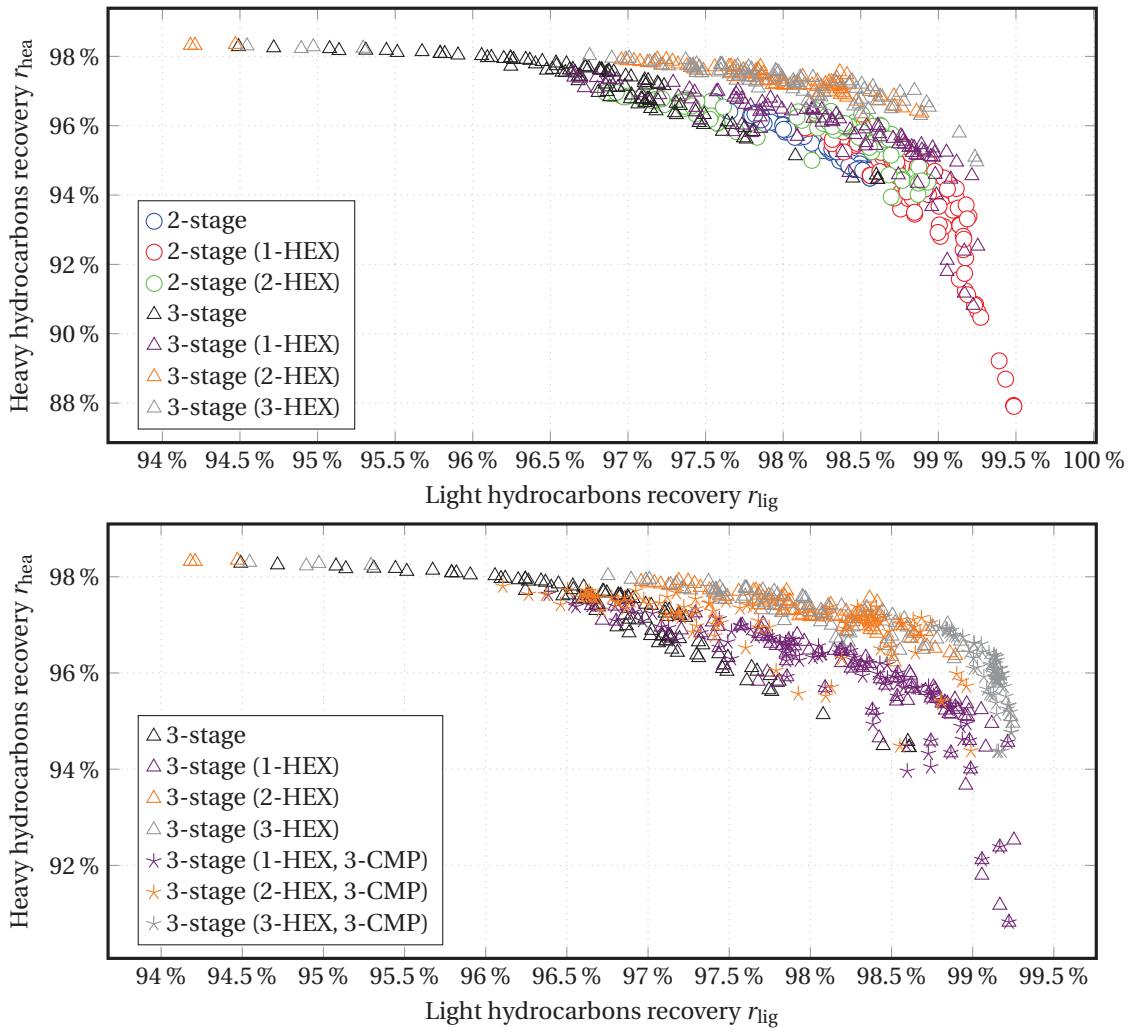

Figure 11.3: Trade-off between the recovery of light and of heavy hydrocarbons with a different number of separation (top) and recompression (bottom) stages.

The addition of separation stages results in a smaller exergy (power and heat) consumption for the same separation performance. The integration of an intermediate pressure level allows for flashing a fraction of the medium-weight hydrocarbons, which are thereby not separated in the last separation stage, resulting in a smaller compressor loading and power consumption, as medium-weight hydrocarbons are not processed through the next compressors.

Feed temperature conditions

The feed temperature at the inlet of the production manifolds has a clear impact on the performance of the separation plant. Lower temperatures result in smaller gas production, especially if no heat exchanger is implemented, and this limits the maximum recovery of light hydrocarbons (Figure 11.4).

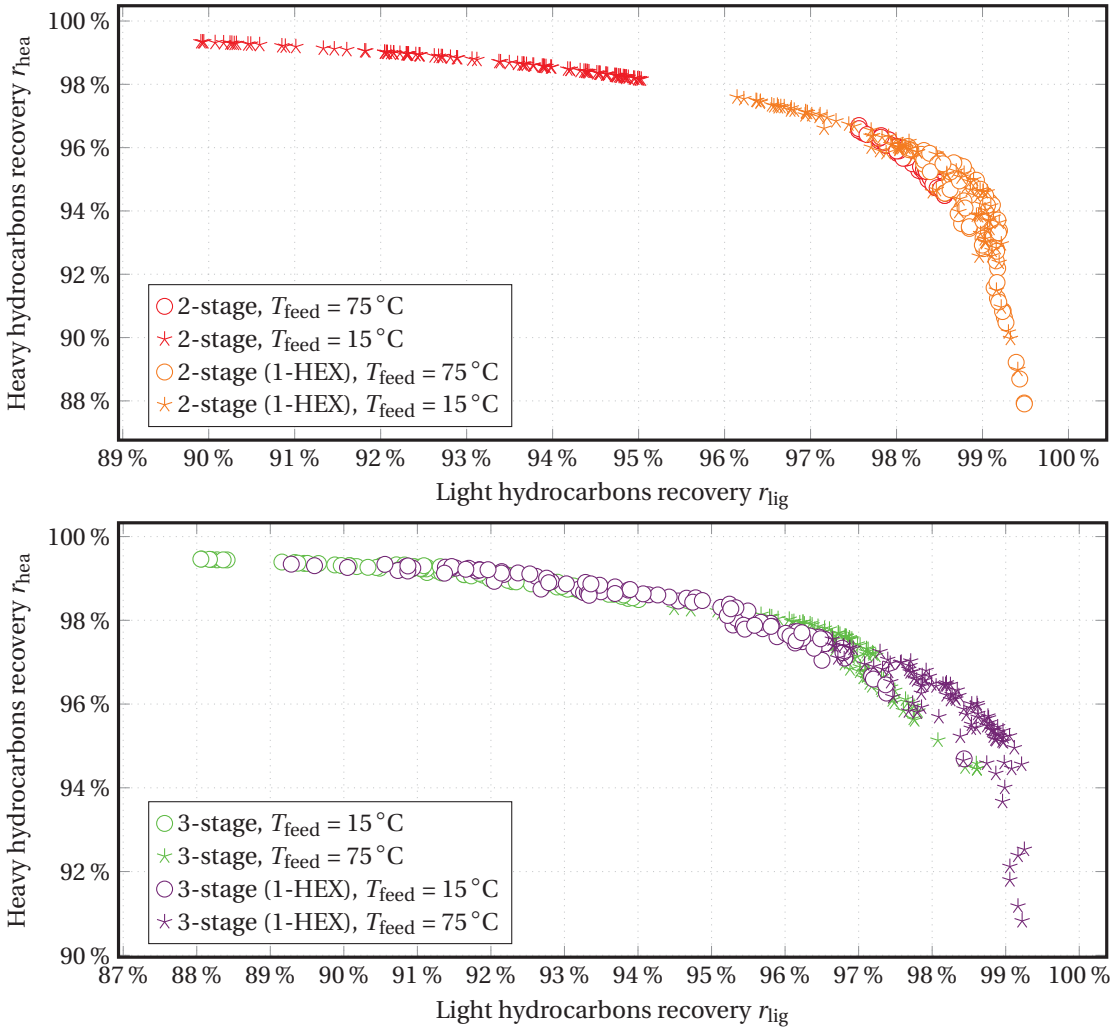

Figure 11.4: Trade-off between the recovery of light and heavy hydrocarbons with different feed temperatures, with two (top) or three (bottom) separation stages.

However, the specific exergy consumption differs significantly from one layout to another (Figure 11.5) although the same quality of separation between light and heavy hydrocarbons can be achieved by integrating an additional heat exchanger. More power needs to be consumed in the layouts without heaters, because a greater amount of light hydrocarbons is recovered at the final separation stage.

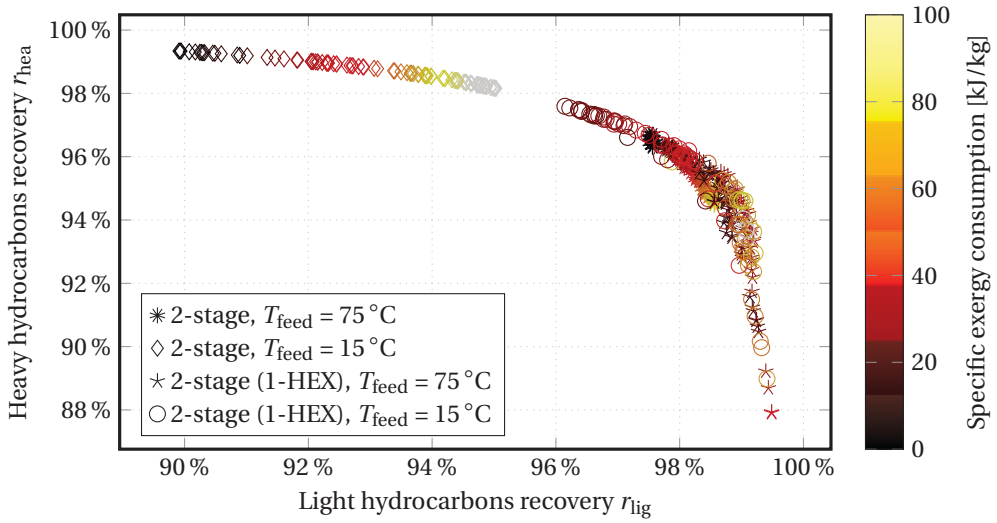

Figure 11.5: Trade-off between the recovery of light and heavy hydrocarbons with different feed temperatures, regarding the specific exergy consumption.

11.3.3 Integrated processing plant

The analysis of the cost build-up (Figure 11.6) for the whole processing plant shows that the fuel gas (utility) cost dominates the expenses related to the offshore platform, followed by the discounted grassroot costs and ended by the tax and maintenance costs. The comparison of the economic evaluations of the 2 and 3-stage layouts shows that there is a clear trade-off between the utility and tax costs, which decrease because of the lower power consumption, and the investment costs, that increase with a higher number of separation and compression stages.

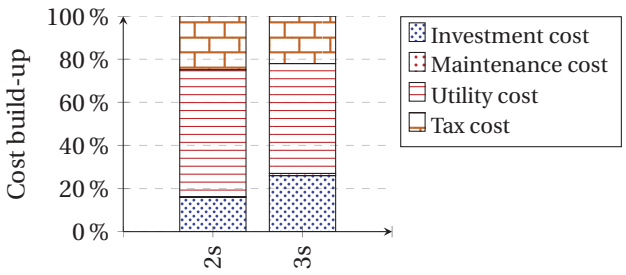

Figure 11.6: Cost build-up for integrated processing plants based on two- and three-stages separation layouts.

The Pareto-curves (Figure 11.7) demonstrate that, in practice, the addition of the scrubbers in the gas treatment section results in a better recovery of the heavy hydrocarbons by 1.5 to 2 %-points for the same quality of gas recovery, which can exceed more than 98 % with an appropriate system layout and proper operating conditions.

Moreover, the system layout with a 3-stage separation scheme, including a heater at the 2nd stage, seems to be the most efficient process layout for the volatile feed composition (Composition 1). It displays a large flexibility with respect to the recovery of light (88–99.5 %) and heavy (95.5–99 %) hydrocarbons (Figure 11.8), and it offers good compromise solutions with high quality of separation between oil and gas (solutions with r_{lig} above 98 % and r_{hea} above 96.5 %). The solution suggested by the performance analysis of isolated separation plants corresponds to a 3-stage scheme with a heater at the 1st stage and is shown to be sub-optimum.

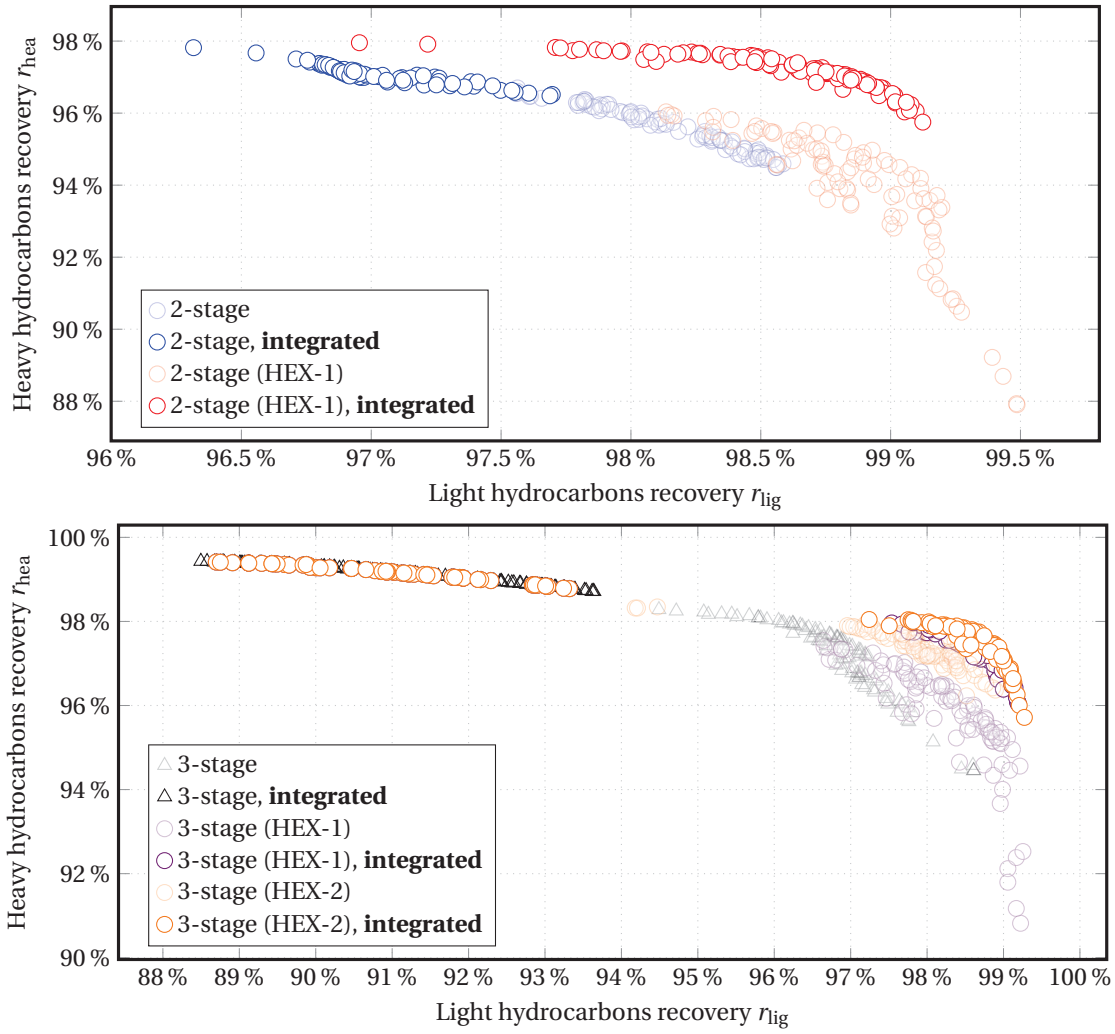

Figure 11.7: Trade-off between the recovery of light and of heavy hydrocarbons for an isolated and integrated separation plant, with two (top) or three (bottom) separation stages.

Optimum compromises that present the highest separation performance, i.e. the highest combined recoveries of light and heavy hydrocarbons, with the lowest exergy consumption, are presented for the volatile oil case (Table 11.6).

Table 11.6: Examples of compromise solutions for an isolated processing plant.

Operating conditions	Variable	Unit	C1	C2	C3	C4
Separation						
Number of stages	$N_{\text{stages}}^{\text{sep}}$	-	2	2	3	3
Stage pressure 1	p_1^{sep}	bar	13.9	14.2	45.5	37.6
Stage pressure 2	p_2^{sep}	bar	1.8	1.8	17.5	17.5
Stage pressure 3	p_3^{sep}	bar	-	-	1.75	1.75
Heating stage		[-]	1	-	3	2
Stage temperature	T^{sep}	°C	95	-	102	117
Recompression						
Number of stages	$N_{\text{stages}}^{\text{rec}}$	-	1	1	2	2
Stage pressure 1	p_1^{rec}	bar	13.9	14.2		20
Stage pressure 2	p_2^{rec}	bar	-	-	45.5	37.6
Stage temperature	$T_{1,2,3,4}^{\text{sep}}$	°C	20.4	17.6		
Treatment						
Number of stages	$N_{\text{stages}}^{\text{tre}}$	-	3	3	3	3
Stage pressure 1	p_1^{tre}	bar	32.3	37.7	45.5	59.2
Stage pressure 2	p_2^{tre}	bar	107	86.2	98.9	81.8
Stage pressure 3	p_3^{tre}	bar	180	180	180	180
Stage temperature	$T_{1,2,3}^{\text{tre}}$	°C	[21–29]	[20–22]	[20–30]	[20–30]
Indicators						
Gas recovery	r_{lig}	-	98.5 %	97.4 %	97.6 %	98.1 %
Oil recovery	r_{hea}	-	97.2 %	96.9 %	98.0 %	97.9 %
Specific power consumption	σ	kJ/kg	77.6	88.1	57.3	52.0
Specific energy use	SEU	kJ/kg	172	88.1	101.5	117.3
Specific exergy consumption	SEC	kJ/kg	103	88.1	68.3	70.4

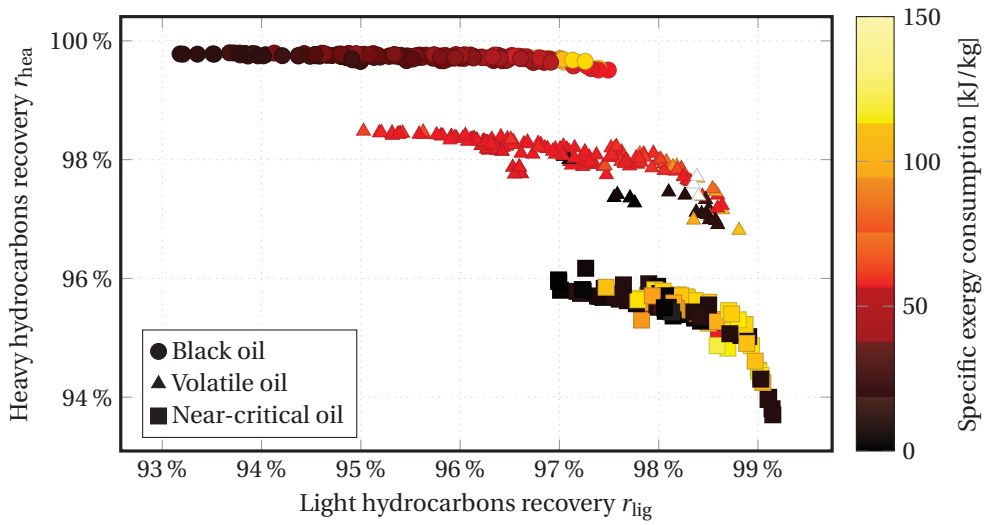

Figure 11.8: Trade-off between the recovery of light and heavy hydrocarbons with different petroleum compositions, regarding the specific exergy consumption.

11.4 Solution under uncertainty

Seven possible configurations (Table 11.7) have been selected for further evaluations, which differ by the number of separation and gas treatment stages, and by the inclusion and placement of a heater. The aim is to evaluate the robustness of each process layout and to investigate whether one prevails over the others when uncertainties are included in the optimisation procedure.

Table 11.7: Investigated configurations for decision-making under uncertainty.

Operating conditions	C1	C2	C3	C4	C5	C6	C7
Separation							
Number of stages	2	2	2	3	3	3	3
Heater	n	y	y	n	y	y	y
Heating stage	-	1	2	-	1	2	3
Treatment							
Number of stages	3	3	3	3	3	3	3

11.4.1 Process uncertainties

In practice, the exact feed conditions and composition are unknown, and this results in a large dispersion of the Pareto-optimal solutions (Figure 11.9). In this context, it is challenging to select the most appropriate processing plant layout: a robust set-up should be efficient with respect to the separation of the light and heavy hydrocarbons, while the power consumption and exergy use should be minimised. Moreover, the optimum operating conditions (e.g. pressure and temperature) are likely to be different from the ones in the deterministic solutions.

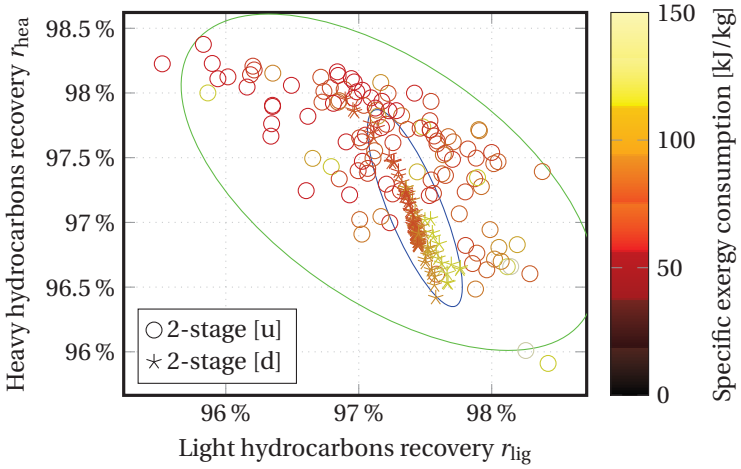

Figure 11.9: Trade-off between the recovery of light and heavy hydrocarbons with [u] and without [d] uncertainty.

The results displayed in Figures 11.3–11.7 indicate that several process layouts seem equivalent from a process and energy perspective, and a deterministic optimisation is therefore performed for every single and random scenario generated by applying uncertainty distribution functions.

The combined optimisation and uncertainty analyses (Figure 11.10) show that the configurations including 3 stages of separation are the most promising ones even in uncertain conditions, from a process and energy efficiency perspective. In the case of black oil, the highest separation performance is reached for a 2-stage separation set-up, because the benefits of a better light hydrocarbon recovery with 3 stages are counterbalanced by the greater losses of medium hydrocarbons with the exported gas flow. The layouts that include a heater are favoured for all types of petroleum and for any number of stages, and the difference is particularly marked for the black oil cases. An additional heat exchanger can increase the separation efficiency by up to 2, 1.5 and 0.8 %-point for black, volatile and near-critical petroleum.

The impact of these uncertainties on the platform performance is underlined by the large variability (Table 11.8) in the values for each objective function. For example, for a heavy oil, the separation efficiency varies between 92.5 and 97 % along the Pareto front for the deterministic case, while it varies between 91.5 and 97.5 % when the uncertainties on the feed conditions are added.

Table 11.8: Variability of the objective functions with [u] and without [d] uncertainty mapping.

	ε_{sep} [d], %	ε_{sep} [u], %	σ [d], kJ/kg	σ [u], kJ/kg
Heavy oil	92.5–97	91.5–97.5	5–90	10–120
Volatile oil	93.6–95.6	92.5–96.6	10–135	20–150
Near-critical oil	92.5–93.5	91.5–95.4	10–440	20–150

Finally, the aim is to suggest a set of optimum design layouts, considering the process uncertainties: this is performed by assessing quantitatively the frequency of each configuration to be an optimum design set-up (Figure 11.11) and by analysing the Pareto frontiers.

For example, for the heavy oil case, the configuration 3 has a frequency of about 22 % to be a Pareto-optimal solution and of about 52 % to be one of the 10 % best configurations with respect to the separation efficiency. However, these numbers fall down to 8 and 22 % when the process uncertainties are included, and the configuration 5 has the highest frequency (58 %) to be one of the 10 %-best performing layouts.

The same analysis performed for the volatile and near-critical petroleums suggests that the configurations with three stages and one heater are favoured in both deterministic and uncertain conditions, because of the higher flexibility given by the additional separation stage and heat exchanger. The placement of the heater is also revealed to be important, and it seems that integrating this component at the 2nd or 3rd stage separation is generally better.

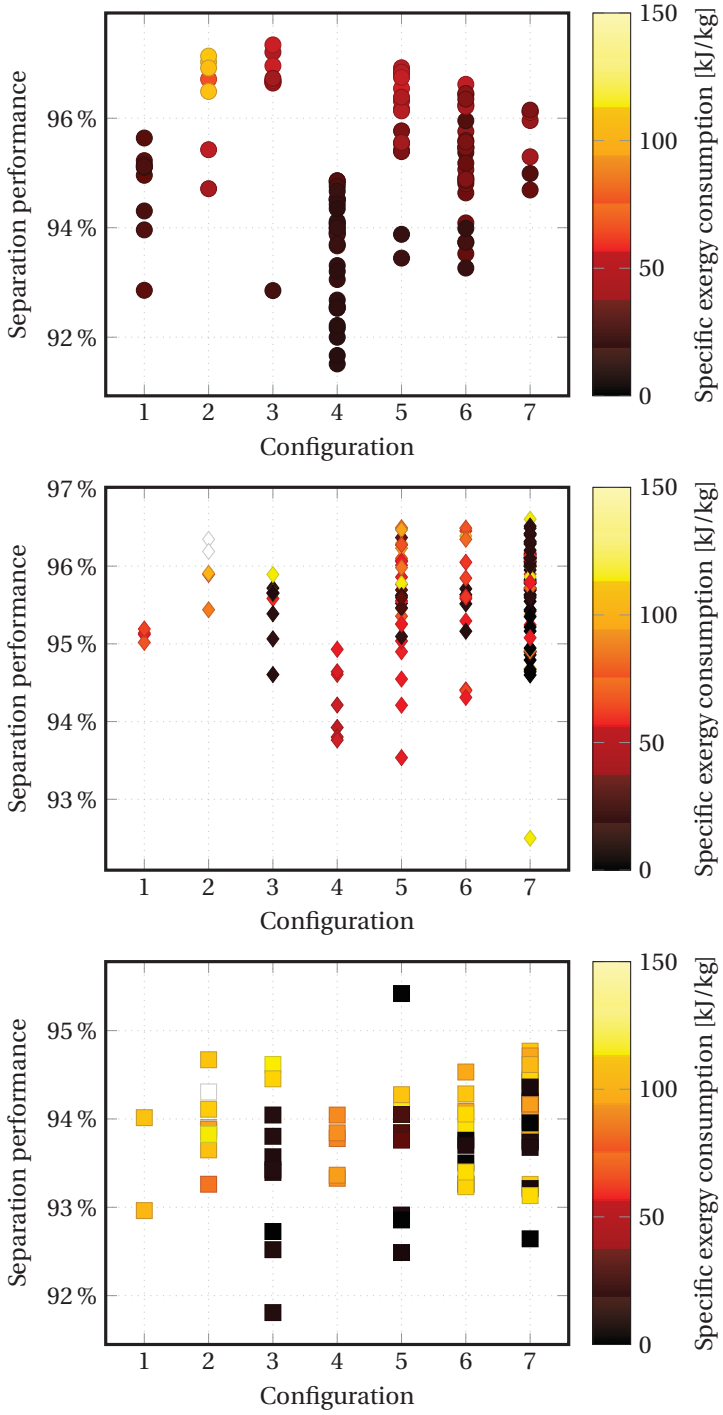

Figure 11.10: Dispersion of the Pareto-optimal solutions per configuration for heavy (top), volatile (middle) and near-critical (bottom) oil with process uncertainties.

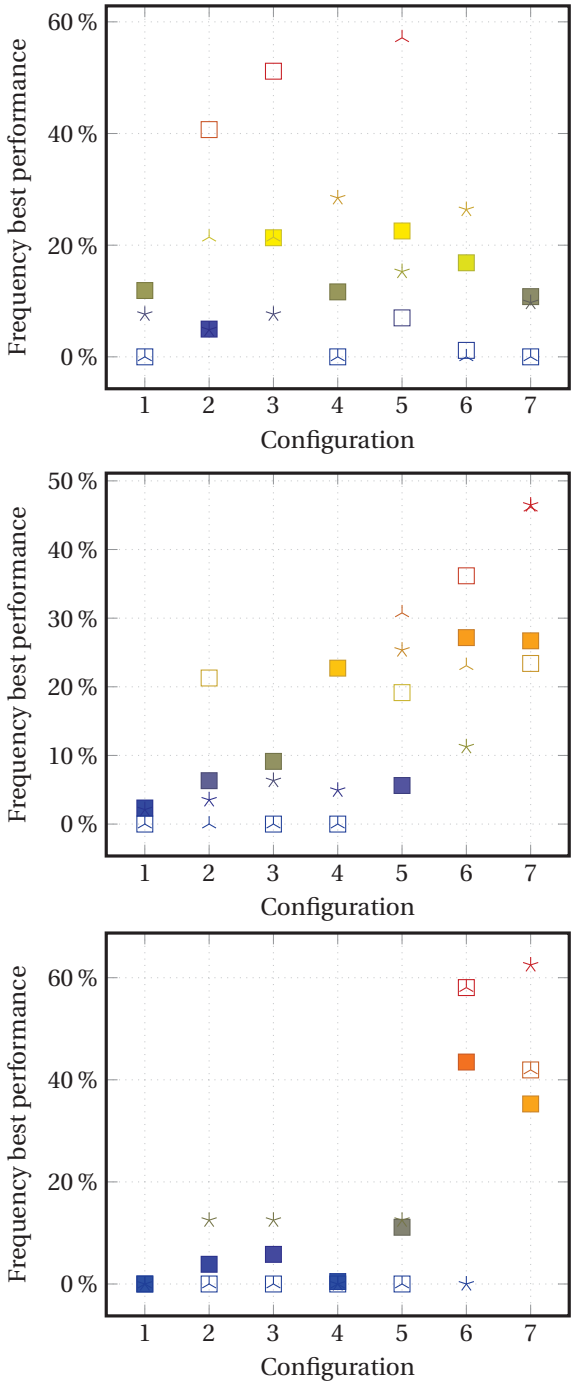

Figure 11.11: Frequency of the Pareto-optimal solutions per configuration for heavy (top), volatile (middle) and near-critical (bottom) oil with [u] and without [d] process uncertainties.

11.4.2 Economic uncertainties

The same approach used to identify the most promising system layouts with regards to the process uncertainties can be applied (Figure 11.12), accounting for the economic uncertainties on the investment costs, resource prices, CO_2-taxes, platform lifetime and interest rate. The results from the uncertainty mapping differ strongly whether the analysis deals with the process or economic uncertainties, and with the type of petroleum processed on-site.

In the case of heavy oil, the process schemes that include a heater largely prevail over the others, as they can achieve a higher degree of separation by about 2.5 %-points, at the expense of slightly higher investment costs associated with the additional heat exchanger. The fuel and tax costs stay unchanged, because the heat contained in the exhaust gases is revealed to be sufficient enough to cover the heating demand of the oil separation process. The comparison of the two- and three-stage layouts suggests that the 2-stage separation processes are preferred from an economic perspective, and the frequency that such set-ups achieve the best separation and economic performances exceeds 90 %. However, the pressure at the first stage separator should be lower by about 5 to 10 bar to avoid too large power consumption in the gas recompression section.

On the contrary, for volatile petroleums, the 3-stage scheme is clearly preferable from both an economic and a process perspective because of the higher content in light- and medium-weight hydrocarbons that flows in the recompression section. These schemes are Pareto-optimum in more than 65 % of the generated economic scenarios and achieve the highest separation efficiency for more than 95 %.

Similar conclusions can be drawn for the case of near-critical petroleums, and the main difference lies in the frequency that the 2-stage separation layout with a 1st stage heater (configuration 2) prevails over the other set-ups. This scheme may be interesting because large amounts of gas are already recovered at the 1st separation stage, but, since oil operators generally prefer larger liquid production, the implementation of three separation stages with one operating at high pressure may be more interesting from a practical point of view.

11.4.3 Combined uncertainties

In a final attempt to find and select optimal process configurations for oil and gas processing plants, this multi-objective optimisation strategy is applied with consideration to both process and economic uncertainties. The findings suggest that three-stage configurations are better with respect to process, energetic and economic aspects: these layouts are more robust over large ranges of feed conditions and properties and under various sets of economic scenarios. The advantage of these designs is particularly marked for volatile and near-critical petroleums, where the frequency that such layouts are Pareto-optimum solutions exceeds 80 and 85 %, and the frequency that they display the best separation and production performance goes beyond 90 % in both cases.

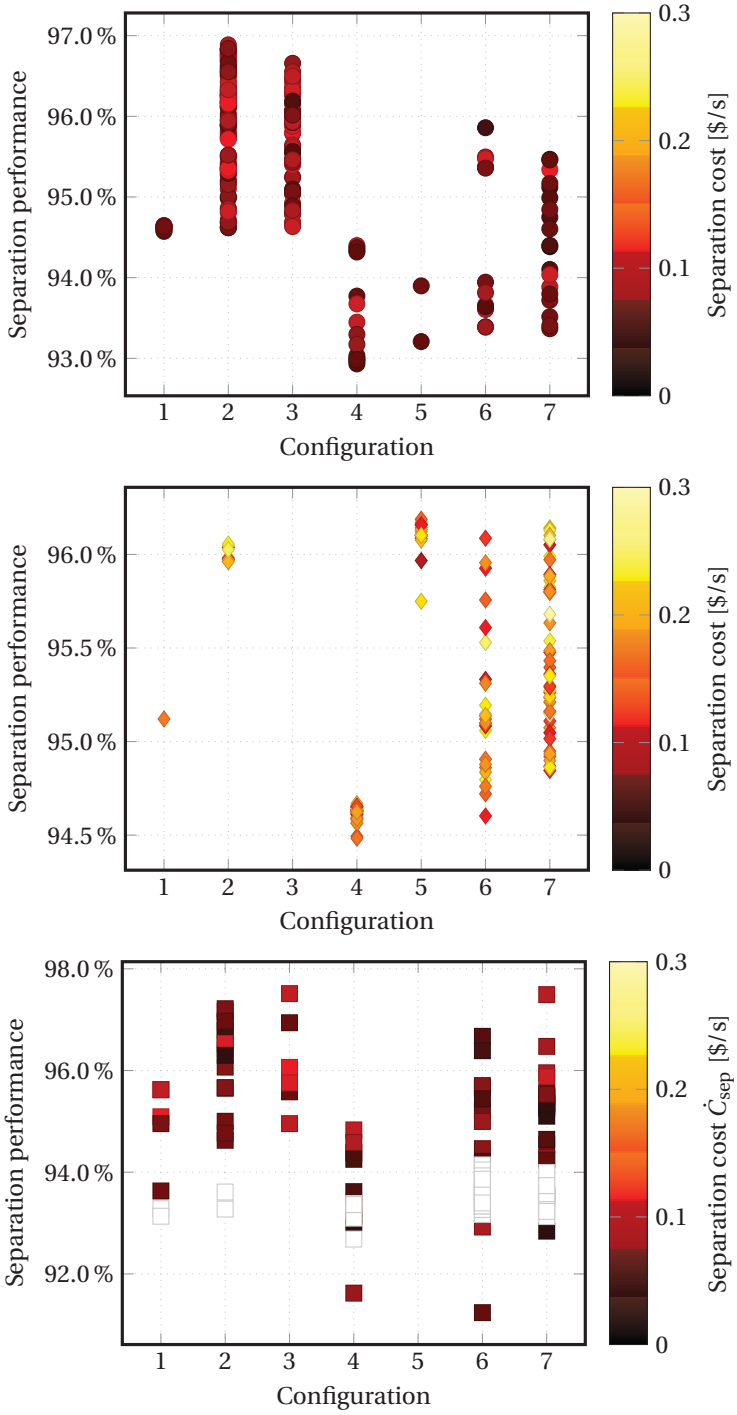

Figure 11.12: Dispersion of the Pareto-optimal solutions per configuration for heavy (top), volatile (middle) and near-critical (bottom) oil with economic uncertainties.

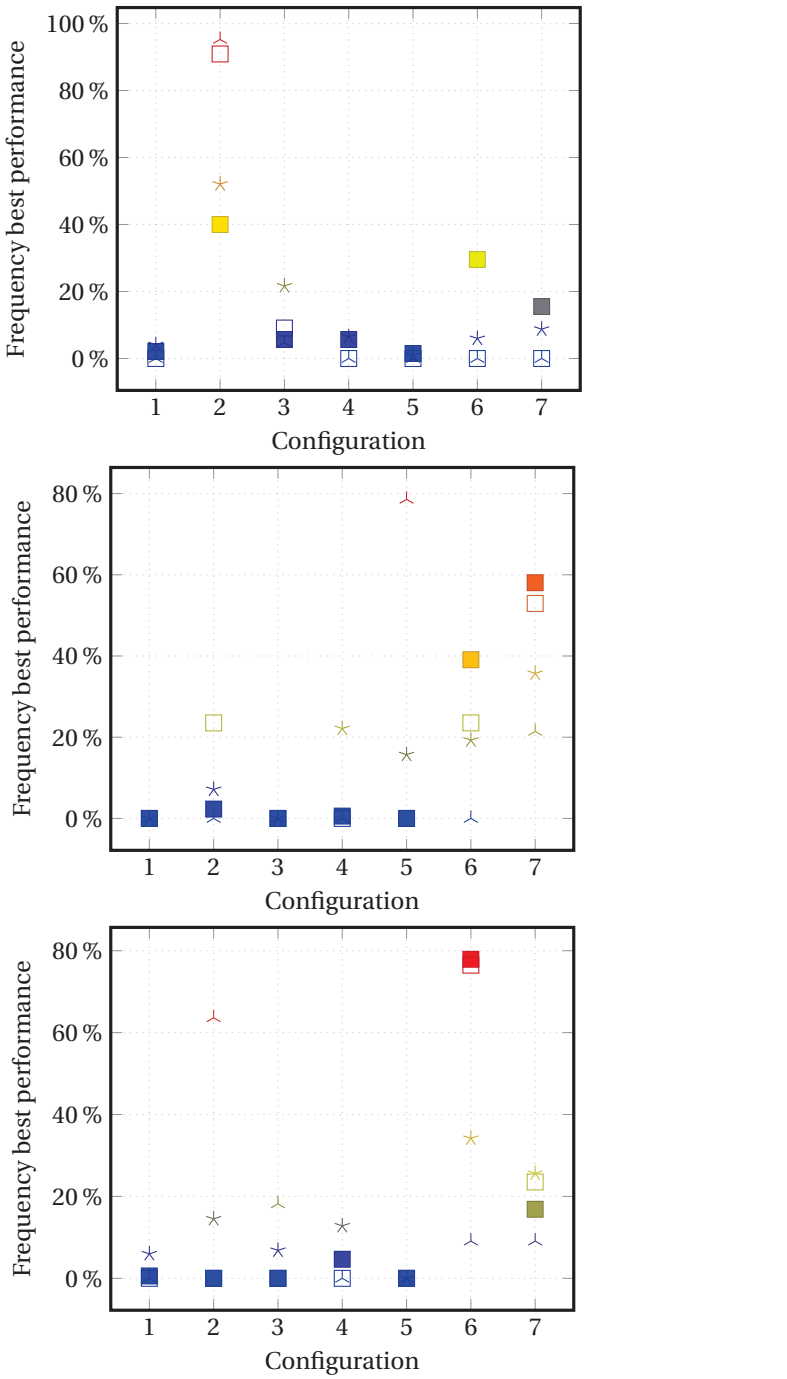

Figure 11.13: Frequency of the Pareto-optimal solutions per configuration for heavy (top), volatile (middle) and near-critical (bottom) oil with [u] and without [d] economic uncertainties.

11.5 Conclusion

Two different approaches for designing an oil and gas processing plant have been applied, analysing the advantages of designing the separation process at a local and a system level. The system performance depends strongly on the level of mass integration within the platform: the recoveries of the light and heavy hydrocarbons are markedly impacted by the number of separation stages and the addition of a heat exchanger.

Disregarding the interactions between the several plant sections can lead to the choice of an inadequate configuration and result in excessive losses of oil and gas, greater power and exergy consumption, and thus in smaller economic benefits. These findings are similar for the three types of petroleums that were considered in this work, although the specific exergy consumption and the selection of the temperature and pressure levels differs significantly from one case to another.

A preliminary economic analysis pinpoints that the production cost is dominated by the natural gas sales price, followed by the tax penalty and investment costs. The selection of an optimum two- or three-stage layout is therefore directly impacted by the petroleum properties and economic environment, and the findings highlight that three-stage separation processes are generally more robust and prevail over other configurations. However, this picture may be different for feeds that are processed at lower temperatures because of the additional fuel demand needed to sustain the heating consumption of the separation process.

The application of this combined mass- and energy-integration framework, together with multi-objective optimisation tools, uncertainty mapping, and economic assessment is proved to be useful. It is particularly valuable for performing a preliminary process analysis and for identifying adequate design solutions, which should be further verified and simulated.

12 Conclusion

Offshore platforms are complex and possibly highly integrated systems that face significant changes in the field properties and operating strategies over time. Today, petroleum-based fuels represent most of our primary energy supply, and concerns on the significant energy use and greenhouse gas emissions of the offshore extraction sector have risen. In this regard, it is particularly relevant to investigate the performance of oil and gas facilities, and this requires the use of a systematic approach for modelling, evaluating and optimising them.

The present thesis builds on the application of an advanced computational framework, which integrates together process design and performance assessment techniques, and takes into account thermodynamic, economic and environmental aspects. It is based on, among other methods, flow-sheeting modelling, exergy and pinch analyses, life cycle assessments and multi-objective optimisations. It allows therefore for a consistent evaluation of the existing oil and gas plants, and can be used as a helping tool.

Summary of findings

Modelling (Chapter 3). One key aspect of the approach used in this work is the dissociation between the process unit models, the system design tools, and the performance assessment methods. The interconnections between the models are not defined explicitly, and this allows for the development of a general system superstructure, which embraces multiple process configurations and eases the assembling of models built on different simulation software.

This database of process technologies is enriched with the thermo-environomic models, which are connected to the physical models by data transfer through a Matlab-based platform. Each plant layout can thereby be evaluated with respect to thermodynamic (process integration and exergy efficiency), economic (investment, operating and total costs), and environmental (global warming potential and eco-indicators) performance indicators. The use of multi-objective optimisation routines helps discarding system set-ups that are sub-optimum, and the implementation of uncertainty functions helps eliminating solutions that are not robust or flexible enough.

Case studies (Chapters 4–6). Six main physical models of oil and gas platforms were developed in the present work:

- a generic offshore facility built on literature data;
- Draugen, the core case study of this thesis (Platform D);
- an oil platform with a high gas-to-oil ratio (Platform A), exporting a volatile light oil;
- a gas and condensate platform (Platform B), with a high reservoir pressure;
- an oil platform with a low gas-to-oil ratio (Platform C), importing gas;
- an oil platform processing a petroleum at low temperatures (Platform E).

The generic model was developed to represent the layout of typical North Sea platforms and analyse the impact of different petroleum compositions and the influence of diverse water- and gas-to-oil ratios. The Draugen platform is operated by Norske Shell and is located in the Norwegian Sea, while the three next ones (Platforms A, B and C) are operated by Statoil in the North Sea, and the last one (Platform E) is operated by Petrobras in the Brazilian Gulf. Measured data were used for all platforms, with the exception of the generic one. These platforms illustrate some of the diversity across these facilities.

Despite these differences, the overall platform layout stays similar and can be subdivided into two main sub-systems. The first is the oil and gas processing plant where feed streams are depressurised (production manifolds), oil, gas and water are separated (separation), oil is pumped and exported to the shore (oil treatment), produced gas is recompressed (gas recompression) and possibly dehydrated, compressed and cooled (gas treatment), and a fraction is treated apart for local power generation (fuel gas handling). Additional processes such as seawater injection and condensate treatment may be implemented. The second is the utility plant, where the power and heat required in the processing plant are generated. It generally consists of gas turbines, possibly complemented by a waste heat recovery process.

Energy demands (Chapters 4–6). The power consumption of the North Sea platforms ranges between 5.5 and 30 MW, and between 20 and 660 MJ/Sm^{3}o.e.. The major electrical demand, even for the fields with low gas-to-oil ratio, corresponds to the gas compressors, and possibly to the seawater injection pumps if these are installed on-site. The heating demand is smaller than 2 MW for two of these platforms, and exceeds 5 MW for the two others, because of the oil heating operations in the separation sub-system. The cooling demand is greater than 20 MW for all platforms, because of the large needs for gas cooling. In comparison, the Brazilian platform has lower power and cooling demands, but high heating use. These differences result mainly from the petroleum properties (temperature, pressure and viscosity) and the export specifications (purity and pressure).

The thermal energy demands vary greatly over the lifetime of a platform, since they are directly affected by the oil and gas flow rates. For instance, the heating demand decreased by 75 % on the Draugen platform between the peak and end-life production stages. The power consumption is not as affected by the variations of the gas production rate, because the flow of gas through the compressors is maintained constant by gas recirculation to prevent surge. However, it is greatly impacted by modifications of the facility, such as the implementation of gas and water injection processes to ease petroleum recovery.

Exergy profiles (Chapters 4–6). Most exergy entering an offshore platform (≥ 97 %) is associated with the feed streams and transits through the processing plant with very little transformation, while most exergy leaving it corresponds to the oil and gas flows. Most exergy destruction (60–65 %) takes place in the utility plant because of the combustion process in the gas turbines. The remaining destruction (35–40 %) occurs in the oil and gas processing plant. Most exergy losses are related to the rejection of the exhausts from the power turbines because of their high temperature, and the remaining ones are caused by the flaring and venting operations, as well as by the discharge of produced water.

The exergy destruction within the processing plant ranges between 12 and 32 MW and between 43 and 517 MJ/Sm^3 o.e.. The distribution of these irreversibilities varies widely across oil and gas facilities: it is sensitive to the boundary and operating conditions, plant layouts, and to the production stages in the field lifetime. In general, thermodynamic irreversibilities are likely significant in processes where pressure is substantially decreased (production manifolds, 10–28 %) or increased (gas recompression and treatment, 11–29 % and 8–57 %), heat is transferred (oil heating and gas cooling), and where gas is recirculated The amounts of exergy destruction in the heat exchangers are likely to decrease over time because of the smaller petroleum extraction rates. The irreversibilities caused by the anti-surge recycling are important in the early- and end-life stages. The exergy losses are dominated by the energy lost with the exhaust gases (≥ 70 %), except for shut-down situations where large quantities of produced gas are flared, and in end-life production stages where high amounts of produced water are discharged to the sea.

Performance indicators (Chapter 7). Performance indicators of different types, such as the energy efficiency and intensity, are used in the oil and gas industry, but the present work shows that they cannot be used to compare consistently different facilities. They do not account for the differences in natural and export conditions and penalise platforms that process low-pressure or low-temperature petroleum. A combination of indicators, including the specific exergy consumption, the best-available-technology and the exergetic efficiencies, is suggested to evaluate adequately the performance of such systems, with regards to their real improvement potentials. An alternative formulation of exergy efficiency is proposed, applied and tested, to overcome the limitations of the definitions previously found in the literature.

Energy savings (Chapter 8). The exergy destruction in the production manifolds can hardly be avoided, since multiphase expanders and ejectors are currently not mature technologies. A possibility, but which is only feasible for some platform layouts, is to implement an additional pressure level. This may result in savings of 5 to 10 % of the total power consumption, at the expense of a greater loading of the scrubber and cooler loads at some compression stages.

The exergy destruction in the gas recompression and treatment sections may be reduced by eliminating anti-surge recirculation, using alternative control methods, downsizing or re-wheeling the compressors, and having several compressors in parallel. The power consumption can be reduced by up to 7 MW, which represents 15 to 20 % of the total demand, and the exergy destruction for the processing plant solely can be decreased by 0.8 to 3.8 MW, which represents 10 to 20 % of the total irreversibilities of the oil and gas plant.

The exergy destruction by heat transfer may only be reduced by enhancing the total site integration, because each individual sub-system generally has only heating or cooling requirements. However, most cooling takes place between 40 and 120 °C, while most heating is required between 60 and 220 °C. These temperature mismatches limit the possibilities for energy integration or would involve the design of a complex heat exchanger network, which may not be interesting for economic and control-related reasons.

The integration of a low-temperature organic Rankine cycle may be interesting, but only for the gas and condensate platform, since large quantities of low-temperature heat are discharged through the gas aftercooler. The thermal efficiency of such cycle does not exceed more than 12 %, using a mixture of ethane and propane as working fluid, and this results in a power production of about 4 MW.

Waste heat recovery (Chapter 9). Most exergy destruction within the utility plant is unavoidable, as the combustion inefficiencies are in essence irreversible. The exergy losses with the exhaust gases can be decreased by integrating a bottoming cycle, transforming the utility plant into a combined cycle or cogeneration plant.

For the Draugen platform, the integration of a steam network improves the efficiency of the utility plant at both design and part-load conditions from about 22 to 31–33 %. A steam Rankine cycle with extraction appears promising, but only for platforms with a high heating demand, such as the ones processing low-temperature or viscous petroleum. Instead of a steam network, organic Rankine cycles may be interesting if the turbine exhausts have a low temperature, and may reach the same level of efficiency.

System integration is crucial for improving the performance of the offshore platform. For example, the bottoming cycle may be designed without analysing the possible interactions with the rest of the offshore system. An inadequate selection of the cooling utility system, for the Draugen platform, would result in a thermodynamic penalty of 20 to 25 % or an economic penalty of 10 %.

Important trade-off between the thermodynamic, economic and environmental performance can be assessed by means of multi-objective optimisations. The Pareto frontiers illustrate the challenges in decision-making processes for bottoming cycles: integrating such cycles results in greater weight and volume on-site, but in greater operating benefits and higher system flexibility.

CO_2-capture (Chapter 10). The implementation of CO_2-capture processes on offshore platforms is a step towards the decarbonisation of oil and gas processing, possibly resulting in lower global warming potential. Post-combustion capture from the turbine exhausts, using monoethanolamine, is feasible, despite the low CO_2 partial pressure. It should be introduced together with a bottoming cycle upstream, because the absorption of CO_2 is improved with lower temperatures, and more electricity is available, reducing the energy penalty of the capture process. The reductions in CO_2-emissions for the entire platform can reach 70 % for a carbon capture rate of 85 %, and the captured CO_2 may be used for enhanced oil recovery.

Pre-combustion capture may be attractive for future offshore platforms, as it cannot be implemented as a retrofit option. Conversion of the produced natural gas into hydrogen is feasible either by steam methane or autothermal reforming, and actual separation between hydrogen and carbon dioxide is mostly competitive with physical and chemical absorption. However, such processes result in a refrigeration demand below ambient temperatures to regenerate the physical solvent or a heating demand at about 100–150 °C for a chemical one.

Pre-combustion units may be more compact because of the smaller flows that need to be processed in the power generation system, which may be interesting considering the space and weight limitations on offshore facilities. However, post-combustion options may be favoured from an economic prospective, since they are well-known technologies. Further analyses have indicated that the economic competitiveness highly depends on the CO_2-taxes, the capital costs associated with the injection wells, and the market value of natural gas.

Design of new platforms (Chapter 11). A detailed design study was performed to analyse the impact of the petroleum feed properties on the optimal system layout of an oil and gas platform, with regards to the number of separation and compression stages, and to the introduction of heaters and coolers. Site integration is crucial: designing the separation process individually leads to sub-optimal solutions if the interactions between the different system sections are not considered.

The most optimal system layouts depend on the possibilities for energy integration and cogeneration, the future economic scenarios, and the expected uncertainties on the petroleum properties. The latter were shown to have a high effect on the selection of the most optimum process layout, and a configuration with an additional separation heater is generally the most robust and flexible layout.

Future work

The approach of the present work seems to be promising for modelling, evaluating and optimising offshore systems. The five facilities that are presented and analysed can be more accurately assessed if more measurements are provided from the operators and stakeholders. This would allow for a more in-depth analysis and lead to thorough discussions on the technical feasibility of the improvements suggested in this work.

Generalisation. Other offshore facilities, either operating in the North Sea or located in other regions of the globe, could be analysed to verify whether the conclusions drawn in the present work can be extended. The differences in system layouts are, nonetheless, expected to be minor: they are related to the export specifications and the possible introduction of processes such as desalting.

Gas offshore plants, which process lighter feeds, but have different requirements in terms of gas purity, could be assessed as well. Processes such as liquefaction and mercury treatment are examples of processes that are typical on such facilities. The energy profiles are expected to differ from oil and gas platforms, because of the large need for refrigeration in liquefaction plants. A possibility could be to investigate the performance of oil and gas onshore facilities, and evaluate whether they differ from offshore ones.

Database. The database of process models could be enlarged to other processes that may be installed on offshore platforms, such as sulphur treatment and natural gas liquids recovery, and to include more working fluids in the analysis of the organic Rankine cycles. The economic models may be improved by evaluating more accurately the costs associated with the construction of the facility, although it is difficult to make an accurate estimate of the grassroot costs of waste heat recovery and CO_2-capture processes. The environmental models could be updated to account for the differences in location and resource impacts between different countries. Uncertainties may be accounted at an earlier stage of the design process.

Design. The design problem may be extended to consider both component design and multi-period aspects. As mentioned, the gas- and water-to-oil ratios vary to a large extent, and the facilities are designed to handle the peak production rates. An optimal processing plant design is therefore not necessarily a plant layout that is the most efficient at peak conditions, but rather a set-up that stays performant for the entire field exploitation. Further multi-objective optimisations should then consider the off-design behaviour of separators, heat exchangers and turbo-machinery components when designing future offshore plants.

Finally, the performance of oil and gas processing on stationary platforms could be evaluated considering alternative options, such as subsea production, and against extraction of other fossil fuel resources such as shale gas.

Final statement

Driving towards more process- and energy-efficient offshore systems is a necessity in the perspective of a future marked by the depletion of fossil fuels, a global climate change challenge and a market shaped by the oil price volatility and carbon dioxide taxes. Oil and gas platforms present similar design set-ups, and the systematic approach applied in this thesis shows that the sources and locations of the performance losses are alike. However, the differences in the field and operating conditions make each platform unique, indicating that no generic improvement can be proposed. The implementation of waste heat recovery cycles may be a step forward towards more sustainable oil and gas processing, but the design of such processes must take into consideration site integration aspects to actually be efficient.

Bibliography

[1] Independent Statistics & Analysis. International Energy Outlook 2013. Technical report, U.S. Energy Information Administration (EIA), 2013.

[2] IEA Statistics. CO_2 emissions from fuel combustion – Highlights. Technical report, International Energy Agency, 2013.

[3] International Energy Agency. World Energy Outlook 2011 – Special Report: Are we entering a golden age of gas? Technical report, OECD/IEA, 2011.

[4] Independent Statistics & Analysis. Norway. Technical report, U.S. Energy Information Administration, 2014.

[5] Mikael Höök and Kjell Aleklett. A decline rate study of Norwegian oil production. *Energy Policy*, 36(11):4262–4271, 2008.

[6] Olje- og energidepartementet. Utslepp til luft frå petroleumsverksemda, 2007. URL www.regjeringen.no/nb/dep/oed/tema/co2/utslepp-til-luft-fra-petroleumsverksemda.html?id=443519.

[7] Fæhn, Taran and Hagem, Cathrine and Rosendahl, Knut E. Norsk olje- og gassproduksjon – Effekter på globale CO_2-utslipp og energisituasjonen i lavinntektsland. Technical report, Statistisk sentralbyrå, 2013.

[8] Statistisk Sentralbyrå. Lavere klimagassutslipp i 2011, 2012. URL http://www.ssb.no/emner/01/04/10/klimagassn/.

[9] Faktasider, 2014. URL factpages.npd.no/factpages/.

[10] Norsk Oljemuseum. Oil and gas field in Norway – Industrial heritage plan, 2008.

[11] Mark Bothamley. Offshore Processing Options for Oil Platforms. In *Proceedings of the SPE Annual Technical Conference and Exhibition*, pages 1–17 (Paper SPE 90325), Houston, USA, 2004. Society of Petroleum Engineers.

[12] Danish Energy Agency. Danmarks olie og gas produktion. Technical report, Energistyrelsen, København, Denmark, 2011.

[13] Norwegian Ministry of Petroleum and Energy. Facts 2012 – The Norwegian Petroleum Sector. Technical report, Norwegian Petroleum Directorate, Oslo, Norway, 2012.

[14] David S. Jones and Peter R. Pujadó, editors. *Handbook of Petroleum Processing*. Springer, 2006.

[15] Francis S. Manning and Richard E. Thompson. *Oilfield processing of petroleum: Natural Gas*, volume 1. PennWell Books, 1991.

[16] William C. Lyons and Gary Plisga, editors. *Standard Handbook of Petroleum & Natural Gas Engineering*. Gulf Professional Publishing, 2nd edition, 2004.

[17] Hussein K. Abdel-Aal, Mohamed Aggour, and Mohamed A. Fahim. *Petroleum and Gas Field Processing*. Chemical Industries. Marcel Dekker, 2003.

[18] Eilan A. Vik and Anthony J. Dinning. Produced Water Re-Injection - The Potential to Become an Improved Oil Recovery Method. Technical report, Aquatem A/S, Oslo, Norway, 2009.

[19] Stig M. Svalheim and Dave C. King. Life of Field Energy Performance. In *Proceedings of the SPE Offshore Europe Conference*, pages 1–10 (Paper SPE 83993), Aberdeen, UK, 2003. Society of Petroleum Engineers.

[20] Robin Vanner. Energy Use in Offshore Oil and Gas Production: Trends and Drivers for Efficiency from 1975 to 2025. PSI Working Paper, Policy Studies Institute, 2005.

[21] Stig M. Svalheim. Environmental Regulations and Measures on the Norwegian Continental Shelf. In *Proceedings of the SPE International Conference on Health, Safety and Environment in Oil and Gas Exploration and Production*, pages 1–10 (Paper SPE 73982), Kuala Lumpur, Malaysia, 2002. Society of Petroleum Engineers.

[22] Oljedirektoratet. Nei til fakling – en internasjonal utfordring, 2008. URL www.npd.no/no/Publikasjoner/Norsk-sokkel/Nr2-2008/Nei-til-fakling/.

[23] Carey Bylin, Zachary Schaffer, Vivek Goel, Donald Robinson, Alexandre do N. Campos, and Fernando Borensztein. Designing the Ideal Offshore Platform Methane Mitigation Strategy. In *Proceedings of the SPE International Conference on Health, Safety and Environment in Oil and Gas Exploration and Production*, pages 1–27 (Paper SPE 126964), Rio de Janeiro, 2010. Society of Petroleum Engineers.

[24] Kristian Sandengen. *Prediction of mineral scale formation in wet gas condensate pipelines and in MEG (mono-ethylene glycol) regeneration plants*. PhD thesis, Norges teknisk-naturvitenskapelige universitet - NTNU, 2006.

[25] Muhammad Riaz, Mustafe A. Yussuf, Michael Frost, Georgios M. Kontogeorgis, Erling H. Stenby, Wei Yan, and Even Solbraa. Distribution of Gas Hydrate Inhibitor Monoethylene

Glycol in Condensate and Water Systems: Experimental Measurement and Thermodynamic Modeling Using the Cubic-Plus-Association Equation of State. *Energy & Fuels*, 28 (5):3530–3538, 2014.

[26] Linda Garverick, editor. *Corrosion in the Petrochemical Industry*. ASM International, 1994.

[27] Srdjan Nešić. Key issues related to modelling of internal corrosion of oil and gas pipelines – A review. *Corrosion Science*, 49(12):4308–4338, 2007.

[28] Tina Puntervold and Tor Austad. Injection of seawater and mixtures with produced water into North Sea chalk formation: Impact on wettability, scale formation and rock mechanics caused by fluid-rock interaction. *Journal of Petroleum Science and Engineering*, 63(1-4):23–33, December 2008.

[29] International Union of Pure and Applied Chemistry Organic Chemistry Division. *A Guide to IUPAC Nomenclature of Organic Compounds (recommendations 1993)*. Blackwell Science, 1993.

[30] Curtis H. Whitson and Michael R. Brulé. *Phase Behavior*, volume 20 of *SPE Monograph Series*. Society of Petroleum Engineers, 2000.

[31] Econ Pöyri. CO_2-emissions effect of electrification. Technical Report R-2011-041, Statoil ASA, 2011.

[32] Magnus Korpås, Leif Warland, Wei He, and John Olav Giæver Tande. A Case-Study on Offshore Wind Power Supply to Oil and Gas Rigs. *Energy Procedia*, 24:18–26, 2012.

[33] Wei He, Kjetil Uhlen, Mahesh Hadiya, Zhe Chen, Gang Shi, and Emilio del Rio. Case study of Integrating an Offshore Wind Farm with Offshore Oil and Gas Platforms and with an Onshore Electrical Grid. *Journal of Renewable Energy*, 2013(ID 607165):1–11, 2013.

[34] Atle R. Ardal, Kamran Sharifabadi, Oyvind Bergvoll, and Vidar Berge. Challenges with integration and operation of offshore oil & gas platforms connected to an offshore wind power plant. In *Proceedings of the Petroleum and Chemical Industry Conference Europe*, pages 1–9. IEEE, 2014.

[35] Bernhard Thomé, editor. *Principles and Practice of Computer-based Systems Engineering*. Software Based Systems. John Wiley and Sons, 1993.

[36] Arthur W. Westerberg, H. P. Hutchison, Rodolphe L. Motard, and Peter Winter. *Process Flowsheeting*. Cambridge Universities Press, 1979.

[37] Invensys Systems. *Pro/II Academic manual*. Lake Forest, USA, 2007.

[38] WinSim. *DESIGN II for Windows – Tutorial and Samples – Version 12.0*. ChemShare Corporation, Richmond, USA, 2014.

[39] Aspen Technology. *Aspen Plus – Modelling Petroleum Processes*. Burlington, USA, 1999.

[40] Belsim. *Belsim VALI User's Guide*. Belsim, 2011.

[41] Process Systems Enterprise. *gPROMS Introductory User Guide*. London, UK, 2004.

[42] Aspen Technology. *Aspen Energy Analyzer*. Burlington, USA, 2008.

[43] Aspen Technology. *Aspen Flare System Analyzer – Getting Started Guide*. Burlington, USA, 2011.

[44] Jan Szargut, David R. Morris, and Frank R. Steward. *Exergy Analysis of Thermal, Chemical, and Metallurgical Processes*. Hemisphere, 1st edition, 1988.

[45] Von P. Grassmann. Zur allgemeinen Definition des Wirkungsgrades. *Chemie Ingenieur Technik*, 4(1):77–80, 1950.

[46] Kurt Nesselmann. Der Wirkungsgrad thermodynamischer Prozesse und sein Zusammenhang mit der Umgebungtemperatur. *Allgemeine Wärmetechnik*, 4(7):141–147, 1953.

[47] Hans D. Baehr. *Energie und Exergie – Die Anwendung des Exergiebegriffs in der Energietechnik*. VDI-Verlag, 1965.

[48] Hans D. Baehr. Zur Definition exergetischer Wirkungsgrade – Eine systematische Untersuchung. *Brennstoff-Wärme-Kraft*, 20(5):197–200, 1968.

[49] G. Kostenko. Efficiency of Heat Processes (in Russian). *Promishlenaya Teplotechnika*, 4: 70–73, 1983.

[50] George Tsatsaronis. Combination of Exergetic and Economic Analysis in Energy-Conversion Processes. In *Energy Economics and Management in Industry, Proceedings of the European Congress*, volume 1, pages 151–157, Oxford, UK, 1984. Pergamon Press.

[51] Andrea Lazzaretto and George Tsatsaronis. On the calculation of efficiencies and costs in thermal systems. In Salvador M. Aceves, S. Garimella, and Richard B. Peterson, editors, *Proceedings of the ASME Advanced Energy Systems Division*, volume 39, pages 421–430, New York, USA, 1999.

[52] Andrea Lazzaretto and George Tsatsaronis. SPECO: A systematic and general methodology for calculating efficiencies and costs in thermal systems. *Energy*, 31:1257–1289, 2006.

[53] Michael J. Moran. *Availability analysis: a guide to efficient energy use*. ASME Press, 2nd edition, 1989.

[54] Tadeusz J. Kotas. *The Exergy Method of Thermal Plant Analysis*. Krieger Publishing, 1995.

[55] Ricardo Rivero and Alejandro Anaya. Exergy analysis of a distillation tower for crude oil fractionation. In George Tsatsaronis, editor, *Computer Aided Energy Systems Analysis*, pages 55–62, New York, USA, 1990.

[56] Reinerus L. Cornelissen. *Thermodynamics and sustainable development – The use of exergy analysis and the reduction of irreversibility*. PhD thesis, Universiteit Twente, Enschede, The Netherlands, 1997.

[57] Yaşar Demirel. Thermodynamic Analysis of Separation Systems. *Separation science and technology*, 39(16):3897–3942, 2004.

[58] Husain Al-Muslim and Ibrahim Dincer. Thermodynamic analysis of crude oil distillation systems. *International Journal of Energy Research*, 29(7):637–655, 2005.

[59] Silvio de Oliveira Jr. and Marco Van Hombeeck. Exergy Analysis of Petroleum Separation Processes in Offshore Platforms. *Energy Conversion and Management*, 38(15-17):1577–1584, 1997.

[60] Bodo Linnhoff. New concepts in thermodynamics for better chemical process design. *Chemical Engineering Research and Design*, 61(4):207–223, 1983.

[61] Bodo Linnhoff. Pinch technology for the synthesis of optimal heat and power systems. *Journal of Energy Resources Technology, Transactions of the ASME*, 111(3):137–147, 1989.

[62] Bodo Linnhoff and Francisco J. Alanis. Integration of a new process into an existing site. a case study in the application of pinch technology. *Journal of Engineering for Gas Turbines and Power*, 113(2):159–169, 1991.

[63] Ian C. Kemp. *Pinch Analysis and Process Integration – A User Guide on Process Integration for the Efficient Use of Energy*. Elsevier, 2nd edition, 2006.

[64] Vikas Dhole and Bodo Linnhoff. Total site targets for fuel co-generation, emissions, and cooling. *Computers and Chemical Engineering*, 17:101–109, 1993.

[65] Bodo Linnhoff and Vikas R. Dhole. Targeting for CO_2 emissions for total sites. *Chemical Engineering and Technology*, 16(4):252–259, 1993.

[66] Bodo Linnhoff and Alan R. Eastwood. Overall site optimization by pinch technology. *Process Safety and Environmental Protection: Transactions of the Institution of Chemical Engineers, Part B*, 75(Suppl):S138–S144, 1997.

[67] Jiři J. Klemeš, Vikas R. Dhole, Kalliopi Raissi, Simon J. Perry, and Luis Puigjaner. Targeting and design methodology for reduction of fuel, power and co_2 on total sites. *Applied Thermal Engineering*, 7(8-10):993–1003, 1997.

[68] Jiři J. Klemeš, Ferenc Friedler, Igor Bulatov, and Petar S. Varbanov. *Sustainability in the process industry: integration and optimization*. McGraw-Hill Professional, 2011.

[69] Yaping Wang and Robin Smith. Wastewater minimisation. *Chemical Engineering Science*, 49(7):981–1006, 1944.

[70] Alberto Alva-Argáez, Antonis C. Kokossis, and Robin Smith. Wastewater minimisation of industrial systems using an integrated approach. *Computers & Chemical Engineering*, 22(1):S741–S744, 1998.

[71] Joao J. Alves and Gavin P. Towler. Analysis of Refinery Hydrogen Distribution Systems. *Industrial & Engineering Chemistry Research*, 41(23):5759–5769, 2002.

[72] Nick Hallale, Ian Moore, and Dennis Vauk. Hydrogen optimisation at minimal investment. Technical report, Petroleum Technology Quarterly (PTQ), 2003.

[73] Xiao Feng, Jing Pu, Junkun Yang, and Khim Hoong Chu. Energy recovery in petrochemical complexes through heat integration retrofit analysis. *Applied Energy*, 88:1965–1982, 2011.

[74] Kazuo Matsuda, Yoshiichi Hirochi, Hiroyuki Tatsumi, and Tim Shire. Applying heat integration total site based pinch technology to a large industrial area in Japan to further improve performance of highly efficient process plants. *Energy*, 34(10):1687–1692, 2009.

[75] Kew H. Chew, Jiři J. Klemeš, Sharifah R. Wan Alwi, and Zainuddin Abdul Manan. Industrial implementation issues of total site heat integration. *Applied Thermal Engineering*, 2013.

[76] Adrian Bejan, George Tsatsaronis, and Michael J. Moran. *Thermal Design & Optimization*. John Wiley & Sons, 1996.

[77] Klaus D. Timmerhaus, Max S. Peters, and Ronald E. West. *Plant design and economics for chemical engineers*, volume 4. McGraw-Hill, 1991.

[78] Gael D. Ulrich. *A guide to chemical engineering process design and economics*. Wiley, 1984.

[79] Richard Turton, Richard C. Bailie, Wallace B. Whiting, Joseph A. Shaeiwitz, and Debangsu Bhattacharyya. *Analysis, Synthesis and Design of Chemical Processes*. Prentice Hall International Series in the Physical and Chemical Engineering Sciences. Prentice Hall, 4th edition, 2012.

[80] Steve Begg and Reidar Bratvold. The Value of Flexibility in Managing Uncertainty in Oil and Gas Investments. In *Proceedings of the SPE Annual Technical Conference and Exhibition*, pages 1–10 (Paper SPE 77586), San Antonio, USA, 2002. Society of Petroleum Engineers.

[81] Norwegian Ministry of Petroleum and Energy. The Petroleum Resources on the Norwegian Continental Shelf. Technical report, Norwegian Petroleum Directorate, Oslo, Norway, 1997.

[82] Klaus Mohn and Bård Misund. Investment and uncertainty in the international oil and gas industry. *Energy Economics*, 31(2):240–248, 2009.

[83] Irene Henriques and Perry Sadorsky. The effect of oil price volatility on strategic investment. *Energy Economics*, 33(1):79–87, 2011.

[84] Saul B. Suslick, Denis Schiozer, and Monica R. Rodriguez. Uncertainty and risk analysis in petroleum exploration and production. *Terræ*, 6(1):30–41, 2009.

[85] Hans P. Bieker, Olav Slupphaug, and Tor A. Johansen. Well Management Under Uncertain Gas or Water Oil Ratios. In *Proceedings of the SPE Digital Energy Conference and Exhibition*, pages 1–6 (Paper SPE 106959), Houston, USA, 2007. Society of Petroleum Engineers.

[86] Pierre Senécal, Bernice Goldsmith, Shirley Conover, Barry Sadler, and Karen Brown. Principles of environmental impact assessment best practice. Special Publication, International Association for Impact Assessment, Fargo, USA, 1999.

[87] Life cycle assessment – Principles and framework, 2006.

[88] Gerald Rebitzer, Tomas Ekvall, Rolf Frischknecht, Davis Hunkeler, Gregory A. Norris, Tomas Rydberg, Wulf-Peter Schmidt, Sangwon Suh, Bo P. Weidema, and David W. Pennington. Life cycle assessment: Part 1: Framework, goal and scope definition, inventory analysis, and applications. *Environment International*, 30(5):701–720, 2004.

[89] Gerald Rebitzer, Olivier Jolliet, Tomas Ekvall, Tomas Rydberg, David W. Pennington, Göran Finnveden, Erwin Leinjeijer, and José Potting. Life cycle assessment Part 2: Current impact assessment practice. *Environment International*, 30(5):721–739, 2004.

[90] Hans-Jörg Althaus, Christian Bauer, Gabor Doka, Roberto Dones, Rolf Frischknecht, Stefanie Hellweg, Sébastien Humbert, Niels Jungbluth, Thomas Köllner, Yves Loerincik, Manuele Margni, and Thomas Nemecek. Implementation of Life Cycle Impact Assessment Methods. Ecoinvent data v2.1 3, Swiss Centre for Life Cycle Inventories, St. Gallen, Switzerland, 2009.

[91] Göran Finnveden, Michael Z. Hauschild, Tomas Ekvall, Jeroen Guinée, Reinout Heijungs, Stefanie Hellweg, Annette Koehler, David Pennington, and Sangwon Suh. Recent developments in Life Cycle Assessment. *Journal of Environmental Management*, 91(1): 1–21, 2009.

[92] Tom McCann and Phil Magee. Crude Oil Greenhouse Gas Life Cycle Analysis Helps Assign Values for CO_2 Emissions Trading. *Oil & Gas Journal*, 97(8):1–5, 1999.

[93] U.S. Environmental Protection Agency. An Assessment of the Environmental Implications of Oil and Gas Production: A Regional Case Study. Working Draft, U.S. Environmental Protection Agency, 2008.

[94] Aranya Venkatesh, Paulina Jaramillo, W. Michael Griffin, and H. Scott Matthews. Uncertainty Analysis of Life Cycle Greenhouse Gas Emissions from Petroleum-Based Fuels and Impacts on Low Carbon Fuel Policies. *Environmental Science & Technology*, 45(1): 125–131, 2011.

[95] Andrew Burnham, Jeongwoo Han, Corrie E. Clark, Michael Wang, Jennifer B. Dunn, and Ignasi Palou-Rivera. Life-Cycle Greenhouse Gas Emissions of Shale Gas, Natural Gas, Coal, and Petroleum. *Environmental Science & Technology*, 46(2):619–627, 2011.

[96] Joseph H. Keenan. A steam chart for second law analysis. *ASME Mechanical Engineering*, 54(3):195–204, 1932.

[97] Antonio Valero, Miguel A. Lozano, and Rodríguez Muñoz. A General Theory of Exergy Saving: Part I. On the Exergetic Cost, Part II. On the Thermoeconomic Cost, Part III. Energy Saving and Thermoeconomics. In Richard A. Gaggioli, editor, *Computer-Aided Engineering of Energy Systems*, volume 3, pages 1–22, New York, USA, 1986.

[98] Andrea Toffolo and Andrea Lazzaretto. A New Thermoeconomic Method for the Location of Causes of Malfunctions in Energy Systems. *Journal of Energy Resources Technology*, 129(1):1–9, 2007.

[99] Vittorio Verda and Romano Borchiellini. Exergy method for the diagnosis of energy systems using measured data. *Energy*, 32(4):490–498, 2007.

[100] Ricardo Rivero, Consuelo Rendón, and Salvador Gallegos. Exergy and exergoeconomic analysis of a crude oil combined distillation unit. *Energy*, 29(12–15):1909–1927, 2004.

[101] Celso Y. Nakashima, Silvio de Oliveira Jr., and Elisio F. Caetano. Subsea multiphase pumping system x gas lift: an exergo-economic comparison. *Engenharia Térmica*, 3(3): 107–114, 2004.

[102] Julio A.M. Silva, Daniel Flórez-Orrego, and Silvio de Oliveira Jr. An exergy based approach to determine production cost and CO_2 allocation for petroleum derived fuels. *Energy*, 67:490–495, 2014.

[103] Marc A. Rosen and Ibrahim Dincer. On exergy and environmental impact. *International Journal of Energy Research*, 21(7):643–654, 1998.

[104] Marc A. Rosen and Ibrahim Dincer. Exergy analysis of waste emissions. *International Journal of Energy Research*, 23(13):1153–1163, 1999.

[105] Jo Dewulf, Herman Van Langenhove, and Jeroen Dirckx. Exergy analysis in the assessment of the sustainability of waste gas treatment systems. *Science of the Total Environment*, 273(1–3):41–52, 2001.

[106] Jo Dewulf and Herman Van Langenhove. Assessment of the Sustainability of Technology by Means of a Thermodynamically Based Life Cycle Analysis. *Environmental Science and Pollution Research*, 9(4):267–273, 2002.

[107] Jan Szargut and David R. Morris. Cumulative exergy consumption and cumulative degree of perfection of chemical processes. *Energy Research*, 11(2):245–261, 1987.

[108] Jan Szargut, Andrzej Ziebik, and Wojciech Stanek. Depletion of the non-renewable natural exergy resources as a measure of the ecological cost. *Energy Conversion and Management*, 43(9–12):1149–1163, 2002.

[109] Mei Gong and Göran Wall. On exergetics, economics and optimization of technical processes to meet environmental conditions. In Ruixian Cai, editor, *Proceedings of TAIES'97, the International Conference on Thermodynamic Analysis and Improvement of Energy Systems, Thermodynamic Analysis and Improvement of Energy Systems*, pages 453–460, Beijing, China, 1997. Chinese Society of Engineering Thermophysics and American Society of Mechanical Engineers.

[110] Reinerus L. Cornelissen and Gerard G. Hirs. The value of the exergetic life cycle assessment besides the LCA. *Energy Conversion and Management*, 43(9–12):1417–1424, 2002.

[111] Bram De Meester, Jo Dewulf, Arnold Janssens, and Herman Van Langenhove. An improved calculation of the energy of natural resources for exergetic life cycle assessment (ELCA). *Environmental Science & Technology*, 40(21):6844–6851, 2006.

[112] Lutz Meyer, George Tsatsaronis, Jens Buchgeister, and Liselotte Schebek. Exergoenvironmental analysis for evaluation of the environmental impact of energy conversion systems. *Energy*, 34(1):75–89, 2009.

[113] Jo Dewulf, Michael E. Bösch, Bram De Meester, Geert Van der Vorst, Herman Van Langenhove, Stephanie Hellweg, and Mark A.J. Huijbregts. Cumulative Exergy Extraction from the Natural Environment (CEENE): a comprehensive Life Cycle Impact Assessment method for resource accounting. *Environmental Science & Technology*, 41(24):8477–8483, 2007.

[114] Morris Muskat. *Physical Principles of Oil Production*. Springer, 1981.

[115] Stortinget. Lov om petroleumsvirksomhet [petroleumsloven]. Technical Report 72, OED (Olje- og energidepartementet), 29 November 1996.

[116] Finansdepartementet. Skatter og avgifter: green taxes, 2011. URL www.regjeringen.no/nb/dep/fin/tema/skatter_og_avgifter/green-taxes-2011.html?id=609076.

[117] Mari Voldsund, Wei He, Audun Røsjorde, Ivar S. Ertesvåg, and Signe Kjelstrup. Evaluation of the Oil and Gas Processing at a Real Production day on a North Sea Oil Platform Using Exergy Analysis. In Umberto Desideri, Giampaolo Manfrida, and Enrico Sciubba, editors, *Proceedings of ECOS 2012 – The 25th International Conference on Efficiency, Cost, Optimization, Simulation and Environmental Impact of Energy Systems*, volume II, pages 153–166, Perugia, Italy, 2012. Firenze University Press.

[118] Lars O. Nord and Olav Bolland. Steam bottoming cycles offshore – challenges and possibilities. *Journal of Power Technologies*, 92(3):201–207, 2013.

[119] Lars O. Nord and Olav Bolland. Design and off-design simulations of combined cycles for offshore oil and gas installations. *Applied Thermal Engineering*, 54:85–91, 2013.

[120] Pål Kloster. Energy Optimization on Offshore Installations with Emphasis on Offshore and Combined Cycle Plants. In *Proceedings of the Offshore Europe Conference*, pages 1–9 (Paper SPE 56964), Aberdeen, UK, 1999. Society of Petroleum Engineers.

[121] Pål Kloster. Reduction of Emissions to Air Through Energy Optimisation on Offshore Installations. In *Proceedings of the SPE International Conference on Health, Safety, and the Environment in Oil and Gas Exploration and Production*, pages 1–7 (Paper SPE 61651), Stavanger, Norway, 2000. Society of Petroleum Engineers.

[122] Harald T. Walnum, Petter Nekså, Lars O. Nord, and Trond Andresen. Modelling and simulation of CO_2 (carbon dioxide) bottoming cycles for offshore oil and gas installations at design and off-design conditions. *Energy*, 59:513–520, 2013.

[123] Daniel Rohde, Harald T. Walnum, Trond Andresen, and Petter Nekså. Heat recovery from export gas compression: Analyzing power cycles with detailed heat exchanger models. *Applied Thermal Engineering*, 60(1–2):1–6, 2013.

[124] Audrey Estublier and Alf S. Lackner. Long-term simulation of the snøhvit co_2 storage. *Energy Procedia*, 1(1):3221–3228, 2009.

[125] Klaas van Alphen, Jochem Van Ruijven, Sjur Kasa, Marko Hekkert, and Wim Turkenburg. The performance of the Norwegian carbon dioxide, capture and storage innovation system. *Energy Policy*, 37(1):43–55, 2009.

[126] Klaas van Alphen, Marko P. Hekkert, and Wim C. Turkenburg. Accelerating the deployment of carbon capture and storage technologies by strengthening the innovation system. *International Journal of Greenhouse Gas Control*, 4(2):396–409, 2010.

[127] Alan Baklid, Ragnhild Korbol, and Geir Owren. Sleipner Vest CO_2 Disposal, CO_2 Injection Into A Shallow Underground Aquifer. In *Proceedings of the SPE Annual Technical Conference and Exhibition*, pages 1–9 (Paper SPE 36600), Denver, USA, 1996. Society of Petroleum Engineers.

[128] Olav Falk-Pedersen, Yngvil Bjerve, Geir Glittum, and Svein Rønning. Separation of carbon dioxide from offshore gas turbine exhaust. *Energy Conversion and Management*, 36(6–9):393–396, 1995.

[129] Francis S. Manning and Richard E. Thompson. *Oilfield processing of petroleum: Crude oil*, volume 2. PennWell Books, 1991.

[130] Ricardo Rivero, Consuelo Rendon, and Leodegario Monroy. The Exergy of Crude Oil Mixtures and Petroleum Fractions: Calculation and Application. *International Journal of Applied Thermodynamics*, 2(3):115–123, 1999.

[131] Ricardo Rivero. Application of the exergy concept in the petroleum refining and petrochemical industry. *Energy Conversion and Management*, 43(9-12):1199–1220, June 2002.

[132] Mari Voldsund, Ivar S. Ertesvåg, Audun Røsjorde, Wei He, and Signe Kjelstrup. Exergy Analysis of the Oil and Gas Separation Processes on a North Sea Oil Platform. In Daniel Favrat and François Maréchal, editors, *Proceedings of ECOS 2010 – The 23rd International Conference on Efficiency, Cost, Optimization, Simulation and Environmental Impact of Energy Systems*, volume IV Power plants & Industrial Processes, pages 303–310, Lausanne, Switzerland, 2010. CreateSpace Independent Publishing Platform.

[133] Raffaele Bolliger. *Méthodologie de la synthèse des systèmes énergétiques industriels*. PhD thesis, École Polytechnique Fédérale de Lausanne, 2010.

[134] Göran Wall. *Encyclopedia of Energy*, volume 2, chapter Exergy, pages 593–606. Academic Press, 2004.

[135] Geoffrey P. Hammond. Industrial energy analysis, thermodynamics and sustainability. *Applied Energy*, 84:675–700, 2007.

[136] Michael J. Moran and Howard N. Shapiro. *Fundamentals of Engineering Thermodynamics*. John Wiley & Sons, 6th edition, 2007.

[137] Vadim M. Brodyansky, Mikhaïl V. Sorin, and Pierre Le Goff. *The Efficiency of Industrial Processes: Exergy Analysis and Optimization*. Elsevier, 1994.

[138] Michael J. Moran. Fundamentals of exergy analysis and exergy-based thermal systems design. In Adrian Bejan and Eden Mamut, editors, *Proceedings of the NATO Advanced Study Institute on Thermodynamic Optimization of Complex Energy Systems*, volume 69 of *NATO Science Series*, pages 73–92, Neptun, Romania, 1998. Kluwer Academic Publishers.

[139] Bodo Linnhoff and Robin Smith. Pinch principle. *Mechanical Engineering*, 110(2):70–73, 1988.

[140] François Maréchal and Boris Kalitventzeff. Energy integration of industrial sites: Tools, methodology and application. *Applied Thermal Engineering*, 18(11):921–933, 1998.

[141] Jiři J. Klemeš and Petar S. Varbanov. Heat integration including heat exchangers, combined heat and power, heat pumps, separation processes and process control. *Applied Thermal Engineering*, 43:1–6, 2012.

[142] Jeroen B. Guinée, Marieke Gorrée, Reinout Heijungs, Gjalt Huppes, René Kleijn, Arjan de Koning, Lauran van Oers, Anneke Wegener S., Sangwon Suh, Helias A. Udo de Haes, Hans de Bruijn, Robbert van Duin, and Mark A.J. Huijbregts. *Handbook on life cycle assessment. Operational guide to the ISO standards. I: LCA in perspective. IIa: Guide. IIb: Operational annex. III: Scientific background.* Kluwer Academic Publishers, 2002.

[143] Helen Becker and François Maréchal. Energy integration of industrial sites with heat exchange restrictions. *Computers and Chemical Engineering*, 37:104–118, 2012.

[144] Laurence Tock. *Thermo-environomic optimisation of fuel decarbonisation alternative processes for hydrogen and power production.* PhD thesis, École Polytechnique Fédérale de Lausanne, 2013.

[145] Léda Gerber. *Integration of Life Cycle Assessment in the conceptual design of renewable energy conversion systems.* PhD thesis, École Polytechnique Fédérale de Lausanne, 2012.

[146] Emanuele Facchinetti. *Integrated Solid Oxide Fuel Cell: Gas Turbine Hybrid Systems with or without CO_2 Separation.* PhD thesis, École Polytechnique Fédérale de Lausanne, 2012.

[147] Aspen Technology. *Aspen Hysys 2004.2 ®– User Guide.* Cambridge, USA, 2004.

[148] Aspen Technology. *Aspen Energy Analyzer 7.0 ®– User Guide.* Cambridge, USA, 2008.

[149] Brian Elmegaard and Niels Houbak. DNA – A General Energy System Simulation Tool. In J. Amundsen, editor, *Proceedings of SIMS 2005 - 46th Conference on Simulation and Modeling*, pages 43–52, Trondheim, Norway, 2005. Tapir Academic Press.

[150] Sanford A. Klein. *EES – Engineering Equation Solver for MIcrosoft Windows Operating Software.* F-Chart Software, 2013.

[151] Matlab ®Primer R2013b, 2013.

[152] François Maréchal and Boris Kalitventzeff. Targeting the optimal integration of steam networks: Mathematical tools and methodology. *Computers and Chemical Engineering*, 23(SUPPL. 1):S133–S136, 1999.

[153] Bruce A. Finlayson. *Introduction to chemical engineering computing.* John Wiley & Sons, 2012.

[154] Robin Smith. *Chemical Process: Design and Integration*, volume 50. John Wiley & Sons, 2005.

[155] Ignacio E. Grossmann and Arthur W. Westerberg. Research challenges in process systems engineering. *AIChE Journal*, 46(9):1700–1703, 2000.

[156] Arthur W. Westerberg. A retrospective on design and process synthesis. *Computers & Chemical engineering*, 28(4):447–458, 2004.

[157] Scott D. Barnicki and Jeffrey J. Siirola. Process synthesis prospective. *Computers & Chemical engineering*, 28(4):441–446, 2004.

[158] James G. Speight. *Handbook of industrial hydrocarbon processes*. Gulf Professional Publishing, 2010.

[159] Johannes D. van der Waals. *On the Continuity of the Gaseous and Liquid States*. Elsevier, 2004.

[160] P. H. Van Konynenburg and R. L. Scott. Critical Lines and Phase Equilibria in Binary Van Der Waals Mixtures. *Philosophical Transactions of the Royal Society of London*, 298 (1442):495–540, 1980.

[161] Wolfgang R. Wagner and Andreas Pruβ. The IAPWS formulation 1995 for the thermodynamic properties of ordinary water substance for general and scientific use. *Journal of Physical and Chemical Reference Data*, 31(3):387–535, 2002.

[162] Giorgio Soave. Equilibrium constants from a modified Redlich–Kwong equation of state. *Chemical Engineering Science*, 27(6):1197–1203, 1972.

[163] Ding-Yu Peng and Donald B. Robinson. A New Two-Constant Equation of State. *Industrial & Engineering Chemistry Fundamentals*, 15(1):59–64, February 1976.

[164] Constantine Tsonopoulos and John L. Heidman. From Redlich-Kwong to the present. *Fluid phase equilibria*, 24(1):1–23, 1985.

[165] Giorgio Soave. 20 years of Redlich–Kwong equation of state. *Fluid Phase Equilibria*, 82: 345–359, 1993.

[166] Chorng H. Twu, Wayne D. Sim, and Vince Tassone. A versatile liquid activity model for SRK, PR and a new cubic equation-of-state TST. *Fluid Phase Equilibria*, 194–197: 385–399, 2002.

[167] Jacques Schwartzentruber and Henri Renon. Extension of UNIFAC to High Pressures and Temperatures by the Use of a Cubic Equation of State. *Industrial & Engineering Chemistry Research*, 28(7):1049–1055, 1989.

[168] Jacques Schwartzentruber, Henri Renon, and Suphat Watanasiri. Development of a new cubic equation of state for phase equilibrium calculations. *Fluid Phase Equilibria*, 52: 127–134, 1989.

[169] Henri Renon and John M. Prausnitz. Local compositions in thermodynamic excess functions for liquid mixtures. *AIChE Journal*, 14(1):135–144, January 1968.

[170] Chau-Chyun Chen, Herbert I. Britt, Joseph F. Boston, and Lawrence B. Evans. Local composition model for excess Gibbs energy of electrolyte systems. Part I: Single solvent, single completely dissociated electrolyte systems. *AIChE Journal*, 28(4):588–596, 1982.

[171] Joachim Gross and Gabriele Sadowski. Perturbed-Chain SAFT: An Equation of State Based on a Perturbation Theory for Chain Molecules. *Industrial & Engineering Chemistry Research*, 40(4):1244–1260, 2001.

[172] Mari Voldsund, Ivar S. Ertesvåg, Wei He, and Signe Kjelstrup. Exergy Analysis of the Oil and Gas Processing a Real Production Day on a North Sea Oil Platform. *Energy*, 55: 716–727, 2013.

[173] Mari Voldsund, Tuong-Van Nguyen, Brian Elmegaard, Ivar S. Ertesvåg, Audun Røsjorde, Knut Jøssang, and Signe Kjelstrup. Exergy destruction and losses on four North Sea offshore platforms: A comparative study of the oil and gas processing plants. *Energy*, 2014. doi: 10.1016/j.energy.2014.02.080.

[174] Eivind Dahl, Eivind Dykesteen, Endre Jacobsen, Erik Malde, Frode Flåten, Hallvard Tunheim, Morten Brandt, Ronny Albrechtsen, Ottar Vikingstad, Sidsel E. Corneliussen, and Trond Hjorteland. *Handbook of Water Fraction Metering*. Norsk Forening for Olje og gassmåling, 2004.

[175] LEVON Group and LLC and URS Corporation. Addressing uncertainty in oil and natural gas industry greenhouse gas inventories – Technical considerations and calculation methods. Technical report, International Petroleum Industry Environmental Conservation Association, 2009.

[176] Sidsel Corneliussen, Jean-Paul Couput, Eivind Dahl, Eivind Dykesteen, Kjell-Eivind Frøysa, Erik Malde, Håkon Moestue, Paul O. Moksnes, Lex Scheers, and Hallvard Tunheim. *Handbook of Multiphase Flow Metering*. Norsk Forening for Olje og gassmåling, 2005.

[177] Standards Norway. NORSOK Standard – Fiscal measurement systems for hydrocarbon gas. Technical report, Standards Norway, 2005.

[178] Standards Norway. NORSOK Standard – Fiscal measurement systems for hydrocarbon liquid. Technical report, Standards Norway, 2007.

[179] Norwegian Petroleum Directorate. Standards relating to measurement of petroleum for fiscal purposes and for calculation of CO_2-tax. Technical report, Norwegian Petroleum Directorate, 2012.

[180] Göran Wall. Exergy flows in industrial processes. *Energy*, 13(2):197–208, 1988.

[181] Tadeusz J. Kotas. Exergy concepts for thermal plant: First of two papers on exergy techniques in thermal plant analysis. *International Journal of Heat and Fluid Flow*, 2(3): 105–114, September 1980. ISSN 0142727X.

[182] Tadeusz J. Kotas. Exergy Criteria of Performance for Thermal Plant: Second of two papers on exergy techniques in thermal plant analysis. *International Journal of Heat and Fluid Flow*, 2(4):147–163, 1980.

[183] Adrian Bejan. *Advanced Engineering Thermodynamics*. John Wiley & Sons, 3rd edition, 2006.

[184] Joachim Ahrendts. *Die Exergie chemisch reaktionsfähiger Systeme*, volume 43. VDI-Verlag, 1977.

[185] George Tsatsaronis. Thermoeconomic analysis and optimization of energy systems. *Progress in Energy and Combustion Science*, 19:227–257, 3 1993.

[186] Norio Sato. *Chemical Energy and Exergy: An Introduction to Chemical Thermodynamics for Engineers*. Elsevier, 1st edition, 2004.

[187] George Tsatsaronis. Definitions and nomenclature in exergy analysis and exergoeconomics. *Energy*, 32(4):249–253, 2007.

[188] Jan Szargut. Exergy in the thermal systems analysis. In A. Bejan and E. Mamut, editors, *Proceedings of the NATO Advanced Study Institute on Thermodynamic Optimization of Complex Energy Systems*, volume 69 of *NATO Science Series*, pages 137–150, Neptun, Romania, 1998. Kluwer Academic Publishers.

[189] Lucien Borel and Daniel Favrat. *Thermodynamics and Energy Systems Analysis: From Energy to Exergy*. EPFL Press, 2010.

[190] Solange Kelly, George Tsatsaronis, and Tatiana Morosuk. Advanced exergetic analysis: Approaches for splitting the exergy destruction into endogenous and exogenous parts. *Energy*, 34(3):384–391, March 2009. ISSN 03605442.

[191] George Tsatsaronis and Moung-Ho Park. On avoidable and unavoidable exergy destructions and investment costs in thermal systems. *Energy Conversion and Management*, 43:1259–1270, 2002.

[192] George Tsatsaronis, Solange Kelly, and Tatiana Morosuk. Endogenous and exogenous exergy destruction in thermal systems. In *Proceedings of IMECE2006 (2006 ASME International Mechanical Engineering Congress and Exposition*, Chicago, USA, 2006. ASME.

[193] Bodo Linnhoff and David Boland. *A user guide on process integration for the efficient use of energy*. Elsevier, 1982.

[194] Zsófia Fodor, Jiři J. Klemeš, and Petar S. Varbanov. Total site targeting accounting for individual process heat transfer characteristics. *Energy*, 44(1):20–28, 2012.

[195] Salmiah Ahmad and Bodo Linnhoff. Supertargeting: different process structures for different economics. *Journal of Energy Resources Technology, Transactions of the ASME*, 111(3):131–136, 1989.

[196] Soterios A. Papoulias and Ignacio E. Grossmann. A structural optimization approach in process synthesis – II: Heat recovery networks. *Computers & Chemical Engineering*, 7 (6):707–721, 1983.

[197] Miguel Bagajewicz and Hernán Rodera. Energy savings in the total site heat integration across many plants. *Computers and Chemical Engineering*, 24(2–7):1237–1242, 2000.

[198] Miguel Bagajewicz and Hernán Rodera. Multiple Plant Heat Integration in a Total Site. *AIChE Journal*, 48(10):2255–2270, 2001.

[199] David W. M. Brown, François Maréchal, and Jean Paris. A dual representation for targeting process retrofit, application to a pulp and paper process. *Applied Thermal Engineering*, 25(7 SPEC. ISS.):1067–1082, 2005.

[200] Léda Gerber, Martin Gassner, and François Maréchal. Systematic integration of lca in process systems design: Application to combined fuel and electricity production from lignocellulosic biomass. *Computers and Chemical Engineering*, 35(7):1265–1280, 2011.

[201] Swiss Centre for Life Cycle Inventories. Ecoinvent, 2013. URL www.ecoinvent.org.

[202] Christopher A. Mattson and Achille Messac. Pareto Frontier Based Concept Selection under Uncertainty, with Visualization. *OPTE: Optimization and Engineering*, 6(1):85–115, 2005.

[203] Geoffrey Basil Leyland. *Multi-objective optimisation applied to industrial energy problems*. PhD thesis, École Polytechnique Fédérale de Lausanne, 2002.

[204] Karl Pearson. Note on Regression and Inheritance in the Case of Two Parents. *Proceedings of the Royal Society of London*, 58:240–242, 1895.

[205] Maurice Kendall and Alan Stuart. *The Advanced Theory of Statistics*, volume 2. Charles Griffin, 1961.

[206] Tuong-Van Nguyen, Leonardo Pierobon, Brian Elmegaard, Fredrik Haglind, Peter Breuhaus, and Mari Voldsund. Exergetic assessment of energy systems on North Sea oil and gas platforms. *Energy*, 62:23–36, 2013.

[207] SIEMENS. SGT-500 Industrial Gas Turbine. Technical report, Siemens Industrial Turbomachinery AB, Finnspong, Sweden, 2011.

[208] Alexandre C. Dimian. *Integrated Design and Simulation of Chemical Processes*. Elsevier, 2003.

[209] Ingeniøren/bøger. *Pumpe Ståbi*. Ingeniøren A/S 2000, 2000.

[210] Sulzer Pumps. *Centrifugal Pump Handbook*. Elsevier, 3rd edition, 2010.

[211] William P. Hancock. Development of a Reliable Gas Injection Operation for the North Sea's Largest-Capacity Production Platform, Statfjord A. *Journal of Petroleum Technology*, 35(11):1963–1972, 1983.

[212] George Tsatsaronis and Michael Winhold. Exergoeconomic analysis and evaluation of energy-conversion plants – I. A new general methodology. *Energy*, 10(1):69–80, 1985.

[213] George Tsatsaronis and Frank Cziesla. *Encyclopedia of Physical Science and Technology*, volume 16, chapter Thermoeconomics, pages 659–680. Academic Press, 3rd edition, 2002.

[214] Tuong-Van Nguyen, Tomasz Jacyno, Peter Breuhaus, Mari Voldsund, and Brian Elmegaard. Thermodynamic analysis of an upstream petroleum plant operated on a mature field. *Energy*, 68:454–469, 2014.

[215] Tuong-Van Nguyen, Tamás Gábor Fülöp, Peter Breuhaus, and Brian Elmegaard. Life performance of oil and gas offshore platforms –site-scale integration and exergy-based assessment. *Energy*, 73:282–301, 2014.

[216] Edgar G. Hertwich, Martin Aaberg, Bhawna Singh, and Anders H. Strømman. Life-cycle assessment of carbon dioxide capture for enhanced oil recovery. *Chinese Journal of Chemical Engineering*, 16(3):343–353, 2008.

[217] Nick Terdre. CO_2 for EOR off Norway under study, 2007. URL www.offshore-mag.com/articles/print/volume-67/issue-9/production/co2-for-eor-off-norway-under-study.html.

[218] REUTERS. Statoil, shell shelve draugen field co_2 injection, 2007. URL www.reuters.com/article/2007/06/29/environment-statoil-shell-co2-dc-idUSL2917344820070629.

[219] Stortinget. Lov om avgift på utslipp av CO_2 i petroleumsvirksomhet på kontinentalsokkelen. Technical Report 72, Finansdepartementet, 21 December 1990.

[220] K. J. Li. Use of a Fractionation Column in an Offshore Environment. In *Proceedings of the SPE Annual Technical Conference and Exhibition*, pages 1–11 (Paper SPE 49121), New Orleans, USA, 1996. Society of Petroleum Engineers.

[221] Jan Szargut. Chemical exergies of the elements. *Applied Energy*, 32(4):269–286, January 1989. ISSN 03062619.

[222] Julian Esteban Barrera, Edson Bazzo, and Eduardo Kami. Energy Improvement Onboard of a Floating Production, Storage and Offloading Unit Using Organic Rankine Cycles. In *Proceedings of ECOS 2014 – The 27th International Conference on Efficiency, Cost, Optimization, Simulation and Environmental Impact of Energy Systems*, Turku, Finland, 2014.

[223] Yamid Alberto Carranza Sánchez and Silvio de Oliveira Jr. Exergy analysis of petroleum offshore platform process plant with CO_2 capture. In *Proceedings of ECOS 2014 – The 27th International conference on Efficiency, Cost, Optimization, Simulation and Environmental Impact of Energy Systems*, Turku, Finland, 2014.

[224] Andreas Mathies Hjorth Jensen. Application of advanced thermodynamic methods to offshore oil and gas platforms: Thermoeconomic and advanced exergetic analysis. Master's thesis, Technical University of Denmark, 2014.

[225] Mikael Höök. *Depletion and Decline Curve Analysis in Crude Oil Production*. Licenciate thesis, Uppsala Universitet, 2009.

[226] Norwegian Meteorological Institute. Mean temperature – ordered report. http://eklima.met.no, October 2012.

[227] Mari Voldsund, Tuong-Van Nguyen, Brian Elmegaard, Ivar S. Ertesvåg, and Signe Kjelstrup. Thermodynamic performance indicators for offshore oil and gas processing: Application to four North Sea facilities. *Oil and Gas Facilities*, 2014.

[228] Tuong-Van Nguyen, Mari Voldsund, Brian Elmegaard, Ivar S. Ertesvåg, and Signe Kjelstrup. On the definition of exergy efficiencies for petroleum systems: Application to offshore oil and gas processing. *Energy*, 73:264–281, 2014.

[229] Michele Margarone, Stefano Magi, Giuseppe Gorla, Stefano Biffi, Paolo Siboni, Gianluca Valenti, Matteo C. Romano, Antonio Giuffrida, Emanuele Negri, and Ennio Macchi. Revamping, Energy Efficiency, and Exergy Analysis of an Existing Upstream Gas Treatment Facility. *Journal of Energy Resources Technology*, 133:012001–1–012001–9, 2011.

[230] Kurt Nesselmann. Über den thermodynamischen Begriff der Arbeitsfähigkeit. *Allgemeine Wärmetechnik*, 3(5–6):97–104, 1952.

[231] Wolfgang Fratzscher and J. Beyer. Stand und Tendenzen bei der Anwendung und Weiterentwicklung des Exergiebegriffs. *Chemische Technik*, 33(1):1–10, 1981.

[232] Noam Lior and Na Zhang. Energy, exergy, and Second Law performance criteria. *Energy*, 32(4):281–296, 2007.

[233] Murray G. Patterson. What is energy efficiency? Concepts, indicators and methodological issues. *Energy Policy*, 24(5):377–390, 1996.

[234] Kanako Tanaka. Assessing measures of energy efficiency performance and their application in industry. IEA Information Paper, International Energy Agency, 2008.

[235] Wolfgang Fratzscher, Viktor M. Brodjanskij, and Klaus Michalek. *Exergie: Theorie und Anwendung*. Deutscher Verlag für Grundstoffindustrie, 1986.

[236] Jan Szargut. International progress in second law analysis. *Energy*, 5(8-9):709–718, August 1980. ISSN 03605442.

[237] Mikhaïl V. Sorin, Vadim M. Brodyansky, and Jean Paris. Observations on exergy efficiency coefficients. In Ennio Carnevale, Giampaolo Manfrida, and F. Martelli, editors, *Proceedings of the Florence World Energy Research Symposium*, volume 94, pages 941–949, Padova, Italy, 1994. SG Editoriali.

[238] Anne Berit Rian and Ivar S. Ertesvåg. Exergy Evaluation of the Arctic Snøhvit Liquefied Natural Gas Processing Plant in Northern Norway – Significance of Ambient Temperature. *Energy & Fuels*, 26:1259–1267, 2012.

[239] Eivind Johannessen and Audun Røsjorde. Equipartition of entropy production as an approximation to the state of minimum entropy production in diabatic distillation. *Energy*, 32(4):467–473, 2007.

[240] Saeid Mokhatab, John Y. Mak, Jaleel V. Valappil, and David A. Wood. *Handbook of Liquefied Natural Gas*. Gulf Professional Publishing, 2013.

[241] Ian K. Smith, Nikola Stosic, and Ahmed Kovacevic. Power recovery from low cost two-phase expanders. *TRANSACTIONS-GEOTHERMAL RESOURCES COUNCIL*, pages 601–606, 2001.

[242] Yves Charron, Philippe Pagnier, Elise Marchetta, and Sylvain Stihlé. Multiphase Flow Helico-Axial turbine: Applications and Performance. In *Proceedings of the 11th Abu Dhabi International Conference and Exhibition*, pages 1–8 (Paper SPE 88643). Society of Petroleum Engineers, 2004.

[243] Jean Falcimaigne and Sandrine Decarre. *Multiphase Production: Pipeline Transport, Pumping and Metering*. Editions OPHRYS, 2008.

[244] Tamás Gábor Fülöp. Evaluation and prospects for site-scale energy integration on oil and gas platforms. Technical report, Technical University of Denmark, 2014.

[245] Tuong-Van Nguyen, Laurence Tock, François Maréchal, and Brian Elmegaard. Oil and gas platforms with steam bottoming cycles: Retrofit integration and thermo-environomic evaluation. *Applied Energy*, 131:222–237, 2014.

[246] Adam Molyneaux. *A practical evolutionary method for the multi-objective optimisation of complex integrated energy systems including vehicle drivetrains*. PhD thesis, École Polytechnique Fédérale de Lausanne, 2002.

[247] Leonardo Pierobon, Rambabu Kandepu, and Fredrik Haglind. Waste Heat Recovery for Offshore Applications. In *Proceedings of the ASME 2012 International Mechanical Engineering Congress and Exposition*, volume 6: Energy, Parts A and B, pages 503–512. ASME, November 2012.

[248] Þór Hardarson. Energy optimisation and evaluation of the lifetime performance of a heavy oil offshore platform. Master's thesis, Technical University of Denmark, 2014.

[249] Bertrand F. Tchanche, Gregory Lambrinos, Antonios Frangoudakis, and George Papadakis. Low-grade heat conversion into power using organic Rankine cycles–a review of various applications. *Renewable and Sustainable Energy Reviews*, 15(8):3963–3979, 2011.

[250] Bo-Tau Liu, Kuo-Hsiang Chien, and Chi-Chuan Wang. Effect of working fluids on organic Rankine cycle for waste heat recovery. *Energy*, 29(8):1207–1217, 2004.

[251] Zhang Shengjun, Wang Huaixin, and Guo Tao. Performance comparison and parametric optimization of subcritical Organic Rankine Cycle (ORC) and transcritical power cycle system for low-temperature geothermal power generation. *Applied Energy*, 88(8):2740–2754, 2011.

[252] Ulli Drescher and Dieter Brüggemann. Fluid selection for the Organic Rankine Cycle (ORC) in biomass power and heat plants. *Applied Thermal Engineering*, 27(1):223–228, 2007.

[253] Ngoc Anh Lai, Martin Wendland, and Johann Fischer. Working fluids for high-temperature organic rankine cycles. *Energy*, 36(1):199–211, 2011.

[254] Norway to set high carbon tax on oil and gas production, 2012. URL www.offshore-technology.com/news/newsnorway-high-carbon-tax-oil-gas.

[255] Barry Burr and Lili Lyddon. A comparison of physical solvents for acid gas removal. In *Proceedings of the 87th Annual Gas Processors Association Convention*, Grapevine, United States, 2008.

[256] Ranjani V. Siriwardane, Ming-Shing Shen, Edward P. Fisher, and James A. Poston. Adsorption of CO_2 on molecular sieves and activated carbon. *Energy & Fuels*, 15(2):279–284, 2001.

[257] Minh T. Ho, Guy W. Allinson, and Dianne E. Wiley. Reducing the cost of CO_2 capture from flue gases using pressure swing adsorption. *Industrial & Engineering Chemistry Research*, 47(14):4883–4890, 2008.

[258] David Berstad, Rahul Anantharaman, and Petter Nekså. Low-temperature CO_2 capture technologies–Applications and potential. *International Journal of Refrigeration*, 36(5):1403–1416, 2013.

[259] Rune Bredesen, Kristin Jordal, and Olav Bolland. High-temperature membranes in power generation with CO_2 capture. *Chemical Engineering and Processing: Process Intensification*, 43(9):1129–1158, 2004.

[260] Adele Brunetti, Francesco Scura, Giuseppe Barbieri, and Enrico Drioli. Membrane technologies for CO_2 separation. *Journal of Membrane Science*, 359(1):115–125, 2010.

[261] Mohamed Kanniche, René Gros-Bonnivard, Philippe Jaud, Jose Valle-Marcos, Jean-Marc Amann, and Chakib Bouallou. Pre-combustion, post-combustion and oxy-combustion in thermal power plant for CO_2 capture. *Applied Thermal Engineering*, 30(1):53–62, 2010.

[262] Stefano Consonni and Federico Vigano. Decarbonized hydrogen and electricity from natural gas. *International Journal of Hydrogen Energy*, 30(7):701–718, 2005.

[263] Cynthia B. Tarun, Eric Croiset, Peter L. Douglas, Murlidhar Gupta, and Mohammad H.M. Chowdhury. Techno-economic study of CO_2 capture from natural gas based hydrogen plants. *International Journal of Greenhouse Gas Control*, 1(1):55–61, 2007.

[264] Stéphanie Hoffmann, Michael Bartlett, Matthias Finkenrath, Andrei Evulet, and Tord Peter Ursin. Performance and cost analysis of advanced gas turbine cycles with precombustion co_2 capture. *Journal of Engineering for Gas Turbines and Power*, 131(2):021701, 2009.

[265] Paolo Chiesa, Giovanni Lozza, and Luigi Mazzocchi. Using hydrogen as gas turbine fuel. In *ASME Turbo Expo 2003, collocated with the 2003 International Joint Power Generation Conference*, pages 163–171. American Society of Mechanical Engineers, 2003.

[266] Vince McDonell. Key combustion issues associated with syngas and high-hydrogen fuels. Technical report, National Energy Technology Laboratory, 2006.

[267] Laurence Tock and François Maréchal. H_2 processes with CO_2 mitigation: Thermo-economic modeling and process integration. *International Journal of Hydrogen Energy*, 37(16):11785–11795, 2012.

[268] Andrew James Sexton. *Amine Oxidation in Carbon Dioxide Capture Processes*. ProQuest, 2008.

[269] Tim Cullinane and Gary T. Rochelle. Carbon dioxide absorption with aqueous potassium carbonate promoted by piperazine. *Chemical Engineering Science*, 59(17):3619–3630, 2004.

[270] Tim Cullinane and Gary T. Rochelle. Kinetics of carbon dioxide absorption into aqueous potassium carbonate and piperazine. *Industrial & engineering chemistry research*, 45(8): 2531–2545, 2006.

[271] Chau-Chyun Chen and Yuhua Song. Generalized Electrolyte-NRTL Model for Mixed-Solvent Electrolyte Systems. *AIChE Journal*, 50(8):1928–1941, 2004.

[272] Otto Redlich and Joseph N. S. Kwong. ON THE THERMODYNAMICS OF SOLUTIONS. V An Equation of State. Fugacities of Gaseous Solutions. *Chemical Reviews*, 44:233–244, 1949.

[273] Olivier Jolliet, Manuele Margni, Raphaël Charles, Sébastien Humbert, Jérôme Payet, Gerald Rebitzer, and Ralph Rosenbaum. IMPACT 2002+: A new life cycle impact assessment methodology. *The International Journal of Life Cycle Assessment*, 8(6):324–330, 2003. ISSN 0948-3349.

[274] Solomon, Susan and Qin, Dahe and Manning, Martin J. and Chen, Zhenlin and Marquis, Melinda and Averyt, Kristen B. and Tignor, Melinda M. B. and Miller, Henry L. IPCC Fourth Assessment Report: Climate Change 2007 (AR4). Technical report, Intergovernmental panel on climate change, 2007.

[275] Mark Goedkoop and Renilde Spriensma. The eco-indicator99: A damage oriented method for life cycle impact assessment: Methodology report. Technical Report 1999/36A, Ministerie van Volkshuisvesting, Ruimtelijke Ordening en Milieu, 2001.

[276] Wayne C. Edmister. Compressibility factors and equations of state. *Petroleum Refiner*, 37(4):173–179, 1958.

[277] Robert H. Cavett. Physical Data for Distillation Calculations, Vapor-Liquid Equilibria. In *Proceedings of the 27th API Meeting, API Division of Refining*, volume 42, pages 351–366, 1962.

[278] Kenneth R. Hall and Lyman Yarborough. A new equation of state for Z-factor calculations. *Oil and Gas Journal*, 71(25):82–92, 1973.

[279] Mohammad R. Riazi and Thomas E. Daubert. Analytical correlations interconvert distillation-curve types. *Oil & Gas Journal*, 84(34):51–57, 1986.

[280] J. B. Maxwell. *Data book on hydrocarbons*. Van Nostrand, 1968.

[281] James G. Speight. *Handbook of petroleum product analysis*. Wiley, 2002.

[282] Daubert, Thomas E. and Danner, Ronald P. *Technical Data Book – Petroleum Refining*. American Petroleum Institute, Refining Department, 1992.

[283] Michael L. Michelsen and Jørgen M. Mollerup. *Thermodynamic models: fundamentals & computational aspects*. Tie-Line, 2nd edition, 2007.

[284] André Péneloux, Evelyne Rauzy, and Richard Fréze. A consistent correction for redlich-kwong-soave volumes. *Fluid Phase Equilibria*, 8:7–23, 1982.

[285] Chau-Chyun Chen and Lawrence B. Evans. A Local Composition Model for the Excess Gibbs Energy of Aqueous Electrolyte Systems. *AICHE Journal*, 32(3):444–454, 1986.

[286] Kenneth S. Pitzer. Electrolytes. From dilute solutions to fused salts. *Journal of the American Chemical Society*, 102(9):2902–2906, 1980.

[287] Aurel Stodola. *Dampf- und Gasturbinen*. Springer, 6th edition, 1924.

[288] Na Zhang and Ruixian Cai. Analytical solutions and typical characteristics of part-load performances of single shaft gas turbine and its cogeneration. *Energy Conversion and Management*, 43(9):1323–1337, 2002.

[289] Leonardo Pierobon, Tuong-Van Nguyen, Ulrik Larsen, Fredrik Haglind, and Brian Elmegaard. Multi-objective optimization of organic rankine cycles for waste heat recovery: Application in an offshore platform. *Energy*, 58:538 – 549, 2013. ISSN 0360-5442.

[290] Taewon Song, Tongseop Kim, Jaeheun Kim, and Sungtack Ro. Performance prediction of axial flow compressors using stage characteristics and simultaneous calculation of interstage parameters. In *Proceedings of the Institution of Mechanical Engineers*, volume 215 Part A, pages 89–98, London, UK, 2001. Institution of Mechanical Engineers.

[291] Dave E. Muir, Herbert I. H. Saravanamuttoo, and D. J. Marshall. Health Monitoring of Variable Geometry Gas Turbines for the Canadian Navy. *ASME Journal of Engineering for Gas Turbines and Power*, 111(2):244–250, 1989.

[292] Piero R. Spina. Gas Turbine performance prediction by using generalized performance curves of compressor and turbine stages. In *Proceedings of the ASME Turbo Expo 2002: Power for Land, Sea, and Air (GT2002)*, volume 2, pages 1073–1082, Amsterdam, The Netherlands, 2002.

[293] Ioannis Templalexis, Pericles Pilidis, Vassilios Pachidis, and Petros Kotsiopoulos. Development of a two-dimensional streamline curvature code. *ASME Journal of Turbomachinery*, 133(1):011003, 2011.

[294] Seymour Lieblein. *Analysis of experimental low-speed loss and stall characteristics of two-dimensional compressor blade cascades*. NACA RM E57A28, 1957.

[295] Herbert I. H. Saravanamuttoo, G. F. C. Rogers, Henry Cohen, and Paul Straznicky. *Gas Turbine Theory*. Pearson Prentice Hall, 6th edition, 2008.

[296] Walter Traupel. *Thermische Turbomaschinen*. Springer, 3rd edition, 1977.

[297] Fredrik Haglind and Brian Elmegaard. Methodologies for predicting the part-load performance of aero-derivative gas turbines. *Energy*, 34(10):1484–1492, 2009.

[298] Shankar Narasimhan and Cornelius Jordache. *Data Reconciliation and Gross Error Detection – An Intelligent Use of Proces Data*. Elsevier, 1999.

[299] John R. Taylor. *An introduction to error analysis – The study of uncertainties in physical measurements*. University Science Books, 2nd edition, 1997.

[300] Mari Voldsund, Tuong-Van Nguyen, Brian Elmegaard, Ivar S. Ertesvåg, Audun Røsjorde, Wei He, and Signe Kjelstrup. Performance indicators for evaluation of North Sea oil and gas platforms. In *Proceedings of ECOS 2013 - The 26th International Conference on Efficiency, Cost, Optimization, Simulation and Environmental Impact of Energy Systems*, Guilin, China, 2013.

A Petroleum properties

Crude oils are mixtures composed of a large number of chemical compounds, including hydrocarbons and impurities such as carbon dioxide, hydrogen sulphide and heavy metals. This appendix goes through the correlations used to calculate petroleum properties, such as the heating value and chemical exergy of hypotheticals, and of the whole crude.

A.1 Boiling point, specific gravity and molecular weight

The exact chemical composition of a crude oil is generally unknown, and only the bulk properties obtained from distillation tests are known. The heavy fractions are therefore modelled using pseudo- or hypothetical components, each representing a certain number of real chemical compounds, and characterised by a given boiling point. It is particularly important to derive properly the properties of those heavy fractions, especially in the case of heavy oils, which have high molecular weight and density.

Each heavy fraction can be characterised by thermophysical properties such as the critical pressure p_c and temperature T_c, the molecular weight M, the specific gravity SG and the boiling point T_b. In general, the physical properties of each fraction are deduced from the three last properties, from semi-empirical correlations found in the literature [276–279].

A first glance into the pseudo-components used in the industry shows a fair agreement between the boiling point temperature on one side, and the specific gravity and molecular weight on the other side (Figure A.1). Simplified polynomial regressions can be deduced, with an accuracy of about 92.1 and 99.7 %, respectively:

$$M = 1 \cdot 10^{-6} T_b^3 - 0.0025 T_b^2 + 2.1342 T_b - 83.859 \tag{A.1}$$

$$\mathrm{SG} = 1 \cdot 10^{-9} T_b^3 - 2 \cdot 10^{-6} T_b^2 + 0.0015 T_b + 0.6229 \tag{A.2}$$

A second possibility is to estimate the specific gravity of each distillation cut, or, in other words, of each hypothetical component, by using the Watson factor K_W, which is constant for all cuts,

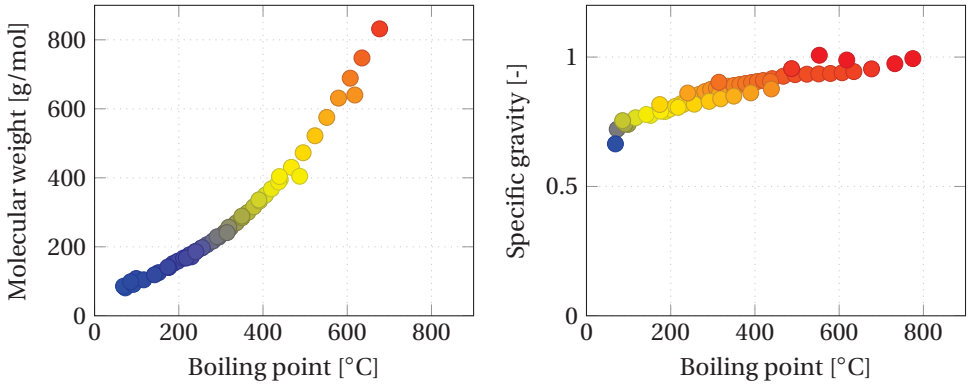

Figure A.1: Fitted regressions of the boiling point, specific gravity and molecular weight of hypothetical components.

and thus equal to the value obtained for the whole crude.

$$K_W = \frac{(1.8T_\mathrm{b})^{\frac{1}{3}}}{\mathrm{SG}} \tag{A.3}$$

where the boiling point temperature is expressed in K and corresponds to the so-called mean average boiling point, and the specific gravity is calculated for a temperature of 15.5 °C.

A third possibility, which is the most common, is to use correlations proposed in the literature, such as the ones proposed by Riazi and Daubert [279]. These ones are based on the measurements of the molecular weight and specific gravity of each heavy fraction, and are in the form of:

$$\Theta = aM^b\mathrm{SG}^c\exp\left(dM + e\mathrm{SG} + f(M\cdot\mathrm{SG})\right) \tag{A.4}$$

where Θ is the physical property of interest, and a, b, c, d, e and f are regression coefficients.

A.2 Carbon-to-hydrogen ratio

Other properties that are of interest for further modelling of the pseudo-components are the carbon-to-hydrogen ratio, defined as the weight of the carbon atoms over the weight of the hydrogen ones, as well as the sulphur, nitrogen and metals contents.

$$\frac{x_C}{x_H} = 8.7746\cdot10^{-10}\{\exp\left(7.176\cdot10^{-3}T_\mathrm{b} + 30.06242\mathrm{SG} - 7.35\cdot10^{-3}T_\mathrm{b}\mathrm{SG}\right)\}T_\mathrm{b}^{-0.98445}\mathrm{SG}^{-18.2753} \tag{A.5}$$

This correlation, proposed by Riazi and Daubert [279] has an absolute average deviation of 2 % and is valid only for distillation fractions that contain hydrocarbons with a carbon number comprised between 20 and 50.

A.3 Heating value

The measurement of properties such as the heating value, using, for instance, a bomb calorimeter, may be time-consuming or impracticable. In the cases that the chemical composition of the petroleum blend is known with a reasonable accuracy, or that physical properties such as the API gravity are known, empirical correlations may be used to estimate the missing properties, such as the one proposed in Maxwell [280]:

$$\mathrm{HHV} = 2.326\left(17,721 + 89.08(^{\circ}\mathrm{API}) - 0.348(^{\circ}\mathrm{API})^2 + 0.009518(^{\circ}\mathrm{API})^3\right) \tag{A.6}$$

$$\mathrm{LHV} = 2.326\left(16,840 + 76.60(^{\circ}\mathrm{API}) - 1.230(^{\circ}\mathrm{API})^2 + 0.008974(^{\circ}\mathrm{API})^3\right) \tag{A.7}$$

or in Speight [281]:

$$\mathrm{HHV} = 4.184(12,400 - 2100\mathrm{SG}^2) \tag{A.8}$$

The deviation of the last correlation is claimed to be generally less than 1 %, but can be expected to be higher for highly aromatic crude oils.

A comparison between the measured and correlated values of the heat of combustion (HHV), based on the correlations of Maxwell [280] and of Speight [281] show a fairly good agreement for the two tested oil blends (Figure A.2). The first one is a volatile oil, with an API gravity of about 37, while the second one is a heavy oil, with an API gravity lower than 20. In both cases, the smallest deviation is observed in the case of the Speight's correlation, which suggests that it is satisfying enough for estimating the heating values and chemical exergies of crude oils.

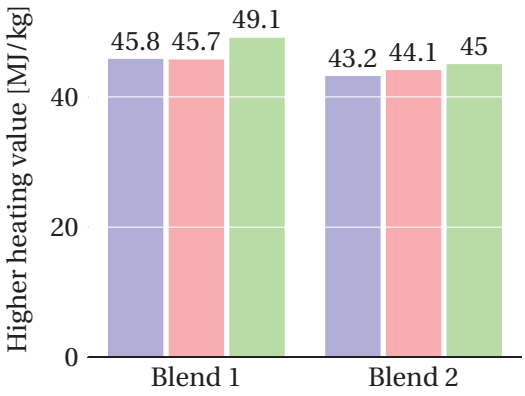

Figure A.2: Comparison of the measured and correlated values of the higher heating value for two types of North Sea crude oils.

The ratio of higher to lower heating values for liquid fuels can be expressed as [282]:

$$\frac{\mathrm{HHV}}{\mathrm{LHV}} = 1.0525 + 4.43 \cdot 10^{-4}(^{\circ}\mathrm{API}) - 2.04 \cdot 10^{-6}(^{\circ}\mathrm{API})^2 \tag{A.9}$$

A.4 Chemical exergy

The standard chemical exergy of pure hydrocarbon fuels C_aH_b, even if not present in the environment, can be calculated using the approach presented in Bejan et al. [76]. It considers an idealised combustion reaction with references substances such as oxygen, entering at the dead state conditions, and forming carbon dioxide and liquid water.

$$C_aH_b + (a + \frac{b}{4}O_2) \longrightarrow aCO_2 + \frac{b}{2}H_2O \tag{A.10}$$

The molar chemical exergy can then expressed as:

$$\bar{e}^{ch}_{fuel} = \left(\frac{\dot{W}_{cv}}{\dot{n}_{fuel}}\right)_{rev} + a\bar{e}^{ch}_{CO_2} + \frac{b}{2}\bar{e}^{ch}_{H_2O(l)} - \left(a + \frac{b}{4}\right)\bar{e}^{ch}_{O_2} \tag{A.11}$$

$$= H\bar{H}V(T_0, p_0) - T_0\left\{\bar{s}_{fuel} + \left(a + \frac{b}{4}\right)\bar{s}_{O_2} - a\bar{s}_{CO_2} - \frac{b}{2}\bar{s}_{H_2O(l)}\right\}(T_0, p_0) \tag{A.12}$$

$$+ \left\{a\bar{e}^{ch}_{CO_2} + \frac{b}{2}\bar{e}^{ch}_{H_2O(l)} - \left(a + \frac{b}{4}\right)\bar{e}^{ch}_{O_2}\right\}$$

$$= \left\{\bar{g}_{fuel} + \left(a + \frac{b}{4}\right)\bar{g}_{O_2} - a\bar{g}_{CO_2} - \frac{b}{2}\bar{g}_{H_2O(l)}\right\}(T_0, p_0) \tag{A.13}$$

$$+ \left\{a\bar{e}^{ch}_{CO_2} + \frac{b}{2}\bar{e}^{ch}_{H_2O(l)} - \left(a + \frac{b}{4}\right)\bar{e}^{ch}_{O_2}\right\}$$

However, this approach requires the use of a measured or estimated fuel heating value, as well as an estimated value for the fuel absolute entropy.

In the case that the fuel absolute entropy cannot be estimated properly, correlations that express the ratio of the standard chemical exergy to the lower heating value can be used [44]. This ratio, called β, depends on the atomic ratios of hydrogen $\frac{H}{C}$, oxygen $\frac{O}{C}$, nitrogen $\frac{N}{C}$ and sulphur $\frac{S}{C}$ to carbon, and can be derived from regression equations:

- for pure liquid hydrocarbons, with a mean accuracy of ± 0.21 %:

$$\beta = 1.0406 + 0.0144\frac{H}{C} \tag{A.14}$$

- for liquid compounds with carbon, hydrogen and oxygen, valid only if $\frac{O}{C}$ is smaller than 1, and with a mean accuracy of ± 0.34 %:

$$\beta = 1.0374 + 0.0159\frac{H}{C} + 0.0567\frac{O}{C} \tag{A.15}$$

- for liquid compounds with carbon, hydrogen, oxygen and sulphur, valid only if $\frac{O}{C}$ is smaller than 1, and with a mean accuracy of ± 0.5 %:

$$\beta = 1.0407 + 0.0154\frac{H}{C} + 0.0562\frac{O}{C} + 0.5904\frac{S}{C}\left(1 - 0.175\frac{H}{C}\right) \tag{A.16}$$

- for liquid technical fuels, as suggested as well in Rivero et al. [130], and with a mean accuracy of ± 0.5 %:

$$\beta = 1.0401 + 0.1728\frac{x_{H_2}}{x_C} + 0.0432\frac{x_{O_2}}{x_C} + 0.2169\frac{x_S}{x_C}\left(1 - 2.0628\frac{x_{H_2}}{x_C}\right) + 0.0428\frac{x_{N_2}}{x_C} \quad \text{(A.17)}$$

In the particular case of pseudo-components, which also contain solid impurities such as nickel and vanadium, the standard chemical exergy can be calculated applying the expressions presented in Rivero et al. [130]:

$$\bar{e}^{\text{ch}}_{\text{hyp}} = \frac{1}{M_{\text{hyp}}}\left(\beta_{\text{hyp}}\text{LHV}_{\text{hyp}} + \sum_{\text{mt}} x_{\text{mt}} e^{\text{ch}}_{\text{mt}}\right) \quad \text{(A.18)}$$

Finally, the chemical exergy of the whole crude oil can be calculated as:

$$\bar{e}^{\text{ch}}_{\text{oil}} = \sum_i e^{\text{ch}}_i + RT_0 \sum_i \bar{x}_i \ln(\bar{x}_i \gamma_i) \quad \text{(A.19)}$$

The deviation caused by inaccuracies in the activity coefficients was estimated in the work of Rivero et al. [130], using the Scatchard-Hildebrand model for Isthmus and Maya crude oils. It was estimated to be about 6.5 % for the compositional exergy, and about 0.005 % for the total chemical exergy, if all the activity coefficients are taken equal to 1.

It may not be possible to estimate directly the carbon-to-hydrogen ratio of the whole crude, if this information is not provided. In this situation, taking the 1st blend as example, and calculating the carbon-to-hydrogen ratios for each distillation fraction, it is seen that the chemical exergy varies in a range of ± 0.52 % if no information on the sulphur content is given, and in the magnitude of ± 0.53 % otherwise.

B Thermodynamic models

This appendix goes through the theory behind the equations of state and activity models used in the modelling of oil and gas systems, and presents a comparison of the ones that are most used.

B.1 Background

Equations of state are analytical expressions that express the pvT-behaviour. They differ with the substance under study and the process conditions. They present the main advantage of being straightforward and efficient, as no iterative procedure is needed. They can be used in wide ranges of temperature and pressure, including subcritical and supercritical regions.

However, these methods are not recommended for modelling non-ideal solutions, i.e. mixtures where the interactions between dissimilar molecules are significantly different than those between similar molecules. In these cases, the forces (attraction or repulsion) acting between the chemical compounds are not negligible, and the deviations from the ideal and real behaviours of the chemical solution must be accounted for.

The first possibility, which is the most accurate, is to introduce *activity coefficients*, which are correctional parameters depending on the temperature, pressure and mole numbers of the solution. These constants can either be measured (empirical approach) or calculated by using component-specific correlations. The second possibility, which is more computationally-efficient, is to customise the EOS with additional parameters to reproduce similar results.

In the present project, both equations of state and activity models have been used to model petroleum systems and to predict properly state variables such as temperatures and pressures. The decomposition of the overall platform model into smaller sub-models, which are connected by the Matlab-based platform, reveals to be particularly advantageous. Each sub-model can be run independently with the adequate thermodynamic package, and the overall model can be evaluated consistently with a higher degree of accuracy and possibly faster convergence.

B.2 Equations of state

The thermodynamic properties of basic hydrocarbon systems can be derived from cubic equations of state, meaning that the volume term in these EOS is of the 1st, 2nd or 3rd order (Table B.1). They are often considered as the most suitable equations for oil and gas applications, and they can be expressed, following the approach of Michelsen and Mollerup [283], as:

$$p = \frac{RT}{v-b} - \frac{a(T)}{(v+\delta_1 b+\delta_3 c)(v+\delta_2 b+\delta_4 c)} \tag{B.1}$$

where:

p is the absolute pressure, in Pa;

R is the ideal gas constant, in $J \cdot mol^{-1} \cdot K^{-1}$;

T is the temperature, in K;

v is the molar volume, in $m^3 \cdot mol^{-1}$;

a is an attraction-related parameter, expressed as a function of the temperature. It is also, for some EOS, dependent on three temperature- and composition-dependent parameters, which are called the binary mixing parameters;

b is an volume-related parameter, expressed as a function of the size of the molecules. It is also, for some EOS, dependent on the molar fraction of each chemical compound present in the solution, but *not* on any binary mixing parameter;

c is a volume-translation parameter, adjusted to reproduce the molar volume of boiling liquid at normal pressure, but without effect on the vapour-liquid equilibrium calculations. This parameter was not present in the original EOS, but was suggested by Péneloux et al. [284] to improve the SRK EOS;

δ_1, δ_2, δ_3 and δ_4 are empirical constants specific to each EOS.

B.3 Activity models

The thermodynamic properties of non-ideal systems can be derived from activity models, such as the Non-Random-Two-Liquid (NRTL) one [169]:

$$ln(\gamma_i) = \frac{\sum_{j=1}^{n} \bar{x}_j \tau_{ji} G_{ji}}{\sum_{k=1}^{n} \bar{x}_k G_{ki}} + \sum_{j=1}^{n} \frac{\bar{x}_j G_{ij}}{\sum_{k=1}^{n} \bar{x}_k G_{kj}} \left(\tau_{ij} - \frac{\sum_{m=1}^{n} \bar{x}_m \tau_{mj} G_{mj}}{\sum_{k=1}^{n} \bar{x}_k G_{kj}} \right) \tag{B.2}$$

where:

Table B.1: Parameters in cubic equations of state

	Attraction-related	Volume-related	δ_1	δ_2
VDW	a	b	0	0
SRK	$\frac{a}{T^{\frac{1}{2}}}{}^{a}$	b	1	0
PR	$a(T)^{b}$	b	$1+\sqrt{2}$	$1-\sqrt{2}$
TCC	$a(T)$	b	3	0.5
SWR	$a(T, a_{ij}, \bar{x}_i, \bar{x}_j)^{c}$	$b(b_i, \bar{x}_i)^{d}$	0	1

[a] Inclusion of a temperature-dependent term
[b] General temperature-dependency
[c] Chemical composition dependency (binary parameters): pseudo-quadratic mixing rule
[d] Chemical composition dependency (molar fractions): linear mixing rule

γ_i is the activity coefficient of a compound i;

$\bar{x}_i$ is its mole fraction in the relevant liquid phase;

n is the total number of chemical compounds;

G and τ are empirical parameters, which are functions of binary parameters derived from data regression of the vapour- and liquid-liquid equilibria and temperature.

For systems with CO_2-capture, such as *amines and CO_2*, the electrolyte-Non-Random-Two-Liquid (eNRTL) activity model [170] is preferred, as the dissociation of the amines results in the formation of electrolytes, and the ionic activity coefficients must be calculated. The main difference between the NRTL and the eNRTL models lies on the accounting for the long-range ion-ion interactions and the development of the segment interaction concepts, which aims at representing the phase behaviour of aqueous organic electrolytes [285].

$$ln(\gamma_i^*) = ln(\gamma_i^{*,\mathrm{lc}}) + ln(\gamma_i^{*,\mathrm{PDH}}) \tag{B.3}$$

where:

$*$ denotes the unsymmetric reference state in thermochemistry of electrolytes;

lc refers to the local interaction contributions, based on the NRTL theory, and the infinite-dilution activity coefficient of the ionic component i;

PDH corresponds to the use of the unsymmetric Pitzer-Debye-Hückel formula for the accounting of the long-range interactions [286], which are of particular importance when investigating the behaviour and association/dissociation of CO_2 with amine species.

Further details of the derivation of the activity coefficient $\gamma_i^{*,\mathrm{PDH}}$, as the sum of the contributions of the segment interactions, are out of scope of this study, and the reader is referred to Chen and Song [271].

B.4 Comparison

Several thermodynamic property models have been recommended for predicting the behaviour of oil and gas in petrochemical processes, with, on top of them, the Peng-Robinson [163] and Redlich-Kwong with Soave modifications [272] equations of state, the Chao-Seader (CS) and Grayson-Streed (GS) semi-empirical methods, and the Braun K10 (BK10) vapour pressure model. Vapour pressure models are more easy-to-use and computationally more efficient than equations of state, although the difference for modern computers and clusters is negligible. Activity models, as, for example, NRTL, are not considered in this section, since such models are claimed to be poor for hydrocarbon modelling. Their preferred range of application differs with regards to temperature, pressure and chemical compositions, but the properties that are predicted with these models may be extrapolated at the expense of higher inaccuracies.

The Peng-Robinson EOS is the most commonly used one, but discussions with platform and refinery operators have shown that other models such as SRK, CS, GS and BK10 have been of interest. The first one is claimed to be suitable over a large range of temperatures (above -270 °C) and pressures (below 100,000 kPa), including around the critical point, but may be unsuitable when large quantities of polar compounds are found. The second one presents, in theory, a smaller application range (above -143 °C and below 35,000 kPa). The Chao-Seader and Grayson-Seed models are generally suitable for systems with heavy hydrocarbons at low pressures (below 150 bar) and temperatures (between -18 and 260 °C), which is the case of the oil streams and, in some cases, of the feed ones. The Braun K10 model is supposedly valid for heavy hydrocarbon systems at temperatures above -17.78 °C, and for pressures below 700 kPa.

These thermodynamic models are compared based on four types of feed, oil and gas streams that are processed in the North Sea region, and which differ by their chemical composition, temperatures and pressures. They illustrate part of the variety of the chemical compounds that are present in petroleum flows and have highly different thermophysical properties.

The first type may be considered as a standard petroleum feed, which, after processing, results in a methane-rich gas and a volatile oil. The second type is characterised by a much higher gas content and very small water fraction, which, after processing, leads to a methane-rich gas and a condensate/oil poor in heavy hydrocarbons. The third type has a much smaller gas content, yielding a heavy and viscous oil. The fourth type is similar to the first one, but the propane and water contents are much higher. These four types correspond to the reservoir fluids of the platforms named A, B, C and D in the rest of this manuscript.

Excellent agreement of the PR and SRK EOS is observed for the feed, gas (Figure B.1) and oil (Figure B.2) streams analysed for four different North Sea platforms over a wide range of temperatures. The comparison of both EOS illustrates that the predicted T-e^{ph} follow the same trends and show the best agreement at high temperatures. The comparison with the CS and GS methods shows a good match of all these models for the oil streams, and a fair one for the gas flows. In the case of heavy oil, the prediction of the vapour-liquid equilibrium (Figure B.3) is unsatisfactory with the CS and GS methods, with a discrepancy of 15 to 35 %. The use of the

BK10 vapour pressure model seems not to be appropriate for any type of feed or gas, and the large discrepancies for the prediction of the vapour-liquid equilibrium, in particular when the feed displays a high water-to-oil ratio, make this model unsuitable for petroleum upstream processes. A detailed comparison of these thermodynamic models with, for instance, the Twu-Coon-Cunningham and the Schwartzentruber-Renon EOS is not presented here. However, the use of the PR and SRK EOS for modelling chemical systems such as glycol-hydrocarbons is not satisfying.

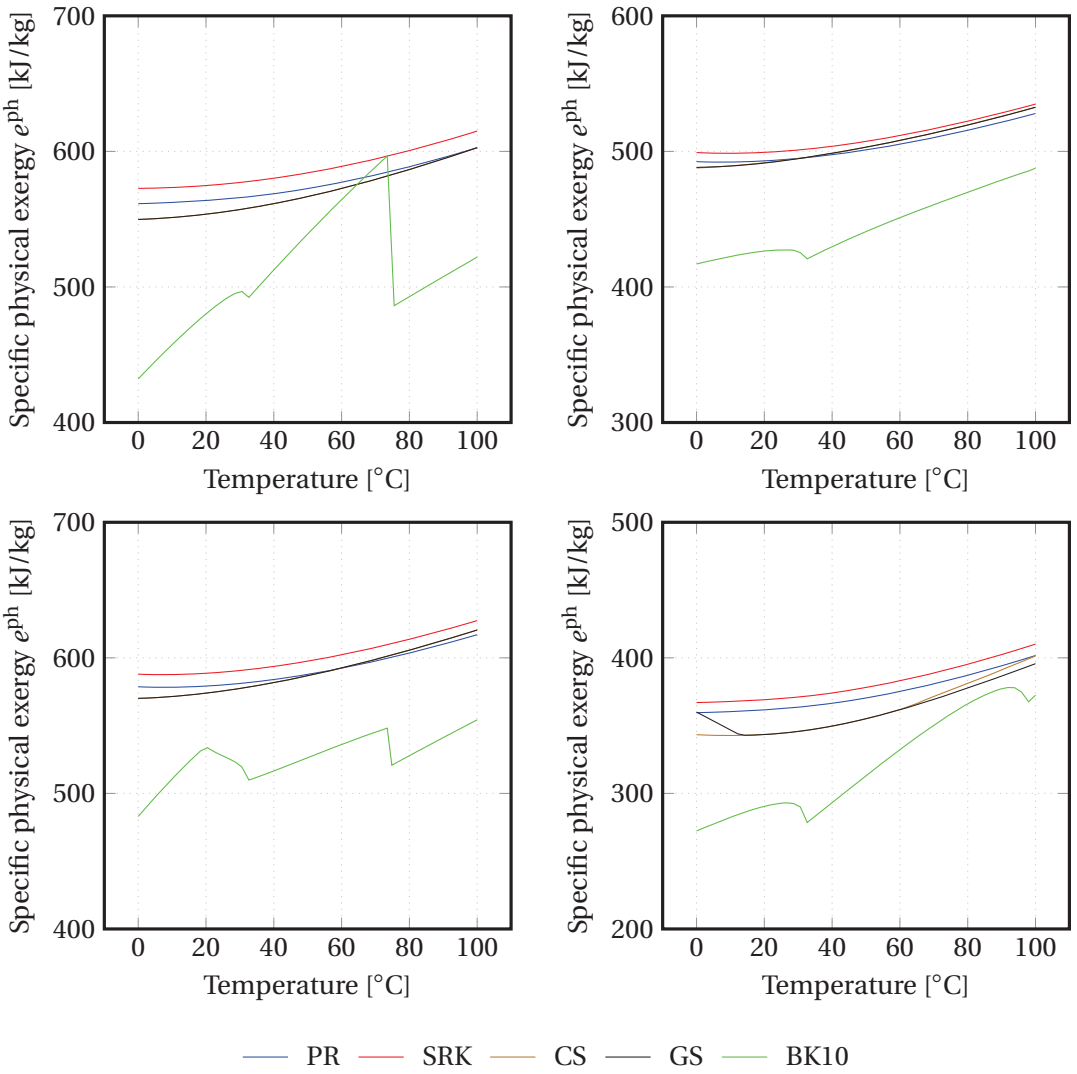

Figure B.1: Predicted temperature–physical exergy profiles for four different types of gases.

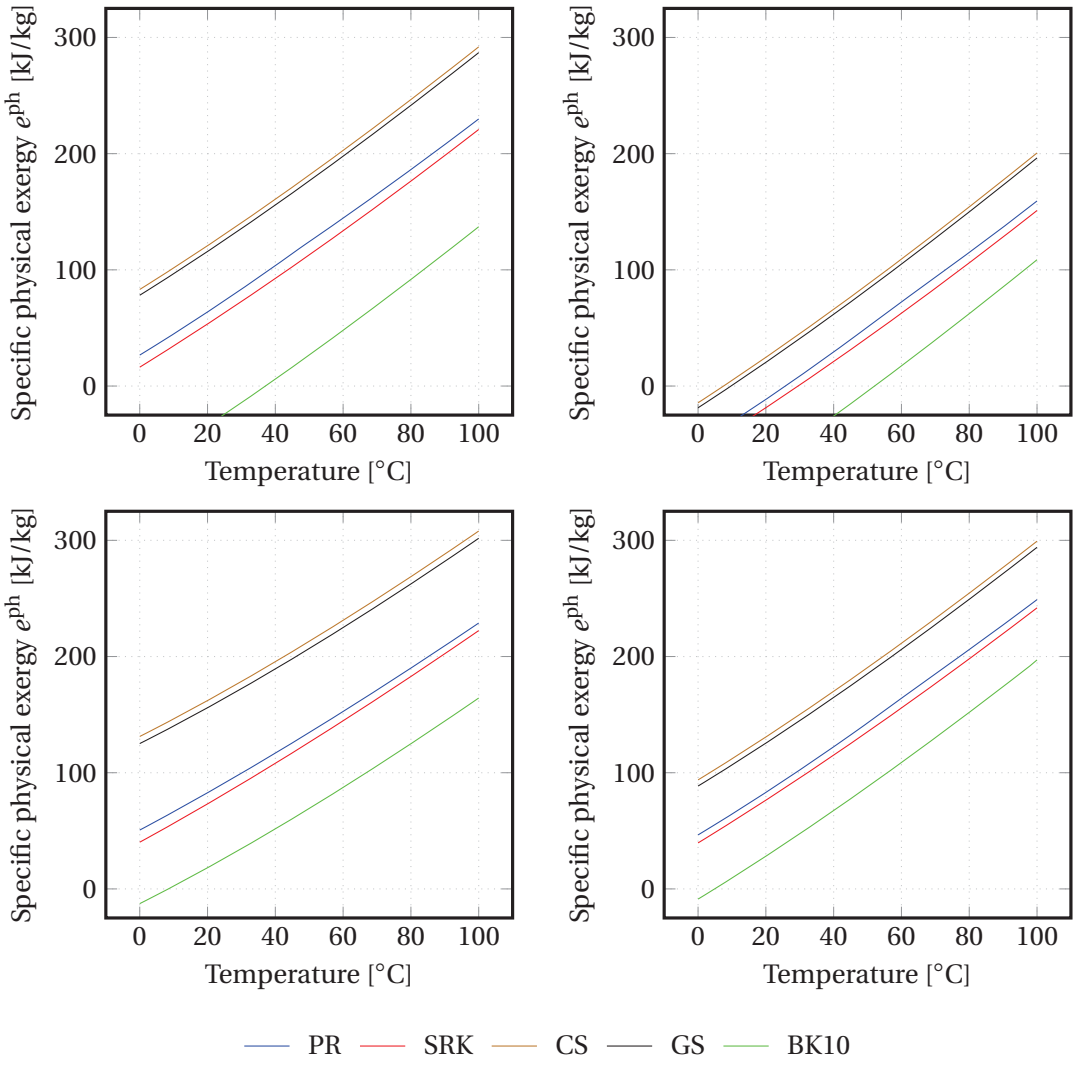

Figure B.2: Predicted temperature–physical exergy profiles for four different types of oils.

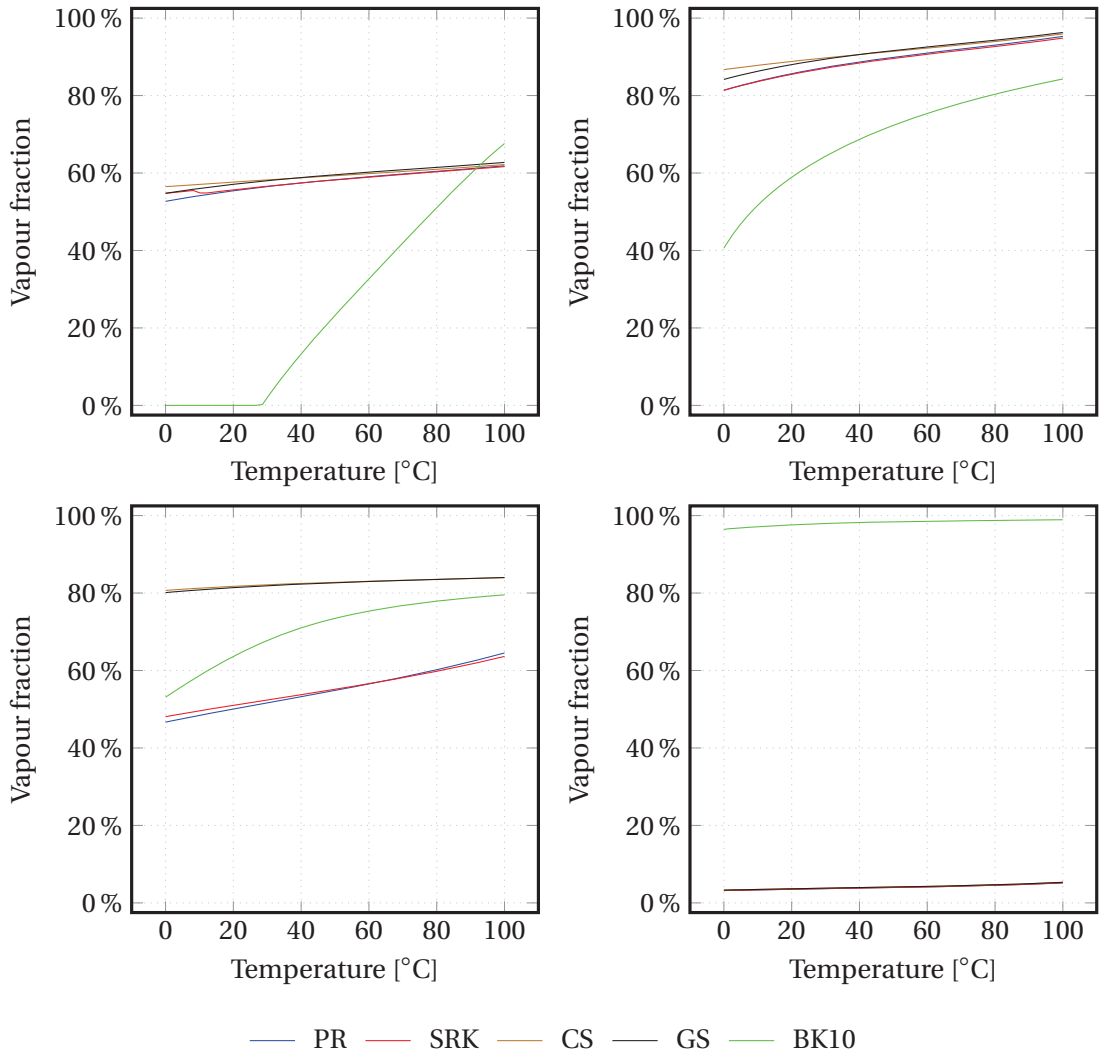

Figure B.3: Predicted vapour liquid-equilibrium for four different feeds.

C Component modelling

Offshore facilities are subject to changes in operating conditions and production flows over time. They mainly run in part-load conditions, and this implies that each component should be modelled carefully so that their behaviour is reproduced carefully. This chapter presents the equations and theory behind the component models.

C.1 Heat exchangers

The total rate of heat transfer across a surface can be expressed, using the Fourier's general formulation in steady-state, as:

$$\dot{Q} = UA\Delta T_{\text{MEAN}} \tag{C.1}$$

where:

$\dot{Q}$ is the rate of heat transfer;

U the overall heat transfer coefficient;

A the heat transfer area;

ΔT_{MEAN} the mean temperature difference.

The overall heat transfer coefficient is a function of the individual resistances to heat transfer, which are related to the limited conductivity of the pipe wall material and the fouling effects inside and outside the tubes, and is given by:

$$\frac{1}{U_{\text{o}}} = \frac{1}{h_{\text{o}}} + \frac{1}{h_{\text{od}}} + \frac{d_{\text{o}} \ln \frac{d_{\text{o}}}{d_{\text{i}}}}{2k_{\text{wall}}} + \frac{d_{\text{o}}}{d_{\text{i}}} \cdot \frac{1}{h_{\text{id}}} + \frac{d_{\text{o}}}{d_{\text{i}}} \cdot \frac{1}{h_{\text{i}}} \tag{C.2}$$

where:

U_o is the overall heat transfer coefficient, based on the outside area of the pipe;

h_o and h_i the outside and inside fluid film coefficients;

h_{od} and h_{id} the outside and inside dirt coefficients, also called fouling factors;

k_{wall} the thermal conductivity of the pipe wall material;

d_o and d_i the outside and inside tube diameters.

Assuming that:

(1) the overall heat transfer coefficient is constant (no temperature-dependency);

(2) the flow rate of each fluid is constant (steady-state conditions);

(3) the specific heat capacity of each fluid is constant (no temperature-dependency or phase change);

(4) heat losses are negligible.

The heat transfer rate across a heat exchanger can be expressed as:

$$\dot{Q} = UA \cdot f_T \cdot \Delta T_{LMTD} \tag{C.3}$$

where ΔT_{LMTD} is the logarithmic mean temperature difference (LMTD) and f_T the LMTD correction factor, which accounts for the deviation between the real flow behaviour and a true counter-current flow. The value of the correction factor can be derived empirically or, with a reasonable accuracy, from correlation plots available in the literature:

$$\Delta T_{LMTD} = \frac{\Delta T_I - \Delta T_{II}}{\ln\left(\frac{\Delta T_I}{\Delta T_{II}}\right)} \tag{C.4}$$

where ΔT_I and ΔT_{II} are the temperature differences between the hot and cold fluid at each end of the heat exchanger.

In part-load conditions, i.e. if the heat exchanger is operated with different mass-flows than the ones it is designed for, the overall heat transfer coefficient is expected to decrease. Assuming that each film coefficient follows a power-law expression with the mass flows in the form:

$$h_{o,off-des} = h_{o,des} \cdot \underbrace{\left(\frac{\dot{m}_{o,off-des}}{\dot{m}_{o,des}}\right)^{\alpha_o}}_{r_{\dot{m},o}} \tag{C.5}$$

$$h_{i,off-des} = h_{i,des} \cdot \underbrace{\left(\frac{\dot{m}_{i,off-des}}{\dot{m}_{i,des}}\right)^{\alpha_i}}_{r_{\dot{m},i}} \tag{C.6}$$

where:

$h_{\text{o,off-des}}$ and $h_{\text{i,off-des}}$ are the outside and inside fluid film coefficients;

$\dot{m}_{\text{o,off-des}}$ and $\dot{m}_{\text{i,off-des}}$ the corresponding mass flow rates;

α_{i} and α_{o} are the power coefficients, smaller than 1;

$\Phi_{\dot{m},\text{o}}$ and $\Phi_{\dot{m},\text{i}}$ the mass flow ratios between the off-design and design conditions.

the overall heat transfer coefficient in off-design conditions can be expressed as:

$$U_{\text{o,off-des}} = U_{\text{o,des}} \cdot \frac{\Phi_{\dot{m},\text{i}} \cdot \Phi_{\dot{m},\text{o}} \left(h_{\text{o,off-des}} + h_{\text{i,off-des}} \cdot \frac{d_{\text{o}}}{d_{\text{i}}} \right)}{\Phi_{\dot{m},\text{o}} \cdot h_{\text{o,des}} + \Phi_{\dot{m},\text{i}} \cdot h_{\text{i,des}}} \tag{C.7}$$

C.2 Turbomachinery and electrical components

The turbomachinery components were modelled using the process measurements and relating the temperatures and pressures in- and out- of these components to their operating loads. However, when none of these data were available, the part-load performance of components such as turbines and compressors was predicted using equations and correlations presented in the literature.

C.2.1 Turbines

The flow behaviour in the turbine expansion process is governed by the Stodola's Ellipse, which states the relation between the mass flow coefficient and the pressure ratio. It results into the following relationship, which is derived in Stodola [287]:

$$c_{\text{trb}} = \frac{\dot{m}\sqrt{T_i}}{\sqrt{p_i^2 - p_o^2}} \tag{C.8}$$

where:

c_{trb} is the so-called turbine constant;

$\dot{m}$ is the mass flow rate through the turbine;

T_i is the flow inlet temperature;

p_i and p_o are the inlet and outlet pressures.

The isentropic efficiency in part-load conditions can be calculated as:

$$\eta_{\text{is,turb,off-des}} = \eta_{\text{is,turb,des}} \frac{\omega_{\text{turb,off-des}}}{\omega_{\text{turb,des}}} \sqrt{\frac{\Delta h_{\text{is,turb,des}}}{\Delta h_{\text{is,turb,off-des}}}} \left(2 - \frac{\omega_{\text{turb,off-des}}}{\omega_{\text{turb,des}}} \sqrt{\frac{\Delta h_{\text{is,turb,des}}}{\Delta h_{\text{is,turb,off-des}}}} \right) \tag{C.9}$$

where:

$\eta_{\text{is,turb}}$ is the turbine isentropic efficiency;

Δh_{is} denotes the isentropic enthalpy drop;

ω corresponds to the rotational speed;

the terms des and off-des stand for design and off-design conditions.

For a steam turbine, the isentropic efficiency in off-design conditions may be, as a first approximation, taken equal to the value at the design point, as it varies marginally for operating loads close to the design one.

C.2.2 Compressors

The part-load performance of a compressor can be described based on extrapolation methods, which aim at deriving analytical performance expressions based on parameters such as the corrected mass flow rate and fitting coefficients [288]. The following expressions are used in the rest of the derivations:

$$\dot{G}_{\text{comp}} = \frac{\dot{m}_{\text{comp}}\sqrt{T_{\text{i,comp}}}}{p_{\text{i}}} \tag{C.10}$$

$$\dot{\omega}_{\text{comp}} = \frac{\omega}{\sqrt{T_{\text{i,comp}}}} \tag{C.11}$$

$$\dot{\omega}^{*}_{\text{comp}} = \frac{\dot{\omega}_{\text{comp,off-des}}}{\dot{\omega}_{\text{comp,des}}} \tag{C.12}$$

$$\pi^{*}_{\text{comp}} = \frac{\dot{\pi}_{\text{comp,off-des}}}{\dot{\pi}_{\text{comp,des}}} \tag{C.13}$$

$$\eta^{*}_{\text{is,comp}} = \frac{\eta_{\text{is,comp,off-des}}}{\eta_{\text{is,comp,des}}} \tag{C.14}$$

where:

$\dot{G}_{\text{comp}}$ is corrected mass flow;

$\dot{\omega}_{\text{comp}}$ is the corrected rotational speed;

$\dot{\omega}^{*}_{\text{comp}}$ is the relative expression of the corrected rotational speeds at design and off-design conditions;

π^{*}_{comp} is the relative expression of the pressure ratios at design ($\dot{\pi}_{\text{comp,des}}$) and off-design ($\dot{\pi}_{\text{comp,off-des}}$) conditions;

$\eta^{*}_{\text{is,comp}}$ is the relative expression of the isentropic efficiencies at design ($\eta_{\text{is,comp,des}}$) and off-design ($\eta_{\text{is,comp,off-des}}$) conditions.

The relationships between the compressor's pressure ratio, isentropic efficiency and these reduced parameters are given as:

$$\pi^*_{\text{comp}} = c_1 \dot{m}^2_{\text{comp}} + c_2 \dot{m}_{\text{comp}} + c_3 \tag{C.15}$$

$$\eta^*_{\text{is,comp,off-des}} = \left(1 - c_4(1-\dot{\omega}_{\text{comp}})^2\right)\left(\frac{\dot{\omega}_{\text{comp}}}{\dot{G}_{\text{comp}}}\right)\left(2 - \frac{\dot{\omega}_{\text{comp}}}{\dot{G}_{\text{comp}}}\right) \tag{C.16}$$

where c_1, c_2, c_3 and c_4 are function of the rotational speed:

$$c_1 = \frac{\dot{\omega}^*_{\text{comp}}}{p(1 - m/\dot{\omega}^*_{\text{comp}}) + \dot{\omega}^*_{\text{comp}}(\dot{\omega}^*_{\text{comp}} - m)^2} \tag{C.17}$$

$$c_2 = \frac{(p - 2m(\dot{\omega}^*_{\text{comp}})^2)}{p(1 - m/\dot{\omega}^*_{\text{comp}}) + \dot{\omega}^*_{\text{comp}}(\dot{\omega}^*_{\text{comp}} - m)^2} \tag{C.18}$$

$$c_3 = \frac{-(pm\dot{\omega}^*_{\text{comp}} - m^2(\dot{\omega}^*_{\text{comp}})^3)}{p(1 - m/\dot{\omega}^*_{\text{comp}}) + \dot{\omega}^*_{\text{comp}}(\dot{\omega}^*_{\text{comp}} - m)^2} \tag{C.19}$$

The m and p values should satisfy the following criteria:

$$\sqrt[3]{p} \geq \frac{2m}{3} \tag{C.20}$$

The m, p and c_4 values are set to 1.06, 0.36 and 0.3, respectively, as detailed information on each compressor is not given.

C.2.3 Gas turbines

In the particular case of the gas turbines present on the Draugen platform, another procedure was used for predicting the compressor off-design characteristics. It was derived by Pierobon et al. [289], based, among other methods, on the application of a stage-stacking analysis [290–292]. The calculations of the isentropic efficiency of each stage were based on the pressure drop assumptions presented in Templalexis et al. [293], and in the works of Lieblein [294] and Saravanamuttoo et al. [295]. The gas turbine off-design characteristics were derived following the method described in Stodola [287] and in Traupel [296]. The maximum relative error was found in the prediction of the gas turbine thermal efficiency, which was 3.7 %.

C.2.4 Pumps

The pump behaviour in off-design conditions was derived based on the process measurements when possible, and was deduced from the volumetric flows in design and part-load conditions otherwise, using a polynomial-form expression:

$$\eta_{\text{is,pmp,off-des}} = \eta_{\text{is,pmp,des}} \cdot \left(p_1 \left(\frac{\dot{V}_{\text{off-des}}}{\dot{V}_{\text{des}}} \right)^3 + p_2 \left(\frac{\dot{V}_{\text{off-des}}}{\dot{V}_{\text{des}}} \right)^2 + p_3 \left(\frac{\dot{V}_{\text{off-des}}}{\dot{V}_{\text{des}}} \right) + p_4 \right) \tag{C.21}$$

where:

$\eta_{\text{is,pmp,off-des}}$ and $\eta_{\text{is,pmp,des}}$ stand for the pump isentropic efficiencies in off-design and design point conditions;

$\dot{V}_{\text{off-des}}$ and $\dot{V}_{\text{des}}$ correspond to the volume flow rates in part-load and design conditions;

p_1, p_2, p_3 and p_4 are constants specific to each pump.

C.2.5 Generator

The generator efficiency is a function of the load at design point and is expressed as a second-order function of the electric load [297]:

$$\eta_{\text{gen,off-des}} = \frac{l\eta_{\text{gen,des}}}{l\eta_{\text{gen,des}} + (1-\eta_{\text{gen,des}})((1-f_{\text{Cu}}) + l^2 f_{\text{Cu}})} \tag{C.22}$$

where:

η_{gen} and $\eta_{\text{gen,dp}}$ are the generator efficiencies at part-load and design conditions;

l is the generator load;

f_{Cu} is the fraction of the total generator losses corresponding to the copper losses, here fixed to 23.5 %.

C.2.6 Bottoming cycle

A bottoming cycle can be coupled to a gas turbine in a combined cycle or combined heat and power configuration, implying that the waste heat recovery cycle acts as slave to the topping cycle, and that its performance varies with the gas turbine load. A change in this last parameter results in a different exhaust gas temperature at the inlet of the boiler, and therefore in different operating conditions.

This work assumes that the bottoming cycle to be integrated on-site operates in sliding-pressure mode, meaning that the pressure in the turbine is *not* fixed in relation to a set-point and is *not* directly regulated by valves. On the contrary, this pressure depends on the actual system conditions, and some advantages are an enhanced operational flexibility and a higher efficiency at part-load.

Three different control strategies are applicable, by controlling the pump rotational speed, as three parameters could be kept constant: the exhaust gas temperature at the outlet of the boiler (rejection temperature), the temperature difference between the exhaust gases and working fluid at the other boiler outlet (superheating approach), and the working fluid outlet temperature (turbine inlet temperature).

The third approach is taken in this work, verifying that there is no thermodynamic violation and that the temperature difference between the hot and cold sides does not go under 10 °C at any point, in particular at the inlet of the evaporator. This strategy was satisfying for the range of gas turbines loads covered in this study, but may not be appropriate if the gas turbine is run at very severe part-load conditions, as the gas turbine exhaust temperature drops significantly.

D Platforms data

This chapter goes through the details of the modelling of the different case studies, from the thermochemical modelling to the assumptions related to the process modelling and simulation. All details on process data for Platforms A, B and C can be found in Voldsund et al. [172, 173]. Most process data for Platform D is confidential and is therefore not presented in this manuscript, but the most important facts were presented in Nguyen et al. [214, 215].

D.1 Platform A

D.1.1 Thermochemical modelling

The feed of the system corresponds to the reservoir fluids, including liquid, gas and water fractions, and hypothetical components were used to simulate these streams. Their properties are given in Table D.1 and were derived by the oil company. The compositions of each phase in the reservoir fluids are given in Table D.2.

Table D.1: Molecular weight, M; normal boiling point, T_b; and ideal liquid density, $\rho_{id.liq.}$, for the hypothetical components used to describe the heavy oil fractions of Platform A.

Name	M, g/mol	T_b, °C	$\rho_{id.liq.}$, kg/m^3
HypoA-1	81	73	721.2
HypoA-2	108	99	740.1
HypoA-3	125	152	774.6
HypoA-4	171	230	817.1
HypoA-5	247	316	859.3
HypoA-6	388	437	906.2
HypoA-7	640	618	988.5

D.1.2 Process modelling

The flow rates of oil, gas and water in each well-stream were initially set as the allocated flow rates calculated by the oil company (Table D.3), and were then scaled so that the simulated flow rates of the output streams fitted with the measured data (Table D.4).

Table D.2: Composition of the three phases of the reservoir fluids, given as molar fractions.

Component	Gas	Liquid	Water
CO_2	$9.18{\cdot}10^{-3}$	$8.61{\cdot}10^{-3}$	0
Methane	0.83	0.78	0
Ethane	$6.81{\cdot}10^{-2}$	$6.41{\cdot}10^{-2}$	0
Propane	$3.74{\cdot}10^{-2}$	$3.55{\cdot}10^{-2}$	0
i-Butane	$5.71{\cdot}10^{-3}$	$5.52{\cdot}10^{-3}$	0
n-Butane	$1.34{\cdot}10^{-2}$	$1.30{\cdot}10^{-2}$	0
i-Pentane	$4.28{\cdot}10^{-3}$	$4.39{\cdot}10^{-3}$	0
n-Pentane	$5.51{\cdot}10^{-3}$	$5.80{\cdot}10^{-3}$	0
H_2O	0	0	1
N_2	$9.18{\cdot}10^{-3}$	$8.61{\cdot}10^{-3}$	0
HypoA-1	$9.07{\cdot}10^{-3}$	$1.34{\cdot}10^{-2}$	0
HypoA-2	$3.47{\cdot}10^{-3}$	$1.17{\cdot}10^{-2}$	0
HypoA-3	$7.14{\cdot}10^{-4}$	$1.49{\cdot}10^{-2}$	0
HypoA-4	0	$1.24{\cdot}10^{-2}$	0
HypoA-5	0	$9.01{\cdot}10^{-3}$	0
HypoA-6	0	$5.22{\cdot}10^{-3}$	0
HypoA-7	0	$3.44{\cdot}10^{-3}$	0

Table D.3: Allocated flow rates of gas, oil and water for each well-stream for the studied production day.

Well	Gas 10^3 Sm^3/h	Oil Sm^3/h	Water m^3/h
7	57.6	20.6	13.8
16	87.5	27.2	1.5
23	80.5	21.1	13.9
24	81.9	40.1	1.9
26	71.3	23.5	5.4

Table D.4: Measured flow rates in process streams leaving the platform.

Produced fluid	Unit	Flow rate
Export oil	Sm^3/h	132.5 ± 0.4
Injection gas	10^3 Sm^3/h	369 ± 17
Produced water	Sm^3/h	67 ± 5

Temperatures, pressures and flow rates that were set as measured throughout the process are given in Table D.5, Table D.6 and Table D.7.

Table D.5: Measured temperatures for the studied production day. The footnotes indicate which values other than measured ones are used in the simulated process flowsheet.

Description	Temperature, °C	Description	Temperature, °C
Production manifold		*Export pumping*	
From well 7, valve, in	85.8 ± 1.0	2nd pump, in	48.1 ± 1.0
From well 16, valve, in	84.7 ± 1.0	*Reinjection, Train A*	
From well 23, valve, in	87.1 ± 1.0	1st cooler, out	28.0[a]
From well 24, valve, in	81.0 ± 1.0	1st compressor, out	94.0 ± 1.0
From well 26, valve, in	79.6 ± 1.0	2nd cooler, out	28.0 ± 1.0
From well 7[b]	76.6 ± 1.0	2nd compressor, out	77.1 ± 1.0
From well 16[b]	75.6 ± 1.0	*Reinjection, Train B*	
From well 23[b]	71.3 ± 1.0	1st cooler, out	28.0 ± 1.0
From well 24[b]	76.8 ± 1.0	1st compressor, out	95.6 ± 1.0
From well 26[b]	74.3 ± 1.0	2nd cooler, out	28.0 ± 1.0
Separation train		2nd compressor, out	74.4 ± 1.0
Gas from 1st separator[b]	73.6 ± 1.0[c]	*Reinjection, Train C*	
Gas from 2nd separator[b]	59.2 ± 1.0	1st cooler, out	30.0[d]
Gas from 3rd separator[b]	46.9 ± 1.0	1st compressor, out	93.4 ± 1.0
Recompression train		2nd cooler, out	30.0[d]
1st cooler, out	39.9 ± 1.0	2nd compressor, out	80.7 ± 1.0
1st compressor, out	104.9 ± 1.0	*Fuel gas system*	
2nd cooler, out	21.0 ± 1.0	1st scrubber, gas out	35.0 ± 1.0
2nd compressor, out	111.8 ± 1.0	2nd scrubber, in	63.0 ± 1.0
3rd cooler, out	24.0 ± 1.0		
3rd compressor, out	146.5 ± 1.0		

[a] This temperature is not measured for the studied production day, so the set point of the cooler is used.

[b] After heat loss.

[c] The weighted mean based on mass flow rate for the two separators that in the simulated flowsheet is merged into one.

[d] This temperature is not measured and the set point for the cooler is not known for the studied production day, so the set point for the cooler a few weeks earlier is used.

In the reinjection trains, the total gas flow rate is determined by the measured gas injection rate. Flow rates are also measured at several places through each of the injection trains, and the flow rate of each train is set to make the simulated flow rates as close as possible to all of the measured flow rates (Table D.8). In the export pumping and fuel gas sections, not enough process variables were measured, so the efficiencies of the export pumps were found from their performance curves, and the pressure drop over the fuel gas cooler was taken from the cooler datasheet (Table D.9). Data on the cooling water system was retrieved separately (Table D.10). Efficiencies of the small pump in the drain system and the water pump were set to the assumed value of 75 %, and pressure drops over all separators were set to 0 kPa if not given.

Table D.6: Measured pressures for the studied production day. The footnotes indicate which values other than measured ones are used in the simulated process flowsheet.

Description	Pressure, bar	Description	Pressure, bar
Production manifold		*Reinjection, Train A*	
From well 7, valve, in	130.1 ± 1.3	1st compressor, in	68.8 ± 0.7
From well 16, valve, in	113.0 ± 1.1	1st compressor, out	137.4 ± 1.4
From well 23, valve, in	165.1 ± 1.7	2nd compressor, in	137.5 ± 1.4[a]
From well 24, valve, in	87.6 ± 0.9	2nd compressor, out	236 ± 2
From well 26, valve, in	88.8 ± 0.9	*Reinjection, Train B*	
From well 7, valve, out	73.0 ± 0.7	1st compressor, in	68.9 ± 0.7
From well 16, valve, out	73.0 ± 0.7	1st compressor, out	139.8 ± 1.4
From well 23, valve, out	73.1 ±0.7	2nd compressor, in	139.1 ± 1.4
From well 24, valve, out	72.7 ± 0.7	2nd compressor, out	236 ± 2
From well 26, valve, out	72.3 ± 0.7	*Reinjection, Train C*	
Separation train		1st compressor, in	66.1 ± 0.7
1st separator, in	70.4 ± 0.7[b]	1st compressor, out	131.9 ± 1.3
2nd separator, in	8.50 ± 0.08	2nd compressor, in	129.2 ± 1.3
3rd separator, in	2.80 ± 0.03	2nd compressor, out	236 ± 2
Water pump, out	8.77 ± 0.09	*Fuel gas system*	
Recompression train		1st scrubber, in	38.8 ± 0.4
1st compressor, in	2.41 ± 0.02	2nd scrubber, in	38.4 ± 0.4
1st compressor, out	5.72 ± 0.06	2nd scrubber, gas out	38.0 ± 0.4
2nd compressor, in	5.20 ± 0.05	To flare	9.30 ± 0.09
2nd compressor, out	18.75 ± 0.19	To turbine	18.25 ± 0.18
3rd compressor, in	18.29 ± 0.18	*Drain system*	
3rd compressor, out	70.0 ± 0.7	Drain pump, out	8.52 ± 0.09[c]
Export pumping			
1st pump, out	13.30 ± 0.13		
2nd pump, in	12.81 ± 0.13		
2nd pump, out	32.1 ± 0.3		

[a] This pressure was measured to 137.5 ± 1.4 bar, but can not be higher than the pressure out from the 1st separator, so in the simulation it is instead set to 137.4 bar.

[b] The weighted mean based on mass flow rate for the mesured values in the gas flow from the two separators that in the simulated flowsheet is merged into one.

[c] This is the pressure measured in the most recent pumping period.

The following simplifications and manipulations were done when simulating the process flowsheet:

- the 1st separation stage actually consists of two separators: a normal and a test separator, which are are continuously in use, but were merged into one component for simplicity;
- the separators overpredicted the separation of water and oil in the separation train, so in the simulation a part of the separated water from each of the separators was split off and added to the oil stream, to correct for this;
- in the drain system small amounts of liquid from knock-out drums in the flare system and from scrubbers with low liquid flow rates are collected in a reclaimed oil sump. The liquid is pumped to the 2nd separation stage after reaching a certain level, but it was simulated as a small pump that is continuously operating. Liquid from the flare system is neglected.

Table D.7: Measured flow rates set in the simulated process flowsheet for the studied production day.

Description	Unit	Flow rate
Separation train		
Water from 1st separator	Sm^3/h	54 ± 5
Water from 2nd separator	m^3/h	12.6 ± 1.3
Water pump, out	m^3/h	0.53 ± 0.05
Recompression train		
1st compressor, in	m^3/h	7100 ± 700
2nd compressor, in	m^3/h	5800 ± 600
3rd compressor, in	m^3/h	1560 ± 160
Export pumping section		
1st pump, out	m^3/h	230 ± 20
2nd pump, out	m^3/h	176 ± 18
Fuel gas system		
To flares	Sm^3/h	335 ± 14[a]
To power turbines	Sm^3/h	9630 ± 170

[a]Sum of pilot flame for high pressure and low pressure flare, where it is assumed that half of the measured flow rate for low pressure flare is for pilot flame while the rest is from other places in the system, and is negligible these places.

Measured flow rates are compared with simulated flow rates in Table D.8 and Table D.11. The simulated flow rates were within the uncertainty of the measured flow rates, when the uncertainty was known.

A measured pressure in the separation train was compared with a simulated pressure in Table D.12. The deviation between these numbers is due to the fact that height differences are not included in the simulation. The pressure difference corresponds to a height difference of 17 m within the separation train.

Table D.8: Measured and simulated flow rates of gas for the studied production day in the reinjection trains.

Description	Measured flow rate, m^3/h	Simulated flow rate, m^3/h
Train A		
1st compressor, in	1210 ± 120	1140
1st compressor, out	750 ± 70	750
2nd compressor, in	510 ± 50	503
Train B		
1st compressor, in	1300 ± 130	1213
1st compressor, out	770 ± 80	790
2nd compressor, in	530 ± 50	529
Train C		
1st compressor, in	2400 ± 200	2348
2nd compressor, in	1040 ± 100	1059

Table D.9: Efficiencies, η, of pumps in the export pumping section found from the performance curves of the pumps; and pressure drop, Δp, of cooler found from its datasheet.

Process unit	Variable	Value
Booster export pump	η, %	55
Main export pump	η, %	48
Fuel gas cooler	Δp, kPa	50

In Table D.13 the measured power consumption of each compression train is compared with the summed enthalpy change, ΔH, over the compressors in each train. The differences between the power consumption and the enthalpy changes are electric and mechanical losses. The numbers indicate that 84–90 % of the power consumed in each train end up in the process streams, and this is considered realistic.

Table D.10: Pressure, p; pressure drop, Δp; temperatures, T; and mass fractions, x, from the oil company's documentation of the cooling system set in the simulation of the cooling water system of Platform A.

Process unit	Variable	Value
Cooling medium to coolers	p, bar	7.8
Pressure drop on cold side in coolers	Δp, bar	0.5
Cooling medium to coolers	T, °C	17
Cooling medium (after mixing)	T, °C	30
Cooling medium, TEG	x_{TEG}, -	0.3
Cooling medium, water	x_{water}, -	0.7

Table D.11: Measured and simulated flow rates of gas for the studied production day in the separation train. The uncertainties for the two last gas flows in the separation train are not known, because the flow rates are lower than what the flowmeters are designed for.

Description	Measured flow rate, ton/h	Simulated flow rate, ton/h
Gas from 1st separator	320 ± 30^a	318
Gas from 2nd separator	8.1	10.4
Gas from 3rd separator	2.2	2.2

[a]The sum of the gas flow from the two separators that in the simulated flowsheet is merged into one.

Table D.12: Measured and simulated pressures for the studied production day in the separation train.

Description	Measured pressure, bar	Simulated pressure, bar
Oil from electrostatic coalescer	4.25 ± 0.04	2.80

Table D.13: Measured power consumption in compression trains and sum of simulated enthalpy change, $\Delta \dot{H}$, over the compressors for each train.

Compressor train	Measured power consumption, kW	Sum of simulated ΔH, kW
Recompression	5200 ± 100	4703
Reinjection A	5550 ± 110	4781
Reinjection B	5940 ± 120	5008
Reinjection C	9800 ± 200	8847

D.2 Platform B

D.2.1 Thermochemical modelling

Composition data was available for the reservoir fluids at the start of the field lifetime, and for the export gas from a few months before the simulated production day. It was not possible to get these composition data for the same production day, and it was then assumed that the composition of the gas phase has not changed significantly over time.

To simulate the well streams, the composition of the reservoir fluids was used, but to get the correct water-to-oil ratio, water was mixed in, while to get the correct gas-to-oil ratio, gas with the composition of the export gas was removed. The compositions of the three fluids used to simulate the well streams are given in Table D.14. Hypothetical components (developed by the oil company) were used to describe the heavy fractions of the reservoir fluids, and the properties set for these hypothetical components are given in Table D.15.

Table D.14: Composition of fluids used for simulation of feed streams of Platform B. The composition of gas is a measured composition of the exported gas a few months before the simulated production day. The composition of reservoir fluids is the composition of the reservoir at start the start of the field lifetime.

Component	Gas	Reservoir fluids	Water
Nitrogen	$1.89 \cdot 10^{-3}$	$1.80 \cdot 10^{-3}$	0
CO_2	$3.78 \cdot 10^{-2}$	$3.53 \cdot 10^{-2}$	0
Water	0	0	1
Methane	0.831	0.801	0
Ethane	$6.98 \cdot 10^{-2}$	$7.00 \cdot 10^{-2}$	0
Propane	$3.02 \cdot 10^{-2}$	$3.09 \cdot 10^{-2}$	0
i-Butane	$4.56 \cdot 10^{-3}$	$4.80 \cdot 10^{-3}$	0
n-Butane	$9.04 \cdot 10^{-3}$	$1.01 \cdot 10^{-2}$	0
i-Pentane	$2.71 \cdot 10^{-3}$	$3.50 \cdot 10^{-3}$	0
n-Pentane	$2.91 \cdot 10^{-3}$	$4.00 \cdot 10^{-3}$	0
HypoB-1	$1.03 \cdot 10^{-2}$	$5.10 \cdot 10^{-3}$	0
HypoB-2	0	$7.90 \cdot 10^{-3}$	0
HypoB-3	0	$8.50 \cdot 10^{-3}$	0
HypoB-4	0	$4.90 \cdot 10^{-3}$	0
HypoB-5	0	$4.50 \cdot 10^{-3}$	0
HypoB-6	0	$3.10 \cdot 10^{-3}$	0
HypoB-7	0	$2.00 \cdot 10^{-3}$	0
HypoB-8	0	$1.20 \cdot 10^{-3}$	0
HypoB-9	0	$8.00 \cdot 10^{-4}$	0
HypoB-10	0	$6.00 \cdot 10^{-4}$	0
HypoB-11	0	$3.00 \cdot 10^{-4}$	0
HypoB-12	0	$1.00 \cdot 10^{-4}$	0

Table D.15: Molecular weight, M; normal boiling point, T_b; ideal liquid density, $\rho_{id.liq.}$; critical temperature, T_c; critical pressure, p_c; critical volume, V_c; and acentric factor, ω, for the hypothetical components used to describe the heavy oil fractions of Platform B.

	M, g/mol	T_b, °C	$\rho_{id.liq.}$, kg/m^3	T_c, °C	p_c, bar	V_c, m^3/kmol	ω
HypoB-1	85.65	68.75	664.5	234.2	29.69	0.37	0.296
HypoB-2	91.13	91.95	741	255	34.49	0.3938	0.454
HypoB-3	104.3	116.7	765.5	279.3	30.35	0.4153	0.492
HypoB-4	118.9	142.2	778	302.2	26.38	0.4571	0.534
HypoB-5	140.1	176.3	790.7	331.6	22.35	0.5269	0.594
HypoB-6	167.5	217.6	805.5	365.2	19.12	0.6203	0.669
HypoB-7	197.5	255.9	818	397.8	16.87	0.7285	0.747
HypoB-8	229	291.1	828.9	429	15.3	0.8467	0.825
HypoB-9	256.6	318.6	838.6	454.5	14.38	0.952	0.89
HypoB-10	289	349.8	849.1	483	13.61	1.081	0.963
HypoB-11	336	390.1	861.8	521.5	12.81	1.271	1.059
HypoB-12	403.6	439	876.9	573.2	12.09	1.555	1.177

D.2.2 Process modelling

The process at Platform B was simulated for a real production day with stable and typical process conditions. Calculated flow rates of gas, condensate and water in each well-stream are given in Table D.16, while measured flow rates of exported gas, exported condensate and produced water are given in Table D.17. The well-stream flow rates were set such that the flow rates of the simulated product streams of the process fitted with the measured product streams in Table D.17 after all other input data in the simulation was set. The more uncertain calculated flow rates of the well streams in Table D.16 were used to set the ratio of flow from the different wells for each of the phases.

Table D.16: Calculated flow rates of gas, oil and water for each well-stream entering the production manifold at Platform B. These flow rates are estimated by the oil company, based on measurements, and they have a high uncertainty.

Well	Gas, 10^3 Sm^3/h	Condensate, Sm^3/h	Water, Sm^3/h
5	153.9	73.61	1.72
6	88	41.9	0.76
11	136	65.1	1.53
12	10.6	5.09	7.11
13	42.1	22.64	0.37
14	180.3	85.94	1.85

Measured temperatures, pressures and flow rates set within the process are given in Table D.18, while values set based on assumptions and information from documentation of the equipment are given in Table D.19. Measured process variables are compared with simulated process variables in Table D.20.

Table D.17: Measured flow rates in process steams leaving Platform B with uncertainty at 95 % confidence level.

Produced fluid	Variable	Value
Exported condensate	$\dot{F}$, Sm^3/h	238.9 ± 0.7
Exported gas	$\dot{F}$, 10^3 Sm^3/h	761 ± 8
Produced water	$\dot{F}$, m^3/h	12.6 ± 0.9

The following simplifications and manipulations were done in the simulation:

- in the real process there is an additional test separator in the 1st separation stage. This separator was merged into the main 1st stage separator;
- all identical parallel coolers, pumps and scrubbers were merged into one;
- the individual temperature of the return cooling medium from each of the coolers was set to the measured temperature of the mixed cooling medium from all coolers, unless this gave a temperature difference to the inlet gas temperature lower than 10 °C. In the latter case the temperature was set to get a difference of 10 °C;
- the gas fraction in the oil from the phase splitter was modified by splitting a part of the gas outlet stream and adding it to the oil stream;
- pressure drop in tubes and separators and heat loss from tubes are neglected. Pressure drop in heat exchangers, where this is not a function of measured pressures are set to 0.5 bar.

Table D.18: Measured process variables set in the simulated process flowsheet of Platform B.

Process stream description	Variable	Value	Process stream description	Variable	Value
Production manifold			*Recompression*		
From well 5, valve, in	p, bar	131.2	1st compressor, in	p, bar	2.26
From well 6, valve, in	p, bar	155.2	1st compressor, out	p, bar	9.35
From well 11, valve, in	p, bar	127.4	2nd compressor, in	p, bar	8.9
From well 12, valve, in	p, bar	123.2	2nd compressor, out	p, bar	27.88
From well 13, valve, in	p, bar	124.4	3rd compressor, in	p, bar	27.15
From well 14, valve, in	p, bar	145.9	3rd compressor, out	p, bar	62.87
From well 5, valve, out	p, bar	122	4th compressor, in	p, bar	61.87
From well 6, valve, out	p, bar	121.3	4th compressor, out	p, bar	118.4
From well 11, valve, out	p, bar	122.4	Condensate pump, out	p, bar	5.7
From well 12, valve, out	p, bar	121.1	1st cooler, out	T, °C	29.4
From well 13, valve, out	p, bar	121.7	1st compressor, out	T, °C	101.3
From well 14, valve, out	p, bar	121.6	2nd cooler, out	T, °C	31.6
From well 5, valve, in	T, °C	109.6	2nd compressor, out	T, °C	115.1
From well 6, valve, in	T, °C	107	3rd cooler, out	T, °C	30.0[a]
From well 11, valve, in	T, °C	110.1	3rd compressor, out	T, °C	95.5
From well 12, valve, in	T, °C	63.9	4th cooler, out	T, °C	35.0[a]
From well 13, valve, in	T, °C	101	4th compressor, out	T, °C	88.4
From well 14, valve, in	T, °C	110.5	1st compressor, in	$\dot{F}$, m^3/h	7200
Separation			2nd compressor, in	$\dot{F}$, m^3/h	1200
1st stage separator	p, bar	119.6	3rd compressor, in	$\dot{F}$, m^3/h	1410
2nd stage separator	p, bar	27.8	4th compressor, in	$\dot{F}$, m^3/h	650
3rd stage separator	p, bar	2.4	*Flare system*		
Phase splitter, gas out	$\dot{F}$, Sm^3/h	74,000	To flare	$\dot{F}$, Sm^3/h	94.3
Water pump, out	p, bar	61.06	*Condensate treatment*		
Fuel gas system			2nd pump, in	p, bar	18.78
After inlet valve	p, bar	39	2nd pump, out	p, bar	106.7
Fuel gas cooler, out	T, °C	29.8	Condensate cooler, out	T, °C	49.4
Fuel gas heater, out	T, °C	49.8	2nd pump, out	T, °C	56.4
To power turbines	$\dot{F}$, Sm^3/h	2300	*Cooling system*		
Gas treatment			Cooling medium (in)	p, bar	12.9
Wet gas scrubber	p, bar	118.2	Cooling medium (in)	T, °C	24.5
Wet gas cooler, out	T, °C	32	Cooling medium (out)	T, °C	55

[a] Set point for cooler

Table D.19: Values for efficiency, η; overall heat transfer coefficient, U; heat transfer surface area, A; temperature, T; pressure, p; mass fraction, x; and electric work, $\dot{W}_{el}$, assumed or from documentation from process equipment for Platform B.

Process unit	Variable	Value	Source
Separation			
Water pump	η, %	75	Assumed
Recompression			
Cross heat exchanger	Overall UA, kJ/(°C·h)	580,000	Assumed, operators
Condensate treatment			
1st pump	η, %	55	Pump performance curves
Cooling system			
Cooling medium, MEG	x_{MEG}, -	0.35	Documentation of cooling system
Cooling medium, water	x_{water}, -	0.65	Documentation of cooling system
Fuel gas system			
Fuel gas heater	$\dot{W}_{el}$, kW	0	Assumed, system description

Table D.20: Measured values for temperature, T; pressure, p; and flow, $\dot{F}$, compared with simulated values for Platform B.

Process stream description	Variable	Measured value	Simulated value
Separation			
1st stage separator	T, °C	105.5 ± 1.0	105.8
2nd stage separator	T, °C	86.9 ± 1.0	79.4
3rd stage separator	T, °C	67.3 ± 1.0	62.2
1st stage separator, water out	$\dot{F}$, m^3/h	4.8 ± 0.5	4.3
3rd stage separator, water out	$\dot{F}$, m^3/h	7.8 ± 0.8	8.3
Water pump, in	p, bar	3.75 ± 0.04	2.4
Gas treatment			
Wet gas scrubber, out	$\dot{F}$, 10^3 Sm^3/h	690 ± 70	725
Condensate treatment			
1st pump, in	p, bar	3.86 ± 0.04	2.4
1st pump, out	$\dot{F}$, m^3/h	250 ± 20	253
2nd pump, out	$\dot{F}$, m^3/h	250 ± 20	248

D.3 Platform C

D.3.1 Thermochemical modelling

Composition data was available for the reservoir fluids at the start of the field lifetime and for the imported gas. These two fluids plus water were mixed to produce well streams, giving realistic water-to-oil and gas-to-oil ratios (Table D.21). Properties of hypothetical components (developed by the oil company) used to describe the heavy fractions are given in Table D.22.

Table D.21: Composition of fluids (molar fraction) used for simulation of feed streams of Platform C. The 'gas' composition is the typical composition of the imported gas. The composition of the 'reservoir fluids' corresponds to the start of the field lifetime.

Component	Gas	Reservoir fluids	Water
Nitrogen	$8.2{\cdot}10^{-3}$	$2.7{\cdot}10^{-3}$	0
CO_2	$1.4{\cdot}10^{-2}$	$6.0{\cdot}10^{-4}$	0
Water	$1.0{\cdot}10^{-6}$	0	1
Methane	$8.6{\cdot}10^{-1}$	$1.6{\cdot}10^{-1}$	0
Ethane	$7.8{\cdot}10^{-2}$	$1.1{\cdot}10^{-2}$	0
Propane	$3.1{\cdot}10^{-2}$	$2.8{\cdot}10^{-3}$	0
i-Butane	$2.6{\cdot}10^{-3}$	$5.8{\cdot}10^{-3}$	0
n-Butane	$4.0{\cdot}10^{-3}$	$1.6{\cdot}10^{-3}$	0
i-Pentane	$4.7{\cdot}10^{-4}$	$3.7{\cdot}10^{-3}$	0
n-Pentane	$4.3{\cdot}10^{-4}$	$1.0{\cdot}10^{-3}$	0
HypoA-1	$2.4{\cdot}10^{-4}$	0	0
HypoC-1	0	$5.5{\cdot}10^{-2}$	0
HypoC-2	0	$8.3{\cdot}10^{-2}$	0
HypoC-3	0	$1.4{\cdot}10^{-1}$	0
HypoC-4	0	$2.4{\cdot}10^{-1}$	0
HypoC-5	0	$2.0{\cdot}10^{-1}$	0
HypoC-6	0	$9.5{\cdot}10^{-2}$	0

Table D.22: Molecular weight, M; normal boiling point, T_b; ideal liquid density, $\rho_{id.liq.}$; critical temperature, T_c; and critical pressure, p_c, for the hypothetical components used to describe the heavy oil fractions of Platform C.

Component	M, g/mol	T_b, °C	$\rho_{id.liq.}$, kg/m^3	T_c, °C	p_c, bar
HypoA-1	81.00	73.00	721.2	247.9	33.46
HypoC-1	98.78	85.76	754.3	269.3	35.50
HypoC-2	141.2	173.9	816.6	365.7	27.19
HypoC-3	185.8	240.5	861.0	434.1	22.71
HypoC-4	241.1	314.5	902.5	505.2	18.54
HypoC-5	404.5	487.1	955.3	647.0	10.45
HypoC-6	907.0	552.8	1007	710.0	9.610

D.3.2 Process modelling

The process at Platform C was simulated for a real production day with stable conditions, and the measured data given for this process is measured at 12.00 for this day. The day was a typical day with the exception that the produced water injection system was not in operation, so the water was discharged to the sea. The petroleum production was high enough to avoid by-pass of any of the oil heaters operating in the separation section, which may happen if the oil flow rate is considered too small.

Calculated flow rates for each well-stream are given in Table D.23. Calculated flow rates are flow rates for each phase in the three-phase well streams estimated by the oil company. Measured flow rates for product streams are given in Table D.24. The oil and gas flow rates in each well were set to make the simulated product streams fit with the measured product streams (Table D.24) after all other input data in the simulation was set.

The more uncertain calculated flow rates in the well streams were used to set the ratio of gas flow rates from each well and the ratio of oil flow rate from each well. Since the produced water was discharged to the sea, and not injected as usual, the flow rate of the produced water was not measured. The water flow rates in each well was therefore set equal to the calculated flow rate.

Measured temperatures, pressures and flow rates set in the simulation are given in Table D.25 and Table D.26, while values set based on assumptions and information from the equipment documentation are given in Table D.27.

The following simplifications were done in the simulation:

- all identical parallel coolers, pumps and scrubbers were merged into one;
- the delivery and return temperatures of the cooling medium in each cooler were set to the values for delivery and return temperature given in the documentation of the seawater system (Table D.27);
- pressure drops and heat losses in tubes and separators were neglected;
- for heat exchangers where values for pressure drops were not direct functions of measured pressures (Tables D.25 and D.26), the pressure drops were set equal to values found in datasheets (Table D.27) or to 1.0 bar;
- a dummy pump was included to increase the pressure of the condensate from the 1st scrubber in the recompression train, to avoid inconsistencies in the flowsheet.
- the pressure out of the pump was set to the pressure out from the 2nd stage separator. In reality, the pressure is increased because of the height differences.

Table D.23: Calculated flow rates of the gas (10^3 Sm^3/h), oil (Sm^3/h) and water (Sm^3/h) phases for each well-stream entering the production manifolds at Platform C.

Well	Gas	Oil	Water
High pressure production manifold			
2	18.06	43.69	9.59
6	6.84	17.49	4.10
8	7.29	17.56	0.54
9	3.97	11.49	0.01
10	7.35	20.03	0.83
15	30.52	133.09	18.15
16	30.51	106.90	5.63
17	3.88	7.41	0.01
18	6.85	13.49	0.01
19	7.22	33.02	0.33
21	2.72	7.81	0.00
25	4.43	22.91	3.42
26	6.59	20.60	0.42
27	3.71	14.40	0.45
28	15.51	41.93	2.21
30	6.15	19.17	4.21
35	18.62	48.19	3.08
40	6.40	27.01	1.42
Low pressure production manifold			
3	2.88	183.26	29.83
12	9.14	24.28	2.40
13	1.65	105.37	89.76
22	0.39	14.28	0.60
34	0.21	14.15	0.44
39	0.68	43.17	54.94
Test manifold			
1	22.08	91.81	27.42

Table D.24: Measured flow rates, $\dot{F}$, in process steams leaving Platform C.

Produced fluid	Variable	Value
Oil	$\dot{F}$, m^3/h	1147
Injected gas	$\dot{F}$, 10^3 Sm^3/h	360
Gas lift	$\dot{F}$, 10^3 Sm^3/h	22

Simulated values are compared with measured values in Table D.28. The following points can be noted:

- most simulated temperatures (21 out of 28) are within the uncertainty of 1 °C of the measured temperatures. The maximum deviation between measured and simulated temperature is 3.7 °C, and this is either due to measurements with higher errors than the assumed uncertainty, or due to inaccuracies in the equation of state. Since deviations higher than 1 °C only take place in a few of the wells, the effect of this is assumed to be negligible compared to other error sources;
- simulated pressure of water and oil entering the water and 1st oil pumps, are 2.75 bar, while the measured values are 4.20 and 3.96 bar, respectively. These deviations are found because height differences are not taken into consideration in the simulation. As discussed for Platform A in Voldsund et al. [172], this has little impact on the overall results;
- simulated flow rates in the oil export and gas treatment sections are within an uncertainty of the measured values of 10 %.

Table D.25: Measured values for pressure, p; temperature, T; and flow rate, $\dot{F}$, set in the simulated process flowsheet of Platform C. Part I.

Process stream	Variable	Value	Process stream	Variable	Value
High pressure production manifold			Well 21, valve, in	T, °C	50.5
Well 2, valve, in	p, bar	85.8	Well 25, valve, in	T, °C	58.5
Well 6, valve, in	p, bar	95.9	Well 26, valve, in	T, °C	60.9
Well 8, valve, in	p, bar	93.9	Well 27, valve, in	T, °C	57.0
Well 9, valve, in	p, bar	92.1	Well 28, valve, in	T, °C	60.9
Well 10, valve, in	p, bar	95.6	Well 30, valve, in	T, °C	64.2
Well 15, valve, in	p, bar	65.4	Well 35, valve, in	T, °C	67.8
Well 16, valve, in	p, bar	77.0	Well 40, valve, in	T, °C	64.4
Well 17, valve, in	p, bar	110.5	*Low pressure production manifold*		
Well 18, valve, in	p, bar	105.4	Well 3, valve, in	p, bar	14.61
Well 19, valve, in	p, bar	83.7	Well 12, valve, in	p, bar	90.2
Well 21, valve, in	p, bar	96.5	Well 13, valve, in	p, bar	13.04
Well 25, valve, in	p, bar	87.4	Well 22, valve, in	p, bar	70.2
Well 26, valve, in	p, bar	94.1	Well 34, valve, in	p, bar	48.4
Well 27, valve, in	p, bar	80.8	Well 39, valve, in	p, bar	22.5
Well 28, valve, in	p, bar	94.5	Well 3, valve, out	p, bar	9.20
Well 30, valve, in	p, bar	94.0	Well 12, valve, out	p, bar	8.08
Well 35, valve, in	p, bar	96.6	Well 13, valve, out	p, bar	9.36
Well 40, valve, in	p, bar	88.5	Well 22, valve, out	p, bar	7.85
Well 2, valve, out	p, bar	47.1	Well 34, valve, out	p, bar	8.05
Well 6, valve, out	p, bar	47.0	Well 39, valve, out	p, bar	8.22
Well 8, valve, out	p, bar	47.0	Well 3, valve, in	T, °C	71.1
Well 9, valve, out	p, bar	47.0	Well 12, valve, in	T, °C	61.7
Well 10, valve, out	p, bar	47.1	Well 13, valve, in	T, °C	70.9
Well 15, valve, out	p, bar	47.8	Well 22, valve, in	T, °C	56.0
Well 16, valve, out	p, bar	47.4	Well 34, valve, in	T, °C	57.2
Well 17, valve, out	p, bar	47.2	Well 39, valve, in	T, °C	71.8
Well 18, valve, out	p, bar	47.0	*Test manifold*		
Well 19, valve, out	p, bar	46.9	Well 1, valve, in	p, bar	60.4
Well 21, valve, out	p, bar	46.9	Well 1, valve, out	p, bar	14.76
Well 25, valve, out	p, bar	46.9	Well 1, valve, in	T, °C	68.4
Well 26, valve, out	p, bar	46.9	*Recompression*		
Well 27, valve, out	p, bar	46.8	1st compressor, in	p, bar	1.24
Well 28, valve, out	p, bar	47.0	1st compressor, out	p, bar	7.14
Well 30, valve, out	p, bar	47.2	2nd compressor, in	p, bar	5.84
Well 35, valve, out	p, bar	47.1	2nd compressor, out	p, bar	17.5
Well 40, valve, out	p, bar	47.0	3rd compressor, in	p, bar	16.8
Well 2, valve, in	T, °C	64.5	3rd compressor, out	p, bar	45.7
Well 6, valve, in	T, °C	66.1	1st cooler, out	T, °C	30.5
Well 8, valve, in	T, °C	58.0	1st compressor, out	T, °C	164.7
Well 9, valve, in	T, °C	60.6	2nd cooler, out	T, °C	28.3
Well 10, valve, in	T, °C	62.4	2nd compressor, out	T, °C	123.0
Well 15, valve, in	T, °C	71.8	3rd cooler, out	T, °C	26.5
Well 16, valve, in	T, °C	66.8	3rd compressor, out	T, °C	125.1
Well 17, valve, in	T, °C	51.7	1st compressor, in	$\dot{F}$, 10^3 Sm^3/h	6.3
Well 18, valve, in	T, °C	57.9	2nd compressor, in	$\dot{F}$, 10^3 Sm^3/h	101
Well 19, valve, in	T, °C	61.9	3rd compressor, in	$\dot{F}$, 10^3 Sm^3/h	87

Table D.26: Measured values for pressure, p; temperature, T; and flow rate, $\dot{F}$, set in the simulated process flowsheet of Platform C. Part II.

Process stream	Variable	Value	Process stream	Variable	Value
Separation and oil export			Import compressor, out	p, bar	184.3
HP degasser	p, bar	46.0	1st cooler, out	T, °C	27.0
Test separator	p, bar	12.9	1st compressor, out	T, °C	91.9
1st stage separator	p, bar	7.22	2nd cooler, out	T, °C	30.0
2nd stage separator	p, bar	2.75	2nd compressor, out	T, °C	91.6
Water pump, out	p, bar	13.48	Imported gas	T, °C	4.4
1st oil pump, out	p, bar	12.48	Import cooler, out	T, °C	29.0
2nd oil pump, in	p, bar	9.46	Import compressor, in	T, °C	9.0
2nd oil pump, out	p, bar	99.1	Import compressor, out	T, °C	52.5
Oil heater, out	T, °C	98.0	Imported gas	$\dot{F}$, 10^3 Sm^3/h	159
Export cooler, in	T, °C	80.8	For gas lift, HP	$\dot{F}$, 10^3 Sm^3/h	0
Export cooler, out	T, °C	74.0	For gas lift, LP	$\dot{F}$, 10^3 Sm^3/h	22
Gas treatment			For injection	$\dot{F}$, 10^3 Sm^3/h	360
1st compressor, in	p, bar	44.4	*Fuel gas system*		
1st compressor, out	p, bar	94.3	Scrubber, in	p, bar	39.0
2nd compressor, in	p, bar	93.1	Heater, out	T, °C	60.9
2nd compressor, out	p, bar	184.9	To flare	$\dot{F}$, Sm^3/h	0
Imported gas	p, bar	110.2	To turbines	$\dot{F}$, Sm^3/h	9650
Import compressor, in	p, bar	108.7			

Table D.27: Split flow ratios, values for split flow ratios, r; overall heat transfer coefficient, U; heat transfer surface area, A; pressure drop, Δp; efficiency, η; mass fraction, x; pressure, p; and temperature, T, assumed or from documentation from process equipment for Platform C.

Process unit	Variable	Value	Source
Separation and oil export			
Flow splitter	r, -	0.5	Separation system manual
Oil-water heat exchanger, UA	UA, kJ/C-h	$1.85 \cdot 10^6$	Assumed, operators
Electrostatic coalescer, water in oil	%	0.5	Product flow specification
Oil-oil heat exchanger, hot side	Δp, bar	1.5	Datasheet
Oil-oil heat exchanger, cold side	Δp, bar	1.5	Datasheet
Oil-water heat exchanger, hot side	Δp, bar	1.5	Datasheet
Oil-water heat exchanger, cold side	Δp, bar	1.5	Datasheet
Oil heater, hot side	Δp, bar	1.0	Datasheet
Oil heater, cold side	Δp, bar	1.5	Datasheet
Water pump	η, %	75	Assumed
1st oil pump	η, %	76	Pump performance curves
2nd oil pump	η, %	74	Pump performance curves
Gas treatment			
1st flow splitter, recirculation	r, -	0	Assumed, operators
2nd flow splitter, recirculation	r, -	0	Assumed, operators
Hot water system			
Heating medium	x_{water}, -	1.00	Hot water system manual
Delivery pressure	p, bar	25.9	Hot water system manual
Delivery temperature	T, °C	170	Hot water system manual
Return temperature	T, °C	120	Hot water system manual
Cooling system			
Cooling medium	x_{water}, -	1.00	Assumed
Delivery pressure	p, bar	11.4	Seawater system manual
Delivery temperature	T, °C	10	Seawater system manual
Return temperature	T, °C	45	Seawater system manual

Table D.28: Measured values for temperature, T; pressure, p; and flow, $\dot{F}$, compared with simulated values for Platform C.

Process stream	Variable	Measured value	Simulated value
High pressure production manifold			
Well 2, valve, out	T, °C	61.5	61.6
Well 6, valve, out	T, °C	62.7	62.9
Well 8, valve, out	T, °C	53.9	53.2
Well 9, valve, out	T, °C	58.6	56.5
Well 10, valve, out	T, °C	58.5	58.2
Well 15, valve, out	T, °C	70.7	70.9
Well 16, valve, out	T, °C	64.7	64.7
Well 17, valve, out	T, °C	43.4	43.6
Well 18, valve, out	T, °C	51.6	50.7
Well 19, valve, out	T, °C	59.9	59.8
Well 21, valve, out	T, °C	47.0	45.9
Well 25, valve, out	T, °C	56.7	57.1
Well 26, valve, out	T, °C	57.8	57.1
Well 27, valve, out	T, °C	55.5	54.7
Well 28, valve, out	T, °C	57.1	56.8
Well 30, valve, out	T, °C	61.5	61.6
Well 35, valve, out	T, °C	63.7	63.6
Well 40, valve, out	T, °C	62.1	62.1
Low pressure production manifold			
Well 3, valve, out	T, °C	70.5	71.0
Well 12, valve, out	T, °C	53.0	51.3
Well 13, valve, out	T, °C	70.6	70.9
Well 22, valve, out	T, °C	52.0	55.7
Well 34, valve, out	T, °C	54.9	57.4
Well 39, valve, out	T, °C	70.8	71.9
Test manifold			
Well 1, valve, out	T, °C	64.9	65.0
Separation and oil export			
Water pump, in	p, bar	4.20	2.75
1st oil pump, in	p, bar	3.96	2.75
1st separator, in	T, °C	65.1	65.5
2nd separator, in	T, °C	96.6	97.2
2nd oil pump, out	$\dot{F}$, Sm^3/h	1000	1100
Gas treatment			
1st compressor, in	$\dot{F}$, Sm^3/h	240,000	230,000
2nd compressor, in	$\dot{F}$, Sm^3/h	260,000	230,000
Fuel gas system			
Heater, in	T, °C	23.1	24.2

D.4 Platform D

D.4.1 Thermochemical modelling

The exact composition of the crude oil processed on the Draugen platform is unknown, and petroleum is therefore modelled as a blend of real and hypothetical components (Table D.29), for which the properties are deduced from assays available in the public domain.

Table D.29: Normal boiling point, T_b; API gravity, API; specific gravity, SG; characterisation factor, UOPK; molecular weight, M; critical temperature, T_c; and pressure, p_c, for the hypothetical components used to describe the heavy oil fractions of Platform D.

Hypotheticals	T_b, °C	API	SG	UOPK	M, g/mol	T_c, °C	p_c, MPa
HypoD-1	186.4	47.72	0.7895	11.89	151.4	372.5	2.2283
HypoD-2	197.5	45.66	0.7987	11.846	158.3	384.3	2.1664
HypoD-3	211.4	43.24	0.8098	11.799	167.3	399.0	2.0906
HypoD-4	225.3	40.95	0.8205	11.755	176.7	413.6	2.0188
HypoD-5	239.3	38.68	0.8315	11.707	186.4	428.2	1.9531
HypoD-6	253.2	36.30	0.8433	11.647	196.2	442.9	1.897
HypoD-7	267.0	33.92	0.8554	11.582	206.1	457.7	1.8466
HypoD-8	280.8	31.80	0.8665	11.53	216.6	472.1	1.7948
HypoD-9	294.7	30.25	0.8748	11.514	228.1	485.6	1.7333
HypoD-10	308.5	29.25	0.8803	11.535	240.8	498.1	1.6633
HypoD-11	322.5	28.56	0.8840	11.578	254.7	510.2	1.5899
HypoD-12	336.4	28.00	0.8872	11.626	269.3	521.9	1.52
HypoD-13	350.2	27.43	0.8904	11.671	284.3	533.5	1.4553
HypoD-14	364.0	26.79	0.8939	11.71	299.9	545.1	1.3961
HypoD-15	377.9	26.09	0.8979	11.742	315.9	556.9	1.3419
HypoD-16	391.9	25.42	0.9017	11.775	332.6	568.7	1.2903
HypoD-17	405.8	24.77	0.9055	11.807	349.9	580.3	1.2418
HypoD-18	419.9	24.10	0.9094	11.837	367.9	591.9	1.1963
HypoD-19	441.0	22.88	0.9166	11.862	395.2	609.9	1.1367
HypoD-20	467.3	21.31	0.9260	11.885	430.4	632.2	1.0704
HypoD-21	495.3	20.31	0.9321	11.954	472.7	654.3	0.9976
HypoD-22	523.4	20.03	0.9338	12.076	521.9	674.8	0.9218
HypoD-23	551.4	19.86	0.9349	12.201	575.1	694.7	0.8534
HypoD-24	579.2	19.58	0.9366	12.314	631.0	714.4	0.7937
HypoD-25	607.1	19.12	0.9395	12.409	688.9	734.4	0.7421
HypoD-26	635.0	18.42	0.9438	12.481	747.4	754.8	0.6979
HypoD-27	676.9	16.77	0.9543	12.531	831.8	786.6	0.6451
HypoD-28	732.2	13.70	0.9745	12.505	931.7	830.8	0.594
HypoD-29	775.0	10.85	0.9940	12.431	996.6	866.3	0.5649

The reservoir fluid composition for each well, as well as the split between the oil, gas and water phases, vary with time and depend on the wells – they were adjusted in the model to fit the flow rates and compositions of the gas, oil and water flows exiting the processing plant (Table D.30–Table D.32). Oil composition is based on crude oil assays from 2002 and gas composition on measurements of the fuel gas composition from 2010–2013.

Table D.30: Chemical composition of the fluids used for simulation of the reservoir well-streams, given on a molar basis (main compounds).

Component	Oil	Gas	Water
Carbon dioxide	0	$8.03 \cdot 10^{-3}$	0
Oxygen	0	$1.06 \cdot 10^{-3}$	0
Nitrogen	0	$7.05 \cdot 10^{-3}$	0
Water	0	0	1
Argon	0	$1.63 \cdot 10^{-5}$	0
Hydrogen sulphide	$7.84 \cdot 10^{-6}$	$1.00 \cdot 10^{-4}$	0
Methane	$1.22 \cdot 10^{-3}$	$5.53 \cdot 10^{-1}$	0
Ethane	$1.95 \cdot 10^{-3}$	$1.57 \cdot 10^{-1}$	0
Propane	$2.35 \cdot 10^{-2}$	$1.99 \cdot 10^{-1}$	0
n–Butane	$5.95 \cdot 10^{-2}$	$3.58 \cdot 10^{-2}$	0
i–Butane	0	$3.10 \cdot 10^{-2}$	0
n–Pentane	$5.68 \cdot 10^{-2}$	0	0
n–Hexane	$3.81 \cdot 10^{-2}$	0	0
n–Heptane	$2.59 \cdot 10^{-2}$	0	0
n–Octane	$1.62 \cdot 10^{-2}$	0	0
n–Nonane	$5.94 \cdot 10^{-3}$	0	0

D.4.2 Process modelling

The lack of data and information on the Draugen platform has led to the elaboration of several assumptions to ensure that the modelling and reconciliation problems become solvable:

- in the well-heads and production manifold section, pressures and temperatures were measured at the tubing head (THPs and THTs), i.e. at the outlet of the master valves placed before the production manifold and along the well-head structure. No measurements were available at the inlet and therefore the exergy destruction taking place in/between the wells and the production manifold is unknown. Significant pressure drops take place, as a lower pressure is required to allow the well-streams to flow to the plant;

  In order to estimate the exergy destruction that can take place in this part of the plant, the pressures were extrapolated to the gas lift pressures, and the temperatures were calculated to fit the measurements at the outlet, neglecting heat losses in the pipes. The assumed values are higher than the real ones, as the pressure at the inlet of the master valves must be lower than the gas lift pressures to ensure that the crude oil can flow;

  This lack of knowledge results in a high uncertainty and overestimations of the exergy destruction taking place in the well-heads. Carefulness should be exercised when discussing the efficiency of these systems. Investigating only the production manifolds without considering the well-heads would unfairly favour platforms with a low inlet pressure, even if a greater amount of pressure-based exergy is destroyed between the reservoir and the separation process;

Table D.31: Chemical composition of the fluids used for simulation of the reservoir well-streams, given on a molar basis (additional compounds).

Component	Oil	Gas	Water
2,2–Dimethyl–Propane	$4.09 \cdot 10^{-2}$	0	0
2–Methyl–Butane	0	$8.00 \cdot 10^{-2}$	0
Methylcyclopentane	$4.41 \cdot 10^{-3}$	0	0
2,2–Dimethyl–Butane	$9.06 \cdot 10^{-4}$	0	0
2,3–Dimethyl–Butane	$2.72 \cdot 10^{-3}$	0	0
2–Methyl–Pentane	$2.24 \cdot 10^{-2}$	0	0
3–Methyl–Pentane	$1.34 \cdot 10^{-2}$	0	0
Cyclohexane	$3.20 \cdot 10^{-2}$	0	0
Benzene	$5.00 \cdot 10^{-4}$	0	0
2,2,3–Trimethylbutane	$1.95 \cdot 10^{-4}$	0	0
3,3–Dimethylpentane	$3.90 \cdot 10^{-4}$	0	0
2,4–Dimethylpentane	$1.56 \cdot 10^{-3}$	0	0
2–Methylhexane	$1.17 \cdot 10^{-2}$	0	0
2,3–Dimethylpentane	$9.74 \cdot 10^{-4}$	0	0
3–Methylhexane	$1.09 \cdot 10^{-2}$	0	0
Cis–1,3–Dimethylcyclopentane	$4.97 \cdot 10^{-3}$	0	0
Trans–1,3–Dimethylcyclopentane	$4.57 \cdot 10^{-3}$	0	0
Trans–1,2–Dimethylcyclopentane	$8.75 \cdot 10^{-3}$	0	0
Methylcyclohexane	$5.01 \cdot 10^{-2}$	0	0
Ethylcyclopentane	$2.59 \cdot 10^{-3}$	0	0
Toluene	$9.54 \cdot 10^{-3}$	0	0
2,2,4–Trimethylpentane	$1.71 \cdot 10^{-4}$	0	0
2,5–Dimethylhexane	$1.20 \cdot 10^{-3}$	0	0
2,4–Dimethylhexane	$1.54 \cdot 10^{-3}$	0	0
3,4–Dimethylhexane	$1.71 \cdot 10^{-4}$	0	0
3,3–Dimethylhexane	$3.42 \cdot 10^{-4}$	0	0
2,3–Dimethylhexane	$1.88 \cdot 10^{-3}$	0	0
2–Methyl–3–Ethylpentane	$3.42 \cdot 10^{-4}$	0	0
2–Methylheptane	$8.55 \cdot 10^{-3}$	0	0
4–Methylheptane	$2.91 \cdot 10^{-3}$	0	0
3–Methylheptane	$1.54 \cdot 10^{-2}$	0	0
2,3,4–Trimethylpentane	$1.71 \cdot 10^{-4}$	0	0
1,1–Dimethylcyclohexane	$5.05 \cdot 10^{-3}$	0	0
Isopropylcyclopentane	$1.60 \cdot 10^{-2}$	0	0
Ethylcyclohexane	$1.74 \cdot 10^{-3}$	0	0
2,2–Dimethylheptane	$2.13 \cdot 10^{-3}$	0	0
2,6–Dimethylheptane	$1.25 \cdot 10^{-2}$	0	0
1–Trans–3,5–Trimethylcyclohexane	$1.24 \cdot 10^{-2}$	0	0

- in the separation system, the pressures measured at the outlet of two 1st stage separators are measured higher than at the inlet, which likely results from height differences of the sensors. In these cases, as potential energies and exergies are not considered within this study, the pressure drops were set equal to 0.15 bar, as it is the case in the 2nd train separator. The by-pass fraction around the crude oil heater is measured only for the oil

Table D.32: Chemical composition of the fluids used for simulation of the reservoir well-streams, given on a molar basis (hypotheticals).

Component	Oil	Gas	Water
HypoD-1	$1.57 \cdot 10^{-2}$	0	0
HypoD-2	$2.46 \cdot 10^{-2}$	0	0
HypoD-3	$2.34 \cdot 10^{-2}$	0	0
HypoD-4	$2.31 \cdot 10^{-2}$	0	0
HypoD-5	$2.40 \cdot 10^{-2}$	0	0
HypoD-6	$2.57 \cdot 10^{-2}$	0	0
HypoD-7	$2.70 \cdot 10^{-2}$	0	0
HypoD-8	$2.70 \cdot 10^{-2}$	0	0
HypoD-9	$2.53 \cdot 10^{-2}$	0	0
HypoD-10	$2.24 \cdot 10^{-2}$	0	0
HypoD-11	$1.99 \cdot 10^{-2}$	0	0
HypoD-12	$1.89 \cdot 10^{-2}$	0	0
HypoD-13	$1.68 \cdot 10^{-2}$	0	0
HypoD-14	$1.42 \cdot 10^{-2}$	0	0
HypoD-15	$1.19 \cdot 10^{-2}$	0	0
HypoD-16	$1.04 \cdot 10^{-2}$	0	0
HypoD-17	$9.67 \cdot 10^{-3}$	0	0
HypoD-18	$9.62 \cdot 10^{-3}$	0	0
HypoD-19	$2.30 \cdot 10^{-2}$	0	0
HypoD-20	$1.78 \cdot 10^{-2}$	0	0
HypoD-21	$1.07 \cdot 10^{-2}$	0	0
HypoD-22	$7.17 \cdot 10^{-3}$	0	0
HypoD-23	$5.63 \cdot 10^{-3}$	0	0
HypoD-24	$4.60 \cdot 10^{-3}$	0	0
HypoD-25	$3.88 \cdot 10^{-3}$	0	0
HypoD-26	$3.47 \cdot 10^{-3}$	0	0
HypoD-27	$6.39 \cdot 10^{-3}$	0	0
HypoD-28	$5.90 \cdot 10^{-3}$	0	0
HypoD-29	$3.04 \cdot 10^{-3}$	0	0

flowing from the 1st stage separator assigned to the 2nd train of the production manifold and is roughly equal to 3 %. The other oil flows are not heated and are directly mixed at the inlet of the 2nd stage separator. Water entrainment with oil at the 1st stage separator was calculated assuming equal fugacities of the two liquid phases, and gas entrainment was determined to meet the same volume flow at the inlet of the booster compressor;

- several pumps are used in the gas recompression and treatment section to drain the gas condensate back to the separation system, the efficiencies were unknown and assumed equal to 30 %, as for the other hydrocarbon pumps present on the plant. Heat losses in the scrubbers were neglected, as they resulted in a temperature drop of less than 1 °C in all cases, which is smaller than the uncertainty of these measurements;
- little information on the gas-glycol dehydration system was available: pressure drops were retrieved from the process information datasheets given by the operators, with

the exceptions of the temperature of the reflux condenser and reboiler, which were measured and equal to 98.4 and 204 °C. The volume flow of the glycol entering the contactor was estimated to 3.73 m^3/h. The contactor is a packed column and the glycol temperature at the inlet was set to be 3.5 °C higher than the gas one, as recommended by the operators. The pump efficiency was set to 90 %, as estimated in the corresponding datasheet. The anti-surge flow was neglected, since the power consumption of this component is negligible in any case;

- in the fuel gas handling system, the temperatures measured at the outlet of some scrubbers are higher than at the inlet, which suggests either supplementary heat addition not indicated in the flowchart, or issues with the sensors, such as improper location, calibration errors or noise. In the simulations, these temperatures were not set but calculated assuming adiabatic scrubbing, since the differences between the simulated and measured values may be imputable to measurement errors;

- gas lift is not used on seven of the production and subsea wells, and therefore the associated measurements were not considered in the simulations;

- the condensate treatment system includes two columns, including 15 (fractionation) and 16 (dehydration) trays. The pressure drops inside the columns were smaller than 0.01 bar and were neglected, with the exception of the kettle reboiler where it was set to 0.05 bar. No measurement of the stripping gas flow entering the dehydrator was available, and the value was set based on the process information diagrams and datasheets. The pump efficiencies were set to 30 %, as estimated by the manufacturers. The anti-surge flow was neglected, since the current circulating flow is close to the nominal one;

- limited data was available on the oil pumping section and the pump efficiency was set to 65 %, based on estimations from the performance maps;

- no recent measurement was available on the pressure drops in the cooling water system: the simulated values were chosen based on the calculated values from the manufacturer;

- the *low* and *high energy use* production days were chosen in the same time frame. The well-fluid flows and field conditions were similar between both days: differences on the average values and standard deviations were smaller than 1 %. The time period considered as representative for the *high energy use* production day excludes the start-up and the shut-down of the oil export system. The system was run at steady-state with a power consumption in the window of the maximum value minus 10 %, which is about 50 % of the duration of the complete loading period.

D.5 Platform E

D.5.1 Thermochemical modelling

At the difference of the models derived for the four North Sea platforms presented in this appendix, the model of Platform E is not based on the use of hypothetical compounds. The feed, oil and gas compositions (Table D.33) were given in de Oliveira Jr. and Van Hombeeck [59] and the medium to heavy fractions of the petroleum streams were simulated by a mixture of known chemical compounds (hexane to undecane).

The properties of the heaviest fraction, denoted C12+, were not given, and this fraction of the feed is simulated using n-pentadecane ($C_{15}H_{32}$), as it gives the closest results to the ones presented in the literature for matching the flow rates of the outlet streams (Table D.34). The largest discrepancy corresponds to the mass flow rate of the recycled condensate mixed with the feed, which is found to be about 15 %.

Table D.33: Composition of fluids (molar fraction) used for simulation of feed and outlet streams of Platform E. The 'gas' and 'oil' compositions are the typical composition of the outlet exported gas and oil.

Component	Feed	Gas	Oil
Methane	$1.3{\cdot}10^{-1}$	$8.5{\cdot}10^{-1}$	$3.7{\cdot}10^{-3}$
Ethane	$9.2{\cdot}10^{-3}$	$6.1{\cdot}10^{-2}$	$2.2{\cdot}10^{-3}$
Propane	$6.6{\cdot}10^{-3}$	$4.2{\cdot}10^{-2}$	$6.1{\cdot}10^{-3}$
i-Butane	$1.6{\cdot}10^{-3}$	$9.4{\cdot}10^{-3}$	$3.5{\cdot}10^{-3}$
n-Butane	$3.4{\cdot}10^{-3}$	$1.9{\cdot}10^{-2}$	$9.7{\cdot}10^{-3}$
i-Pentane	$1.4{\cdot}10^{-3}$	$6.2{\cdot}10^{-3}$	$8.0{\cdot}10^{-3}$
n-Pentane	$1.8{\cdot}10^{-3}$	$7.2{\cdot}10^{-3}$	$1.2{\cdot}10^{-2}$
n-Hexane	$3.1{\cdot}10^{-3}$	$5.6{\cdot}10^{-3}$	$3.7{\cdot}10^{-2}$
n-Heptane	$3.4{\cdot}10^{-3}$	$1.4{\cdot}10^{-3}$	$5.2{\cdot}10^{-2}$
n-Octane	$4.2{\cdot}10^{-3}$	$2.0{\cdot}10^{-4}$	$6.8{\cdot}10^{-2}$
n-Nonane	$6.6{\cdot}10^{-3}$	0	$1.1{\cdot}10^{-1}$
n-Decane	$1.9{\cdot}10^{-3}$	0	$3.1{\cdot}10^{-2}$
n-Undecane	$3.9{\cdot}10^{-3}$	0	$6.4{\cdot}10^{-2}$
C12+	$3.6{\cdot}10^{-2}$	0	$5.9{\cdot}10^{-1}$
Water	$7.9{\cdot}10^{-1}$	$8.0{\cdot}10^{-4}$	$1.8{\cdot}10^{-3}$

Table D.34: Measured flow rates, $\dot{m}$, in process steams leaving Platform E.

Produced fluid	Variable	Value
Oil	$\dot{m}$, t/h	285
Gas	$\dot{m}$, t/h	29
Water	$\dot{m}$, t/h	136

D.5.2 Process modelling

No information on the process and measurement uncertainties was given, so the exact values (Table D.35) were inserted in the process simulation software. Similarly, the component data (Table D.36) was used to calibrate the model, and it should be noticed that there are apparently no recirculation flows around the compressors.

Table D.35: Measured values for pressure, p; temperature, T; and flow rate, $\dot{m}$, set in the simulated process flowsheet of Platform E.

Process stream	Variable	Value	Process stream	Variable	Value
Separation train			4th scrubber	p, bar	173.9
1st stage separator	p, bar	9.3	Exported gas	p, bar	173.87
2nd stage separator	p, bar	2.2	Condensate from all scrubbers	p, bar	1.7
1st stage separator	T, °C	90	1st scrubber	T, °C	40
2nd stage separator	T, °C	89.9	2nd scrubber	T, °C	40
Gas from 1st separator	$\dot{m}$, t/h	34.23	3rd scrubber	T, °C	40
Water from 1st separator	$\dot{m}$, t/h	136	4th scrubber	T, °C	40
Water from 2nd separator	$\dot{m}$, t/h	0	Exported gas	T, °C	40
Recompression train			Condensate from all scrubbers	T, °C	30.9
Cooler, in	$\dot{m}$, t/h	0.852	Condensate from 1st scrubber	$\dot{m}$, t/h	3.857
Scrubber	p, bar	1.7	Condensate from 2nd scrubber	$\dot{m}$, t/h	1.3095
Scrubber	T, °C	40	Condensate from 3rd scrubber	$\dot{m}$, t/h	0.774
Condensate from scrubber	$\dot{m}$, t/h	0.115	Condensate from 4th scrubber	$\dot{m}$, t/h	0.014
Gas treatment			Condensate from all scrubbers	$\dot{m}$, t/h	6.069
1st scrubber	p, bar	8.6	*Oil pumping*		
2nd scrubber	p, bar	22.9	Exported oil	p, bar	68.65
3rd scrubber	p, bar	69.9	Exported oil	T, °C	92.7

Table D.36: Efficiencies of pumps in the export pumping section, of compressors in the gas recompression and treatment processes, and of gas turbines and furnaces in the utility plant.

Process unit	Variable	Value
Compressor	η_{pol}, %	75
Compressor	η_{mec}, %	90
Pump	η_{pp}, %	75
Gas turbine	η_{th}, %	30
Furnace	η_{th}, %	95
HRSG	η_{th}, %	60

E Data validation and reconciliation

The systems of balance equations over industrial chemical processes such as oil and gas platforms are basic, meaning that inconsistencies of the mass and energy balances are related to erroneous process models or to measurement errors. In order to ensure a consistent evaluation of the system, the data must be validated and adjusted to satisfy the mass and energy balance constraints. The adjustment method based on statistical theory of errors is called data validation and reconciliation, and the theory and an example of this method are presented in this appendix.

E.1 Theory

The data reconciliation method assumes that there are only *random errors*, i.e. errors due to measurement noise, and that there are no *systematic errors*, i.e. errors due to imperfect calibration or observation methods.

Performing a data reconciliation allows therefore for exploiting properly the information retrieved from the measurements, taking into account the errors associated with each sensor. However, the number of unmeasured variables (m) must be smaller than the number of equations used to describe the system (p), and the level of redundancy (R) illustrates whether the model is possibly solvable:

$$R = p - m \tag{E.1}$$

The problem is then solvable if the level of redundancy is higher than 0, and if all the measurements provide information on the missing variables. This situation is called *positive* redundancy. In this case, the data reconciliation problem can be formulated as [298]:

$$\min_{x_i, u_j} \sum_{i=1}^{n} w_i \cdot (x_i^* - x_i)^2 \quad \text{subject to } g_l(x_i, u_j) = 0 \text{ and } l = 1, ..., m \tag{E.2}$$

where:

n is the number of measured variables;

x_i is the measured value of the variable i;

x_i^* is the corresponding reconciled value;

w_i is the weight related to the measurement accuracy;

u_j is the estimate of the unmeasured variable j;

$w_i \cdot (x_i^* - x_i)^2$ is the penalty of the measurement of the variable i;

$g_l(x_i, u_j)$ is the vector of process equations.

This problem is called a constrained weighted least-squares optimisation problem, for which the objective is to minimise the weighted errors on the measurements, i.e. the sum of the measurement penalties, under the constraints describing the physical behaviour of the process. These constraints are generally related to the material and energy balances, and possibly to the practical issues associated with the process operations. Assuming that the *random errors* are stochastically independent and normally distributed, this problem can be reformulated as:

$$\min_{x_i, u_j} \sum_{i=1}^{n} \frac{\left(x_i^* - x_i\right)^2}{\sigma_i^2} \tag{E.3}$$

where σ_i is the standard deviation of the variable i.

Several types of standard deviations (uncorrected sample, corrected sample, unbiased sample) can be calculated. The ones considered in this work are the sample standard deviations for one production day, given at 95 % confidence interval. This implies that there is a 95 % probability that a measurement taken in that day falls in the range $\bar{x} \pm 2\,\sigma_i$ [299]:

$$\sigma_i = \sqrt{\frac{1}{N_{\text{obs}} - 1} \sum_{N_{\text{obs}}} (x_k - \bar{x})^2} \tag{E.4}$$

where:

k is the kth observation;

N_{obs} is the number of observations of the variable i;

$\bar{x}$ is the arithmetic mean of the variable x_k for N observations.

The sample standard deviation gives information on the variations of the flow and field conditions over a production day but does *not* reflect systematic errors caused by calibration

imperfections. Redundant measurements that can be used for data reconciliation were only available for the flow rates of the input and output streams. However, other measured variables, such as temperatures and pressures, are used in this study to calculate the energy and exergy flows.

The data reconciliation method builds on the assumption that only random errors are present. If this assumption is not justified, data reconciliation may result into improper data adjustments and faulty estimates. The detection of gross errors may be based on engineer's experience and on statistical tests. For example, the *global* test, also called *Chi-square* test, can be used to evaluate a set of measured values, by comparing the sum of the penalty terms to a percentile of the probability density function of a chi-square distribution. It is particularly useful to detect whether one or more gross errors are present in the measurements, but does not give a clear indication on the location of these errors.

E.2 Data reconciliation

The data reconciliation method was applied on Platforms A and D, and the application of this technique is presented for the first case study. The standard deviations suggested by the platform operators are used in the reconciliation problem, and the allocation fractions of the gas, water and oil flows to each well are assumed to have an accuracy of ± 5 %.

The overall processing plant, excluding the fuel gas handling sub-system, was modelled and simulated using the software Vali® [40]. The convergence goodness and speed depend strongly on the model initialisation, and the results obtained with the models developed on Aspen Plus were used at first, together with the measurements.

The process model can be described by 1139 equations, while the numbers of unmeasured variables, constants and measured variables amount to 1117, 259 and 99, respectively. The total number of redundancies is only 22, of which 1 is trivial. As a consequence, only the values of a few variables, such as the flowrates (Table E.1, and Table E.2) are corrected in the reconciliation process, while the values of others, such as the temperatures (Table E.3) and pressures (Table E.4), cannot be improved. The values obtained with the backwards approach of Voldsund et al. [117] and in this work (Table E.5, Table E.6, and Table E.7) are strongly similar.

Table E.1: Reconciled outflows, accuracies and penalties.

Produced fluid	Unit	Reconciled flowrate	Reconciled accuracy	Penalty
Export oil	Sm^3/h	132.3	0.4	0.2
Injection gas	$10^3\ Sm^3/h$	365	4	0.06
Produced water	Sm^3/h	65	2	0.09

Table E.2: Reconciled flowrates for the studied production day.

Flow	Unit	Reconciled flowrate	Reconciled accuracy	Penalty
Separation				
Gas from 1st separator	m^3/h	318	3	0.003
Gas from 2nd separator	m^3/h	10.4	0.1	8
Gas from 3rd separator	m^3/h	1.8	0.1	5
Water from 1st separator	Sm^3/h	65	2	5
Water from 2nd separator	m^3/h	0	10	90
Recompression train				
Gas, 1st compressor, in	m^3/h	7100	700	0
Gas, 2nd compressor, in	m^3/h	5800	600	0
Gas, 3rd compressor, in	m^3/h	1560	160	0
Export pumping section				
Oil, 1st pump, out	m^3/h	231	20	0.003
Oil, 2nd pump, out	m^3/h	176	18	0.001
Reinjection Train A				
Gas, 1st compressor, in	m^3/h	1140	50	0.3
Gas, 1st compressor, out	m^3/h	750	35	2
Gas, 2nd compressor, in	m^3/h	501	23	0.03
Reinjection Train B				
Gas, 1st compressor, in	m^3/h	1180	60	0.8
Gas, 1st compressor, out	m^3/h	770	40	0
Gas, 2nd compressor, in	m^3/h	510	20	0.1
Reinjection Train C				
Gas, 1st compressor, in	m^3/h	2300	80	0.3
Gas, 2nd compressor, in	m^3/h	1030	40	0.04

Table E.3: Reconciled temperatures for the studied production day.

Description	Reconciled temperature, °C	Reconciled accuracy	Penalty
Production manifold			
From well 7, valve, in	85.8	1.0	0
From well 16, valve, in	84.7	1.0	0
From well 23, valve, in	87.1	1.0	0
From well 24, valve, in	81.0	1.0	0
From well 26, valve, in	79.6	1.0	0
From well 7	67.7	0.43	78
From well 16	75.6	0.28	0.012
From well 23	74.4	0.38	9.4
From well 24	85.2	0.66	71
From well 26	75.9	0.24	2.6
Separation train			
Gas from 1st separator	73.7	1.0	0.010
Gas from 2nd separator	58.3	0.2	0.74
Gas from 3rd separator	46.9	1.0	0
Recompression train			
1st cooler, out	39.9	1.0	0
1st compressor, out	104.9	1.0	0
2nd cooler, out	21.0	1.0	0
2nd compressor, out	111.8	1.0	0
3rd cooler, out	23.9	1.0	0.0045
3rd compressor, out	146.5	1.0	0
Oil pumping			
2nd pump, in	48.1	1.0	0
Reinjection, Train A			
1st cooler, out	28.0	1.0	0
1st compressor, out	94.0	1.0	0
2nd cooler, out	28.0	1.0	0
2nd compressor, out	77.1	1.0	0
Reinjection, Train B			
1st cooler, out	28.0	1.0	0
1st compressor, out	95.6	1.0	0
2nd cooler, out	28.0	1.0	0
2nd compressor, out	74.4	1.0	0
Reinjection, Train C			
1st cooler, out	30.0	1.0	0
1st compressor, out	93.4	1.0	0
2nd cooler, out	30.0	1.0	0
2nd compressor, out	80.7	1.0	0

Table E.4: Reconciled pressures for the studied production day.

Description	Reconciled pressure, bar	Reconciled accuracy	Penalty
Production manifold			
From well 7, valve, in	128.4	1.3	1.7
From well 16, valve, in	113	1.1	0
From well 23, valve, in	166.0	1.7	0.27
From well 24, valve, in	89.2	0.89	3.3
From well 26, valve, in	89.1	0.89	0.09
From well 7	74.1	0.69	2.7
From well 16	73.0	0.69	0
From well 23	72.8	0.69	0.16
From well 24	71.6	0.69	2.6
From well 26	72.1	0.69	0.070
Separation train			
Gas from 1st separator	70.4	0.7	0
Gas from 2nd separator	8.5	0.08	0
Gas from 3rd separator	2.8	0.0	0
Recompression train			
1st compressor, in	2.41	0.02	0
1st compressor, out	5.72	0.06	0
2nd compressor, in	5.2	0.05	0
2nd compressor, out	18.75	0.19	0
3rd compressor, in	18.29	0.18	0.00033
3rd compressor, out	70	0.7	0
Export pumping			
1st pump, out	13.30	0.13	0
2nd pump, in	12.81	0.13	0
2nd pump, out	32.1	0.3	0
Reinjection, Train A			
1st compressor, in	68.7	0.7	0.007
1st compressor, out	137.4	1.4	0
2nd compressor, in	137.4	1.4	0
2nd compressor, out	236	2	0
Reinjection, Train B			
1st compressor, in	68.8	0.7	0.01
1st compressor, out	139.8	1.4	0
2nd compressor, in	139.1	1.4	0
2nd compressor, out	236	2	0
Reinjection, Train C			
1st compressor, in	66.0	0.7	0.01
1st compressor, out	131.9	1.3	0
2nd compressor, in	129.2	1.3	0
2nd compressor, out	236	2	0

Table E.5: Reconciled recycling fractions for the studied production day.

Description	Reconciled fraction
Oil pumping	
1st pump	0.24
2nd pump	0.22
Recompression	
1st compressor	0.94
2nd compressor	0.67
3rd compressor	0.71

Table E.6: Reconciled isentropic efficiencies for the studied production day.

Description	Reconciled efficiency
Recompression	
1st compressor	0.41
2nd compressor	0.71
3rd compressor	0.57
Reinjection Train A	
1st compressor	0.64
2nd compressor	0.54
Reinjection Train B	
1st compressor	0.64
2nd compressor	0.56
Reinjection Train C	
1st compressor	0.66
2nd compressor	0.63

Table E.7: Reconciled power consumption in compression trains.

Compressor train	Reconciled power consumption, kW
Recompression	4760
Reinjection A	4770
Reinjection B	4880
Reinjection C	8990

E.3 Data validation

A good match between the measured and reconciled flowrates is found, with the exception of the gas and water flows out of the 1st and 2nd separation stages. The *global test* shows that the sum of the penalty terms reaches 350 and a critical chi-square value of 33, for a significance level of 95 %, which suggests that there are measurements biasing the data reconciliation problem. However, the comparison of different process software suggests that the model developed with Vali® overpredicts the water separation at the 1st stage by about 15 %.

An adjustment of the process model to correct this issue improves the model quality, with a total penalty sum of 265 and a critical chi-square value of 31. The next step is therefore to validate the data, by gross error *elimination* or *relaxation*. This can be performed in three different ways, by considering at first the measurements with the highest penalty, or the measurements with the highest impact on the overall penalty.

Removing the measurements with the highest penalty or with the highest correction penalty results in the same reconciled values, an overall penalty of 22 and a critical chi-square value of 28. The measurements that are eliminated, though in a different order, are:

- the temperature at the outlet of Well 7;
- the temperature at the outlet of Well 23;
- the temperature at the outlet of Well 24.

Removing the measurements with the highest impact results in an overall penalty of 16 and a critical chi-square value of 28, but the measurements that are eliminated are different:

- the allocated water flowrate at Well 24;
- the temperature at the outlet of Well 7;
- the allocated gas flowrate at Well 23.

The comparison of the two approaches illustrates significant differences (Table E.8).

Relaxing gross errors, instead of eliminating them, means relaxing the uncertainty estimates for the doubtful measurements (Table E.9). The overall penalty falls down to 19.6 and the critical chi-square value to 31.4, and the measurements that are relaxed are:

- the pressures and temperatures of Well 7, inlet and outlet;
- the pressures and allocated flowrate of Well 24, inlet and outlet;
- the allocated gas flowrate of Well 23.

Table E.8: Reconciled variables for the studied production day, after gross error elimination using the highest penalty and highest impact approaches.

Variable	Unit	Measured value	Reconciled value (highest penalty)	Reconciled value (highest impact)
Outflows				
Export oil	Sm^3/h	132.5 ± 0.4	132.3	132.3
Injection gas	$10^3\ Sm^3/h$	369 ± 17	361	386
Produced water	Sm^3/h	67 ± 5	64	62
Power consumption				
Recompression	kW	5200 ± 100	4750	4780
Reinjection Train A	kW	5550 ± 110	4730	4960
Reinjection Train B	kW	5940 ± 120	4830	5100
Reinjection Train C	kW	9800 ± 200	8860	9700
Anti-surge fractions				
Compressor 1		N/A	0.94	0.94
Compressor 2		N/A	0.67	0.68
Compressor 3		N/A	0.70	0.71
Pump 1		N/A	0.24	0.24
Pump 2		N/A	0.22	0.22

Table E.9: Reconciled variables for the studied production day, after gross error relaxation.

Variable	Unit	Measured value	Reconciled value
Outflows			
Export oil	Sm^3/h	132.5 ± 0.4	132.3
Injection gas	$10^3\ Sm^3/h$	369 ± 17	384
Produced water	Sm^3/h	67 ± 5	63
Power consumption			
Recompression	kW	5200 ± 100	4780
Reinjection Train A	kW	5550 ± 110	4940
Reinjection Train B	kW	5940 ± 120	5080
Reinjection Train C	kW	9800 ± 200	9620
Anti-surge fractions			
Compressor 1		N/A	0.94
Compressor 2		N/A	0.67
Compressor 3		N/A	0.70
Pump 1		N/A	0.24
Pump 2		N/A	0.22

F Simulation software

The simulations of several offshore platforms have been implemented on Aspen Plus and Hysys, which are widely used in industrial applications. Discussions with engineers in oil and gas companies suggest that the latter is more commonly used for modelling upstream petroleum processes, whilst the second may be preferred for complex chemical systems. This appendix reports some of the differences found between both software.

Although both software build on similar thermodynamic models (e.g. Peng-Robinson) and convergence methods (e.g. Newton-Raphson), they may present different numerical resolution sequences and feature minor to major differences in terms of thermodynamic models (e.g. interaction coefficients between chemical compounds). The two software are compared based on the simulations of four oil and gas platforms, for which only the final outflows, temperatures and pressures across the systems are set equal, using real data measurements.

The major differences correspond to the prediction of the flow rates at the outlet of the 3-phase separators in the petroleum separation process, despite the high similarities with regards to the composition of these streams. In Aspen Plus, the light- and medium-weight hydrocarbon recovery is overestimated (up to 9 %) for volatile oils and gases, while it is underestimated (up to 3 %) for heavy oils.

The flow rate discrepancy reaches nearly 20 % when it comes to the prediction of the gas recovered at the last separation stage, but is below 3 % in all cases for the calculations of the gas entering the gas treatment section. These discrepancies suggest that one of the main differences lies in the prediction of the separation efficiency between the liquid and vapour phases, or, in the entrainment of the light hydrocarbons and water with the petroleum stream.

These differences stress the importance of getting additional process data to adjust the efficiencies of the 3-phase separators and scrubbers in the separation, gas recompression and treatment sections. These issues were corrected by considering the power measurements for the compressors in the gas recompression process, and by the use of the flow measurements of the gas and oil flows at the outlet of the 1st stage separator.

G Production manifold

The introduction of an additional pressure level in the production manifolds can result in further energy savings. The problem may be reformulated as a MINLP problem, aiming at maximising the oil and gas production and minimising the power consumption. This appendix highlights the main equations.

Each well unit is associated with two types of variables: an integer variable, $y_{\text{well,PM}}$, which defines whether the well is connected (1) or not (0) to a given pressure level of the separation or gas compression sections, and a continuous variable, Δp_{well}, which corresponds to the pressure drop over the production manifold valves. Four pressure levels are considered, corresponding to the low (LP), test (TP), high (HP) and very high pressure (VHP) ones. The objective function is subject to practical and thermodynamic constraints, such as:

- the feed from a given well cannot be split between several production manifolds;

$$\forall \text{well} \sum_{\text{PM}}^{N_{\text{PM}}} y_{\text{well,PM}} = 1 \tag{G.1}$$

- the low (LP) and test (TP) pressures are fixed based on Voldsund et al. [300];

$$p_{\text{LP}} = 7.85;\ p_{\text{TP}} = 14.76 \tag{G.2}$$

- the pressure of each level equals the lowest pressure of the feed streams of that level;

$$\forall \text{PM}\ p_{\text{PM}} = \min \sum_{\text{well}}^{N_{\text{well}}} \left(y_{\text{well,PM}} (p_{\text{well,in}} - \Delta p_{\text{well}}) \right) \tag{G.3}$$

- the streams from the wells with an original pressure higher than the LP manifold can only be routed to the VHP or HP levels.

$$p_{\text{well,in}} - \Delta p_{\text{well}} \geq p_{\text{LP}}, p_{\text{TP}} \tag{G.4}$$

If I was young, I'd flee this town
I'd bury my dreams underground
As did I, we drink to die, we drink tonight.

— Beirut

DTU Mechanical Engineering
Section of Thermal Energy
Technical University of Denmark

Nils Koppels Allé, Bld. 403
DK- 2800 Kgs. Lyngby
Denmark
Phone (+45) 4525 4131
Fax (+45) 4588 4325
www.mek.dtu.dk
ISBN: 978-87-7475-392-6

DCAMM
Danish Center for Applied Mathematics and Mechanics

Nils Koppels Allé, Bld. 404
DK-2800 Kgs. Lyngby
Denmark
Phone (+45) 4525 4250
Fax (+45) 4593 1475
www.dcamm.dk
ISSN: 0903-1685